NOTICE

The quality of this microform is heavily dependent upon the quality of the original thesis submitted for microfilming. Every effort has been made to ensure the highest quality of reproduction possible.

If pages are missing, contact the university which granted the degree.

Some pages may have indistinct print especially if the original pages were typed with a poor typewriter ribbon or if the university sent us an inferior photocopy.

Previously copyrighted materials (journal articles, published tests, etc.) are not filmed.

Reproduction in full or in part of this microform is governed by the Canadian Copyright Act, R.S.C. 1970, c. C-30.

AVIS

La qualité de cette microforme dépend grandement de la qualité de la thèse soumise au microfilmage. Nous avons tout fait pour assurer une qualité supérieure de reproduction.

S'il manque des pages, veuillez communiquer avec l'université qui a conféré le grade.

La qualité d'impression de certaines pages peut laisser à désirer, surtout si les pages originales ont été dactylographiées à l'aide d'un ruban usé ou si l'université nous a fait parvenir une photocopie de qualité inférieure.

Les documents qui font déjà l'objet d'un droit d'auteur (articles de revue, tests publiés, etc.) ne sont pas microfilmés.

La reproduction, même partielle, de cette microforme est soumise à la Loi canadienne sur le droit d'auteur, SRC 1970, c. C-30.

Canada

THE UNIVERSITY OF ALBERTA

SIMULATION OF MODIFIED STEAM INJECTION PROCESSES APPLIED TO BOTTOM WATER RESERVOIRS

by

MAHNAZ KASRAIE

A THESIS

SUBMITTED TO THE FACULTY OF GRADUATE STUDIES AND RESEARCH

IN PARTIAL FULFILLMENT OF THE REQUIREMENTS FOR THE DEGREE

OF DOCTOR OF PHILOSOPHY

IN

PETROLEUM ENGINEERING

DEPARTMENT OF MINING, METALLURGICAL AND PETROLEUM

ENGINEERING

EDMONTON, ALBERTA

FALL 1987

ISBN 0-315-40867-7

THE UNIVERSITY OF ALBERTA

RELEASE FORM

NAME OF AUTHOR Mahnaz Kasraie

TITLE OF THESIS Simulation of Modified Steam Injection Processes Applied to Bottom Water Reservoirs

DEGREE FOR WHICH THESIS WAS PRESENTED DOCTOR OF PHILOSOPHY

YEAR THIS DEGREE WAS GRANTED 1987

Permission is hereby granted to THE UNIVERSITY OF ALBERTA LIBRARY to reproduce single copies of this thesis and to lend or sell such copies for private, scholarly or scientific research purposes only.

The author reserves other publication rights, and neither the thesis nor extensive extracts from it may be printed or otherwise reproduced without the author's written permission.

M. Kasraie

Permanent address: Box 633 SUB 11
Edmonton, Alberta
T6G 2E0

DATED Sept. 10, 1987

THE UNIVERSITY OF ALBERTA

FACULTY OF GRADUATE STUDIES AND RESEARCH

The undersigned certify that they have read, and recommend to the Faculty of Graduate Studies and Research, for acceptance, a thesis entitled SIMULATION OF MODIFIED STEAM INJECTION PROCESSES APPLIED TO BOTTOM WATER RESERVOIRS by MAHNAZ KASRAIE in partial fulfillment of the requirements for the degree of Doctor in Philosophy in Petroleum Engineering

.....
Dr. S.M. Farouq Ali (Supervisor)

.....
Dr. R.G. Bentsen

.....
Prof. P.M. Dranchuk

.....
Dr. J.M. Whiting

.....
Dr. J. Masliyah

.....
Dr. G.S. Reddy (External Examiner)

DATED Aug 6, 1987

To My Father Ahmad Kasraie,

To My Mother,

and

To Mary, Manijeh, Mohamad Reza, Mitra, and Mozhgan

ABSTRACT

Steam injection in the form of cyclic steam stimulation and steamflooding has been highly successful as an enhanced oil recovery technique. This study deals with the mathematical simulation of steam injection processes, with special reference to several phenomena, thus far not considered. These are: thermal upgrading of oil, non-Newtonian oil rheology and injection of foam. In addition, a number of steam injection strategies were studied for bottom water heavy oil reservoirs. One of these is the case of partial penetration in formations containing a bottom water layer. Both steamfloods and cyclic steam stimulation were simulated for partially penetrating wells. Another new feature studied in this work is the case of multiple layer steam injection from a single tubing. For this purpose, a wellbore heat loss model was developed for multiple offtake. It was found that the steam quality can vary considerably in such a case, with the lower zone taking steam of lower quality than the upper zone. Finally, the case of gas injection with steam was also investigated for cyclic steam stimulation. The simulator was also used to simulate a scaled model experiment.

Three-phase, two- and three-dimensional, multicomponent simulators and a wellbore model were developed for the above studies. A fully implicit formulation was employed. The finite difference equations were solved using a block matrix band equation solving algorithm. Thermal upgrading, non-Newtonian flow, and foam injection were incorporated into the mathematical model, using the published experimental data. The purpose here was to show the qualitative effects in each of these cases, rather than a comprehensive study of each of these effects. It was found that if the oil is shear thinning, the oil recovery and oil-steam ratio are likely to increase. Thermal upgrading may lead to a small recovery increase, if long times are involved. Foam was not particularly effective in increasing oil recovery. In this work, the foam was considered as an agent for decreasing gas phase mobility. Injection of natural gas with steam, in cyclic steam stimulation, was found to increase the oil-steam ratio only marginally.

ACKNOWLEDGMENTS

I wish to express my thanks to Dr. S.M. Farouq Ali for providing guidance throughout the course of this study.

I would like to thank Dr. R.G. Bentsen, Prof. P.M. Dranchuk, Dr. Jacob Masliyah, and Dr. J.M. Whiting for helpful suggestions for improvements.

Thanks are expressed to Dr. Jamal Abou-Kassem, for reviewing Chapter IV, and for giving valuable suggestions regarding the solution scheme.

The assistance of Mr. Kacheong Yeung and Mrs. Darlene Spel[illegible]aration of the final copy is greatly appreciated.

This research was carried out under a contract with Energy, Mines and Resources Canada, Department of Supply and Services. Special thanks are expressed to Dr. Albert George and EMR for making this work possible.

TABLE OF CONTENTS

CHAPTER Page

IV. DEVELOPMENT OF THE MATHEMATICAL MODEL (continued)

CHAPTER — Page

LIST OF TABLES

LIST OF FIGURES

NOMENCLATURE

A	bulk area of cross-section m^2 (ft^2)
c_{pi}	specific heat of component i kJ/kg-C (Btu/lb-F)
c_s	specific heat of rock matrix kJ/kg-C (Btu/lb-F)
$C_{i\alpha}$	concentration of component i in phase α mass frac
D	depth below sea level, positive downwards m (ft)
$D_{i\alpha}$	diffusion rate of i in phase α m^2/s (ft^2/ hr)
f_{iog}	ratio of the mass fraction of component i in the oleic phase in equilibrium with the mass fraction in the vapour phase
f_{iow}	ratio of the mass fraction of component i in the oleic phase in equilibrium with the mass fraction in the aqueous phase
g	acceleration due to gravity m/s^2
$h_{i\alpha}$	enthalpy of component i in phase α kJ/kmole (Btu/lbmole)
k	absolute permeability in a given direction m^2 (1.127darcy)
k_h	thermal conductivity in a given direction kW/m-K (Btu/day-ft-F)
$k_{r\alpha}$	relative permeability to α phase frac
L_{vi}	latent heat of component i kJ/kg (Btu/lb)
m_i^*	injection rate of component i kg/s-m^3 (lb/day-ft^3)
M_i	molecular weight of component i kg/kmole (lb/lbmole)
M_α	molecular weight of α phase kg/kmole (lb/lbmole)
p	pressure Pa (psia)
P_{cgo}	gas-oil capillary pressure Pa (psia)
P_{cow}	oil-water capillary pressure Pa (psia)
q_α^*	injection rate of α phase sm^3/m^3-s (STB/ft^3-day
q_L^*	heat loss rate kJ/s-m^3 (Btu/day-ft^3)
S_α	saturation of α phase fraction pore volume
t	time s (day)
v_α	phase pore velocity in a given direction m/s (ft/day)
w	weighting factor for the upstream direction, 0 or 1
x	coordinate m (ft)
y	coordinate m (ft)
z	coordinate m (ft)
ϕ	porosity fraction
Φ	potential of the particular phase= $p + \rho_\alpha g D$, Pa (psia)
ρ_α	density of the α phase kg/m^3 (lb/ft^3)
μ_α	viscosity of the α phase Pa.s (centipoise)

Chapter I

INTRODUCTION

Steam injection is currently responsible for the production of over one million barrels/day of heavy oil. There are two principal variations of steam injection: cyclic steam stimulation, which has been successful in Cold Lake oil sands formations, and is the only proven commercial heavy oil recovery method to-date for that area, and steamflooding, which has been highly successful in California, and is lately finding application in Saskatchewan. Eventually, some form of steamflooding may be applicable to Cold Lake reservoirs. This would, however, require the use of an additive with steam, which could be a gas, liquid, or a suitable foam; because steam alone cannot adequately mobilize the highly viscous oil. A suitable gas or liquid could lower oil viscosity under cold conditions, while a steam-based foam would improve sweep efficiency. The present study partly addresses this question.

Previous works dealing with steam injection simulation have not dealt with thermal upgrading, non-Newtonian oil rheology, and foam injection. These effects can be important. But the main purpose in this work is to show the incorporation of such effects in a steam injection simulator.

The principal field problem considered in this work is bottom water, which is a common problem in Alberta and Saskatchewan heavy oil formations. This can take many forms, ranging from an oil-water transition zone to 100% water, with full or partial communication with the overlying oil zone. These aspects are covered in this study. Bottom water heavy oil reservoirs may be exploited by special techniques, such as partial penetration, which was also considered in this work. Other strategies may involve injection of blocking agents such as foam. Steam is often injected into multiple oil zones from a single steam injection tubing. As a result, different zones take steam of different

qualities. This problem has not been examined in the literature thus far, and is considered in this work, using a wellbore simulator developed for this situation.

Chapter II

REVIEW OF THE LITERATURE

This chapter provides a review of the numerical simulators developed to date for steam injection studies. Various applications have been reported, mainly steamflooding. Cyclic steam simulations have been reported for simpler cases, e.g. effect of bottom water has been neglected. A number of steam simulators have been developed. Computational difficulties and the machine time requirements have limited the use of such simulators to relatively small grids, consisting of a few hundred, or fewer, blocks. A few investigators have examined the use of steam additives, mainly gases. The following survey is designed to highlight the main features of steam injection simulators in chronological order and indicate the current status. Table 2.1 gives a summary of all the steam injection models reported to date, indicating the main features of the models and the solution technique used.

Shutler (1968 and 1969) developed three phase, one- and two-dimensional models for steam injection. The mass balance equations for the three-phase (oleic, aqueous and vapour) flow were solved simultaneously, using Newtonian iteration for the steam condensation term, while the energy balance equation was solved separately by the non-iterative ADIP method. He allowed for the interphase mass transfer between water and steam phases, but considered the oil phase to be nonvolatile, and the hydrocarbon gas to be insoluble in the liquid phases.

Abdalla and Coats (1971) developed a three-phase (oil, water and gas), two-dimensional steam drive simulator. In this model the implicit-pressure, explicit saturation (IMPES) method was used. The model was relatively unstable in view of the approximate treatment of the nonlinearities.

Vinsome (1974) developed a three-phase (oil, water and steam) model for steam injection. A stabilized IMPES method was employed. While this was simpler than the implicit method, it provided second-order accuracy in the space derivatives, and large time

Table 2.1

MAIN FEATURES OF EXISTING THERMAL SIMULATORS

Model	Features	Solution Technique.
Shutler (1969)	One-dimensional three-phase; included effects	Three-step solution technique for
capillary	fluid flow, heat transfer and gas	of three-phase relative permeability,
Newtonian iteration		pressure. composition.
condensation		employed for steam
		term.
Shutler (1970)	Three-phase, two-dimensional steamflood model. Considers effect of gravity, reservoir heterogeneity, and non uniform initial fluid phase distribution.	Three-stage solution technique in each time step to obtain pressure and saturation, then temperature and finally gas composition.
Abdalla and Coats (1971)	Three-phase steamflood, dead oil	Explicit solution, unstable for most situations.
Coats et al. (1974)	Three-dimensional steam injection, three-phase.	Simultaneous solution of the mass
Dead oil, no solution gas.		and
energy balances. Accounts for		the effect of temperature on relative permeability.

Table 2.1 (continued)

MAIN FEATURES OF EXISTING THERMAL SIMULATORS

Model	Features	Solution Technique
Patel, Masliyah and Mathews (1977)	Steam injection, one-dimensional, radial.	Fully implicit solution of the pressure equation. Very stable.
Ferrer and Farouq Ali (1977)	Two-dimensional, three-phase, multicomponent thermal, compositional steam injection.	The mass and heat balance as well as compositional constraint equations were solved sequentially. Direct solution technique. Implicit pressure and explicit production rate. Slow to converge.
Weinstein et al. (1977)	One-dimensional, three-phase steam stimulation model.	Semi-implicit formulation. Sequential solution technique.
Coats (1978)	Three-dimensional steamflooding with distillation or solution gas.	Three-dimensional, highly implicit. Direct solution.
Crookston et al. (1978)	Thermal simulator one-dimensional, basically for fire flooding.	Direct solution technique, semi-implicit.

Table 2.1 (continued)

MAIN FEATURES OF EXISTING THERMAL SIMULATORS

Model	Features	Solution Technique
Abou-Kassem (1981)	Two-dimensional, three-phase steam model with solution gas. Nine-point difference scheme used.	Fully implicit treatment of all terms. Newtonian formulation, Gaussian elimination. Much computational work required.
Harding (1986)	One-dimensional, included nitrogen and CO_2 as steam additives. Primarily to simulate laboratory steamfloods.	Highly implicit, direct solution method.

steps were utilized. A Runge-Kutta integration scheme was employed. It was claimed that this technique could be incorporated into the existing simulators to increase their efficiency.

Coats, George, Chu and Marcum (1974) developed a three-phase (oil, water and steam), three-dimensional simulator for steam injection. In their work, the mass and energy balance equations were solved simultaneously. They combined the water and steam equations in order to avoid iteration on the mass transfer condensation term. This model did not account for the distillation of oil.

Patel, Masliyah, and Mathews (1977) developed a one-dimensional radial steam model for three-phase (oil-water-gas) flow. They used a fully implicit scheme for the solution of the pressure equation. The model proved to be very stable for cyclic steam injection in oil sands.

Ferrer and Farouq Ali (1977) developed a three-phase compositional simulator that described the steam injection process in two dimensions. In this work, interphase mass and heat transfer were considered: thus, the oil composition changed during the steam injection process. The partial differential equations obtained for mass balance for each component, as well as the heat balance equation, were solved sequentially. The use of the model for cyclic steam stimulation and steamflooding was illustrated by several examples. The sensitivity of the model to the input parameters was also examined. This model indicated that steam distillation and gravity segregation are important factors in the steam injection processes.

Weinstein, Wheeler and Woods (1977) presented a three-phase, one-dimensional steam injection model to simulate a cyclic steam stimulation process. Interphase mass transfer was allowed between water and vapour, and oil and vapour. This model accounts for steam condensation, solution gas, and distillation effects. However, it does not consider gravity and capillary pressure, or temperature dependence of relative permeability. Also, this model accounts for two-dimensional heat transfer. An explicit mass transfer rate between the oil and vapour rather than a gas solubility factor suggested a new method of

treating solution gas and distillation effects. On the other hand, explicit treatment of this type can induce instability. The "sequential solution" scheme (Spillette, Hillstead and Stone, 1973) was used for solving the equations. Recent work has shown that such a procedure is less stable for steam injection simulations than implicit schemes. It was concluded that gas injection has a favourable effect on performance and that gas injection following steam is the best alternative.

Coats (1978) reported a three-dimensional, highly implicit numerical model for simulating steamflooding with distillation or solution gas. This model was an improvement over his previous works. He employed a direct solution technique to simultaneously solve three and four equations for the dead-oil and two-component oil cases, respectively. This model was more stable than the previous model, and required less computing time.

Crookston, Culham and Chen (1979) presented a semi-implicit numerical model for simulating thermal recovery processes. This model was used for one-dimensional *in situ* combustion studies. This three-phase, (oleic, aqueous, vapour), one-dimensional model included gravity (vertical runs) and capillary effects. Heat transfer by conduction, convection, and vapourization-condensation of both water and hydrocarbons were considered. A direct solution procedure was used to simultaneously solve the system of equations. This consisted of the alternating diagonal ordering Gaussian elimination scheme, which was utilized by Price and Coats (1974) as well.

Abou-Kassem (1981) developed a compositional steam injection model, suitable for two dimensions, with an implicit solution scheme. The main feature of this approach was in the use of a nine-point difference scheme instead of the five-point difference schemes used by other investigators. The nine-point formulation approximates flow in a plane much better, since the fluid is permitted to move in four additional directions. As a result, the grid orientation effects are minimized. Abou-Kassem showed that by using the nine-point scheme, the calculated saturation and temperature profiles were almost identical for parallel and diagonal grids. On the other hand, use of the nine-point scheme increases the

computational work enormously. Furthermore, a nine-point scheme becomes a twenty seven-point scheme in three dimensions. But this has not been tried as yet in view of the vast amount of computations needed on one hand, and numerical problems on the other. It was also shown that the method of two-point upstream relative permeabilities may not be valid for thermal simulators.

Harding (1986) developed a highly implicit thermal numerical simulator. This steam and gas injection model was designed to aid in the interpretation of one-dimensional laboratory experimental steamfloods. The model was employed for a variety of history matching runs and process sensitivity studies. Harding used a direct solution method in his simulator. The simulator was designed to represent special features, such as heat loss from a cylindrical core, heat loss from flanges, etc. The possibility of using nitrogen and CO_2 as steam additives were among the features incorporated into the numerical model. An important result of Harding's experimental-theoretical study was that the experimental results were unreliable due to very high heat loss. The numerical model pointed out the importance of heat loss. Thus, Harding's simulator proved to be a useful means for interpreting experimental data, indicating improvements to be made in the experimental design.

Steam Injection in the Presence of Bottom Water

Many heavy oil formations in Alberta and Saskatchewan as well as in California are characterized by a bottom water layer below the oil zone which is often in communication with it. This bottom layer may consist of merely a high water saturation zone, or a transition zone. In the following, this layer will be referred to as "bottom water". The extent of bottom water may be different for various reservoirs. It could be a thin sand, a few meters in thickness, or it may be an aquifer. The permeability of the water layer may be considerably different from that of the oil zone, if clays are present in the water-bearing sand. The presence of bottom water is likely to have two significant but competing effects

on thermal recovery processes. On one hand it could be a means of providing initial injectivity in the highly viscous oil sands. On the other hand, this zone may act as a heat sink, thereby, reducing the efficiency of heating the oil formation above.

In secondary and tertiary recovery methods, any injected fluid, which could be air, steam, solvent etc., will exhibit a tendency to migrate into the low resistance water sand. As a consequence, the displacement and sweep efficiencies will be poor. A variety of factors will determine the magnitude of such migration, such as oil viscosity, relative water sand thickness, injection rate, oil saturation in the water sand, relative permeability and well completion. Presence of a barrier between the oil and water zone will reduce the channeling tendency if the barrier extends to at least one-half the distance between injector and producer, and the bottom water is not active. Vertical permeability thus plays an important role and any shale breaks, silt zones, or other heterogeneities restricting vertical permeability at the base of the oil zone would be beneficial in the oil recovery performance.

Flow of heat from the water zone into the oil formation is a complicated situation to handle, if a hot fluid is injected. This situation will be still more complex if air is chosen as the injection fluid. In heavy oil thermal recovery processes, presence of a limited water zone could be an advantage, since it could serve as a means of initial injectivity.

Laboratory Experimentation

Several investigators have conducted laboratory experiments with bottom water steamfloods. Pursley (1974) carried out experiments with a scaled model to simulate a 1.25 acre pattern. The sand thickness was 140 ft, with 15% bottom water and oil viscosity was 100,000 cp. Upon injection of one pore volume of steam, 36% recovery was obtained. Steam override was observed; on the whole, it contacted a large proportion of the oil. The presence of bottom water was helpful in providing injectivity. This way the base of the oil zone was heated. Vertical permeability was also an important factor.

Ehrlich (1977) and Huygen and Lowry (1979) investigated the recovery process of a 5 million cp bitumen, with a bottom water layer. They observed that the heated bitumen was carried into the bottom water by the condensate.

Stegemeier, Laumbach and Volek (1980) as well as Prats (1977), and Doscher and Huang (1979), have reported experiments of bottom water steamfloods with low pressure scaled models. Prats conducted experiments for Peace River conditions (200,000 cp oil), with water-to-oil zone thickness ratios of 0.50, 0.25 and 0.10. The oil saturation in the water zone was 0.55-0.65. The operational procedure consisted of injecting steam into the water zone, pressurizing, and blowing down to raise the temperature of the overlying oil zone, and to carry the oil flowing by gravity into the water zone to the production wells with limited steam production. Different bottom water layers required a different optimal operating strategies. In all cases, oil-steam ratios were between 0.2 and 0.3.

Stegemeier et al. (1980) conducted experiments to simulate the Mt. Poso field, which has a water drive. They developed a successful operating technique for a typically marginal steamflood process. It consisted in injecting steam updip as the downdip wells watered-out. A line drive pattern was employed.

Doscher and Huang (1979) conducted steamflood experiments with a water zone. They observed that an increase in the steam injection rate delayed the oil production and decreased the oil-steam ratio. Gravity segregation of steam occurred at long times.

Farouq Ali, Abad and Snyder (1974, 1976) conducted a series of experimental studies, where bottom water simulation was carried out by means of a high permeability sand placed at the base of a vertical tar sand pack. Initially, steam was propagating at the base of the sand, advancing upward, and eventually the entire sand was heated, resulting in a recovery of almost 50%.

A few investigators have reported laboratory studies of *in situ* combustion in the presence of a water zone. Garon, Geisbrecht and Lowry (1980) carried out scaled model experiments using a 5 million cp bitumen. It was found that the combustion zone advanced

near the base of the oil zone, where there was no communication between the oil and water layers, as a result of preheating of the water layer by steam. In addition to a firefront advancing in the direction of air flow, a second front was observed which was moving slowly in the perpendicular direction. In cases where there was communication between the oil and water layers, the sweep was good, but the air-oil ratio was much higher (20,000 vs. 13,000 scf/bbl). Recovery was 11-12% in both cases.

Proctor (1986) carried out a series of scaled model experiments for steamflooding bottom water models under a variety of conditions. The operational strategies for thin reservoirs (20-40 ft), with the presence of bottom water were studied in this work. Oil viscosity of 1275 cp was employed in most cases. His studies included steamfloods in bottom water situations, gas injection in bottom water studies, where a small volume of gas was injected into the top of the pack followed by steam injection, and steamflood experiments employing horizontal wells. It was concluded that gas injection prior to steamflooding in reservoirs underlain with bottom water would create a high conductivity zone and divert steam from bottom water into the oil zone, hence improving oil recovery. Also, horizontal well runs exhibited a more efficient recovery.

Numerical Simulation of Bottom Water Reservoirs

Numerical simulations of cyclic steam injection for oil reservoirs underlain by water have been conducted by Bowen and Patel (1982) as well as Prats (1974). It was found that for the bottom water thickness-to-oil zone thickness ratios of about 0.2, the oil-steam ratio may fall in the acceptable range (0.1 to 0.2 bbl/bbl). Beyond that, the oil-steam ratio dropped rapidly. When this ratio reached 1.0, oil recovery became very low. These numbers were valid for a 50,000 cp oil, and would change for different operating parameters and conditions.

It was also reported that for thin water zones, a smaller slug is more efficient, since it has a tendency to create a heated zone rather than being dissipated into the water zone. It

appears that the performance was better for lower viscosity oils, but bottom water can have adverse effects for any oil viscosity. Study of saturation and temperature distributions in the developed simulators indicates steam channeling as well as oil migration into the water zone. These results were obtained from the first cycle. In subsequent cycles, however, the performance improves to some extent, and this is a result of radial heat conduction into the cold oil sand away from the hot zone.

Several simulations of steamflooding in the presence of bottom water were reported by Prats (1977). A study of this type for a 50,000 cp oil in a 50 ft sand with 10 ft of water shows that the oil-steam ratio initially tends to increase with cumulative steam injected, and then starts to decrease. Also, a strong rate dependence has been reported. Study of saturation and temperature shows that steam has a tendency to flow through the water zone, with heating of the overlying oil, causing the oil to gravitate to the water zone, from where it will be directed to the producing wells by hot water. Given enough time, steam will segregate by gravity in the oil zone, mobilizing the oil, and also channelling into the water zone. It was found that water zone thickness has a pronounced effect on the oil recovery, and for a water sand thickness equal to oil sand thickness, recovery was insignificant and virtually nil. Both sands had the same absolute permeability.

Crookston, Culham and Chen (1979) studied one example of a two-dimensional bottom water steamflood, which was a special case of a one-dimensional fireflood simulator.

Singh (1985) used a three component, implicit steamflood model. The mass and energy balance equations were solved simultaneously. The three components were: 1) heavy oil, 2) water and 3) an additive. The Peng-Robinson equation of state was used to obtain phase behaviour data. Capillary pressure was neglected. This model was designed to study oil recovery in the Athabasca tar sand area in Alberta, where the oil viscosity is over one million cp. The reservoir consisted of an oil zone 60 ft thick underlain by a water

zone with negligible oil saturation. This model was concerned with 1) the bottom water thickness, 2) steam injection rate, and 3) additive injection rate.

It was reported that application of a blocking agent would decrease the flow of steam in more conductive parts of the reservoir, thereby improving the oil-steam ratio. In the simulation, it was assumed that the blocking agent would reduce the permeability of the bottom water zone to zero. Two simulation runs were conducted to study the effect of a blocking agent on sweep efficiency, oil-steam ratio and oil formation heating. In these runs, steam was initially injected into the bottom water zone to mobilize the overlying oil and create adequate injectivity in the oil formation. Sbusequently, the bottom water layer was assumed to be completely blocked, and steam injection was continued through the heated oil zone.

It was found that initially the injection of a blocking agent reduced the oil-steam ratio. It was postulated that by the time the oil above the bottom water was mobile enough to have injected steam flow through it, (the time at which the blocking agent was injected), a large amount of oil would be mobilized and flow downwards into the bottom water zone. Some of this oil was produced, while a considerable volume was trapped in the blocked water zone. This was responsible for the initially lower oil-steam ratio as compared with the cases where no blocking agent was employed. However, after some 50 additional days, higher oil-steam ratios were obtained, because the use of a blocking agent for a long enough time resulted in improved heating of the oil bearing-formation and a considerable amount of bitumen was produced from the oil zone.

It was concluded that a bottom water zone is helpful in improving injectivity, but too large a thickness of bottom water will delay response in oil production and will result in an increased amount of water production and, therefore, yield poorer sweep efficiency. It was also concluded that in a bottom water containing reservoir, a higher rate of steam injection results in considerable heat production together with fluid production, but very low rates cause considerable delay in oil production. It was also concluded that blocking agents can

improve sweep efficiency by providing efficient heating of the oil formations but they may result in oil entrapment in areas from which it cannot be produced.

Kasraie and Farouq Ali (1984, 1984, 1985, 1987) have discussed the problem of steamflooding and cyclic steaming in the presence of bottom water. For the oil viscosities and formation permeabilities considered, they concluded that heavy oil formations with bottom water not exceeding one-fifth of the oil zone thickness may be commercially amenable to steam injection.

Chapter III

STATEMENT OE THE PROBLEM

Although a number of steam injection simulators have been developed, as reviewed in Chapter II, a number of important features of steam injection processes have not been considered. It is the purpose of this work to develop steam injection simulators in order to examine the following problems: —

1. To investigate the features of thermal upgrading, non-Newtonian oil rheology, and steam-foam flow in a three-dimensional, multicomponent simulator, and determine the effects of these features in selected steamflood simulations, and to examine the effect of gas injection with steam on cyclic steaming response.
2. To examine the effect of a bottom water zone on steamflooding and cyclic steam stimulation performance. In this regard, the effects of partial penetration, relative water zone thickness, oil and water zone absolute permeabilities and vertical permeability are to be studied.
3. To simulate a scaled laboratory steamflood, and determine the extent of necessary adjustments to field relative permeabilities for obtaining a reasonable match.
4. To develop a wellbore model for determining the effect of multiple offtake in a steam injection well on wellbore steam quality and pressure. Then to use the steam quality and pressure, as functions of time, in steamflood simulations to determine the effect on oil recovery and other parameters.

Chapter IV

DEVELOPMENT OF THE MATHEMATICAL MODEL

Introduction

In this research, two three-phase, multicomponent thermal simulators for steam injection were developed. These consist of (i) a three-dimensional, two-component simulator, and (ii) a two- dimensional, four-component simulator. The model development given below is for a generalized three-dimensional, multicomponent, three-phase steam injection simulator, all the groundwork for which was accomplished. The aforesaid simulators employed similar development, being subsets. The simulators were employed for a variety of steam injection situations, including foam flow, thermal upgrading, use of additives, and non-Newtonian oil rheology. In addition, a wellbore simulator was developed, with the feature of fluid flow regime changes, which was used to examine steam quality variations when steam is injected into two separate layers from a single tubing. The aforementioned are new features, not reported before.

The three-dimensional, three-phase, multicomponent simulator employs a fully implicit formulation. Newtonian iteration is used to solve the resulting nonlinear difference equations. The algebraic equations for the grid have a block band matrix structure, with a 6 x 6 block size. In the following section, the model formulation, the finite difference approximations, derivation of the Jacobians, and the overall solution scheme will be discussed. SI units are used in the following development.

Simulator Equations

Assumptions

This thermal model represents non-isothermal flow of three phases (oleic, aqueous, and vapour) in three dimensions. Each phase can consist of as many as five components, and interphase mass transfer of all components is allowed. In the mass balance equation, molecular diffusion within each phase is allowed for, however instantaneous equilibrium is assumed between phases. Thermal equilibrium is also assumed between phases, as well as between the fluids and the rock matrix. Heat transfer to the impermeable, adjacent formations above and below is governed by the diffusivity equation. The composition of a particular phase is determined by the K-values. Mild thermal cracking of the heavy hydrocarbon is allowed to occur, and is taken to be a function of temperature and time, based upon published laboratory data. It is assumed that the volume of carbon formed as a result is negligible.

While heat loss to the formations above and below is allowed, lateral heat flow is assumed to be zero. In the energy balance, the terms for kinetic energy, work done by viscous forces, and work done by body forces have been neglected, being small.

As one example, the components are: (1) non-volatile hydrocarbon, (2) water, (3) surfactant, (4) non-condensable gas, and (5) electrolyte (salt). Other components may be employed, as needed, so long as the respective K-values are available.

The three-phase relative permeabilities to oil, water, and gas were calculated by Naar-Wygal-Henderson and Stone methods, as discussed below. In some cases, the relative permeabilities were made temperature-dependent.

Mass Balance for a Component

In order to derive the mass balance for component i, consider a volume element of sides $\Delta x, \Delta y, \Delta z$, with flow of the three phases into and out of the element in the x-, y-, and z-directions. Molecular diffusion within each phase is allowed for. Instantaneous phase equilibrium is assumed.

Diffusion of component i is described by Fick's law of diffusion. For example, the mass diffusion rate of component i in the x-direction in the oleic phase is given by

$$m_{i_o} = -AD_{io}\frac{\partial \rho_o C_{io}}{\partial x}, \tag{4.1}$$

where m_i is the mass diffusion rate of component i in kg/s, A is total area in m^2, D_{io} is the rate of diffusion of component i in the oleic phase in m^2/s, ρ_o is the oleic phase density in kg/m^3, and C_{io} is the mass concentration of component i in the oleic phase.

The mass balance on component i for flow in all three directions can be written as follows:

Net mass throughput + Net mass change = 0

For example, the mass balance for one dimensional flow gives the following equation:

$$\begin{aligned}
&[(\rho_o q_o C_{i_o})\big|_{x+\Delta x} + (\rho_w q_w C_{i_w})\big|_{x+\Delta x} + (\rho_g q_g C_{i_g})\big|_{x+\Delta x} \\
&-(\rho_o q_o C_{i_o})\big|_x - (\rho_w q_w C_{i_w})\big|_x - (\rho_g q_g C_{i_g})\big|_x + m_{io}|_{x+\Delta x} - m_{io}|_x + m_{iw}|_{x+\Delta x} \\
&-m_{iw}|_x + m_{ig}|_{x+\Delta x} - m_{ig}|_x - m_i^* - m_{si}^*]\Delta t \\
&+[(\phi S_o \rho_o C_{i_o})\big|_{t+\Delta t} + (\phi S_w \rho_w C_{i_w})\big|_{t+\Delta t} + (\phi S_g \rho_g C_{i_g})\big|_{t+\Delta t}
\end{aligned}$$

$$-(\phi S_o \rho_o C_{i_o})\Big|_t - (\phi S_w \rho_w C_{i_w})\Big|_t - (\phi S_g \rho_g C_{i_g})\Big|_t] \cdot A\Delta x = 0. \tag{4.2}$$

The q-terms are replaced by velocities, using Darcy's equation for multiphase flow. Rearranging, and taking the limits of Δx (and similarly, Δy and Δz, for three dimensions) and Δt to zero, the following equation results:

$$\nabla \cdot \left(\frac{k k_{ro} \rho_o C_{i_o}}{\mu_o} \nabla \Phi_o\right) + \nabla \cdot \left(\frac{k k_{rw} \rho_w C_{i_w}}{\mu_w} \nabla \Phi_w\right) + \nabla \cdot \left(\frac{k k_{rg} \rho_g C_{i_g}}{\mu_g} \nabla \Phi_g\right)$$
$$+\nabla \cdot (D_{i_o} \nabla(\rho_o C_{i_o})) + \nabla \cdot (D_{i_w} \nabla(\rho_w C_{i_w})) + \nabla \cdot (D_{i_g} \nabla(\rho_g C_{i_g})) + m_i^* + m_{si}^* + \sum_{j=1}^{J} P_{ji}$$
$$= \frac{\partial}{\partial t}(\phi S_o \rho_o C_{i_o} + \phi S_w \rho_w C_{i_w} + \phi S_g \rho_g C_{i_g}), \tag{4.3}$$

where P_{ji} is the rate of generation of component i from the jth reaction, with J reactions taking place. The remaining symbols are defined in the Nomenclature.

At this stage, the Φs are replaced by phase pressures as follows

$$\Phi_o = p_o - \rho_o g D, \tag{4.4}$$

where D is depth below sea level, in m. Next, the capillary pressure relations are used to reduce the water and gas phase pressures to oil pressure, which is taken to be the principal unknown:

$$P_{cow} = p_o - p_w, \tag{4.5}$$

$$P_{cgo} = p_g - p_o. \tag{4.6}$$

The final form of the mass balance equation for component i is:

$$\nabla \cdot [(\frac{k k_{ro} \rho_o C_{i_o}}{\mu_o} + \frac{k k_{rw} \rho_w C_{i_o}}{\mu_w f_{iow}} + \frac{k k_{rg} \rho_g C_{i_o}}{\mu_g f_{iog}}) \nabla p_o]$$
$$-\nabla \cdot [(\frac{k k_{ro} \rho_o C_{i_o}}{\mu_o} \rho_o g + \frac{k k_{rw} \rho_w C_{i_o}}{\mu_w f_{iow}} \rho_w g + \frac{k k_{rg} \rho_g C_{i_o}}{\mu_g f_{iog}} \rho_g g) \nabla D]$$
$$-\nabla \cdot (\frac{k k_{rw} \rho_w C_{i_o}}{\mu_w f_{iow}} \nabla P_{cow}) + \nabla \cdot (\frac{k k_{rg} \rho_g C_{i_o}}{\mu_g f_{iog}} \nabla P_{cgo})$$

$$+\nabla\cdot(D_{i_o}\nabla(\rho_o C_{i_o}))+\nabla\cdot(D_{iw}\nabla(\rho_w\frac{C_{i_o}}{f_{iow}}))+\nabla\cdot(D_{ig}\nabla(\rho_g\frac{C_{i_o}}{f_{iog}}))+m_i^*+m_{si}^*-\sum_{j=1}^{J}P_{ji}$$
$$=\frac{\partial}{\partial t}(\phi(1-S_w-S_g)\rho_o C_{io}+\phi S_w\rho_w\frac{C_{io}}{f_{iow}}+\phi S_g\rho_g\frac{C_{io}}{f_{iog}}). \qquad (4.7)$$

The finite difference approximation to this equation is discussed in a subsequent section.

Heat Balance

The heat balance equation takes into account heat conduction within the reservoir in all three directions. Besides, it considers heat convection due to the flow of the oleic, aqueous, and vapour phases. In the general case, each phase contains five components, as mentioned previously. The heat balance also includes the feature of heat transport due to the molecular diffusion of the components. Heat loss to the overlying and underlying adjacent formations is allowed, assuming conductive transfer only because these boundaries are impermeable to flow. Lateral heat loss is neglected in the present model, because we are considering elements of symmetry, with no-flow boundaries. Where this is not the case, it is possible to include a heat loss term to account for such a loss. In practice, because the heat flow in the lateral direction is confined to the formation, it is usually not considered a loss.

As for mass balance, consider flow of heat in the x-direction; a similar treatment could be used for the y- and z-directions. The heat balance can be written as

Net heat throughput in time Δt=Net change in heat content

The heat flow consists of conduction, convection, and that due to molecular diffusion. Writing the heat balance for an element with dimensions $\Delta x, \Delta y$, and Δz, we have

$$[q_{cond_{x+\Delta x}}-q_{cond_x}+q_{cond_{y+\Delta y}}-q_{cond_y}+q_{cond_{z+\Delta z}}-q_{cond_z}]\Delta t$$
$$+[q_{conv_{x+\Delta x}}-q_{conv_x}+q_{conv_{y+\Delta y}}-q_{conv_y}+q_{conv_{z+\Delta z}}-q_{conv_z}]\Delta t$$
$$+[q_{diff_{x+\Delta x}}-q_{diff_x}+q_{diff_{y+\Delta y}}-q_{diff_y}+q_{diff_{z+\Delta z}}-q_{diff_z}]\Delta t$$
$$+[\frac{q_o^*\rho_o}{M_o}\sum_i x_{i_o}h_{i_o i,j,k}^{n+1}+\frac{q_w^*\rho_w}{M_w}\sum_i x_{i_w}h_{i_w i,j,k}^{n+1}+\frac{q_g^*\rho_g}{M_g}\sum_i x_{i_g}h_{i_g i,j,k}^{n+1}-q_L^*+r_H^*]\Delta t$$
$$+\Delta x\Delta y\Delta z\{(1-\phi)\frac{\rho_s}{M_s}h_s+\frac{\phi\rho_o S_o}{M_o}\sum_i x_{io}h_{io}+\frac{\phi\rho_w S_w}{M_w}\sum_i x_{iw}h_{iw}+\frac{\phi\rho_g S_g}{M_g}\sum_i x_{ig}h_{ig}\}_{t+\Delta t}$$
$$-\Delta x\Delta y\Delta z\{(1-\phi)\frac{\rho_s}{M_s}h_s+\frac{\phi\rho_o S_o}{M_o}\sum_i x_{io}h_{io}+\frac{\phi\rho_w S_w}{M_w}\sum_i x_{iw}h_{iw}+\frac{\phi\rho_g S_g}{M_g}\sum_i x_{ig}h_{ig}\}_t=0, \qquad (4.8)$$

where q_{cond_x}, for example, is the heat conducted in the x-direction, and is given by

$$q_{cond_x} = -Ak_{hx}\frac{\partial T}{\partial x}. \tag{4.9}$$

Similarly, q_{conv_x} is heat convection in the x-direction, given by

$$q_{conv_x} = \frac{v_o\rho_o}{M_o}\sum_i x_{i_o}h_{i_o} \tag{4.10}$$

In the same way,

$$q_{diff_x} = m_i h_{iox}, \tag{4.11}$$

where m_i is given by Eq.(4.1). Other symbols are defined in the Nomenclature; $q^*{}_L$ is the heat loss rate to the adjacent formations, in kJ/s-m^3, and r_H is the heat of any reactions occurring, in the same units.

Dividing Eq.(4.8) by $\Delta x\Delta y\Delta z\Delta t$, and taking the limit for $\Delta x, \Delta y, \Delta z, \Delta t \rightarrow 0$, the following equation is obtained:

$$\begin{aligned}
&\nabla\cdot(k_h\nabla T_r) - \nabla[\frac{v_o\rho_o}{M_o}\sum_i x_{i_o}h_{i_o} + \frac{v_w\rho_w}{M_w}\sum_i x_{i_w}h_{i_w} + \frac{v_g\rho_g}{M_g}\sum_i x_{i_g}h_{i_g}] \\
&\qquad -\nabla\cdot\sum_i[J_{i_o}h_{i_o} + J_{i_w}h_{i_w} + J_{i_g}h_{i_g}] - q_L{}^* + r_H{}^* \\
&\quad + \frac{q_{o^*}\rho_o}{M_o}\sum_i x_{i_o}h_{i_o}{}^{n+1}_{i,j,k} + \frac{q_{w^*}\rho_w}{M_w}\sum_i x_{i_w}h_{i_w}{}^{n+1}_{i,j,k} + \frac{q_{g^*}\rho_g}{M_g}\sum_i x_{i_g}h_{i_g}{}^{n+1}_{i,j,k} \\
&= \frac{\partial}{\partial t}[(1-\phi)\frac{\rho_s}{M_s}h_s + \frac{\phi\rho_o S_o}{M_o}\sum_i x_{io}h_{io} + \frac{\phi\rho_w S_w}{M_w}\sum_i x_{iw}h_{iw} + \frac{\phi\rho_g S_g}{M_g}\sum_i x_{ig}h_{ig}],
\end{aligned} \tag{4.12}$$

The above equation is adequate for all practical purposes; however, for completeness, the following terms should be added to the right-hand side:

$$\begin{aligned}
&\frac{\partial}{\partial t}[\frac{1}{2Jg_c}(\frac{\rho_o v_o{}^2}{M_o} + \frac{\rho_w v_w{}^2}{M_w} + \frac{\rho_g v_g{}^2}{M_g})] \\
&\qquad -\frac{1}{2Jg_c}\nabla(\frac{\rho_o v_o}{M_o}v_o^2 + \frac{\rho_w v_w}{M_w}v_w^2 + \frac{\rho_g v_g}{M_g}v_g^2) \\
&\qquad\qquad -\nabla(\tau_o v_o + \tau_w v_w + \tau_g v_g)
\end{aligned}$$

The above terms are negligibly small under most conditions. These terms respectively represent the kinetic energy, the body force work, kinetic energy again, and work done by viscous forces. Before expanding Eq.(4.12), the following substitutions are made:

$$h_{i_o} = c_{p_i}(T - T_R)M_i, \tag{4.13}$$

and

$$h_{i_g} = (c_{p_i}(T - T_R) + L_{v_i})M_i, \tag{4.14}$$

where the units of each term are kJ/kmole. The final form of Eq.(4.12) before discretization by finite differences is as follows:

$$\begin{aligned}
&\nabla \cdot (k_h \nabla T) - \nabla(\rho_o v_o T \sum_i c_{p_i} C_{i_o} + \rho_w v_w T \sum_i c_{p_i} C_{i_w} + \rho_g v_g \sum_i (c_{p_i} T + L_{v_i}) C_{ig}) \\
&-\nabla \cdot (\rho_o \sum_i c_{p_i} T D_{i_o} \nabla C_{i_o} + \rho_w \sum_i c_{p_i} T D_{i_w} \nabla C_{i_w} + \rho_g \sum_i (c_{p_i} T + L_{v_i}) D_{i_g} \nabla C_{i_g}) \\
&-q_L{}^* + r_H{}^* + \frac{q_o{}^* \rho_o}{M_o} \sum_i x_{i_o} h_{i_o i,j,k}^{n+1} + \frac{q_w{}^* \rho_w}{M_w} \sum_i x_{i_w} h_{i_w i,j,k}^{n+1} + \frac{q_g{}^* \rho_g}{M_g} \sum_i x_{i_g} h_{i_g i,j,k}^{n+1} \\
&= \frac{\partial}{\partial t}[(1-\phi)\frac{\rho_s}{M_s} c_s T + \phi \rho_o S_o \sum_i c_{p_i} T C_{i_o} + \phi \rho_w S_w \sum_i c_{p_i} T C_{i_w} + \phi \rho_g S_g \sum_i (c_{p_i} T + L_{v_i}) C_{i_g}].
\end{aligned} \tag{4.15}$$

Formulation of the Problem

We shall now state the muliphase, multicomponent flow problem completely for a block, containing a well (source/sink). Consider a system of N components in three phases. The unknowns are as follows:

p_o =oleic phase pressure

p_w =aqueous phase pressure

p_g =vapour phase pressure

S_o =oleic phase saturation

S_w =aqueous phase saturation

S_g =vapour phase saturation

T =temperature

C_{i_o} =mass fraction of component i in the oleic phase $(i = 1, 2, ..., N)$

C_{i_w} =mass fraction of component i in the aqueous phase $(i = 1, 2, ..., N)$

C_{i_g} =mass fraction of component i in the vapour phase $(i = 1, 2, ..., N)$

q^*_o =oleic phase injection rate (+) or production rate (-)

q^*_w =aqueous phase injection rate (+) or production rate (-)

q^*_g =vapour phase injection rate (+) or production rate (-)

Thus the total number of unknowns is $3N + 10$ in the most general case. The equations to be solved are as follows:

Mass balance for component i, Eq.(4.7), $(i = 1, 2, ..., N)$ N equations,

Energy balance, Eq.(4.15) 1 equation,

Saturation constraint $S_o + S_w + S_g = 1$ 1 equation,

Capillary pressure relationships $P_{cow} = p_o - p_w$, 1 equation,

$P_{cgo} = p_g - p_o$ 1 equation,

Mole fraction constraints $\sum_{i=1}^{N} x_{io} = 1$ 1 equation,

$\sum_{i=1}^{N} x_{iw} = 1$ 1 equation,

$\sum_{i=1}^{N} x_{ig} = 1$ 1 equation,

K-values for the oleic/aqueous and oleic/vapour phases

$$K_{iow} = \frac{x_{io}}{x_{iw}} \quad (i = 1, 2, ..., N) \quad \text{N equations,}$$

$$K_{iog} = \frac{x_{ig}}{x_{io}} \quad (i = 1, 2, ..., N) \quad \text{N equations.}$$

Well flow rate relationships

$$q_w^* = \left(\frac{k_{rw}\rho_w\rho_{osc}\mu_o}{k_{ro}\rho_o\rho_{wsc}\mu_w}\frac{\frac{\partial\Phi_w}{\partial r}}{\frac{\partial\Phi_o}{\partial r}}\right)q_o^* \quad \text{1 equation}$$

$$q_g^* = \left(\frac{k_{rg}\rho_g\rho_{osc}\mu_o}{k_{ro}\rho_o\rho_{gsc}\mu_g}\frac{\frac{\partial\Phi_g}{\partial r}}{\frac{\partial\Phi_o}{\partial r}}\right)q_o^* \quad \text{1 equation}$$

The oil rate is specified, or one of the other rates, or the total rate could be specified. The total number of equations is thus seen to be $3N+10$, same as the total number of unknowns. The problem is properly formulated, given appropriate boundary and initial conditions. It should be noted that in this work, mass fractions of the components i, i.e. C_{i_o}, C_{i_w}, and C_{i_g} were used in place of mole fractions. These are related to the mole fractions by equations of the following type

$$C_{i_o} = \frac{x_{io} M_i}{M_o}$$

Boundary and Initial Conditions

In this model, the reservoir boundaries are assumed to be closed to flow of fluids, flow of heat (except at the top and base of the formation), and diffusional transfer. Each of the dependent variables is a function of x, y, z, and t, e.g. $p_o = p_o(x, y, z, t)$. The boundary conditions can be stated as follows:

$$\left.\frac{\partial p_o}{\partial x}\right|_{C_x} = 0,$$

$$\left.\frac{\partial p_o}{\partial y}\right|_{C_y} = 0,$$

$$\left.\frac{\partial p_o}{\partial z}\right|_{C_z} = 0,$$

$$\left.\frac{\partial T}{\partial x}\right|_{C_x} = 0,$$

$$\left.\frac{\partial T}{\partial y}\right|_{C_y} = 0,$$

$$\left.\frac{\partial T}{\partial z}\right|_{b} \neq 0,$$

$$\left.\frac{\partial C_{1o}}{\partial x}\right|_{C_x} = 0,$$

$$\left.\frac{\partial C_{1o}}{\partial y}\right|_{C_y} = 0,$$

$$\left.\frac{\partial C_{1o}}{\partial z}\right|_{C_z} = 0,$$

$$\left.\frac{\partial C_{2o}}{\partial x}\right|_{C_x} = 0,$$

$$\left.\frac{\partial C_{2o}}{\partial y}\right|_{C_y} = 0,$$

$$\left.\frac{\partial C_{2o}}{\partial z}\right|_{C_z} = 0,$$

where C is the entire exterior surface of the reservoir normal to the x, y, and z directions, and b is a subset consisting of the top and the base of the reservoir.

Initial conditions can be stated as follows:

$$p_o(x, y, z, 0) = p_{oi},$$

$$S_w(x,y,z,0) = S_{wi},$$

$$S_g(x,y,z,0) = S_{gi},$$

$$T(x,y,z,0) = T_i,$$

$$C_{1o}(x,y,z,0) = C_{1o_i},$$

$$C_{2o}(x,y,z,0) = C_{2o_i},$$

$$C_{3o}(x,y,z,0) = C_{3o_i},$$

$$C_{4o}(x,y,z,0) = C_{4o_i},$$

$$C_{5o}(x,y,z,0) = C_{5o_i}.$$

The initial water and gas pressure values are based upon the capillary pressure and temperature data. In the case of the injection and production wells, the boundary and initial conditions are given by the source-sink terms, as discussed previously. It is important to note that the initial mass fractions of all components in each phase must add to 1 separately. This is done by carrying out an initial flash equilibrium calculation for the mixture.

Finite Difference Approximations

Component Mass Balance

The partial differential equations obtained for each component as well as the heat balance equation were discretized for the fully implicit formulation, i.e. all transmissibilities, nonlinear coefficients, and source/sink terms (mass as well as heat terms) were taken at time level $n+1$. All variable parts of fluid and heat transmissibilities were taken at the upstream conditions.

The mass balance equation for component i can be expressed as

$$F_{i,j,k} = 0, \tag{4.15}$$

where the single i refers to a particular component ($i = 1,2,...,5$), and the subscript (i,j,k) refers to a particular block in a three-dimensional grid, and F is given by

$$F_{i,j,k} = T_x\Big|^{n+1}_{i+\frac{1}{2},j,k} p_{o_{i+1,j,k}}^{n+1} + T_x\Big|^{n+1}_{i-\frac{1}{2},j,k} p_{o_{i-1,j,k}}^{n+1} + T_y\Big|^{n+1}_{i,j+\frac{1}{2},k} p_{o_{i,j+1,k}}^{n+1}$$

$$
\begin{aligned}
&+T_y\Big|^{n+1}_{i,j-\frac{1}{2},k} p_{o_{i,j-1,k}}^{n+1} + T_z\Big|^{n+1}_{i,j,k+\frac{1}{2}} p_{o_{i,j,k+1}}^{n+1} + T_z\Big|^{n+1}_{i,j,k-\frac{1}{2}} p_{o_{i,j,k-1}}^{n+1} \\
&-(T_x\Big|^{n+1}_{i+\frac{1}{2},j,k} + T_x\Big|^{n+1}_{i-\frac{1}{2},j,k} + T_y\Big|^{n+1}_{i,j+\frac{1}{2},k} + T_y\Big|^{n+1}_{i,j-\frac{1}{2},k} + T_z\Big|^{n+1}_{i,j,k+\frac{1}{2}} + T_z\Big|^{n+1}_{i,j,k-\frac{1}{2}}) p_{o_{i,j,k}}^{n+1} \\
&-T_{ggx}\Big|^{n+1}_{i+\frac{1}{2},j,k} D_{i+1,j,k}^{n+1} - T_{ggx}\Big|^{n+1}_{i-\frac{1}{2},j,k} D_{i-1,j,k}^{n+1} - T_{ggy}\Big|^{n+1}_{i,j+\frac{1}{2},k} D_{i,j+1,k}^{n+1} \\
&-T_{ggy}\Big|^{n+1}_{i,j-\frac{1}{2},k} D_{i,j-1,k}^{n+1} - T_{ggz}\Big|^{n+1}_{i,j,k+\frac{1}{2}} D_{i,j,k+1}^{n+1} - T_{ggz}\Big|^{n+1}_{i,j,k-\frac{1}{2}} D_{i,j,k-1}^{n+1} \\
&-(T_{ggx}\Big|^{n+1}_{i+\frac{1}{2},j,k} + T_{ggx}\Big|^{n+1}_{i-\frac{1}{2},j,k} + T_{ggy}\Big|^{n+1}_{i,j+\frac{1}{2},k} + T_{ggy}\Big|^{n+1}_{i,j-\frac{1}{2},k} - T_{ggz}\Big|^{n+1}_{i,j,k+\frac{1}{2}} - T_{ggz}\Big|^{n+1}_{i,j,k-\frac{1}{2}}) D_{i,j,k}^{n+1} \\
&-T_{wx}\Big|^{n+1}_{i+\frac{1}{2},j,k} P_{cow_{i+1,j,k}}^{n+1} - T_{wx}\Big|^{n+1}_{i-\frac{1}{2},j,k} P_{cow_{i-1,j,k}}^{n+1} - T_{wy}\Big|^{n+1}_{i,j+\frac{1}{2},k} P_{cow_{i,j+1,k}}^{n+1} \\
&-T_{wy}\Big|^{n+1}_{i,j-\frac{1}{2},k} P_{cow_{i,j-1,k}}^{n+1} - T_{wz}\Big|^{n+1}_{i,j,k+\frac{1}{2}} P_{cow_{i,j,k+1}}^{n+1} - T_{wz}\Big|^{n+1}_{i,j,k-\frac{1}{2}} P_{cow_{i,j,k-1}}^{n+1} \\
&+(T_{wx}\Big|^{n+1}_{i+\frac{1}{2},j,k} + T_{wx}\Big|^{n+1}_{i-\frac{1}{2},j,k} + T_{wy}\Big|^{n+1}_{i,j+\frac{1}{2},k} + T_{wy}\Big|^{n+1}_{i,j-\frac{1}{2},k} + T_{wz}\Big|^{n+1}_{i,j,k+\frac{1}{2}} + T_{wz}\Big|^{n+1}_{i,j,k-\frac{1}{2}}) P_{cow_{i,j,k}}^{n+1} \\
&+T_{gx}\Big|^{n+1}_{i+\frac{1}{2},j,k} P_{cgo_{i+1,j,k}}^{n+1} + T_{gx}\Big|^{n+1}_{i-\frac{1}{2},j,k} P_{cgo_{i-1,j,k}}^{n+1} + T_{gy}\Big|^{n+1}_{i,j+\frac{1}{2},k} P_{cgo_{i,j+1,k}}^{n+1} \\
&+T_{gy}\Big|^{n+1}_{i,j-\frac{1}{2},k} P_{cgo_{i,j-1,k}}^{n+1} + T_{gx}\Big|^{n+1}_{i,j,k+\frac{1}{2}} P_{cgo_{i,j,k+1}}^{n+1} + T_{gx}\Big|^{n+1}_{i,j,k-\frac{1}{2}} P_{cgo_{i,j,k-1}}^{n+1} \\
&+(T_{gx}\Big|^{n+1}_{i+\frac{1}{2},j,k} + T_{gx}\Big|^{n+1}_{i-\frac{1}{2},j,k} + T_{gy}\Big|^{n+1}_{i,j+\frac{1}{2},k} + T_{gy}\Big|^{n+1}_{i,j-\frac{1}{2},k} + T_{gz}\Big|^{n+1}_{i,j,k+\frac{1}{2}} + T_{gz}\Big|^{n+1}_{i,j,k-\frac{1}{2}}) P_{cgo_{i,j,k}}^{n+1} \\
&+\frac{A_x D_{io}}{\Delta x}\Big|^{n+1}_{i+\frac{1}{2},j,k} (\rho_o C_{io})_{i+1,j,k}^{n+1} + \frac{A_x D_{io}}{\Delta x}\Big|^{n+1}_{i-\frac{1}{2},j,k} (\rho_o C_{io})_{i-1,j,k}^{n+1} + \frac{A_y D_{io}}{\Delta y}\Big|^{n+1}_{i,j+\frac{1}{2},k} (\rho_o C_{io})_{i,j+1,k}^{n+1} \\
&+\frac{A_y D_{io}}{\Delta y}\Big|^{n+1}_{i,j-\frac{1}{2},k} (\rho_o C_{io})_{i,j-1,k}^{n+1} + \frac{A_z D_{io}}{\Delta z}\Big|^{n+1}_{i,j,k+\frac{1}{2}} (\rho_o C_{io})_{i,j,k+1}^{n+1} + \frac{A_z D_{io}}{\Delta z}\Big|^{n+1}_{i,j,k-\frac{1}{2}} (\rho_o C_{io})_{i,j,k-1}^{n+1} \\
&-(\frac{A_x D_{io}}{\Delta x}\Big|^{n+1}_{i+\frac{1}{2},j,k} + \frac{A_x D_{io}}{\Delta x}\Big|^{n+1}_{i-\frac{1}{2},j,k} + \frac{A_y D_{io}}{\Delta y}\Big|^{n+1}_{i,j+\frac{1}{2},k} + \frac{A_y D_{io}}{\Delta y}\Big|^{n+1}_{i,j-\frac{1}{2},k} + \frac{A_z D_{io}}{\Delta z}\Big|^{n+1}_{i,j,k+\frac{1}{2}} + \frac{A_z D_{io}}{\Delta z}\Big|^{n+1}_{i,j,k-\frac{1}{2}}) (\rho_o C_{io})_{i,j,k}^{n+1} \\
&+\frac{A_x D_{iw}}{\Delta x}\Big|^{n+1}_{i+\frac{1}{2},j,k} (\frac{\rho_o C_{io}}{f_{i_{ow}}})_{i+1,j,k}^{n+1} + \frac{A_x D_{iw}}{\Delta x}\Big|^{n+1}_{i-\frac{1}{2},j,k} (\frac{\rho_o C_{io}}{f_{i_{ow}}})_{i-1,j,k}^{n+1} + \frac{A_y D_{iw}}{\Delta y}\Big|^{n+1}_{i,j+\frac{1}{2},k} (\frac{\rho_o C_{io}}{f_{i_{ow}}})_{i,j+1,k}^{n+1} \\
&+\frac{A_y D_{iw}}{\Delta y}\Big|^{n+1}_{i,j-\frac{1}{2},k} (\frac{\rho_o C_{io}}{f_{i_{ow}}})_{i,j-1,k}^{n+1} + \frac{A_z D_{iw}}{\Delta z}\Big|^{n+1}_{i,j,k+\frac{1}{2}} (\frac{\rho_o C_{io}}{f_{i_{ow}}})_{i,j,k+1}^{n+1} + \frac{A_z D_{iw}}{\Delta z}\Big|^{n+1}_{i,j,k-\frac{1}{2}} (\frac{\rho_o C_{io}}{f_{i_{ow}}})_{i,j,k-1}^{n+1} \\
&-(\frac{A_x D_{iw}}{\Delta x}\Big|^{n+1}_{i+\frac{1}{2},j,k} + \frac{A_x D_{iw}}{\Delta x}\Big|^{n+1}_{i-\frac{1}{2},j,k} + \frac{A_y D_{iw}}{\Delta y}\Big|^{n+1}_{i,j+\frac{1}{2},k} + \frac{A_y D_{iw}}{\Delta y}\Big|^{n+1}_{i,j-\frac{1}{2},k} + \frac{A_z D_{iw}}{\Delta z}\Big|^{n+1}_{i,j,k+\frac{1}{2}} + \frac{A_z D_{iw}}{\Delta z}\Big|^{n+1}_{i,j,k-\frac{1}{2}}) (\frac{\rho_o C_{io}}{f_{i_{ow}}})_{i,j,k}^{n+1} \\
&+\frac{A_x D_{ig}}{\Delta x}\Big|^{n+1}_{i+\frac{1}{2},j,k} (\frac{\rho_g C_{io}}{f_{i_{og}}})_{i+1,j,k}^{n+1} + \frac{A_x D_{ig}}{\Delta x}\Big|^{n+1}_{i-\frac{1}{2},j,k} (\frac{\rho_g C_{io}}{f_{i_{og}}})_{i-1,j,k}^{n+1} + \frac{A_y D_{ig}}{\Delta y}\Big|^{n+1}_{i,j+\frac{1}{2},k} (\frac{\rho_g C_{io}}{f_{i_{og}}})_{i,j+1,k}^{n+1} \\
&+\frac{A_y D_{ig}}{\Delta y}\Big|^{n+1}_{i,j-\frac{1}{2},k} (\frac{\rho_g C_{io}}{f_{i_{og}}})_{i,j-1,k}^{n+1} + \frac{A_z D_{ig}}{\Delta z}\Big|^{n+1}_{i,j,k+\frac{1}{2}} (\frac{\rho_g C_{io}}{f_{i_{og}}})_{i,j,k+1}^{n+1} + \frac{A_z D_{ig}}{\Delta z}\Big|^{n+1}_{i,j,k-\frac{1}{2}} (\frac{\rho_g C_{io}}{f_{i_{og}}})_{i,j,k-1}^{n+1} \\
&-(\frac{A_x D_{ig}}{\Delta x}\Big|^{n+1}_{i+\frac{1}{2},j,k} + \frac{A_x D_{ig}}{\Delta x}\Big|^{n+1}_{i-\frac{1}{2},j,k} + \frac{A_y D_{ig}}{\Delta y}\Big|^{n+1}_{i,j+\frac{1}{2},k} + \frac{A_y D_{ig}}{\Delta y}\Big|^{n+1}_{i,j-\frac{1}{2},k} + \frac{A_z D_{ig}}{\Delta z}\Big|^{n+1}_{i,j,k+\frac{1}{2}} + \frac{A_z D_{ig}}{\Delta z}\Big|^{n+1}_{i,j,k-\frac{1}{2}}) (\frac{\rho_g C_{io}}{f_{i_{og}}})_{i,j,k}^{n+1} \\
&+V_{b_{i,j,k}} m_i^{*n+1} + V_{b_{i,j,k}} m_{si}^{*n+1} - V_{b_{i,j,k}} \sum_{j\prime=1}^{J} P_{ij\prime i,j,k} \\
&-\frac{V_{b_{i,j,k}}}{\Delta t}[(\phi S_w \rho_w \frac{C_{io}}{f_{i_{ow}}}\Big|^{n+1}_{i,j,k} - \phi S_w \rho_w \frac{C_{io}}{f_{i_{ow}}}\Big|^{n}_{i,j,k}) + ([\phi(1-S_w-S_g)\rho_o C_{io}]\Big|^{n+1}_{i,j,k} \\
&-[\phi(1-S_w-S_g)\rho_o C_{io}]\Big|^{n}_{i,j,k}) + (\phi S_g \rho_g \frac{C_{io}}{f_{i_{og}}}\Big|^{n+1}_{i,j,k} - \phi S_g \rho_g \frac{C_{io}}{f_{i_{og}}}\Big|^{n}_{i,j,k})] \qquad (4.16)
\end{aligned}
$$

where

$$T_x = T_{o_x} + T_{w_x} + T_{g_x},$$

$$T_{o_x} = \frac{A_x k_x k_{r_o} \rho_o C_{i_o}}{\mu_o \Delta x}\Big|_{i\pm\frac{1}{2},j,k},$$

$$T_{w_x} = \frac{A_x k_x k_{r_w} \rho_w C_{i_w}}{\mu_w \Delta x}\Big|_{i\pm\frac{1}{2},j,k},$$

$$T_{g_x} = \frac{A_x k_x k_{r_g} \rho_g C_{i_g}}{\mu_g \Delta x}\Big|_{i\pm\frac{1}{2},j,k},$$

and

$$T_{gg_x} = T_{o_x}\rho_o g + T_{w_x}\rho_w g + T_{g_x}\rho_g g,$$

where, for example,

$$T_{o_x}\Big|_{i+\frac{1}{2},j,k} = \frac{2A_{x_{i+1,j,k}} k_{x_{i+1,j,k}} A_{x_{i,j,k}} k_{x_{i,j,k}}}{A_{x_{i+1,j,k}} k_{x_{i+1,j,k}} \Delta x_{i,j,k} + A_{x_{i,j,k}} k_{x_{i,j,k}} \Delta x_{i+1,j,k}} \left(\frac{k_{r_o}\rho_o C_{i_o}}{\mu_o}\right)_l^{(n+1)},$$

where

l is $i+1,j,k$: if ${\Phi_{o_{i+1,j,k}}}^{n+1} > {\Phi_{o_{i,j,k}}}^{n+1}$, or, l is i,j,k: if ${\Phi_{o_{i+1,j,k}}}^{n+1} \leq {\Phi_{o_{i,j,k}}}^{n+1}$.

Similar terms can be written for the y and z directions also. The above choice of l is based upon the well-known concept of upstream saturations.

Energy Balance

The energy balance equation (Eq.(4.12)) is discretized for a fully implicit formulation, as follows:

$$G_{i,j,k} = 0, \tag{4.17}$$

where G is given by

$$G_{i,j,k} = \frac{A_x k_{hx}}{\Delta x}\Big|_{i+\frac{1}{2},j,k}^{n+1}(T_{i+1,j,k}^{n+1} - T_{i,j,k}^{n+1}) - \frac{A_x k_{hx}}{\Delta x}\Big|_{i-\frac{1}{2},j,k}^{n+1}(T_{i,j,k}^{n+1} - T_{i-1,j,k}^{n+1}) + \frac{A_y k_{hy}}{\Delta y}\Big|_{i,j+\frac{1}{2},k}^{n+1}(T_{i,j+1,k}^{n+1} - T_{i,j,k}^{n+1})$$
$$- \frac{A_y k_{hy}}{\Delta y}\Big|_{i,j-\frac{1}{2},k}^{n+1}(T_{i,j,k}^{n+1} - T_{i,j-1,k}^{n+1}) + \frac{A_z k_{hz}}{\Delta z}\Big|_{i,j,k+\frac{1}{2}}^{n+1}(T_{i,j,k+1}^{n+1} - T_{i,j,k}^{n+1}) - \frac{A_z k_{hz}}{\Delta z}\Big|_{i,j,k-\frac{1}{2}}^{n+1}(T_{i,j,k}^{n+1} - T_{i,j,k-1}^{n+1})$$

$$-V_{b_{i,j,k}}\Delta_x\left(\rho_o v_{ox}T\sum_i(c_{p_i}C_{i_o})\right)^{n+1}_{i,j,k}-V_{b_{i,j,k}}\Delta_y\left(\rho_o v_{oy}T\sum_i(c_{p_i}C_{i_o})\right)^{n+1}_{i,j,k}-V_{b_{i,j,k}}\Delta_z\left(\rho_o v_{oz}T\sum_i(c_{p_i}C_{i_o})\right)^{n+1}_{i,j,k}$$

$$-V_{b_{i,j,k}}\Delta_x\left(\rho_w v_{wx}T\sum_i(c_{p_i}\frac{C_{i_o}}{f_{i_{ow}}})\right)^{n+1}_{i,j,k}-V_{b_{i,j,k}}\Delta_y\left(\rho_w v_{wy}T\sum_i(c_{p_i}\frac{C_{i_o}}{f_{i_{ow}}})\right)^{n+1}_{i,j,k}$$

$$-V_{b_{i,j,k}}\Delta_z\left(\rho_w v_{wz}T\sum_i(c_{p_i}\frac{C_{i_o}}{f_{i_{ow}}})\right)^{n+1}_{i,j,k}-V_{b_{i,j,k}}\Delta_x\left(\rho_g v_{gx}T\sum_i(c_{p_i}T+L_{v_i})\frac{C_{i_o}}{f_{i_{og}}}\right)^{n+1}_{i,j,k}$$

$$-V_{b_{i,j,k}}\Delta_y\left(\rho_g v_{gy}T\sum_i(c_{p_i}T+L_{v_i})\frac{C_{i_o}}{f_{i_{og}}}\right)^{n+1}_{i,j,k}-V_{b_{i,j,k}}\Delta_z\left(\rho_g v_{gz}T\sum_i(c_{p_i}T+L_{v_i})\frac{C_{i_o}}{f_{i_{og}}}\right)^{n+1}_{i,j,k}$$

$$+\sum_i\Big[\frac{A_xD_{i_o}\rho_o c_{p_i}T}{\Delta x}\Big|^{n+1}_{i+\frac{1}{2},j,k}(C_{io}{}^{n+1}_{i+1,j,k}-C_{io}{}^{n+1}_{i,j,k})-\frac{A_xD_{i_o}\rho_o c_{p_i}T}{\Delta x}\Big|^{n+1}_{i-\frac{1}{2},j,k}(C_{io}{}^{n+1}_{i,j,k}-C_{io}{}^{n+1}_{i-1,j,k})\Big]$$

$$+\sum_i\Big[\frac{A_yD_{i_o}\rho_o c_{p_i}T}{\Delta y}\Big|^{n+1}_{i,j+\frac{1}{2},k}(C_{io}{}^{n+1}_{i,j+1,k}-C_{io}{}^{n+1}_{i,j,k})-\frac{A_yD_{i_o}\rho_o c_{p_i}T}{\Delta y}\Big|^{n+1}_{i,j-\frac{1}{2},k}(C_{io}{}^{n+1}_{i,j,k}-C_{io}{}^{n+1}_{i,j-1,k})\Big]$$

$$+\sum_i\Big[\frac{A_zD_{i_o}\rho_o c_{p_i}T}{\Delta z}\Big|^{n+1}_{i,j,k+\frac{1}{2}}(C_{io}{}^{n+1}_{i,j,k+1}-C_{io}{}^{n+1}_{i,j,k})-\frac{A_zD_{i_o}\rho_o c_{p_i}T}{\Delta z}\Big|^{n+1}_{i,j,k-\frac{1}{2}}(C_{io}{}^{n+1}_{i,j,k}-C_{io}{}^{n+1}_{i,j,k-1})\Big]$$

$$+\sum_i\Big[\frac{A_xD_{i_w}\rho_w c_{p_i}T}{\Delta x}\Big|^{n+1}_{i+\frac{1}{2},j,k}(\frac{C_{i_o}{}^{n+1}}{f_{i_{ow}\,i+1,j,k}}-\frac{C_{i_o}{}^{n+1}}{f_{i_{ow}\,i,j,k}})-\frac{A_xD_{i_w}\rho_w c_{p_i}T}{\Delta x}\Big|^{n+1}_{i-\frac{1}{2},j,k}(\frac{C_{i_o}{}^{n+1}}{f_{i_{ow}\,i,j,k}}-\frac{C_{i_o}{}^{n+1}}{f_{i_{ow}\,i-1,j,k}})\Big]$$

$$+\sum_i\Big[\frac{A_yD_{i_w}\rho_w c_{p_i}T}{\Delta y}\Big|^{n+1}_{i,j+\frac{1}{2},k}(\frac{C_{i_o}{}^{n+1}}{f_{i_{ow}\,i,j+1,k}}-\frac{C_{i_o}{}^{n+1}}{f_{i_{ow}\,i,j,k}})-\frac{A_yD_{i_w}\rho_w c_{p_i}T}{\Delta y}\Big|^{n+1}_{i,j-\frac{1}{2},k}(\frac{C_{i_o}{}^{n+1}}{f_{i_{ow}\,i,j,k}}-\frac{C_{i_o}{}^{n+1}}{f_{i_{ow}\,i,j-1,k}})\Big]$$

$$+\sum_i\Big[\frac{A_zD_{i_w}\rho_w c_{p_i}T}{\Delta z}\Big|^{n+1}_{i,j,k+\frac{1}{2}}(\frac{C_{i_o}{}^{n+1}}{f_{i_{ow}\,i,j,k+1}}-\frac{C_{i_o}{}^{n+1}}{f_{i_{ow}\,i,j,k}})-\frac{A_zD_{i_w}\rho_w c_{p_i}T}{\Delta z}\Big|^{n+1}_{i,j,k-\frac{1}{2}}(\frac{C_{i_o}{}^{n+1}}{f_{i_{ow}\,i,j,k}}-\frac{C_{i_o}{}^{n+1}}{f_{i_{ow}\,i,j,k-1}})\Big]$$

$$+\sum_i\Big[\frac{A_xD_{i_g}\rho_g(c_{p_i}T+L_{v_i})}{\Delta x}\Big|^{n+1}_{i+\frac{1}{2},j,k}(\frac{C_{i_o}{}^{n+1}}{f_{i_{og}\,i+1,j,k}}-\frac{C_{i_o}{}^{n+1}}{f_{i_{og}\,i,j,k}})-\frac{A_xD_{i_g}\rho_g(c_{p_i}T+L_{v_i})}{\Delta x}\Big|^{n+1}_{i-\frac{1}{2},j,k}(\frac{C_{i_o}{}^{n+1}}{f_{i_{og}\,i,j,k}}-\frac{C_{i_o}{}^{n+1}}{f_{i_{og}\,i-1,j,k}})\Big]$$

$$+\sum_i\Big[\frac{A_yD_{i_g}\rho_g(c_{p_i}T+L_{v_i})}{\Delta y}\Big|^{n+1}_{i,j+\frac{1}{2},k}(\frac{C_{i_o}{}^{n+1}}{f_{i_{og}\,i,j+1,k}}-\frac{C_{i_o}{}^{n+1}}{f_{i_{og}\,i,j,k}})-\frac{A_yD_{i_g}\rho_g(c_{p_i}T+L_{v_i})}{\Delta y}\Big|^{n+1}_{i,j-\frac{1}{2},k}(\frac{C_{i_o}{}^{n+1}}{f_{i_{og}\,i,j,k}}-\frac{C_{i_o}{}^{n+1}}{f_{i_{og}\,i,j-1,k}})\Big]$$

$$+\sum_i\Big[\frac{A_zD_{i_g}\rho_g(c_{p_i}T+L_{v_i})}{\Delta z}\Big|^{n+1}_{i,j,k+\frac{1}{2}}(\frac{C_{i_o}{}^{n+1}}{f_{i_{og}\,i,j,k+1}}-\frac{C_{i_o}{}^{n+1}}{f_{i_{og}\,i,j,k}})-\frac{A_zD_{i_g}\rho_g(c_{p_i}T+L_{v_i})}{\Delta z}\Big|^{n+1}_{i,j,k-\frac{1}{2}}(\frac{C_{i_o}{}^{n+1}}{f_{i_{og}\,i,j,k}}-\frac{C_{i_o}{}^{n+1}}{f_{i_{og}\,i,j,k-1}})\Big]$$

$$+V_{b_{i,j,k}}[-q^*_L+r^{*v}_H+\frac{q_{o^*}\rho_o}{M_o}\sum_i x_{i_o}h_{i_o}{}^{n+1}_{i,j,k}+\frac{q_{w^*}\rho_w}{M_w}\sum_i x_{i_w}h_{i_w}{}^{n+1}_{i,j,k}+\frac{q_{g^*}\rho_g}{M_g}\sum_i x_{i_g}h_{i_g}{}^{n+1}_{i,j,k}]\Big|^{n+1}_{i,j,k}]$$

$$-\frac{V_{b_{i,j,k}}}{\Delta t}[((1-\phi)\frac{\rho_s}{M_s}h_s\Big|^{n+1}_{i,j,k}-(1-\phi)\frac{\rho_s}{M_s}h_s\Big|^{n}_{i,j,k})+(\phi\rho_o(1-S_w-S_g)\sum_i c_{p_i}C_{i_o}T\Big|^{n+1}_{i,j,k}-$$

$$\phi\rho_o(1-S_w-S_g)\sum_i c_{p_i}C_{i_o}T\Big|^{n}_{i,j,k})+(\phi\rho_w S_w\sum_i c_{p_i}\frac{C_{i_o}}{f_{i_{ow}}}T\Big|^{n+1}_{i,j,k}-\phi\rho_w S_w\sum_i c_{p_i}\frac{C_{i_o}}{f_{i_{ow}}}T\Big|^{n}_{i,j,k})$$

$$+(\phi\rho_g S_g\sum_i(c_{p_i}T+L_{v_i})\frac{C_{i_o}}{f_{i_{og}}}\Big|^{n+1}_{i,j,k}-\phi\rho_g S_g\sum_i(c_{p_i}T+L_{v_i})\frac{C_{i_o}}{f_{i_{og}}}\Big|^{n}_{i,j,k})] \qquad (4.18)$$

The convection terms in the above equation are given by the following expressions:

$$V_{b_{i,j,k}}\Delta_x\left(\rho_o v_{ox}T\sum_i(c_{p_i}C_{i_o})\right)^{n+1}_{i,j,k}=-\frac{A_xk_xk_{ro}\rho_o}{\mu_o\Delta x}\Big|^{n+1}_{i,j,k}(s_{i+1}p_o{}^{n+1}_{i+1,j,k}+s_ip_o{}^{n+1}_{i,j,k}+s_{i-1}p_o{}^{n+1}_{i-1,j,k}$$

$$-s_{i+1}gD_{i+1,j,k}\rho_o{}^{n+1}_{i+1,j,k}-s_igD_{i,j,k}\rho_o{}^{n+1}_{i,j,k}-s_{i-1}gD_{i-1,j,k}\rho_o{}^{n+1}_{i-1,j,k})$$

$$\cdot(s_{i+1}T^{n+1}_{i+1,j,k}\sum_i(c_{p_i}C_{i_o})|^{n+1}_{i+1,j,k}+s_iT^{n+1}_{i,j,k}\sum_i(c_{p_i}C_{i_o})|^{n+1}_{i,j,k}+s_{i-1}T^{n+1}_{i-1,j,k}\sum_i(c_{p_i}C_{i_o})|^{n+1}_{i-1,j,k})$$

$$-T^{n+1}_{i,j,k}\sum_i(c_{p_i}C_{i_o})|^{n+1}_{i,j,k}\Big[\{w_{o_x}\frac{A_xk_xk_{ro}\rho_o}{\mu_o\Delta x}|^{n+1}_{i,j,k}+(1-w_{o_x})\frac{A_xk_xk_{ro}\rho_o}{\mu_o\Delta x}|^{n+1}_{i+1,j,k}\}(p_{o^{n+1}_{i+1,j,k}}-p_{o^{n+1}_{i,j,k}})$$

$$-\{w^*{}_{o_x}\frac{A_xk_xk_{ro}\rho_o}{\mu_o\Delta x}|^{n+1}_{i,j,k}+(1-w^*{}_{oy})\frac{A_xk_xk_{ro}\rho_o}{\mu_o\Delta x}|^{n+1}_{i-1,j,k}\}(p_{o^{n+1}_{i,j,k}}-p_{o^{n+1}_{i-1,j,k}})$$

$$-\{w_{o_x}\frac{A_xk_xk_{ro}\rho_o}{\mu_o\Delta x}|^{n+1}_{i,j,k}+(1-w_{o_x})\frac{A_xk_xk_{ro}\rho_o}{\mu_o\Delta x}|^{n+1}_{i+1,j,k}\}g(\rho_{o^{n+1}_{i+1,j,k}}D_{i+1,j,k}-\rho_{o^{n+1}_{i,j,k}}D_{i,j,k})$$

$$+\{w^*{}_{o_x}\frac{A_xk_xk_{ro}\rho_o}{\mu_o\Delta x}|^{n+1}_{i,j,k}+(1-w^*{}_{o_x})\frac{A_xk_xk_{ro}\rho_o}{\mu_o\Delta x}|^{n+1}_{i-1,j,k}\}g(\rho_{o^{n+1}_{i-1,j,k}}D_{i-1,j,k}-\rho_{o^{n+1}_{i,j,k}}D_{i,j,k})\Big] \tag{4.19}$$

$$V_{b_{i,j,k}}\Delta_y\left(\rho_o v_{oy}T\sum_i(c_{p_i}C_{i_o})\right)^{n+1}_{i,j,k}=-\frac{A_yk_yk_{ro}\rho_o}{\mu_o\Delta y}\Big|^{n+1}_{i,j,k}(s_{j+1}p_{o^{n+1}_{i,j+1,k}}+s_jp_{o^{n+1}_{i,j,k}}+s_{j-1}p_{o^{n+1}_{i,j-1,k}}$$

$$-s_{j+1}gD_{i,j+1,k}\rho_{o^{n+1}_{i,j+1,k}}-s_{[illegible]}{}^{n+1}_{i,j,k}-s_{j-1}gD_{i,j-1,k}\rho_{o^{n+1}_{i,j-1,k}})$$

$$\cdot(s_{j+1}T^{n+1}_{i,j+1,k}\sum_i(c_{p_i}C_{i_o})|^{n+1}_{i,j+1,k}+s_jT^{n+1}_{i,j,k}\sum_i(c_{p_i}C_{i_o})|^{n+1}_{i,j,k}+s_{j-1}T^{n+1}_{i,j-1,k}\sum_i(c_{p_i}C_{i_o})|^{n+1}_{i,j-1,k})$$

$$-T^{n+1}_{i,j,k}\sum_i(c_{p_i}C_{i_o})|^{n+1}_{i,j,k}\Big[\{w_{o_y}\frac{A_yk_yk_{ro}\rho_o}{\mu_o\Delta y}|^{n+1}_{i,j,k}+(1-w_{o_y})\frac{A_yk_yk_{ro}\rho_o}{\mu_o\Delta y}|^{n+1}_{i,j+1,k}\}(p_{o^{n+1}_{i,j+1,k}}-p_{o^{n+1}_{i,j,k}})$$

$$-\{w^*{}_{o_y}\frac{A_yk_yk_{ro}\rho_o}{\mu_o\Delta y}|^{n+1}_{i,j,k}+(1-w^*{}_{o_y})\frac{A_yk_yk_{ro}\rho_o}{\mu_o\Delta y}|^{n+1}_{i,j-1,k}\}(p_{o^{n+1}_{i,j,k}}-p_{o^{n+1}_{i,j-1,k}})$$

$$-\{w_{o_y}\frac{A_yk_yk_{ro}\rho_o}{\mu_o\Delta y}|^{n+1}_{i,j,k}+(1-w_{o_y})\frac{A_yk_yk_{ro}\rho_o}{\mu_o\Delta y}|^{n+1}_{i,j+1,k}\}g(\rho_{o^{n+1}_{i,j+1,k}}D_{i,j+1,k}-\rho_{o^{n+1}_{i,j,k}}D_{i,j,k})$$

$$+\{w^*{}_{o_y}\frac{A_yk_yk_{ro}\rho_o}{\mu_o\Delta y}|^{n+1}_{i,j,k}+(1-w^*{}_{o_y})\frac{A_yk_yk_{ro}\rho_o}{\mu_o\Delta y}|^{n+1}_{i,j-1,k}\}g(\rho_{o^{n+1}_{i,j-1,k}}D_{i,j-1,k}-\rho_{o^{n+1}_{i,j,k}}D_{i,j,k})\Big] \tag{4.20}$$

$$V_{b_{i,j,k}}\Delta_z\left(\rho_o v_{oz}T\sum_i(c_{p_i}C_{i_o})\right)^{n+1}_{i,j,k}=-\frac{A_zk_zk_{ro}\rho_o}{\mu_o\Delta z}\Big|^{n+1}_{i,j,k}(s_{k+1}p_{o^{n+1}_{i,j,k+1}}+s_kp_{o^{n+1}_{i,j,k}}+s_{k-1}p_{o^{n+1}_{i,j,k-1}}$$

$$-s_{k+1}gD_{i,j,k+1}\rho_{o^{n+1}_{i,j,k+1}}-s_kgD_{i,j,k}\rho_{o^{n+1}_{i,j,k}}-s_{k-1}gD_{i,j,k-1}\rho_{o^{n+1}_{i,j,k-1}})$$

$$\cdot(s_{k+1}T^{n+1}_{i,j,k+1}\sum_i(c_{p_i}C_{i_o})|^{n+1}_{i,j,k+1}+s_kT^{n+1}_{i,j,k}\sum_i(c_{p_i}C_{i_o})|^{n+1}_{i,j,k}+s_{k-1}T^{n+1}_{i,j,k-1}\sum_i(c_{p_i}C_{i_o})|^{n+1}_{i,j,k-1})$$

$$-T^{n+1}_{i,j,k}\sum_i(c_{p_i}C_{i_o})|^{n+1}_{i,j,k}\Big[\{w_{o_z}\frac{A_zk_zk_{ro}\rho_o}{\mu_o\Delta z}|^{n+1}_{i,j,k}+(1-w_{o_z})\frac{A_zk_zk_{ro}\rho_o}{\mu_o\Delta z}|^{n+1}_{i,j,k+1}\}(p_{o^{n+1}_{i,j,k+1}}-p_{o^{n+1}_{i,j,k}})$$

$$-\{w^*{}_{o_z}\frac{A_zk_zk_{ro}\rho_o}{\mu_o\Delta z}|^{n+1}_{i,j,k}+(1-w^*{}_{o_z})\frac{A_zk_zk_{ro}\rho_o}{\mu_o\Delta z}|^{n+1}_{i,j,k-1}\}(p_{o^{n+1}_{i,j,k}}-p_{o^{n+1}_{i,j,k-1}})$$

$$-\{w_{o_z}\frac{A_zk_zk_{ro}\rho_o}{\mu_o\Delta z}|^{n+1}_{i,j,k}+(1-w_{o_z})\frac{A_zk_zk_{ro}\rho_o}{\mu_o\Delta z}|^{n+1}_{i,j,k+1}\}g(\rho_{o^{n+1}_{i,j,k+1}}D_{i,j,k+1}-\rho_{o^{n+1}_{i,j,k}}D_{i,j,k})$$

$$+\{w^*{}_{o_z}\frac{A_zk_zk_{ro}\rho_o}{\mu_o\Delta z}|^{n+1}_{i,j,k}+(1-w^*{}_{o_z})\frac{A_zk_zk_{ro}\rho_o}{\mu_o\Delta z}|^{n+1}_{i,j,k-1}\}g(\rho_{o^{n+1}_{i,j,k-1}}D_{i,j,k-1}-\rho_{o^{n+1}_{i,j,k}}D_{i,j,k})\Big]$$

(4.21)

$$
\begin{aligned}
V_{b_{i,j,k}}\Delta_x\Big(\rho_w v_{wx} T\sum_i (c_{p_i}\frac{C_{i_o}}{f_{i_{ow}}})\Big)^{n+1}_{i,j,k} &= -\frac{A_x k_x k_{rw}\rho_w}{\mu_w \Delta x}\Big|^{n+1}_{i,j,k}(s_{i+1}p_{o}{}^{n+1}_{i+1,j,k} + s_i p_{o}{}^{n+1}_{i,j,k} + s_{i-1}p_{o}{}^{n+1}_{i-1,j,k} \\
&\quad - s_{i+1}P_{cow}{}^{n+1}_{i+1,j,k} - s_i P_{cow}{}^{n+1}_{i,j,k} + s_{i-1}P_{cow}{}^{n+1}_{i-1,j,k} \\
&\quad - s_{i+1}gD_{i+1,j,k}\rho_w{}^{n+1}_{i+1,j,k} - s_i g D_{i,j,k}\rho_w{}^{n+1}_{i,j,k} - s_{i-1}gD_{i-1,j,k}\rho_w{}^{n+1}_{i-1,j,k}) \\
&(s_{i+1}T^{n+1}_{i+1,j,k}\sum_i (c_{p_i}\frac{C_{i_o}}{f_{iow}})|^{n+1}_{i+1,j,k} + s_i T^{n+1}_{i,j,k}\sum_i (c_{p_i}\frac{C_{i_o}}{f_{iow}})|^{n+1}_{i,j,k} + s_{i-1}T^{n+1}_{i-1,j,k}\sum_i (c_{p_i}\frac{C_{i_o}}{f_{iow}})|^{n+1}_{i-1,j,k}) \\
&-T^{n+1}_{i,j,k}\sum_i (c_{p_i}\frac{C_{i_o}}{f_{iow}})|^{n+1}_{i,j,k}\Big[\{w_{w_x}\frac{A_x k_x k_{rw}\rho_w}{\mu_w\Delta x}|^{n+1}_{i,j,k} + (1-w_{w_x})\frac{A_x k_x k_{rw}\rho_w}{\mu_w\Delta x}|^{n+1}_{i+1,j,k}\}(p_{o}{}^{n+1}_{i+1,j,k} - p_{o}{}^{n+1}_{i,j,k}) \\
&\quad -\{w_{w_x}\frac{A_x k_x k_{rw}\rho_w}{\mu_w\Delta x}|^{n+1}_{i,j,k} + (1-w_{w_x})\frac{A_x k_x k_{rw}\rho_w}{\mu_w\Delta x}|^{n+1}_{i+1,j,k}\}(P_{cow}{}^{n+1}_{i+1,j,k} - P_{cow}{}^{n+1}_{i,j,k}) \\
&\quad -\{w^*{}_{w_x}\frac{A_x k_x k_{rw}\rho_w}{\mu_w\Delta x}|^{n+1}_{i,j,k} + (1-w^*{}_{w_x})\frac{A_x k_x k_{rw}\rho_w}{\mu_w\Delta x}|^{n+1}_{i-1,j,k}\}(p_{o}{}^{n+1}_{i,j,k} - p_{o}{}^{n+1}_{i-1,j,k}) \\
&\quad +\{w^*{}_{w_x}\frac{A_x k_x k_{rw}\rho_w}{\mu_w\Delta x}|^{n+1}_{i,j,k} + (1-w^*{}_{w_x})\frac{A_x k_x k_{rw}\rho_w}{\mu_w\Delta x}|^{n+1}_{i-1,j,k}\}(P_{cow}{}^{n+1}_{i,j,k} - P_{cow}{}^{n+1}_{i-1,j,k} \\
&\quad -\{w_{w_x}\frac{A_x k_x k_{rw}\rho_w}{\mu_w\Delta x}|^{n+1}_{i,j,k} + (1-w_{w_x})\frac{A_x k_x k_{rw}\rho_w}{\mu_w\Delta x}|^{n+1}_{i+1,j,k}\}g(\rho_w{}^{n+1}_{i+1,j,k}D_{i+1,j,k} - \rho_w{}^{n+1}_{i,j,k}D_{i,j,k}) \\
&\quad +\{w^*{}_{w_x}\frac{A_x k_x k_{rw}\rho_w}{\mu_w\Delta x}|^{n+1}_{i,j,k} + (1-w^*{}_{w_x})\frac{A_x k_x k_{rw}\rho_w}{\mu_w\Delta x}|^{n+1}_{i-1,j,k}\}g(\rho_w{}^{n+1}_{i-1,j,k}D_{i-1,j,k} - \rho_w{}^{n+1}_{i,j,k}D_{i,j,k})\Big]
\end{aligned}
$$

(4.22)

$$
\begin{aligned}
V_{b_{i,j,k}}\Delta_y\Big(\rho_w v_{wy} T\sum_i (c_{p_i}\frac{C_{i_o}}{f_{i_{ow}}})\Big)^{n+1}_{i,j,k} &= -\frac{A_y k_y k_{rw}\rho_w}{\mu_w \Delta y}\Big|^{n+1}_{i,j,k}(s_{j+1}p_{o}{}^{n+1}_{i,j+1,k} + s_j p_{o}{}^{n+1}_{i,j,k} + s_{j-1}p_{o}{}^{n+1}_{i,j-1,k} \\
&\quad - s_{j+1}P_{cow}{}^{n+1}_{i,j+1,k} - s_j P_{cow}{}^{n+1}_{i,j,k} + s_{j-1}P_{cow}{}^{n+1}_{i,j-1,k} \\
&\quad - s_{j+1}gD_{i,j+1,k}\rho_w{}^{n+1}_{i,j+1,k} - s_j g D_{i,j,k}\rho_w{}^{n+1}_{i,j,k} - s_{j-1}gD_{i,j-1,k}\rho_w{}^{n+1}_{i,j-1,k}) \\
&(s_{j+1}T^{n+1}_{i,j+1,k}\sum_i (c_{p_i}\frac{C_{i_o}}{f_{iow}})|^{n+1}_{i,j+1,k} + s_j T^{n+1}_{i,j,k}\sum_i (c_{p_i}\frac{C_{i_o}}{f_{iow}})|^{n+1}_{i,j,k} + s_{j-1}T^{n+1}_{i,j-1,k}\sum_i (c_{p_i}\frac{C_{i_o}}{f_{iow}})|^{n+1}_{i,j-1,k}) \\
&-T^{n+1}_{j,j,k}\sum_i (c_{p_i}\frac{C_{i_o}}{f_{iow}})|^{n+1}_{i,j,k}\Big[\{w_{w_y}\frac{A_y k_y k_{rw}\rho_w}{\mu_w\Delta y}|^{n+1}_{i,j,k} + (1-w_{w_y})\frac{A_y k_y k_{rw}\rho_w}{\mu_w\Delta y}|^{n+1}_{i,j+1,k}\}(p_{o}{}^{n+1}_{i,j+1,k} - p_{o}{}^{n+1}_{i,j,k}) \\
&\quad -\{w_{w_y}\frac{A_y k_y k_{rw}\rho_w}{\mu_w\Delta y}|^{n+1}_{i,j,k} + (1-w_{w_y})\frac{A_y k_y k_{rw}\rho_w}{\mu_w\Delta y}|^{n+1}_{i,j+1,k}\}(P_{cow}{}^{n+1}_{i,j+1,k} - P_{cow}{}^{n+1}_{i,j,k}) \\
&\quad -\{w^*{}_{w_y}\frac{A_y k_y k_{rw}\rho_w}{\mu_w\Delta y}|^{n+1}_{i,j,k} + (1-w^*{}_{w_y})\frac{A_y k_y k_{rw}\rho_w}{\mu_w\Delta y}|^{n+1}_{i,j-1,k}\}(p_{o}{}^{n+1}_{i,j,k} - p_{o}{}^{n+1}_{i,j-1,k}) \\
&\quad +\{w^*{}_{w_y}\frac{A_y k_y k_{rw}\rho_w}{\mu_w\Delta y}|^{n+1}_{i,j,k} + (1-w^*{}_{w_y})\frac{A_y k_y k_{rw}\rho_w}{\mu_w\Delta y}|^{n+1}_{i,j-1,k}\}(P_{cow}{}^{n+1}_{i,j,k} - P_{cow}{}^{n+1}_{i,j-1,k}
\end{aligned}
$$

$$-\{w_{w_y}\frac{A_y k_y k_{rw}\rho_w}{\mu_w \Delta y}|_{i,j,k}^{n+1}+(1-w_{w_y})\frac{A_y k_y k_{rw}\rho_w}{\mu_w \Delta y}|_{i,j+1,k}^{n+1}\}g(\rho_w{}_{i,j+1,k}^{n+1}D_{i,j+1,k}-\rho_w{}_{i,j,k}^{n+1}D_{i,j,k})$$
$$+\{w^*{}_{w_y}\frac{A_y k_y k_{rw}\rho_w}{\mu_w \Delta y}|_{i,j,k}^{n+1}+(1-w^*{}_{w_y})\frac{A_y k_y k_{rw}\rho_w}{\mu_w \Delta y}|_{i,j-1,k}^{n+1}\}g(\rho_w{}_{i,j-1,k}^{n+1}D_{i,j-1,k}-\rho_w{}_{i,j,k}^{n+1}D_{i,j,k})\Big] \tag{4.23}$$

$$V_{b_{i,j,k}}\Delta_z\Big(\rho_w v_{wz}T\sum_i(c_{p_i}\frac{C_{i_o}}{f_{i_{ow}}})\Big)_{i,j,k}^{n+1}=-\frac{A_z k_z k_{rw}\rho_w}{\mu_w \Delta z}\Big|_{i,j,k}^{n+1}(s_{k+1}p_{o_{i,j,k+1}}^{n+1}+s_k p_{o_{i,j,k}}^{n+1}+s_{k-1}p_{o_{i,j,k-1}}^{n+1}$$
$$-s_{k+1}P_{cow_{i,j,k+1}}^{n+1}-s_k P_{cow_{i,j,k}}^{n+1}+s_{k-1}P_{cow_{i,j,k-1}}^{n+1}$$
$$-s_{k+1}gD_{i,j,k+1}\rho_w{}_{i,j,k+1}^{n+1}-s_k gD_{i,j,k}\rho_w{}_{i,j,k}^{n+1}-s_{k-1}gD_{i,j,k-1}\rho_w{}_{i,j,k-1}^{n+1})$$
$$\cdot(s_{k+1}T_{i,j,k+1}^{n+1}\sum_i(c_{p_i}\frac{C_{i_o}}{f_{iow}})|_{i,j,k+1}^{n+1}+s_k T_{i,j,k}^{n+1}\sum_i(c_{p_i}\frac{C_{i_o}}{f_{iow}})|_{i,j,k}^{n+1}+s_{k-1}T_{i,j,k-1}^{n+1}\sum_i(c_{p_i}\frac{C_{i_o}}{f_{iow}})|_{i,j,k-1}^{n+1})$$
$$-T_{i,j,k}^{n+1}\sum_i(c_{p_i}\frac{C_{i_o}}{f_{iow}})|_{i,j,k}^{n+1}\Big[\{w_{w_z}\frac{A_z k_z k_{rw}\rho_w}{\mu_w \Delta z}|_{i,j,k}^{n+1}+(1-w_{w_z})\frac{A_z k_z k_{rw}\rho_w}{\mu_w \Delta z}|_{i,j,k+1}^{n+1}\}(p_{o_{i,j,k+1}}^{n+1}-p_{o_{i,j,k}}^{n+1})$$
$$-\{w_{w_z}\frac{A_z k_z k_{rw}\rho_w}{\mu_w \Delta z}|_{i,j,k}^{n+1}+(1-w_{w_z})\frac{A_z k_z k_{rw}\rho_w}{\mu_w \Delta z}|_{i,j,k+1}^{n+1}\}(P_{cow_{i,j,k+1}}^{n+1}-P_{cow_{i,j,k}}^{n+1})$$
$$-\{w^*{}_{w_z}\frac{A_z k_z k_{rw}\rho_w}{\mu_w \Delta z}|_{i,j,k}^{n+1}+(1-w^*{}_{w_z})\frac{A_z k_z k_{rw}\rho_w}{\mu_w \Delta z}|_{i,j,k-1}^{n+1}\}(p_{o_{i,j,k}}^{n+1}-p_{o_{i,j,k-1}}^{n+1})$$
$$+\{w^*{}_{w_z}\frac{A_z k_z k_{rw}\rho_w}{\mu_w \Delta z}|_{i,j,k}^{n+1}+(1-w^*{}_{w_z})\frac{A_z k_z k_{rw}\rho_w}{\mu_w \Delta z}|_{i,j,k-1}^{n+1}\}(P_{cow_{i,j,k}}^{n+1}-P_{cow_{i,j,k-1}}^{n+1}$$
$$-\{w_{w_z}\frac{A_z k_z k_{rw}\rho_w}{\mu_w \Delta z}|_{i,j,k}^{n+1}+(1-w_{w_z})\frac{A_z k_z k_{rw}\rho_w}{\mu_w \Delta z}|_{i,j,k+1}^{n+1}\}g(\rho_w{}_{i,j,k+1}^{n+1}D_{i,j,k+1}-\rho_w{}_{i,j,k}^{n+1}D_{i,j,k})$$
$$+\{w^*{}_{w_z}\frac{A_z k_z k_{rw}\rho_w}{\mu_w \Delta z}|_{i,j,k}^{n+1}+(1-w^*{}_{w_z})\frac{A_z k_z k_{rw}\rho_w}{\mu_w \Delta z}|_{i,j,k-1}^{n+1}\}g(\rho_w{}_{i,j,k-1}^{n+1}D_{i,j,k-1}-\rho_w{}_{i,j,k}^{n+1}D_{i,j,k})\Big] \tag{4.24}$$

$$V_{b_{i,j,k}}\Delta_x\Big(\rho_g v_{gx}T\sum_i(c_{p_i}T+L_{v_i})\frac{C_{i_o}}{f_{i_{og}}}\Big)_{i,j,k}^{n+1}=-\frac{A_x k_x k_{rg}\rho_g}{\mu_g \Delta x}\Big|_{i,j,k}^{n+1}(s_{i+1}p_{o_{i+1,j,k}}^{n+1}+s_i p_{o_{i,j,k}}^{n+1}+s_{i-1}p_{o_{i-1,j,k}}^{n+1}$$
$$+s_{i+1}P_{cgo_{i+1,j,k}}^{n+1}+s_i P_{cgo_{i,j,k}}^{n+1}+s_{i-1}P_{cgo_{i-1,j,k}}^{n+1}$$
$$-s_{i+1}gD_{i+1,j,k}\rho_g{}_{i+1,j,k}^{n+1}-s_i gD_{i,j,k}\rho_g{}_{i,j,k}^{n+1}-s_{i-1}gD_{i-1,j,k}\rho_g{}_{i-1,j,k}^{n+1})$$
$$\cdot(s_{i+1}\sum_i(c_{p_i}T+L_{vi})\frac{C_{i_o}}{f_{iog}}|_{i+1,j,k}^{n+1}+s_i\sum_i(c_{p_i}T+L_{vi})\frac{C_{i_o}}{f_{iog}}|_{i,j,k}^{n+1}+s_{i-1}\sum_i(c_{p_i}T+L_{vi})\frac{C_{i_o}}{f_{iog}}|_{i-1,j,k}^{n+1})$$
$$-\sum_i(c_{p_i}T+L_{vi})\frac{C_{i_o}}{f_{iog}}|_{i,j,k}^{n+1}\Big[\{w_{g_x}\frac{A_x k_x k_{rg}\rho_g}{\mu_g \Delta x}|_{i,j,k}^{n+1}+(1-w_{g_x})\frac{A_x k_x k_{rg}\rho_g}{\mu_g \Delta x}|_{i+1,j,k}^{n+1}\}(p_{o_{i+1,j,k}}^{n+1}-p_{o_{i,j,k}}^{n+1})$$

$$
\begin{aligned}
&+\{w_{g_x}\frac{A_xk_xk_{rg}\rho_g}{\mu_g\Delta x}|_{i,j,k}^{n+1}+(1-w_{g_x})\frac{A_xk_xk_{rg}\rho_g}{\mu_g\Delta x}|_{i+1,j,k}^{n+1}\}(P_{cgo_{i+1,j,k}}^{n+1}-P_{cgo_{i,j,k}}^{n+1})\\
&-\{w^*{}_{g_x}\frac{A_xk_xk_{rg}\rho_g}{\mu_g\Delta x}|_{i,j,k}^{n+1}+(1-w^*{}_{g_x})\frac{A_xk_xk_{rg}\rho_g}{\mu_g\Delta x}|_{i-1,j,k}^{n+1}\}(p_{o_{i,j,k}}^{n+1}-p_{o_{i-1,j,k}}^{n+1})\\
&-\{w^*{}_{g_x}\frac{A_xk_xk_{rg}\rho_g}{\mu_g\Delta x}|_{i,j,k}^{n+1}+(1-w^*{}_{g_x})\frac{A_xk_xk_{rg}\rho_g}{\mu_g\Delta x}|_{i-1,j,k}^{n+1}\}(P_{cgo_{i,j,k}}^{n+1}-P_{cgo_{i-1,j,k}}^{n+1}\\
&-\{w_{g_x}\frac{A_xk_xk_{rg}\rho_g}{\mu_g\Delta x}|_{i,j,k}^{n+1}+(1-w_{g_x})\frac{A_xk_xk_{rg}\rho_g}{\mu_g\Delta x}|_{i+1,j,k}^{n+1}\}g(\rho_{g_{i+1,j,k}}^{n+1}D_{i+1,j,k}-\rho_{g_{i,j,k}}^{n+1}D_{i,j,k})\\
&+\{w^*{}_{g_x}\frac{A_xk_xk_{rg}\rho_g}{\mu_g\Delta x}|_{i,j,k}^{n+1}+(1-w^*{}_{g_x})\frac{A_xk_xk_{rg}\rho_g}{\mu_g\Delta x}|_{i-1,j,k}^{n+1}\}g(\rho_{g_{i-1,j,k}}^{n+1}D_{i-1,j,k}-\rho_{g_{i,j,k}}^{n+1}D_{i,j,k})\Big]
\end{aligned}
\tag{4.25}
$$

$$
\begin{aligned}
V_{b_{i,j,k}}\Delta_y\Big(\rho_g v_{gy}T\sum_i(c_{p_i}T+L_{v_i})\frac{C_{i_o}}{f_{io_g}}\Big)_{i,j,k}^{n+1}&=-\frac{A_yk_yk_{rg}\rho_g}{\mu_g\Delta y}\Big|_{i,j,k}^{n+1}(s_{j+1}p_{o_{i,j+1,k}}^{n+1}+s_jp_{o_{i,j,k}}^{n+1}+s_{j-1}p_{o_{i,j-1,k}}^{n+1}\\
&+s_{j+1}P_{cgo_{i,j+1,k}}^{n+1}+s_jP_{cgo_{i,j,k}}^{n+1}+s_{j-1}P_{cgo_{i,j-1,k}}^{n+1}\\
&-s_{j+1}gD_{i,j+1,k}\rho_{g_{i,j+1,k}}^{n+1}-s_jgD_{i,j,k}\rho_{g_{i,j,k}}^{n+1}-s_{j-1}gD_{i,j-1,k}\rho_{g_{i,j-1,k}}^{n+1})\\
(s_{j+1}\sum_i(c_{p_i}T+L_{vi})\frac{C_{i_o}}{f_{iog}}|_{i,j+1,k}^{n+1}+s_j\sum_i(c_{p_i}T+L_{vi})\frac{C_{i_o}}{f_{iog}}|_{i,j,k}^{n+1}+s_{j-1}\sum_i(c_{p_i}T+L_{vi})\frac{C_{i_o}}{f_{iog}}|_{i,j-1,k}^{n+1})\\
-\sum_i(c_{p_i}T+L_{vi})\frac{C_{i_o}}{f_{iog}}|_{i,j,k}^{n+1}\Big[&\{w_{g_y}\frac{A_yk_yk_{rg}\rho_g}{\mu_g\Delta y}|_{i,j,k}^{n+1}+(1-w_{g_y})\frac{A_yk_yk_{rg}\rho_g}{\mu_g\Delta y}|_{i,j+1,k}^{n+1}\}(p_{o_{i,j+1,k}}^{n+1}-p_{o_{i,j,k}}^{n+1})\\
&+\{w_{g_y}\frac{A_yk_yk_{rg}\rho_g}{\mu_g\Delta y}|_{i,j,k}^{n+1}+(1-w_{g_y})\frac{A_yk_yk_{rg}\rho_g}{\mu_g\Delta y}|_{i,j+1,k}^{n+1}\}(P_{cgo_{i,j+1,k}}^{n+1}-P_{cgo_{i,j,k}}^{n+1})\\
&-\{w^*{}_{g_y}\frac{A_yk_yk_{rg}\rho_g}{\mu_g\Delta y}|_{i,j,k}^{n+1}+(1-w^*{}_{g_y})\frac{A_yk_yk_{rg}\rho_g}{\mu_g\Delta y}|_{i,j-1,k}^{n+1}\}(p_{o_{i,j,k}}^{n+1}-p_{o_{i,j-1,k}}^{n+1})\\
&-\{w^*{}_{g_y}\frac{A_yk_yk_{rg}\rho_g}{\mu_g\Delta y}|_{i,j,k}^{n+1}+(1-w^*{}_{g_y})\frac{A_yk_yk_{rg}\rho_g}{\mu_g\Delta y}|_{i,j-1,k}^{n+1}\}(P_{cgo_{i,j,k}}^{n+1}-P_{cgo_{i,j-1,k}}^{n+1}\\
&-\{w_{g_y}\frac{A_yk_yk_{rg}\rho_g}{\mu_g\Delta y}|_{i,j,k}^{n+1}+(1-w_{g_y})\frac{A_yk_yk_{rg}\rho_g}{\mu_g\Delta y}|_{i,j+1,k}^{n+1}\}g(\rho_{g_{i,j+1,k}}^{n+1}D_{i,j+1,k}-\rho_{g_{i,j,k}}^{n+1}D_{i,j,k})\\
&+\{w^*{}_{g_y}\frac{A_yk_yk_{rg}\rho_g}{\mu_g\Delta y}|_{i,j,k}^{n+1}+(1-w^*{}_{g_y})\frac{A_yk_yk_{rg}\rho_g}{\mu_g\Delta y}|_{i,j-1,k}^{n+1}\}g(\rho_{g_{i,j-1,k}}^{n+1}D_{i,j-1,k}-\rho_{g_{i,j,k}}^{n+1}D_{i,j,k})\Big]
\end{aligned}
\tag{4.26}
$$

$$
\begin{aligned}
V_{b_{i,j,k}}\Delta_z\Big(\rho_g v_{gz}T\sum_i(c_{p_i}T+L_{v_i})\frac{C_{i_o}}{f_{io_g}}\Big)_{i,j,k}^{n+1}&=-\frac{A_zk_zk_{rg}\rho_g}{\mu_g\Delta z}\Big|_{i,j,k}^{n+1}(s_{k+1}p_{o_{i,j,k+1}}^{n+1}+s_kp_{o_{i,j,k}}^{n+1}+s_{k-1}p_{o_{i,j,k-1}}^{n+1}\\
&+s_{k+1}P_{cgo_{i,j,k+1}}^{n+1}+s_kP_{cgo_{i,j,k}}^{n+1}+s_{k-1}P_{cgo_{i,j,k-1}}^{n+1}
\end{aligned}
$$

$$-s_{k+1}gD_{i,j,k+1}\rho_{g\,i,j,k+1}^{n+1} - s_k gD_{i,j,k}\rho_{g\,i,j,k}^{n+1} - s_{k-1}gD_{i,j,k-1}\rho_{g\,i,j,k-1}^{n+1})$$

$$(s_{k+1}\sum_i (c_{p_i}T + L_{vi})\frac{C_{i_o}}{f_{iog}}|_{i,j,k+1}^{n+1} + s_k\sum_i (c_{p_i}T + L_{vi})\frac{C_{i_o}}{f_{iog}}|_{i,j,k}^{n+1} + s_{k-1}\sum_i (c_{p_i}T + L_{vi})\frac{C_{i_o}}{f_{iog}}|_{i,j,k-1}^{n+1})$$

$$-\sum_i (c_{p_i}T + L_{vi})\frac{C_{i_o}}{f_{iog}}|_{i,j,k}^{n+1}\Big[\{w_{g_s}\frac{A_z k_z k_{rg}\rho_g}{\mu_g \Delta z}|_{i,j,k}^{n+1} + (1-w_{g_s})\frac{A_z k_z k_{rg}\rho_g}{\mu_g \Delta z}|_{i,j,k+1}^{n+1}\}(p_{o\,i,j,k+1}^{n+1} - p_{o\,i,j,k}^{n+1})$$

$$+\{w_{g_s}\frac{A_z k_z k_{rg}\rho_g}{\mu_g \Delta z}|_{i,j,k}^{n+1} + (1-w_{g_s})\frac{A_z k_z k_{rg}\rho_g}{\mu_g \Delta z}|_{i,j,k+1}^{n+1}\}(P_{cgo\,i,j,k+1}^{n+1} - P_{cgo\,i,j,k}^{n+1})$$

$$-\{w^*_{g_s}\frac{A_z k_z k_{rg}\rho_g}{\mu_g \Delta z}|_{i,j,k}^{n+1} + (1-w^*_{g_s})\frac{A_z k_z k_{rg}\rho_g}{\mu_g \Delta z}|_{i,j,k-1}^{n+1}\}(p_{o\,i,j,k}^{n+1} - p_{o\,i,j,k-1}^{n+1})$$

$$-\{w^*_{g_s}\frac{A_z k_z k_{rg}\rho_g}{\mu_g \Delta z}|_{i,j,k}^{n+1} + (1-w^*_{g_s})\frac{A_z k_z k_{rg}\rho_g}{\mu_g \Delta z}|_{i,j,k-1}^{n+1}\}(P_{cgo\,i,j,k}^{n+1} - P_{cgo\,i,j,k-1}^{n+1})$$

$$-\{w_{g_s}\frac{A_z k_z k_{rg}\rho_g}{\mu_g \Delta z}|_{i,j,k}^{n+1} + (1-w_{g_s})\frac{A_z k_z k_{rg}\rho_g}{\mu_g \Delta z}|_{i,j,k+1}^{n+1}\}g(\rho_{g\,i,j,k+1}^{n+1}D_{i,j,k+1} - \rho_{g\,i,j,k}^{n+1}D_{i,j,k})$$

$$+\{w^*_{g_s}\frac{A_z k_z k_{rg}\rho_g}{\mu_g \Delta z}|_{i,j,k}^{n+1} + (1-w^*_{g_s})\frac{A_z k_z k_{rg}\rho_g}{\mu_g \Delta z}|_{i,j,k-1}^{n+1}\}g(\rho_{g\,i,j,k-1}^{n+1}D_{i,j,k-1} - \rho_{g\,i,j,k}^{n+1}D_{i,j,k})\Big] \tag{4.27}$$

The derivation of the above approximation is given in Appendix A.

Mass Fraction Constraints

The sum of the mass fractions of each component in oleic, aqueous, and vapor phases is separately equal to 1, which can be stated as follows:

$$\sum_{i=1}^{n} C_{i_o} = 1 \tag{4.28}$$

$$\sum_{i=1}^{n} C_{i_w} = 1 \tag{4.29}$$

$$\sum_{i=1}^{n} C_{i_g} = 1 \tag{4.30}$$

Equations (4.29) and (4.30) can be written as follows:

$$\sum_{i=1}^{n} \frac{C_{i_o}}{f_{i_{ow}}} = 1 \tag{4.31}$$

$$\sum_{i=1}^{n} \frac{C_{i_o}}{f_{i_{og}}} = 1 \tag{4.32}$$

For the simulator, it is more convenient to write the above equations in the following form:

$$H_{i,j,k} = \sum_{i=1}^{n} \frac{C_{i_o}}{f_{i_{ow}}} - 1 \tag{4.33}$$

$$I_{i,j,k} = \sum_{i=1}^{n} \frac{C_{i_o}}{f_{i_{og}}} - 1 \tag{4.34}$$

Solution Scheme

At this point, we have nine nonlinear equations, which can be stated as follows:

$$F_{i_{i,j,k}} = 0 \qquad (i = 1,2,...,5) \tag{4.35}$$

$$G_{i,j,k} = 0 \tag{4.36}$$

$$\sum_{i=1}^{5} C_{io} = 1 \tag{4.37}$$

$$H_{i,j,k} = 0 \tag{4.38}$$

$$I_{i,j,k} = 0 \tag{4.39}$$

The unknowns in the above nine equations are $p_o, S_w, S_g, T, C_{1o}, C_{2o}, C_{3o}, C_{4o}$, and C_{5o} for blocks $(i,j,k),(i+1,j,k),(i-1,j,k),(i,j+1,k),(i,j-1,k),(i,j,k+1)$, and $(i,j,k-1)$, i.e. 63 unknowns.

The above nonlinear equations were solved by generalized Newtonian iteration, using a block matrix band algorithm. For this purpose, the above equations take the following form:

$$\sum_{l=1}^{7} \frac{\partial F_p}{\partial p_{o_l}} \delta p_{o_l} + \sum_{l=1}^{7} \frac{\partial F_p}{\partial S_{w_l}} \delta S_{w_l} + \sum_{l=1}^{7} \frac{\partial F_p}{\partial S_{g_l}} \delta S_{g_l} + \sum_{l=1}^{7} \frac{\partial F_p}{\partial T_l} \delta T_l$$
$$+ \sum_{i=1}^{5} \Big(\sum_{l=1}^{7} \frac{\partial F_p}{\partial C_{io_l}} \delta C_{io_l} \Big) = -F_{p_{i,j,k}} \qquad (p = 1,2,...,5) \tag{4.40}$$

where p=1,2,...,5, represents each of the components.

$$\sum_{i=1}^{7} \frac{\partial G_p}{\partial p_{o_l}} \delta p_{o_l} + \sum_{i=1}^{7} \frac{\partial G_p}{\partial S_{w_l}} \delta S_{w_l} + \sum_{i=1}^{7} \frac{\partial G_p}{\partial S_{g_l}} \delta S_{g_l} + \sum_{i=1}^{7} \frac{\partial G_p}{\partial T_l} \delta T_l$$
$$+ \sum_{i=1}^{5} \Big(\sum_{i=1}^{7} \frac{\partial G_p}{\partial C_{io_l}} \delta C_{io_l} \Big) = -G_{i,j,k} \tag{4.41}$$

$$\frac{\partial H}{\partial p_o}\delta p_o + \frac{\partial H}{\partial T}\delta T + \sum_{i=1}^{5}\frac{\partial H}{\partial C_{i_o}}\delta C_{i_o}\Big|_{i,j,k} = -H_{i,j,k} \tag{4.42}$$

$$\frac{\partial I}{\partial p_o}\delta p_o + \frac{\partial I}{\partial T}\delta T + \sum_{i=1}^{5}\frac{\partial I}{\partial C_{i_o}}\delta C_{i_o}\Big|_{i,j,k} = -I_{i,j,k} \tag{4.43}$$

$$\sum_{i=1}^{5}\delta C_{i_o}\Big|_{i,j,k} = 0 \tag{4.44}$$

$$H_{i,j,k} = \sum_{i=1}^{5}\frac{C_{i_o}}{f_{i_{ow}}} - 1 \tag{4.45}$$

$$I_{i,j,k} = \sum_{i=1}^{5}\frac{C_{i_o}}{f_{i_{og}}} - 1 \tag{4.46}$$

Here l stands for blocks $(i,j,k-1),(i,j-1,k),(i-1,j,k),(i,j,k),(i+1,j,k),(i,j+1,k)$, and $(i,j,k+1)$. Equations (4.44) to (4.46) involve only one particular block that can be $(i,j,k),(i-1,j,k)$, etc. Therefore we can solve for C_{3o}, C_{4o}, and C_{5o} in terms of C_{1o} and C_{2o}, which are two of the nine main variables. The expressions for C_{3o}, C_{4o}, and C_{5o} are as follows:

$$\delta C_{3o} = (b_0 - C_1 a_0) + (b_1 - C_1 a_1)\delta C_{1o} + (b_2 - C_1 a_2)\delta C_{2o} + (b_3 - C_1 a_3)\delta p_o + (b_4 - C_1 a_4)\delta T \tag{4.47}$$

$$\delta C_{4o} = -\delta C_{1o} - \delta C_{2o} - \delta C_{3o} - \delta C_{5o} \tag{4.48}$$

$$\begin{aligned}\delta C_{5o} = &\left[\frac{H f_{4ow}}{Den_1\left(1-\frac{f_{4ow}}{f_{3ow}}\right)}\right] - \left[\frac{1-\frac{f_{4ow}}{f_{1ow}}}{Den_1\left(1-\frac{f_{4ow}}{f_{3ow}}\right)}\right]\delta C_{1o} - \left[\frac{1-\frac{f_{4ow}}{f_{2ow}}}{Den_1\left(1-\frac{f_{4ow}}{f_{3ow}}\right)}\right]\delta C_{2o} \\ &- \left[\frac{f_{4ow}\sum_{i=1}^{5}\frac{C_{i_o}}{f_{i_{ow}}^2}\frac{\partial f_{i_{ow}}}{\partial p_o}}{Den_1\left(1-\frac{f_{4ow}}{f_{3ow}}\right)}\right]\delta p_o - \left[\frac{f_{4ow}\sum_{i=1}^{5}\frac{C_{i_o}}{f_{i_{ow}}^2}\frac{\partial f_{i_{ow}}}{\partial T}}{Den_1\left(1-\frac{f_{4ow}}{f_{3ow}}\right)}\right]\delta T\end{aligned} \tag{4.49}$$

where

$$Den_1 = \frac{1-\frac{f_{4ow}}{f_{1ow}}}{\left(1-\frac{f_{4ow}}{f_{3ow}}\right)} - \frac{1-\frac{f_{4og}}{f_{3og}}}{Den_2} \tag{4.50}$$

$$Den_2 = 1 - \frac{f_{4og}}{f_{3og}} \tag{4.51}$$

$$b_0 = If_{4og}/Den_2 \tag{4.52}$$

$$b_1 = (1 - \frac{f_{4og}}{f_{1og}})/Den_2 \tag{4.53}$$

$$b_2 = (1 - \frac{f_{4og}}{f_{2og}})/Den_2 \tag{4.54}$$

$$b_3 = f_{4og} \sum_{i=1}^{5} \frac{C_{i_o}}{f_{iog}^2} \frac{\partial f_{iog}}{\partial p_o}/Den_2 \tag{4.55}$$

$$b_4 = f_{4og} \sum_{i=1}^{5} \frac{C_{i_o}}{f_{iog}^2} \frac{\partial f_{iog}}{\partial T}/Den_2 \tag{4.56}$$

$$c_1 = (1 - \frac{f_{4og}}{f_{5og}})/Den_2 \tag{4.57}$$

$$Den_3 = (1 - \frac{f_{4ow}}{f_{3ow}}) \cdot Den_1 \tag{4.58}$$

$$a_0 = Hf_{4ow}/Den_3 \tag{4.59}$$

$$a_1 = (1 - \frac{f_{4ow}}{f_{1ow}})/Den_3 \tag{4.60}$$

$$a_2 = (1 - \frac{f_{4ow}}{f_{2ow}})/Den_3 \tag{4.61}$$

$$a_3 = f_{4ow} \sum_{i=1}^{5} \frac{C_{i_o}}{f_{iow}^2} \frac{\partial f_{iow}}{\partial p_o}/Den_3 \tag{4.62}$$

$$a_4 = f_{4ow} \sum_{i=1}^{5} \frac{C_{i_o}}{f_{iow}^2} \frac{\partial f_{iow}}{\partial T}/Den_3 \tag{4.63}$$

Substituting the above in Eqs.(4.40) through (4.46), six equations in six unknowns p_o, S_w, S_g, T, C_{1o}, and C_{2o} are obtained. The first five equations are given by

$$\sum_l \Big[\frac{\partial F_i}{\partial p_o} + \{\frac{f_{4og}\sum_{i=1}^5 \frac{C_{io}}{f_{iog}^2}\frac{\partial f_{iog}}{\partial p_o}}{Den_2} + C_1\frac{f_{4ow}\sum_{i=1}^5 \frac{C_{io}}{f_{iow}^2}\frac{\partial f_{iow}}{\partial p_o}}{Den_1\left(1-\frac{f_{4ow}}{f_{3ow}}\right)}\}(\frac{\partial F_i}{\partial C_{3o_l}} - \frac{\partial F_i}{\partial C_{4o_l}}) + \frac{f_{4ow}\sum_{i=1}^5 \frac{C_{io}}{f_{iow}^2}\frac{\partial f_{iow}}{\partial p_o}}{Den_1\left(1-\frac{f_{4ow}}{f_{3ow}}\right)}$$
$$\cdot(\frac{\partial F_i}{\partial C_{4o_l}} - \frac{\partial F_i}{\partial C_{5o_l}})\Big]\delta p_{o_l} + \sum_l \frac{\partial F_i}{\partial S_{w_l}}\delta S_{w_l} + \sum_l \frac{\partial F_i}{\partial S_{g_l}}\delta S_{g_l}$$
$$+\sum_l \Big[\frac{\partial F_i}{\partial T_l} + \{\frac{f_{4og}\sum_{i=1}^5 \frac{C_{io}}{f_{iog}^2}\frac{\partial f_{iog}}{\partial T}}{Den_2} + C_1\frac{f_{4ow}\sum_{i=1}^5 \frac{C_{io}}{f_{iow}^2}\frac{\partial f_{iow}}{\partial T}}{Den_1\left(1-\frac{f_{4ow}}{f_{3ow}}\right)}\}(\frac{\partial F_i}{\partial C_{3o_l}} - \frac{\partial F_i}{\partial C_{4o_l}})$$
$$+\frac{f_{4ow}\sum_{i=1}^5 \frac{C_{io}}{f_{iow}^2}\frac{\partial f_{iow}}{\partial T}}{Den_1\left(1-\frac{f_{4ow}}{f_{3ow}}\right)}(\frac{\partial F_i}{\partial C_{4o_l}} - \frac{\partial F_i}{\partial C_{5o_l}})\Big]\delta T_l + \sum_l \Big[\frac{\partial F_i}{\partial C_{1o_l}} + \{-\frac{1-\frac{f_{1og}}{f_{1ow}}}{Den_2} + C_1\frac{1-\frac{f_{4ow}}{f_{1ow}}}{Den_1\left(1-\frac{f_{4ow}}{f_{3ow}}\right)}\}$$
$$\cdot(\frac{\partial F_i}{\partial C_{3o_l}} - \frac{\partial F_i}{\partial C_{4o_l}}) - \frac{\partial F_i}{\partial C_{4o_l}} + \frac{1-\frac{f_{4ow}}{f_{1ow}}}{Den_1\left(1-\frac{f_{4ow}}{f_{3ow}}\right)}(\frac{\partial F_i}{\partial C_{4o_l}} - \frac{\partial F_i}{\partial C_{5o_l}})\Big]\delta C_{1o_l} + \sum_l \Big[\frac{\partial F_i}{\partial C_{2o_l}} + \{-\frac{1-\frac{f_{1og}}{f_{2og}}}{Den_2}$$
$$+C_1\frac{1-\frac{f_{4ow}}{f_{2ow}}}{Den_1\left(1-\frac{f_{4ow}}{f_{3ow}}\right)}\}(\frac{\partial F_i}{\partial C_{3o_l}} - \frac{\partial F_i}{\partial C_{4o_l}}) - \frac{\partial F_i}{\partial C_{4o_l}} + \frac{1-\frac{f_{4ow}}{f_{2ow}}}{Den_1\left(1-\frac{f_{4ow}}{f_{3ow}}\right)}(\frac{\partial F_i}{\partial C_{4o_l}} - \frac{\partial F_i}{\partial C_{5o_l}})\Big]\delta C_{2o_l}$$
$$= -F_i - \sum_l \Big[\{\frac{If_{4og}}{Den_2} - C_1\frac{Hf_{4ow}}{Den_2\left(1-\frac{f_{4ow}}{f_{3ow}}\right)}\}\cdot(\frac{\partial F_i}{\partial C_{3o_l}} - \frac{\partial F_i}{\partial C_{4o_l}}) - \frac{Hf_{4ow}}{Den_1\left(1-\frac{f_{4ow}}{f_{3ow}}\right)}(\frac{\partial F_i}{\partial C_{4o_l}} - \frac{\partial F_i}{\partial C_{5o_l}})\Big] \quad (4.64)$$

The sixth equation is

$$\sum_l \Big[\frac{\partial G}{\partial p_o} + \{\frac{f_{4og}\sum_{i=1}^5 \frac{C_{io}}{f_{iog}^2}\frac{\partial f_{iog}}{\partial p_o}}{Den_2} + C_1\frac{f_{4ow}\sum_{i=1}^5 \frac{C_{io}}{f_{iow}^2}\frac{\partial f_{iow}}{\partial p_o}}{Den_1\left(1-\frac{f_{4ow}}{f_{3ow}}\right)}\}(\frac{\partial G}{\partial C_{3o_l}} - \frac{\partial G}{\partial C_{4o_l}}) + \frac{f_{4ow}\sum_{i=1}^5 \frac{C_{io}}{f_{iow}^2}\frac{\partial f_{iow}}{\partial p_o}}{Den_1\left(1-\frac{f_{4ow}}{f_{3ow}}\right)}$$
$$\cdot(\frac{\partial G}{\partial C_{4o_l}} - \frac{\partial G}{\partial C_{5o_l}})\Big]\delta p_{o_l} + \sum_l \frac{\partial G}{\partial S_{w_l}}\delta S_{w_l} + \sum_l \frac{\partial G}{\partial S_{g_l}}\delta S_{g_l}$$
$$+\sum_l \Big[\frac{\partial G}{\partial T_l} + \{\frac{f_{4og}\sum_{i=1}^5 \frac{C_{io}}{f_{iog}^2}\frac{\partial f_{iog}}{\partial T}}{Den_2} + C_1\frac{f_{4ow}\sum_{i=1}^5 \frac{C_{io}}{f_{iow}^2}\frac{\partial f_{iow}}{\partial T}}{Den_1\left(1-\frac{f_{4ow}}{f_{3ow}}\right)}\}(\frac{\partial G}{\partial C_{3o_l}} - \frac{\partial G}{\partial C_{4o_l}})$$
$$+\frac{f_{4ow}\sum_{i=1}^5 \frac{C_{io}}{f_{iow}^2}\frac{\partial f_{iow}}{\partial T}}{Den_1\left(1-\frac{f_{4ow}}{f_{3ow}}\right)}(\frac{\partial G}{\partial C_{4o_l}} - \frac{\partial G}{\partial C_{5o_l}})\Big]\delta T_l + \sum_l \Big[\frac{\partial G}{\partial C_{1o_l}} + \{-\frac{1-\frac{f_{1og}}{f_{1ow}}}{Den_2} + C_1\frac{1-\frac{f_{4ow}}{f_{1ow}}}{Den_1\left(1-\frac{f_{4ow}}{f_{3ow}}\right)}\}$$
$$\cdot(\frac{\partial G}{\partial C_{3o_l}} - \frac{\partial G}{\partial C_{4o_l}}) - \frac{\partial G}{\partial C_{4o_l}} + \frac{1-\frac{f_{4ow}}{f_{1ow}}}{Den_1\left(1-\frac{f_{4ow}}{f_{3ow}}\right)}(\frac{\partial G}{\partial C_{4o_l}} - \frac{\partial G}{\partial C_{5o_l}})\Big]\delta C_{1o_l} + \sum_l \Big[\frac{\partial G}{\partial C_{2o_l}} + \{-\frac{1-\frac{f_{1og}}{f_{2og}}}{Den_2}$$
$$+C_1\frac{1-\frac{f_{4ow}}{f_{2ow}}}{Den_1\left(1-\frac{f_{4ow}}{f_{3ow}}\right)}\}(\frac{\partial G}{\partial C_{3o_l}} - \frac{\partial G}{\partial C_{4o_l}}) - \frac{\partial G}{\partial C_{4o_l}} + \frac{1-\frac{f_{4ow}}{f_{2ow}}}{Den_1\left(1-\frac{f_{4ow}}{f_{3ow}}\right)}(\frac{\partial G}{\partial C_{4o_l}} - \frac{\partial G}{\partial C_{5o_l}})\Big]\delta C_{2o_l}$$
$$= -G - \sum_l \Big[\{\frac{If_{4og}}{Den_2} - C_1\frac{Hf_{4ow}}{Den_2\left(1-\frac{f_{4ow}}{f_{3ow}}\right)}\}\cdot(\frac{\partial G}{\partial C_{3o_l}} - \frac{\partial G}{\partial C_{4o_l}}) - \frac{Hf_{4ow}}{Den_1\left(1-\frac{f_{4ow}}{f_{3ow}}\right)}(\frac{\partial G}{\partial C_{4o_l}} - \frac{\partial G}{\partial C_{5o_l}})\Big] \quad (4.65)$$

In the above equations the δ-operator is defined as

$$\delta u_l = u_l^{n+1(m+1)} - u_l^{n+1(m)},$$

where u stands for any of the six variables, n is the time level, and (m) is the iteration level. A convenient notation for the aforesaid six equations is

$$\begin{aligned}
&Z^{p,1}{}_{i,j,k}\delta p_{oi,j,k-1} + B^{p,1}{}_{i,j,k}\delta p_{oi,j-1,k} + D^{p,1}{}_{i,j,k}\delta p_{oi-1,j,k} + E^{p,1}{}_{i,j,k}\delta p_{oi,j,k} \\
&\quad + F^{p,1}{}_{i,j,k}\delta p_{oi+1,j,k} + H^{p,1}{}_{i,j,k}\delta p_{oi,j+1,k} + S^{p,1}{}_{i,j,k}\delta p_{oi,j,k+1} \\
&+ Z^{p,2}{}_{i,j,k}\delta S_{wi,j,k-1} + B^{p,2}{}_{i,j,k}\delta S_{wi,j-1,k} + D^{p,2}{}_{i,j,k}\delta S_{wi-1,j,k} + E^{p,2}{}_{i,j,k}\delta S_{wi,j,k} \\
&\quad + F^{p,2}{}_{i,j,k}\delta S_{wi+1,j,k} + H^{p,2}{}_{i,j,k}\delta S_{wi,j+1,k} + S^{p,2}{}_{i,j,k}\delta S_{wi,j,k+1} \\
&+ Z^{p,3}{}_{i,j,k}\delta S_{gi,j,k-1} + B^{p,3}{}_{i,j,k}\delta S_{gi,j-1,k} + D^{p,3}{}_{i,j,k}\delta S_{gi-1,j,k} + E^{p,3}{}_{i,j,k}\delta S_{gi,j,k} \\
&\quad + F^{p,3}{}_{i,j,k}\delta S_{gi+1,j,k} + H^{p,3}{}_{i,j,k}\delta S_{gi,j+1,k} + S^{p,3}{}_{i,j,k}\delta S_{gi,j,k+1} \\
&+ Z^{p,4}{}_{i,j,k}\delta T_{i,j,k-1} + B^{p,4}{}_{i,j,k}\delta T_{i,j-1,k} + D^{p,4}{}_{i,j,k}\delta T_{i-1,j,k} + E^{p,4}{}_{i,j,k}\delta T_{i,j,k} \\
&\quad + F^{p,4}{}_{i,j,k}\delta T_{i+1,j,k} + H^{p,4}{}_{i,j,k}\delta T_{i,j+1,k} + S^{p,4}{}_{i,j,k}\delta T_{i,j,k+1} \\
&+ Z^{p,5}{}_{i,j,k}\delta C_{1oi,j,k-1} + B^{p,5}{}_{i,j,k}\delta C_{1oi,j-1,k} + D^{p,5}{}_{i,j,k}\delta C_{1oi-1,j,k} + E^{p,5}{}_{i,j,k}\delta C_{1oi,j,k} \\
&\quad + F^{p,5}{}_{i,j,k}\delta C_{1oi+1,j,k} + H^{p,5}{}_{i,j,k}\delta C_{1oi,j+1,k} + S^{p,5}{}_{i,j,k}\delta C_{1oi,j,k+1} \\
&+ Z^{p,6}{}_{i,j,k}\delta C_{2oi,j,k-1} + B^{p,6}{}_{i,j,k}\delta C_{2oi,j-1,k} + D^{p,6}{}_{i,j,k}\delta C_{2oi-1,j,k} + E^{p,6}{}_{i,j,k}\delta C_{2oi,j,k} \\
&\quad + F^{p,6}{}_{i,j,k}\delta C_{2oi+1,j,k} + H^{p,6}{}_{i,j,k}\delta C_{2oi,j+1,k} + S^{p,6}{}_{i,j,k}\delta C_{2oi,j,k+1} = q^{p}{}_{i,j,k},
\end{aligned}$$

where $p = 1, 2, ..., 5$ stands for the five component mass balances, Eq. (4.64), and $p = 6$ corresponds to the energy balance Eq.(4.65). A more stable formulation results if the variables are eliminated at the matrix level. This is same as solving for all nine unknowns, without eliminating three unknowns as done previously.

Derivatives of the Mass Balance Equation

The fully implicit scheme used in this work leads to nonlinear equations. The Newtonian iteration scheme is used to linearize the mass balance and heat balance equations. For this purpose, the derivatives of the mass balance equation $F_{i_{i,j,k}} = 0$, and the heat balance equation $G_{i,j,k} = 0$ need to be obtained. The derivatives of $F_{i_{i,j,k}}$ are taken with respect to p_o, S_w, S_g, T, and C_{i_o}, $(i = 1, 2, ..., 5)$, at points $(i, j, k-1), (i, j-1, k), (i-1, j, k), (i, j, k), (i+1, j, k), (i, j+1, k)$, and $(i, j, k+1)$. All derivatives, except those at (i, j, k) were obtained analytically. The latter derivatives were

computed numerically, because the analytical derivative expressions were very long, and tests showed that the analytical derivative took much longer to calculate than the numerical derivative.

The analytical derivatives of the F_i function are given in the following, only for the block $(i+1, j, k)$. The derivatives at the other five blocks $(i, j, k-1), (i, j-1, k), (i-1, j, k), (i, j+1, k), and (i, j, k+1)$ were obtained by interchanging the subscripts. This has to be done rather carefully because some of the subscripts may remain invariant under such a scheme.

Derivative of F_i with respect to p_o

$$\begin{aligned}
\frac{\partial F_i}{\partial p_o}\Big|_{i+1,j,k} &= \frac{A_x k_x}{\Delta x}\Big|^{n+1}_{i+\frac{1}{2},j,k}\{w_{o_x}\frac{k_{ro}\rho_o C_{i_o}}{\mu_o}i,j,k + (1-w_{b_x})\frac{k_{ro}\rho_o C_{i_o}}{\mu_o}_{i+1,j,k} + w_{\omega_x}\frac{k_{rw}\rho_w C_{i_o}}{\mu_w f_{iow}}\Big|_{i,j,k} \\
&+(1-w_{\omega_x})\frac{k_{rw}\rho_w C_{i_o}}{\mu_w f_{iow}}\Big|_{i+1,j,k} + w_{g_x}\frac{k_{rg}\rho_g C_{i_o}}{\mu_g f_{iog}}\Big|_{i,j,k} + (1-w_{g_x})\frac{k_{rg}\rho_g C_{i_o}}{\mu_g f_{iog}}\Big|_{i+1,j,k}\} \\
&+\frac{A_x k_x}{\Delta x}\Big|^{n+1}_{i+\frac{1}{2},j,k}\{(1-w_{o_x})\Big(\frac{k_{ro}C_{i_o}}{\mu_o}\frac{\partial\rho_o}{\partial p_o}\Big)_{i+1,j,k} + (1-w_{\omega_x})\frac{k_{rw}C_{i_o}}{\mu_w}\Big(\frac{1}{f_{iow}}\frac{\partial\rho_w}{\partial p_o} - \frac{\rho_w}{f^2_{iow}}\frac{\partial f_{iow}}{\partial p_o}\Big)\Big|_{i+1,j,k} \\
&+(1-w_{g_x})\frac{k_{rg}C_{i_o}}{\mu_g}\Big(\frac{1}{f_{iog}}\frac{\partial\rho_g}{\partial p_o} - \frac{\rho_g}{f^2_{iog}}\frac{\partial f_{iog}}{\partial p_o}\Big)\Big|_{i+1,j,k}\}(p_{o_{i+1,j,k}} - p_{o_{i,j,k}}) \\
&+\frac{A_x k_x}{\Delta x}\Big|^{n+1}_{i+\frac{1}{2},j,k}\{2(1-w_{o_x})g\Big(\frac{k_{ro}\rho_o C_{i_o}}{\mu_o}\frac{\partial\rho_o}{\partial p_o}\Big)_{i+1,j,k} + (1-w_{\omega_x})g\frac{k_{rw}C_{i_o}}{\mu_w}\Big(\frac{2\rho_w}{f_{iow}}\frac{\partial\rho_w}{\partial p_o} - \frac{\rho^2_w}{f^2_{iow}}\frac{\partial f_{iow}}{\partial p_o}\Big)\Big|_{i+1,j,k} \\
&+(1-w_{g_x})g\frac{k_{rg}C_{i_o}}{\mu_g}\Big(\frac{2\rho_g}{f_{iog}}\frac{\partial\rho_g}{\partial p_o} - \frac{\rho^2_g}{f^2_{iog}}\frac{\partial f_{iog}}{\partial p_o}\Big)\Big|_{i+1,j,k}(D_{i,j,k} - D_{i+1,j,k}) \\
&+\frac{A_x k_x}{\Delta x}\Big|^{n+1}_{i+\frac{1}{2},j,k}(1-w_{\omega_x})\frac{k_{rw}C_{i_o}}{\mu_w}\Big(\frac{1}{f_{iow}}\frac{\partial\rho_w}{\partial p_o} - \frac{\rho_w}{f^2_{iow}}\frac{\partial f_{iow}}{\partial p_o}\Big)\Big|_{i+1,j,k}(P_{cow_{i,j,k}} - P_{cow_{i+1,j,k}}) \\
&+\frac{A_x k_x}{\Delta x}\Big|^{n+1}_{i+\frac{1}{2},j,k}(1-w_{g_x})\frac{k_{rg}C_{i_o}}{\mu_g}\Big(\frac{1}{f_{iog}}\frac{\partial\rho_g}{\partial p_o} - \frac{\rho_g}{f^2_{iog}}\frac{\partial f_{iog}}{\partial p_o}\Big)\Big|_{i+1,j,k}(P_{cgo_{i,j,k}} - P_{cgo_{i+1,j,k}}) \\
&+\frac{A_x D_{io}}{\Delta x}C_{i_o}\frac{\partial\rho_o}{\partial p_o}\Big|_{i+1,j,k} + \frac{A_x D_{iw}}{\Delta x}C_{i_o}\frac{k_{rw}C_{i_o}}{\mu_w}\Big(\frac{1}{f_{iow}}\frac{\partial\rho_w}{\partial p_o} - \frac{\rho_w}{f^2_{iow}}\frac{\partial f_{iow}}{\partial p_o}\Big)\Big|_{i+1,j,k} \\
&+\frac{A_x D_{ig}}{\Delta x}C_{i_o}\frac{k_{rg}C_{i_o}}{\mu_g}\Big(\frac{1}{f_{iog}}\frac{\partial\rho_g}{\partial p_o} - \frac{\rho_g}{f^2_{iog}}\frac{\partial f_{iog}}{\partial p_o}\Big)\Big|_{i+1,j,k}
\end{aligned} \tag{4.66}$$

Derivative of F_i with respect to S_w

$$\begin{aligned}
\frac{\partial F_{i_{i,j,k}}}{\partial S_{w_{i+1,j,k}}} &= \frac{A_x k_x}{\Delta x}\Big|^{n+1}_{i+\frac{1}{2},j,k}\{(1-w_{o_x})\frac{\rho_o C_{i_o}}{\mu_o}\frac{\partial k_{ro}}{\partial S_w}\Big|_{i+1,j,k}[(p_{o^{n+1}_{i+1,j,k}} - p_{o^{n+1}_{i,j,k}}) \\
&-\rho_{o_{i+1,j,k}}g(D_{i+1,j,k} - D_{i,j,k})] + (1-w_{\omega_x})\Big(\frac{k_{rw}C_{i_o}}{\mu_w}\frac{\partial\rho_w}{\partial p_o}\Big)_{i+1,j,k} \\
&[(p_{o^{n+1}_{i+1,j,k}} - p_{o^{n+1}_{i,j,k}}) - \rho_{w_{i+1,j,k}}g(D_{i+1,j,k} - D_{i,j,k}) - (P_{cow_{i+1,j,k}} - P_{cow_{i,j,k}})]\} \\
&-T_{wx_{i+\frac{1}{2},j,k}}\frac{\partial P_{cow}}{\partial S_w}\Big|_{i+1,j,k}
\end{aligned} \tag{4.67}$$

Derivative of F_i with respect to S_g

$$\frac{\partial F_{i_{i,j,k}}}{\partial S_{g_{i+1,j,k}}} = \frac{A_x k_x}{\Delta x}\Big|^{n+1}_{i+\frac{1}{2},j,k}\{(1-w_{o_x})\frac{\rho_o C_{i_o}}{\mu_o}\frac{\partial k_{ro}}{\partial S_g}\Big|_{i+1,j,k}[(p_{o^{n+1}_{i+1,j,k}} - p_{o^{n+1}_{i,j,k}})$$
$$-\rho_{o_{i+1,j,k}} g(D_{i+1,j,k} - D_{i,j,k})] + (1-w_{g_x})\Big(\frac{k_{rg}C_{i_o}}{\mu_g}\frac{\partial \rho_g}{\partial p_o}\Big)_{i+1,j,k}$$
$$[(p_{o^{n+1}_{i+1,j,k}} - p_{o^{n+1}_{i,j,k}}) - \rho_{g_{i+1,j,k}} g(D_{i+1,j,k} - D_{i,j,k}) - (P_{cgo_{i+1,j,k}} - P_{cgo_{i,j,k}})]\}$$
$$-T_{gx_{i+\frac{1}{2},j,k}}\frac{\partial P_{cgo}}{\partial S_g}\Big|_{i+1,j,k} \qquad (4.68)$$

Derivative of F_i with respect to T

$$\frac{A_x k_x}{\Delta x}\Big|^{n+1}_{i+\frac{1}{2},j,k}\{(1-w_{o_x})[\frac{k_{ro}C_{i_o}}{\mu_o}\frac{\partial \rho_o}{\partial T}\Big|_{i+1,j,k} + \frac{\rho_o C_{i_o}}{\mu_o}\frac{\partial k_{ro}}{\partial T}\Big|_{i+1,j,k} - \frac{k_{ro}\rho_o C_{i_o}}{\mu_o^2}\frac{\partial \mu_o}{\partial T}\Big|_{i+1,j,k}]$$
$$+(1-w_{w_x})[\frac{k_{rw}C_{i_o}}{\mu_w f_{iow}}\frac{\partial \rho_w}{\partial T}\Big|_{i+1,j,k} + \frac{\rho_w C_{i_o}}{\mu_w f_{iow}}\frac{\partial k_{rw}}{\partial T}\Big|_{i+1,j,k} - \frac{k_{rw}\rho_w C_{i_o}}{\mu_w^2 f_{iow}}\frac{\partial \mu_w}{\partial T}\Big|_{i+1,j,k} - \frac{k_{rw}\rho_w C_{i_o}}{\mu_w f_{iow}^2}\frac{\partial f_{iow}}{\partial T}\Big|_{i+1,j,k}]$$
$$+(1-w_{g_x})[\frac{k_{rg}C_{i_o}}{\mu_g f_{iog}}\frac{\partial \rho_g}{\partial T}\Big|_{i+1,j,k} + \frac{\rho_g C_{i_o}}{\mu_g f_{iog}}\frac{\partial k_{rg}}{\partial T}\Big|_{i+1,j,k} - \frac{k_{rg}\rho_g C_{i_o}}{\mu_g^2 f_{iog}}\frac{\partial \mu_g}{\partial T}\Big|_{i+1,j,k} - \frac{k_{rg}\rho_g C_{i_o}}{\mu_g f_{iog}^2}\frac{\partial f_{iog}}{\partial T}\Big|_{i+1,j,k}]\}$$
$$(p_{o_{i+1,j,k}} - p_{o_{i,j,k}}) - \frac{A_x k_x}{\Delta x}\Big|^{n+1}_{i+\frac{1}{2},j,k}\{(1-w_{w_x})[\frac{k_{rw}C_{i_o}}{\mu_w f_{iow}}\frac{\partial \rho_w}{\partial T}\Big|_{i+1,j,k} + \frac{\rho_w C_{i_o}}{\mu_w f_{iow}}\frac{\partial k_{rw}}{\partial T}\Big|_{i+1,j,k} - \frac{k_{rw}\rho_w C_{i_o}}{\mu_w^2 f_{iow}}\frac{\partial \mu_w}{\partial T}\Big|_{i+1,j,k}$$
$$-\frac{k_{rw}\rho_w C_{i_o}}{\mu_w f_{iow}^2}\frac{\partial f_{iow}}{\partial T}\Big|_{i+1,j,k}](P_{cow_{i+1,j,k}} - P_{cow_{i,j,k}}) + (1-w_{g_x})$$
$$[\frac{k_{rg}C_{i_o}}{\mu_g f_{iog}}\frac{\partial \rho_g}{\partial T}\Big|_{i+1,j,k} + \frac{\rho_g C_{i_o}}{\mu_g f_{iog}}\frac{\partial k_{rg}}{\partial T}\Big|_{i+1,j,k} - \frac{k_{rg}\rho_g C_{i_o}}{\mu_g^2 f_{iog}}\frac{\partial \mu_g}{\partial T}\Big|_{i+1,j,k} - \frac{k_{rg}\rho_g C_{i_o}}{\mu_g f_{iog}^2}\frac{\partial f_{iog}}{\partial T}\Big|_{i+1,j,k}](P_{cgo_{i+1,j,k}} - P_{cgo_{i,j,k}})$$
$$+[(1-w_{g_x})\frac{k_{rg}\rho_g C_{i_o}}{\mu_g f_{iog}}\Big|_{i+1,j,k} + w_{g_x}\frac{k_{rg}\rho_g C_{i_o}}{\mu_g f_{iog}}\Big|_{i,j,k}]\frac{\partial P_{cgo}}{\partial T}\Big|_{i+1,j,k}\}$$
$$+\frac{A_x D_{io}}{\Delta x}\Big|^{n+1}_{i+\frac{1}{2},j,k} C_{i_{o_{i+1,j,k}}}\frac{\partial \rho_o}{\partial T}\Big|_{i+1,j,k} + \frac{A_x D_{iw}}{\Delta x}[\frac{C_{i_o}}{f_{iow}}\Big|_{i+1,j,k} - \Big(-\frac{\rho_o C_{i_o}}{f_{ioo}^2}\frac{\partial f_{ioo}}{\partial T}\Big)_{i+1,j,k}]$$
$$+\frac{A_x D_{ig}}{\Delta x}[\frac{C_{i_o}}{f_{iog}}\Big|_{i+1,j,k}\Big(-\frac{\rho_g C_{i_o}}{f_{iog}^2}\frac{\partial f_{iog}}{\partial T}\Big)_{i+1,j,k}] \qquad (4.69)$$

Derivative of F_i with respect to C_{io}

$$\frac{\partial F_{i_{i,j,k}}}{\partial C_{io_{i+1,j,k}}} = \frac{A_x k_x}{\Delta x}\Big|^{n+1}_{i+\frac{1}{2},j,k}\{(1-w_{o_x})k_{ro}|_{i+1,j,k}[\frac{\rho_o}{\mu_o}\Big|_{i+1,j,k} - \frac{\rho_o C_{i_o}}{\mu_o^2}\frac{\partial \mu_o}{\partial C_{i_o}}\Big|_{i+1,j,k} + \frac{C_{i_o}}{\mu_o}\frac{\partial \rho_o}{\partial C_{i_o}}\Big|_{i+1,j,k}]$$
$$+(1-w_{w_x})\frac{k_{rw}}{f_{iow}}[\frac{\rho_w}{\mu_w}\Big|_{i+1,j,k} - \frac{\rho_w C_{i_o}}{\mu_w^2}\frac{\partial \mu_w}{\partial C_{i_o}}\Big|_{i+1,j,k} + \frac{C_{i_o}}{\mu_w}\frac{\partial \rho_w}{\partial C_{i_o}}\Big|_{i+1,j,k}]$$
$$+(1-w_{g_x})\frac{k_{rg}}{f_{iog}}[\frac{\rho_g}{\mu_g}\Big|_{i+1,j,k} - \frac{\rho_g C_{i_o}}{\mu_g^2}\frac{\partial \mu_g}{\partial C_{i_o}}\Big|_{i+1,j,k} + \frac{C_{i_o}}{\mu_g}\frac{\partial \rho_g}{\partial C_{i_o}}\Big|_{i+1,j,k}](p_{o^{n+1}_{i+1,j,k}} - p_{o^{n+1}_{i,j,k}})$$
$$-\frac{A_x k_x}{\Delta x}\Big|^{n+1}_{i+\frac{1}{2},j,k}\{(1-w_{o_x})k_{ro}|_{i+1,j,k} g[\frac{\rho_o^2}{\mu_o}\Big|_{i+1,j,k} - \rho_o^2 C_{i_o}\Big|_{i+1,j,k}\frac{1}{\mu_o^2}\frac{\partial \mu_o}{\partial C_{i_o}}\Big|_{i+1,j,k} + \frac{2\rho_o C_{i_o}}{\mu_o}\frac{\partial \rho_o}{\partial C_{i_o}}\Big|_{i+1,j,k}]$$
$$+(1-w_{w_x})\frac{k_{rw}}{f_{iow}}\Big|_{i+1,j,k} g[\frac{\rho_w^2}{\mu_w}\Big|_{i+1,j,k} - \rho_w^2 C_{i_o}\Big|_{i+1,j,k}\frac{1}{\mu_w^2}\frac{\partial \mu_w}{\partial C_{i_o}}\Big|_{i+1,j,k} + \frac{2\rho_w C_{i_o}}{\mu_w}\frac{\partial \rho_w}{\partial C_{i_o}}\Big|_{i+1,j,k}]$$

$$+(1-w_{g_x})\frac{k_{rg}}{f_{iog}}\Big|_{i+1,j,k} g[\frac{\rho_g^2}{\mu_g}\Big|_{i+1,j,k} - \rho_g^2 C_{i_o}\Big|_{i+1,j,k}\frac{1}{\mu_g^2}\frac{\partial\mu_g}{\partial C_{i_o}}\Big|_{i+1,j,k} + \frac{2\rho_g C_{i_o}}{\mu_g}\frac{\partial\rho_g}{\partial C_{i_o}}\Big|_{i+1,j,k}]](D_{i+1,j,k} - D_{i,j,k})$$

$$-\{(1-w_{w_x})\frac{k_{rw}}{f_{iow}}[\frac{\rho_w}{\mu_w}\Big|_{i+1,j,k} - \frac{\rho_w C_{i_o}}{\mu_w^2}\frac{\partial\mu_w}{\partial C_{i_o}}\Big|_{i+1,j,k} + \frac{C_{i_o}}{\mu_w}\frac{\partial\rho_w}{\partial C_{i_o}}\Big|_{i+1,j,k}](P_{cow_{i+1,j,k}} - P_{cow_{i,j,k}})$$

$$+(1-w_{g_x})\frac{k_{rg}}{f_{iog}}[\frac{\rho_g}{\mu_g}\Big|_{i+1,j,k} - \frac{\rho_g C_{i_o}}{\mu_g^2}\frac{\partial\mu_g}{\partial C_{i_o}}\Big|_{i+1,j,k} + \frac{C_{i_o}}{\mu_g}\frac{\partial\rho_g}{\partial C_{i_o}}\Big|_{i+1,j,k}](P_{cgo_{i+1,j,k}} - P_{cgo_{i,j,k}})$$

$$+\frac{A_x D_{io}}{\Delta x}[\rho_{o_{i+1,j,k}} + C_{i_o}\frac{\partial\rho_o}{\partial C_{i_o}}\Big|_{i+1,j,k}$$

$$+\frac{A_x D_{iw}}{\Delta x}\frac{1}{f_{iow}}\Big|_{i+1,j,k}[\frac{\rho_w}{\mu_w}\Big|_{i+1,j,k} - \frac{\rho_w C_{i_o}}{\mu_w^2}\frac{\partial\mu_w}{\partial C_{i_o}}\Big|_{i+1,j,k} + \frac{C_{i_o}}{\mu_w}\frac{\partial\rho_w}{\partial C_{i_o}}\Big|_{i+1,j,k}]$$

$$+\frac{A_x D_{ig}}{\Delta x}\frac{1}{f_{iog}}\Big|_{i+1,j,k}[\frac{\rho_g}{\mu_g}\Big|_{i+1,j,k} - \frac{\rho_g C_{i_o}}{\mu_g^2}\frac{\partial\mu_g}{\partial C_{i_o}}\Big|_{i+1,j,k} + \frac{C_{i_o}}{\mu_g}\frac{\partial\rho_g}{\partial C_{i_o}}\Big|_{i+1,j,k}] \qquad (4.70)$$

Derivatives of the Energy Balance Equation

Derivatives of the energy balance equation $G_{i,j,k} = 0$ were obtained in a manner similar to the mass balance equations. These are given below:

Derivative of G with respect to p_o

$$\frac{\partial G_{i,j,k}}{\partial p_{oi+1,j,k}} = \frac{A_x k_x k_{ro}\rho_w}{\mu_o \Delta x}\Big|_{i,j,k}(s_{i+1} - s_{i+1} g D_{i+1,j,k}\frac{\partial\rho_o}{\partial p_o}\Big|_{i+1,j,k})$$

$$\cdot(s_{i+1}T_{i+1,j,k}\sum_i (c_{p_i}C_{i_o})|_{i+1,j,k} + s_i T_{kji}\sum_i (c_{p_i}C_{i_o})|_{kji} + s_{i-1}T_{i-1,j,k}\sum_i (c_{p_i}C_{i_o})|_{i-1,j,k})$$

$$+T_{i,j,k}\sum_i (c_{p_i}C_{i_o})|_{i,j,k}\{(w_{o_x}\frac{A_x k_x k_{ro}\rho_w}{\mu_o\Delta x}\Big|_{i,j,k} + (1-w_{o_x})\frac{A_x k_x k_{ro}\rho_w}{\mu_o\Delta x}\Big|_{i+1,j,k})$$

$$+(1-w_{o_x})\frac{A_x k_x k_{ro}\rho_w}{\mu_o\Delta x}\Big|_{i+1,j,k}\frac{\partial\rho_o}{\partial p_o}\Big|_{i+1,j,k}(p_{o^{n+1}_{i+1,j,k}} - p_{o^{n+1}_{i,j,k}})$$

$$-(w_{o_x}\frac{A_x k_x k_{ro}\rho_w}{\mu_o\Delta x}\Big|_{i,j,k} + (1-w_{o_x})\frac{A_x k_x k_{ro}\rho_w}{\mu_o\Delta x}\Big|_{i+1,j,k})\frac{\partial\rho_o}{\partial p_o}\Big|_{i+1,j,k} g D_{i+1,j,k}$$

$$-(1-w_{o_x})\frac{A_x k_x k_{ro}\rho_w}{\mu_o\Delta x}\Big|_{i+1,j,k}\frac{\partial\rho_o}{\partial p_o}\Big|_{i+1,j,k} g(\rho_{oi+1,j,k}D_{i+1,j,k} - \rho^{n+1}_{oi,j,k}D_{i,j,k})\}$$

$$+\frac{A_x k_x k_{rw}\rho_w}{\mu_w\Delta x}\Big|_{i,j,k}(s_{i+1} - s_{i+1}gD_{i+1,j,k}\frac{\partial\rho_w}{\partial p_o}\Big|_{i+1,j,k})$$

$$\cdot(s_{i+1}T^{n+1}_{i+1,j,k}\sum_i (c_{p_i}\frac{C_{i_o}}{f_{iow}})|^{n+1}_{i+1,j,k} + s_i T^{n+1}_{i,j,k}\sum_i (c_{p_i}\frac{C_{i_o}}{f_{iow}})|^{n+1}_{i,j,k} + s_{i-1}T^{n+1}_{i-1,j,k}\sum_i (c_{p_i}\frac{C_{i_o}}{f_{iow}})|^{n+1}_{i-1,j,k})$$

$$+\frac{A_x k_x k_{rw}\rho_w}{\mu_w\Delta x}\Big|_{i,j,k}(s_{i+1}p^{n+1}_{oi+1,j,k} + s_i p^{n+1}_{oi,j,k} + s_{i-1}p^{n+1}_{oi-1,j,k}$$

$$-s_{i+1}P^{n+1}_{cowi+1,j,k} - s_i P^{n+1}_{cowi,j,k} + s_{i-1}P^{n+1}_{cowi-1,j,k}$$

$$-s_{i+1}gD_{i+1,j,k}\rho^{n+1}_{wi+1,j,k} - s_i gD_{i,j,k}\rho^{n+1}_{wi,j,k} - s_{i-1}gD_{i-1,j,k}\rho^{n+1}_{wi-1,j,k})$$

$$\cdot(s_{i+1}T_{i+1,j,k}\sum_i (c_{g_i}(-\frac{C_{i_o}}{f^2_{iow}}\frac{\partial f_{iow}}{\partial p_o})_{i+1,j,k})$$

$$T_{i,j,k}\sum_i(c_{p_i}\frac{C_{i_o}}{f_{iow}})|_{i,j,k}\{(w_{o_x}\frac{A_x k_x k_{rw}\rho_w}{\mu_w\Delta x}\Big|_{i,j,k}+(1-w_{w_x})\frac{A_x k_x k_{rw}\rho_w}{\mu_w\Delta x}\Big|_{i+1,j,k}$$

$$+(1-w_{w_x})\frac{A_x k_x k_{rw}\rho_w}{\mu_w\Delta x}\Big|_{i+1,j,k}\frac{\partial\rho_w}{\partial p_o}\Big|_{i+1,j,k}(p_{o^{n+1}_{i+1,j,k}}-p_{o^{n+1}_{i,j,k}})$$

$$-(1-w_{w_x})\frac{A_x k_x k_{rw}\rho_w}{\mu_w\Delta x}\Big|_{i+1,j,k}\frac{\partial\rho_w}{\partial p_o}\Big|_{i+1,j,k}(P_{cow^{n+1}_{i+1,j,k}}-P_{cow^{n+1}_{i,j,k}})$$

$$-(w_{o_x}\frac{A_x k_x k_{rw}\rho_w}{\mu_w\Delta x}\Big|_{i,j,k}+(1-w_{w_x})\frac{A_x k_x k_{rw}\rho_w}{\mu_w\Delta x}\Big|_{i+1,j,k}\frac{\partial\rho_w}{\partial p_o}\Big|_{i+1,j,k}gD_{i+1,j,k}$$

$$-(1-w_{w_x})\frac{A_x k_x k_{rw}\rho_w}{\mu_w\Delta x}\Big|_{i+1,j,k})\frac{\partial\rho_w}{\partial p_o}\Big|_{i+1,j,k}g(\rho_{wi+1,j,k}D_{i+1,j,k}-\rho_{w^{n+1}_{i,j,k}}D_{i,j,k})\}$$

$$+\frac{A_x k_x k_{rg}\rho_w}{\mu_g\Delta x}\Big|_{i,j,k}(s_{i+1}-s_{i+1}gD_{i+1,j,k}\frac{\partial\rho_g}{\partial p_o}\Big|_{i+1,j,k})$$

$$\cdot(s_{i+1}\sum_i(c_{p_i}T+L_{vi})\frac{C_{i_o}}{f_{iog}}|^{n+1}_{i+1,j,k}+s_i\sum_i(c_{p_i}T+L_{vi})\frac{C_{i_o}}{f_{iog}}|^{n+1}_{i,j,k}+s_{i-1}\sum_i(c_{p_i}T+L_{vi})\frac{C_{i_o}}{f_{iog}}|^{n+1}_{i-1,j,k})$$

$$+\frac{A_x k_x k_{rg}\rho_w}{\mu_g\Delta x}\Big|_{i,j,k}(s_{i+1}p_{o^{n+1}_{i+1,j,k}}+s_i p_{o^{n+1}_{i,j,k}}+s_{i-1}p_{o^{n+1}_{i-1,j,k}}$$

$$+s_{i+1}P_{cgo^{n+1}_{i+1,j,k}}+s_i P_{cgo^{n+1}_{i,j,k}}+s_{i-1}P_{cgo^{n+1}_{i-1,j,k}}$$

$$-s_{i+1}gD_{i+1,j,k}\rho_{g^{n+1}_{i+1,j,k}}-s_i gD_{i,j,k}\rho_{g^{n+1}_{i,j,k}}-s_{i-1}gD_{i-1,j,k}\rho_{g^{n+1}_{i-1,j,k}})$$

$$\cdot(s_{i+1}\sum_i((T_{i+1,j,k}c_{p_i}+L_{vi})\Big(-\frac{C_{i_o}}{f^2_{iog}}\frac{\partial f_{iog}}{\partial p_o}\Big)_{i+1,j,k})$$

$$\sum_i(c_{p_i}T+L_{vi})\frac{C_{i_o}}{f_{iog}}|_{i,j,k}\{(w_{g_x}\frac{A_x k_x k_{rg}\rho_w}{\mu_g\Delta x}\Big|_{i,j,k}+(1-w_{g_x})\frac{A_x k_x k_{rg}\rho_w}{\mu_g\Delta x}\Big|_{i+1,j,k})$$

$$+(1-w_{g_x})\frac{A_x k_x k_{rg}\rho_w}{\mu_g\Delta x}\Big|_{i+1,j,k}\frac{\partial\rho_g}{\partial p_o}\Big|_{i+1,j,k}(p_{o^{n+1}_{i+1,j,k}}-p_{o^{n+1}_{i,j,k}})$$

$$+(1-w_{g_x})\frac{A_x k_x k_{rg}\rho_w}{\mu_g\Delta x}\Big|_{i+1,j,k}\frac{\partial\rho_g}{\partial p_o}\Big|_{i+1,j,k}(P_{cgo^{n+1}_{i+1,j,k}}-P_{cgo^{n+1}_{i,j,k}})$$

$$-(w_{g_x}\frac{A_x k_x k_{rg}\rho_w}{\mu_g\Delta x}\Big|_{i,j,k}+(1-w_{g_x})\frac{A_x k_x k_{rg}\rho_w}{\mu_g\Delta x}\Big|_{i+1,j,k})\frac{\partial\rho_g}{\partial p_o}\Big|_{i+1,j,k}gD_{i+1,j,k}$$

$$-(1-w_{g_x})\frac{A_x k_x k_{rg}\rho_w}{\mu_g\Delta x}\Big|_{i+1,j,k})\frac{\partial\rho_g}{\partial p_o}\Big|_{i+1,j,k}g(\rho_{gi+1,j,k}D_{i+1,j,k}-\rho_{g^{n+1}_{i,j,k}}D_{i,j,k})\}$$

$$+\frac{A_x}{\Delta x_{i+\frac{1}{2},j,k}}\{(1-w_{o_x})\frac{\partial\rho_o}{\partial p_o}\Big|_{i+1,j,k}\sum_i[Tc_{pi}D_{io}\Big|^{n+1}_{i+1,j,k}(C_{io^{n+1}_{i+1,j,k}}-C_{io^{n+1}_{i,j,k}})]$$

$$(1-w_{w_x})\frac{\partial\rho_w}{\partial p_o}\Big|_{i+1,j,k}\sum_i[Tc_{pi}D_{iw}\Big|^{n+1}_{i+1,j,k}(\frac{C_{i_o}{}^{n+1}}{f_{iow\,i+1,j,k}}-\frac{C_{i_o}{}^{n+1}}{f_{iow\,i,j,k}})]$$

$$(1-w_{g_x})\frac{\partial\rho_g}{\partial p_o}\Big|_{i+1,j,k}\sum_i[(Tc_{pi}+L_{vi})D_{ig}\Big|^{n+1}_{i+1,j,k}(\frac{C_{i_o}{}^{n+1}}{f_{iog\,i+1,j,k}}-\frac{C_{i_o}{}^{n+1}}{f_{iog\,i,j,k}})]$$

$$\sum_i[w_{w_x}T\rho_w c_{p_i}D_{iw}\Big|^{n+1}_{i,j,k}+(1-w_{w_x})T\rho_w c_{p_i}D_{iw}\Big|^{n+1}_{i+1,j,k}\Big(-\frac{C_{i_o}}{f^2_{iow}}\frac{\partial f_{iow}}{\partial p_o}\Big)_{i+1,j,k}\cdot$$

$$\sum_i[w_{g_x}\rho_g(Tc_{p_i}+L_{vi})D_{ig}\Big|^{n+1}_{i,j,k}+(1-w_{g_x})T\rho_g(Tc_{p_i}+L_{vi})D_{ig}\Big|^{n+1}_{i+1,j,k}\Big(-\frac{C_{i_o}}{f^2_{iog}}\frac{\partial f_{iog}}{\partial p_o}\Big)_{i+1,j,k}\}. \quad (4.7)$$

Derivative of G with respect to S_w

$$\frac{\partial G_{i,j,k}}{\partial S_{w\,i+1,j,k}} = \frac{A_x k_x k_{rw} \rho_w}{\mu_w \Delta x}\Big|_{i,j,k} s_{i+1}\left(-\frac{\partial P_{cow}}{\partial S_w}\Big|_{i+1,j,k}\right)$$

$$\cdot\left(s_{i+1} T^{n+1}_{i+1,j,k} \sum_i (c_{p_i} \frac{C_{i_o}}{f_{iow}})\Big|^{n+1}_{i+1,j,k} + s_i T^{n+1}_{i,j,k} \sum_i (c_{p_i} \frac{C_{i_o}}{f_{iow}})\Big|^{n+1}_{i,j,k} + s_{i-1} T^{n+1}_{i-1,j,k} \sum_i (c_{p_i} \frac{C_{i_o}}{f_{iow}})\Big|^{n+1}_{i-1,j,k}\right)$$

$$+T_{i,j,k} \sum_i (c_{p_i} C_{i_o})\Big|_{i,j,k} [(1-w_{o_x}) \frac{A_x k_x \rho_o}{\mu_o \Delta x} \frac{\partial k_{ro}}{\partial S_w}\Big|_{i+1,j,k} (p^{n+1}_{o\,i+1,j,k} - p^{n+1}_{o\,i,j,k} - \rho^{n+1}_{o\,i+1,j,k} g D_{i+1,j,k} + \rho^{n+1}_{o\,i,j,k} g D_{i,j,k})]$$

$$+T_{i,j,k} \sum_i (c_{p_i} \frac{C_{i_o}}{f_{iow}})\Big|_{i,j,k} [(1-w_{w_x}) \frac{A_x k_x \rho_w}{\mu_w \Delta x} \frac{\partial k_{rw}}{\partial S_w}\Big|_{i+1,j,k}$$

$$\cdot(p^{n+1}_{o\,i+1,j,k} - p^{n+1}_{o\,i,j,k} - \rho_{w\,i+1,j,k} g D_{i+1,j,k} + \rho_{w\,i,j,k} D_{i,j,k} - P_{cow\,i+1,j,k} + P_{cow\,i,j,k})$$

$$-\{w_{w_x} \frac{A_x k_x k_{rw} \rho_w}{\mu_w \Delta x}\Big|^{n+1}_{i,j,k} + (1-w_{w_x}) \frac{A_x k_x k_{rw} \rho_w}{\mu_w \Delta x}\Big|^{n+1}_{i+1,j,k}\} \frac{\partial P_{cow}}{\partial S_w}\Big|_{i+1,j,k}] \qquad (4.72)$$

Derivative of G with respect to S_g

$$\frac{\partial G_{i,j,k}}{\partial S_{g\,i+1,j,k}} = T_{i,j,k} \sum_i (c_{p_i} C_{i_o})\Big|_{i,j,k} [(1-w_{o_x}) \frac{A_x k_x \rho_o}{\mu_o \Delta x} \frac{\partial k_{ro}}{\partial S_g}\Big|_{i+1,j,k}$$

$$\cdot(p^{n+1}_{o\,i+1,j,k} - p^{n+1}_{o\,i,j,k} - \rho^{n+1}_{o\,i+1,j,k} g D_{i+1,j,k} + \rho^{n+1}_{o\,i,j,k} g D_{i,j,k})] + s_{i+1} \frac{A_x k_x k_{rg} \rho_w}{\mu_g \Delta x}\Big|_{i,j,k} \frac{\partial P_{cgo}}{\partial S_g}\Big|_{i+1,j,k}$$

$$\cdot\left(s_{i+1} \sum_i (c_{p_i} T + L_{vi}) \frac{C_{i_o}}{f_{iog}}\Big|^{n+1}_{i+1,j,k} + s_i \sum_i (c_{p_i} T + L_{vi}) \frac{C_{i_o}}{f_{iog}}\Big|^{n+1}_{i,j,k} + s_{i-1} \sum_i (c_{p_i} T + L_{vi}) \frac{C_{i_o}}{f_{iog}}\Big|^{n+1}_{i-1,j,k}\right)$$

$$+\sum_i (c_{p_i} T + L_{vi}) \frac{C_{i_o}}{f_{iog}}\Big|_{i,j,k} [(1-w_{g_x}) \frac{A_x k_x \rho_g}{\mu_g \Delta x} \frac{\partial k_{rg}}{\partial S_g}\Big|_{i+1,j,k}$$

$$\cdot(p^{n+1}_{o\,i+1,j,k} - p^{n+1}_{o\,i,j,k} - \rho_{g\,i+1,j,k} g D_{i+1,j,k} + \rho_{g\,i+1,j,k} D_{i,j,k} - P_{cgo\,i+1,j,k} - P_{cgo\,i,j,k})$$

$$+\{w_{g_x} \frac{A_x k_x k_{rg} \rho_g}{\mu_g \Delta x}\Big|^{n+1}_{i,j,k} + (1-w_{g_x}) \frac{A_x k_x k_{rg} \rho_g}{\mu_g \Delta x}\Big|^{n+1}_{i+1,j,k}\} \frac{\partial P_{cgo}}{\partial S_g}\Big|_{i+1,j,k}] \qquad (4.73)$$

Derivative of G with respect to T

$$\frac{\partial G_{i,j,k}}{\partial T_{i+1,j,k}} = \frac{A_x k_x}{\Delta x}\Big|^{n+1}_{i+\frac{1}{2},j,k} + \frac{A_x k_x k_{ro} \rho_w}{\mu_o \Delta x}\Big|_{i,j,k} [(-s_{i+1} g D_{i+1} \frac{\partial \rho_o}{\partial T})$$

$$\cdot(s_{i+1} T^{n+1}_{i+1,j,k} \sum_i (c_{p_i} C_{i_o})\Big|^{n+1}_{i+1,j,k} + s_i T^{n+1}_{i,j,k} \sum_i (c_{p_i} C_{i_o})\Big|^{n+1}_{i,j,k} + s_{i-1} T^{n+1}_{i-1,j,k} \sum_i (c_{p_i} C_{i_o})\Big|^{n+1}_{i-1,j,k})$$

$$+(s_{i+1} p^{n+1}_{o\,i+1,j,k} + s_i p^{n+1}_{o\,i,j,k} + s_{i-1} p^{n+1}_{o\,i-1,j,k}$$

$$-s_{i+1} g D_{i+1,j,k} \rho^{n+1}_{o\,i+1,j,k} - s_i g D_{i,j,k} \rho^{n+1}_{o\,i,j,k} - s_{i-1} g D_{i-1,j,k} \rho^{n+1}_{o\,i-1,j,k})$$

$$\cdot(s_{i+1} \sum_i c_{pi} C_{io}|_{i+1,j,k})] + T_{i,j,k} \sum_i (c_{p_i} C_{i_o})\Big|_{i,j,k} [(1-w_{o_x}) \{\frac{A_x k_x}{\Delta x} \frac{\partial}{\partial T} (\frac{k_{ro} \rho_o}{\mu_o})\Big|_{i+1,j,k}$$

$$\cdot(p^{n+1}_{o\,i+1,j,k} - p^{n+1}_{o\,i,j,k} - \rho^{n+1}_{o\,i+1,j,k} g D_{i+1,j,k} + \rho^{n+1}_{o\,i,j,k} g D_{i,j,k}) - \frac{A_x k_x k_{ro} \rho_w}{\mu_o \Delta x}\Big|_{i,j,k} g D_{i+1,j,k} \frac{\partial \rho_o}{\partial T}\Big|_{i+1,j,k}]]$$

$$+\frac{A_x k_x k_{rw}\rho_w}{\mu_w \Delta x}\Big|_{i,j,k}[(s_{i+1}\frac{\partial R_{cow}}{\partial T}\Big|_{i+1,j,k} - s_{i+1} g D_{i+1,j,k}\frac{\partial \rho_w}{\partial T}\Big|_{i+1,j,k})$$

$$(s_{i+1}T^{n+1}_{i+1,j,k}\sum_i (c_{p_i}\frac{C_{i_o}}{f_{iow}})|^{n+1}_{i+1,j,k} + s_i T^{n+1}_{i,j,k}\sum_i (c_{p_i}\frac{C_{i_o}}{f_{iow}})|^{n+1}_{i,j,k} + s_{i-1}T^{n+1}_{i-1,j,k}\sum_i (c_{p_i}\frac{C_{i_o}}{f_{iow}})|^{n+1}_{i-1,j,k})$$

$$+(s_{i+1}p_{o^{n+1}_{i+1,j,k}} + s_i p_{o^{n+1}_{i,j,k}} + s_{i-1}p_{o^{n+1}_{i-1,j,k}}$$

$$-s_{i+1}P_{cow^{n+1}_{i+1,j,k}} - s_i P_{cow^{n+1}_{i,j,k}} + s_{i-1}P_{cow^{n+1}_{i-1,j,k}}$$

$$-s_{i+1}gD_{i+1,j,k}\rho_{w^{n+1}_{i+1,j,k}} - s_i g D_{i,j,k}\rho_{w^{n+1}_{i,j,k}} - s_{i-1}gD_{i-1,j,k}\rho_{w^{n+1}_{i-1,j,k}})(s_{i+1}\sum_i \frac{c_{pi}C_{io}}{f_{iow}})]$$

$$+T_{i,j,k}\sum_i (c_{p_i}\frac{C_{i_o}}{f_{iow}})|_{i,j,k}[(1-w_{w_x})\{\frac{A_x k_x}{\Delta x}\frac{\partial}{\partial T}(\frac{k_{rw}\rho_w}{\mu_w})\Big|_{i+1,j,k}$$

$$(p_{o^{n+1}_{i+1,j,k}} - p_{o^{n+1}_{i,j,k}} - \rho_{w_{i+1,j,k}}gD_{i+1,j,k} + \rho_{w_{i,j,k}}D_{i,j,k} - P_{cow_{i+1,j,k}} + P_{cow_{i,j,k}})$$

$$-\frac{A_x k_x k_{rw}\rho_w}{\mu_w \Delta x}\Big|_{i,j,k}(gD_{i+1,j,k}drtw + dpwt)\}]$$

$$+\frac{A_x k_x k_{rg}\rho_w}{\mu_g \Delta x}\Big|_{i,j,k}[(s_{i+1}\frac{\partial P_{cgo}}{\partial T}\Big|_{i+1,j,k} - s_{i+1}gD_{i+1,j,k}\frac{\partial \rho_g}{\partial T}\Big|_{i+1,j,k})$$

$$(s_{i+1}\sum_i (c_{p_i}T + L_{vi})\frac{C_{i_o}}{f_{iog}}|^{n+1}_{i+1,j,k} + s_i\sum_i (c_{p_i}T + L_{vi})\frac{C_{i_o}}{f_{iog}}|^{n+1}_{i,j,k} + s_{i-1}\sum_i (c_{p_i}T + L_{vi})\frac{C_{i_o}}{f_{iog}}|^{n+1}_{i-1,j,k})$$

$$+(s_{i+1}p_{o^{n+1}_{i+1,j,k}} + s_i p_{o^{n+1}_{i,j,k}} + s_{i-1}p_{o^{n+1}_{i-1,j,k}}$$

$$+s_{i+1}P_{cgo^{n+1}_{i+1,j,k}} + s_i P_{cgo^{n+1}_{i,j,k}} + s_{i-1}P_{cgo^{n+1}_{i-1,j,k}}$$

$$-s_{i+1}gD_{i+1,j,k}\rho_{g^{n+1}_{i+1,j,k}} - s_i g D_{i,j,k}\rho_{g^{n+1}_{i,j,k}} - s_{i-1}gD_{i-1,j,k}\rho_{g^{n+1}_{i-1,j,k}})(s_{i+1}\sum_i (c_{pi} + \frac{\partial L_{v_i}}{\partial T})\frac{C_{io}}{f_{iog\,i+1,j,k}})$$

$$+\sum_i (c_{p_i}T + L_{vi})\frac{C_{i_o}}{f_{iog}}|kji[(1-w_{g_x})\{\frac{A_x k_x}{\Delta x}\frac{\partial}{\partial T}(\frac{k_{rg}\rho_g}{\mu_g})\Big|_{i+1,j,k}$$

$$(p_{o^{n+1}_{i+1,j,k}} - p_{o^{n+1}_{i,j,k}} - \rho_{g_{i+1,j,k}}gD_{i+1,j,k} + \rho_{g_{i+1,j,k}}D_{i,j,k} - P_{cgo_{i+1,j,k}} - P_{cgo_{i,j,k}})$$

$$\cdot(gD_{i+1,j,k}drtg - dpt)\}]$$

$$+\sum_i \frac{A_x}{\Delta x}\Big|^{n+1}_{i+\frac{1}{2},j,k}[(1-w_{o_x})D_{io}\{\rho_o c_{pi} + \rho_o T\frac{\partial c_{p_i}}{\partial T} + c_{pi}T\frac{\partial \rho_o}{\partial T}\Big|_{i+1,j,k}\}]\Big|_{i+1,j,k}(C_{ioi+1,j,k} - C_{ioi,j,k})$$

$$+\sum_i \frac{A_x}{\Delta x}\Big|^{n+1}_{i+\frac{1}{2},j,k}[(1-w_{w_x})D_{iw}\{\rho_w c_{pi} + \rho_w T\frac{\partial c_{p_i}}{\partial T} + c_{pi}T\frac{\partial \rho_w}{\partial T}\Big|_{i+1,j,k}\}]\Big|_{i+1,j,k}(\frac{C_{i_o}}{f_{iow\,i+1,j,k}} - \frac{C_{i_o}}{f_{iow\,i,j,k}})$$

$$+\sum_i \frac{A_x D_{iw}\rho_w c_{pi}T}{\Delta x}\Big|^{n+1}_{i+\frac{1}{2},j,k}\cdot(-\frac{C_{i_o}}{f^2_{iow}}\frac{\partial f_{iow}}{\partial T})_{i+1,j,k}$$

$$+\sum_i \frac{A_x}{\Delta x}\Big|^{n+1}_{i+\frac{1}{2},j,k}[(1-w_{g_x})D_{ig}\{\rho_g c_{pi} + \rho_g T\frac{\partial c_{p_i}}{\partial T} + c_{pi}T\frac{\partial \rho_g}{\partial T}\Big|_{i+1,j,k} + \rho_g\frac{\partial L_{v_i}}{\partial T} + L_{vi}\frac{\partial \rho_g}{\partial T}\Big|_{i+1,j,k}\}]\Big|_{i+1,j,k}$$

$$(\frac{C_{i_o}}{f_{iog\,i+1,j,k}} - \frac{C_{i_o}}{f_{iog\,i,j,k}}) + \sum_i \frac{A_x D_{ig}\rho_g(c_{pi}T + L_{vi})}{\Delta x}\Big|^{n+1}_{i+\frac{1}{2},j,k}\cdot(-\frac{C_{i_o}}{f^2_{iog}}\frac{\partial f_{iog}}{\partial T})_{i+1,j,k} \qquad (4.74)$$

Derivative of G with respect to C_{io}

$$\frac{\partial G_{i,j,k}}{\partial C_{ioi+1,j,k}} = \frac{A_x k_x k_{ro}\rho_w}{\mu_o \Delta x}\Big|_{i,j,k}[(s_{i+1}p_{o^{n+1}_{i+1,j,k}} + s_i p_{o^{n+1}_{i,j,k}} + s_{i-1}p_{o^{n+1}_{i-1,j,k}}$$

$$-s_{i+1}gD_{i+1,j,k}\rho_{o_{i+1,j,k}}^{n+1}-s_igD_{i,j,k}\rho_{o_{i,j,k}}^{n+1}-s_{i-1}gD_{i-1,j,k}\rho_{o_{i-1,j,k}}^{n+1})+s_{i+1}T_{i+1,j,k}\sum_i(c_{p_i}C_{i_o})|_{i+1,j,k}$$

$$-(s_{i+1}T_{i+1,j,k}^{n+1}\sum_i(c_{p_i}C_{i_o})|_{i+1,j,k}^{n+1}+s_iT_{i,j,k}^{n+1}\sum_i(c_{p_i}C_{i_o})|_{i,j,k}^{n+1}+s_{i-1}T_{i-1,j,k}^{n+1}\sum_i(c_{p_i}C_{i_o})|_{i-1,j,k}^{n+1}$$

$$(s_{i+1}gD_{i+1,j,k}\frac{\partial\rho_o}{\partial C_{i_o}}|_{i+1,j,k})]$$

$$+T_{i,j,k}\sum_i(c_{p_i}C_{i_o})|_{i,j,k}[(1-w_{o_x})\frac{A_xk_xk_{ro}}{\Delta x}\frac{\partial\frac{\rho_o}{\mu_o}}{\partial C_{i_o}}|_{i+1,j,k}(p_{o_{i+1,j,k}}^{n+1}-p_{o_{i,j,k}}^{n+1}-\rho_{o_{i+1,j,k}}^{n+1}gD_{i+1,j,k}+\rho_{o_{i,j,k}}^{n+1}gD_{i,j,k})]$$

$$+\frac{A_xk_xk_{rw}\rho_w}{\mu_w\Delta x}|_{i,j,k}[(s_{i+1}p_{o_{i+1,j,k}}^{n+1}+s_ip_{o_{i,j,k}}^{n+1}+s_{i-1}p_{o_{i-1,j,k}}^{n+1}$$

$$-s_{i+1}P_{cow_{i+1,j,k}}^{n+1}-s_iP_{cow_{i,j,k}}^{n+1}+s_{i-1}P_{cow_{i-1,j,k}}^{n+1}$$

$$-s_{i+1}gD_{i+1,j,k}\rho_{w_{i+1,j,k}}^{n+1}-s_igD_{i,j,k}\rho_{w_{i,j,k}}^{n+1}-s_{i-1}gD_{i-1,j,k}\rho_{w_{i-1,j,k}}^{n+1})(s_{i+1}T_{i+1,j,k}c_{pi}/f_{iow}|_{i+1,j,k}$$

$$-(s_{i+1}T_{i+1,j,k}^{n+1}\sum_i(c_{p_i}\frac{C_{i_o}}{f_{iow}})|_{i+1,j,k}^{n+1}+s_iT_{i,j,k}^{n+1}\sum_i(c_{p_i}\frac{C_{i_o}}{f_{iow}})|_{i,j,k}^{n+1}+s_{i-1}T_{i-1,j,k}^{n+1}\sum_i(c_{p_i}\frac{C_{i_o}}{f_{iow}})|_{i-1,j,k}^{n+1}$$

$$(s_{i+1}gD_{i+1,j,k}\frac{\partial\rho_w}{\partial C_{i_o}}|_{i+1,j,k})]+T_{i,j,k}\sum_i(c_{p_i}\frac{C_{i_o}}{f_{iow}})|_{i,j,k}$$

$$[(1-w_{w_x})\frac{A_xk_xk_{rw}}{\Delta x}\frac{\partial\frac{\rho_w}{\mu_w}}{\partial C_{i_o}}|_{i+1,j,k}(p_{o_{i+1,j,k}}^{n+1}-p_{o_{i,j,k}}^{n+1}-\rho_{w_{i+1,j,k}}gD_{i+1,j,k}+\rho_{w_{i,j,k}}D_{i,j,k}-P_{cow_{i+1,j,k}}+P_{cow_{i,j,k}})]$$

$$+\frac{A_xk_xk_{rg}\rho_w}{\mu_g\Delta x}|_{i,j,k}[(s_{i+1}p_{o_{i+1,j,k}}^{n+1}+s_ip_{o_{i,j,k}}^{n+1}+s_{i-1}p_{o_{i-1,j,k}}^{n+1}$$

$$+s_{i+1}P_{cgo_{i+1,j,k}}^{n+1}+s_iP_{cgo_{i,j,k}}^{n+1}+s_{i-1}P_{cgo_{i-1,j,k}}^{n+1}$$

$$-s_{i+1}gD_{i+1,j,k}\rho_{g_{i+1,j,k}}^{n+1}-s_igD_{i,j,k}\rho_{g_{i,j,k}}^{n+1}-s_{i-1}gD_{i-1,j,k}\rho_{g_{i-1,j,k}}^{n+1})(s_{i+1}(T_{i+1,j,k}c_{pi}+L_{vi})/f_{iog})$$

$$-(s_{i+1}\sum_i(c_{p_i}T+L_{vi})\frac{C_{i_o}}{f_{iog}}|_{i+1,j,k}^{n+1}+s_i\sum_i(c_{p_i}T+L_{vi})\frac{C_{i_o}}{f_{iog}}|_{i,j,k}^{n+1}+s_{i+1}\sum_i(c_{p_i}T+L_{vi})\frac{C_{i_o}}{f_{iog}}|_{i-1,j,k}^{n+1}$$

$$(s_{i+1}gD_{i+1,j,k}\frac{\partial\rho_g}{\partial C_{i_o}}|_{i+1,j,k})]+\sum_i(c_{p_i}T+L_{vi})\frac{C_{i_o}}{f_{iog}}|_{i,j,k}[(1-w_{g_x})\frac{A_xk_xk_{rg}}{\Delta x}\frac{\partial\frac{\rho_g}{\mu_g}}{\partial C_{i_o}}|_{i+1,j,k}$$

$$(p_{o_{i+1,j,k}}^{n+1}-p_{o_{i,j,k}}^{n+1}-\rho_{g_{i+1,j,k}}gD_{i+1,j,k}+\rho_{g_{i+1,j,k}}D_{i,j,k}-P_{cgo_{i+1,j,k}}-P_{cgo_{i,j,k}})$$

$$+\frac{A_x}{\Delta x}|_{i+\frac{1}{2},j,k}^{n+1}(1-w_{o_x})D_{io_{i+1,j,k}}c_{pi_{i+1,j,k}}T_{i+1,j,k}\frac{1}{f_{iow_{i+1,j,k}}}(\rho_{o_{i+1,j,k}}+C_{io_{i+1,j,k}}\frac{\partial\rho_o}{\partial C_{i_o}}|_{i+1,j,k})$$

$$+\frac{A_x}{\Delta x}|_{i+\frac{1}{2},j,k}^{n+1}(1-w_{w_x})D_{iw_{i+1,j,k}}c_{pi_{i+1,j,k}}T_{i+1,j,k}\frac{1}{f_{iow_{i+1,j,k}}}(\rho_{w_{i+1,j,k}}+C_{io_{i+1,j,k}}\frac{\partial\rho_w}{\partial C_{i_o}}|_{i+1,j,k})$$

$$+\frac{A_x}{\Delta x}|_{i+\frac{1}{2},j,k}^{n+1}(1-w_{g_x})D_{ig_{i+1,j,k}}c_{pi_{i+1,j,k}}T_{i+1,j,k}\frac{1}{f_{iog_{i+1,j,k}}}(\rho_{g_{i+1,j,k}}+C_{io_{i+1,j,k}}\frac{\partial\rho_g}{\partial C_{i_o}}|_{i+1,j,k}) \quad (4.75)$$

Numerical Derivatives

The numerical derivatives of the F_i and G functions were calculated using the following type of equation, giving $\frac{\partial F_i}{\partial p_o}$ at block i,j,k, for example:

$$\frac{\partial F_i}{\partial p_o}|_{i,j,k}=\frac{F_i(p_{o_{i,j,k}}+\epsilon,\bar{x})-F_i(p_{o_{i,j,k}},\bar{x})}{\epsilon}$$

(4.76)

where $\bar{x}$ represents all other variables, the values of which are held constant at the current iteration.

Source-Sink Terms

The source-sink terms consist of injection/production terms for oleic, aqueous, and vapour phases as well as for enthalpy. The procedure used for injection and production wells is described below. The terms are taken to be fully implicit in all cases.

Injection Well

An injection well is treated rather simply. In this case, the injection rate of a component, or a phase with a given composition, is specified. For example, the injection rate of the aqueous phase q_w^*, sm^3/s, may be given with 100% water. This can be converted into an appropriate source term m_i^*, kg/ s-m^3, in a straightforward manner. The enthalpy term follows directly from this term, given the injected enthaply per unit mass.

Two components, if injected simultaneously, can be treated in the same manner, although it is numerically more convenient to consider alternating injection, as would be the case in the actual field practice.

It should be noted that only Abou-Kassem (1981) has rigorously treated wet steam injection as a two-phase injection problem. Earlier, Ito (1976) employed an approximate approach of this type. The result was pressure oscillation at the injection well, which can lead to solution convergence problems.

Production Well

The case of a production well is more complex than that of an injection well. The present simulator allows for three options: (i)the oil production rate is specified, (ii)the total liquid production rate is specified (e.g. pump capacity), or (iii)the well bottomhole flowing pressure is specified. In each case, the phase production rates are obtained from the basic mobility relationship, as shown below.

If the oil, water, and vapour production rates are q_o^*, q_w^*, q_g^*, then the following relationships hold:

$$\frac{\rho_{osc}q_o^*}{\rho_{wsc}q_w^*} = \frac{\frac{-k_{ro}\rho_o}{\mu_o}\frac{\partial\Phi_o}{\delta r}}{\frac{-k_{rw}\rho_w}{\mu_w}\frac{\partial\Phi_w}{\delta r}} \tag{4.77}$$

and

$$\frac{\rho_{osc}q_o^*}{\rho_{gsc}q_{gsc_{free}}^*} = \frac{\frac{-k_{ro}\rho_o}{\mu_o}\frac{\partial\Phi_o}{\delta r}}{\frac{-k_{rg}\rho_g}{\mu_g}\frac{\partial\Phi_g}{\delta r}} \tag{4.78}$$

Thus, q_w^* and q_g^* can be obtained from:

$$q_g^* = \left(\frac{k_{rg}\rho_g\rho_{osc}\mu_o}{k_{ro}\rho_o\rho_{gsc}\mu_g}\frac{\frac{\partial\Phi_g}{\delta r}}{\frac{\partial\Phi_o}{\delta r}}\right)q_o^* \tag{4.79}$$

or, $q_g^* = g \cdot q_o^*$, where g is the above multiplier.

Similarly,

$$q_w^* = \left(\frac{k_{rw}\rho_w\rho_{osc}\mu_o}{k_{ro}\rho_o\rho_{wsc}\mu_w}\frac{\frac{\partial\Phi_w}{\delta r}}{\frac{\partial\Phi_o}{\delta r}}\right)q_o^* = f \cdot q_o^* \tag{4.80}$$

where f is the expression in the parentheses. If the total liquid production rate q_t^* is given, it can be broken into oil and water phase production rates, as follows:

$$q_w^* = \frac{fq_t}{1+f} \tag{4.81}$$

and

$$q_o^* = \frac{q_w^*}{f} \tag{4.82}$$

The total liquid rate is useful for a pumping well, where q_t^* is less than or equal to the pump capacity. If, on the other hand, the bottomhole flowing pressure p_{wf} is given, the oil production rate is given by (based upon steady state radial flow in terms of average pressure):

$$q_o^* = \frac{2\pi hkk_{ro}(\Phi_b - \Phi_{wf})\rho_o}{\mu_o[ln\frac{r_e}{r_w} - \frac{1}{2} + s]\rho_{osc}}, \tag{4.83}$$

where Φ_b is the well block pressure, and r_e is the drainage radius equivalent to the block area. If the well is producing against a fluid head in the wellbore, the above equation can be used.

Once the phase production rates are calculated, the individual component production rates are obtained from phase compositions, which are known at the well block.

The heat production rates are obtained directly from the enthalpy of the produced components and the phase production rates. Such a term is given below:

$$\rho_{osc}q_o^* \sum_i C_{o_i} c_{p_i} T + \rho_{wsc}q_w^* \sum_i C_{w_i} c_{p_i} T + \rho_{gsc}q_{gsc}^* \sum_i C_{g_i}(c_{p_i} T + L_{v_i}). \tag{4.84}$$

Three-Phase Relative Permeabilities

Determination of three-phase relative permeabilities by laboratory experiments is difficult and time consuming, although both steady and unsteady state methods have been used successfully for obtaining such data. In reservoir simulation, the unsteady state method is used more commonly because of its relative simplicity [Johnson, Bossler, and Nauman (1959)]. This method is based upon the Buckley-Leverett theory, and thus assumes an infinite saturation at the front. Because of this, the results should be used with caution, especially if viscous instabilities are present. Islam and Bentsen (1986) have discussed this question in a number of publications.

Two-phase relative permeabilities used in simulations are usually experimentally obtained. Three-phase values are often synthesized from experimental oil-water and oil-gas relations, employing Stone's method (1970,1973), or one of its variations. We shall briefly discuss Stone's method, and the Naar-Wygal-Henderson (1961,1962) method, as well as a modification of the latter, which was developed for this study.

Stone's Method

The following assumptions are made in developing Stone's method [Stone(1973)]:

1. The water relative permeability is a function of water saturation only, and does not depend on the relative proportions of oil and gas phases. Thus,

$$k_{rw} = k_{rw}(S_w). \tag{4.85}$$

2. The gas relative permeability is a function of gas saturation only, and does not depend on the relative proportions of oil and water phases. Thus,

$$k_{rg} = k_{rg}(S_g). \tag{4.86}$$

3. The oil relative permeability is a function of both water and gas saturations, i.e.

$$k_{ro} = k_{ro}(S_w, S_g). \tag{4.87}$$

Keeping these rules in mind, k_{rw} and k_{rg} can be obtained simply from two-phase oil-water and oil-gas relative permeability data, while k_{ro} is obtained from the following relationship. This is a modified form of Stone's original equation.

$$k_{ro} = k_{row}{}^*[(\frac{k_{row}}{k_{row}{}^*} + k_{rw})(\frac{k_{rog}}{k_{row}{}^*} + k_{rg}) - (k_{row} + k_{rog})], \tag{4.88}$$

where k_{row} and k_{rog} are, respectively, the relative permeabilities to oil in the water-oil and gas-oil systems, and are obtained from two-phase relative permeability curves, and

$$k_{row}{}^* = k_{row}(S_w). \tag{4.89}$$

Shutler (1969) suggested an equation that relates the actual three-phase oil saturation S_o to a two-phase oil saturation S_2 in a gas-oil system, where (S_{wr} is irreducible water saturation)

$$S_2 = \frac{(1 - S_w - S_g)(1 - S_{wr})}{1 - S_w}. \tag{4.90}$$

Then the relative permeability to oil in the three-phase system is given by:

$$k_{ro} = \frac{k_{row}(S_w)k_{rog}(S_2)}{k_{row}(S_{wr})}. \tag{4.91}$$

where

k_{row}=relative permeability to oil in a water-oil system

k_{rog}=relative permeability to oil in a oil-gas-irreducible water system

Naar-Wygal-Henderson Method

Naar, Wygal and Henderson (1961,1962) proposed the following relationships for three-phase relative permeabilities, based upon simplification of their integral equations:

$$k_{rw} = \left[\frac{S_w - S_{wr}}{1 - S_{wr}}\right]^4, \tag{4.92}$$

$$k_{ro} = S_o^3 \frac{(1 - S_g + S_w - 2S_{wr})}{(1 - S_{wr})^4}, \tag{4.93}$$

$$k_{rg} = S_g^3 \frac{(2 - S_g - 2S_{wr})}{(1 - S_{wr})^4}. \tag{4.94}$$

The above equations are used widely in reservoir simulation. These equations are simplifications of more complex forms. It is seen that only a single parameter S_w is required, which often becomes a history matching parameter. Aktan and Farouq Ali (1972) showed that the Naar-Wygal-Henderson equations gave relative permeabilities close to those obtained from Stone's method. Considering the uncertainties in experimental measurements of relative permeabilities, these equations offer a useful alternative.

The above equations give $k_{rw} = 0$ when $S_w = S_{wr}$. However, they do not properly describe the behaviour of k_{ro} and k_{rg} at the critical oil and gas saturations. These effects must be considered in simulation. Most investigators simply make k_{ro} zero, when $S_o \leq S_{or}$, and k_{rg} zero, when $S_g \leq S_{gc}$. This is not satisfactory in solution techniques involving derivatives of relative permeability, as in the fully implicit procedure used in the present work, or in the semi-implicit techniques. In semi- or fully implicit methods, nonlinearities near the critical points are severe, and smooth functions need to be used.

Modified Relative Permeability Equations

A modification of the three-phase relative permeability equations (4.92) to (4.94) is suggested, in order to properly account for the behaviour of the relative permeabilities to oil and gas at their critical saturation values. This modification does not allow for the mobility of oil and gas phases at or below the critical values, and it provides a smooth transition of relative permeability from zero to nonzero values. The proposed modifications are as follows.

Relative permeability to oil:

In Eq.(4.93), the term S_o^3 can be replaced by $C_1(S_o - S_{or})S_o^2$. As a result, the modified relative permeability to oil k_{roM} is given by

$$k_{roM} = C_1(S_o - S_{or})S_o^2 \frac{(1 - S_g + S_w - 2S_{wr})}{(1 - S_{wr})^4}, \tag{4.95}$$

and

$$k_{roM} = 0 \quad \text{if} \quad S_o < S_{or}, \tag{4.96}$$

where C_1 is a constant that is obtained as follows. Equation (4.95) has to be consistent with Eq.(4.93), when $S_g = 0$ and $S_w = S_{wr}$, where S_{wr} is irreducible water satruration. Therefore, we can equate them and solve for C_1. In Eq.(4.93), if $S_g = 0$ and $S_w = S_{wr}$, then $k_{ro} = 1$. In Eq.(4.95):

$$1 = k_{roM} = C_1(S_o - S_{or})S_o^2 \frac{(1 - S_{wr})}{(1 - S_{wr})^4}, \tag{4.97}$$

but when $S_g = 0$ and $S_w = S_{wr}$, $S_o = 1 - S_{wr}$, giving

$$C_1 = \frac{1 - S_{wr}}{1 - S_{wr} - S_{or}}. \tag{4.98}$$

Therefore:

$$k_{roM} = \frac{1 - S_{wr}}{1 - S_{wr} - S_{or}}(S_o - S_{or})S_o^2 \frac{(1 - S_g + S_w - 2S_{wr})}{(1 - S_{wr})^4}. \tag{4.99}$$

Notice that the subscript M stands for the modified form.

Relative permeability to gas:

In this case, the term S_g^3 in Eq.(4.94) can be replaced by $C_2(S_g - S_{gc})S_g^2$, so that the modified equation is writtten as:

$$k_{rgM} = C_2(S_g - S_{gc})S_g^2 \frac{(2 - S_g - 2S_{wr})}{(1 - S_{wr})^4}, \tag{4.100}$$

Again, in this case, in order to keep Eq.(4.100) consistent with Eq.(4.94), when $S_o = 0$ and $S_w = S_{wr}$, the two expressions are considered to be equal; therefore, C_2 is obtained as follows. In Eq.(4.94), $k_{rg} = 1$, thus

$$C_2 = \frac{1 - S_{wr}}{1 - S_{wr} - S_{gc}}, \tag{4.101}$$

and

$$k_{rgM} = \frac{1 - S_{wr}}{1 - S_{wr} - S_{gc}}(S_g - S_{gc})S_g{}^2\frac{(2 - S_g - 2S_{wr})}{(1 - S_{wr})^4}, \tag{4.102}$$

and

$$k_{rgM} = 0 \quad \text{if} \quad S_g < S_{gc}. \tag{4.103}$$

In this manner, the known values of S_{or} and S_{gc} can be incorporated into the original Naar-Wygal-Henderson equations. The form of Eqs.(4.99) and (4.102) is suitable when account has to be taken of temperature dependence of relative permeabilities. In such a case, the residual oil and irreducible water saturations may be taken to be functions of temperature [Diaz and Farouq Ali (1974), Ferrer and Farouq Ali (1977), Weinbrandt, Ramey and Casse (1975)].

Figures 4.1 and 4.2 show a comparison of the Naar-Wygal-Henderson and the modified relative permeabilities. The plots show

$$\frac{k_{roNH} - k_{roM}}{k_{roNH}} = \frac{S_{or}(1 - S_o - S_{wr})}{S_o(1 - S_{or} - S_{wr})}$$

versus S_o in Fig. 4.1, and

$$\frac{k_{rgNH} - k_{rgM}}{k_{rgNH}} = \frac{S_{gc}(1 - S_g - S_{wr})}{S_g(1 - S_{gc} - S_{wr})}$$

versus S_g in Fig. 4.2. It is seen that for high values of S_o and S_g the difference between the Naar-Wygal-Henderson and modified permeabilities is small.

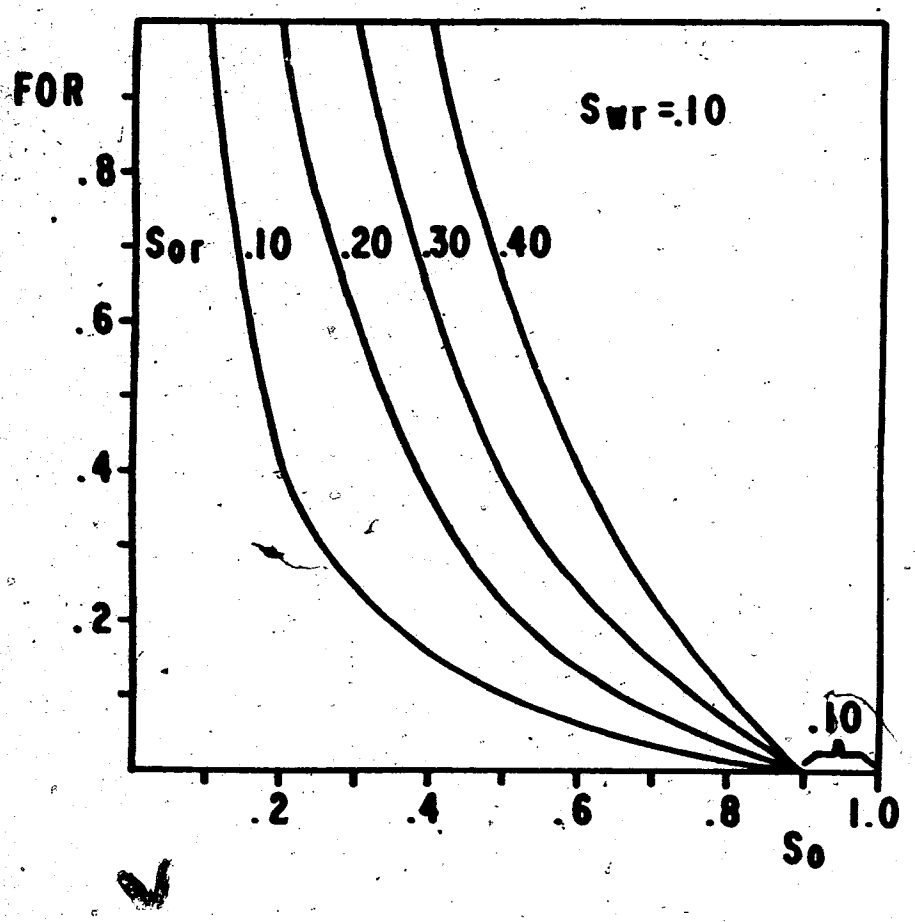

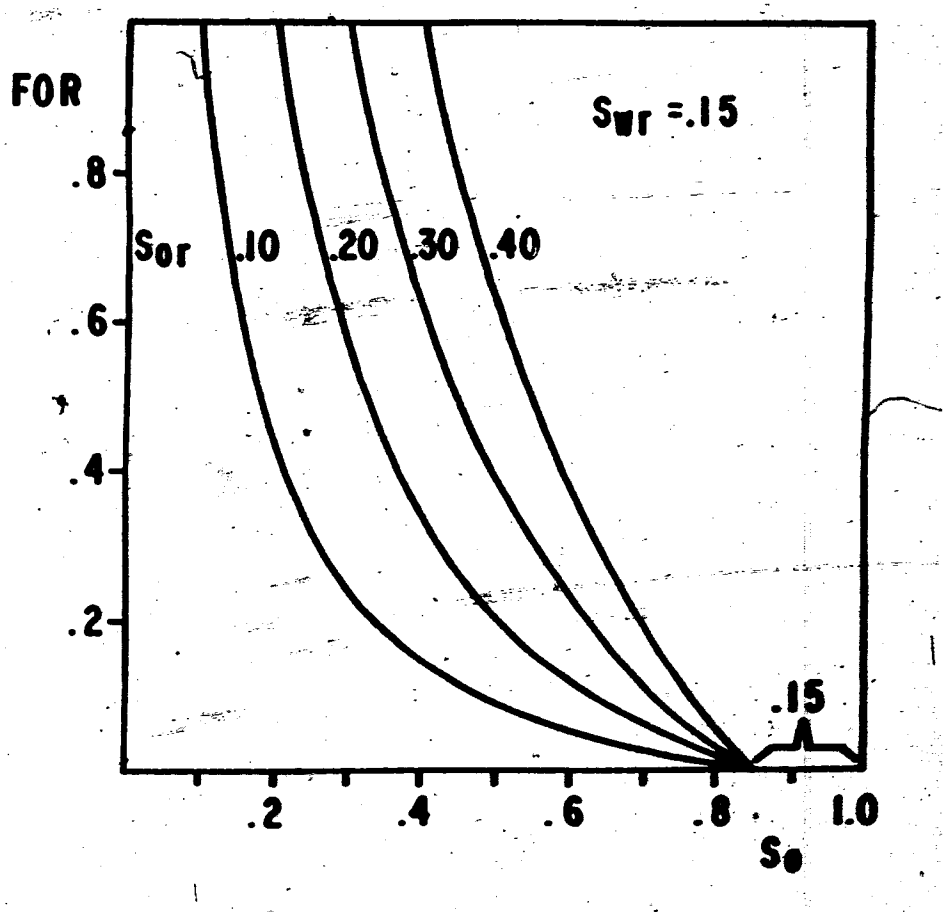

Figure 4.1 Comparison of the Naar-Wygal-Henderson and Modified Oil Relative Permeability Values, FOR = (kroNH-kroM)/kroM

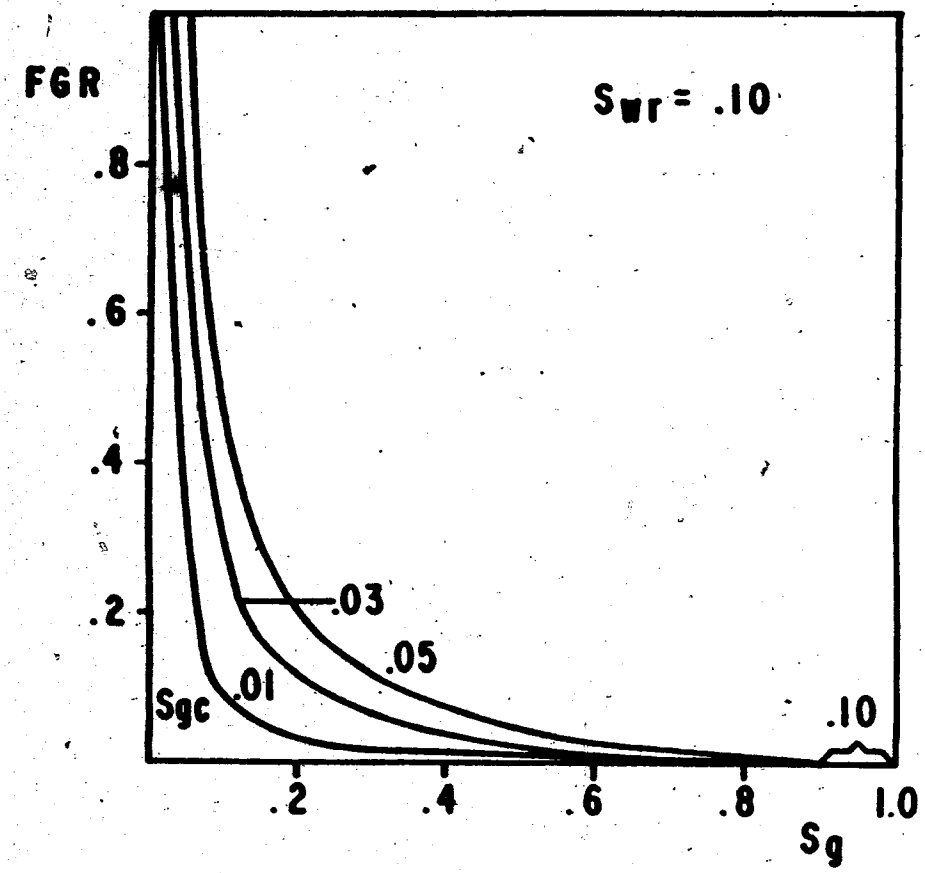

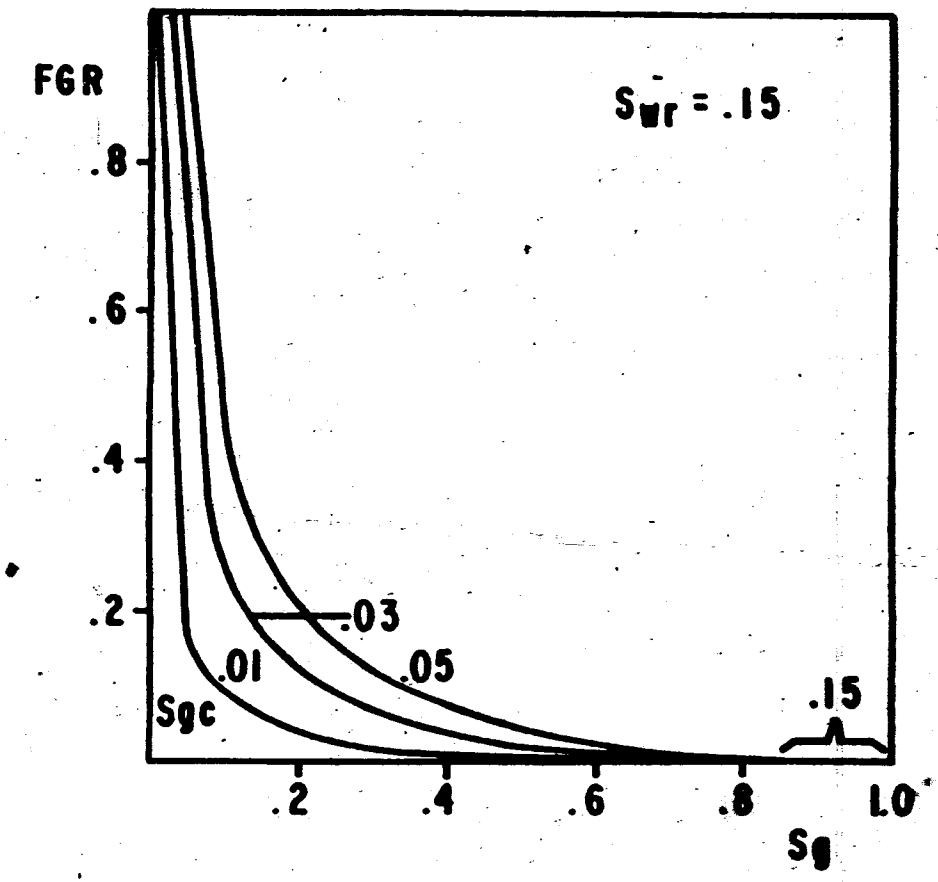

Figure 4.2 Comparison of the Naar-Wygal-Henderson and Modified Gas Relative Permeability Values, FOR = (kroNH-kroM)/kroM

Temperature Dependence of Relative Permeabilities

Several investigators have studied the effect of temperature on relative permeabilities [Poston et al (1970), Weinbrandt et al. (1972), Sufi, Ramey and Brigham (1982), and Polikar et al. (1986)], and have reported conflicting experimental data. The question whether relative permeabilities are temperature dependent is open to controversy. It seems that in clean sand, with no clays present, relative permeabilities are essentially independent of temperature. On the other hand, in naturally occurring sands, with considerable amounts of clay minerals, relative permeabilities are temperature dependent, possibly due to rock-fluid interactions and other effects, such as thermal expansion and grain dislocations. In this work, we will not be concerned with this question. The simulations conducted considered both temperature dependent and temperature invariant relative permeabilities. A few investigators have studied this effect on steam processes [Ferrer and Farouq Ali(1975)]. It was observed that oil recovery increased for the temperature dependent relative permeabilities. Oil recovery was found to increase more noticeably in the case of steam drive than for cyclic steam stimulation. This occurs because production of hot fluids causes temperature reduction and consequently acceleration of pressure depletion in cyclic steaming. Diaz and Farouq Ali (1974) reported similar results for the simulation of cyclic hot water stimulation. In his studies, however, the effect of temperature dependence of relative permeabilities on oil recovery and production rate were less significant than in the case of steam. This could be explained by the lower temperature in the case of hot water injection than for steam soak. Coats and co-workers (1974) reported that difficulties were encountered in matching experimental data when the effect of temperature on relative permeabilities was not taken into account. On the other hand, Shutler (1969,1970) and Weinstein et al. (1974) reported good agreement between calculated and experimental data without considering this effect.

It should be noted that the inclusion of temperature dependence of relative permeabilities provides one more adjustment parameter for obtaining a history match, whether such temperature dependence is real or not.

In the present study, the end-points S_{wr} and S_{or} were made linear functions of temperature, when temperature dependence was to be considered. This agrees with the experimental data of Weinbrandt and Ramey (1972), and is a convenient though not rigourous means of including the effect of temperature on relative permeabilities :

$$S_{or} = a_0 - a_1 T, \tag{4.104}$$

$$S_{wr} = b_0 + b_1 T, \tag{4.105}$$

$$S_{gc} = \text{const.} \tag{4.106}$$

Thermal Upgrading of Heavy Oils

A heavy crude oil, when subjected to mild thermal cracking conditions, exhibits a permanent and considerable reduction in its viscosity and specific gravity. All crudes are susceptible to cracking, however, high temperatures and long times are required to crack heavy crudes, such as the Athabasca bitumen. By subjecting both the original crude and the heat-treated oil to distillation under identical conditions, the amount of upgrading or conversion of crude constituents can be estimated.

Laboratory tests have been conducted on a variety of crude oils, in order to study the time-temperature history, and to obtain specific degrees of viscosity reduction for each sample. At 500 F, the permanent upgrading of physical properties takes place rather slowly. Use of temperatures lower than that will only improve the oil fluidity, which is the case of heated pipelines as currently practiced. Above 700 F, coking may take place, which will cause operating problems.

Crude oils having low API gravities and high viscosities and pour points cause production difficulties both in and out of the reservoir. Thermal cracking offers a solution, which is associated with lowering of pour point and viscosity. Egloff and Morrell (1926) suggested severe cracking of a high pour point oil at the wellhead to eliminate the need for pipeline heaters as well as diluents. Underground thermal processes may subject large volumes of reservoir crude to a temperature, which is high enough to cause mild thermal cracking. The permanent change in the physical properties of heavy oil as a result of mild thermal cracking was observed by Ball (1941) on oil from the Athabasca oil sands.

In a survey by Henderson and Weber (1965), mild thermal cracking experiments carried out on samples of seven different crude oils have been reported. Six of these samples were chosen from conventional oil reservoirs and one was from the Athabasca oil sands. In this study, Henderson and Weber were concerned about (i) the time that a particular crude could be heated at different temperatures; (ii) establishing a relationship between changes in the crude and the period of heating; and (iii) the important variables of the process. These variables are discussed in the next section.

Kinetics of the Cracking Process

In a thermal cracking process large molecules of hydrocarbons are ruptured by thermal energy into smaller molecules. Under normal conditions, some small molecules form, which are relatively stable gases or liquids. Also, some unstable or reactive molecules are produced that can polymerize with one another and yield larger molecules than those in the original crude. Provided the pyrolysis is continued for sufficient time, or the temperature is further increased, the original crude will be almost entirely converted into a mixture of light gases (e.g. methane and hydrogen), which are stable, and a solid material, which is coke.

Henderson and Weber (1965) give the following kinetic equation to describe the cracking reaction of pure hydrocarbons as well as petroleum:

$$\ln(\frac{C_0}{C}) = kt. \tag{4.107}$$

This is the integrated form of the first order rate equation, where C_0= percent weight of reactant initially present, C= percent of reactant remaining at time t, t= time, seconds, and k=specific rate or velocity constant, sec^{-1}. The specific rate k is given by the integrated Arrhenius equation

$$k = Ae^{-\frac{E}{RT}}, \tag{4.108}$$

where A= pre-exponent, sec^{-1}, E= activation energy, Btu/lb-mole, T=absolute temperature, R, and R= gas constant= 1.987 Btu/lb-mole-R.

Representation of Upgrading in the Mathematical Model

For the purpose of this study, the upgrading process was represented via an oil viscosity equation, where the viscosity is a function of the fraction upgraded, as follows:

$$\ln\mu = a + b(1 - e^{-Ate^{-\frac{E}{RT}}}), \tag{4.109}$$

where μ is the viscosity at 150 F in cp, T is in R, and t is in seconds. The constants a and b were taken from Henderson and Weber's experimental data, for three of the oils tested by them. These are listed in Table 4.1.

Table 4.1

KINETICS CONSTANTS USED FOR UPGRADING

Crude Oil	Log_{10} A	Activation Energy, E, kcal/mole	b	a
C	12.13	49.0	-10.067	6.7852
E	9.86	43.6	-6.299	4.2896
Athabasca Bitumen	11.53	49.	-11.16	7.253

Flow of Foams in Porous Media

Rheology of Foam

Foams are complex two-phase, multicomponent fluid systems, with rather unusual flow behaviour in a porous medium. A foam is basically a gas-liquid dispersion that is formed by mixing a gas, such as air or nitrogen, and a liquid to which a surface active agent has been added. A number of previous studies have been devoted to foam rheology in a variety of flow systems, such as laboratory containers, capillary tubes, and porous media (e.g. Bernard (1963), Holm (1968), Raza (1970), and Mast (1972)). Recently, Irani and Solomon (1986) discussed the mechanics of CO_2-foam propagation in a slim tube, and foam stability. A brief description of some of the dominant characteristics of foam are given below. A few studies have also dealt with "oil foams", i.e. dispersions of oil, containing a surface active agent and a gas. Such foams are usually unstable, and will not be considered in this study.

Fried (1961) conducted the first comprehensive study on the flow of foams in a porous medium. Although this work was done over 25 years ago, it is still useful for reasons of its thoroughness. He reported that the mobility of an externally generated foam in a porous medium was considerably lower than that of the gas used for the foam.

Consider first, certain rheological features of a foam. Foam can be generated by injecting gas into a porous medium that initially contains a foaming solution. Raza and Marsden (1967) and Raza (1970), showed that anionic foaming agents produce low quality, stable foams, while nonionic agents yield high quality, unstable foams. (Foam quality is defined as the ratio of gas volume to the total foam volume.) Flow tests in a porous medium showed that the foam quality increased as the surfactant concentration increased until a concentration of 0.1% by weight was reached, after which the quality became constant. The time for foam breakthrough was very small up to a surfactant

concentration of 0.1%. Thereafter, the breakthrough time increased 20-fold, reaching a maximum at a concentration of 1% to 8%, and then decreasing somewhat. Chiang et al. (1980) reported that stable foams formed at 0.6% concentration.

Minssieux (1974) proposed two mechanisms for foam instability, which is strongly influenced by quality. When drainage of liquid and rupture of fluid is the dominant mechanism, foam stability increases with increasing quality. If gas diffusion between adjacent bubbles is the main cause of instability, foam stability will be expected to decrease with increasing quality. The latter effect was dominant in the case of a viscous liquid phase. Possibly, in the flow of an aqueous foam, liquid drainage is the dominant mechanism deciding foam stability. Regarding the effect of temperature and pressure on foam stability, it appears that generally foam stability increases with increasing pressure, and decreases with increasing temperature. The quality decreases with an increase in pressure and/or decrease in temperature, for a given surfactant condition. These results are based upon Wang's (1984) and Maini and Ma's (1984) work.

The mobility reduction factor of foams increases with increasing foam stability due to the similarity in the surface forces affecting the foam properties inside and outside the porous medium. The apparent viscosity of foam depends on a number of factors, including velocity or shear rate, pressure, and temperature. An increase in pressure causes a decrease in the foam quality, and an increase in density. The apparent viscosity of foam is often expressed as a function of foam density, with the viscosity passing thorugh a maximum as the density increases (Grove et al (1951)). It has been shown by Marsden and Khan (1966) that the apparent viscosity decreases with increasing shear rate and increases with increasing quality. Shear stress versus shear rate plots for foams tend to show that foams have pseudoplastic behaviour. Flow experiments in capillary tubes have shown that the apparent viscosity also depends on the tube radius (Raza and Marsden (1967)). Correcting for slippage and compressibility, it was found that the foam viscosity

became independent of quality, but continued to be a function of tube diameter. The apparent viscosity of a foam was found to decrease with temperature.

Hirasaki and Lawson (1983) proposed a mathematical equation for the apparent viscosity of foam. The viscosity was attributed to: (i) the liquid slugs, (ii) resistance to deformation of the interface of a bubble passing through a capillary and (iii) surface tension gradient. The equation consists of two parameters, which must be determined from experimental data. Effect of temperature was not considered in this work.

Flow in Porous Media

The early work of Fried (1961), and later Bernard (1964) showed that the mobility of foam in a porous medium is lower than that of gas or the liquid constituting the foam. The latter study also showed that the displacement efficiency of a foam was higher in sand packs containing water only as compared to sand packs containing oil only. When both oil and water were present, the performance was somewhere in between. Further studies have shown (Bernard (1964)) that the relative permeability to water as a function of water saturation is not altered in the presence of foam, however, that of the gas is lowered, because the effect of foam is to create a higher trapped gas saturation, which indirectly lowers the relative permeability to water. The presence of oil tends to lower the trapped gas saturation.

There is some difference of opinion on the mechanics of flow of a foam in a porous medium. Marsden and Khan (1966) suggested that the foam components flow simultaneously in a porous medium. Thus, foam mobility was found to decrease with increasing quality. On the other hand, Bernard et al. (1964) proposed that water flows as a continuous phase, while the gas is a discontinuous phase. Still another mechanistic picture was described by Holm (1968), who observed in visual studies that the gas and liquid phases flowed separately in a porous medium by the breaking and reforming of the bubbles. Foam generation and quality have been related to absolute permeability (Raza

(1970)). Foam is generated in the longer pores, wherein the foam would tend to flow, with temporary blockage in the smaller pores. In this manner, it is possible to describe the flow of a foam in a porous medium in at least two different ways: as a single body, or as two separate phases. In any case, the flow behaviour is non-Newtonian.

Application of Foam in Steam Injection

A foam is used in steam injection for two purposes, which are not quite distinct. First, injected with steam it can help control steam mobility, because steam will act as a viscous fluid leading to higher displacement efficiency of the mobilized oil. Secondly, foam can also be used as a blocking agent, where gravity override of steam has created a high conductivity path in the upper part of the formation. Steam mobility control by use of foam is likely to be more effective in steamflooding lighter oils, where the steam front is close to vertical. When steam override is present, use of foam as a blocking agent is likely to be more effective. In both cases, formation and flow of foam leads to a large reduction in gas phase mobility.

Elson and Marsden (1978) have reviewed the literature on the use of foam with steam, concluding that foam is best suited as a blocking agent. Chiang et al. (1980) carried out ambient temperature experiments using a surfactant and water, with nitrogen as gas. They reported that *in situ* formation of foam increased liquid recovery and reduced gravity override. Isaacs et al. (1985) reported steam-foam experiments, showing that steam-foams were formed in the case of one of the surfactants, as indicated by the large pressure drop, when steam was injected. On the other hand, no foam was formed in the case of the other surfactant. They reported that the gas phase relative permeability curves had to be shifted depending on gas velocity and surfactant concentration in order to simulate foam flow.

Representation of Foam in the Mathematical Model

In the present mathematical model, foam was considered to have two effects on steam flow: it increases the apparent viscosity of the steam phase, and it reduces the relative permeability to gas. In the existing literature, there are no consistent data describing foam rheology as a function of surfactant concentration, quality, temperature, and pressure. The same is true for the relative permeability to gas in the presence of a foam. The purpose of this work was to put together the available data in a form in which the dominant aspects of foam flow are represented. The input consisted of the surfactant concentration in the steam zone. This was used to calculate the foam quality. The quality was modified for pressure and temperature effects. Finally, the computed quality was used in the viscosity equation, to calculate the apparent viscosity of foam. In a similar way, the relative permeability to gas was based upon the flow velocity, assuming the presence of a foam after Isaacs et al, (1985). The equations used are as follows, and are based upon the experimental data of Wang (1980), Grove (1951), Marsden and Khan (1966), and Best et al. (1985).

$$x = 1.14205\,(0.7975 - 0.90763\,C_s)(0.36 + 3.2 \times 10^{-4}\,p)\exp(-0.001594\,T), \quad (4.110)$$

$(75 \le T \le 140°F,\ 1500 \le p \le 2000\ \text{psia},\ 0.1 \le C_s \le 0.33\%\ \text{by wt})$

where x is foam quality, fraction, C_s is concentration in steam, fraction, p is pressure in psia, and T is temperature in °F. The apparent viscosity of foam is given by

$$\mu_{app} = -386 + 783\,x - 0.4211\,\dot{\gamma}, \quad (0.7 \le x \le 0.95,\ 100 \le \dot{\gamma} \le 300\ \text{min}^{-1}) \quad (4.111)$$

where $\dot{\gamma}$ is the shear rate, related to velocity v by (Jennings et al. (1971))

$$\dot{\gamma} = \frac{299\,v}{\sqrt{k\phi}}, \quad (4.112)$$

where v is in ft/day, k is permeability in darcies; and ϕ is porosity, fraction. Notice that the above equations are valid only over a limited range of the variables involved. The relative permeability to gas is similarly given by

$$k_{rg} = k_{rgo} (0.1 + 0.3092\ v) , \qquad (4.113)$$

where k_{rgo} is relative permeability to gas in the absence of foam. This is a rough approximation, and only reflects the observed trend.

Auxiliary Relationships

Table 4.2 shows the functional dependences of the variables involved in the model. The functions employed for the majority of simulations are discussed below.

Oil Phase and Water Viscosity

The oil phase viscosity μ_o was calculated from the Andrade equation for the Aberfeldy reservoir

$$\mu_o = 1.257 \times 10^{-5} \exp\left(\frac{5573}{T + 460}\right) \qquad (4.114)$$

where T is in °F and μ is in cp, in the case where the other components were not soluble in the nonvolatile oleic phase. The oil viscosity-temperature relations used for the Aberfeldy and M-6 oils are shown in Figs. 4.3 to 4.6, on both semi-logarithmic and arithmetic coordinates. The Aberfeldy water viscosity curves are shown in Figs. 4.7 and 4.8.

Table 4.2

FUNCTIONAL DEPENDENCE OF PHYSICAL PROPERTIES

Variable	Functional Dependence
P_{cow}	S_w, T
P_{go}	S_g, T
k_{rw}	S_w, T
k_{rg}	S_g, T
k_{ro}	S_w, S_g, T
ρ_w	p_o, T, C_{iw}
ρ_g	p_o, T, C_{ig}
ρ_o	p_o, T, C_{io}
μ_w	T, C_{iw}
μ_g	T, p, C_{ig}
μ_o	T, C_{io}
M_g	C_{ig}
M_o	C_{io}
M_w	C_{iw}
k_h	Constant
ϕ	p_o
h_w	T, C_{iw}
h_g	T, C_{ig}
h_o	T, C_{io}
C_g	T, C_{ig}
C_o	T, C_{io}
C_w	T, C_{iw}
c_s	Constant
c_{ob}	Constant

Figure 4.3 Aberfeldy Oil Viscosity-Temperature Relationship (log plot)

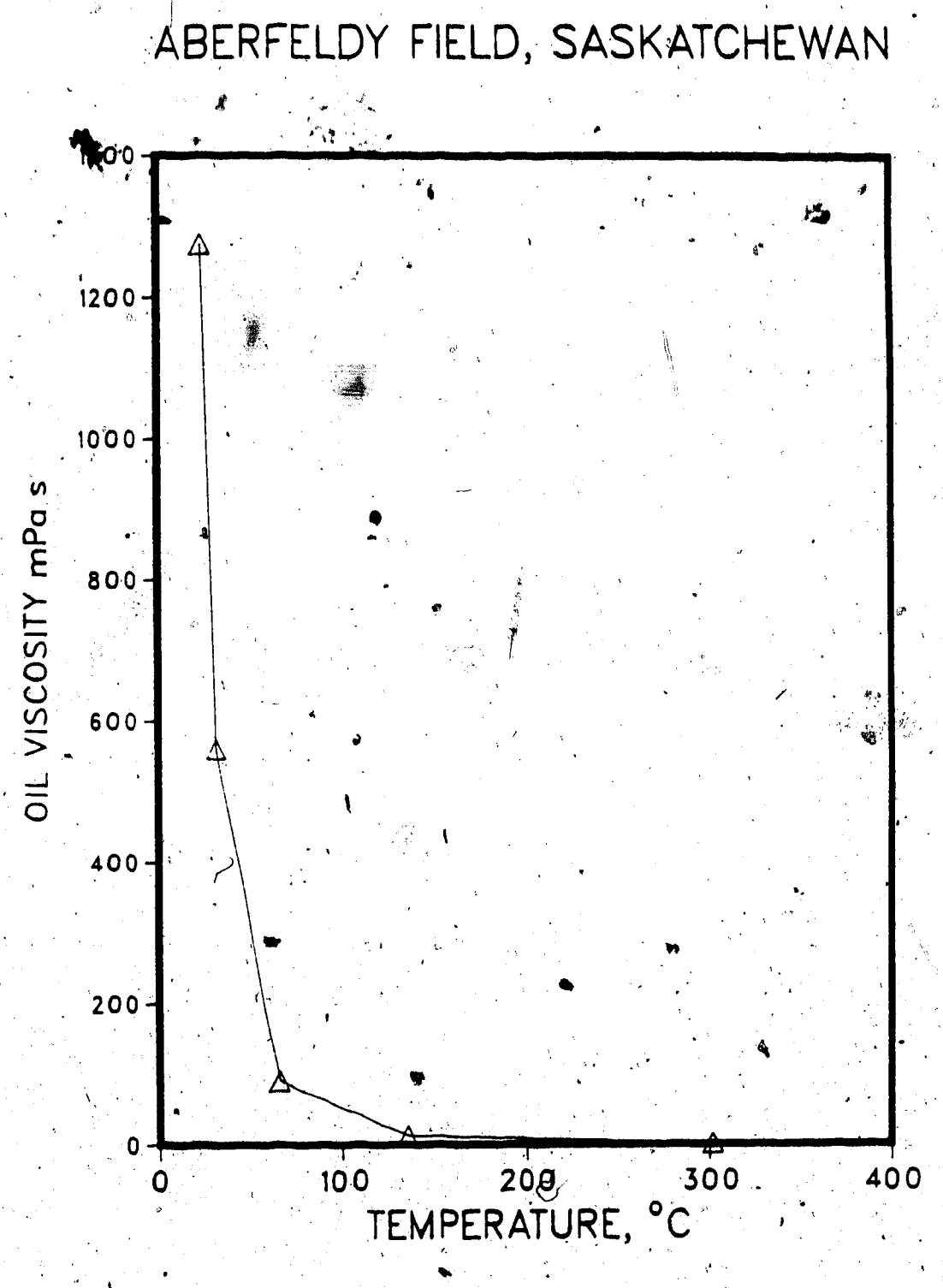

Figure 4.4 Aberfeldy Oil Viscosity-Temperature Relationship (linear plot)

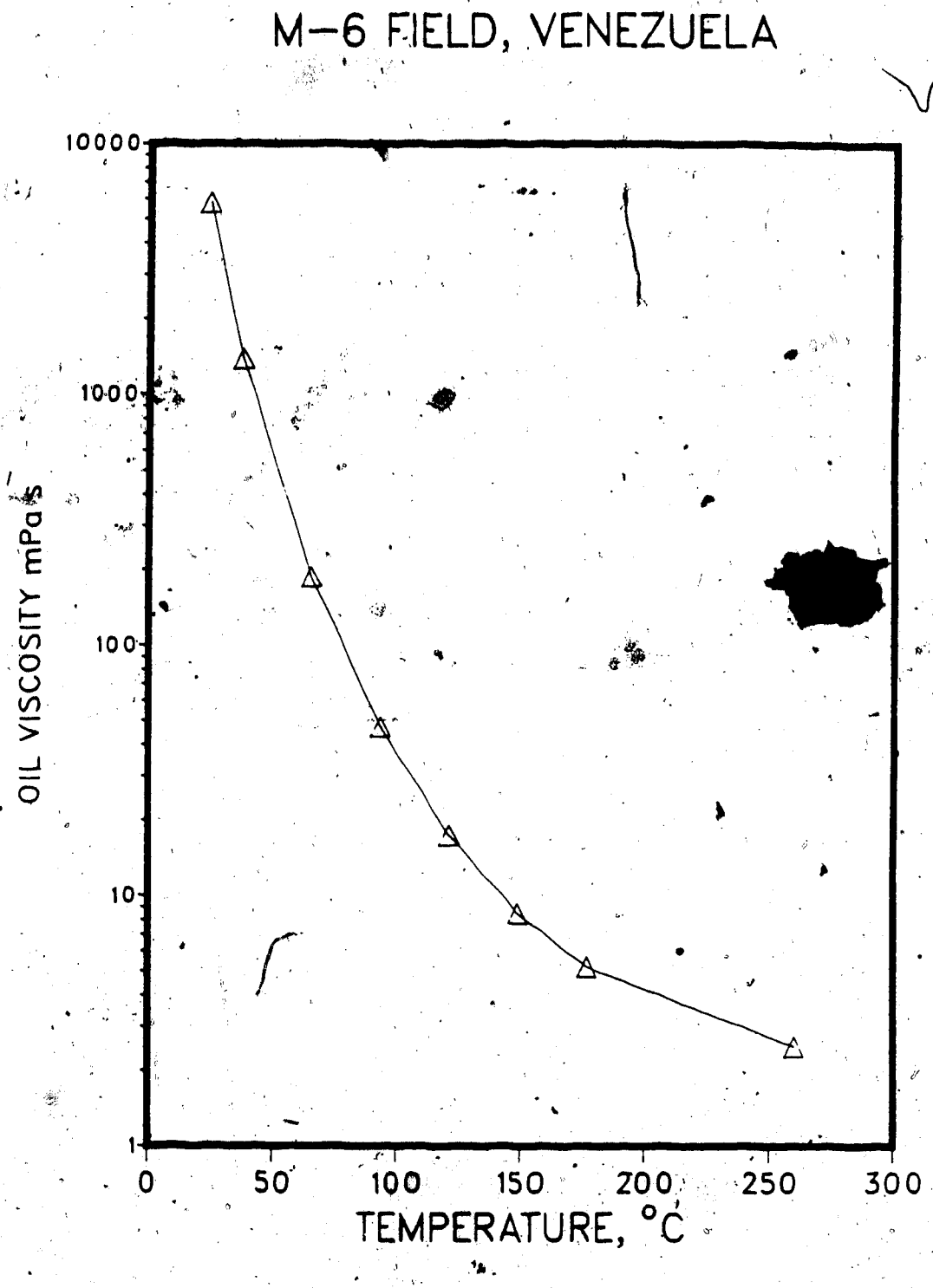

Figure 4.5 M-6 Oil Viscosity-Temperature Relationship (log plot)

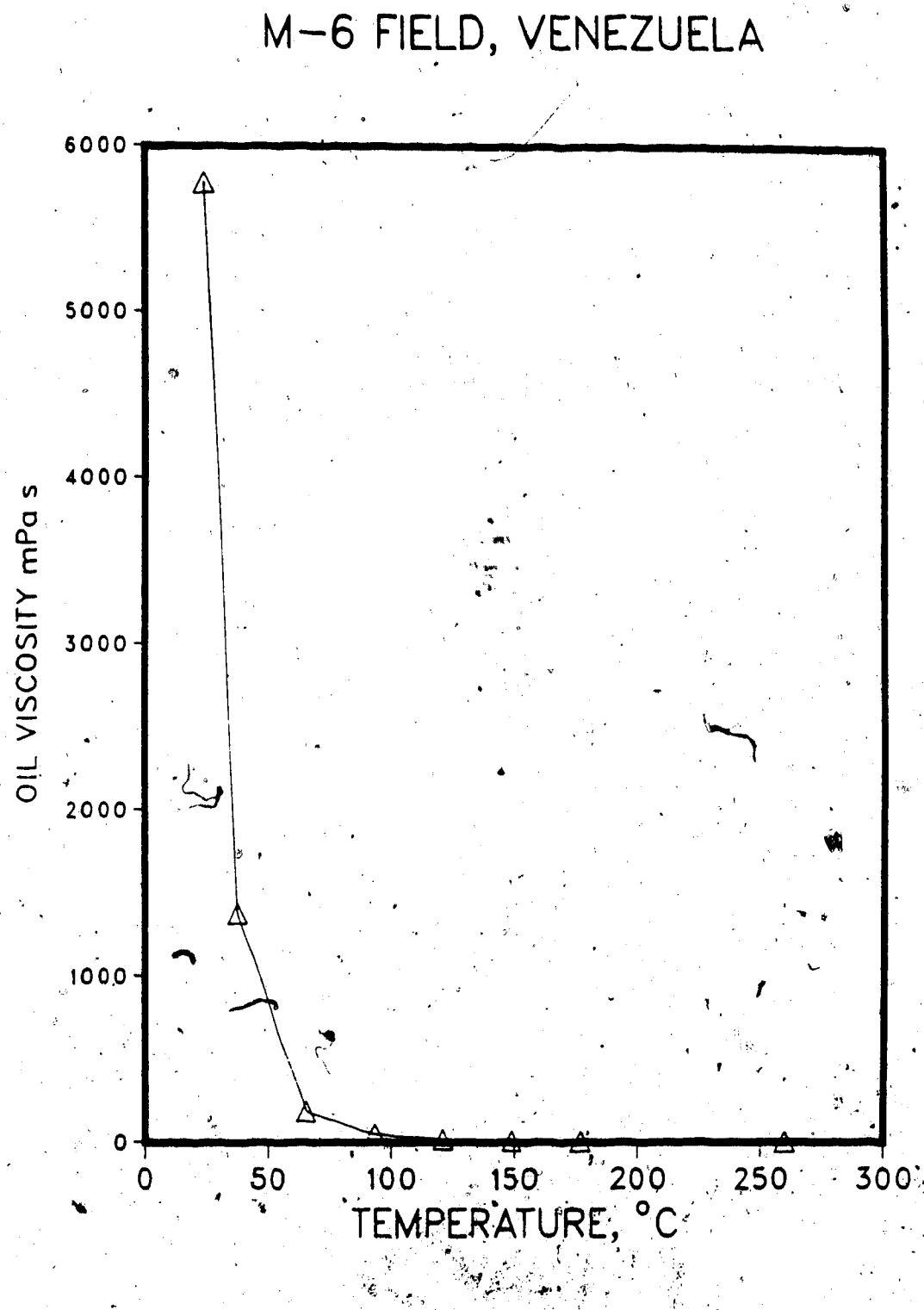

Figure 4.6 M-6 Oil Viscosity-Temperature Relationship (linear plot)

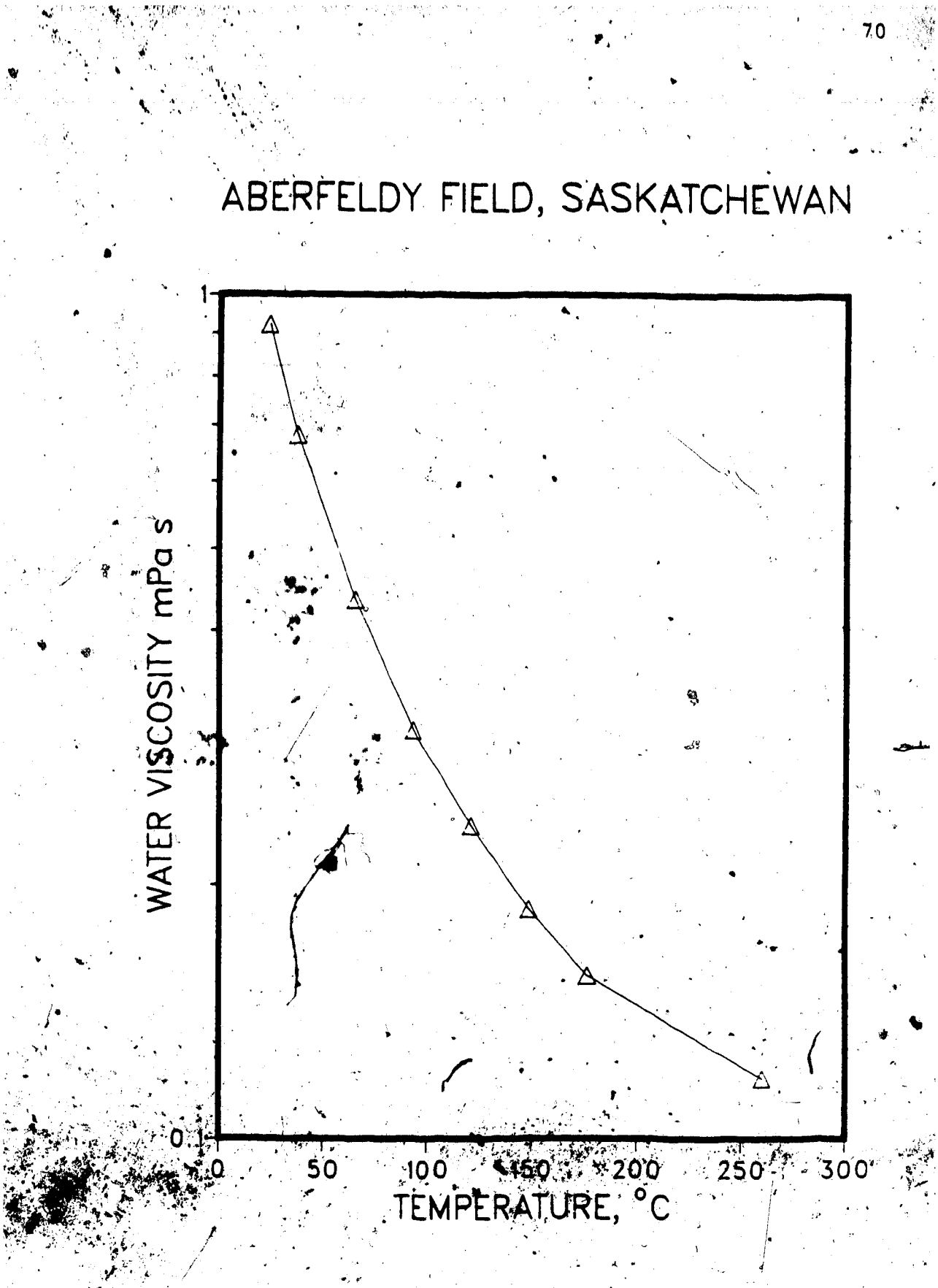

Figure 4.7 Aberfeldy Formation Water Viscosity-Temperature Curve

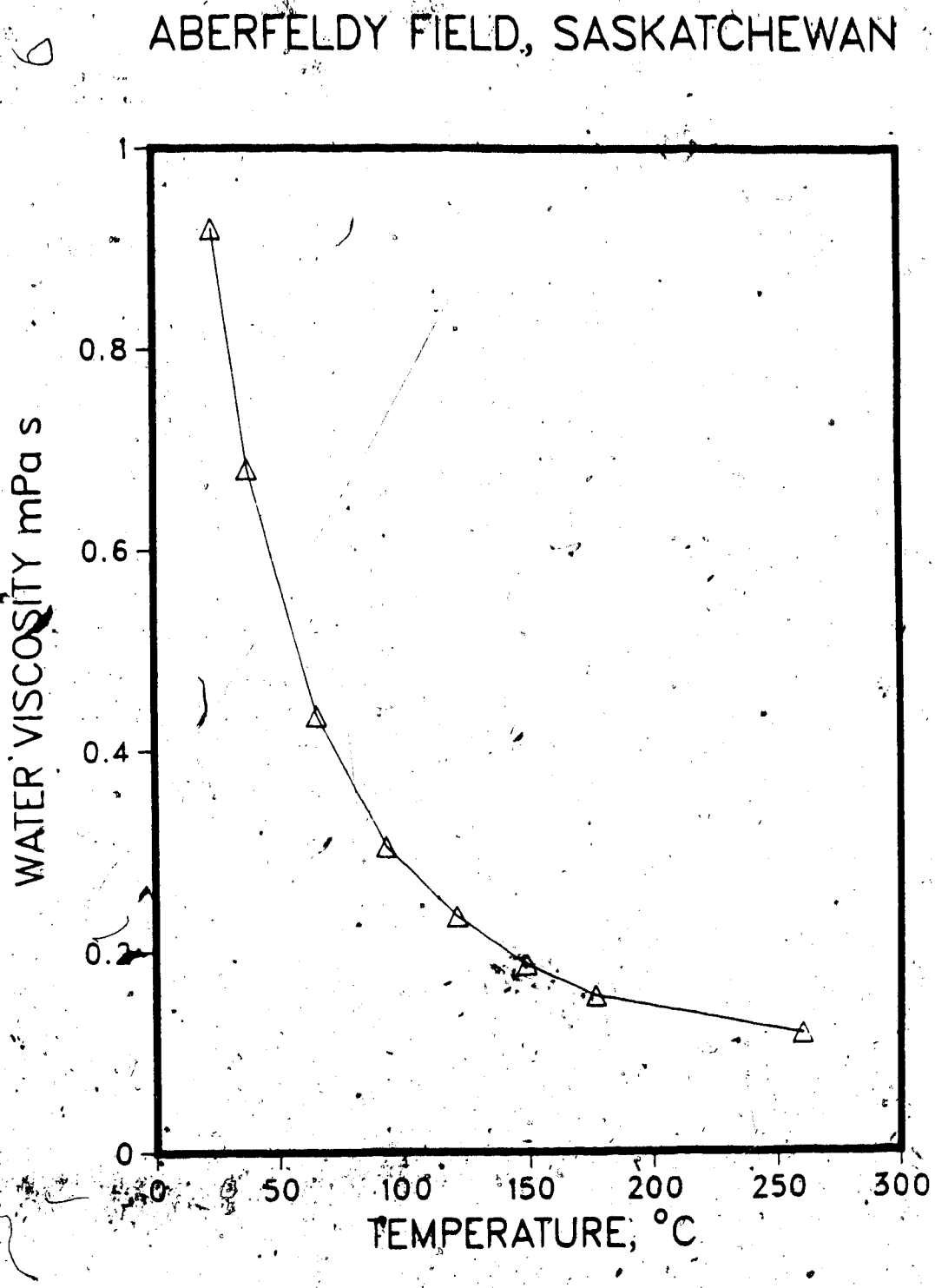

Figure 4.8 Aberfeldy Formation Water Viscosity-Temperature Curve

Non-Newtonian Oil Viscosity

Non-Newtonian oil viscosity is considered to be a function of temperature, pressure, gas solubility, and shear rate. The oil viscosity as a function of temperature is given by Andrade's equation, or Beggs and Robinson's (1975) correlation, if gas in solution is to be taken into consideration. Non-Newtonian oil viscosity was expressed by the following equation, which serves for illustrative purposes only:

$$\mu_o = \mu_{on}^{n} \gamma^{n-1} \tag{4.115}$$

where μ_o is the apparent non-Newtonian viscosity. It is possible to determine whether a fluid exhibits non-Newtonian behaviour by giving a value of shear rate to Equation (4.115) that determines the oil viscosity. With flow in porous media, a range of shear rates occurs at any average throughput. An average shear rate $\bar{\gamma}$ can be used to represent the shear rates that exist within each grid block in the reservoir corresponding to the block velocity. By using $\bar{\gamma}$ and Equation (4.115), a non-Newtonian viscosity for the flowing fluid can be obtained, for the average velocity $\bar{v}$. The average velocity in a three-dimensional block is given by

$$\bar{v} = \frac{\bar{q}_o}{A\phi} \tag{4.116}$$

where $\bar{q}$ is the average flow rate in the block, i.e.,

$$\left(\frac{\bar{q}_o}{A}\right) = \left\{\left[\left(\frac{q_o}{A}\right)_{i+1,\,j,\,k} + \left(\frac{q_o}{A}\right)_{i-1,\,j,\,k}\right]^2 + \left[\left(\frac{q_o}{A}\right)_{i,\,j+1,\,k} + \left(\frac{q_o}{A}\right)_{i,\,j-1,\,k}\right]^2\right.$$

$$+\left[\left(\frac{q_o}{A}\right)_{i,j,k-1} + \left(\frac{q_o}{A}\right)_{i,j,k+1}\right]^2 \Bigg\}^{1/2} \qquad (4.117)$$

The characteristic length in the porous medium is defined by McKinley et al. (1966) to be:

$$l = C\sqrt{k/\phi}\,. \qquad (4.118)$$

The constant C is related to the pore size distribution and tortuosity of the porous medium, and can be expressed as a function of permeability as follows (Gogarty, 1967):

$$l = f(k)\sqrt{k/\phi}\,. \qquad (4.119)$$

The average shear rate, obtained in this manner, can be obtained by dividing Equation (4.116) by Equation (4.119) as follows:

$$\bar{\dot{\gamma}} = \frac{3.55\,\bar{v}}{f(k)\sqrt{k/\phi}}\,, \qquad (4.120)$$

where the functional form of f(K) can be written as:

$$f(k) = \dot{m}\,\log\frac{k}{k_I} + \dot{P} \qquad (4.121)$$

In the above equation, the constants $\dot{m}$ and $\dot{P}$ depend on the fluid properties for a given rock. In this study, f(k) was taken to be unity (Gogarty (1967)). Equation (4.120) can be used to calculate the local shear rate in the porous medium, which is then substituted into Equation (4.115) to obtain the apparent viscosity at that point and time.

Relative Permeabilities and Capillary Pressures

The capillary pressure curve for the steam-oil system is shown in Fig. 4.9. This curve is unlike commonly used gas-oil curves, and is based upon laboratory data. Curves of this type have been employed by other investigators (Coats (1976)) in steamflood simulations. The oil-gas and oil-water relative permeability curves are shown in Fig. 4.10 and 4.12, respectively. These are based upon typical Saskatchewan reservoir data, and are used for the Aberfeldy reservoir. The respective relative permeability ratio plots are shown in Figs. 4.11 and 4.13. The temperature dependence of capillary pressure was included by making endpoints temperature dependent (only in the case of M-6 simulations). The relative permeability curves were interpolated by means of splines.

Aqueous Phase Viscosity

The aqueous phase consists of water, a very small fraction of oil, and possibly a surfactant and salt. The viscosity of this mixture μ_w was approximated as follows:

$$\mu_w = \mu_{wo}(1 + C)$$
$$= (1 + C)\frac{1776 - T}{26.5\,T - 89}, \qquad (4.122)$$

where C is the concentration of the surfactant, μ_w is in cp and T is in °F. For most cases, the Aberfeldy water viscosity curves shown in Figs. 4.6 and 4.7 were used.

Vapour Phase Viscosity

The viscosity of the vapour phase mixture can be obtained from the Herning and Zipperer (1936) equation:

$$\mu_v = \frac{\Sigma \mu_i y_i \sqrt{M_i}}{\Sigma y_i \sqrt{M_i}}, \qquad (4.123)$$

where μ_i = pure component viscosity

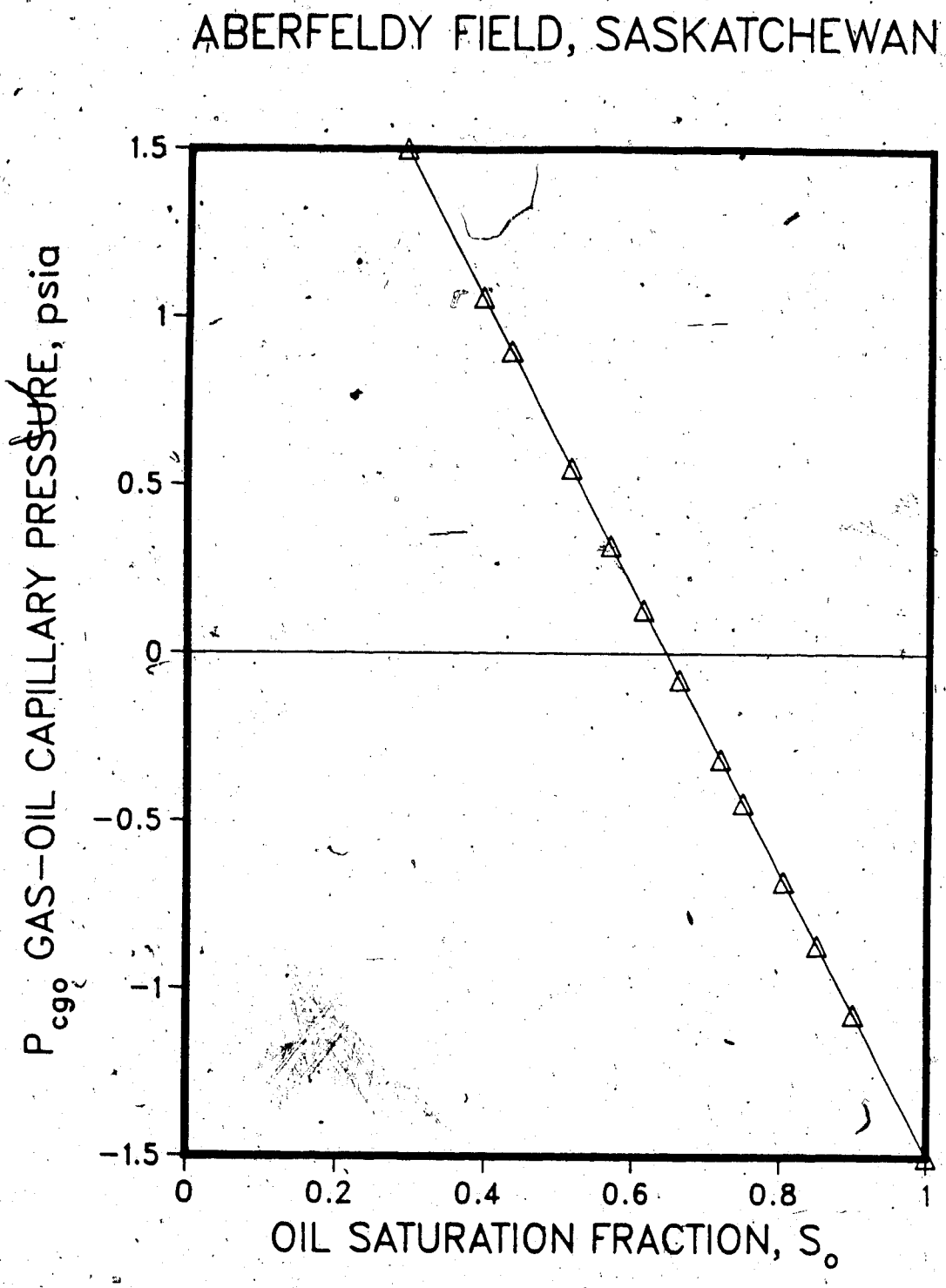

Figure 4.9 Formation Gas-Oil Capillary Pressure Relationship

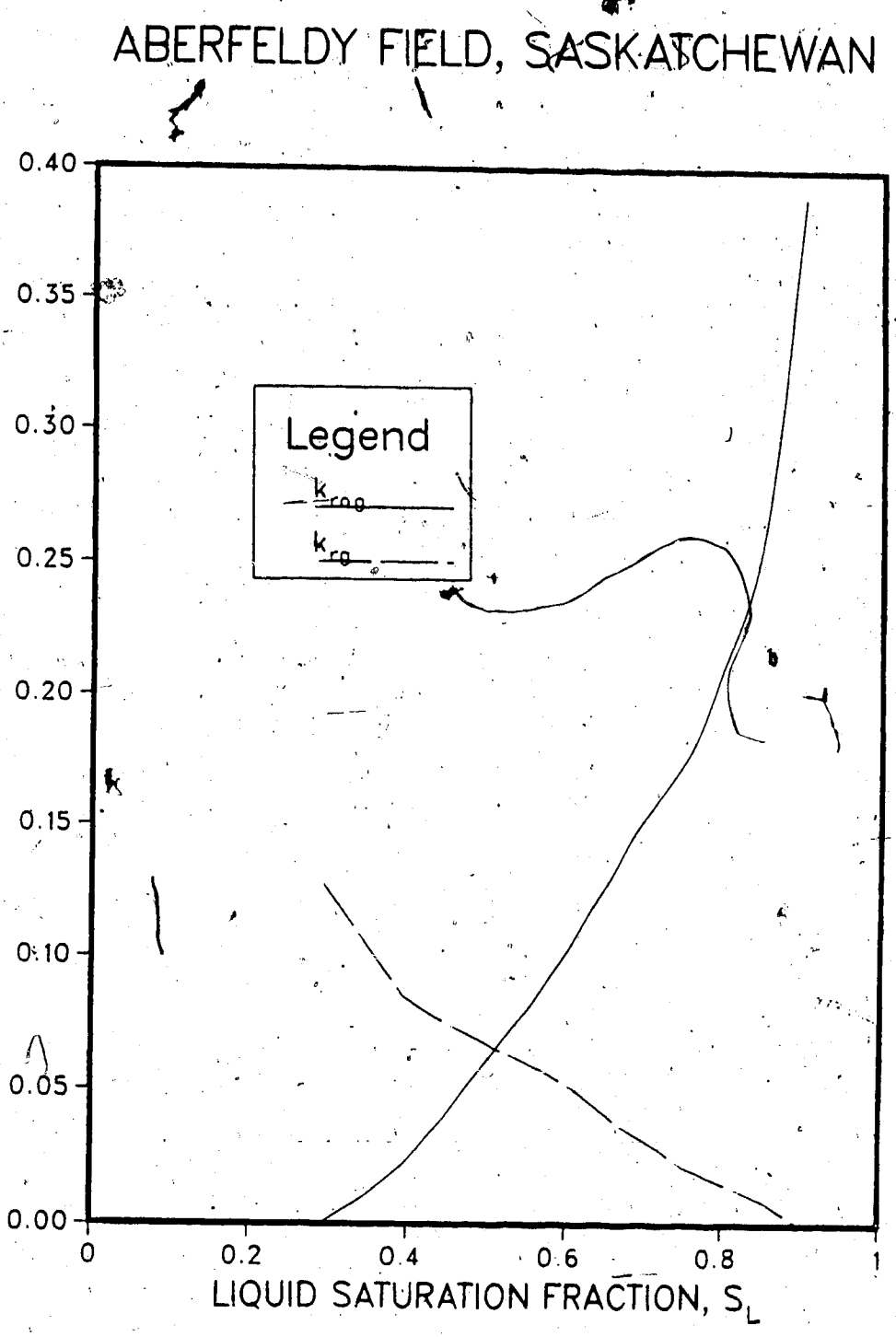

Figure 4.10 Aberfeldy Formation Gas-Oil Relative Permeability Curves.

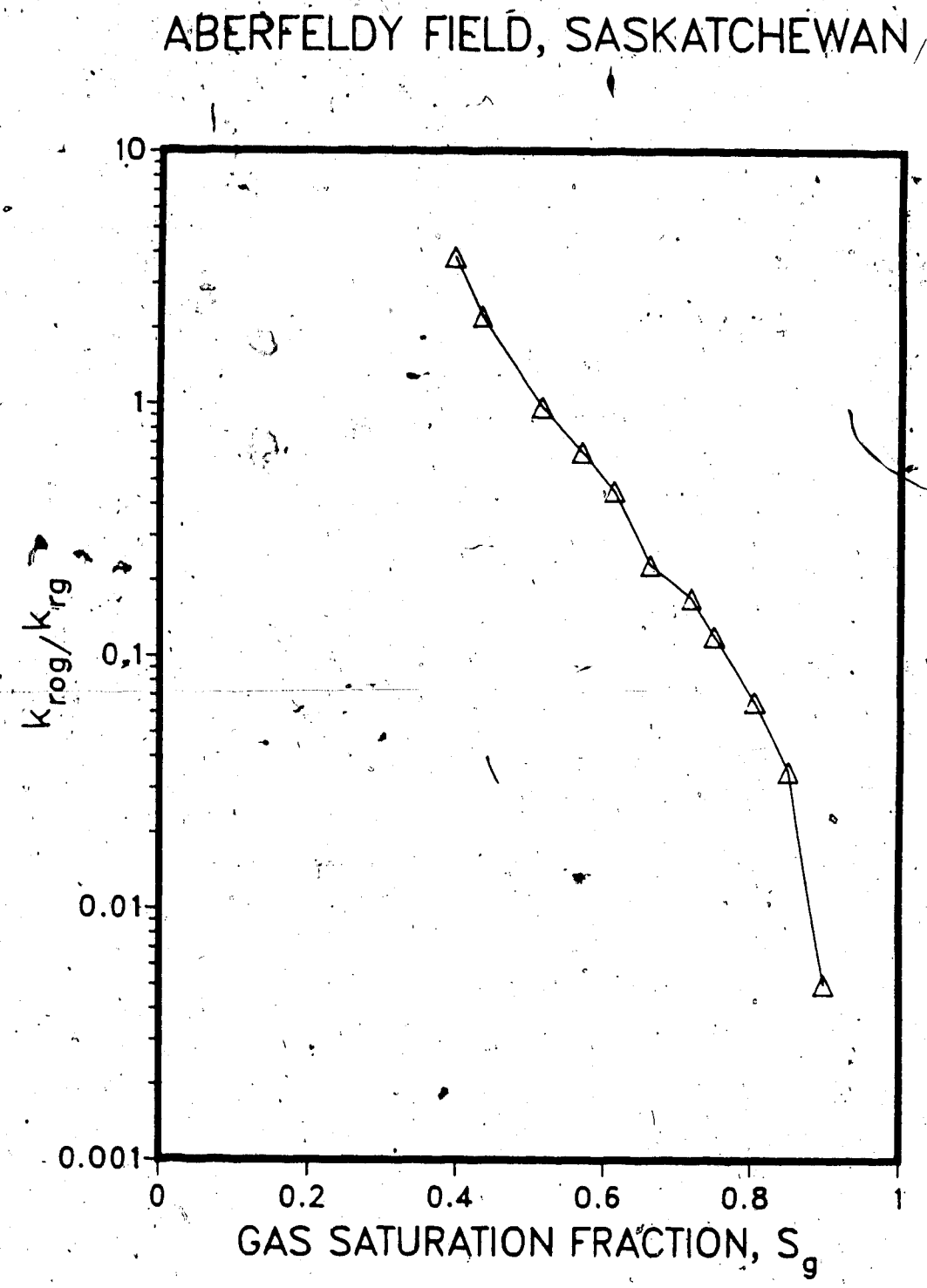

Figure 4.11 Aberfeldy Formation Gas-Oil Relative Permeability Ratio Curves

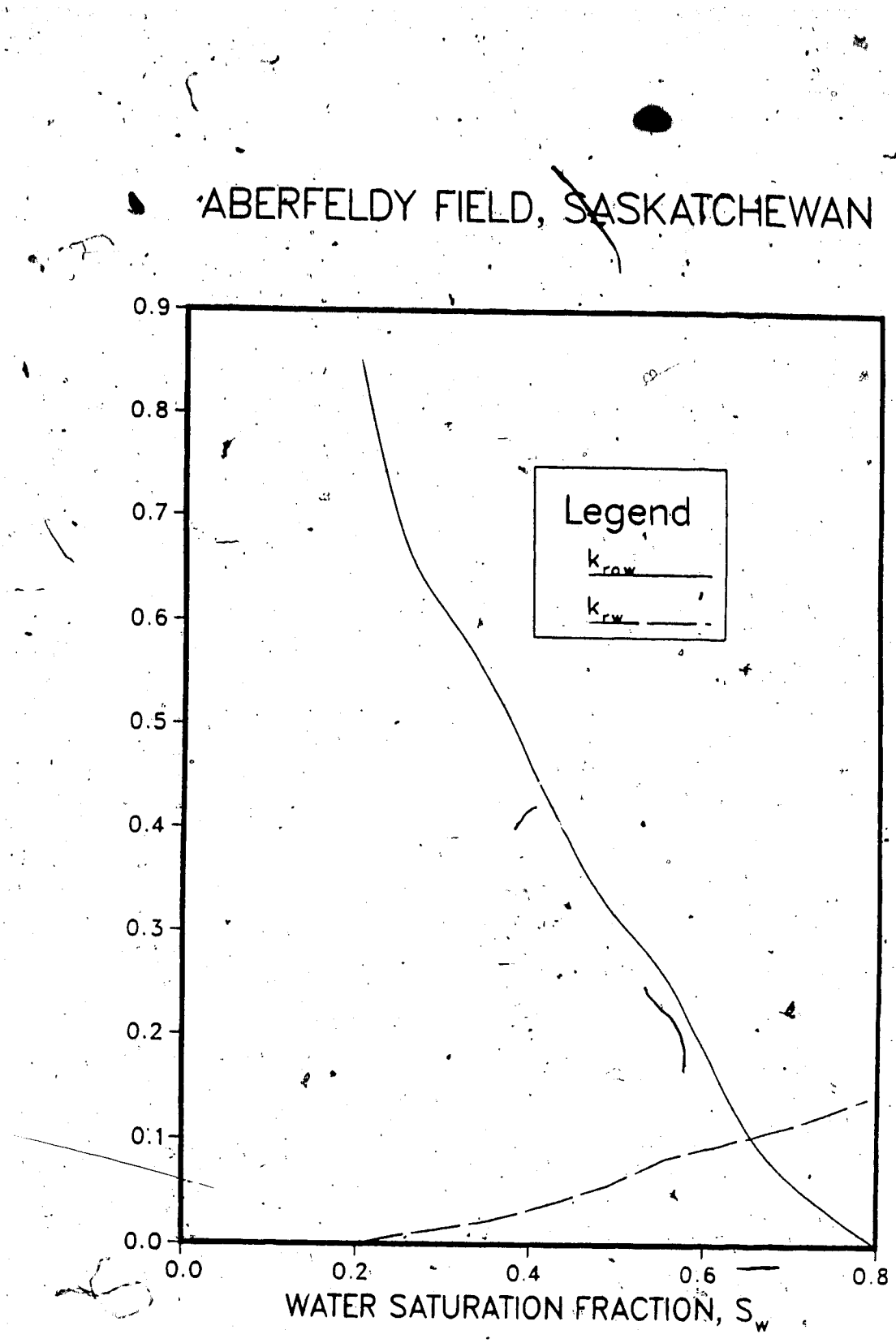

Figure 4.12 Aberfeldy Formation Water-Oil Relative Permeability Curves.

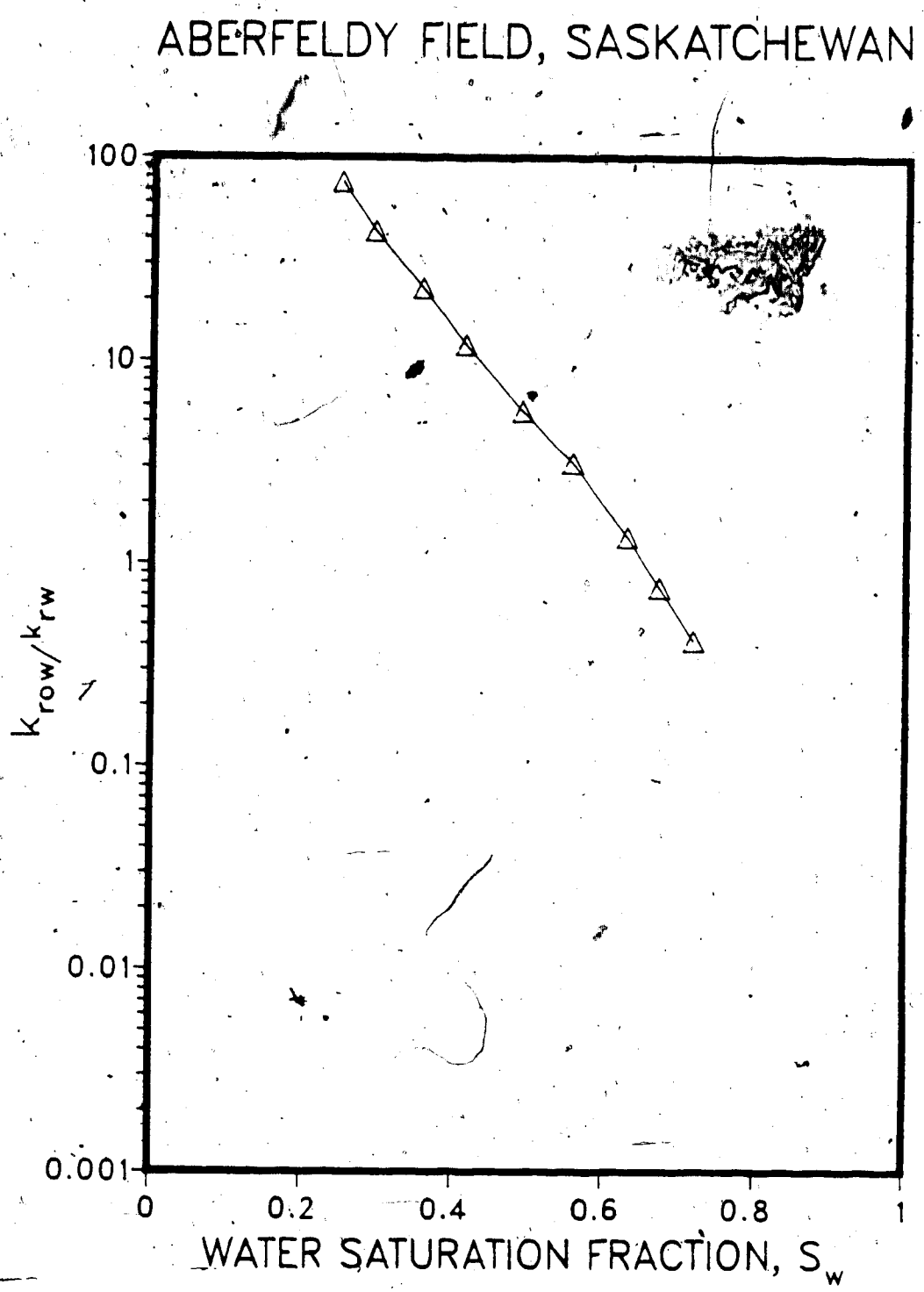

Figure 4.13 Aberfeldy Formation Water-Oil Relative Permeability Ratio Curves

M_i = pure component molecular weight

y_i = gas phase mole fraction of component i

Oil Phase Density

The density of the oil phase, ρ_o, was calculated from the following relationship, as a function of temperature and pressure (Crookston et al. (1979)):

$$\rho_o = (59.4 - 0.012\,T)\exp(10^{-5}p) \qquad (4.124)$$

where ρ_o is in lb/ft^3, p_o is in psia, and T is in °F.

Aqueous Phase Density

The density of the aqueous phase, ρ_w, was calculated from the following relationship as a function of temperature and pressure:

$$\rho_w = (60.5 - 0.0171\,T)\exp(0.004\,p_w) \qquad (4.125)$$

Equilibrium Factors

The mathematical treatment allows for as many as five components, being (1) nonvolatile hydrocarbon, (2) water, (3) surfactant, (4) noncondensable gas and (5) electrolyte. Since, in general, all components may be present in all phases, phase properties, such as molecular weights, can be expressed in terms of component properties. The equilibrium factors are defined as follows:

$$K_{iow} = \frac{x_{io}}{x_{iw}}, \qquad (4.126)$$

$$K_{iog} = \frac{x_{io}}{x_{ig}}, \qquad (4.127)$$

where K_{iow} is the equilibrium factor for oleic-aqueous phase, and K_{iog} for the oleic-vapour phase, x_{io} is the mole fraction of component i in the oleic phase, x_{iw} is the mole fraction in the aqueous phase, and x_{ig} is the mole fraction in the vapour phase. Equation (4.127) is the reciprocal of the usual two-component K-value, and was used in this form for convenience only. The model equations were developed in terms of mass fractions rather than mole fractions. Thus

$$K_{iow} = f_{iow} \frac{M_o}{M_w}, \qquad (4.128)$$

where f_{iow} is the ratio of the mass fraction of the component i in the oleic and aqueous phases, M_o is the molecular weight of the oleic phase, and M_w is the molecular weight of the aqueous phase. The molecular weight is calculated from the phase compositions. Moreover f_{iow} is a function of temperature.

Properties of Steam

Many correlations are available for calculating properties of steam. The following correlations were used in this work. These were reported by Farouq Ali (1965) and Fiori and Ejiogu (1986).

Temperature

$$T_s = 115.1\, p_s^{0.225} \qquad (4.129)$$

where T_S is in °F and p_S is in psia.

Vapour enthalpy

$$h_s = 1204.8 - 0.000197697\,(p - 453.23)^{1.73808} \qquad (4.130)$$

where h_S is in Btu/lb.

Liquid enthalpy

$$h_w = 77.036p^{0.28302} \qquad 500 \le p \le 1500 \qquad (4.131)$$

$$h_w = 0.12038p + 430.984 \qquad 1500 \le p \le 2500 \qquad (4.132)$$

where h_S and h_w are in Btu/lb.

Latent heat of water

$$L_{V_{H_2O}} = h_s - h_w \qquad (4.133)$$

where L_V is in Btu/lb.

Specific volume of steam, in ft^3/lb

$$V_s = \frac{490.386 - 0.04703}{p} \qquad (4.134)$$

Specific volume of liquid

$$V_w = 3.7175 \times 10^{-6}p + 0.01789 \qquad (4.135)$$

The latter two values are valid if $500 \le p \le 1500$; these values will be

$$V_s = \frac{551.74}{p} - 0.0887 \qquad (4.136)$$

$$V_w = 0.017529 \exp\,(1.9302 \times 10^{-4}p) \qquad (4.137)$$

if $1500 \le p \le 2500$.

Wellbore Steam Flow Model

Formulation

The wellbore model developed for this study was designed to predict steam pressure (temperature), quality, and heat loss as functions of depth and time. The sand face steam pressure and quality were then input as functions of time into the steamflood simulator. The model is an improved version of an earlier model reported by Pacheco and Farouq Ali (1972).

The system to be modeled consists of three parts: (i) the fluid flow conduit, tubing or casing-tubing annulus, (ii) casing-tubing annulus, casing wall, and the cement sheath, and (iii) the formation surrounding the wellbore. Within the conduit, steady, homogeneous two-phase flow of water and steam is assumed. This is described by combining a two-phase mass balance with a momentum balance, and is as follows (the vertical coordinate z is taken positive in the downward direction:

$$144\frac{dp}{dz} - \bar{\rho}_m\frac{g}{g_c} + \bar{\rho}_m\frac{dW_f}{dz} + \frac{\bar{\rho}_m v_m}{g_c}\frac{dv_m}{dz} = 0 \tag{4.138}$$

The subscript m in the above equations refers to the steam-water mixture.

The pressure gradient is given by

$$\frac{dp}{dz} = \frac{1}{144}\left(\frac{\bar{\rho}_m\frac{g}{g_c} - \tau_f}{1-\gamma_a}\right), \tag{4.139}$$

where γ_a is the acceleration gradient defined in the manner of Orkiszewski (1967):

$$\gamma_a = \frac{wq_s}{144A^2 g_c \bar{p}}. \tag{4.140}$$

Next, an energy balance is written for the flow under consideration, which is as follows:

$$\frac{\dot{Q}}{3600} + w\frac{d}{dz}\left(h_m + \frac{{v_m}^2}{2g_cJ_c} - \frac{g}{g_cJ_c}z\right) \doteq 0, \tag{4.141}$$

where the enthalpy h_m of a two-phase steam-water mixture is given by

$$h_m = h_m(f_{st}, p) = (1-f_{st})h_w + f_{st}h_s, \tag{4.142}$$

where f_{st} is steam quality, and h_w and h_s are enthalpies of saturated water and steam, respectively. These were calculated from the equations given in the previous section. Using these equations, and allowing for heat loss from the tubing to the cement sheath, given by

$$\dot{Q} = 2\pi r_{te}U_{te}(T - T_{cem}), \tag{4.143}$$

the energy balance equation (4.141) takes the form

$$C_1 \frac{df_{st}}{dz} + C_2 f_{st} + C_3 = 0. \tag{4.144}$$

Here U_{te} represents the net resistance to heat flow offered by the flowing fluid, tubing, insulation, annulus fluid, casing wall, and the cement sheath, and is given by

$$U_{te} = \frac{1}{r_{te}} \left[\frac{\ln \frac{r_{ins}}{r_{te}}}{k_{hins}} + \frac{1}{r_{ins}(h_r + h_c)} + \frac{\ln \frac{r_{cem}}{r_{ce}}}{k_{hcem}} \right]^{-1} \tag{4.145}$$

In the above equations the subscript "cem" refers to the cement sheath, "ins" refers to tubing insulation, if any, "ce" refers to casing exterior, and "te" refers to tubing exterior. The coefficients h_r and h_c are radiation and convection heat transfer coefficients, calculated in the conventional manner, as described by Pacheco and Farouq Ali (1972).

The heat loss term $\dot{Q}$ was calculated by solving the two-dimensional radial heat conduction equation

$$\frac{1}{r}\frac{\partial}{\partial r}\left(r\frac{\partial T_f}{\partial r}\right) + \frac{\partial^2 T_f}{\partial z^2} = \frac{1}{\alpha}\frac{\partial T_f}{\partial t}, \tag{4.146}$$

where T_f is the temperature of the surrounding formations and α is thermal diffusivity. This is a new feature; the previous authors have used the approximation of the Ei-function to estimate the temperatures around the wellbore, and thus derive the heat loss rate.

The boundary and initial conditions for the solution of Eqs.(4.139) and (4.141) are:

Initial Condition $\quad T_f = T_a + \gamma z \quad$ at $\quad t = 0$

Boundary Conditions

$$T_f = T_a \quad \text{at} \quad z = 0$$

$$T_f = T_R \quad \text{at} \quad z = Z$$

$$\dot{Q} = -2\pi r k_{hf} \frac{\partial T_f}{\partial r} \quad \text{at} \quad r = r_{cem}$$

$$\frac{\partial T_f}{\partial r} = 0 \quad \text{at} \quad r = \infty$$

Two-Phase Flow

The existing two-phase flow literature shows that the prevailing flow regime should be considered in determining holdup (and hence the average mixture density) and the friction factor. The following flow regimes were considered, using the correlations given by the authors indicated:

Flow Region Considered	*Correlation*
Bubble/Plug	Gould et al (1974)
Slug/Froth	Chierici et al (1974)
Transition	Duns and Ros (1961)

Mist Duns and Ros (1961)

Solution Procedure

Equations (4.139) and (4.144) were differenced and solved by a procedure similar to that discussed by Pacheco and Farouq Ali (1972). Equation (4.146) was discretized and solved using the backward difference (implicit) scheme. The resulting algebraic equations were solved by a band algorithm. The overall procedure was iterative, which involved updating the nonlinear coefficients and the heat transfer coefficient U_{te} at each iteration.

Chapter V

DEVELOPMENT OF THE COMPUTER MODEL

This chapter will discuss the computer program development and the structure of the computer code. The main sections of the program are discussed in detail in the following paragraphs. The program consists of a main code and two subroutines. The first subroutine calculates the fluid properties and all time-dependent transmissibilities, while the second one solves the block-banded system of linear equations resulting from the Newtonian iteration. The number of subroutines was minimized in order to reduce computational time. The program flow diagram is shown in Fig. 5.1. The program requires total memory of approximately 2 Megabytes.

Initialization

As the first step, the block data program is set to initialize all of the transmissibilities, constant as well as time-dependent. It also initializes all the source-sink terms for heat as well as fluid flow. The main program reads all of the basic data and initializes the remaining variables. An initial time step is read in; afterwards, the program selects its own time step automatically within minimum and maximum limits that are specified. The program has the flexibility of either using a single value of each variable for the entire grid, or values for the individual grid blocks.

Calculation of Transmissibilities

Before starting the calculations for a new time step, all of the time-invariant quantities are calculated, which include constant parts of the heat flow, fluid flow and diffusional transmissibilities. The time-dependent parts of the transmissibilities are calculated at each time step and are updated within each iteration.

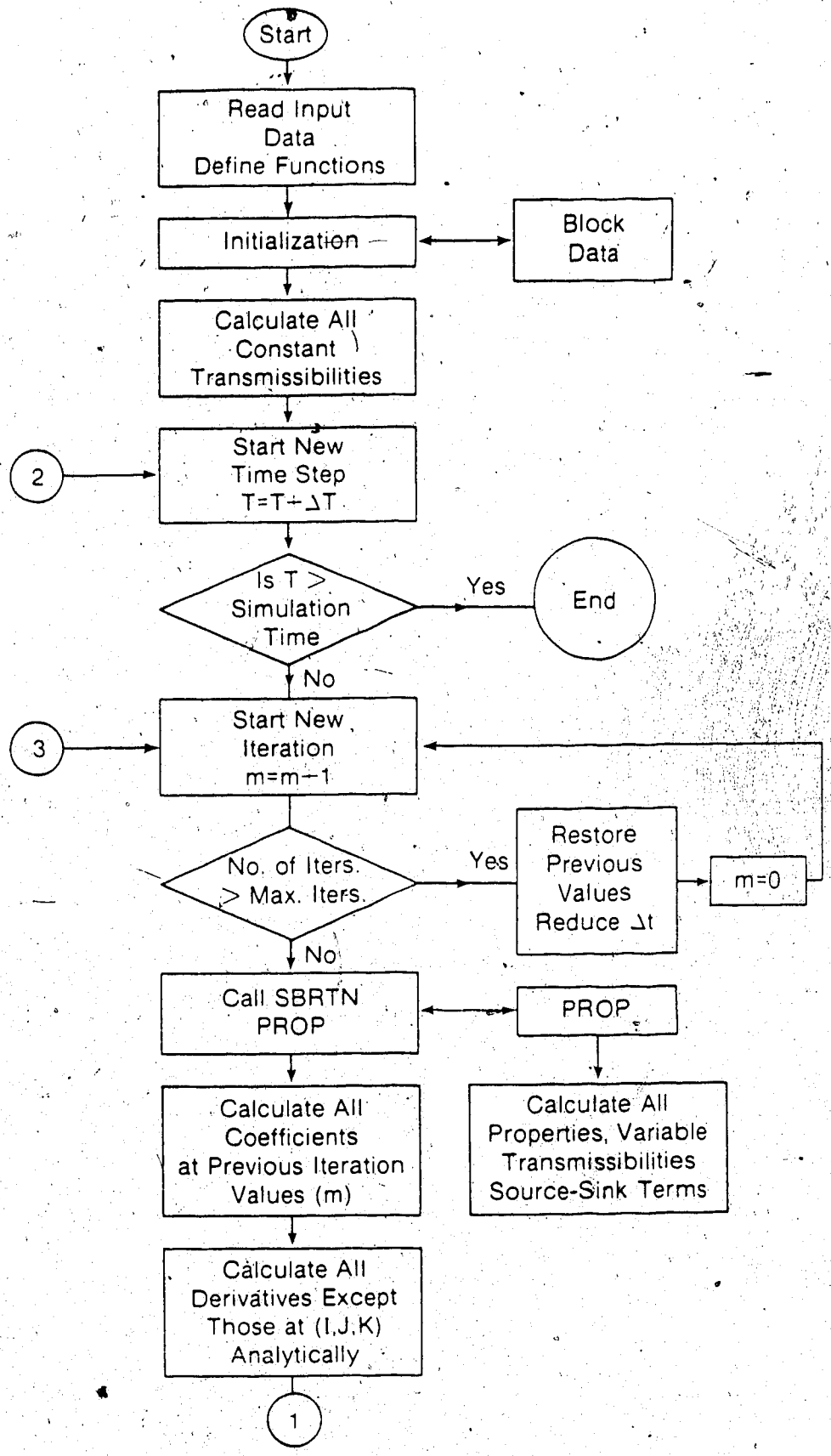

Figure 5.1 Flow Diagram of the Computational Procedure Used in the Program

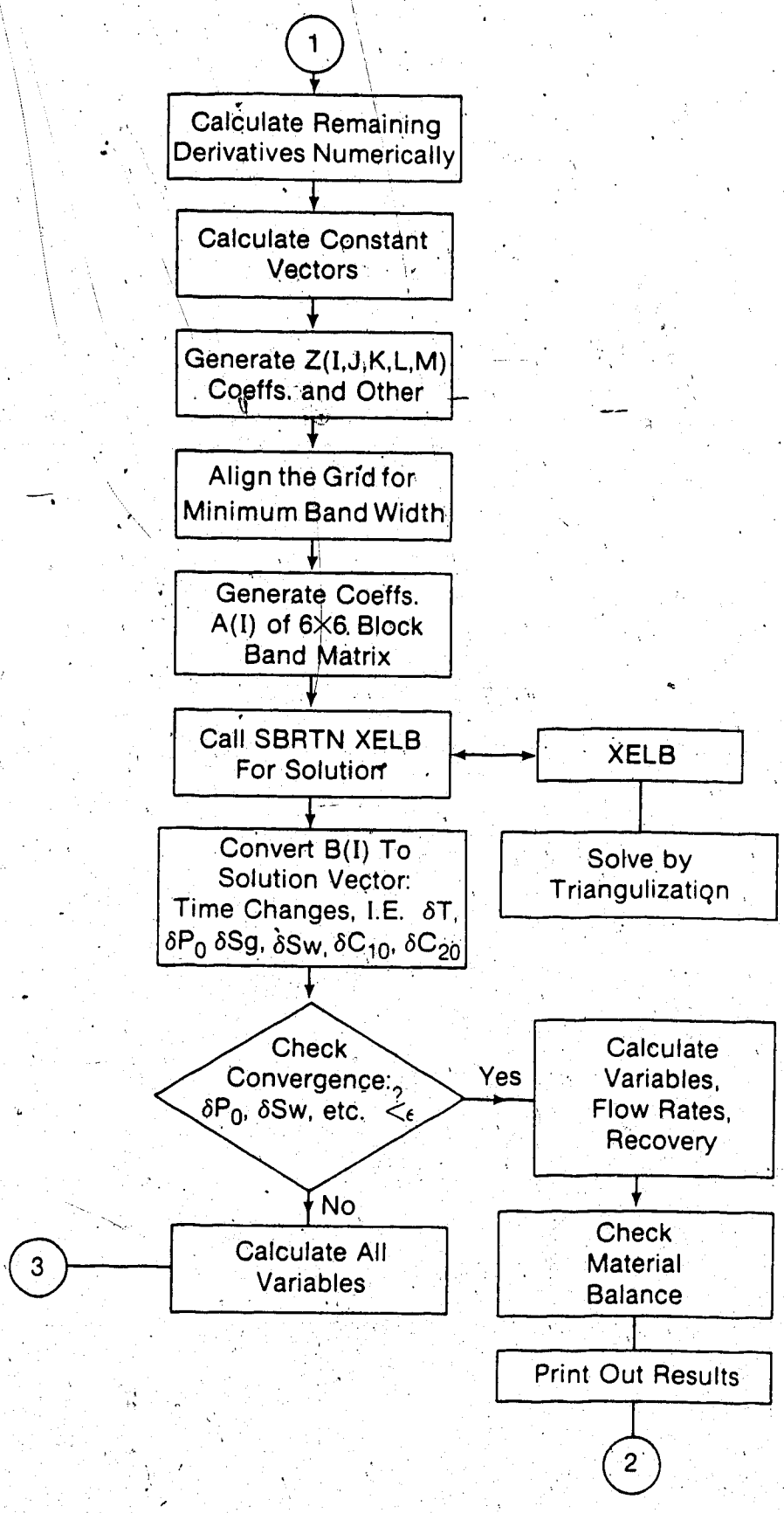

Figure 5.1 (continued) Flow Diagram of the Computational Procedure Used in the Program.

Property Subroutine

The main feature of this program is a subroutine named PROP. Once this subroutine is called, it provides the values of all of the fluid properties, their derivatives, and the coefficients. The time-dependent parts of all variables are calculated in this subfoutine and multiplied by the constant parts transferred from the main program.

The property subroutine also calculates the fluid and heat source/sink terms, using the given well specifications. These are based upon the time level (n+1) transmissibilities. The subroutine computes all arrays of derivatives of the basic properties, such as viscosity and density. Finally, it calculates a variety of summations involving transmissibiliites as well as derivatives.

Calculation of Coefficients

The coefficients Z, B, D, E, F, H, and S in the linearized Newtonian equations are long expressions, involving various derivatives and other properties. The derivatives of the mass balance equations and the heat balance equations, written in functional form, were derived analytically with respect to the variables at blocks ($i \pm 1$, j, k), (i, $j \pm 1$, k), and (i, j, $k \pm 1$). The analytical derivatives at block (i, j; k) were more tedious to obtain. The analytical expressions obtained were so lengthy that it was decided to calculate them numerically. It is believed that the numerical calculation of the derivatives led to considerable savings in computer time. Numerical calculation of derivatives can be simplified, resulting in reducing computer time, by eliminating terms in the function which do not depend on the variable of differentiation. Finite difference approximation of the convective-diffusion terms was mentioned in the previous chapter, and is given in Appendix A.

The coefficients Z, B, D, E, F, H, and S in the equations involve the above-mentioned derivatives as well as other variables. The first five equations are mass balances

for components 1 to 5, the sixth equation being the energy balance. Each equation involves six Z coefficients, six B coefficients, etc. The program generates the Z, B, D, F, H, and S coefficients, first, for the mass balance equations, and then for the energy balance. The E coefficients are calculated next in the same order. This permits writing a more efficient computer code, since the computation of coefficients is linked with the generation of analytical or numerical derivatives, as the case may be. The constant vectors for the equations are generated together with the coefficients, in the same order. The final matrix of coefficients is of the form shown in Fig. 5.2 for a 3 x 3 x 2 grid.

Solution of the System of Equations

The system of linear equations to be solved at eaeh iteration toward the new time level values consists of six times the number of grid blocks. The coefficient matrix of the equations is shown in Fig.5.2. As can be seen, it has a block diagonal structure. The solution can be obtained by Gaussian elimination or other solution techniques. In this study, it was decided to use a band algorithm, which was modified for a block diagonal matrix. This modification is quite tedious, because the transformed matrix must preserve a certain structure. Figure 5.3 shows the transformed matrix. The listing of the program developed for transforming the original block coefficient matrix of any order into a block diagonal matrix of minimum band width is given in Appendix B. It is believed that this program could be useful for any similar system of simultaneous equations arising from an implicit scheme. The program also includes the solution algorithm, which is a band matrix solver, with limited pivoting. The matrix transformation and band solver programs were extensively tested, by themselves, and were also used in a black oil simulator to ensure accuracy of solution.

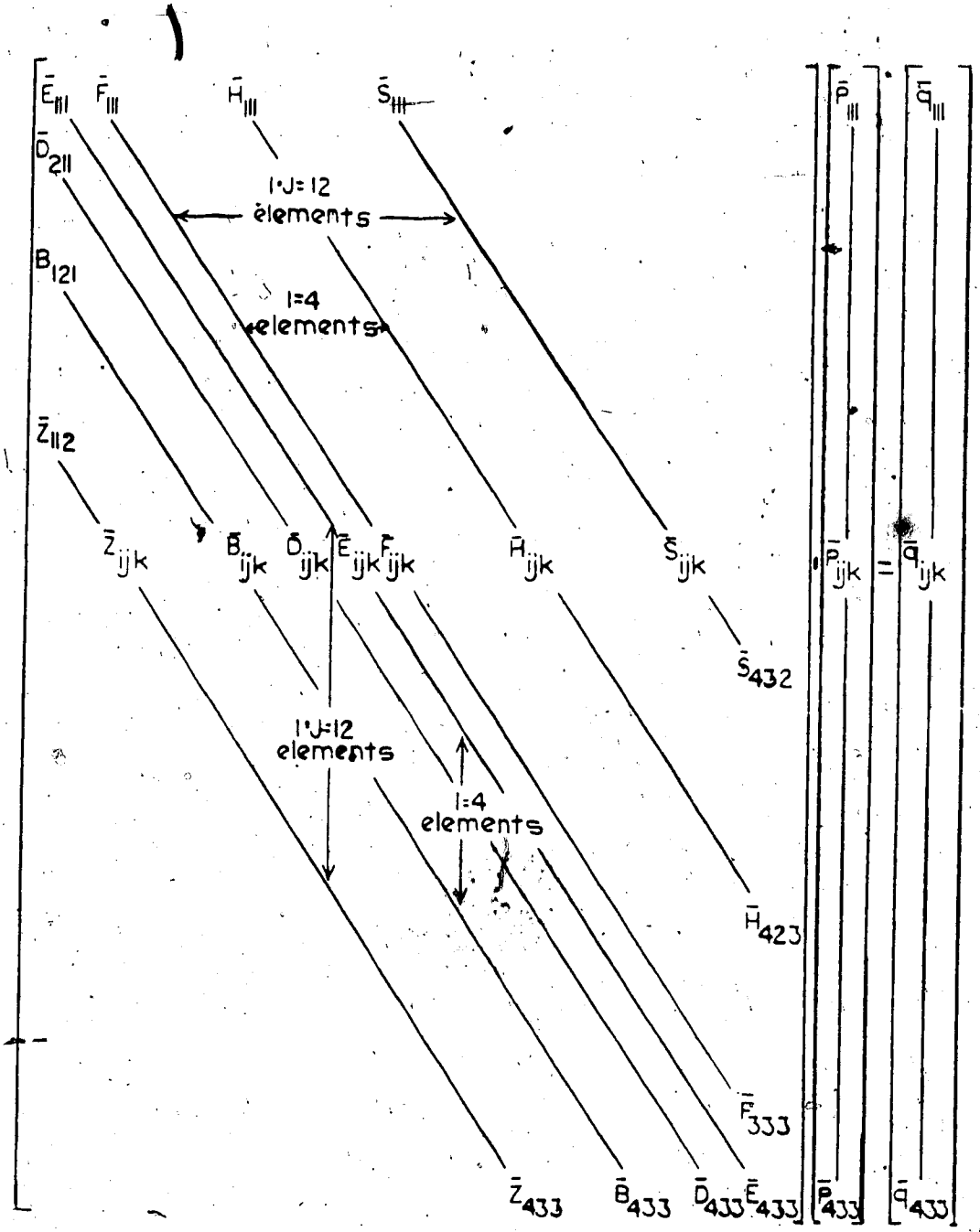

Fig. 5.2 - Matrix Form of the System of Equations, Where Each Element is a 6x6 Matrix.

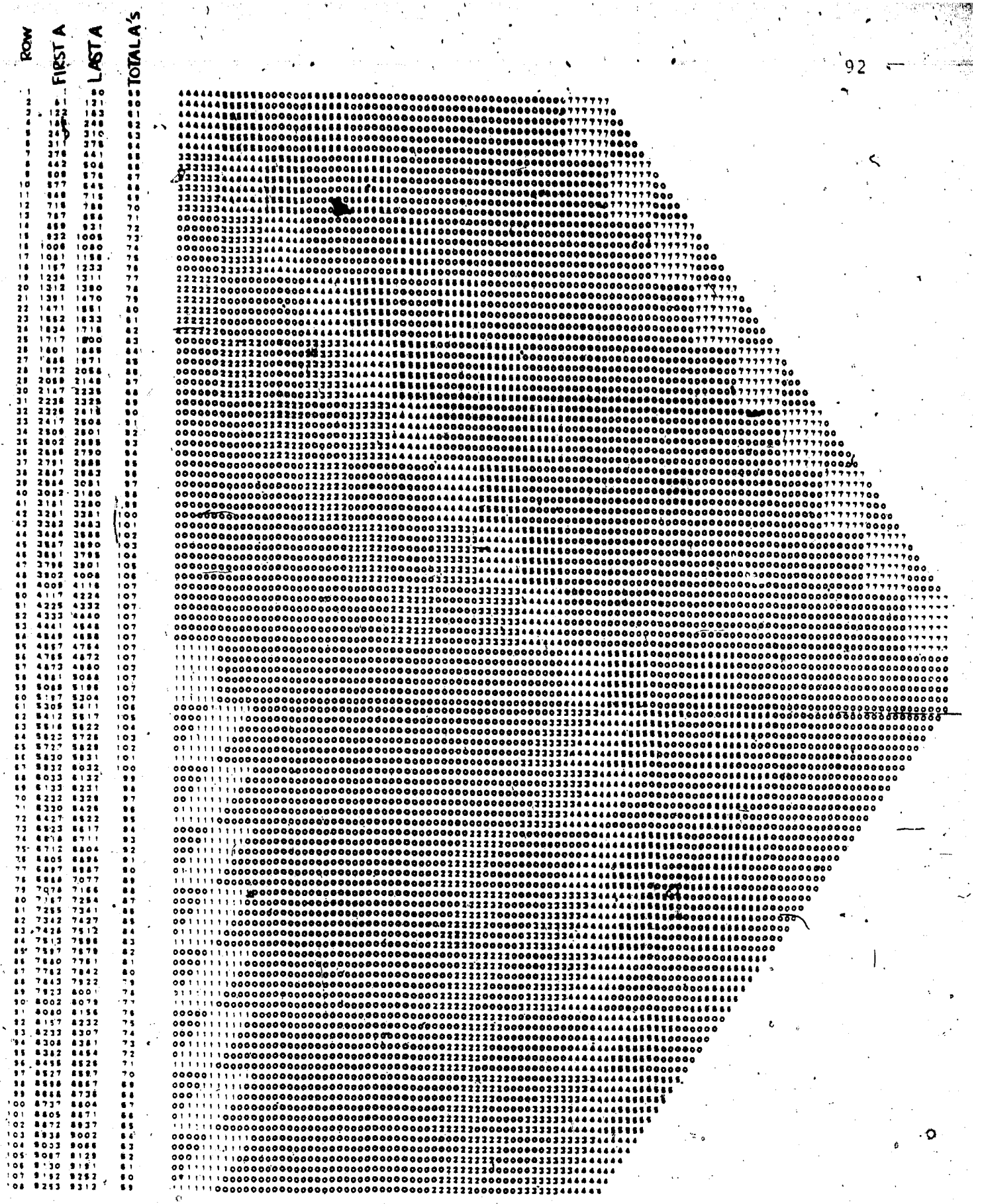

Fig. 5.3 - Form of the COefficient Matrix for Input into the Band Algorithm.

Overall Procedure

The overall solution procedure is illustrated by the program flow diagram shown in Fig.5.1. Briefly, the program first calculates the time-invariant quantities, such as constant parts of the several transmissibilities involved in the equation. The calculation of the main dependent variables, i.e. p_o, S_w, S_g, T, C_{1o} and C_{2o} at the new time level requires Newtonian iteration, which is done in an inner iteration loop. For this purpose, the derivatives, as well as all other time-dependent variables, are calculated at the latest iterates of the new time values of the variables. These are used to generate the coefficients Z, B, D, E, F, H, S, and the constant vectors in all of the equations.

Next, the coefficient matrix is transformed into a block band matrix, which is then solved by a band algorithm. The solution gives the changes in the values of the variables over one iteration, i.e. $\delta\, p_o^{(m)}$, $\delta\, S_w^{(m)}$, $\delta\, S_g^{(m)}$, $\delta\, T^{(m)}$, $\delta\, C_{1o}^{(m)}$ and $\delta\, C_{2o}^{(m)}$, where m indicates the iteration level. These are tested for convergence. If convergence is achieved, the final values of the variables at the new time level are calculated. If convergence is not attained, the derivatives and the coefficients are recalculated, and the procedure is repeated. The solution is advanced to the desired simulation time. The grids used in the simulations are shown in Fig. 5.4.

Computational Details

The program requires a memory of approximately 2 Megabytes for a 5 x 5 x 2 grid. The number of simultaneous equations to solve in this case is 300, which alone takes 11 seconds of CPU time amounting to approximately 2 millisec/grid block/time step. This is rather slow, even for the coarse grid used. The machine time can be reduced through the use of two dimensions and/or fewer number of components. For large grids necessary for commercial simulations, the code must be adapted for a supercomputer.

Grid II

Diagonal grid Areas
Shown is $A/2 = d^2$

Grid III

Diagonal grid Pattern
Area A

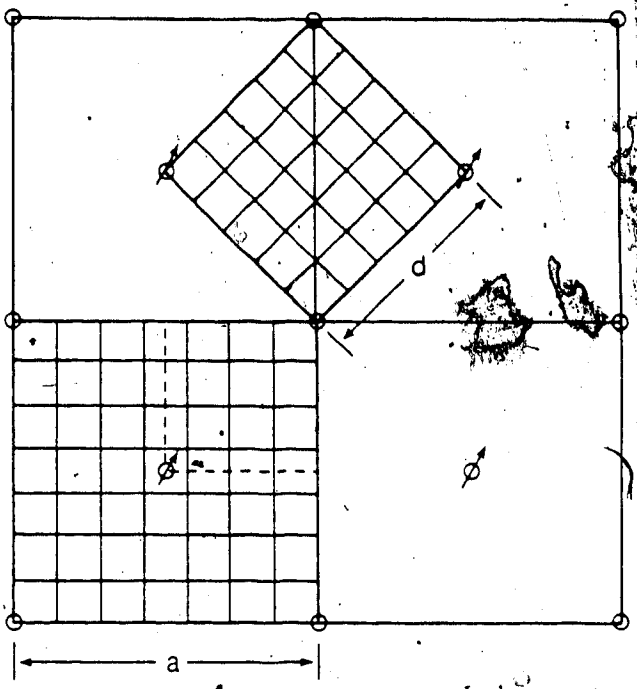

Grid I

Pattern position chosen
to conform with the
grid in parallel orientation
Pattern Area A

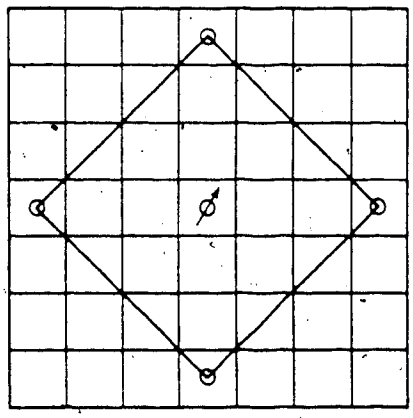

Figure Grids used in the steamflood and cyclic steam stimulation simulations.

Figure 5.4 Types of Grids used in the Simulations

The three-phase, three-dimensional model was validated using the Test Problem 1 given by Coats (1976). The oil, water, and gas saturation distributions and pressure distribution at 1800 days were within 5% of the values quoted. The cumulative oil recovery was 67% vs 66.4%. It can be said that the simulator is valid for at least one previously studied problem. The material balance and the heat balance errors at all times were less than 0.1%, and much smaller in most cases.

Chapter VI

DISCUSSION OF RESULTS

Introduction

This numerical study of steam injection examines steam injection processes in the contexts of foam injection, additive gas, thermal upgrading, and non-Newtonian oil viscosity behaviour; it evaluates the effect of bottom water on steamflooding and cyclic steam stimulation response, with particular attention to partial penetration, and examines the effect of multiple steam offtake from the injection tubing on steamflood response. These are the principal contributions of this work, and are believed to represent new information.

In the following discussion, sample results are presented for each of these aspects of steam injection. The objective is to study the effect of these phenomena in a steam injection simulator, and to provide an idea of the relative importance and magnitudes of such effects. It is not possible to discuss these in depth because of time and other constraints, one of which is the computer time available.

Simulators Developed

Three steam simulators were developed over the period of this study. The fully implicit five-component three-dimensional three-phase simulator was extremely slow, limited to short runs. The other two simulators, viz. three-dimensional two-component and two-dimensional four-component three-phase simulators were used for the runs discussed here. In particular, the first of these simulators was successful in simulating virtually every steam injection situation, with regard to solution stability and fast convergence. Even then a short simulation (e.g. 3 years) consumed over 500 seconds of CPU time.

For wellbore simulations, a wellbore heat loss model was extended for flow regime considerations in the tubing, and in particular, multiple offtake of steam, which has not been simulated heretofore.

Reservoir Data Employed for the Simulations

Three different heavy oil reservoirs were considered in this work: Aberfeldy, Saskatchewan; M-6, Venezuela; and Cold Lake, Alberta. The data used for these simulations are given in Table 6.1. The relative permeability and viscosity-temperature curves are shown in Figs. 4.3 to 4.13. The methods used for foam upgrading, and non-Newtonian oil implementation were described in Chapter IV. The formation thicknesses given in Table 6.1 are realistic for the reservoirs considered. In one or two cases, other thicknesses were also used in order to be able to compare the results. The bottom water thickness varies from zero to equal to the oil zone thickness, because the objective was to examine the effect of bottom water. It is possible to make certain rock properties, such as compressibility, specific heat, thermal conductivity and thermal diffusivity functions of the variables involved, in the simulators. However, this was considered to be unnecessary because of the uncertainty in the data available. Similar considerations hold for the parameters used in the thermal upgrading, foam, and non-Newtonian oil viscosity models, where even less consistent information has been published.

The grids used were coarse, ranging from 18 to 200 grid blocks, in view of the excessive CPU time required for finer grids, particularly because in the fully implicit scheme, three to six equations are solved for each block. A few runs were repeated for short durations using finer grids. The discrepancy in computed oil recoveries was less than 5%, and in oil saturations, etc., less than 10%, for grid size change from 18 to 147 grid blocks.

Types of Simulations Conducted

Several types of simulations were carried out for this study. These are summarized pictorially in Fig. 6.1. Detailed results are given in the tables in Appendix C. It is seen that not all runs were repeated for all three reservoirs considered, because the purpose was to

Table 6.1

RESERVOIR DATA USED IN THE SIMULATIONS

		Aberfeldy Saskatchewan	Cold Lake Alberta	M-6 Venezuela
Formation thickness, ft		36	36 to 150	98
Water zone thickness, ft		3.6 to 36	3.6 to 36	9.8 to 98
Formation permeabilities, darcy	k_x	2.0	2.0	2.0
	k_y	2.0	2.0	2.0
	k_z	0.4 to 2.0	2.0	0.4 to 2.0
Porosity, %		35	35	35
Reservoir pressure, psi		200	500	150
Reservoir temp, °F		74	74	113
Oil viscosity at reservoir temp, cp		1275	125,000	5780
Water compressibility, psi^{-1}		3×10^{-6}	3×10^{-6}	3×10^{-6}
Water thermal expansion coeff., $°F^{-1}$		4.9×10^{-4}	4.9×10^{-4}	4.9×10^{-4}
Oil compressibility, psi^{-1}		5×10^{-6}	5×10^{-6}	5×10^{-6}
Oil thermal expansion coeff., $°F^{-1}$		5×10^{-4}	5×10^{-4}	5×10^{-4}
Rock compressibility, psi^{-1}		1×10^{-4}	1×10^{-4}	1×10^{-4}
Formation thermal conductivity, Btu/hr-ft-°F		1.76	1.76	1.76
Overburden thermal conductivity, Btu/hr-ft-°F		1.47	1.47	1.47
Overburden density, lb/ft^3		165	165	165
Overburden specific heat, Btu/lb-°F		0.20	0.20	0.20
Overburden thermal diffusivity, ft^2/hr		0.04	0.04	0.04
Relative permeabilities		Figs. 4.10 and 4.12	→	→
S_{wc}, fraction		0.20	0.20	0.20
S_{or}, fraction		0.211	0.211	0.211
S_{gc}, fraction		0.1	0.1	0.1

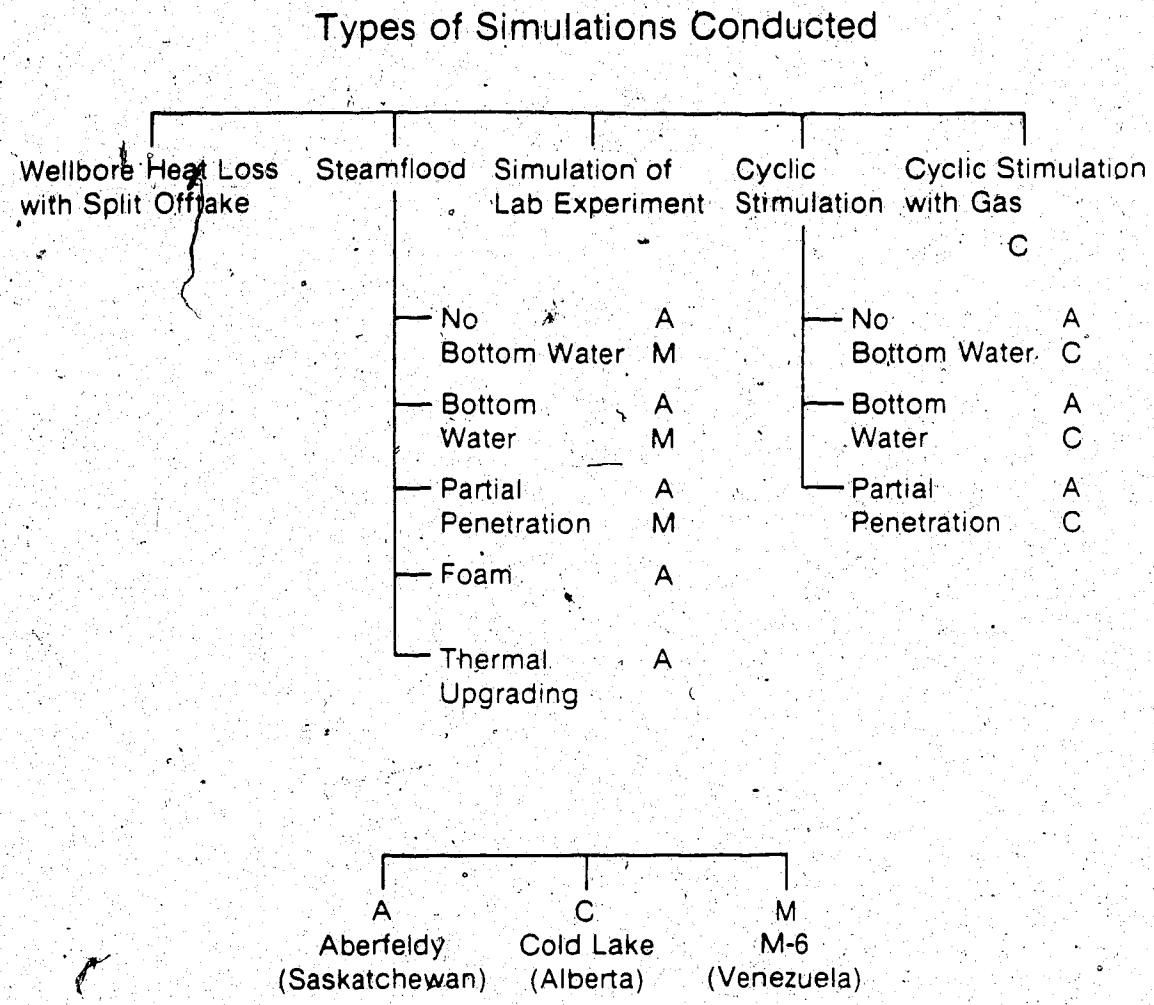

Figure 6.1 Diagram Showing the Types of Simulations Conducted in this Study

show the effects of differences in reservoir characteristics on the steam injection process under consideration. It is seen that a large number of simulations were made in the case of Aberfeldy reservoir, because of the importance of bottom water in this type of reservoir. The runs were more computer time-consuming in the case of the Clearwater formation, Cold Lake, due to very high oil viscosity, which limited the number of runs. No computational difficulties were encountered in any of the cases studied. At times, the automatic time step selection procedure produced very small time steps (order of 0.005 day), which increased the CPU time.

Base Steamflood for Aberfeldy

The base steamflood results for the Aberfeldy reservoir (ABRS1) are listed in Table 6.2, and plotted in Figs. 6.2 to 6.4. Selected time results are given in Table C.1. A 2 acre five-spot pattern was considered in this run, with a steam injection rate of 600 B/D CWE (CWE=Cold Water Equivalent), steam pressure of 500 psia, and sand face steam quality of 70%. Formation thickness was 36 ft, and no bottom water layer was present. The oil and water production histories shown in Fig. 6.2 are typical of steamfloods, with an initially low production rate, increasing to a high value toward the end of the simulation. The water production rate goes through a peak, and then decreasees. Figure 6.3 shows that the WOR (water-oil ratio) peaks at about 18, then steadily declines. This is so because the temperature increase in the producers leads to increasing oil mobility, while water mobility increases much less. This results in a steady increase in the oil-steam ratio, as shown in Fig. 6.4. This trend will continue to a point only. For very large volumes of steam injection, the oil-steam ratio would eventually decrease, since there is not enough mobile oil on one hand, and steam mobility is greatly increased on the other.

Conducting a simulation of this type for very long periods not only requires considerable computer time, but also requires considerable simulation experience. Once the wells get sufficiently hot, the oil mobility increases exponentially, and so does steam

Table 6.2

ABERFELDY STEAMFLOOD RUNS RESULTS SUMMARY

Run No.	Steam Inj. Rate B/D	h_w h_{oil}	Completion	500 days OSR m^3/m^3	500 days Cum. WOR	500 days Oil Rec. %	500 days Inst. WOR	700 days OSR	700 days Cum. WOR	700 days Oil Rec. %	700 days Inst. WOR	Comments
ABRS1	600	0	1-2	0.097	3.79	1.75	9.32	0.250	1.47	6.25	4.2	
ABRS2	600	1.0	1-1	0.028	24.4	0.47	22.70	0.034	20.6	0.81	728.5	
ABRS3	600	0	1-2	0.0878	4.80	1.56	10.15	0.189	2.18	4.81	5.2	
ABRS4	1200	0	1-2	0.131	1.99	4.71	7.40	0.290	1.18	14.56	3.4	S_g = .02
ABRS5	600	0.2	1-1	0.0543	12.1	1.15	16.23	0.113	3.62	3.32	10.7	
ABRS6	600	0.1	1-1	0.075	8.34	1.66	12.97					
ABRS7	600	0.28	1-1	0.0473	13.55	0.988	18.04	0.0745	9.89	2.16	14.6	(note2)
ABRS8	1200	0	1-2	0.164	1.89	5.74	5.92	0.331	1.12	16.2	2.98	S_{gT} = 0 S_{gB} = 0
ABRS11	600	0	1-2	0.648	0.73	11.6	0.98	0.883	0.859	22.17	.88	
ABRS13	300	0	1-2									
ABRS14	1200	0	1-2	0.196	1.60	7.02	5.09	0.355	1.22	17.8	2.8	S_g = .02
ABRS9	600	0.1	-	0.0769	8.31	1.69	12.86		-			(note1)
ABRS10	1200	0	1-2	0.081	6.0	0.721	10.08	0.186	2.73	2.35	5.5	S_{gT} = .05 S_{gB} = .05
ABRS15		0.2	1-1	0.055	12.3	1.17	16.24	0.0922	6.34	2.58	12.5	(note2)
ABRS16		0.2	1-1	0.376	1.53	8.02	1.90	0.627	0.757	18.0	1.5	

Notes: 1. Injection in 2-2, prod. from 1-1 (2-2 is bottom water layer, 1-1 is oil layer).
2. Vertical permeability = 1/5 horizontal permeability.
3. Steam quality in all runs is 70% except in Run ABRS3 it is 30%.

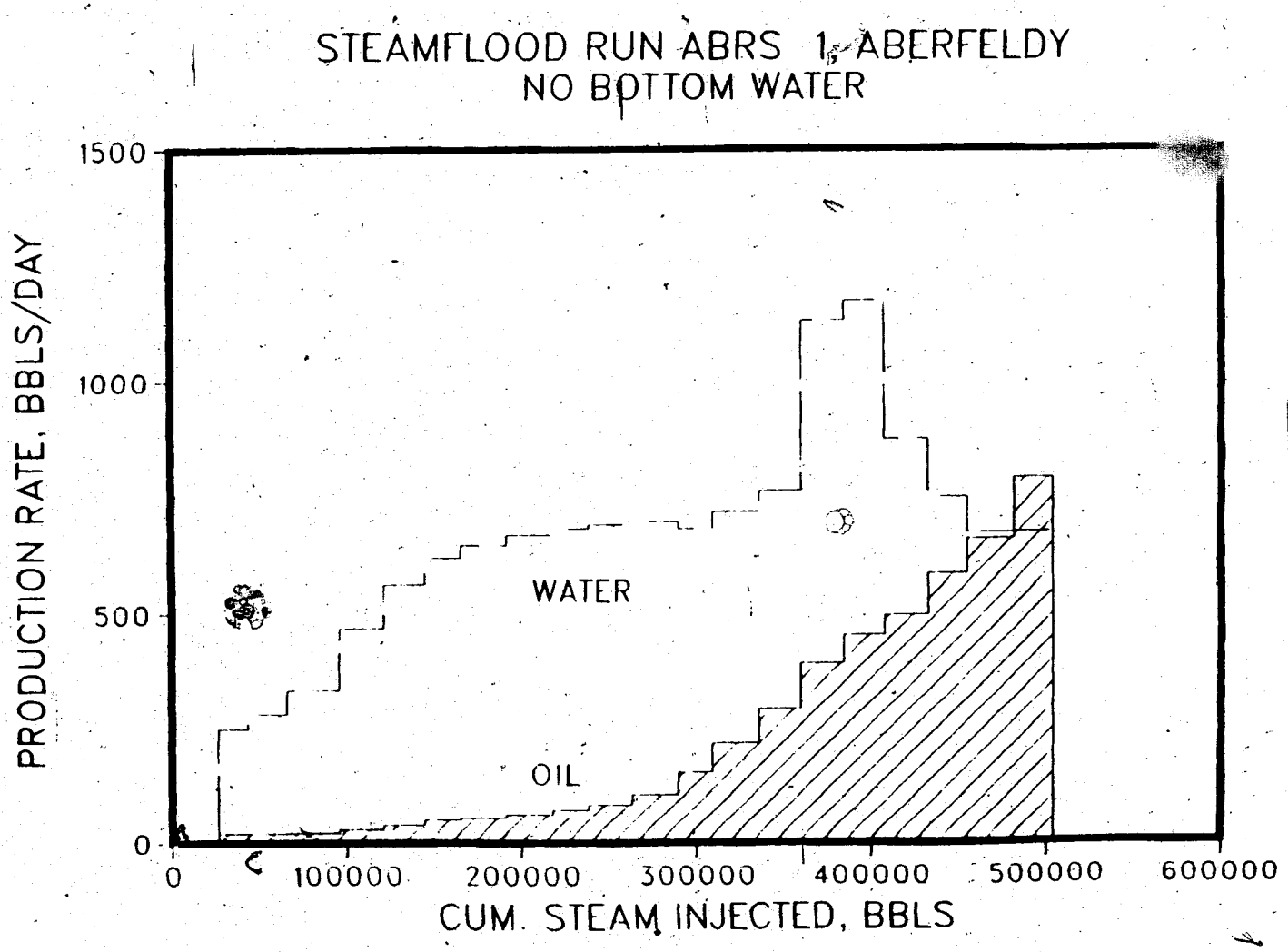

Figure 6.2 Production History of the Aberfeldy Steamflood ABRS1, No Bottom Water

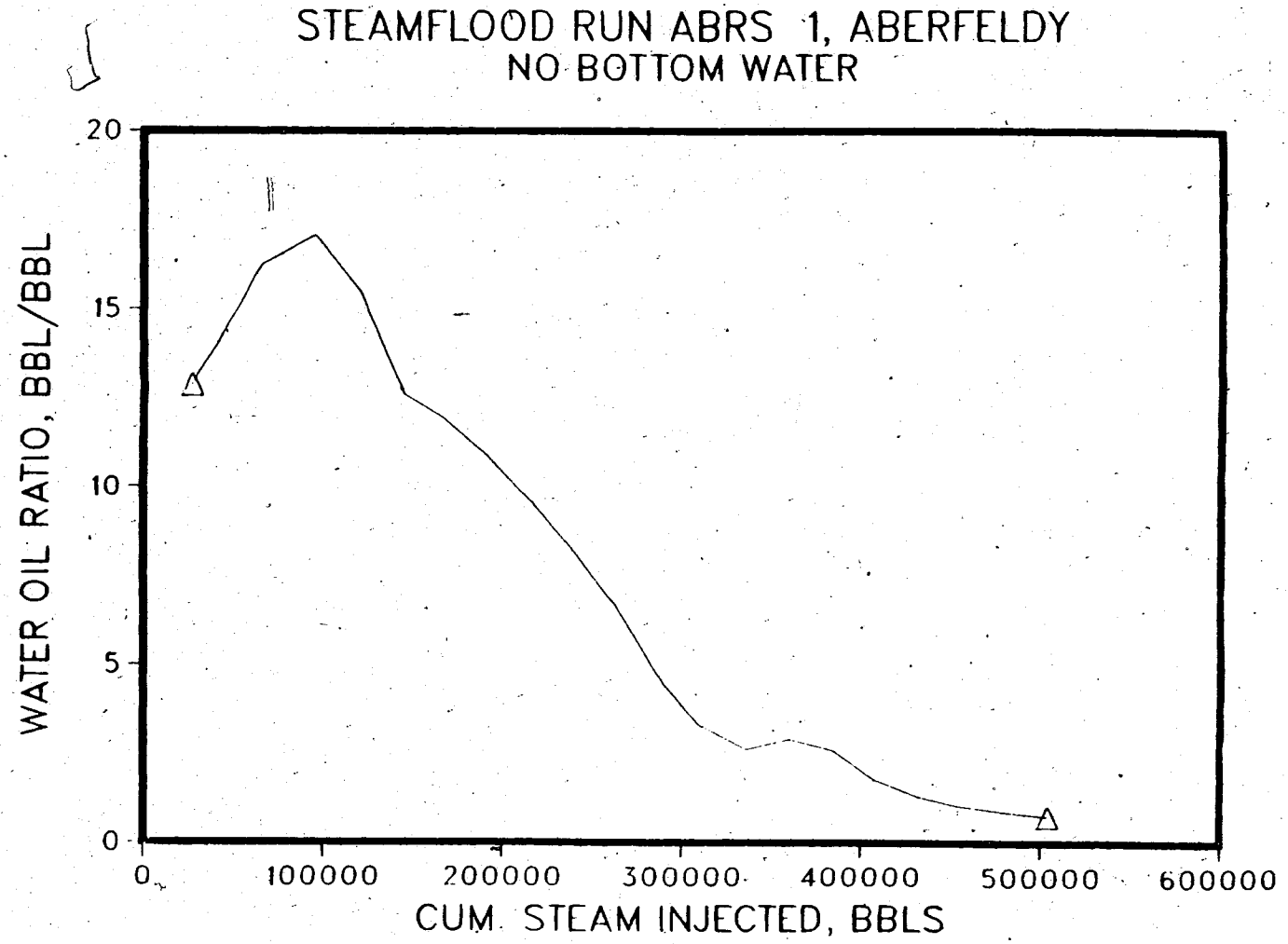

Figure 6.3 Water-Oil Ratio vs. Steam Injected for Aberfeldy Steamflood ABRS1

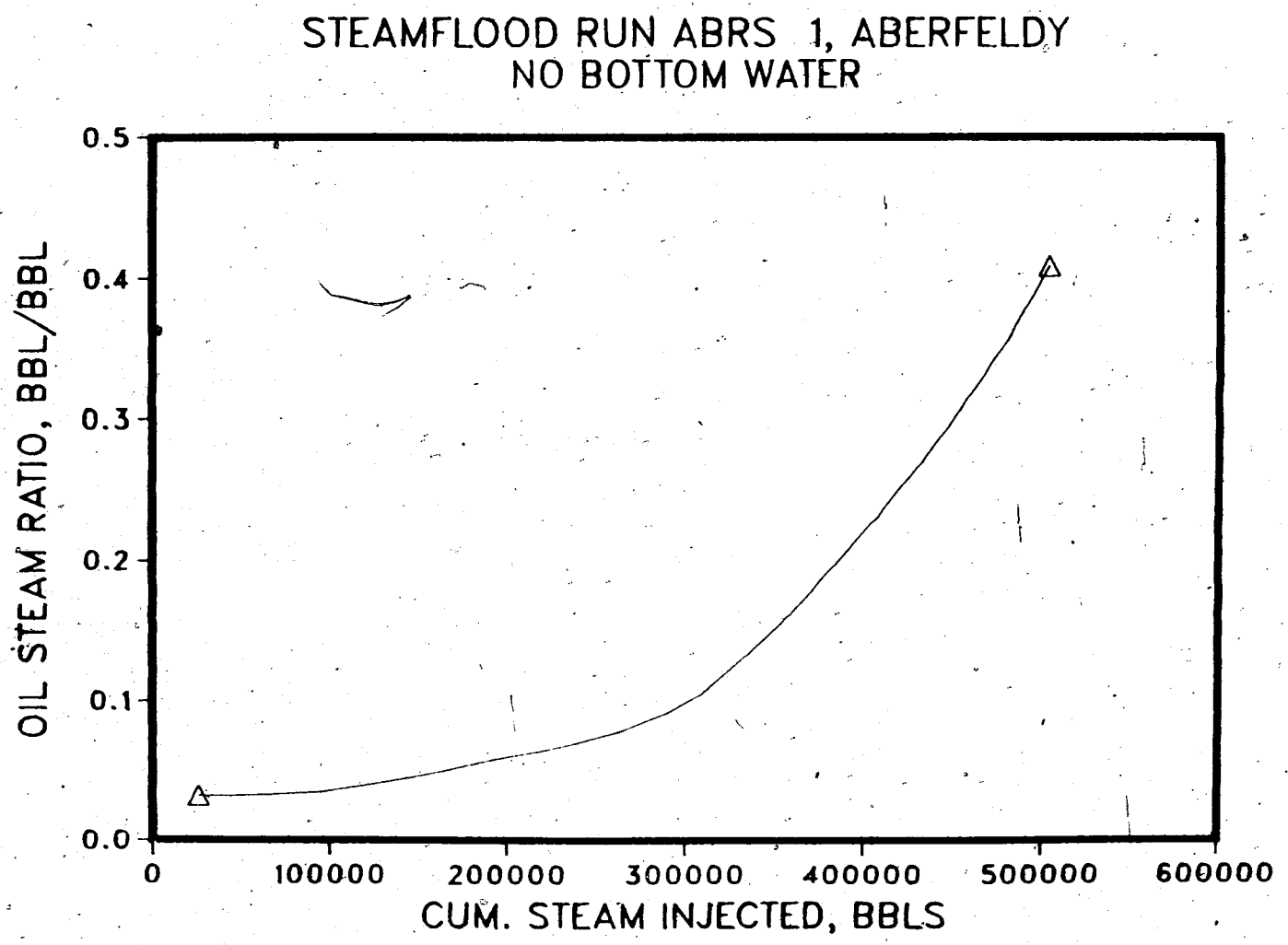

Figure 6.4 Oil-Steam Ratio vs. Steam Injected for Aberfeldy Steamflood ABRS1

injectivity. At such a stage, which can only be identified from previous unsuccessful runs, the steam injection rate and the well production must be reduced (as one does in actual field practice also), to continue to obtain a stable solution. This process needs to be repeated as many times as necessary, as shown by the lack of convergence of the solution, which may be due to excessive physically unrealistic pressure and/or saturation changes.

Temperature, Pressure and Gas Saturation Behaviour in a Multilayer Steamflood

In a steamflood, the formation temperatures, pressures, and saturations vary in a complex manner, depending on the formation characteristics, especially permeability, oil viscosity, and steam injection interval, as well as rate, pressure, and quality. The effects of these variables can be seen from the individual simulation histories. As an example, a detailed analysis is given of Run ABRS10. Figures 6.5 to 6.7 give the oil/water production data, water-oil ratio, and oil-steam ratio, respectively, while Figs. 6.8 through 6.10 show the injection well block pressure, temperature, and gas saturation histories, respectively, versus time. The injection was completed in both layers representing the formation. There was no bottom water in this run.

Initially the reservoir oil has a very low mobility (viscosity 1200cp), and as a result, the steam pressure in the injection block is high. As steam injection proceeds, the steam pressure increases rapidly (Fig. 6.8), and reaches a peak value of about 450 psi at about 400 days. The oil and water production curves (Fig. 6.5) up to this time show that the oil rate is very small, and the water rate is building up, both starting from nearly zero (because of initially immobile water, and very low oil mobility). The temperature curves show (Fig. 6.9) that during this period, the bottom layer temperature was somewhat higher than that of the top layer. This behaviour was evident in many of the runs conducted in the case of a uniform formation, where the perforations were allowed to take steam according to the steam pressure and the prevailing flow resistance. It is partly explained by the fact that, initially, the injected steam condenses, so that much hot water enters the formation. The

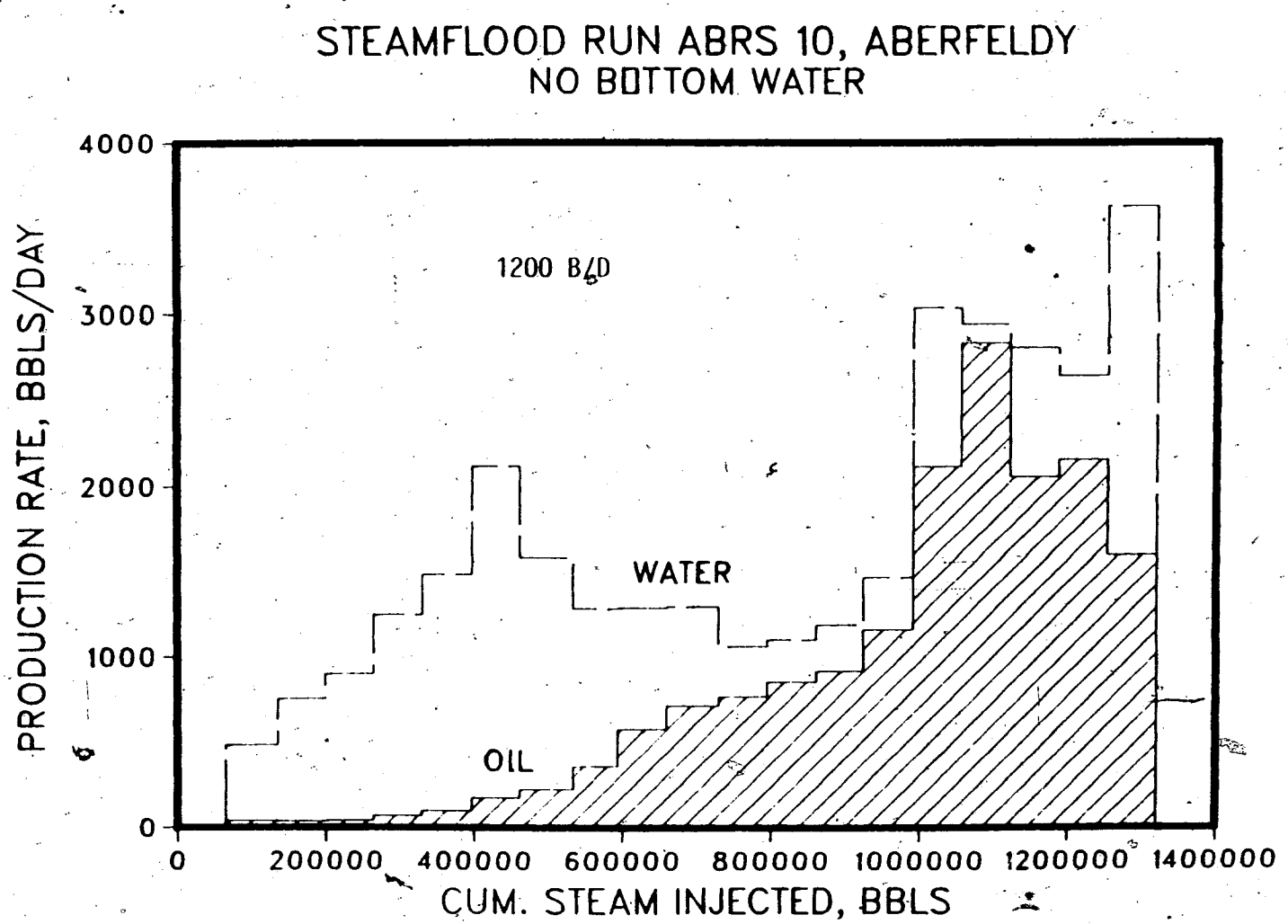

Figure [illegible] Production History of the Aberfeldy Steamflood ABRS10, No Bottom Water

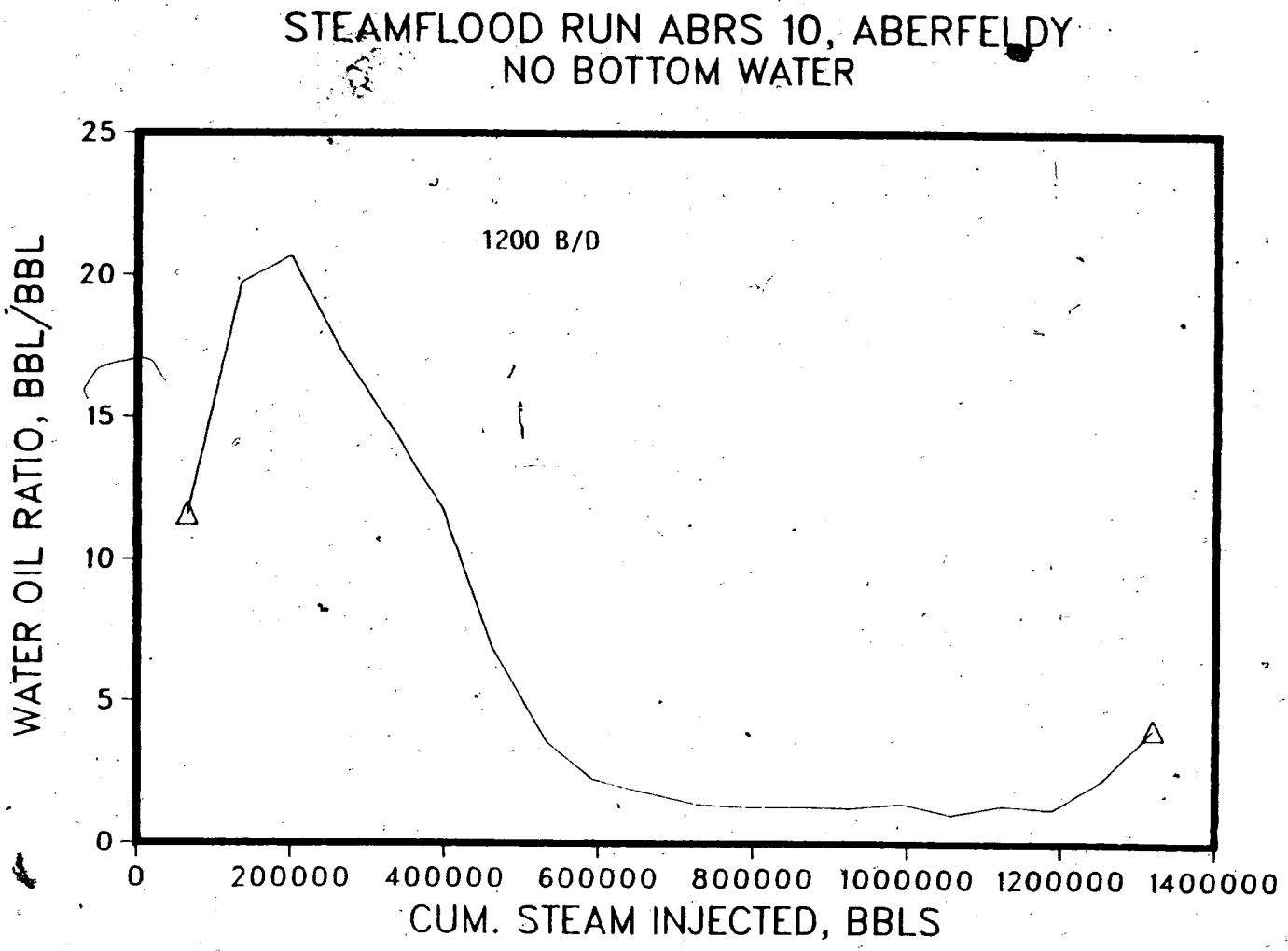

Figure 6.6 Water-Oil Ratio vs. Steam Injected for Aberfeldy Steamflood ABRS10

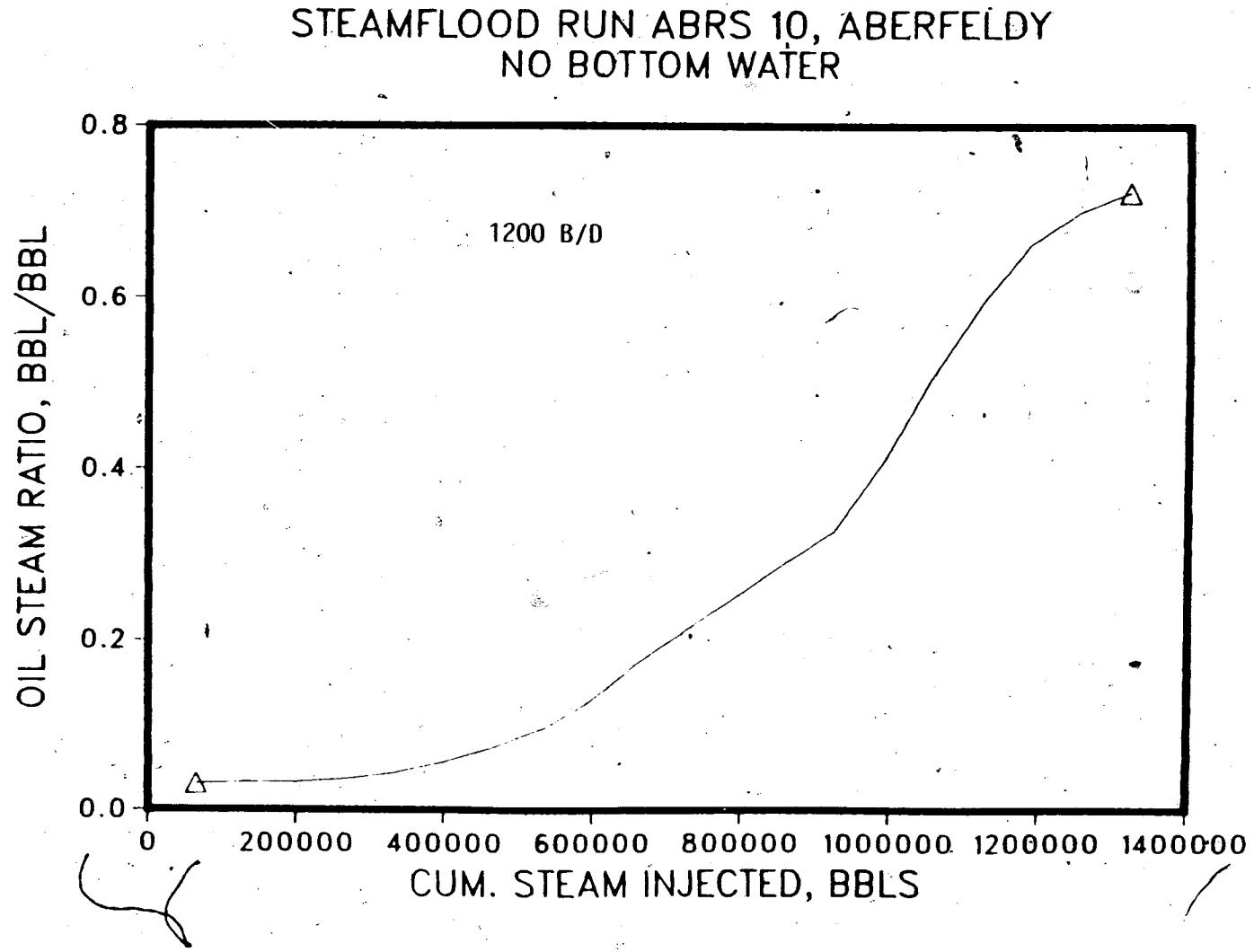

Figure 6.7 Oil-Steam Ratio vs. Steam Injected for Aberfeldy Steamflood ABRS10

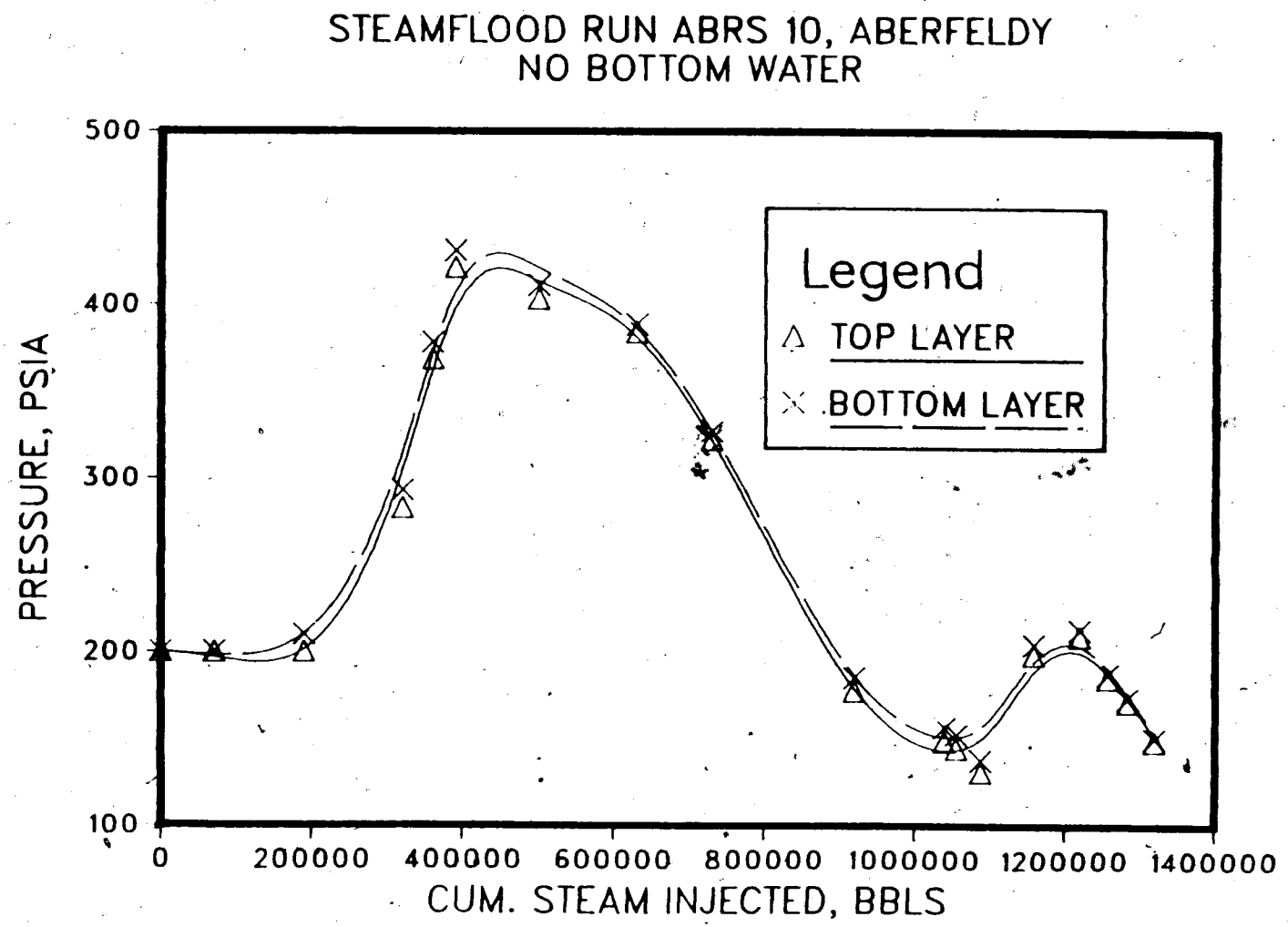

Figure 6.8 Pressure Variation in the Injection Well Block, Steamflood Run ABRS10

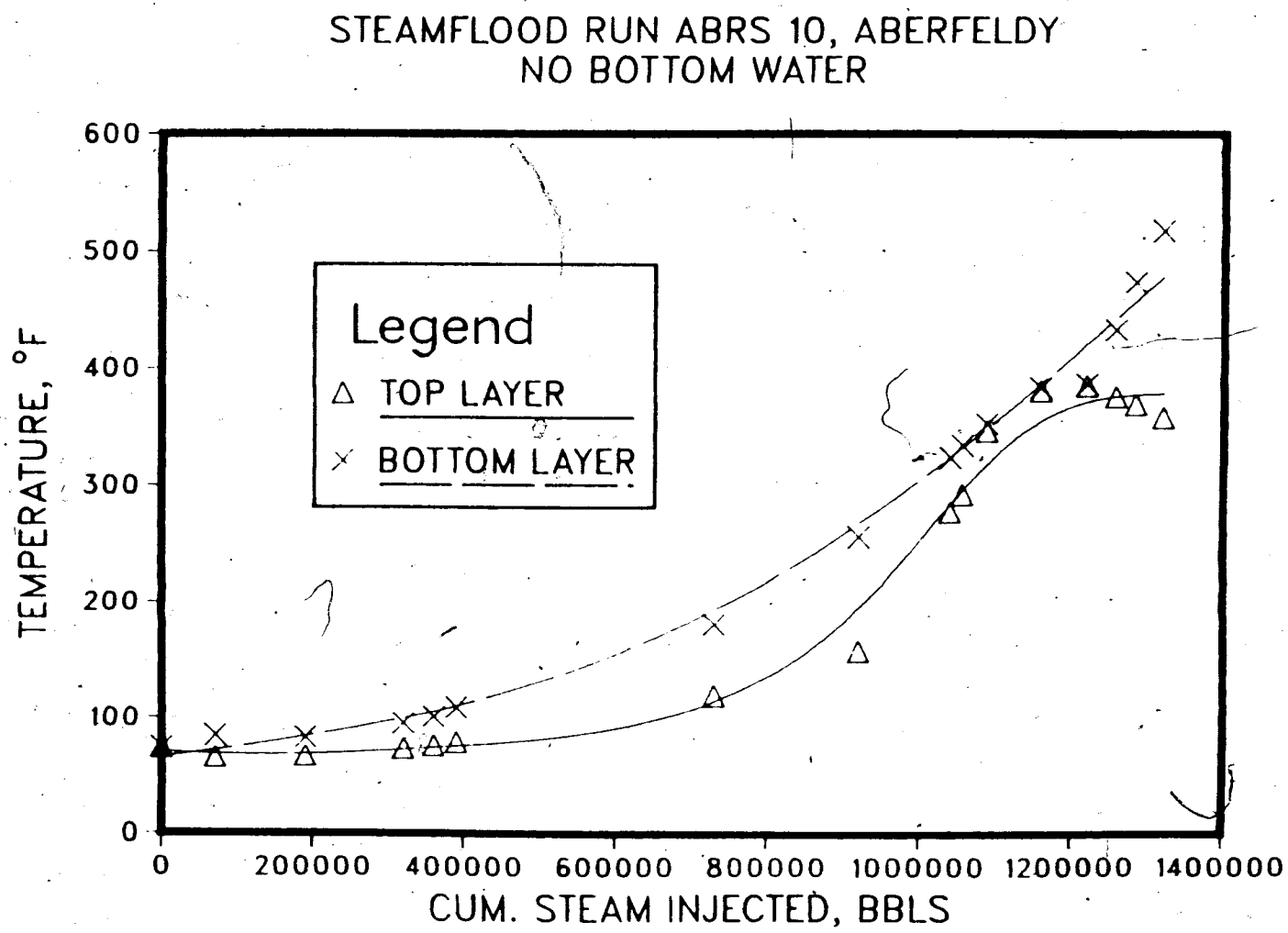

Figure 6.9 Temperature Variation in the Injection Well Block, Steamflood Run ABRS10

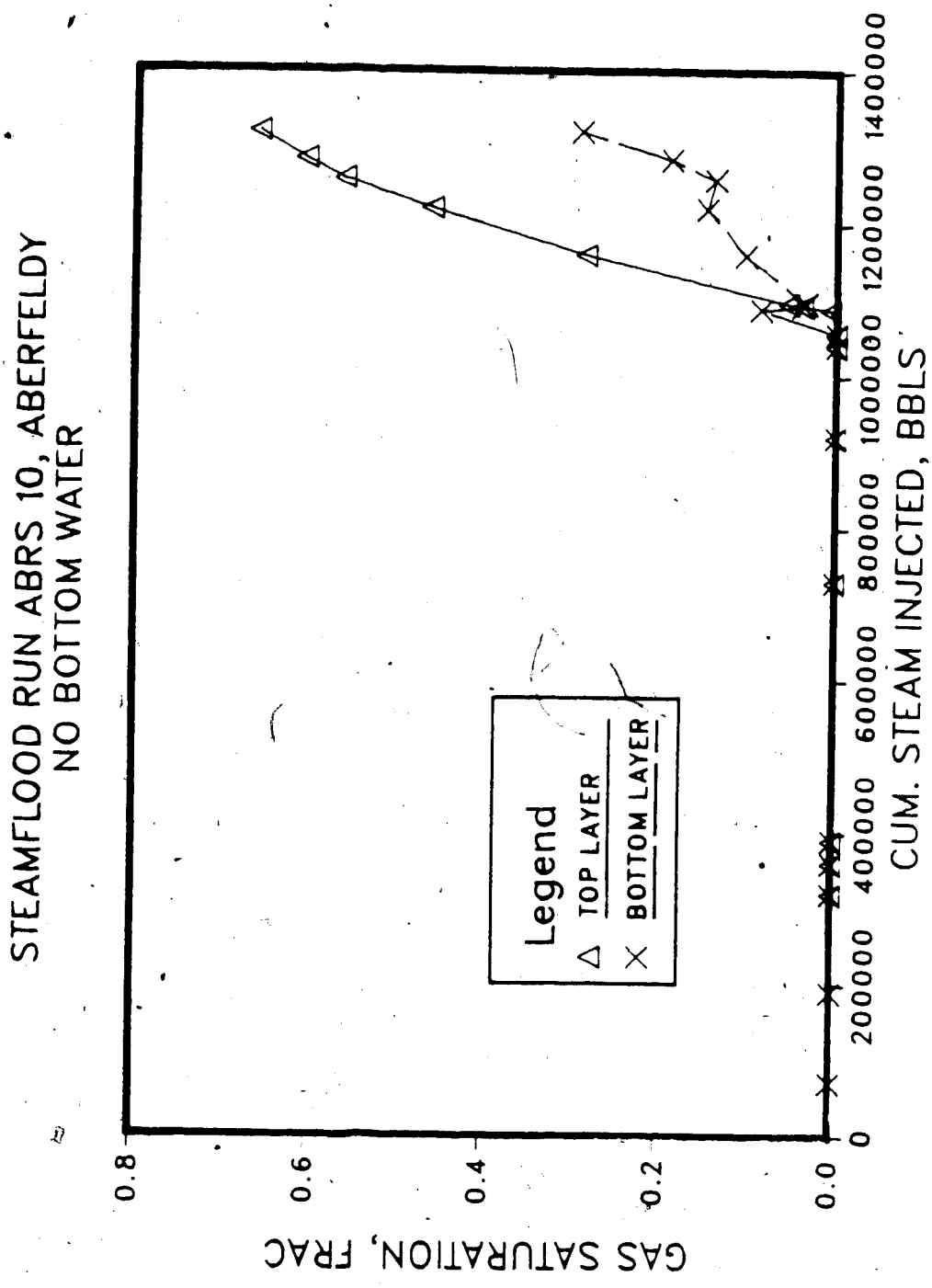

Figure 6.10 Gas Saturation Variation in the Injection Well Block, Steamflood Run ABRS10

segregated hot water tends to create a higher permeability to water in the lower part of the formation, which further helps steam inflow into this part. Initial segregation of steam will occur in the case of (i) low viscosity oils, (ii) an initial gas saturation, or (iii) completion in the upper part of the formation only. Even in the case of high viscosity oils, steam segregation would tend to occur at long times. As a result of low oil mobility, the water-oil ratio increases rapidly during the initial period (Fig. 6.6).

As steam injection continues, the hot condensate arrives at the producers, causing an increase in the oil mobility. Consequently, the oil rate increases rapidly (Fig. 6.5), together with the water rate. The injection block pressure drops during this period also (Fig. 6.8), to a value of about 200 psi. At this point, the temperatures in the upper and lower parts of the formation are nearly equal (Fig. 6.9 at 1.1 MMBbls steam injected). The water-oil ratio declines during this period, and tends to level out at a value of about 2, compared to the peak value of 20. At about this point, the gas saturation, which was higher initially in the lower layer, now starts to increase in the upper part (Fig. 6.10). As a result, more steam is diverted to the upper part. The injection block pressure rises somewhat due to an increase in flow resistance resulting from gas saturation buildup (Fig. 6.9, temperatures beyond 1.2 MMBbls steam injected), coupled with the decreasing oil saturation, both lowering the oil mobility. Thus the small pressure peak seen in Fig. 6.8 is the result of the above mentioned complex interactions.

In the last part of the run, most of the steam continues to flow into the upper part of the formation (gas saturation 56% vs. 14% in the lower part), the temperature of the lower part continues to increase. The pressure declines rapidly after the second peak (Fig. 6.8), because of steam breakthrough, resulting in a marked decline in the formation resistance. The oil production rate declines during this period (Fig 6.5), because there is less oil left in the formation. As a result, the water-oil ratio increases (Fig. 6.6) to 4, but not much more, because the water saturation, hence permeability, is also low.

The cumulative oil-steam ratio curve shows a behaviour consistent with the above discussion. Initially, the increase in the oil-steam ratio is slow, since the steam injection rate is constant, but the oil production rate is low. Later, as the oil is mobilized, the oil-steam ratio increases rapidly. During the last stage of steam injection, the oil-steam ratio tends to level off.

It should be noted that if steam injection is continued beyond the stage at which the run is terminated, steam flow rate increases very rapidly, until steam (gas) is the only flowing phase. In field practice, after steam breakthrough the steam injection rate is greatly turned down. From this point on there is only a decrease in the oil-steam ratio, because no more oil is produced. From a computational point of view, the steam injection rate has to be cut down also, but the solution convergence rate still slows down greatly due to the high gas flow rate.

Bottom Water Steamfloods for Aberfeldy:

Effect of Bottom Water Thickness Table 6.2 (p.101) summarizes selected steamfloods carried out for the Aberfeldy formation. The floods with bottom water present are indicated by a nonzero ratio h_w/h_{oil}, i.e. the ratio of water layer to the oil layer thickness. Figure 6.11 shows plots of oil-steam ratio versus h_w/h_{oil} for Aberfeldy and M-6 steamfloods. In the runs indicated, steam was injected into the oil zone only, with the producers completed in the oil zone also. It is clear that the oil-steam ratio declines steeply with an increase in the h_w/h_{oil} ratio. The decline is much smaller for M-6. It is also seen that the oil-steam ratio reaches a low rather early for the high h_w/h_{oil} ratios, whereas for lower ratios, there is considereable difference between the 500 and 700 day oil-steam ratio curves. This implies that in the thicker water zones, steam penetrates the bottom water zone early, and from then onward, there is little improvement in the oil displacement efficiency.

Figure 6.11 also shows the oil recovery curve for the 700-day period. The recovery drops rapidly with an increase in h_w/h_{oil} ratio, based upon the same reasons as noted for

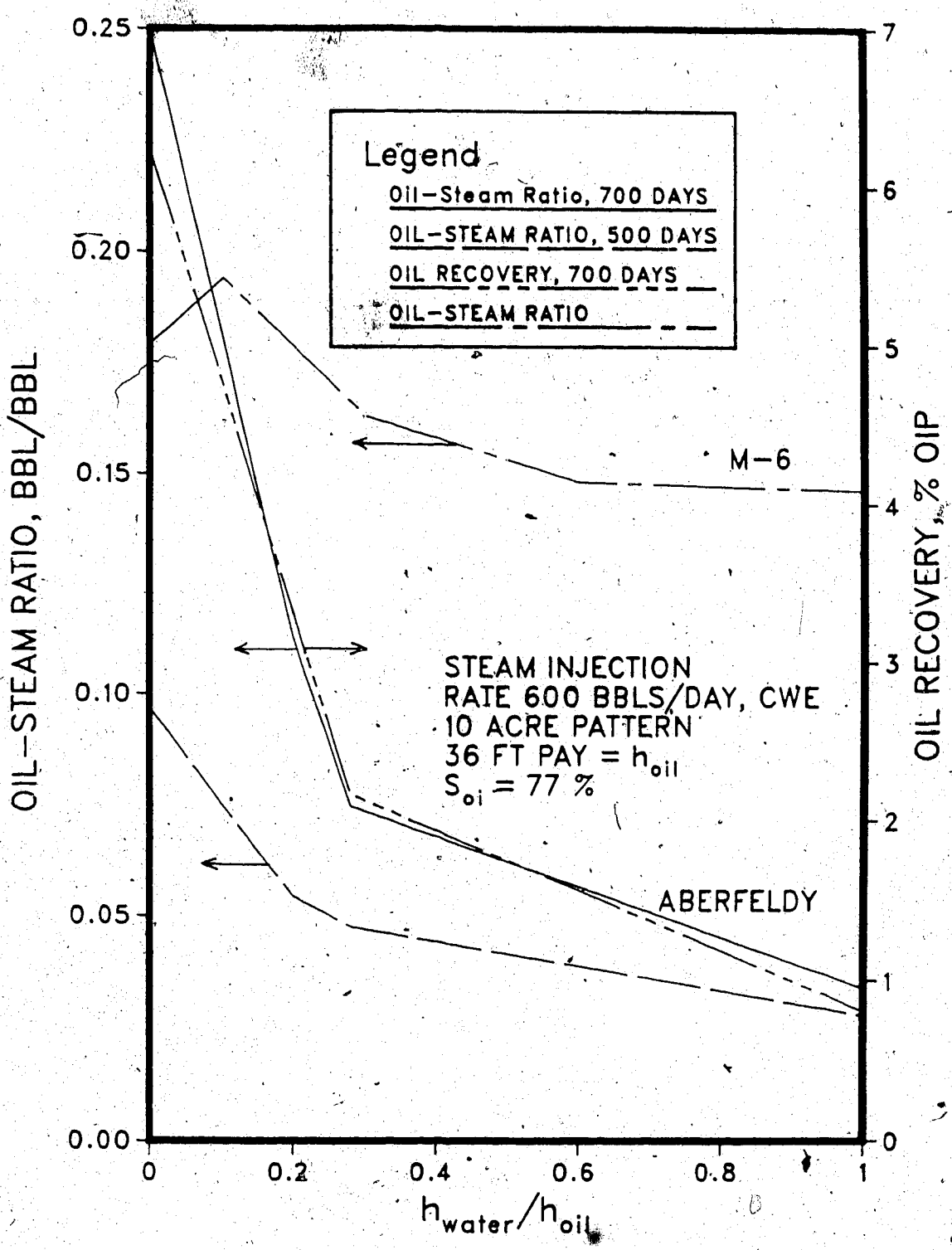

Figure 6.11 Variation of Oil-Steam Ratio and Recovery with Water-Oil Zone Thickness Ratio.

the oil-steam ratio. The cumulative WOR for $h_w/h_{oil} = 1$ (ABRS2) was 20.6, compared to 1.47, when no bottom water was present.

Figures 6.12 through 6.23 show the oil and water production history, water-oil ratio, and oil-steam ratio plots for the bottom water runs ABRS2, ABRS6, ABRS5, and ABRS7, with $h_w/h_o = 1$; 0.1, 0.2, and 0.28, respectively. The trends in all four cases are similar, but the scales are different. In other words, the steam injection process works the same way whether bottom water is present or not. But when bottom water is present, much less steam flows in the oil zone than that in the absence of bottom water. In particular, the slow drop in WOR in Run ABRS2 (Fig. 6.13) is noticeable due to the fact that, even though the oil is mobilized (causing a drop in WOR), considerable amounts of water continue to flow from the water zone into the producers.

Effect of Bottom Water Oil Saturation

In all of the runs conducted, it was assumed that the bottom water contains residual oil only, so that water is the only mobile phase. If a higher oil saturation is assumed, or if it is assumed that the residual oil saturation decreases with an increase in temperature, a small amount of oil will be produced from the "water" zone. An interesting example of this type is the Peace River project, where the bottom "water" layer has an oil saturation of 55-60%, so that steam injection into the bottom water produces a considerable volume of oil. The oil formations in the Cold Lake area often have oil saturations in the same range. However, whereas the water in Peace River is mobile, it is often immobile in Cold Lake because of the fine grained sand and clays present.

One run, ABRS2A, was carried out to determine the effect of bottom water oil saturation on recovery. The data used were the same as for Run ABRS2, except in this case, the oil saturation in the water layer was increased to 50% to simulate a transition zone. Figure 6.24 shows plots of oil and water production rates versus cumulative steam injection. Figure 6.25 shows a similar plot for the oil-steam ratio. (Results are tabulated in

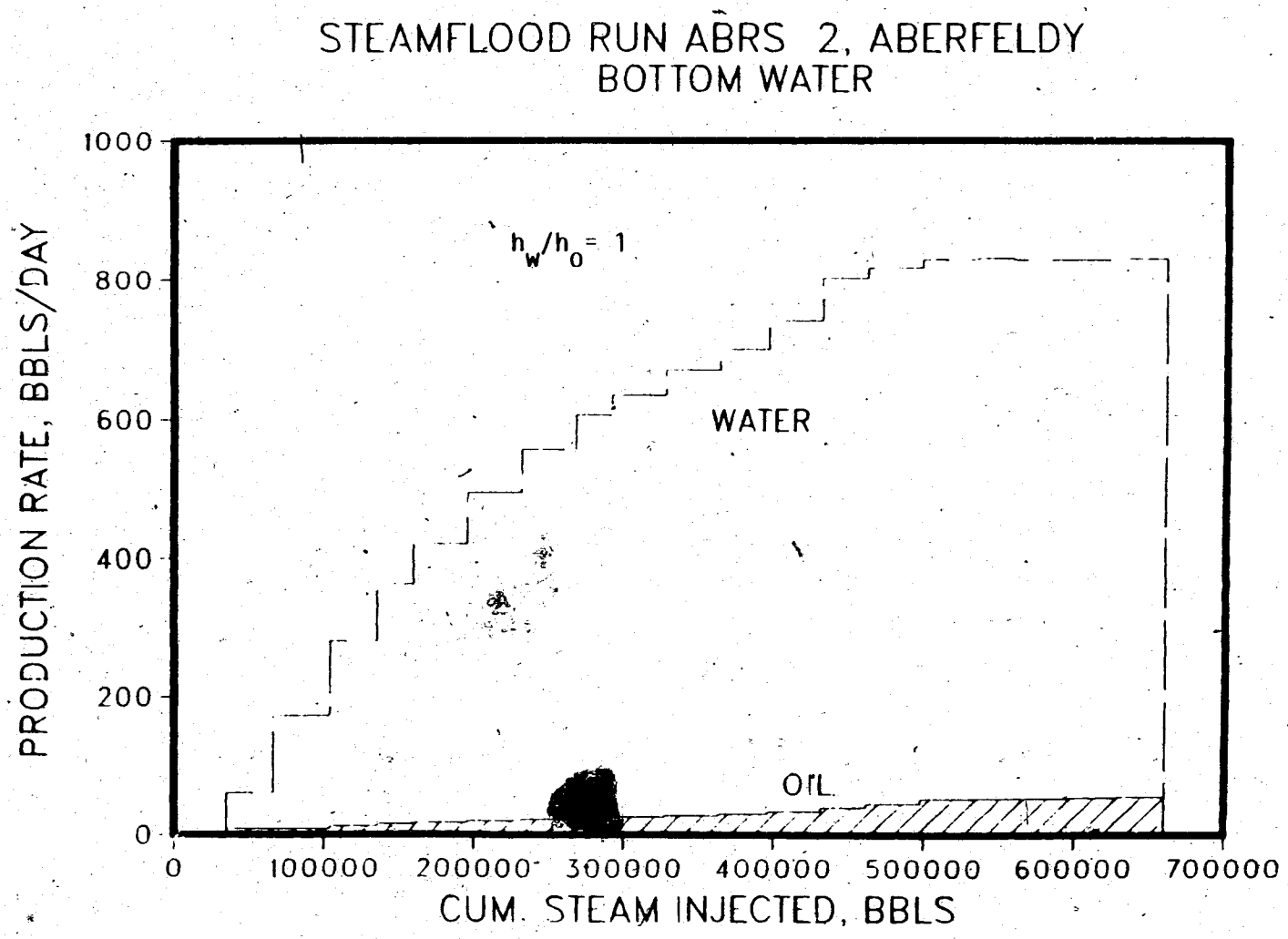

Figure 6.12 Production History of the Aberfeldy Steamflood ABRS2, Bottom Water

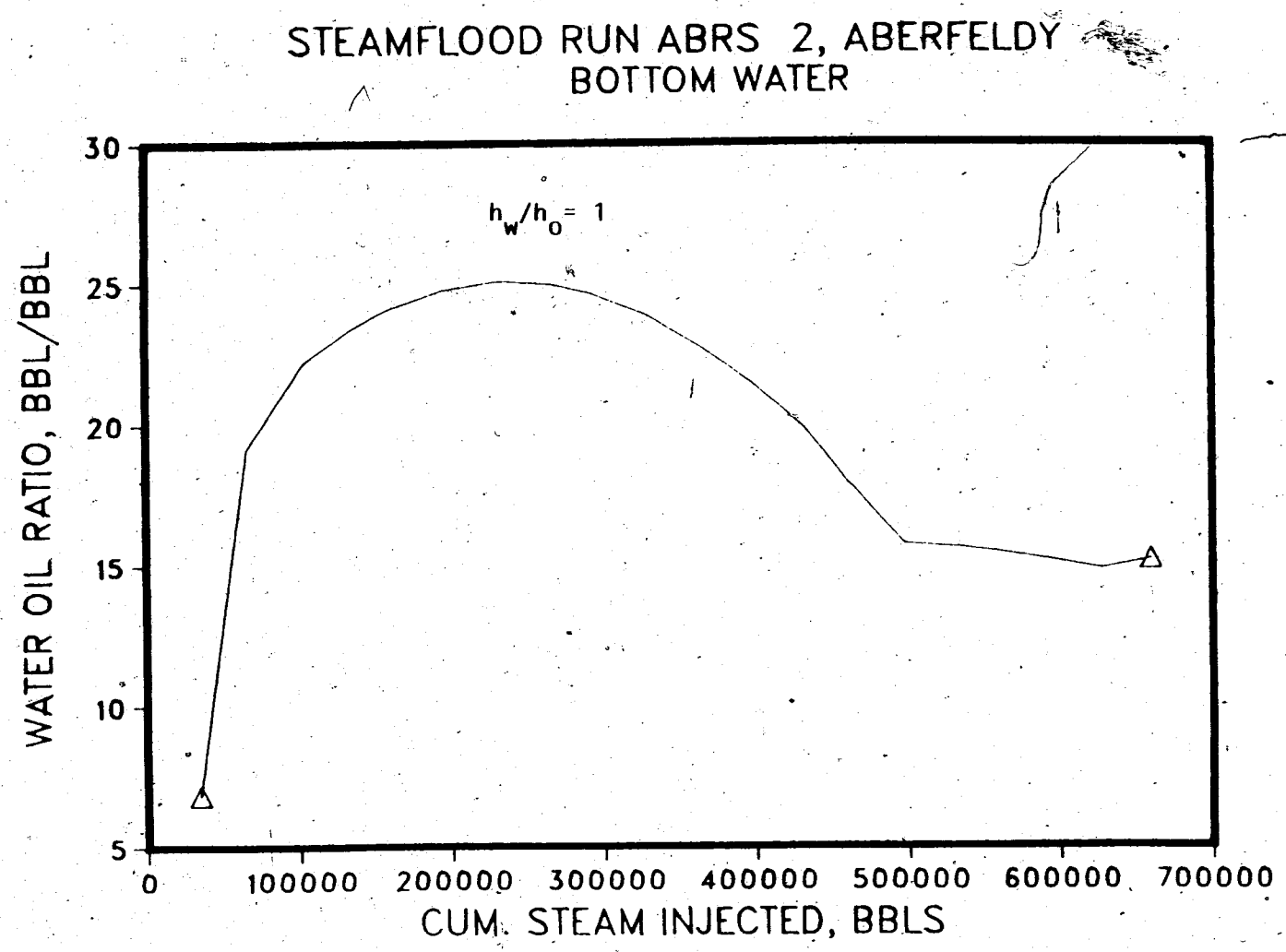

Figure 6.13 Water-Oil Ratio vs. Steam Injected for Aberfeldy Steamflood ABRS2

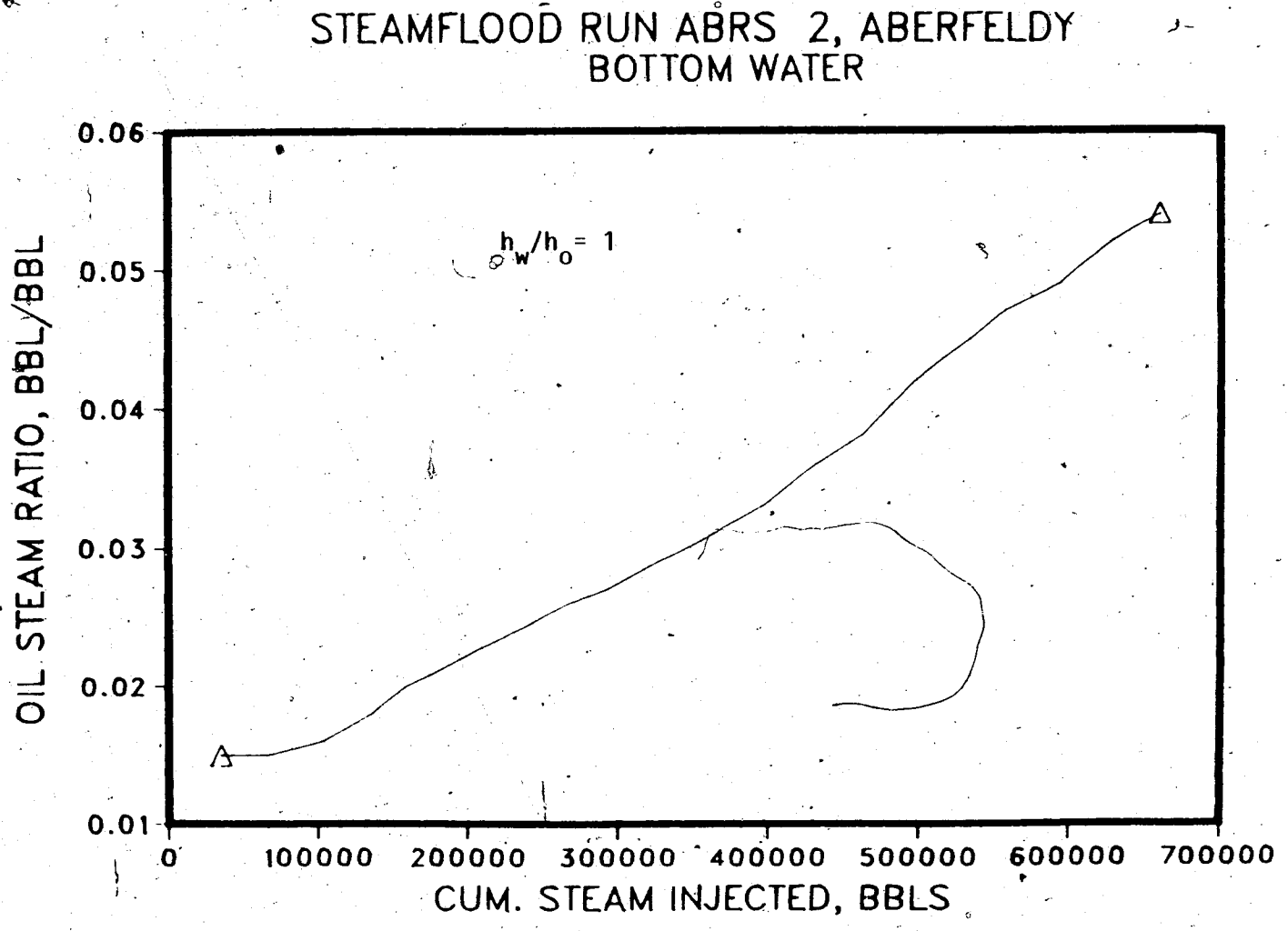

Figure 6.14 Oil-Steam Ratio vs. Steam Injected for Aberfeldy Steamflood ABRS2

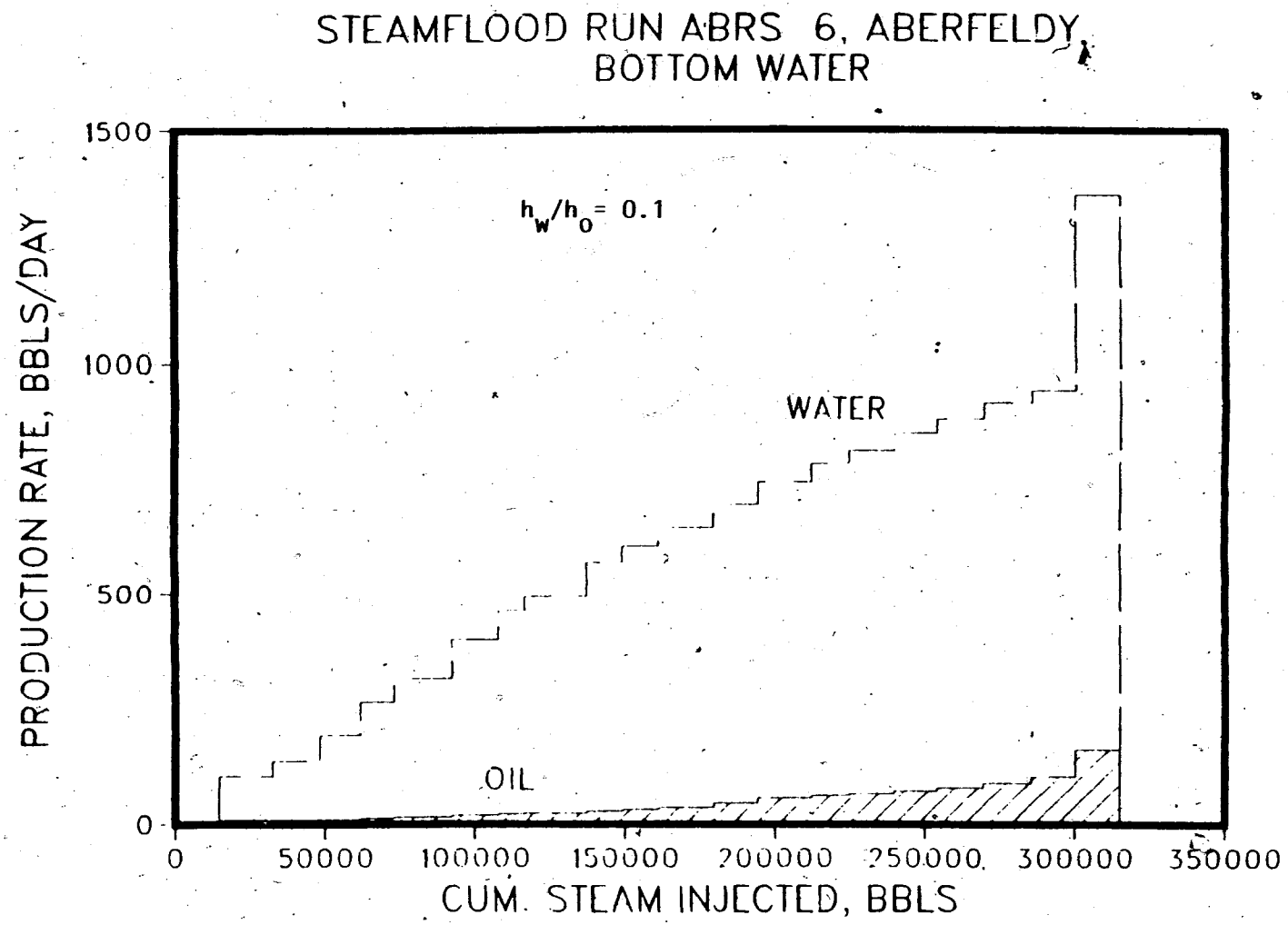

Figure 6.15 Production History of the Aberfeldy Steamflood ABRS6, Bottom Water

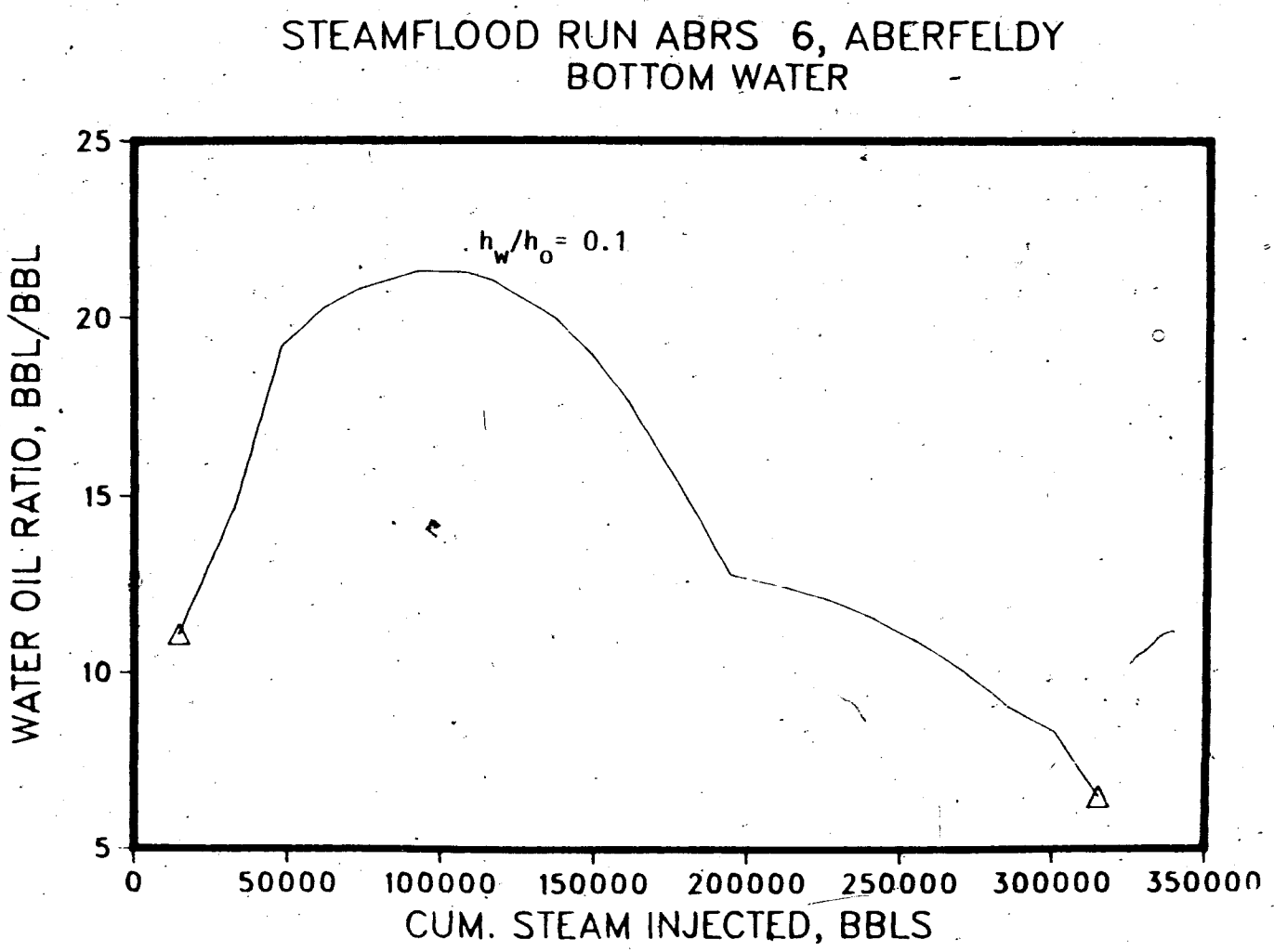

Figure 6.16 Water-Oil Ratio vs. Steam Injected for Aberfeldy Steamflood ABRS6

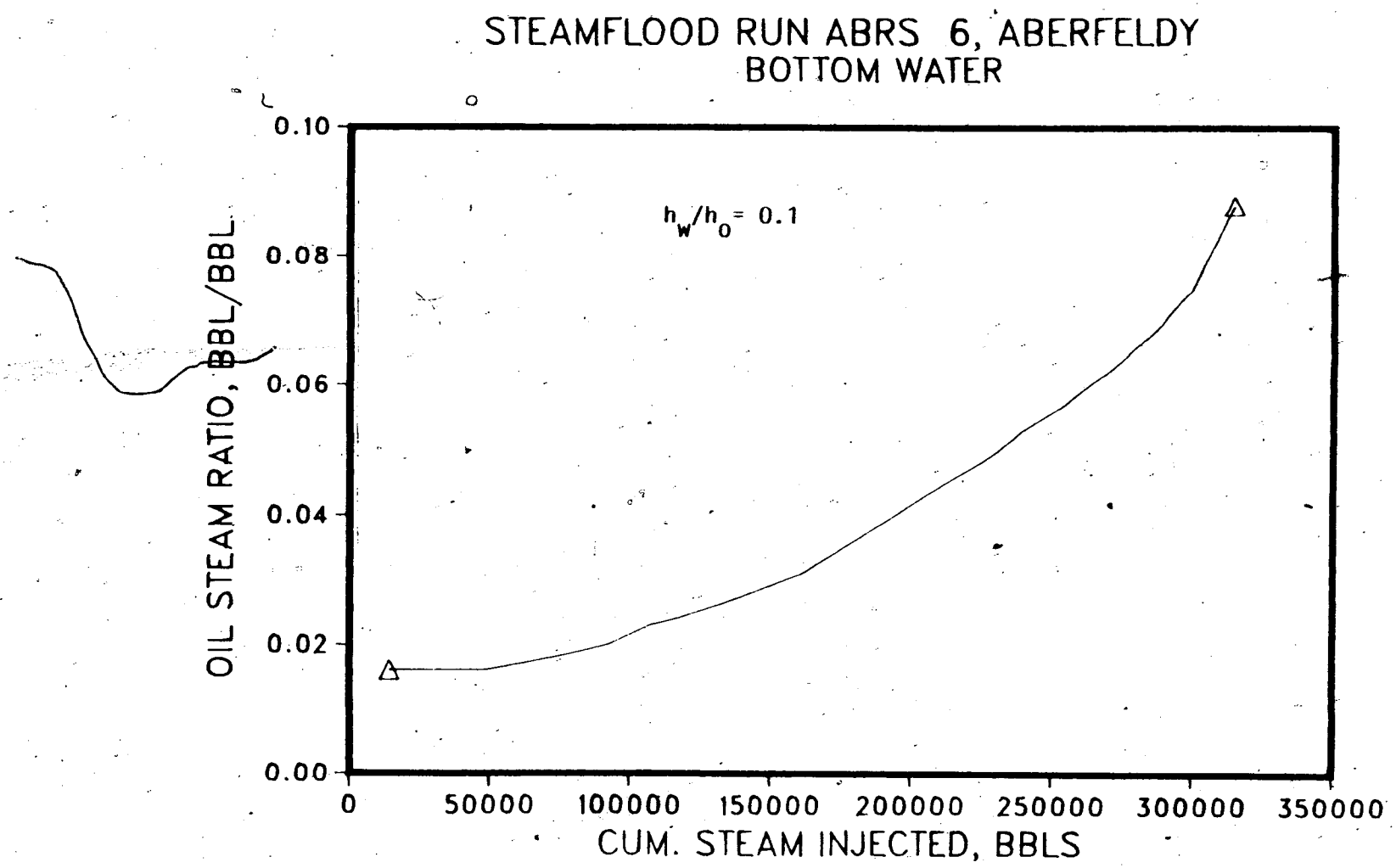

Figure 6.17 Oil-Steam Ratio vs. Steam Injected for Aberfeldy Steamflood ABRS6

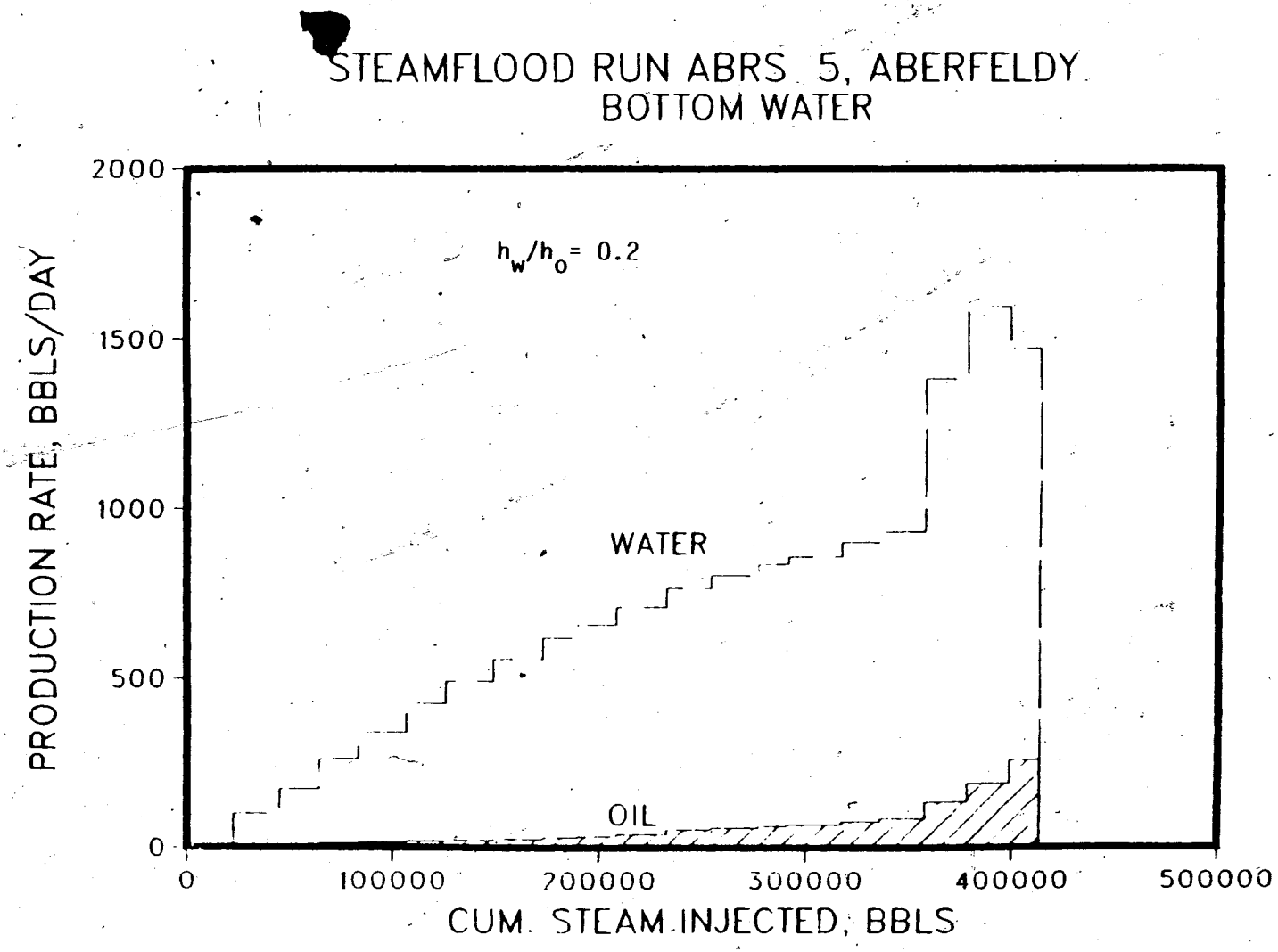

Figure 6.18 Production History of the Aberfeldy Steamflood, ABRS5, Bottom Water

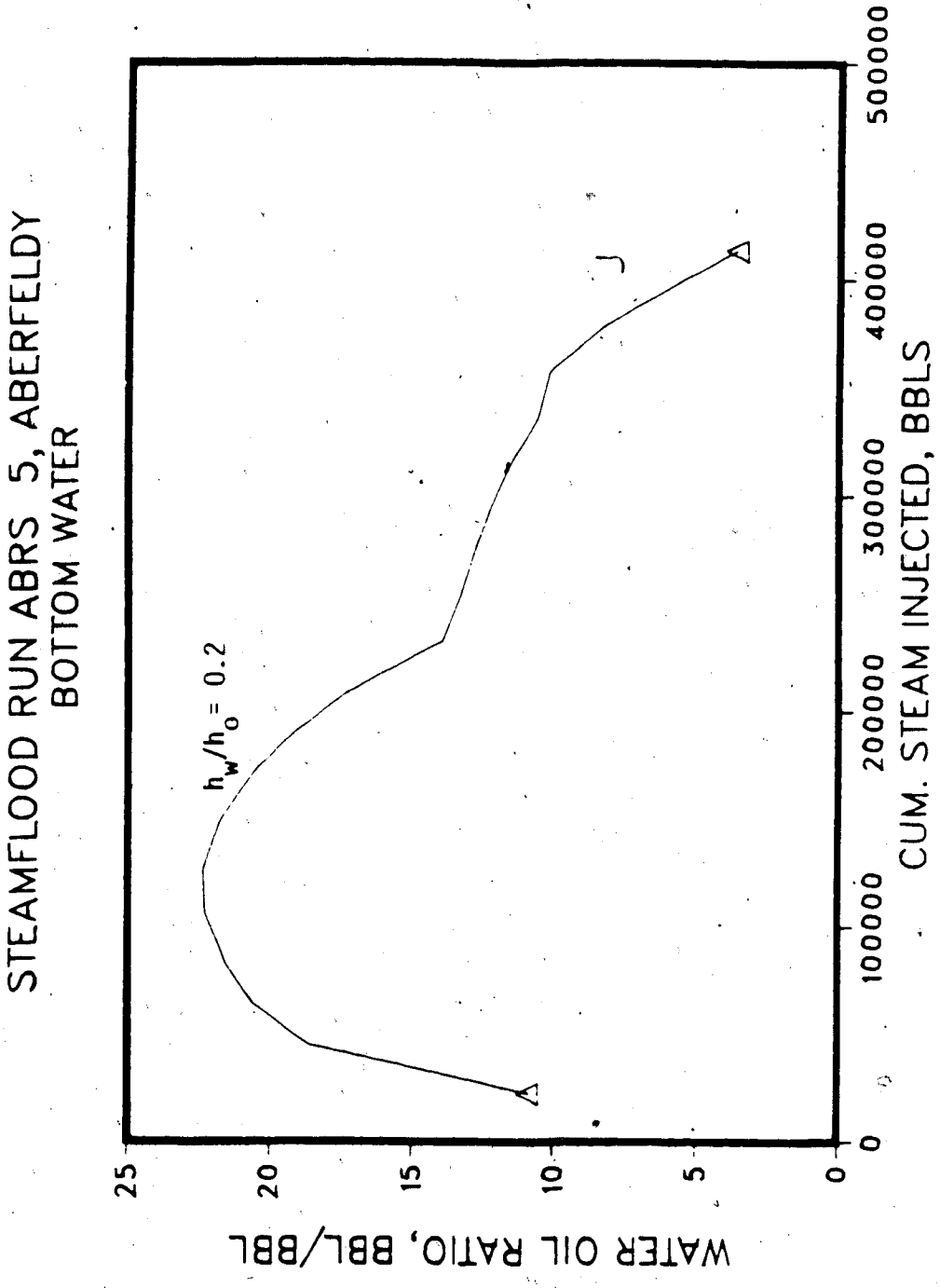

Figure 6.19 Water-Oil Ratio vs. Steam Injected for Aberfeldy Steamflood ABRS5

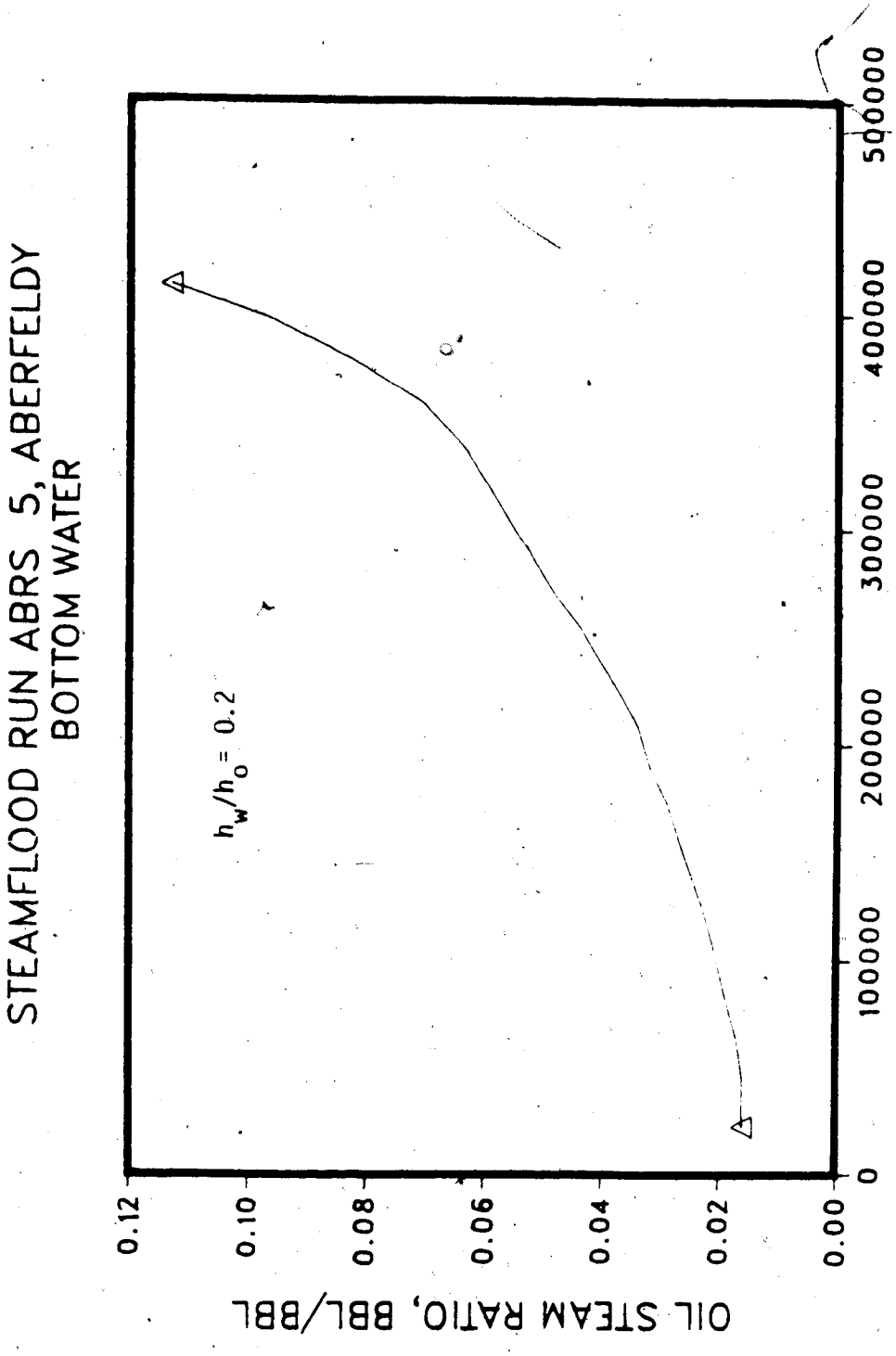

Figure 6.20 Oil-Steam Ratio vs. Steam Injected for Aberfeldy Steamflood ABR55

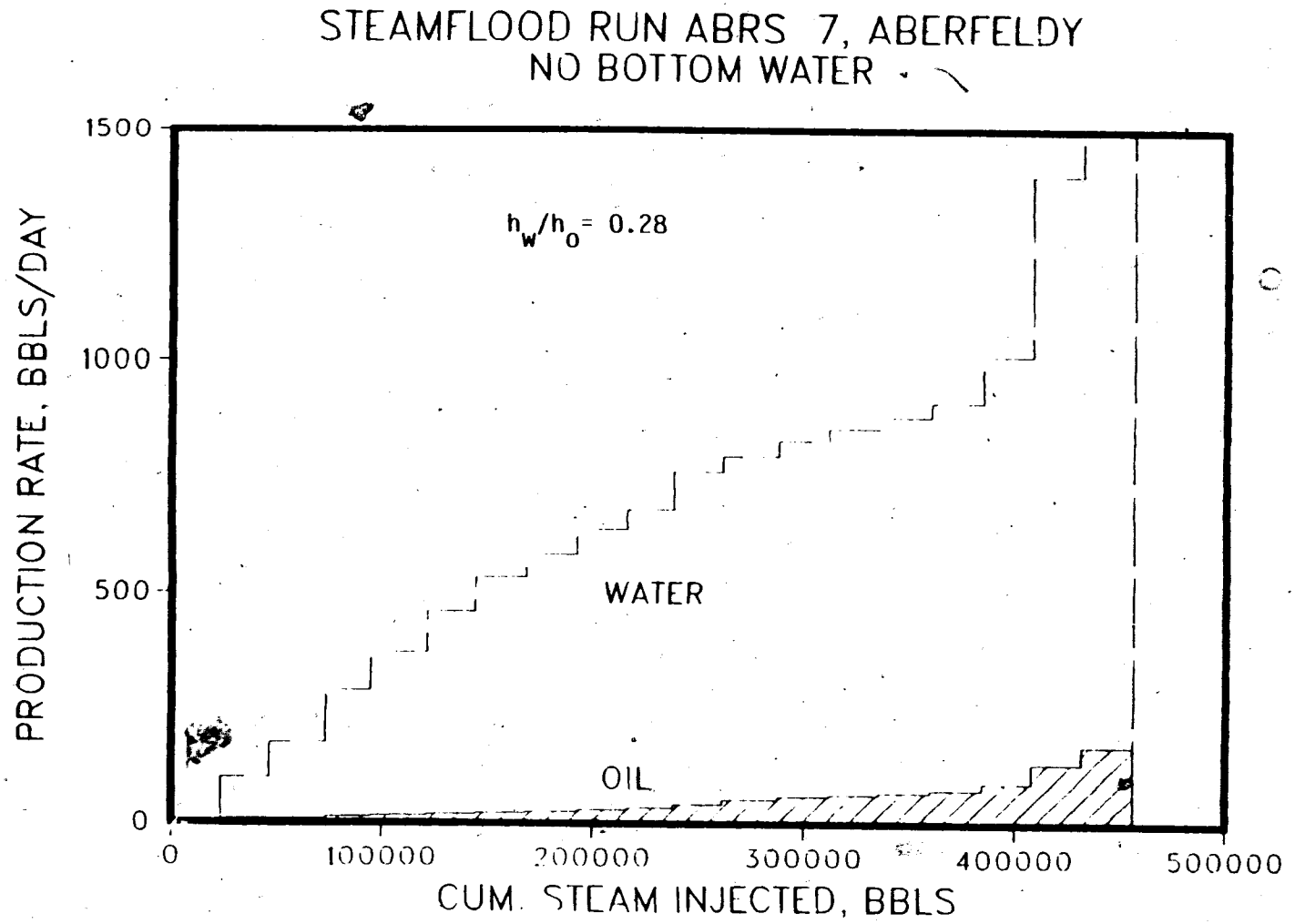

Figure 6.21 Production History of the Aberfeldy Steamflood ABRS7, Bottom Water

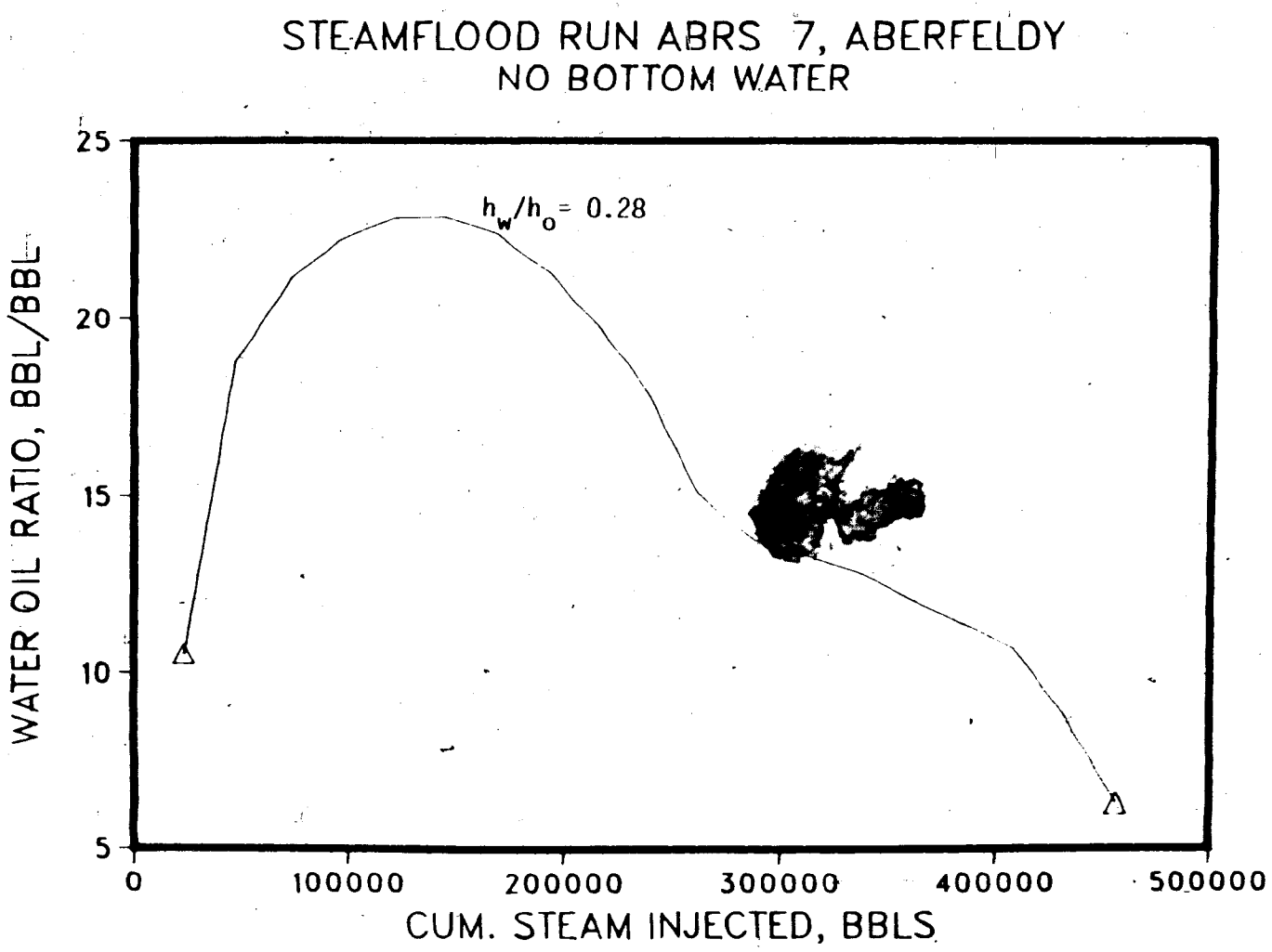

Figure 6.22 Water-Oil Ratio vs. Steam Injected for Aberfeldy Steamflood ABRS7

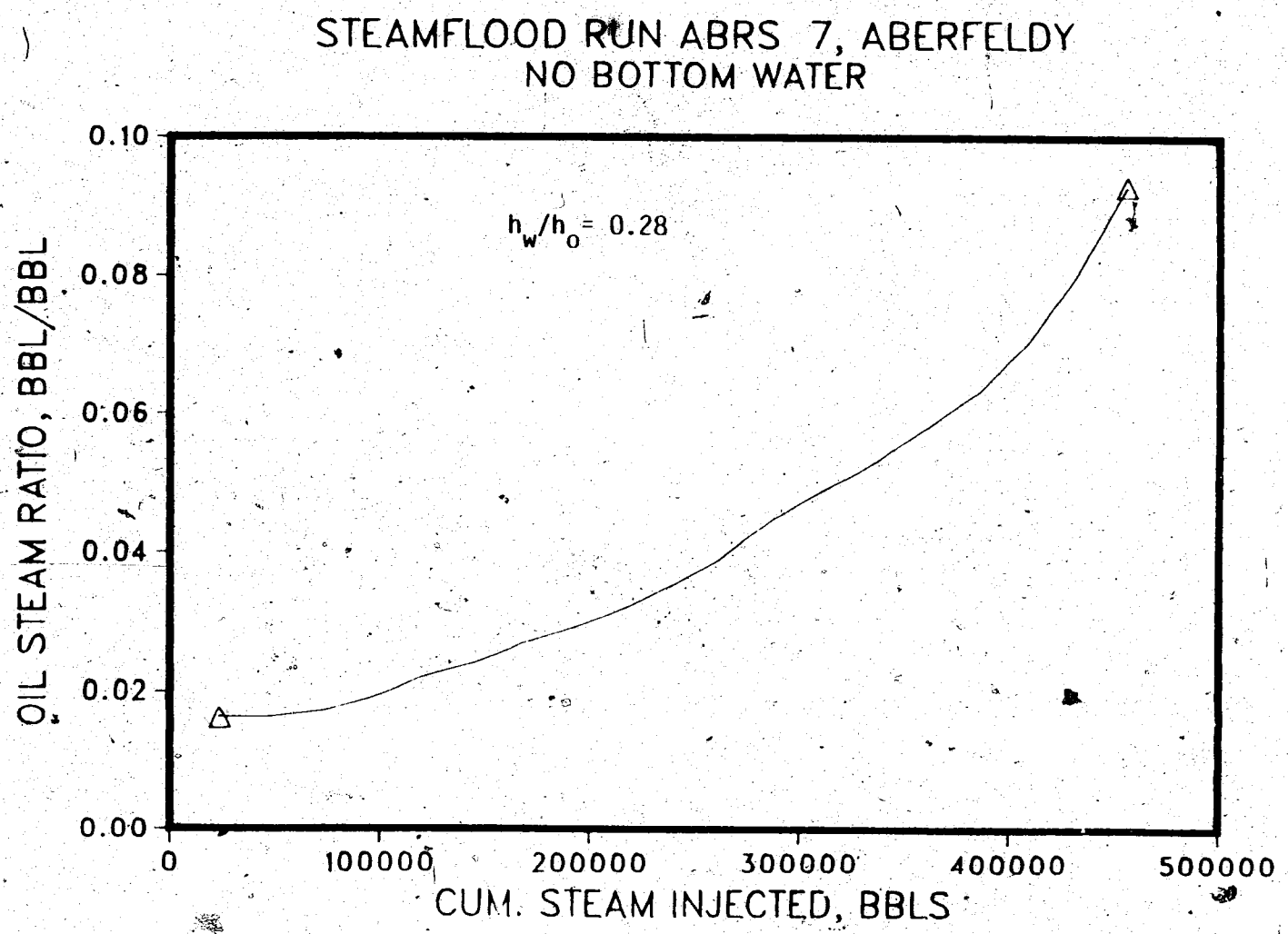

Figure 6.23 . Oil-Steam Ratio vs. Steam Injected for Aberfeldy Steamflood ABRS7

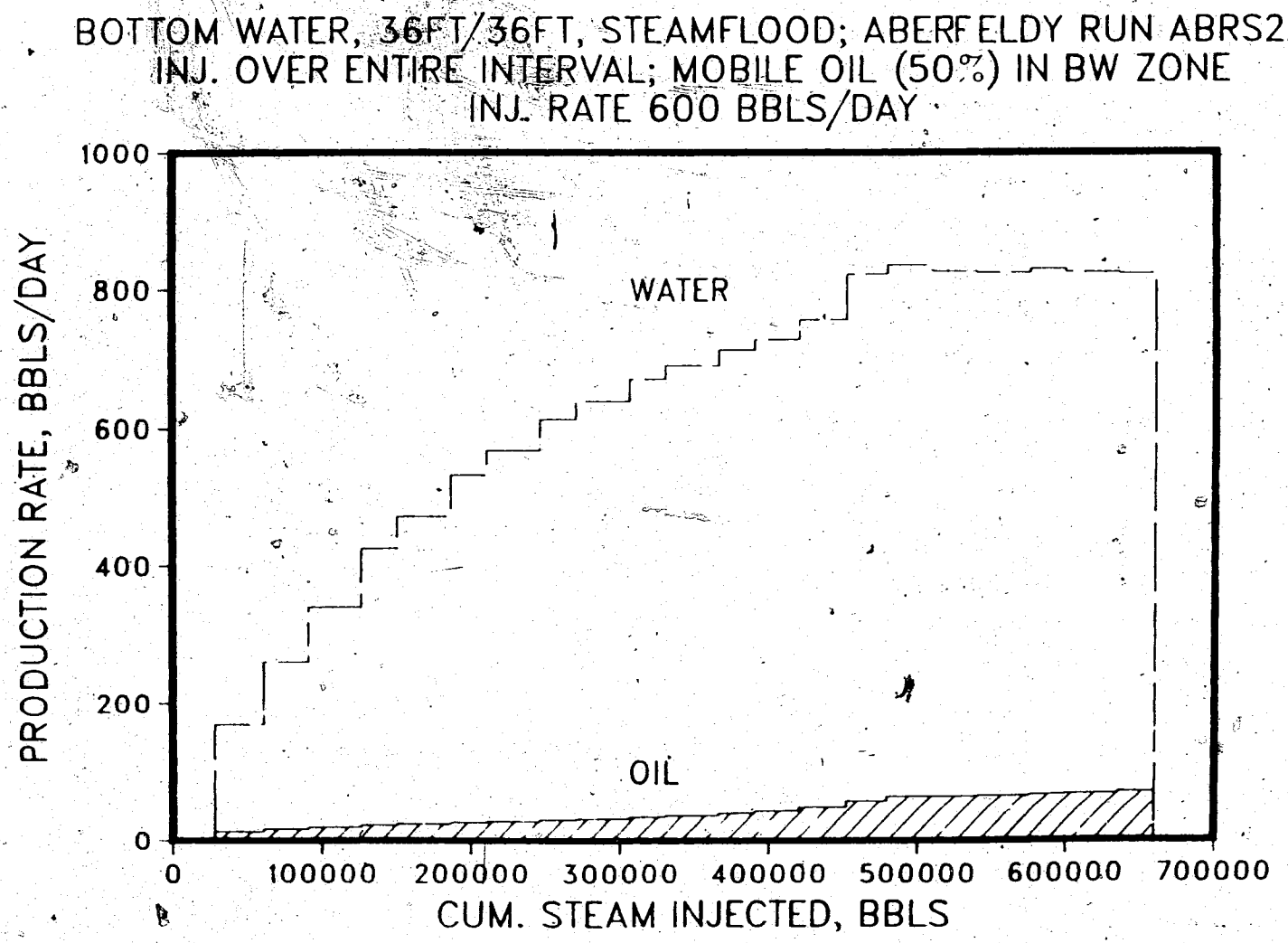

Figure 6.24 Production History of the Aberfeldy Steamflood, ABRS2A, Bottom Water

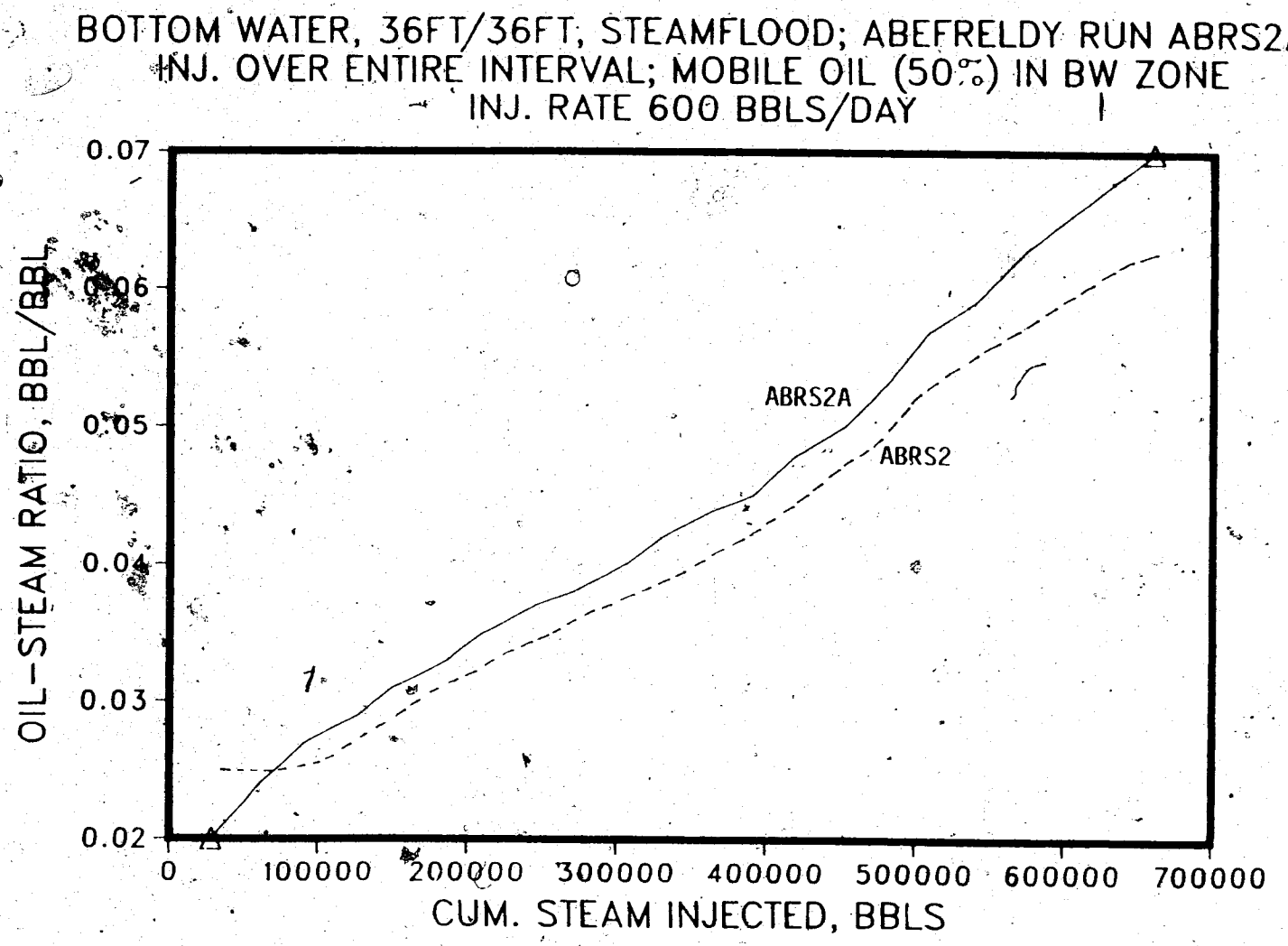

Figure 6.25 Oil-Steam Ratio vs. Steam Injected for Aberfeldy Steamflood ABRS2A

Table C.26.) A comparison with Figs. 6.12 and 6.14 for the case of immobile oil in the water layer shows that a small improvement in the oil production rate and oil-steam ratio occurs. The cumulative oil-steam ratio for the period simulated is nearly 30% higher than that for immobile oil. The oil recovery is 2% (Table C.26) as compared to 0.8% (ABRS2, Table 6.2) for the immobile oil case. As expected, the WOR is also lower because of some oil production from the water zone as well. The temperature profiles showed that heating of the water zone is to some extent greater than that of the oil zone (both have the same thickness and heating properties). It can be conjectured that, if a bottom water zone contains a substantial volume of mobile oil, it may be feasible to develop a profitable steam injection process. Other variables to be examined in this regard are steam injection interval, rate, and quality, as functions of time.

Effect of Steam Injection Rate

Table 6.2 shows four runs (ABRS4, ABRS8, ABRS14, and ABRS10) utilizing twice the steam injection rate of the base run, i.e. 1200 B/D. The oil and water production histories, water-oil ratios, and oil-steam ratio for these runs are shown in Figs. 6.26 through 6.34 and Figs. 6.5 to 6.7. A comparison of the base run ABRS1 (Figs. 6.2 to 6.4) and ABRS4 (Figs. 6.26 to 6.28) shows that the oil recovery in the case of the higher steam injection rate is more than twice as large (14.6% vs. 6.25%) in the same time, i.e. 700 days (cum. inj. 420,000 bbl and 840,000 bbl), when there is no bottom water. This is due to faster and increased heating of the reservoir, with reduced gravity segregation of steam. The effect is noticeable in the oil-steam ratio, which increases from 0.25 (ABRS1) to 0.29 (ABRS4). This is a better criterion, because it shows that the real gain in oil production as a result of an increase in steam injection rate is smaller than the oil recovery figures indicate.

Figures 6.35 to 6.37 show the oil and water production histories, WOR, and oil-steam ratio for Run ABRS4A, which is similar to Run ABRS4, except that a bottom water

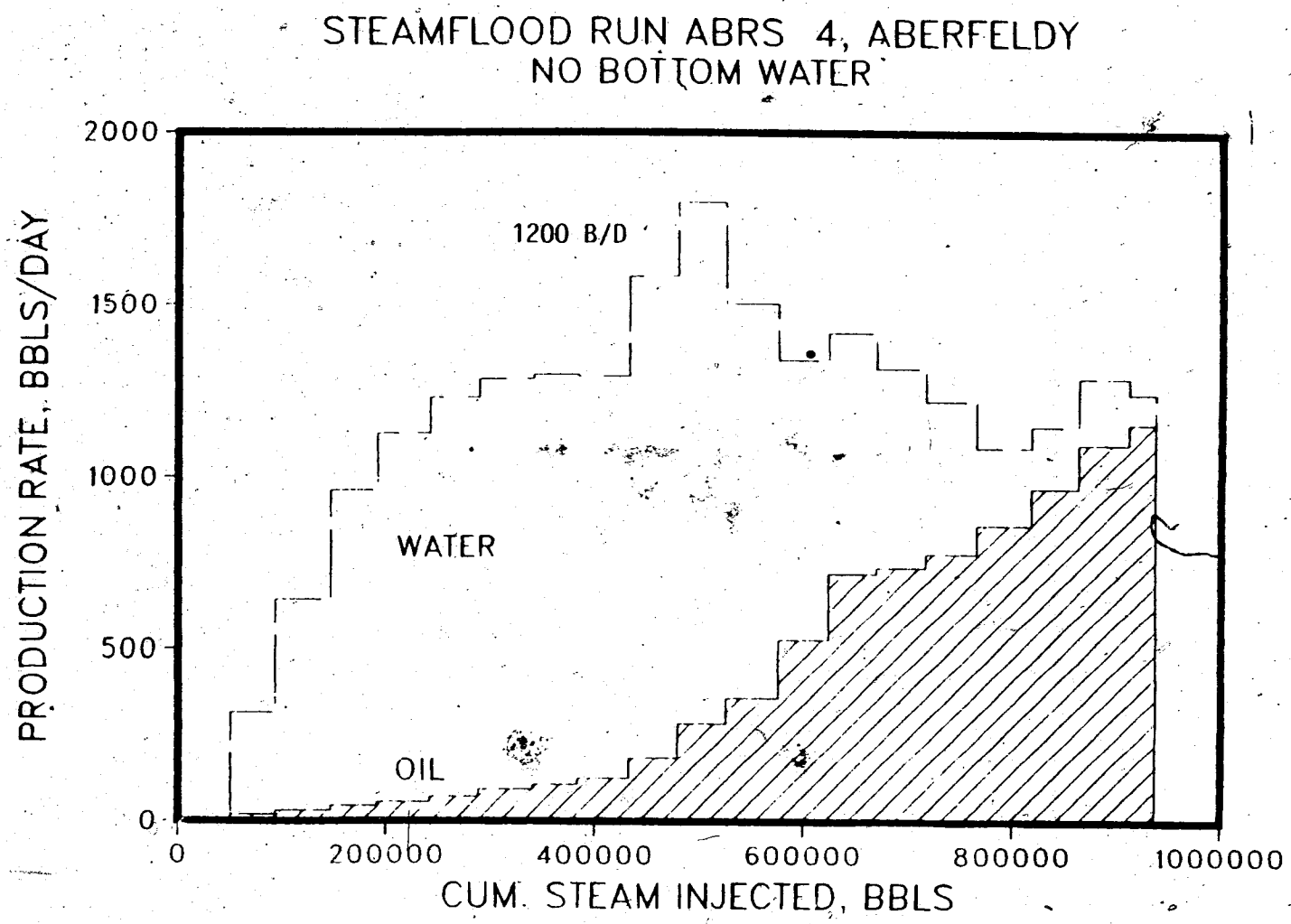

Figure 6.26 Production History of the Aberfeldy Steamflood ABRS4, No Bottom Water

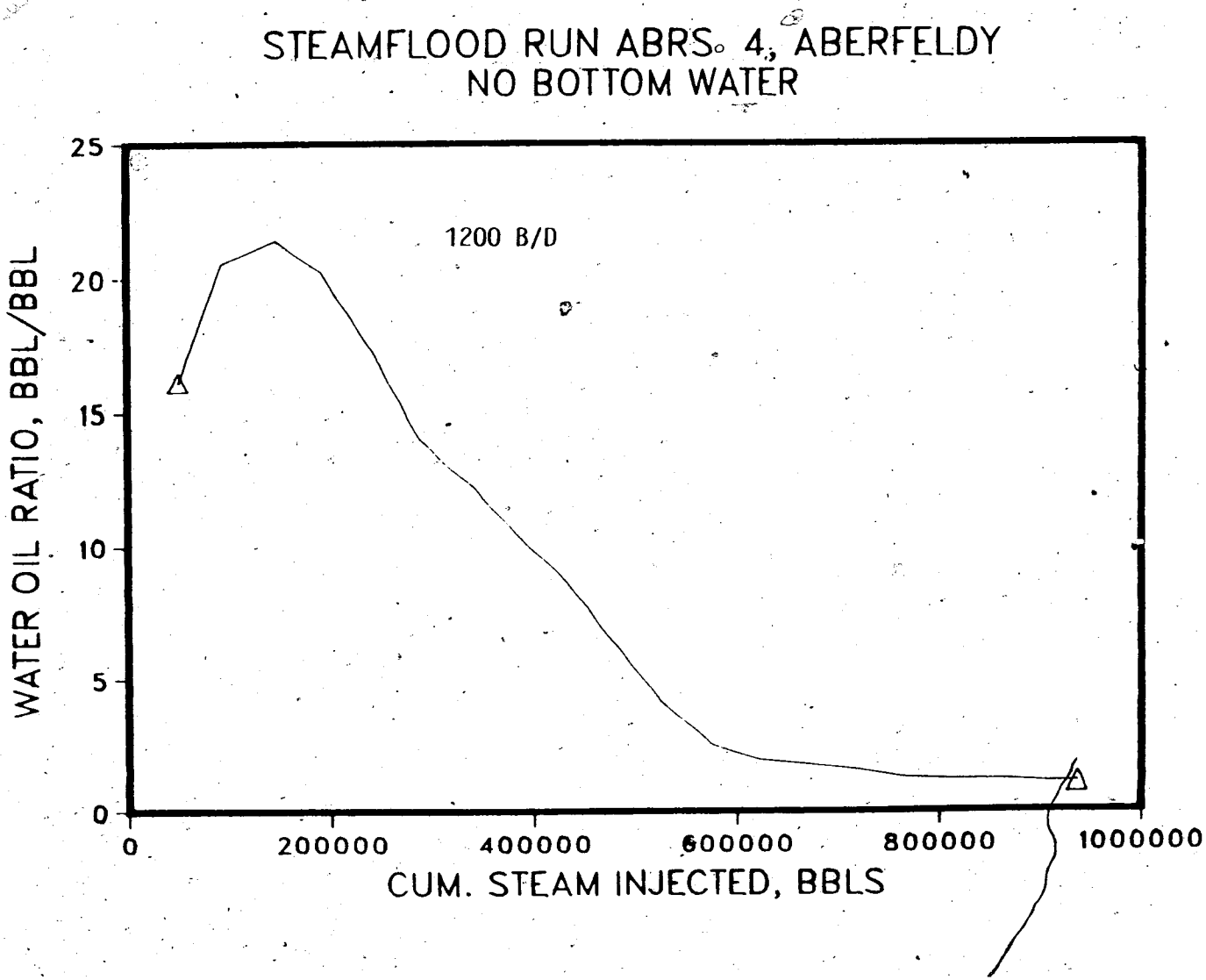

Figure 6.27 Water-Oil Ratio vs. Steam Injected for Aberfeldy Steamflood ABRS4

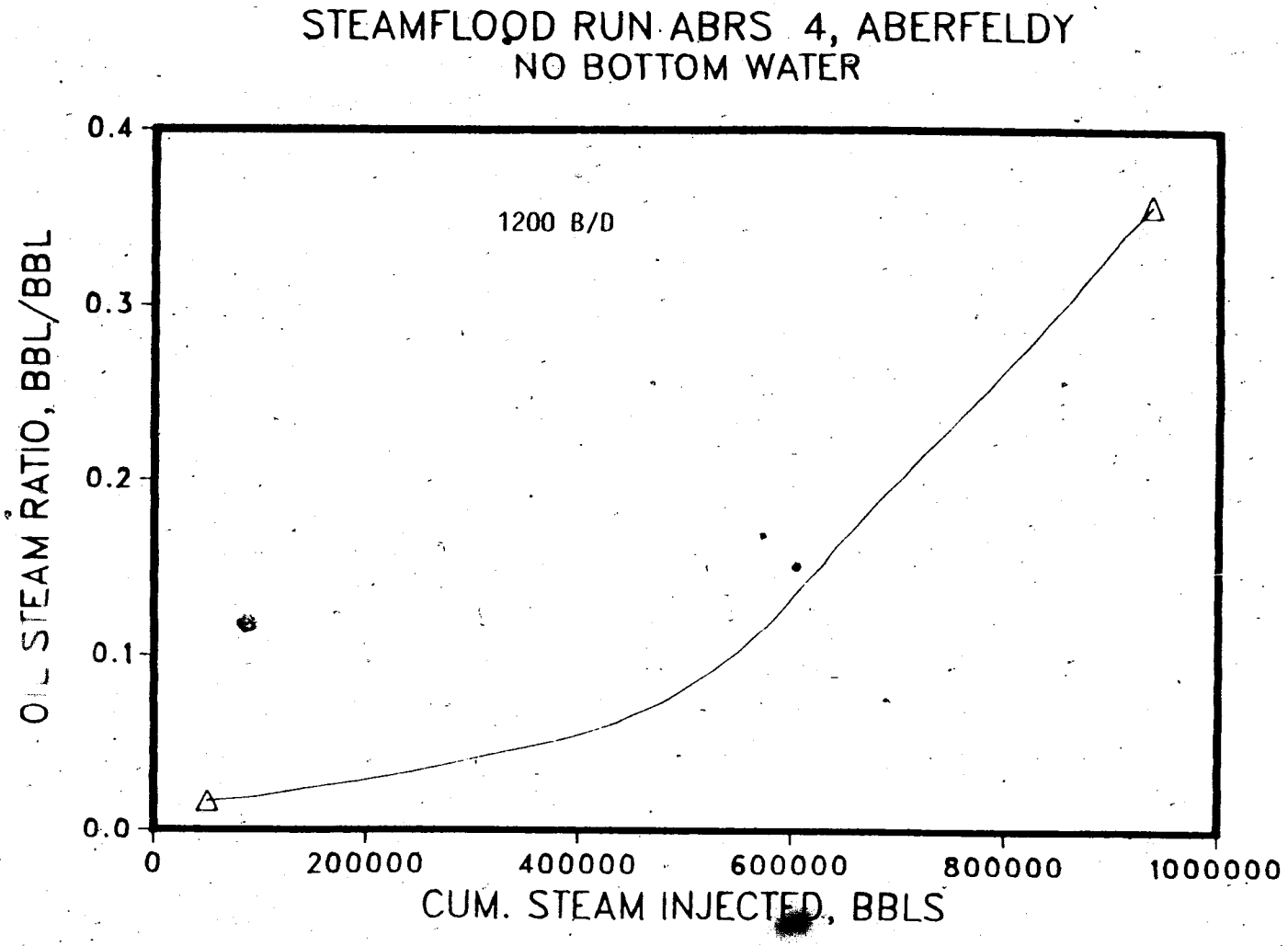

Figure 6.28 Oil-Steam Ratio vs. Steam Injected for Aberfeldy Steamflood ABRS4

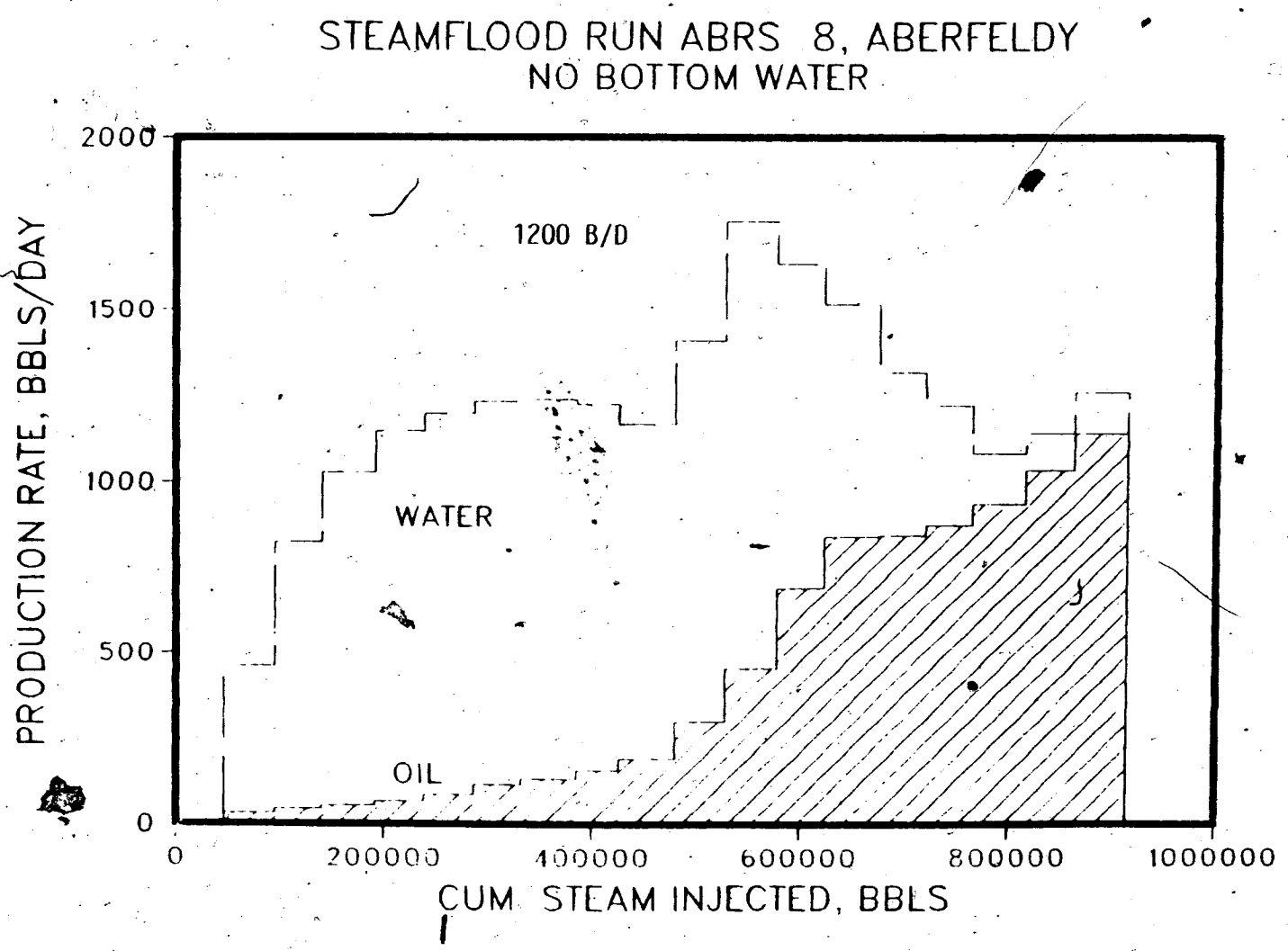

Figure 6.29 Production History of the Aberfeldy Steamflood ABRS8, No Bottom Water

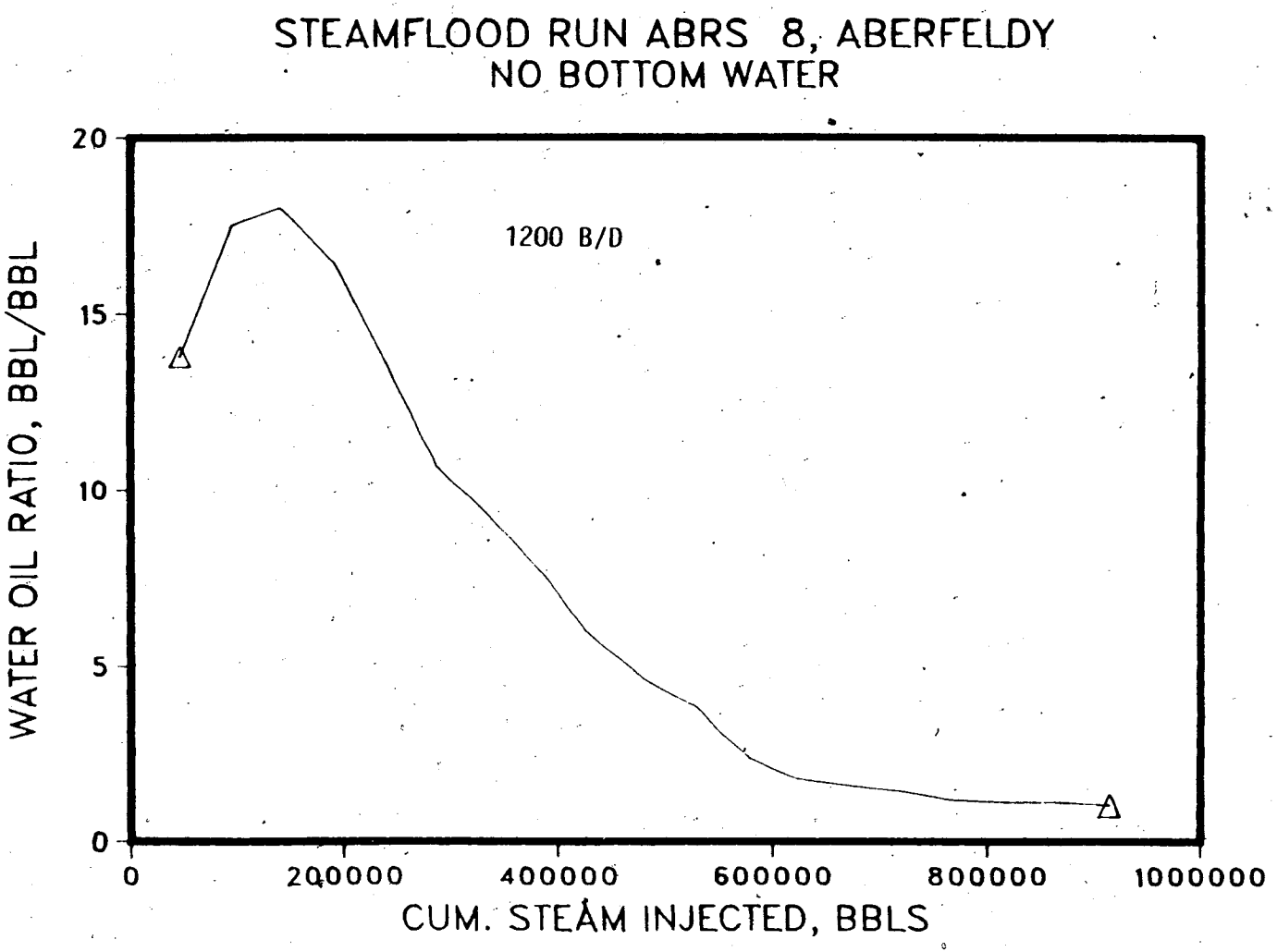

Figure 6.30 Water-Oil Ratio vs. Steam Injected for Aberfeldy Steamflood ABRS8

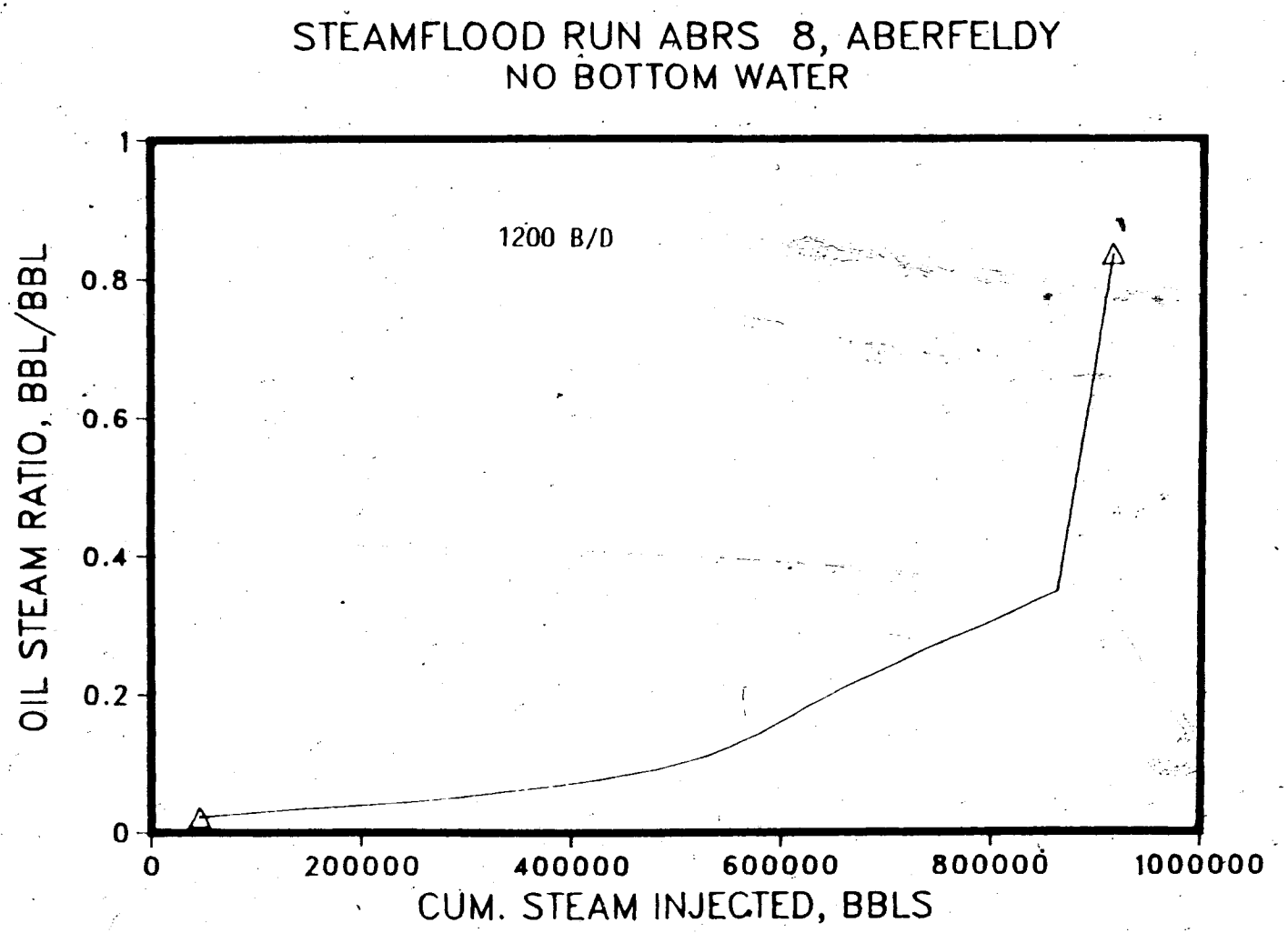

Figure 6.31 Oil-Steam Ratio vs. Steam Injected for Aberfeldy Steamflood ABRS8

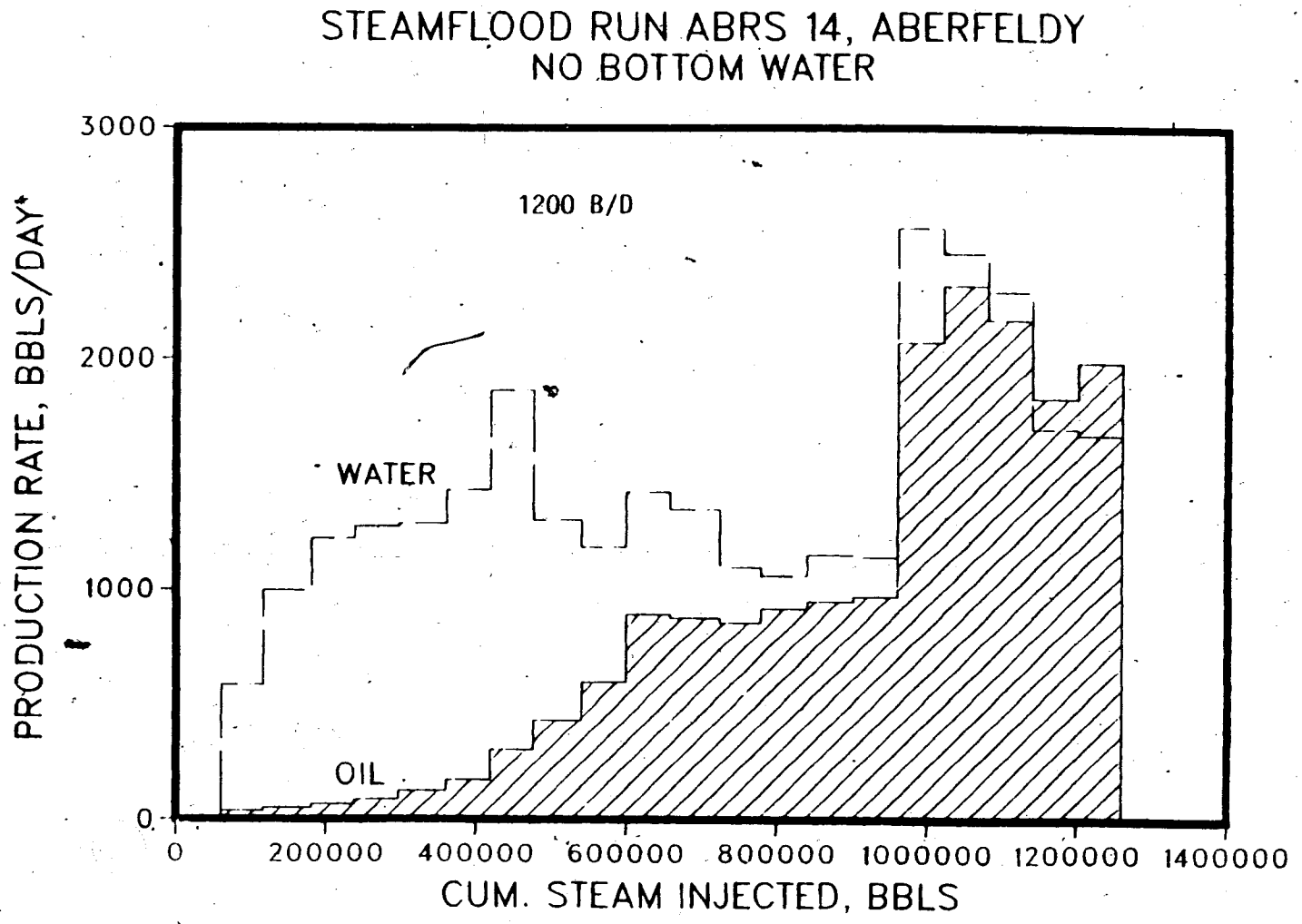

Figure 6.32 Production History of the Aberfeldy Steamflood ABRS14, No Bottom Water

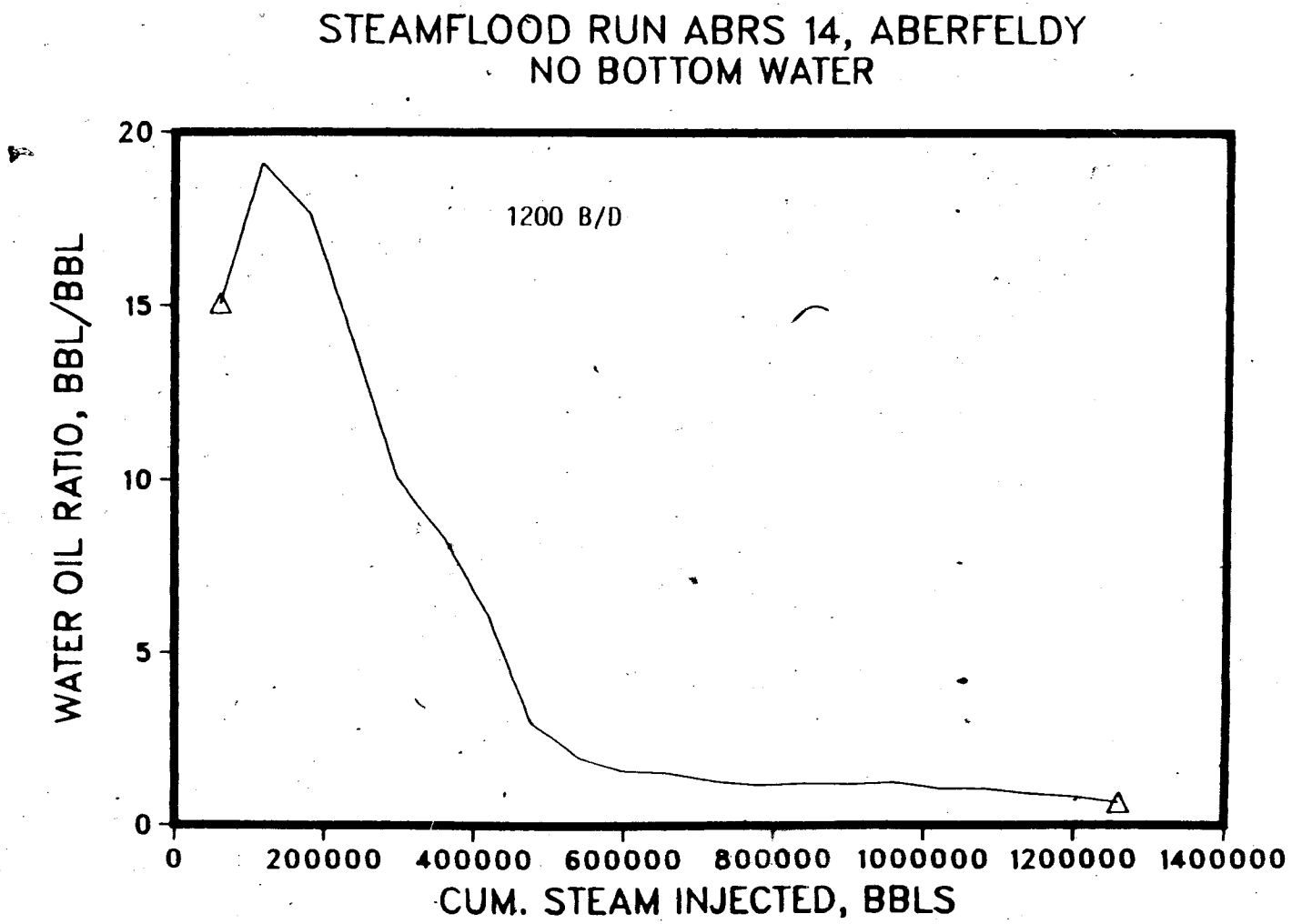

Figure 6.33 Water-Oil Ratio vs. Steam Injected for Aberfeldy Steamflood ABRS14

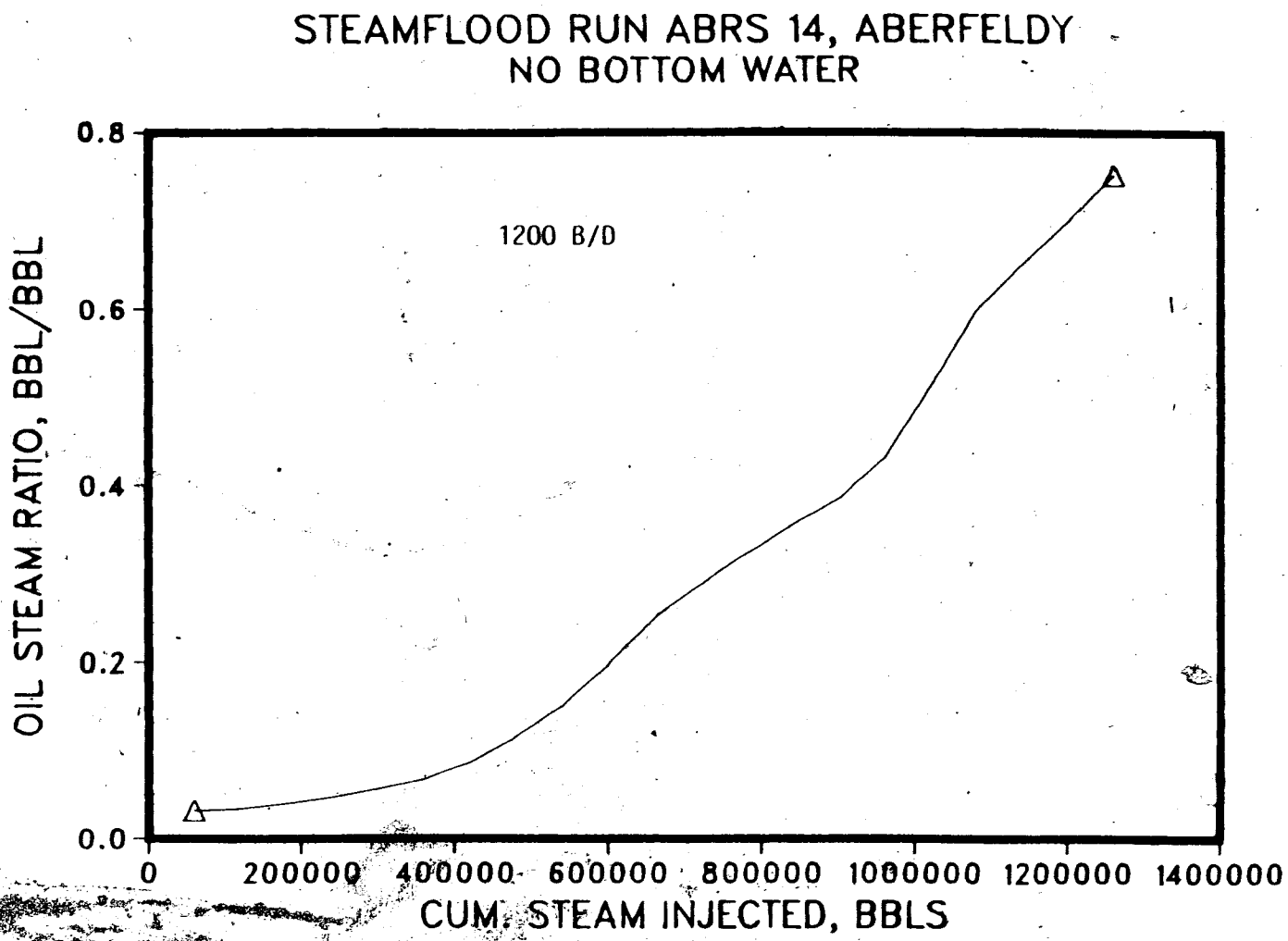

Figure 6.34 Oil-Steam-Ratio vs. Steam Injected for Aberfeldy Steamflood ABRS14

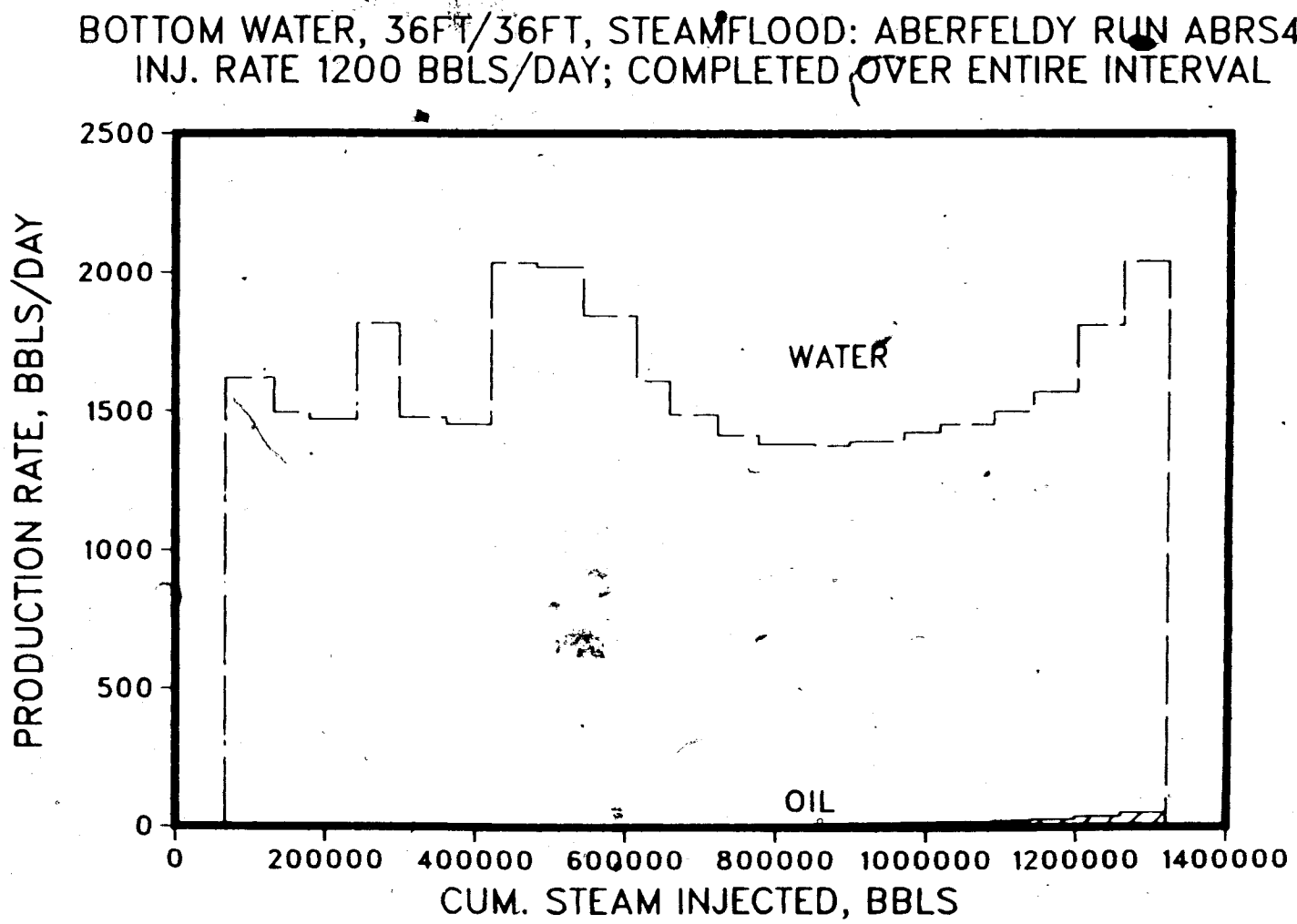

Figure 6.35 Production History of the Aberfeldy Steamflood ABRS4A, Bottom Water

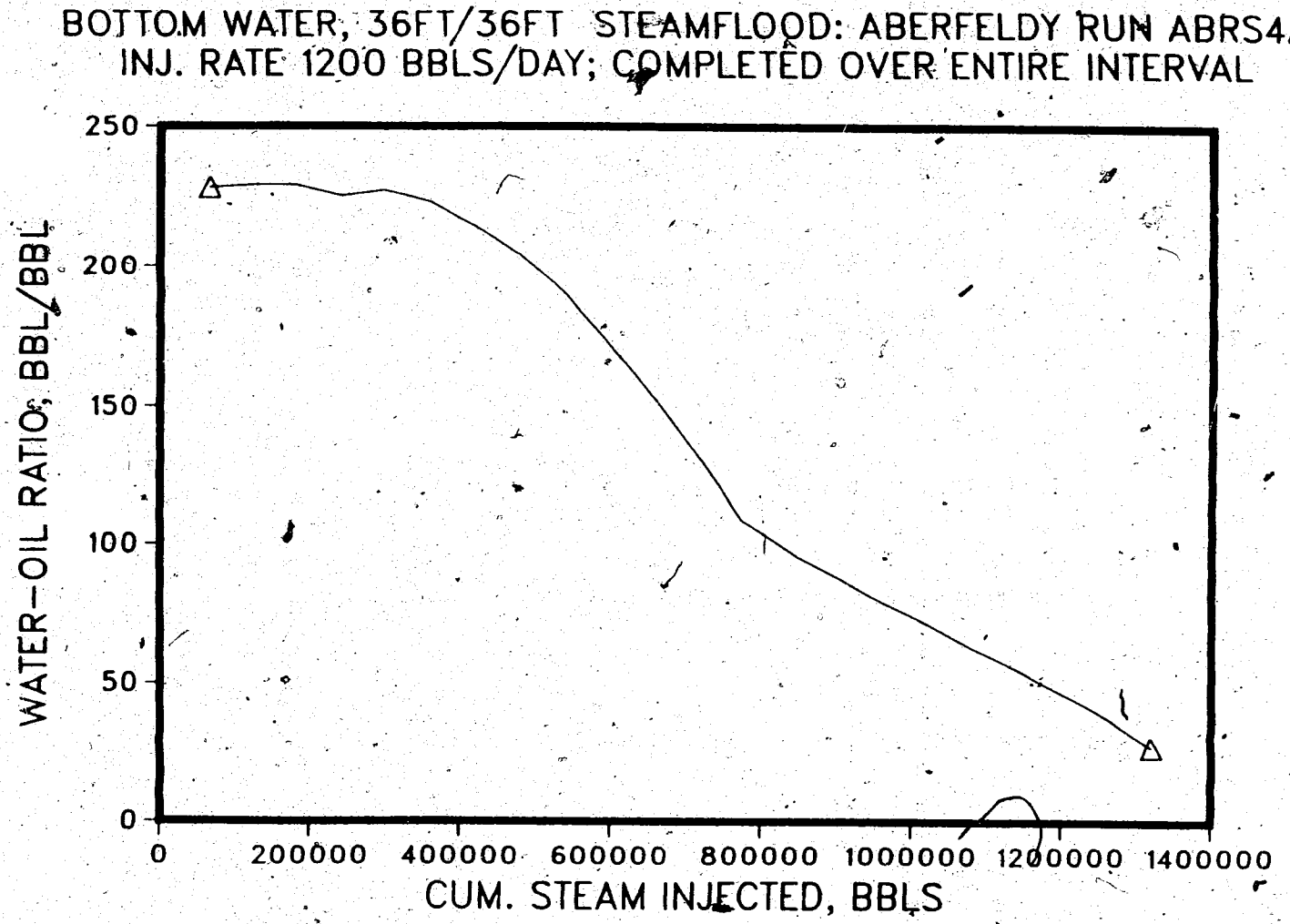

Figure 6.36, Water-Oil Ratio vs. Steam Injected for Aberfeldy Steamflood ABRS4A

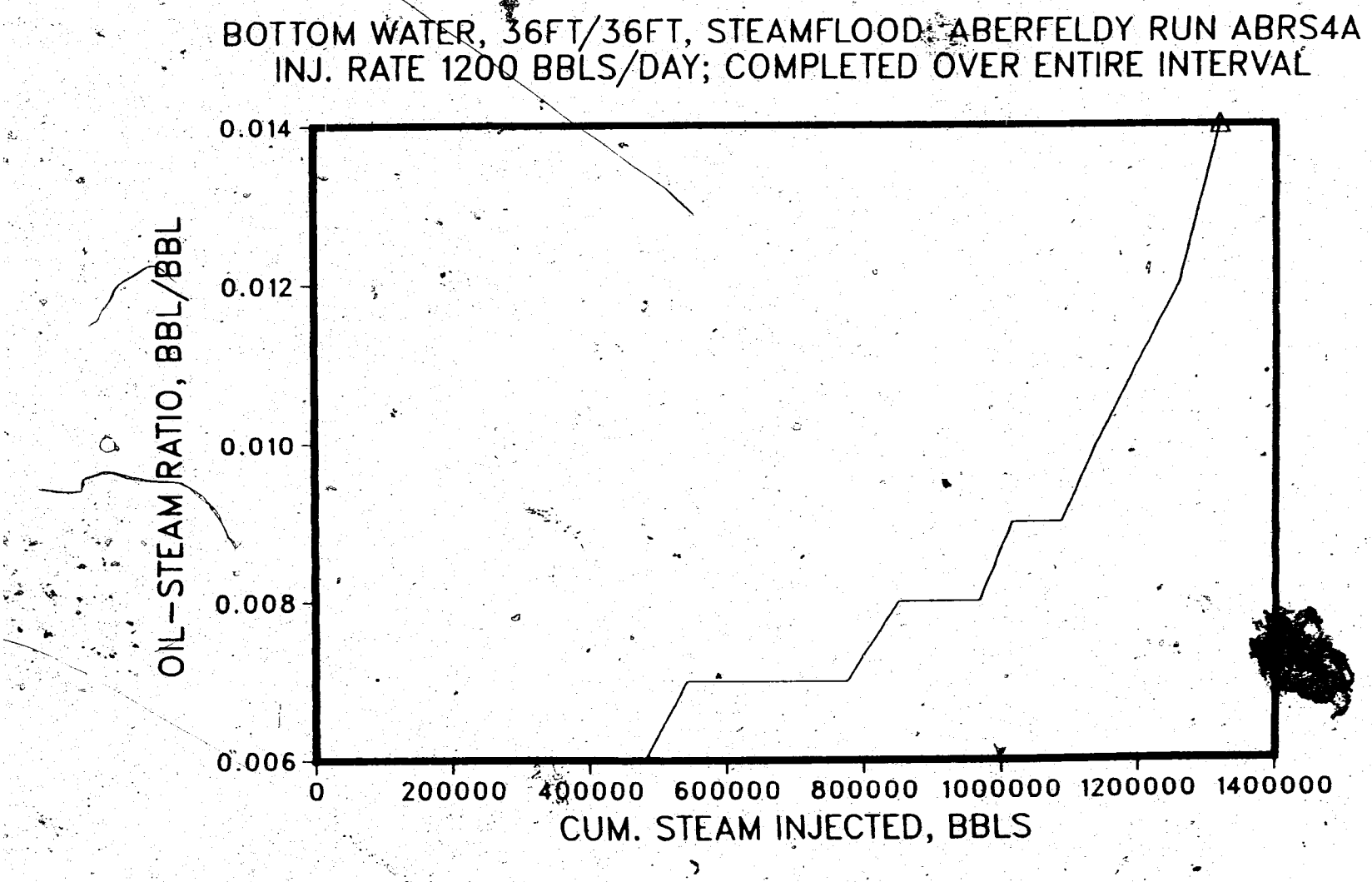

Figure 6.37 · Oil-Steam Ratio vs. Steam Injected for Aberfeldy Steamflood ABRS4A

layer of the same thickness as the oil zone is present. Figures 6.38 to 6.40 show similar plots for Run ABRS4B, in which the bottom water layer is one-tenth of the oil layer thickness. The difference in the performances of the three runs (ABRS4, ABRS4A, and ABRS4B) is remarkable. First, the thick water zone clearly leads to a large drop in the oil-steam ratio (0.0125 for ABRS4A vs. 0.290 for ABRS4) and oil recovery (0.85% for ABRS4A vs. 14.6% for ABRS4). This is due to the flow of steam in the water zone, which was found to be heated more than the oil zone. When the water zone thickness is reduced to one-tenth of the oil zone, the performance is actually improved for the high steam injection rate. The oil-steam ratio is now higher (0.352 for ABRS4B) than in the absence of bottom water. This is due to the fact that there is limited influx of steam into the water zone, with most of the steam going into the oil zone. At the same time, the heat from the water zone is conducted upward, mobilizing the colder oil above. As a result, the overall performance is actually improved due to the presence of water.

For a given oil, and for a given steam injection rate, there would be some bottom water zone thickness that is not detrimental and actually improves overall performance of a steamflood. A thin water zone would be beneficial for promoting steam injectivity in the case of a very viscous oil. But if the water zone is too thin, it will become saturated with the oil driven from the oil zone above, thus leading to a drop in steam injectivity. On the other hand, a thick water zone will act as a heat sink, leading to poor performance.

Effect of Vertical Permeability

An important factor in bottom water steamfloods is the vertical permeability of the oil/water formations. Obviously, a vertical permeability of zero is desirable, which will be the case if a shale barrier is present between the oil and water layers. If the vertical permeability is less than the horizontal permeability, then the performance would depend on the actual value. Up to a point, a reduction in the vertical permeability may not have a noticeable beneficial effect on performance, because steam still reaches the water zone.

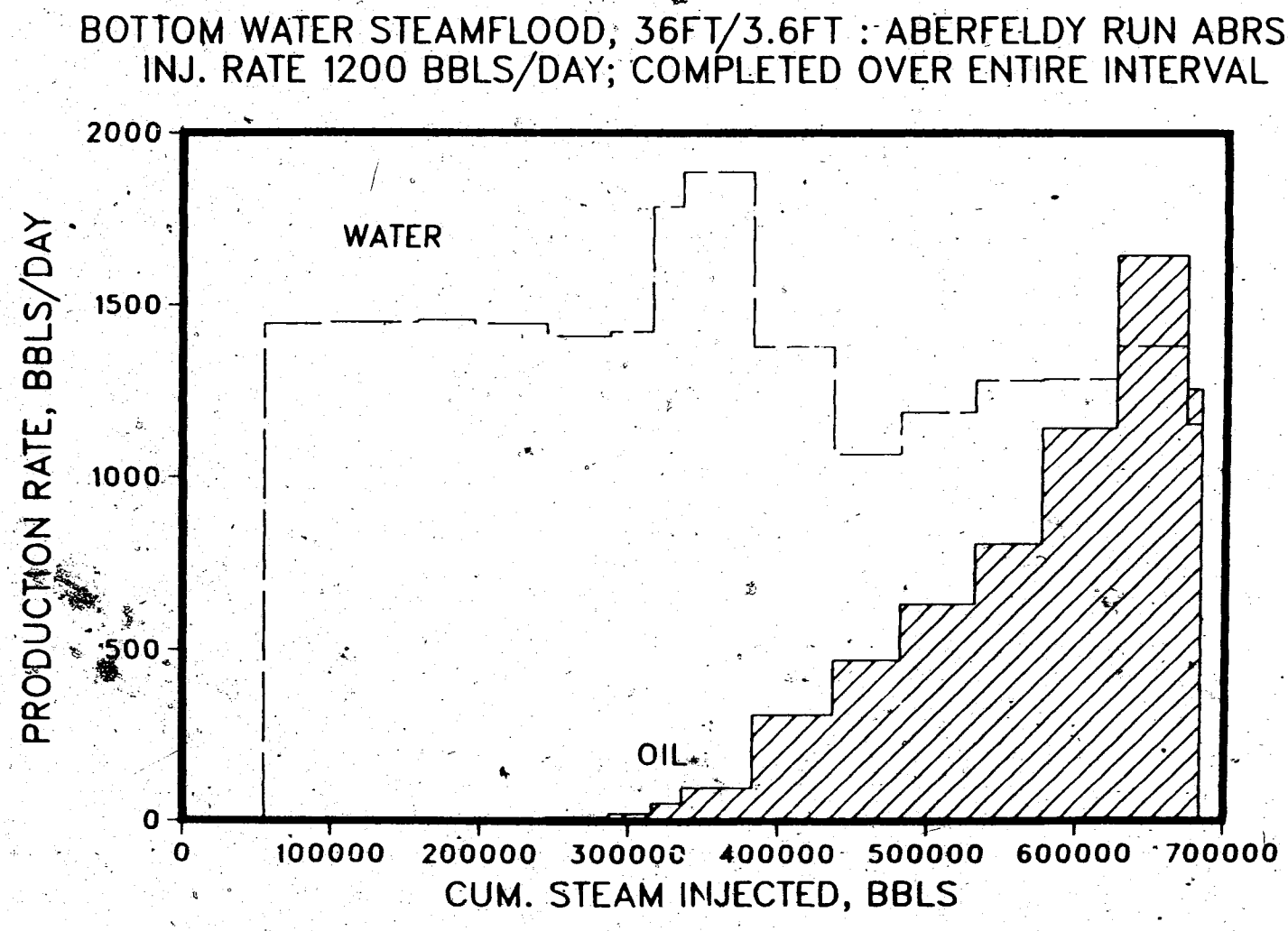

Figure 6.38 Production History of the Aberfeldy Steamflood ABRS4B, Bottom Water

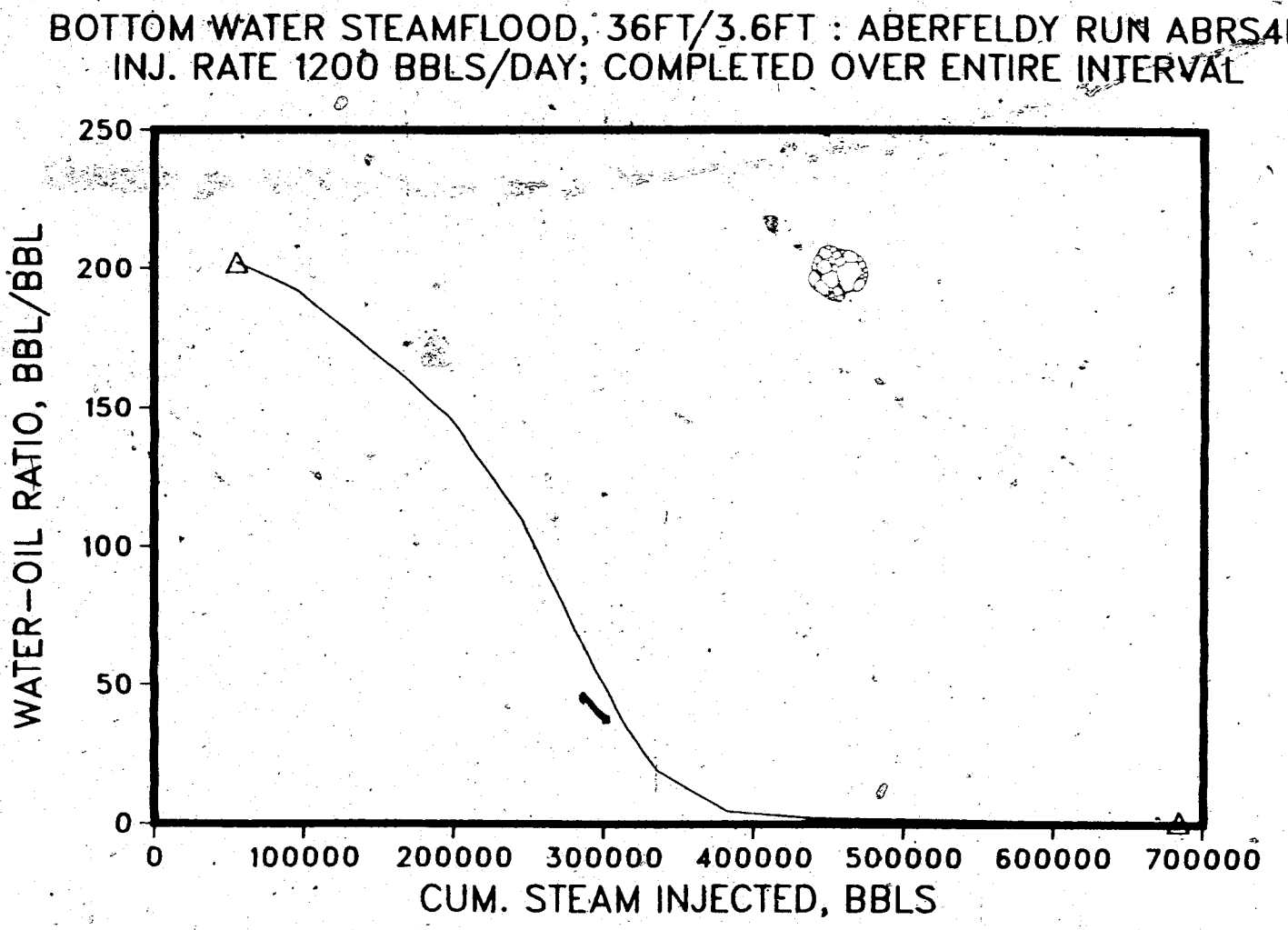

Figure 6.39 Water-Oil Ratio vs. Steam Injected for Aberfeldy Steamflood ABRS4B

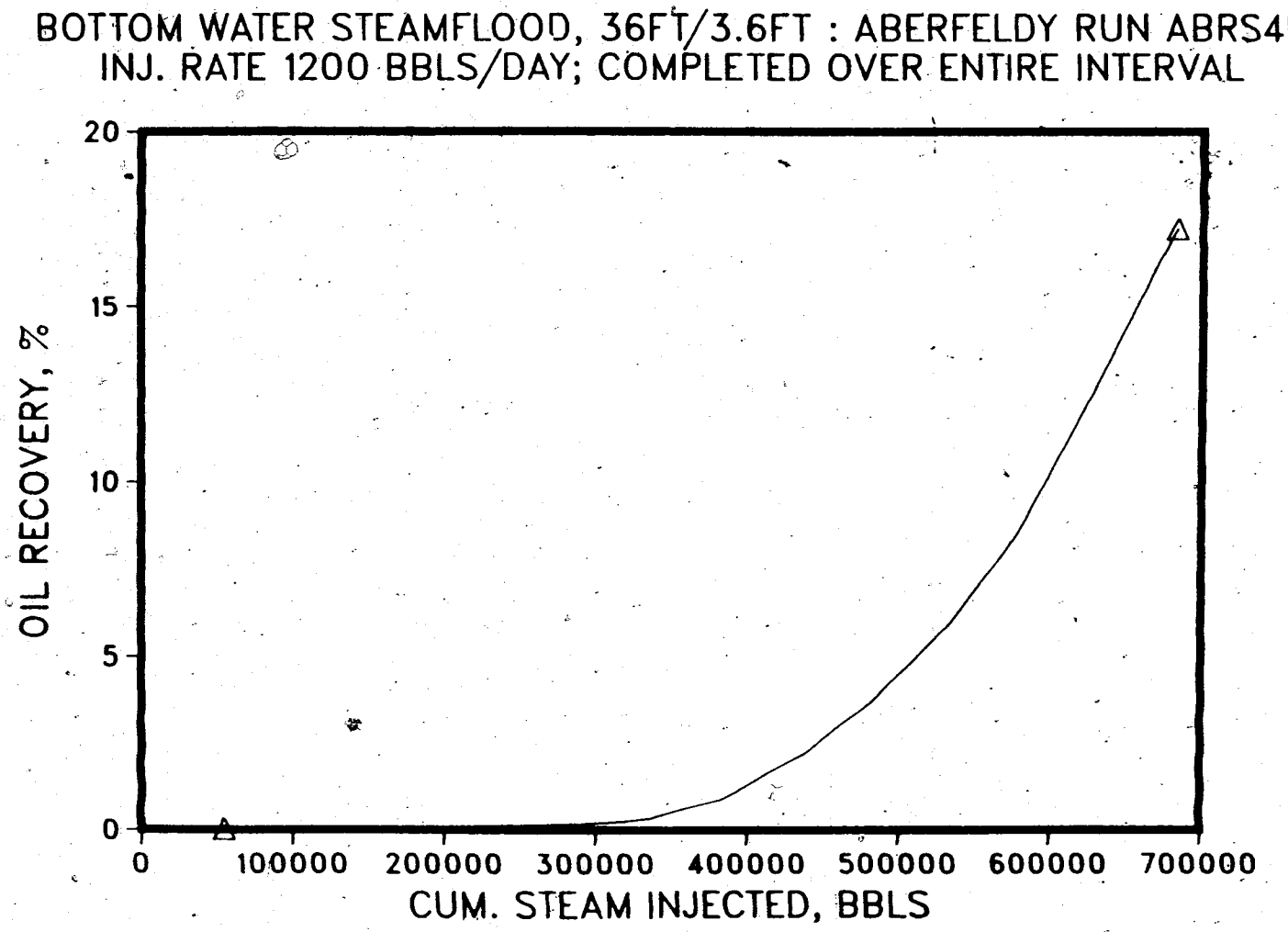

Figure 6.40 Oil Recovery vs. Steam Injected for Aberfeldy-Steamflood,ABRS4B

This was noted in the simulations conducted. Figures 6.21 to 6.23 and 6.41 through 6.43 show the oil and water production, WOR, and oil-steam ratio plots for Runs ABRS7 and ABRS15, in which the vertical permeability was reduced by a factor of 5, compared to the horizontal permeability. The bottom water zone was one-third and one-fifth of the oil zone, respectively. The performance of these two runs can be compared with that of the base Run ABRS1. It is seen that the reduced vertical permeability did not help much. The oil-steam rato is 0.075 and 0.092, respectively, compared to 0.25 in the absence of bottom water. If we compare the performance of ABRS15 (oil-steam ratio 0.092) with reduced vertical permeability (one-fifth) to that of ABRS5 (oil-steam ratio 0.113), with equal permeabilities in all directions, it is seen that the reduced permeability actually gives a slightly lower oil-steam ratio and oil recovery (in both cases $h_w/h_o = 0.2$). While this difference may not be significant because of numerical limitations, one possible explanation is that the oil driven into the water zone below (wells are completed in the oil zone only) is restricted from flowing back into the oil zone due to lower vertical permeability.

In Run ABRS16, the vertical permeability was reduced by a factor of 10 relative to the horizontal permeabilities (Table C.13). The performance is clearly improved in this case (oil-steam ratio is 0.627). It seems that the small amount of steam flowing in the water layer is helpful in conductive heating of the oil zone above, so that the cold oil is mobilized and driven efficiently into the producers.

Effect of Completion Interval

In steamflooding, the completion interval of the steam injection wells and the producers has an important effect on performance (oil recovery, oil-steam ratio, water-oil ratio, etc.). This is so because the vertical sweep, and the fluid and heat distributions will depend on the injection/production intervals. In all of the steamfloods discussed above, where bottom water was not present, the steam injection and production wells were completed in the entire interval. When bottom water was present, the wells were completed

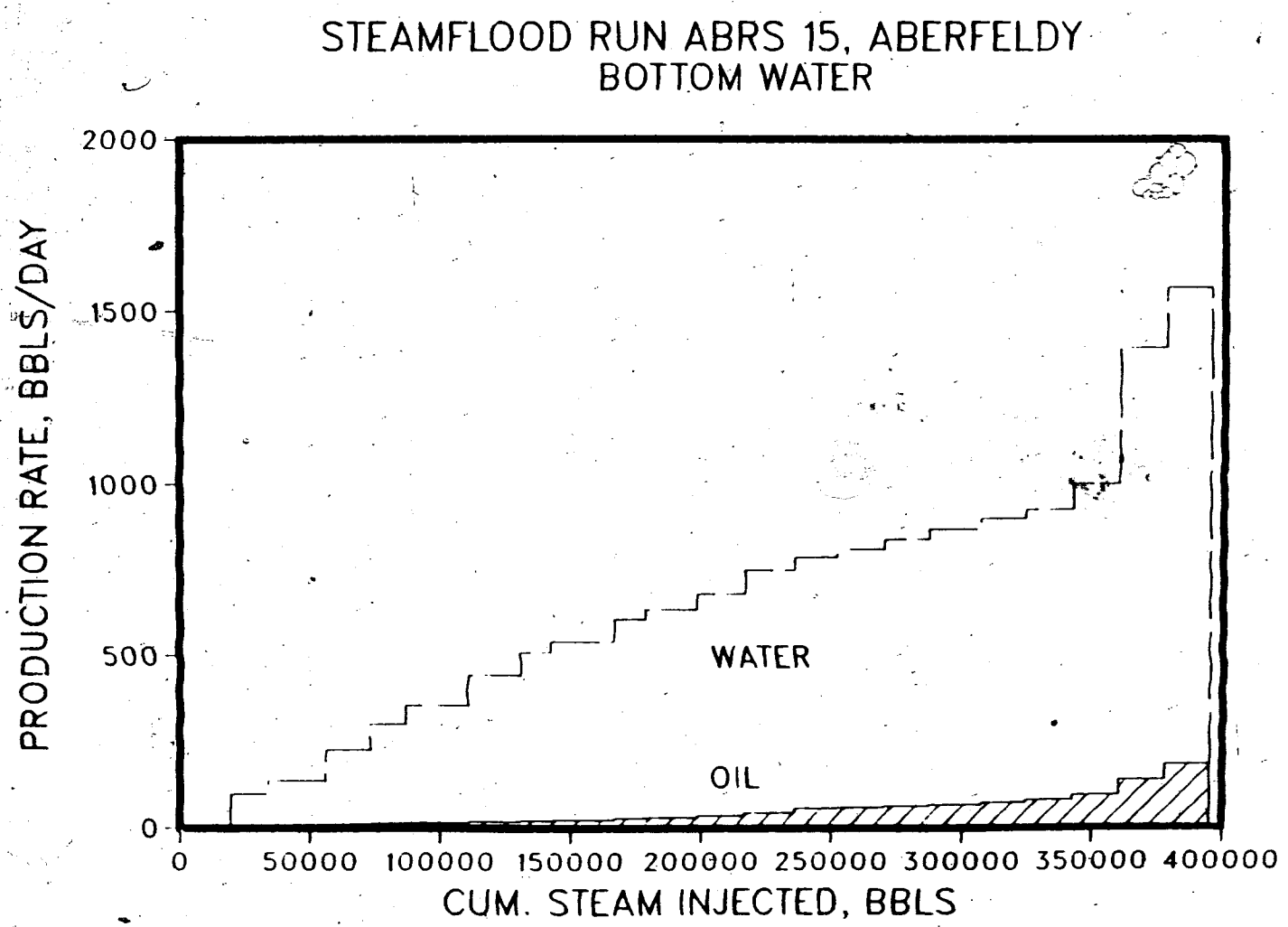

Figure 6.41 Production History of the Aberfeldy Steamflood ABRS15, Bottom Water

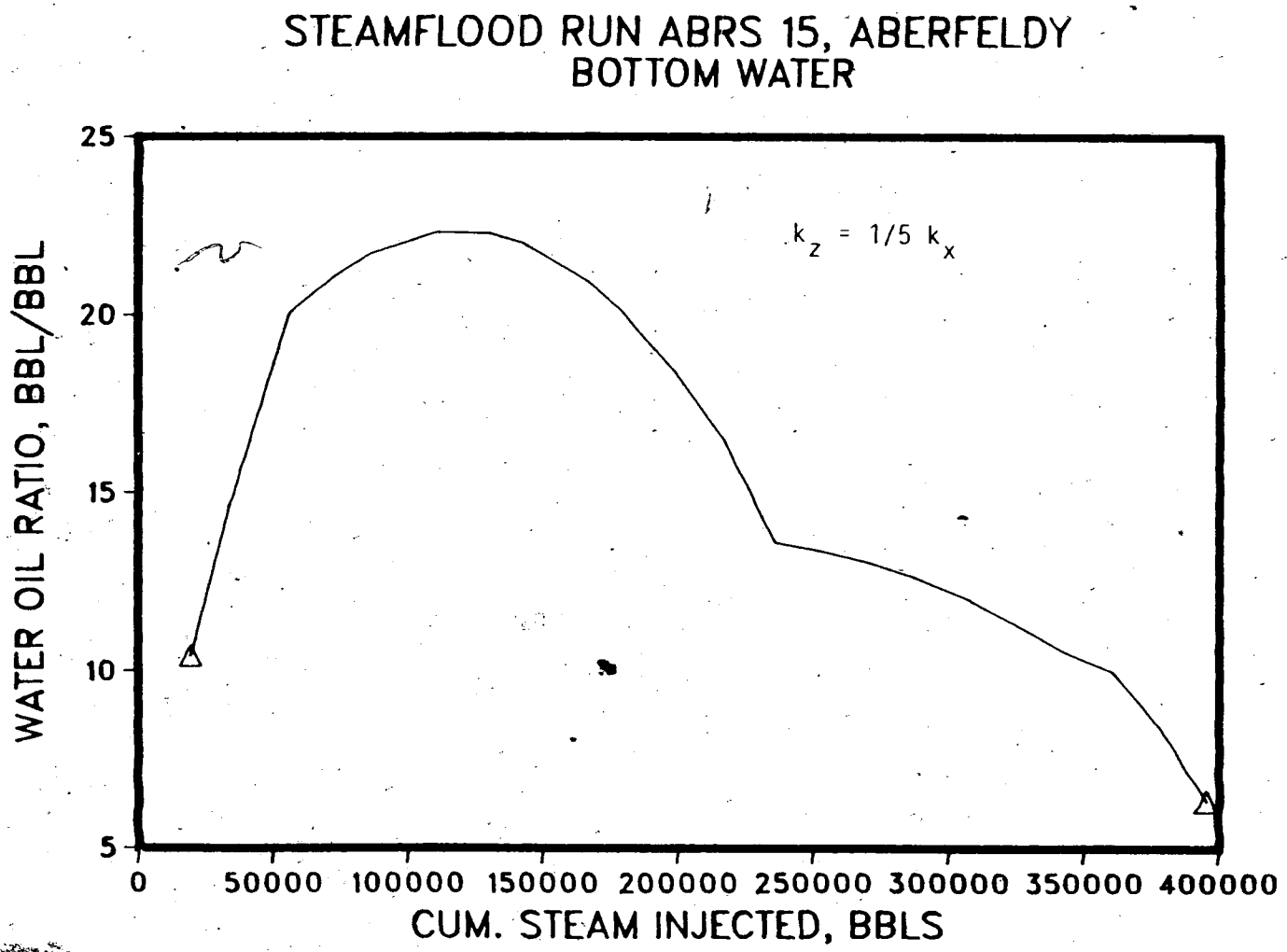

Figure 6.42 Water-Oil Ratio vs. Steam Injected for Aberfeldy Steamflood ABRS15

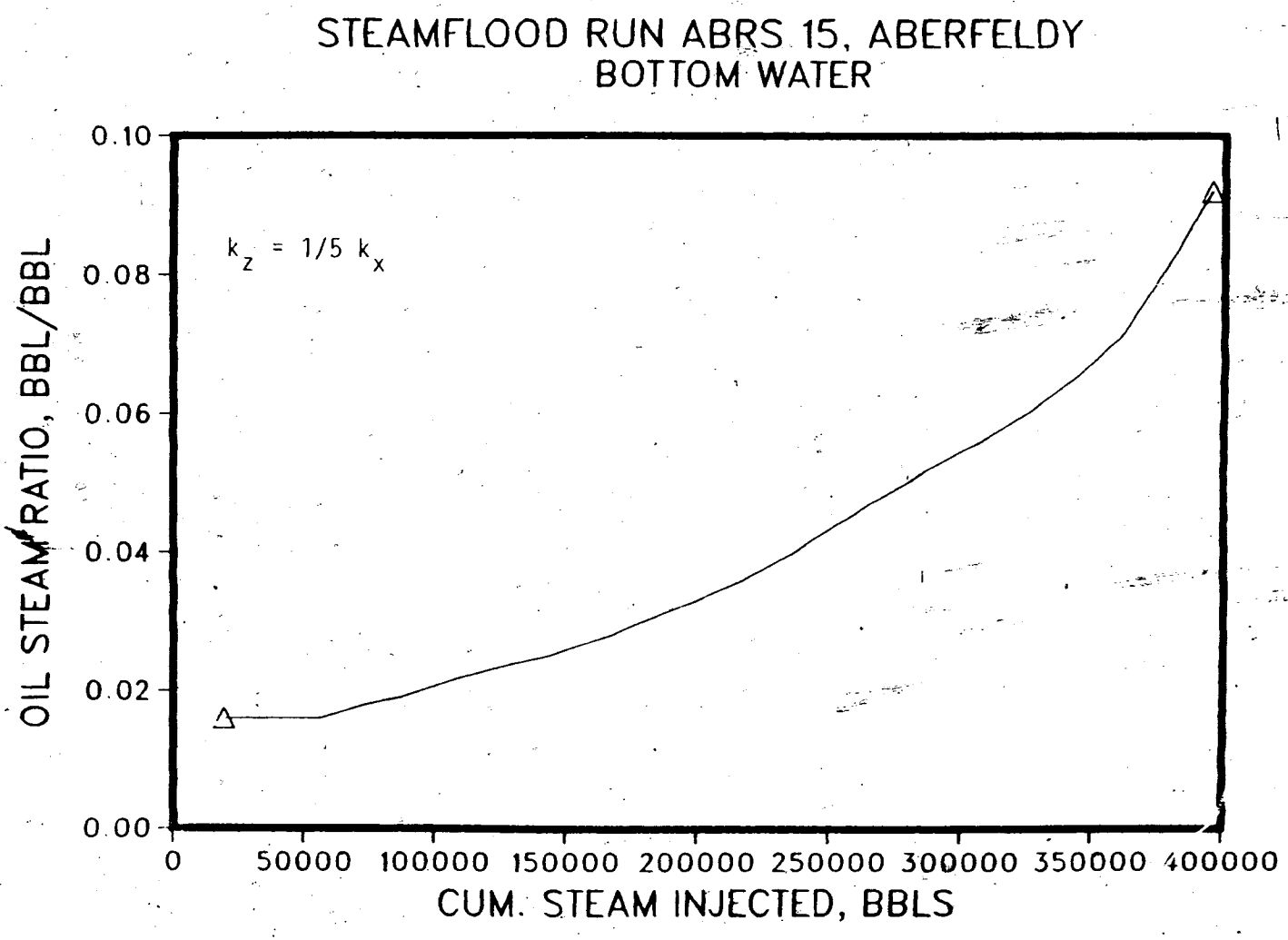

Figure 6.43 Oil-Steam Ratio vs. Steam Injected for Aberfeldy Steamflood ABRS15

only in the oil zone. As an example of a different type of completion, Run ABRS1B (Table C.27) is presented. In this run, there is no bottom water, and the injection well is completed in the lower part of the formation only. In this manner, steam would first heat the lower part of the formation, then rise, and heat the upper part. In contrast, the injection well completion in Run ABRS1 was across the entire formation, and as a result, steam segregation occurred early during the flood. Figures 6.44 to 6.46 show the performance curves for Run ABRS1B, and a comparison with Figs. 6.2 to 6.4 shows that injection in the lower part of the formation did improve oil-steam ratio (0.39 vs. 0.25), oil recovery (11% vs. 6.25%), and WOR. Many other types of completion schemes can be tested: e.g. completion at two points in the oil zone, completion of producers initially in the lower part of the oil zone, and at a later time over the entire interval (when bottom water is present), injection well completion in the oil zone and completion of producers in the water zone (case of reverse coning), as well as various partial penetration schemes.

Cyclic Steam Stimulations: Aberfeldy

Many cyclic steam stimulation simulations were carried out to examine the effects of selected variables, for the Aberfeldy and Cold Lake reservoirs. The main variables in the cyclic steaming process are: steam slug size, steam pressure, quality, injection rate, soak time, injection interval, wellbore completion, production period, well operating conditions, number of cycles, increasing/decreasing/constant steam slug sizes for succeeding cycles, formation fracturing, bottom water effects, use of additives with steam, partial penetration, etc. A few of these variables were studied in this work.

Tables 6.3 (a) and (b) summarize the principal results of cyclic steam stimulation simulations conducted. The run termination criterion was a preset (200 sec) computer time. Only in a few instances were runs as long as 500 sec conducted.

Tables C.14 to C.17 and Figs. 6.47 through 6.58 summarize results of cyclic steam stimulation simulations for the Aberfeldy formation, for the case of no bottom water. The

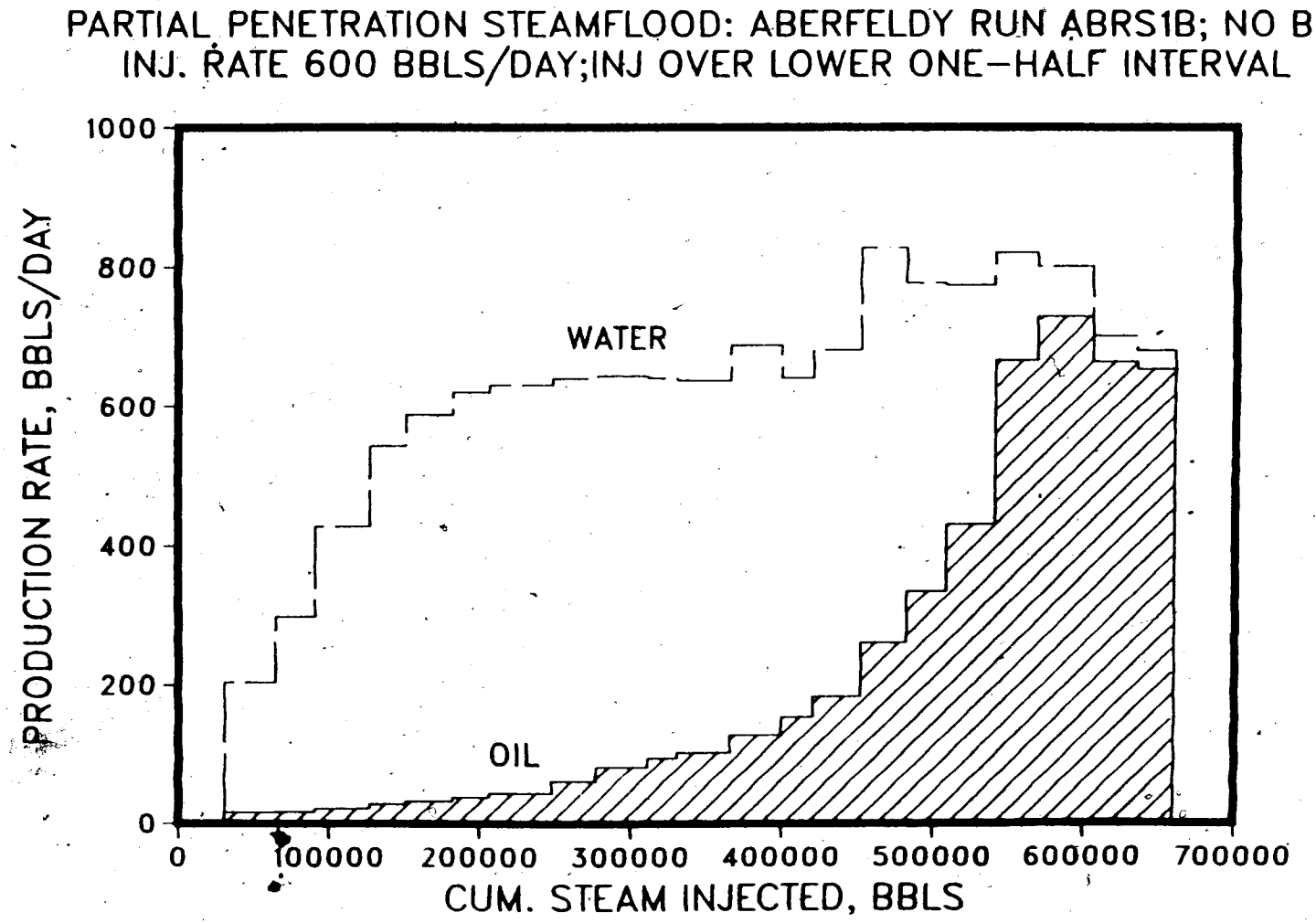

Figure 6.44 Production History of the Aberfeldy Steamflood ABRS1B, No Bottom Water.

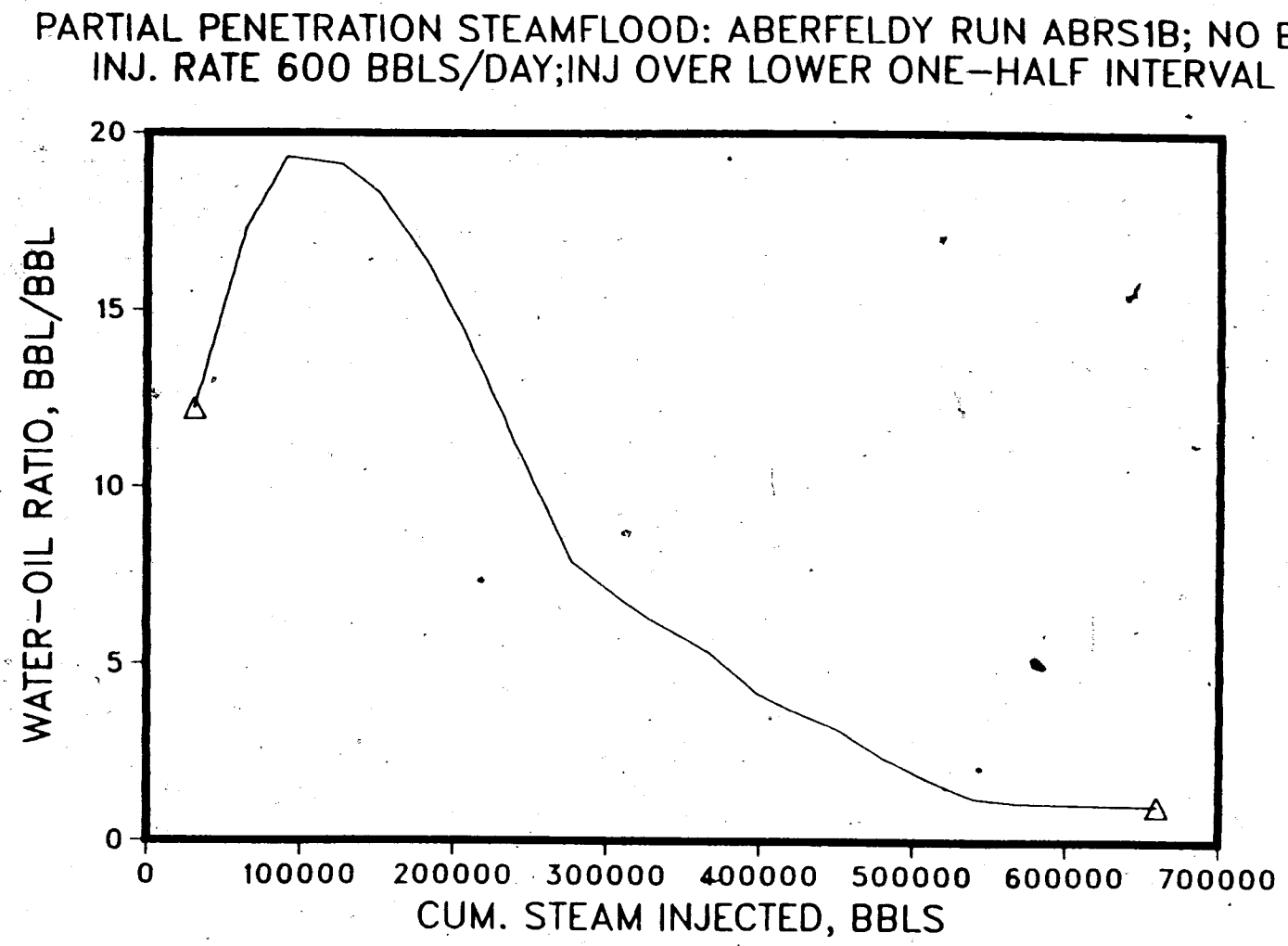

Figure 6.45 Water-Oil Ratio vs. Steam Injected for Aberfeldy Steamflood ABRS1B

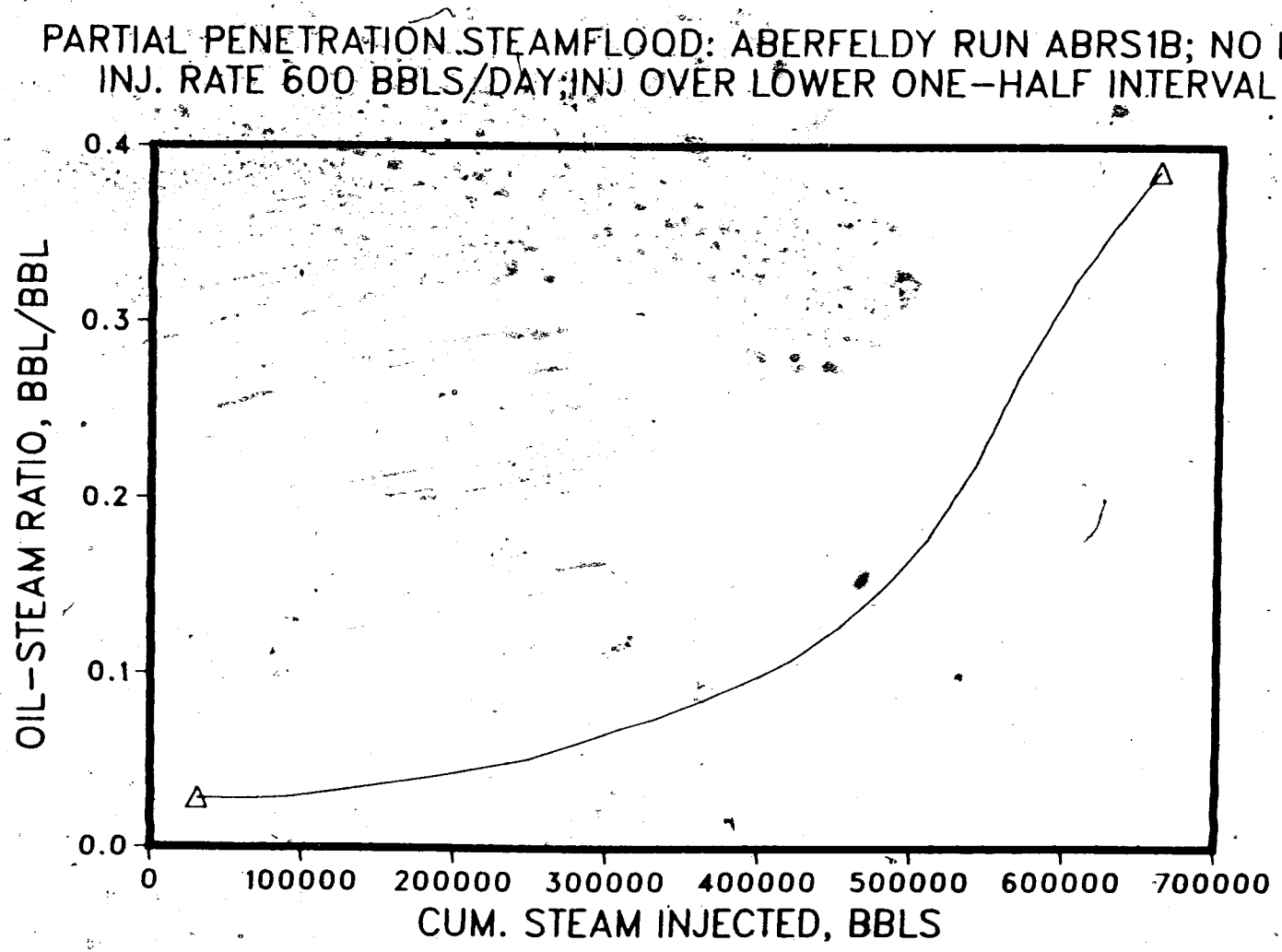

Figure 6.46 Oil-Steam Ratio vs. Steam Injected for Aberfeldy Steamflood ABRS1B

ABERFELDY CYCLIC STEAMING RUNS & CONDITIONS

Run	Cycle 1 Injection Time	Cycle 1 Soak Time	Cycle 1 Production Time	Cycle 2 Injection Time	Cycle 2 Soak Time	Cycle 2 Production Time	Cycle 3 Injection Time	Cycle 3 Soak Time	Cycle 3 Production Time	Conditions	Notes
ABC1	30	5	90	30	5	90	30	5	90	no bottom water	1,2
ABC2	30	5	90	40	5	90	50	5	90	no bottom water	3
ABC3	30	5	90	20	5	90	10	5	90	no bottom water	4
ABC4	30	20	90	30	20	90	30	20	90	no bottom water	5
ABC6	30	5	90	30	5	90	30	5	90	thin bottom water	1,2
ABC8	30	5	90	20	5	90	10	5	90	thin bottom water	3
ABC9	30	20	90	30	20	90	30	20	90	thin bottom water	4
ABC11	30	5	90	30	5	90	30	5	90	thick bottom water	1,2
ABC17	30	5	90	30	5	90	30	5	90	thick botom water	3
ABC18	30	5	90	30	5	90	30	5	90	thick bottom water	4,6

Note 1: Injection time 30 days, soak time 5 days
Note 2: Same condition in all cycles
Note 3: Injection time 30 days in Cycle 1, 40 days in Cycle 2 and 50 days in Cycle 3, soak time, 5 days
Note 4: Injection time 30 days in Cycle 1, 20 days in Cycle 2 and 10 days in Cycle 3, soak time, 5 days
Note 5: Injection time 30 days, long soak times (20 days), in all cycles
Note 6: Well completed in the upper one-half of the oil zone

ABERFELDY CYCLIC RUNS RESULTS SUMMARY

Run	$\frac{h_w}{h_{oil}}$	Perfs.	Cycle 1 Prod. time,day	Cycle 1 OSR Bbl/Bbl	Cycle 1 Cum WOR	Cycle 1 Oil Rec.%	Cycle 2 Prod. time,day	Cycle 2 OSR Bbl/Bbl	Cycle 2 Cum. WOR	Cycle 2 Oil Rec.%	Cycle 3 Prod. time,day	Cycle 3 OSR Bbl/Bbl	Cycle 3 Cum. WOR	Cycle 3 Oil rec.%	N
ABC1	0	1-2	90	0.103	10.2	.32	0	-	-	-	0	-	-	-	1,2
ABC2	0	1-2	90	.151	8.65	.40	90	.086	76.9	.53	7	.053	21.3	.565	3
ABC3	0	1-2	90	.151	8.65	.40	90	.132	26.2	.59	90	.1254	27.62	.67	4
ABC4	0	1-2	90	.1408	8,75	.38	20	.0874	25.11	.47	0	-	-	-	5
ABC6	0.1	1-1	90	.058	31.17	.15	90	.0593	57.6	30	10	.044	24.2	.34	1,2
ABC8	0.1	1-1	90	.058	31.17	.15	90	.079	14.77	.34	90	.091	17.11	.47	3
ABC9	0.1	1-1	90	.055	32.12	.14	17	.0395	20.4	.20	0	-	-	-	4
ABC11	1.0	1-1	90	.082	16.8	.158	90	.0477	374.	.184	0	-	-	-	1,2
ABC17	1.0	1-1	90	.081	16.53	.155	90	.054	132.8	.206	13	.038	126.7	.221	3
ABC18	1.0	1-1	90	.0056	3.85	.011	90	.0114	4.60	.044	90	.022	2.97	.129	3,6

Note 1: Injection time 30 days, soak time 5 days

Note 2: Same condition in all cycles

Table 6.3 (b) continued

Note 3: Injection time 30 days in Cycle 1, 40 days in Cycle 2 and 50 days in Cycle 3, soak time, 5 days

Note 4: Injection time 30 days in Cycle 1, 20 days in Cycle 2 and 10 days in Cycle 3, soak time, 5 days

Note 5: Injection time 30 days, long soak times (20 days), in all cycles

Note 6: Well completed in the upper one-half of the oil zone

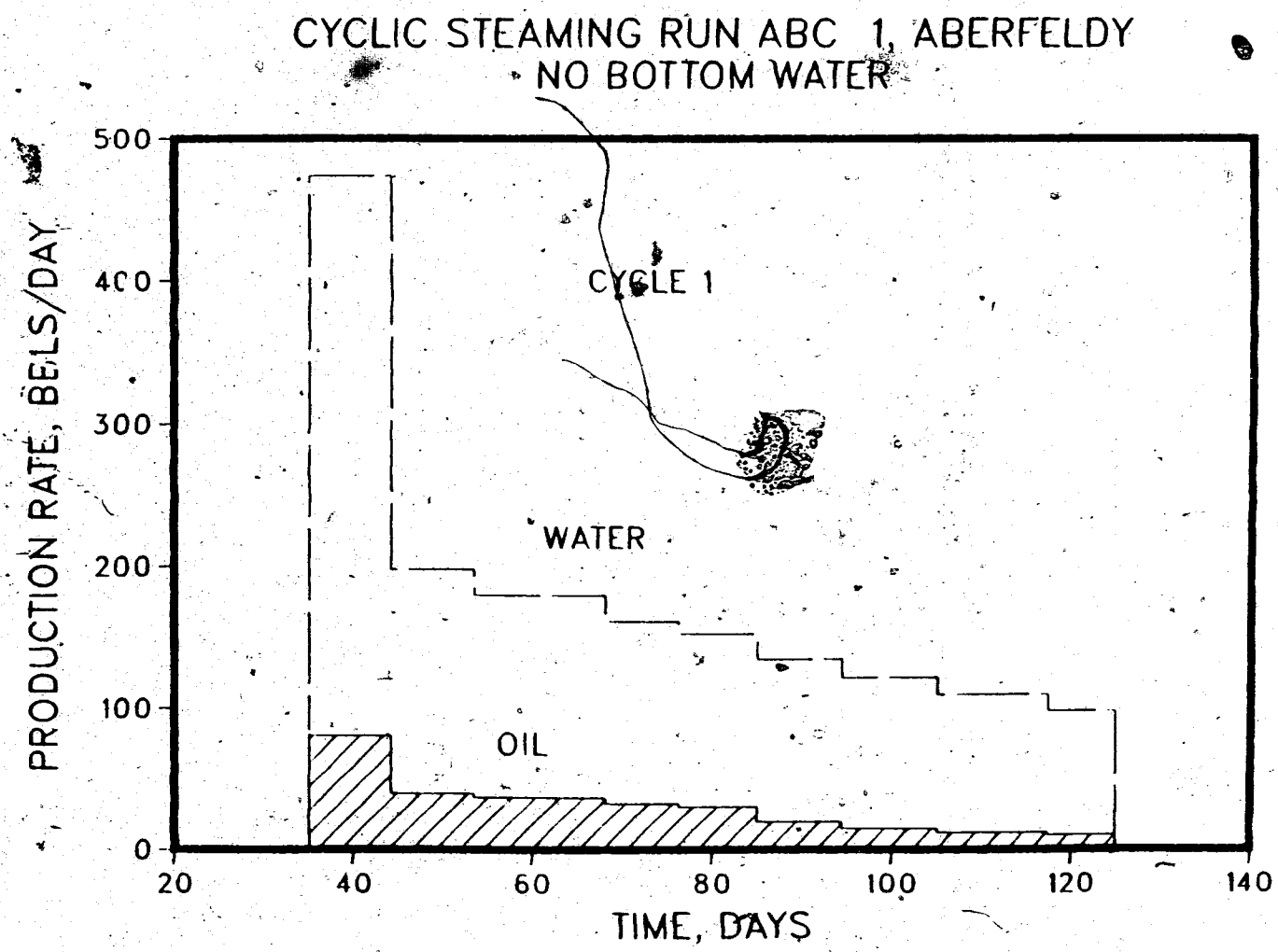

Figure 6.47 Production History for Aberfeldy Cyclic Run ABC1, No Bottom Water

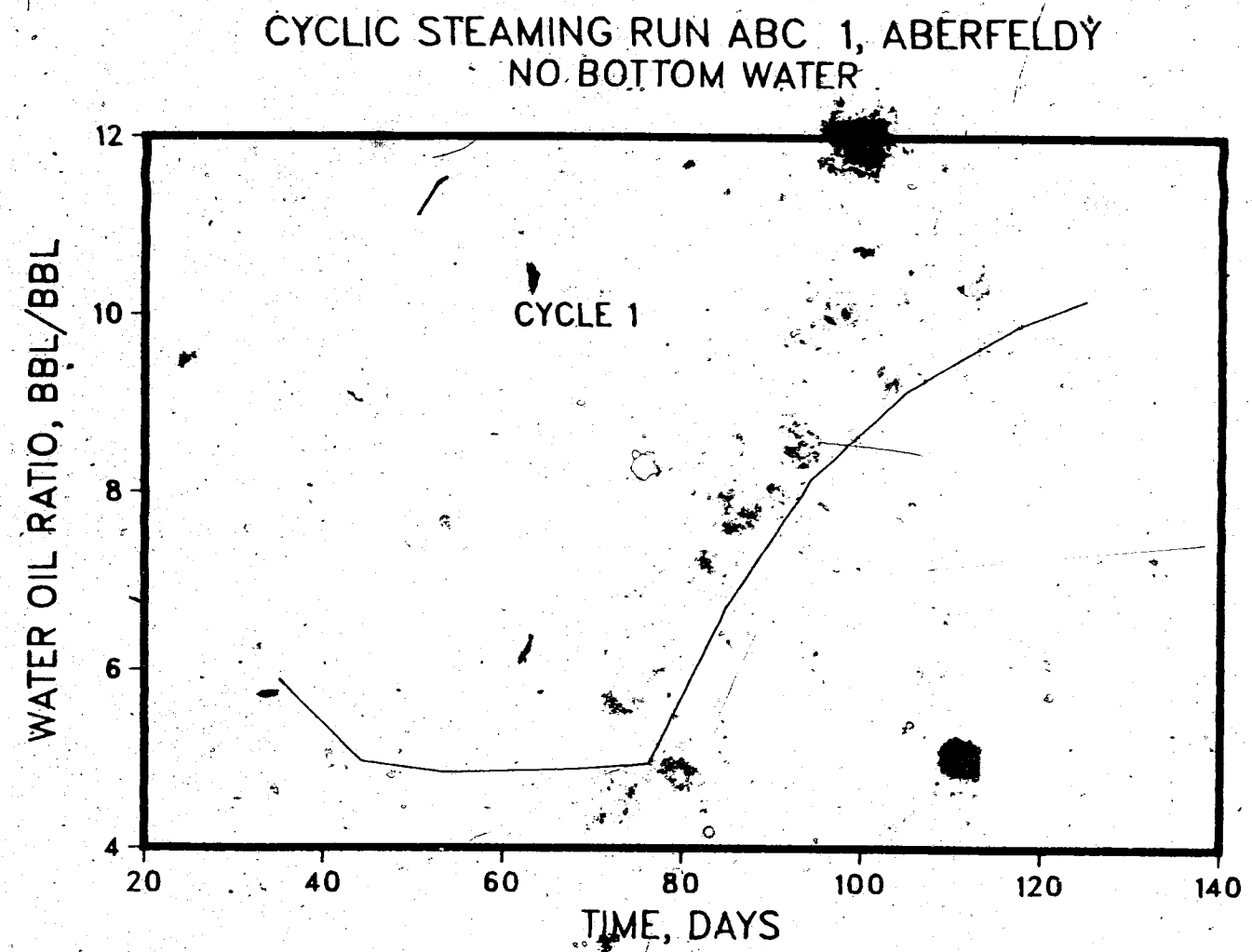

Figure 6.48 Water-Oil Ratio for Aberfeldy Cyclic Run ABC1, No Bottom Water

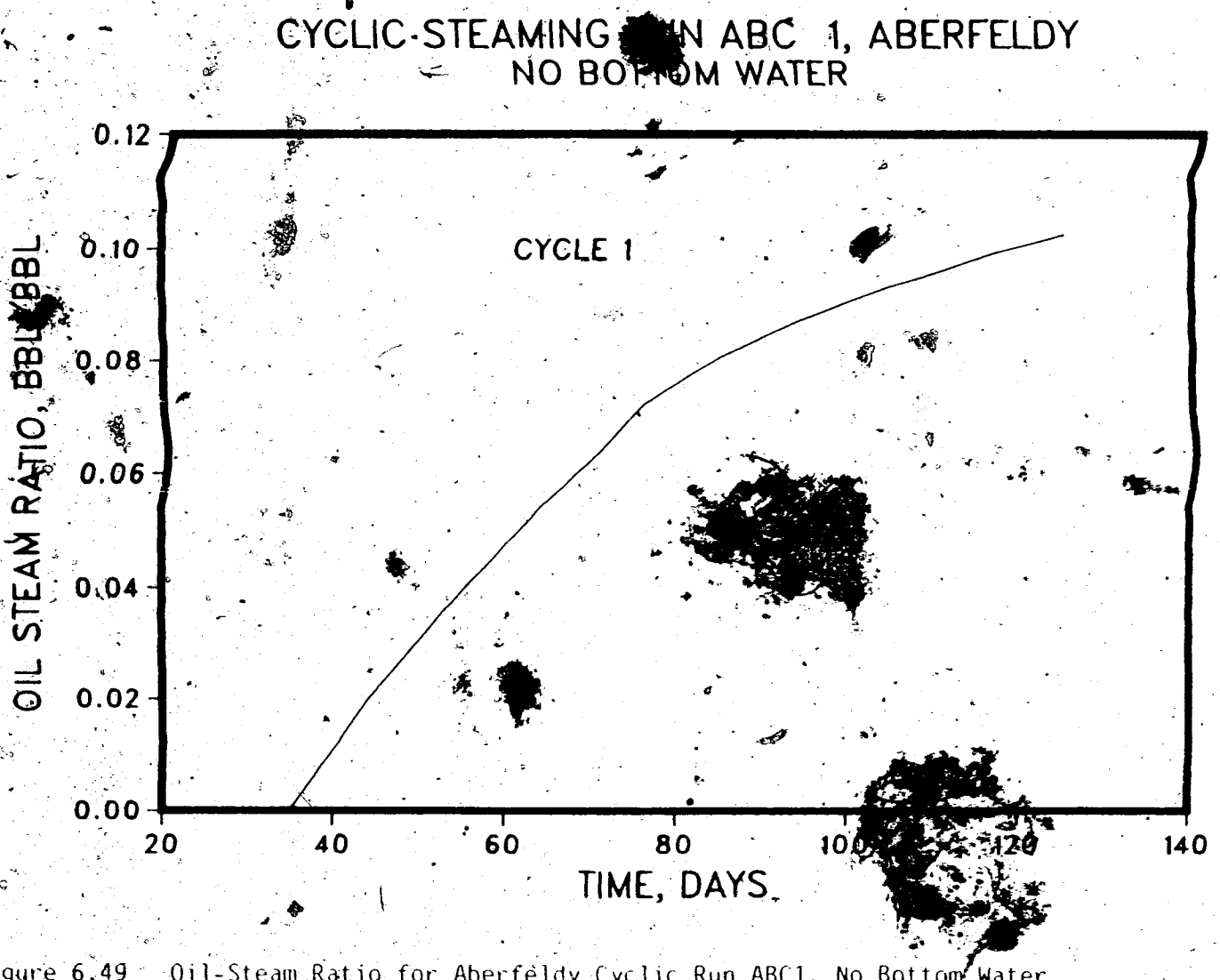

Figure 6.49 Oil-Steam Ratio for Aberfeldy Cyclic Run ABC1, No Bottom Water

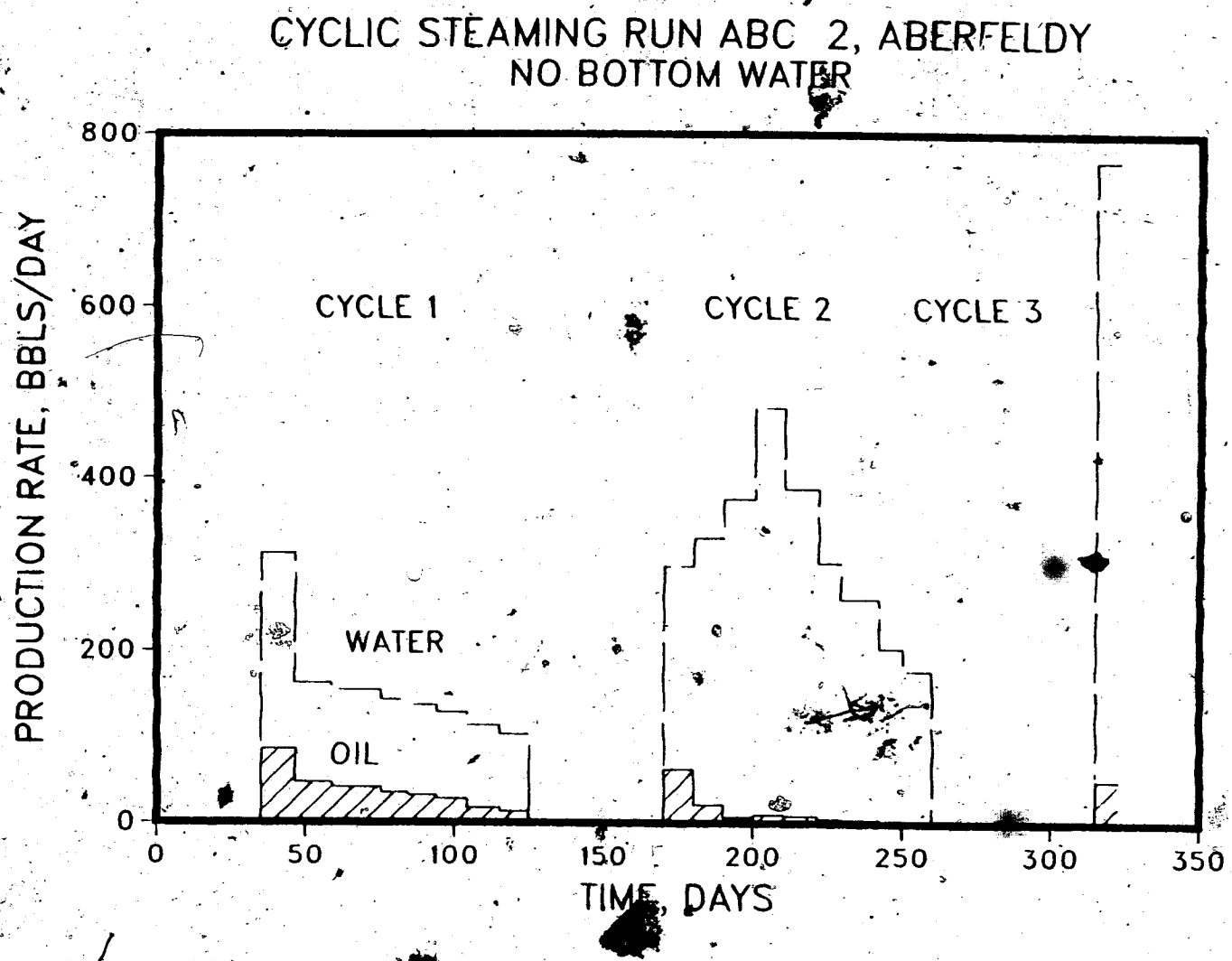

Figure 6.50 : Production History for Aberfeldy Cyclic Run ABC2, No Bottom Water

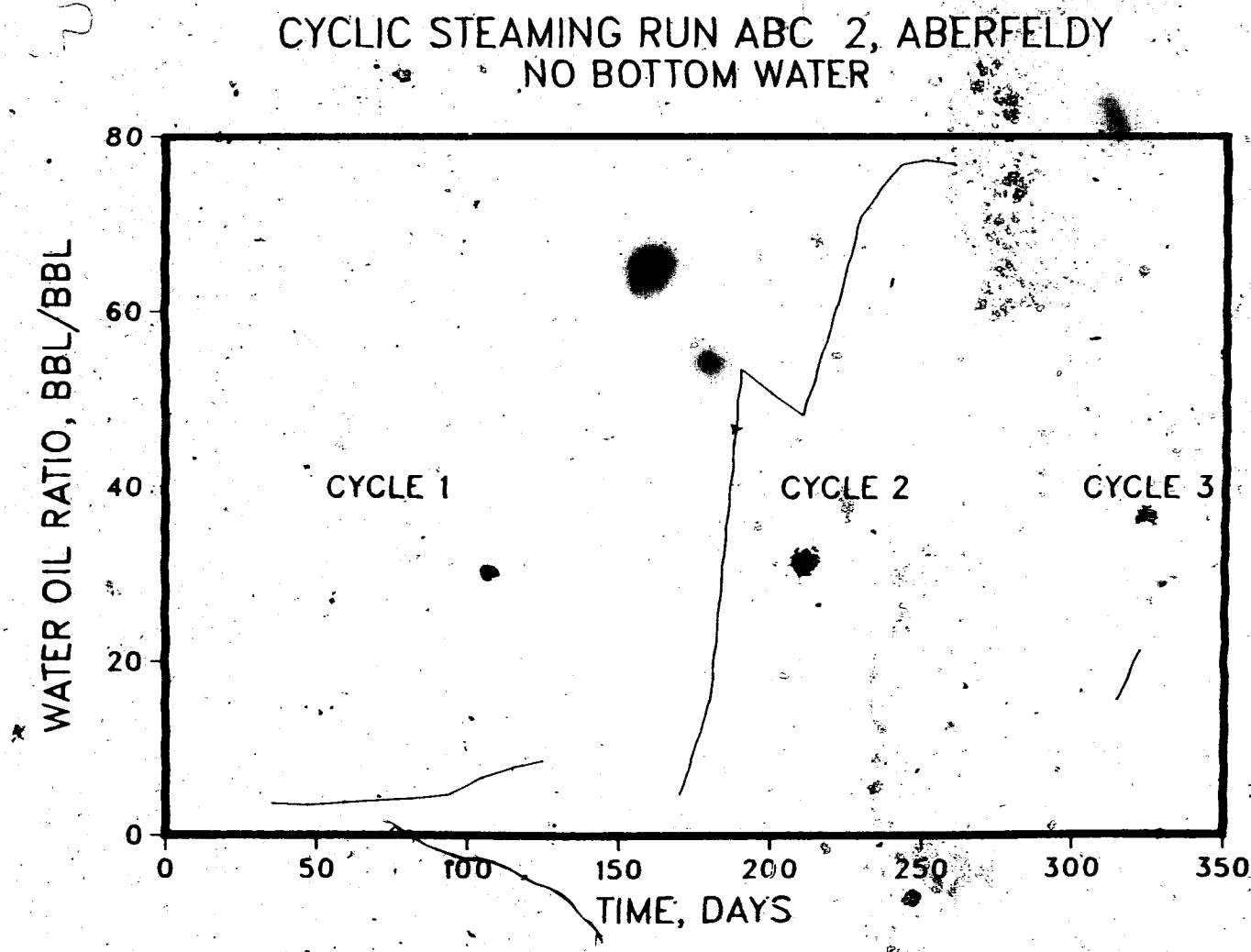

Figure 6.51 Water-Oil Ratio for Aberfeldy Cyclic Run ABC2, No Bottom Water

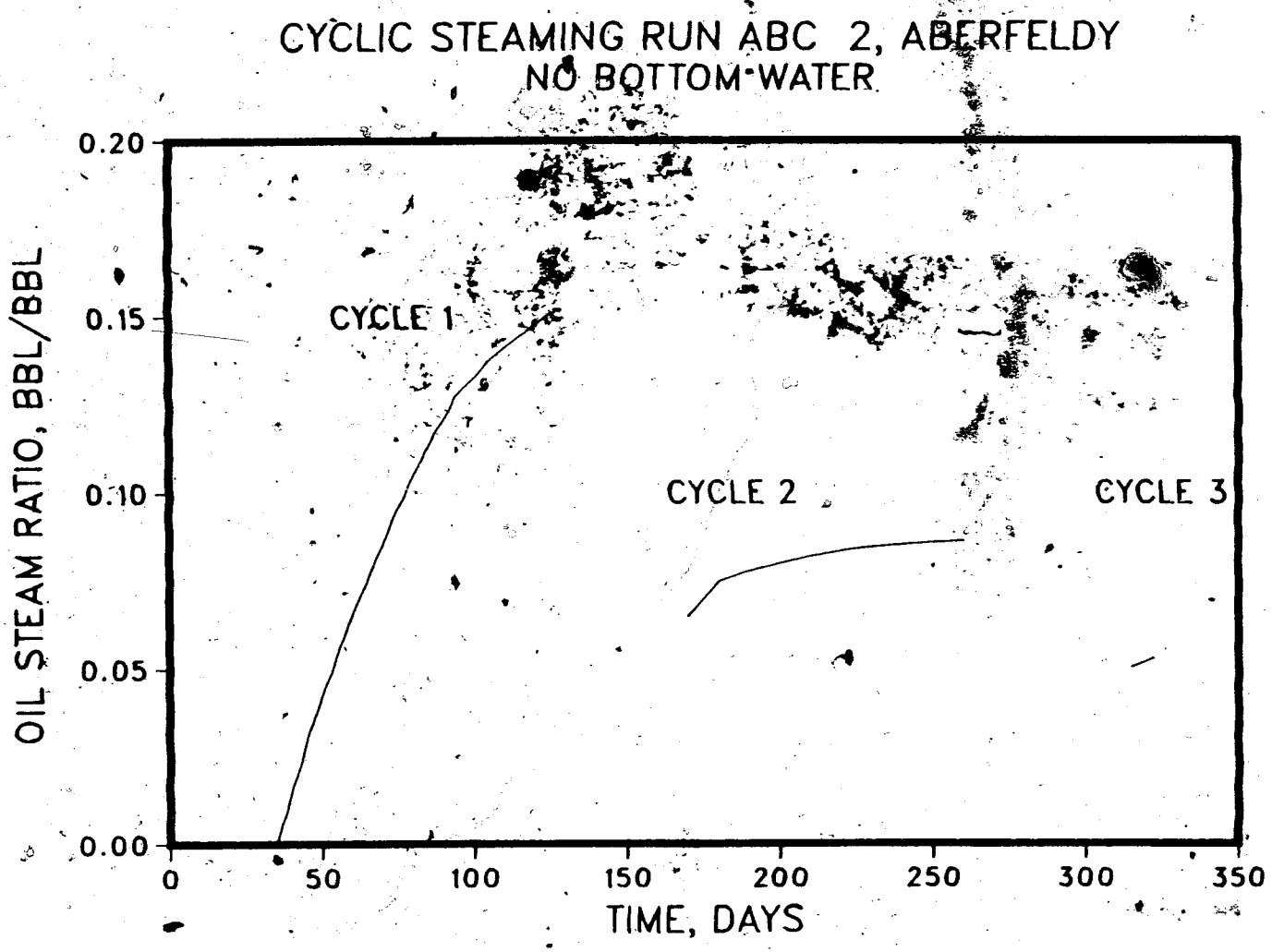

Figure 6.52 . Oil-Steam Ratio for Aberfeldy Cyclic Run ABC2, No Bottom Water

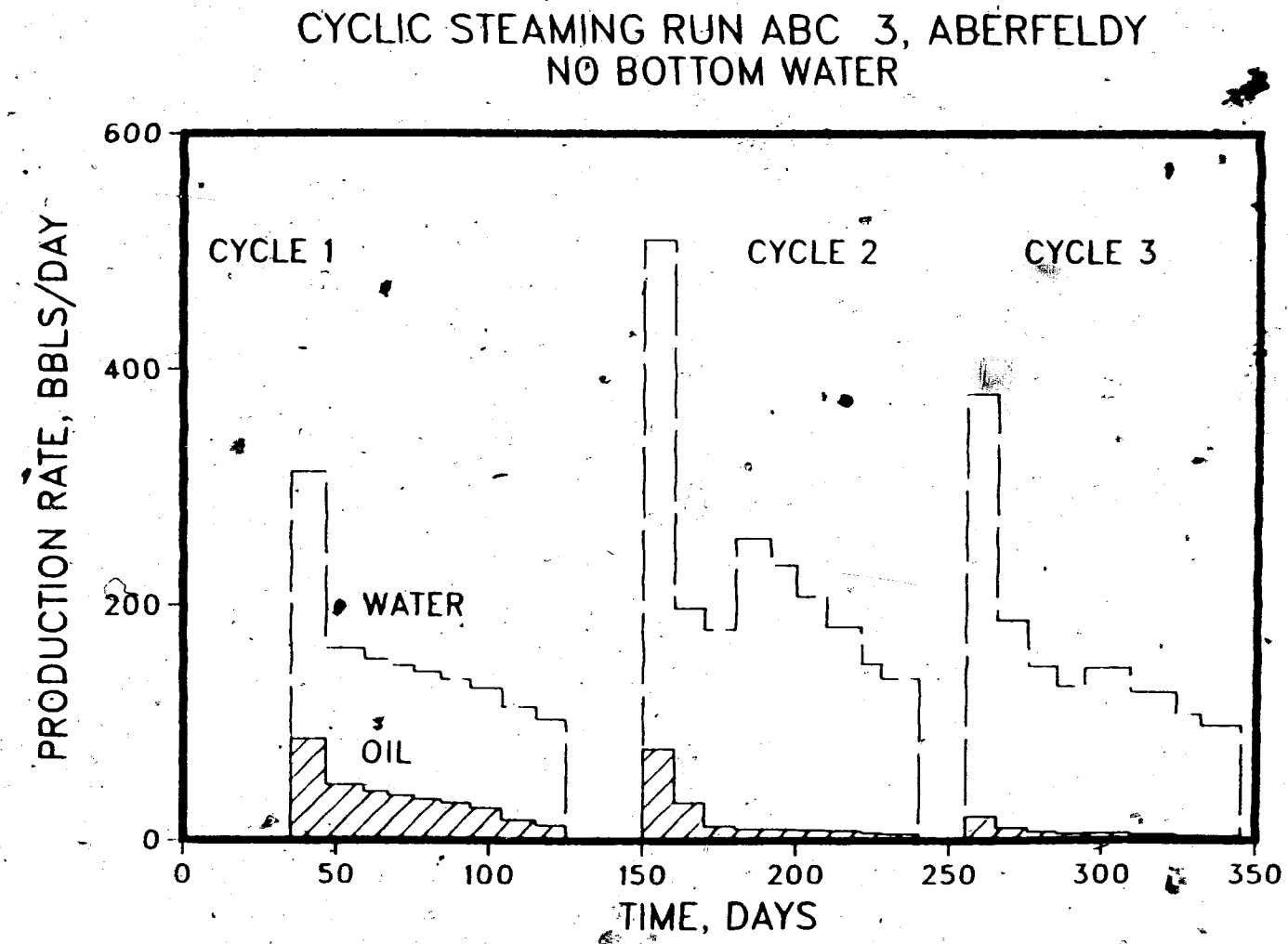

Figure 6.53 Production History for Aberfeldy Cyclic Run ABC3, No Bottom Water

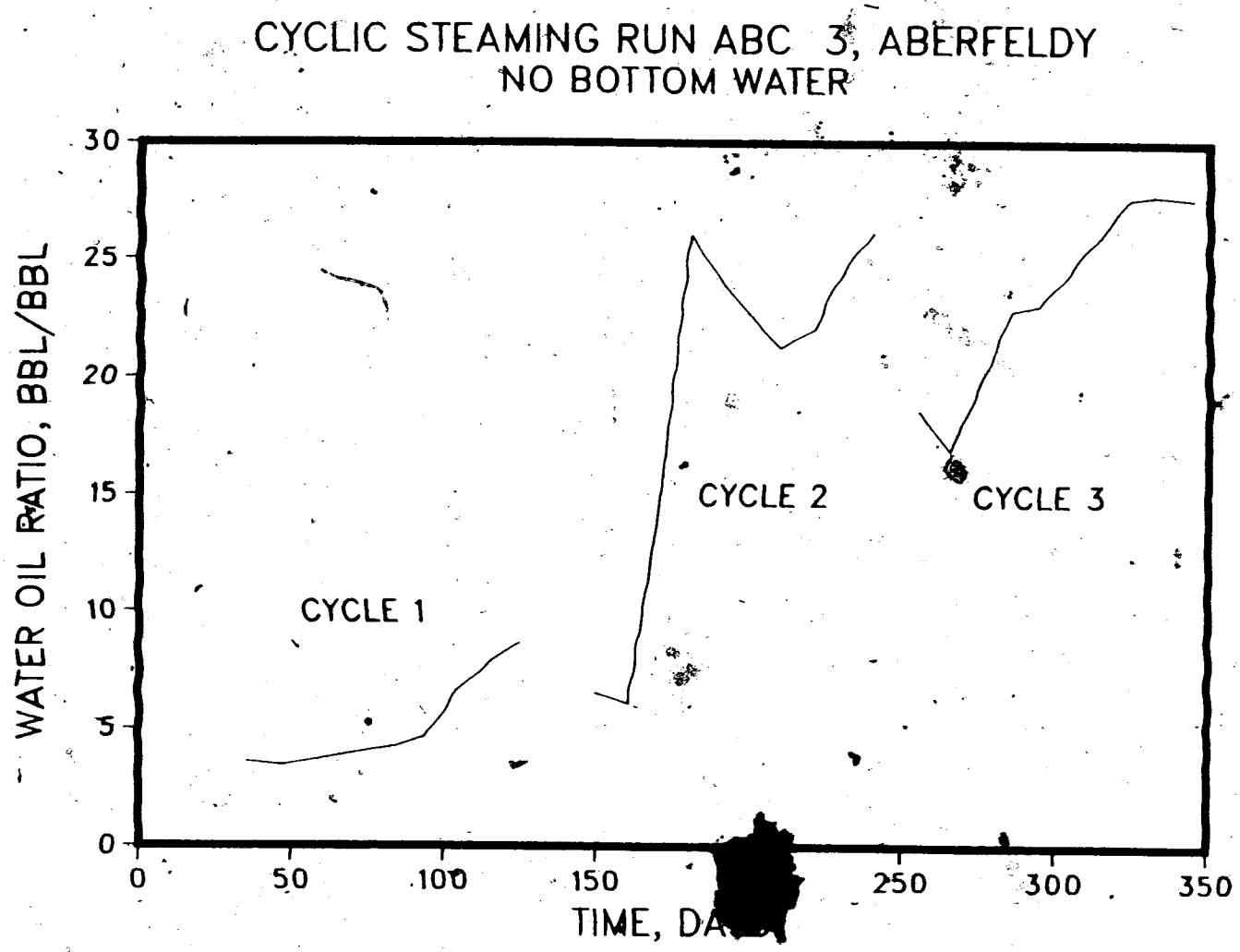

Figure 6.54 Water-Oil Ratio for Aberfeldy Cyclic Run ABC3, No Bottom Water

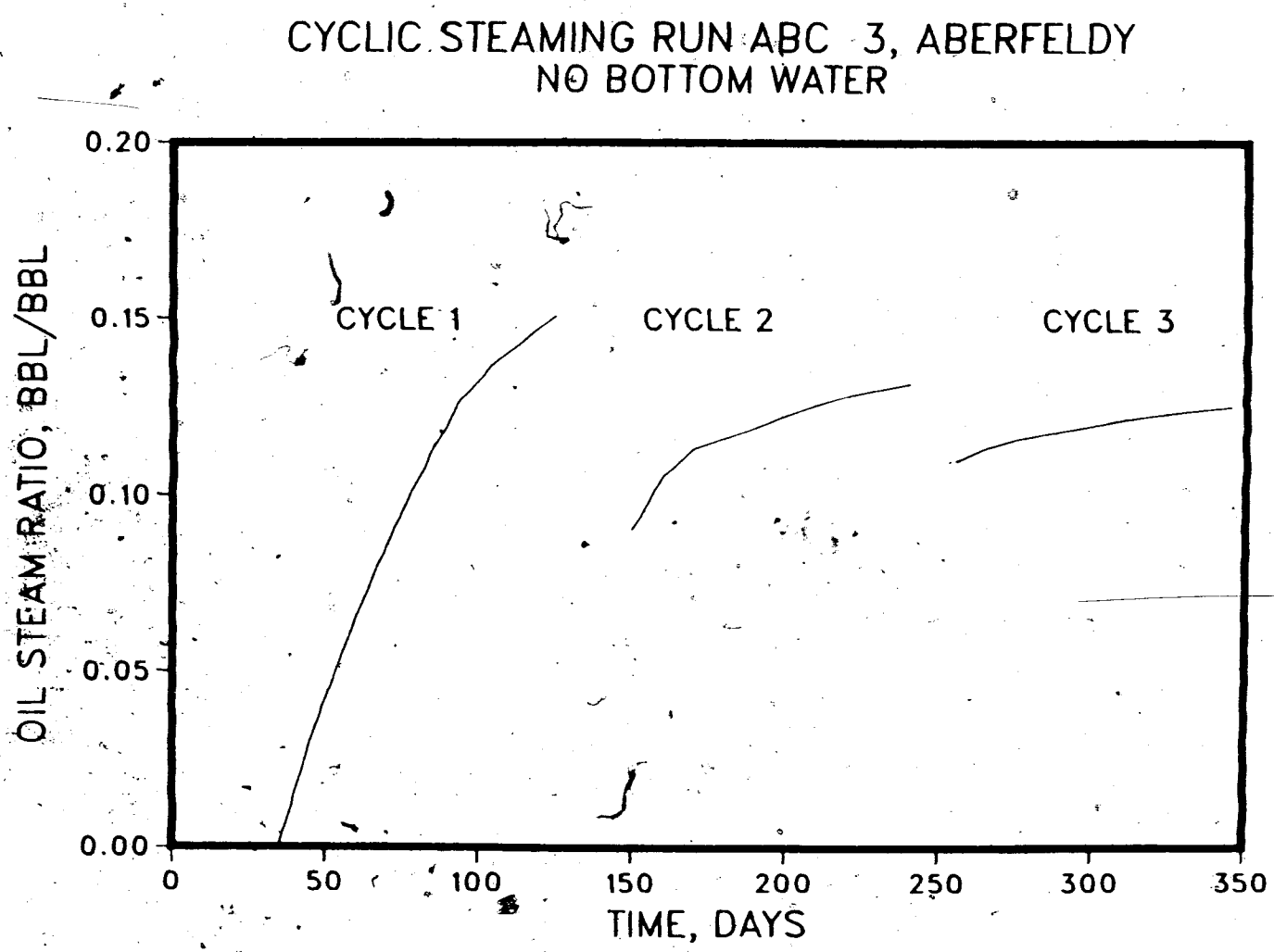

Figure 6.55 Oil-Steam Ratio for Aberfeldy Cyclic Run ABC3, No Bottom Water

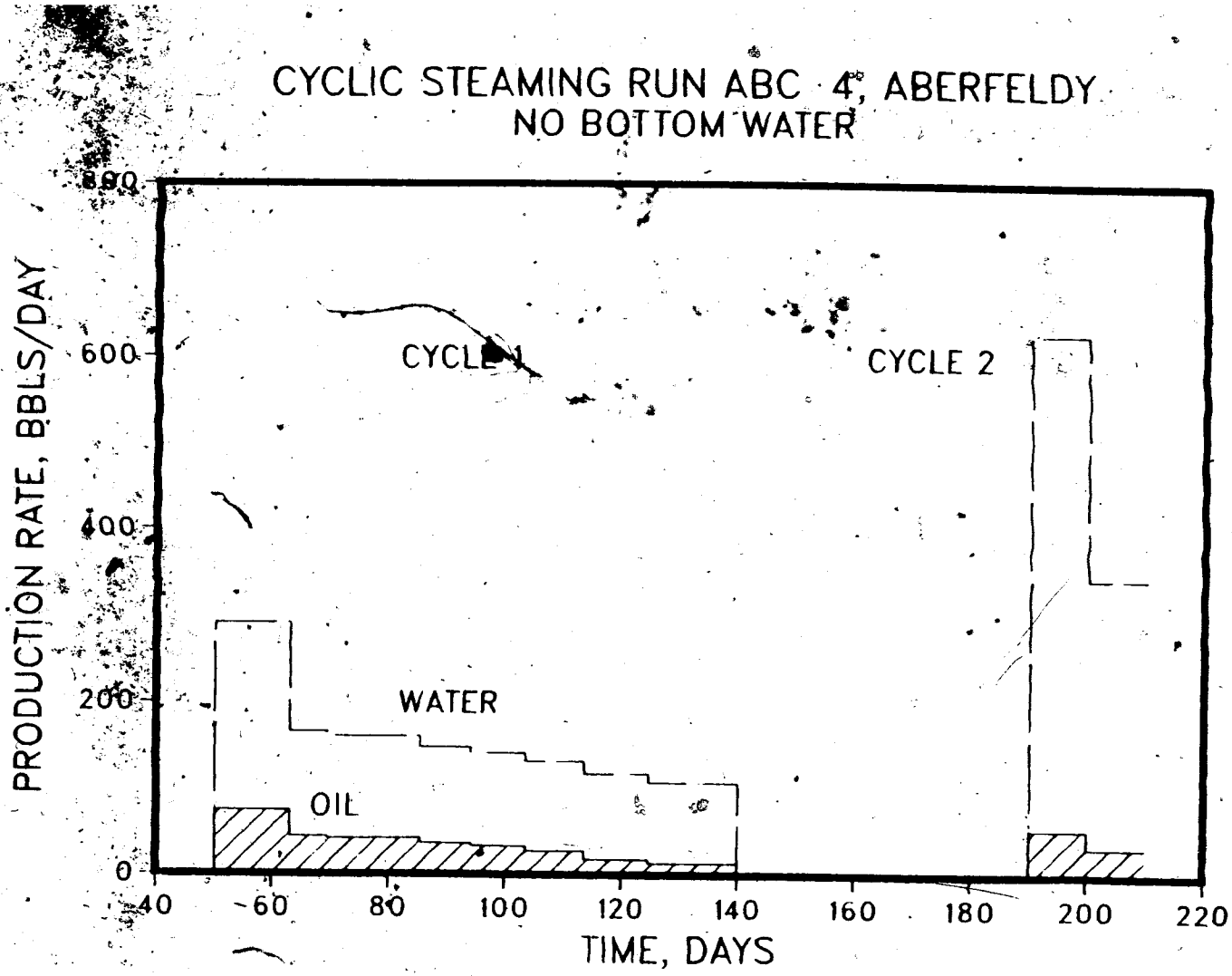

Figure 6.56 - Production History for Aberfeldy Cyclic Run ABC4, No Bottom Water

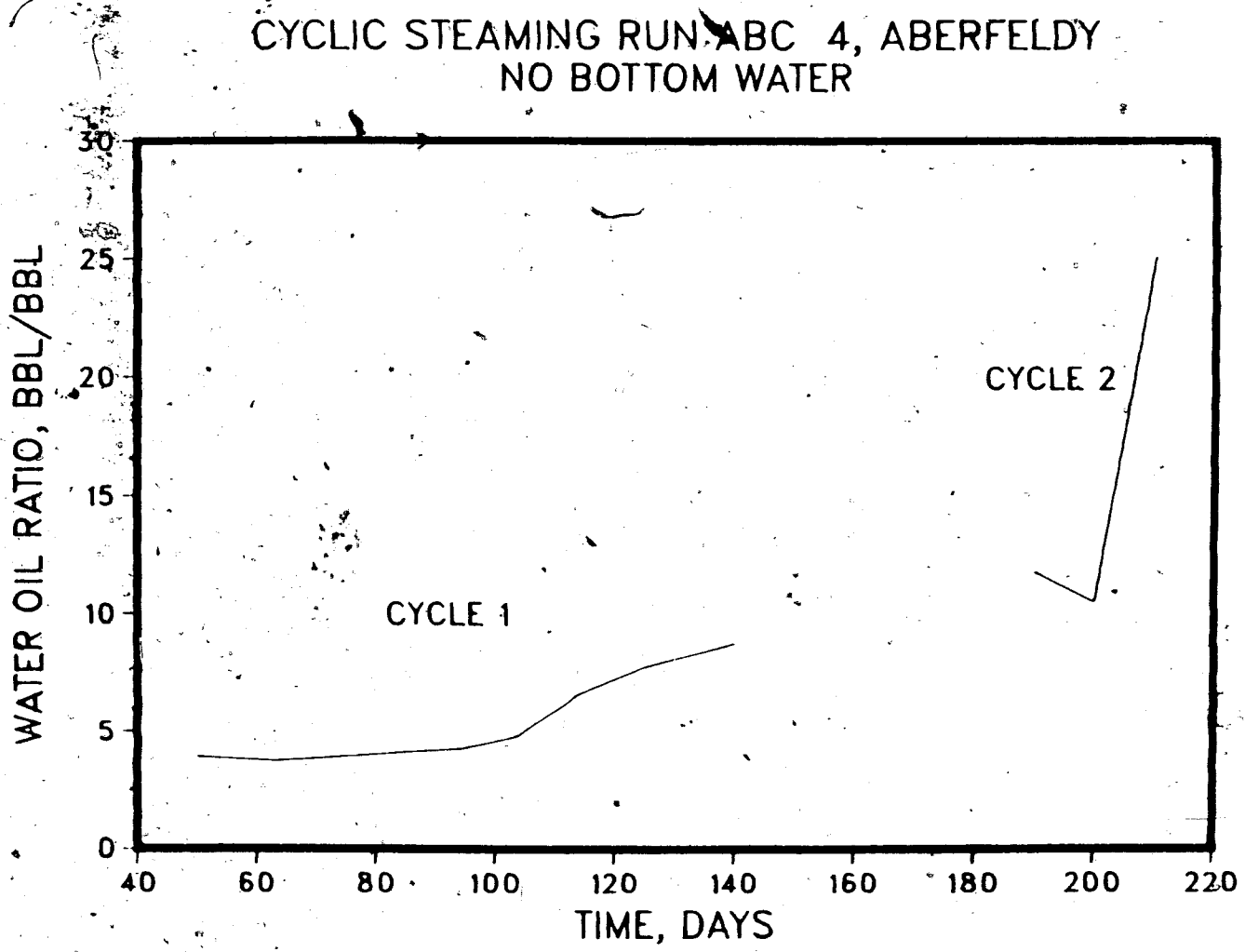

Figure 6.57 Water Oil Ratio for Aberfeldy Cyclic Run ABC4, No Bottom Water

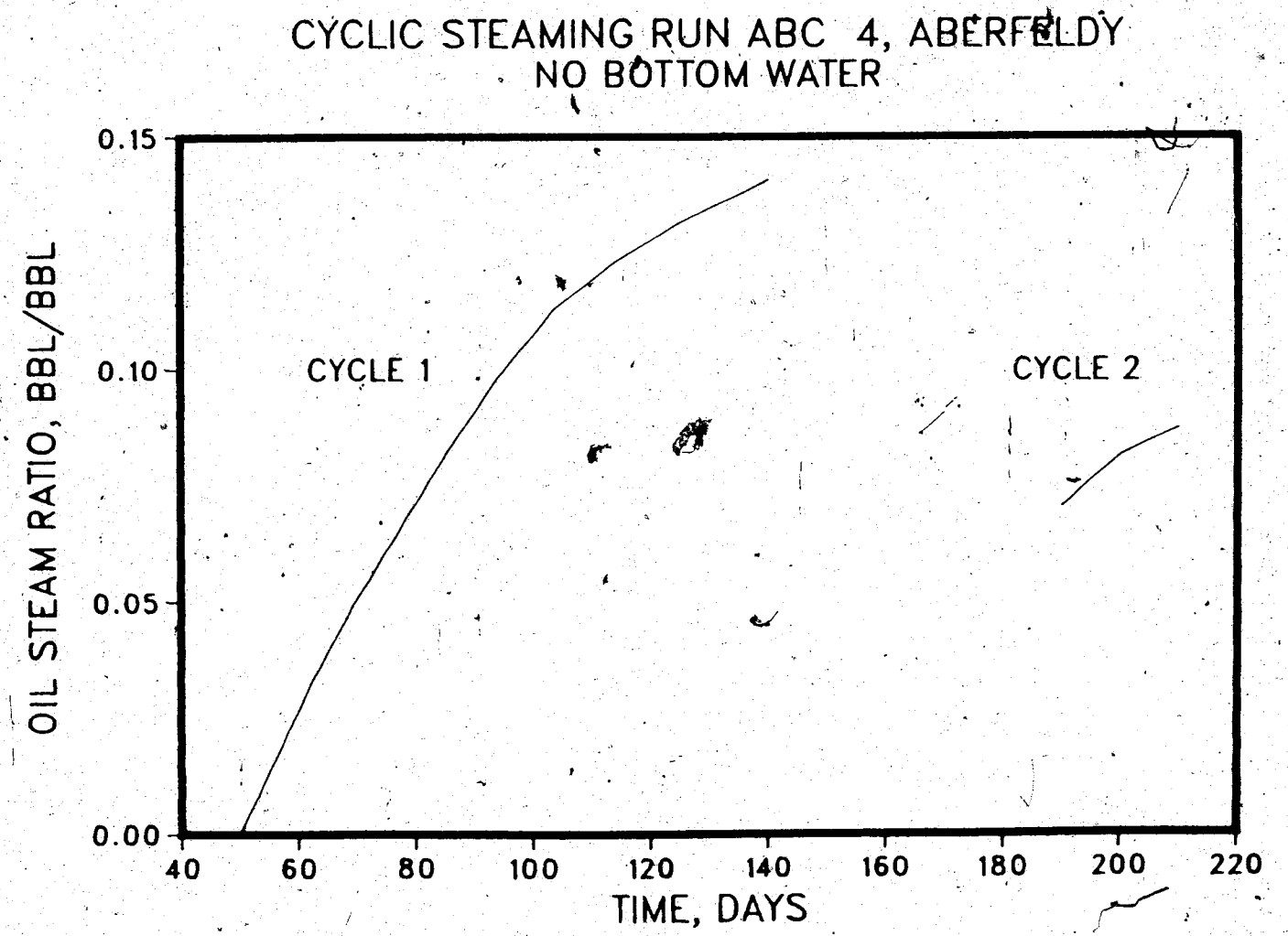

Figure 6.58 Oil-Steam Ratio for Aberfeldy Cyclic Run ABC4, No Bottom Water

runs correspond to the conditions given in the summary Table 6.3. The first run employs a constant steam slug size in each cycle, the second run employs increasing slugs from cycle to cycle, the third run utilizes decreasing slugs from cycle to cycle, and the fourth employs long soak times following steam injection. It is seen that the oil-steam ratio is highest - about 0.15 - in the first cycle. In subsequent cycles it drops because of water saturation buildup. This is expected because the formation thickness is small, so that gravity flow is limited. Furthermore, after the first cycle, the inflow of cold oil from the cooler parts of the formation is limited by the high oil viscosity. This is evidenced by the high WOR values in the first cycle, and in most cases in the second and third cycles. At the end of steam injection, the water saturation around the wellbore is very high, causing the very high WORs. The performance of Run ABC3 (Table C.16, Figs. 6.53-6.55) is most favourable, with steam slugs decreasing: 18, 12, and 6 MBbls, in the three cycles. The corresponding oil-steam ratios are 0.15, 0.13, and 0.12, respectively. In Run ABC2 (Table C.15, Figs. 6.50-6.52) the oil-steam ratios are lower, for the larger steam slugs used. A long soak time (20 days in Run ABC4) has a similar undesirable effect, leading to a drop in the oil-steam ratio, possibly due to cooling of the oil around the wellbore. On the basis of these limited results, it could be said that decreasing steam slugs in succeeding cycles are desirable, but the amount of decrease is a factor to be considered, and that long soak times cause a drop in the oil-steam ratio.

Effect of Bottom Water

The Aberfeldy runs discussed in the previous section were repeated for a bottom water zone (Runs ABC6, ABC8, ABC9). The results are summarized in Tables C.18 to C.22, and are plotted in Figs. 6.59 through 6.73. It is obvious that the performance throughout is poorer than in the absence of bottom water, Runs ABC1 to 4. The oil-steam ratio is seen to be nearly one-half, or less, of that in the absence of bottom water. The water-oil ratios are much higher - two to three times those in the absence of bottom water.

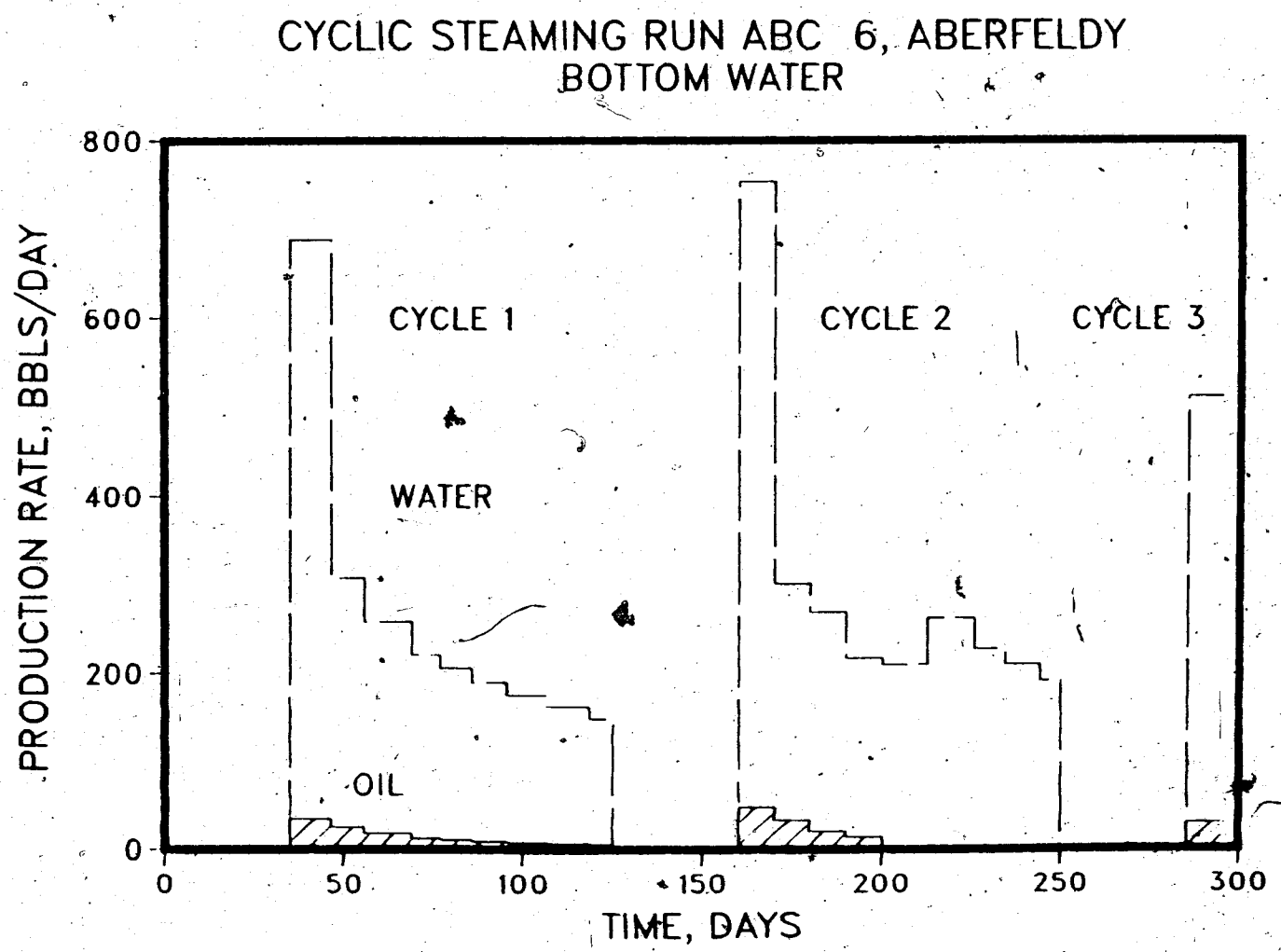

Figure 6.59 Production History for Aberfeldy Cyclic Run ABC6 Bottom Water

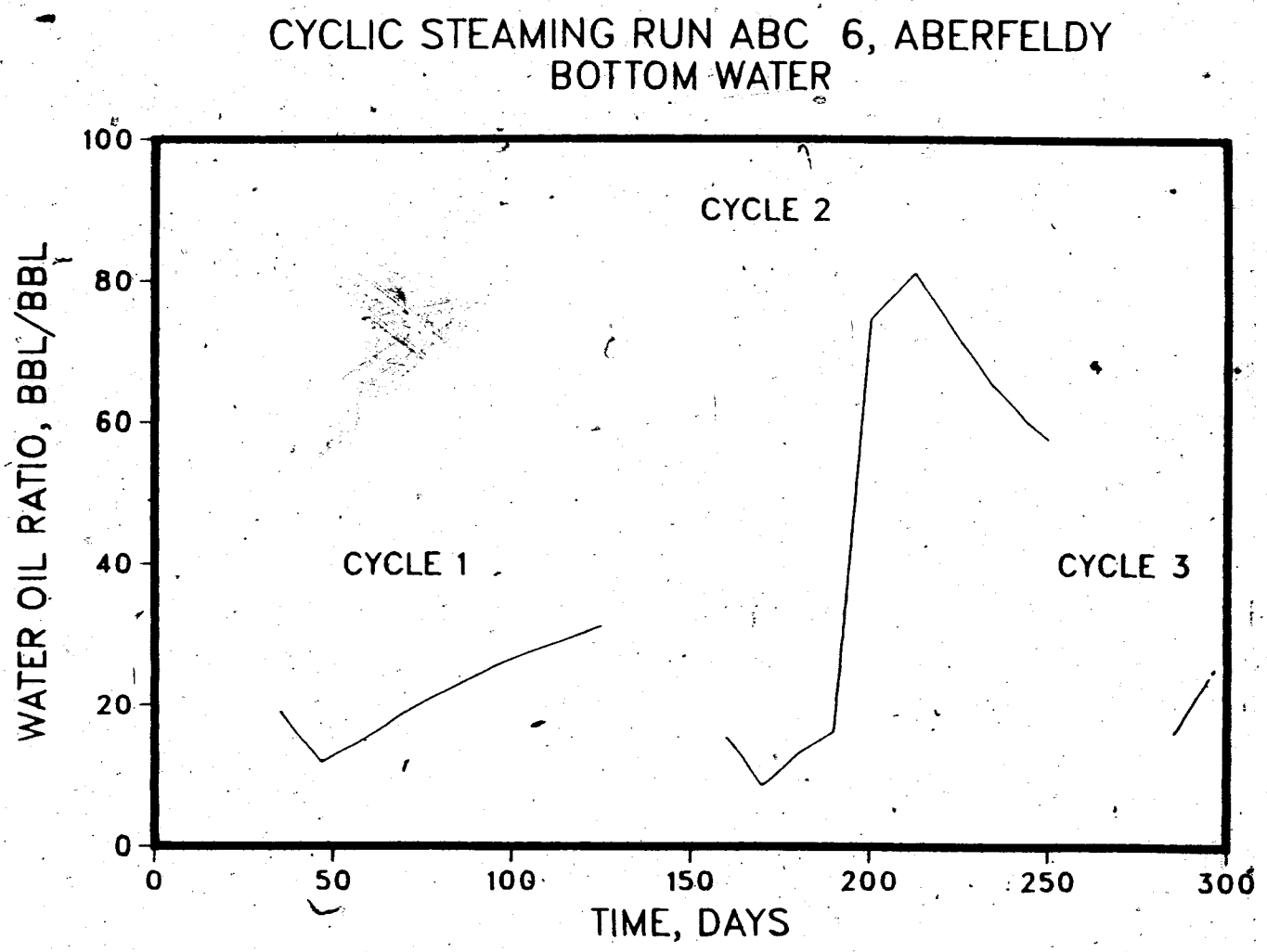

Figure 6.60 Water-Oil Ratio for Aberfeldy Cyclic Run ABC6, Bottom Water

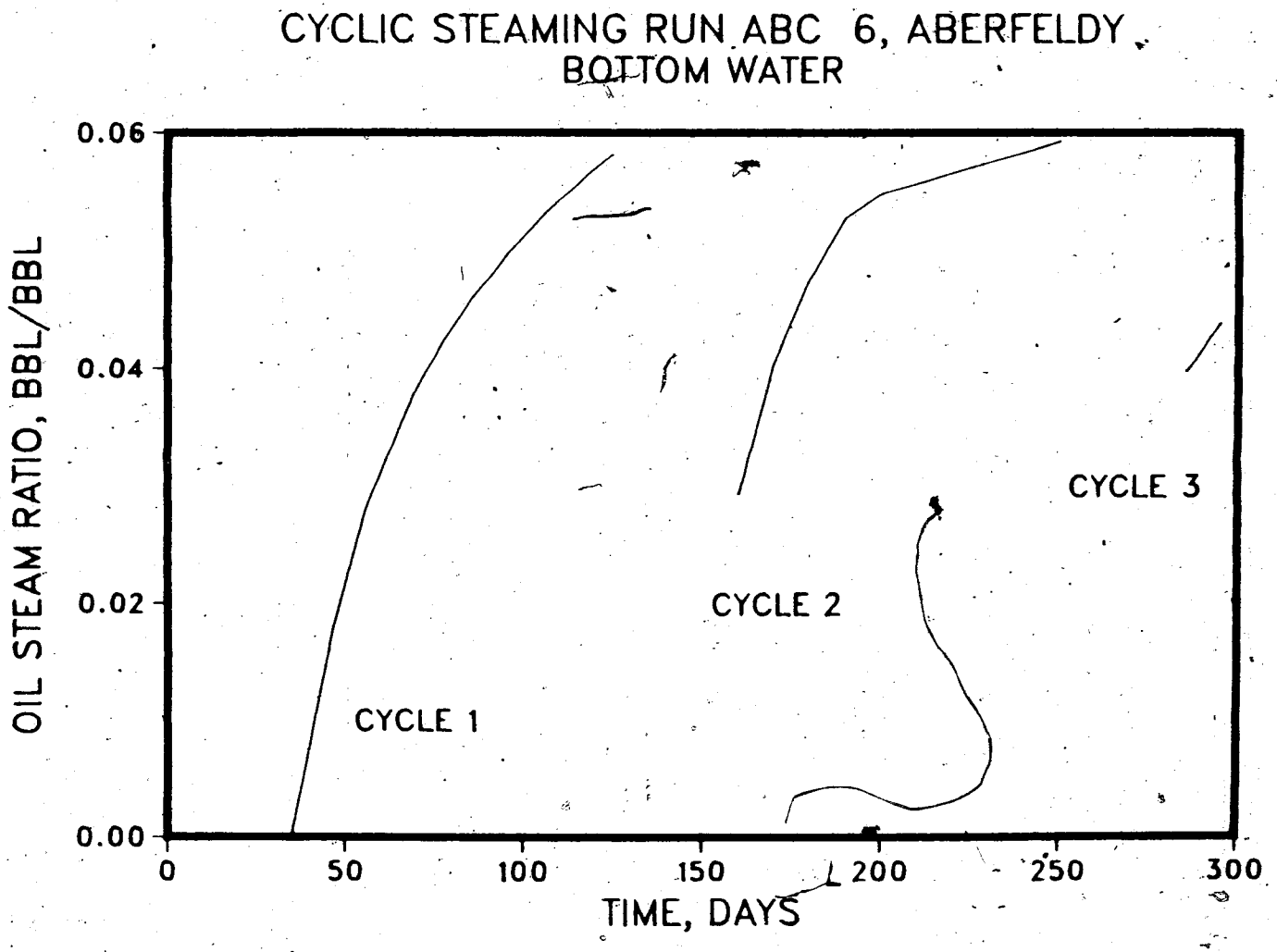

Figure 6.61 Oil-Steam Ratio for Aberfeldy Cyclic Run ABC6, Bottom Water

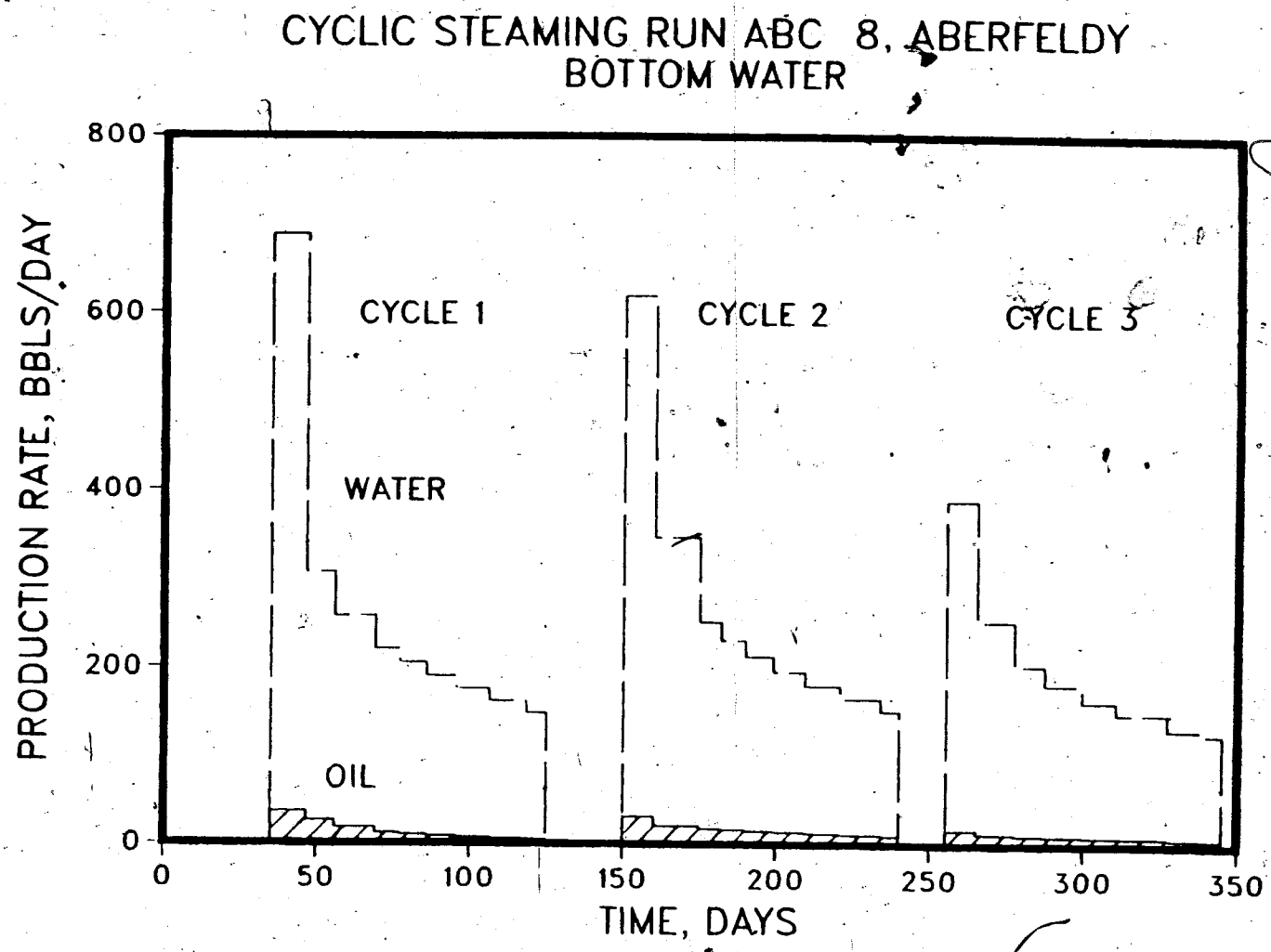

Figure 6.62 Production History for Aberfeldy Cyclic Run ABC8, Bottom Water

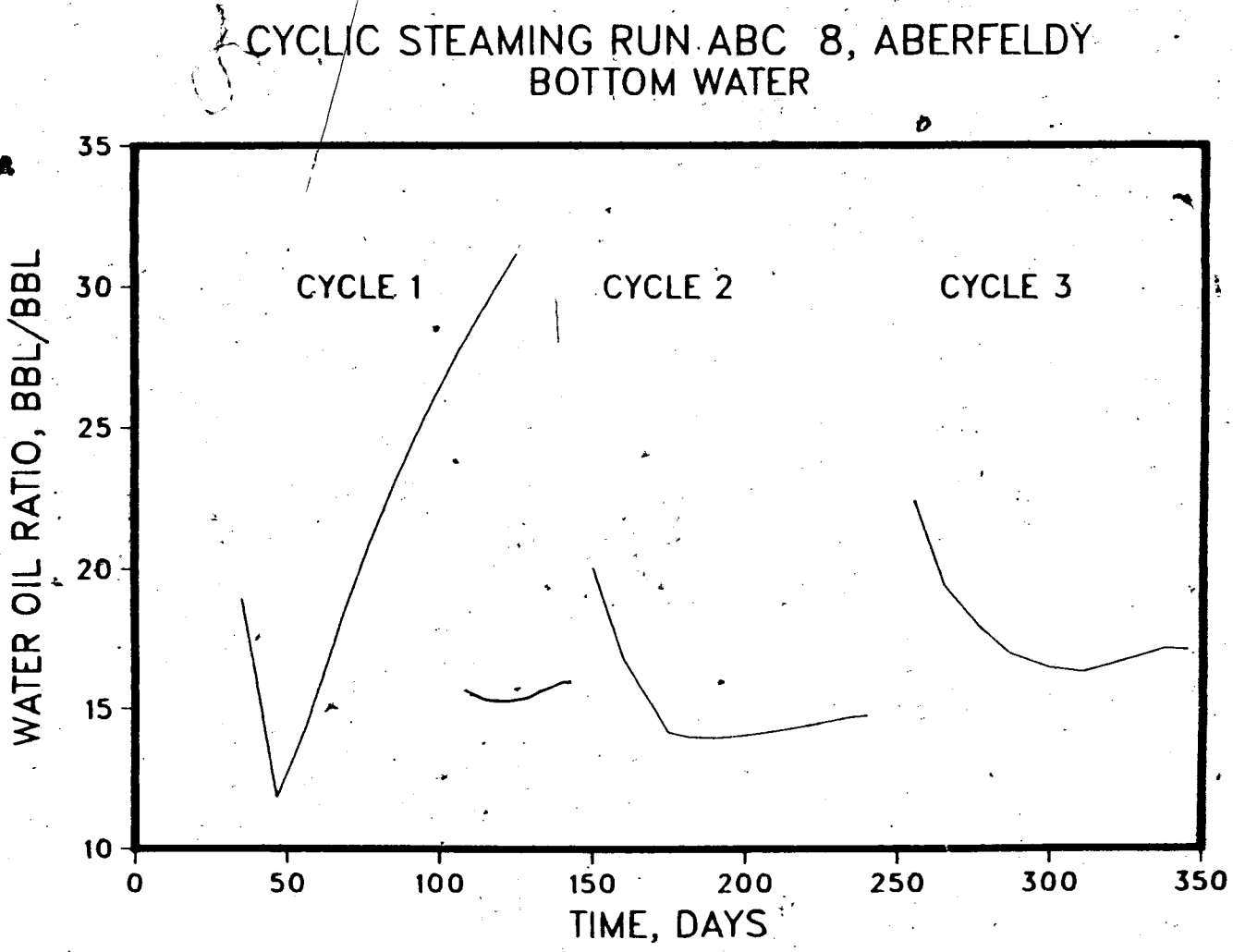

Figure 6.63 Water-Oil Ratio for Aberfeldy Cyclic Run ABC8, Bottom Water

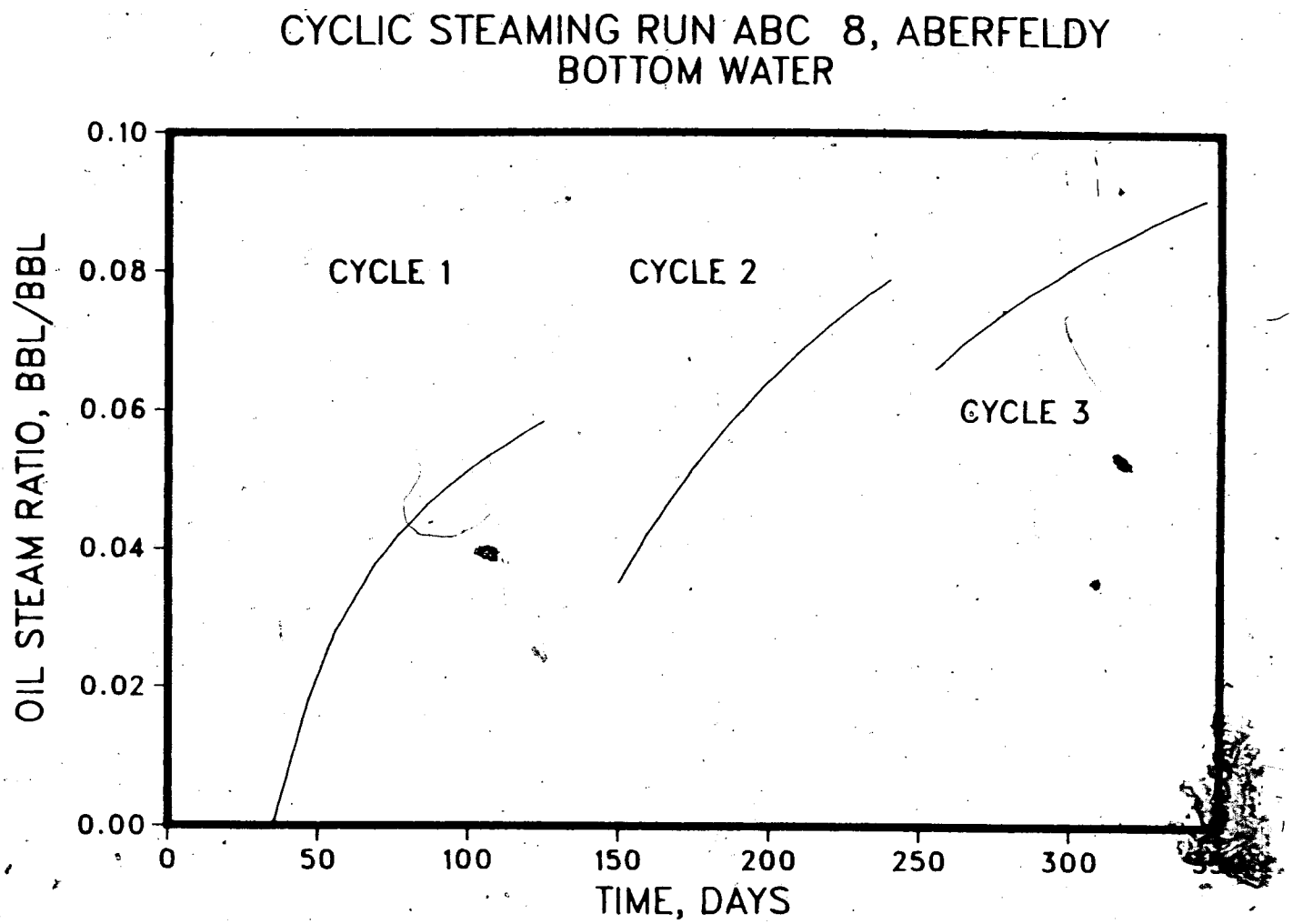

Figure 6.64 Oil-Steam Ratio for Aberfeldy Cyclic Run ABC8, Bottom Water

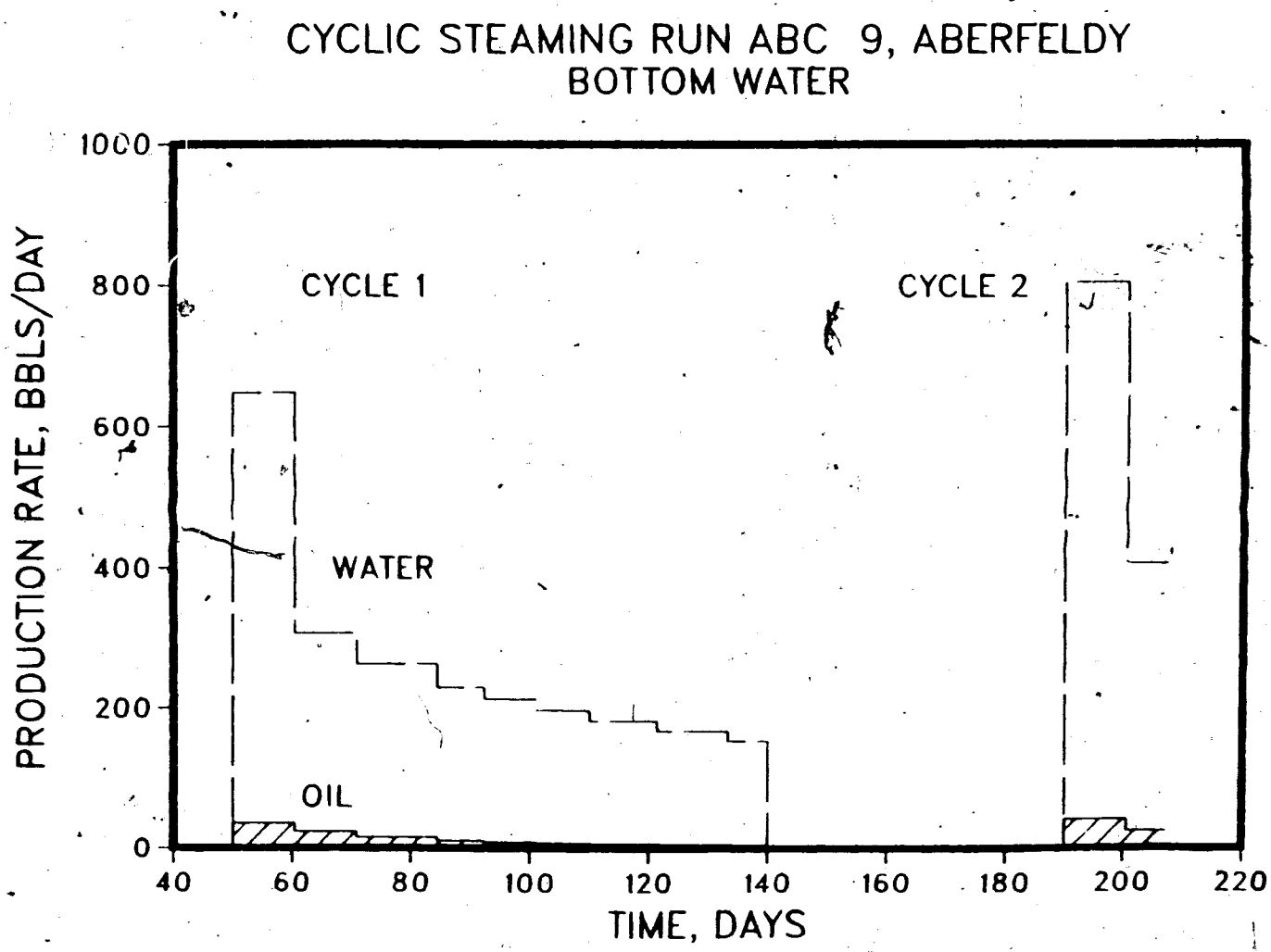

Figure 6.65 Production History for Aberfeldy Cyclic Run ABC9, Bottom Water

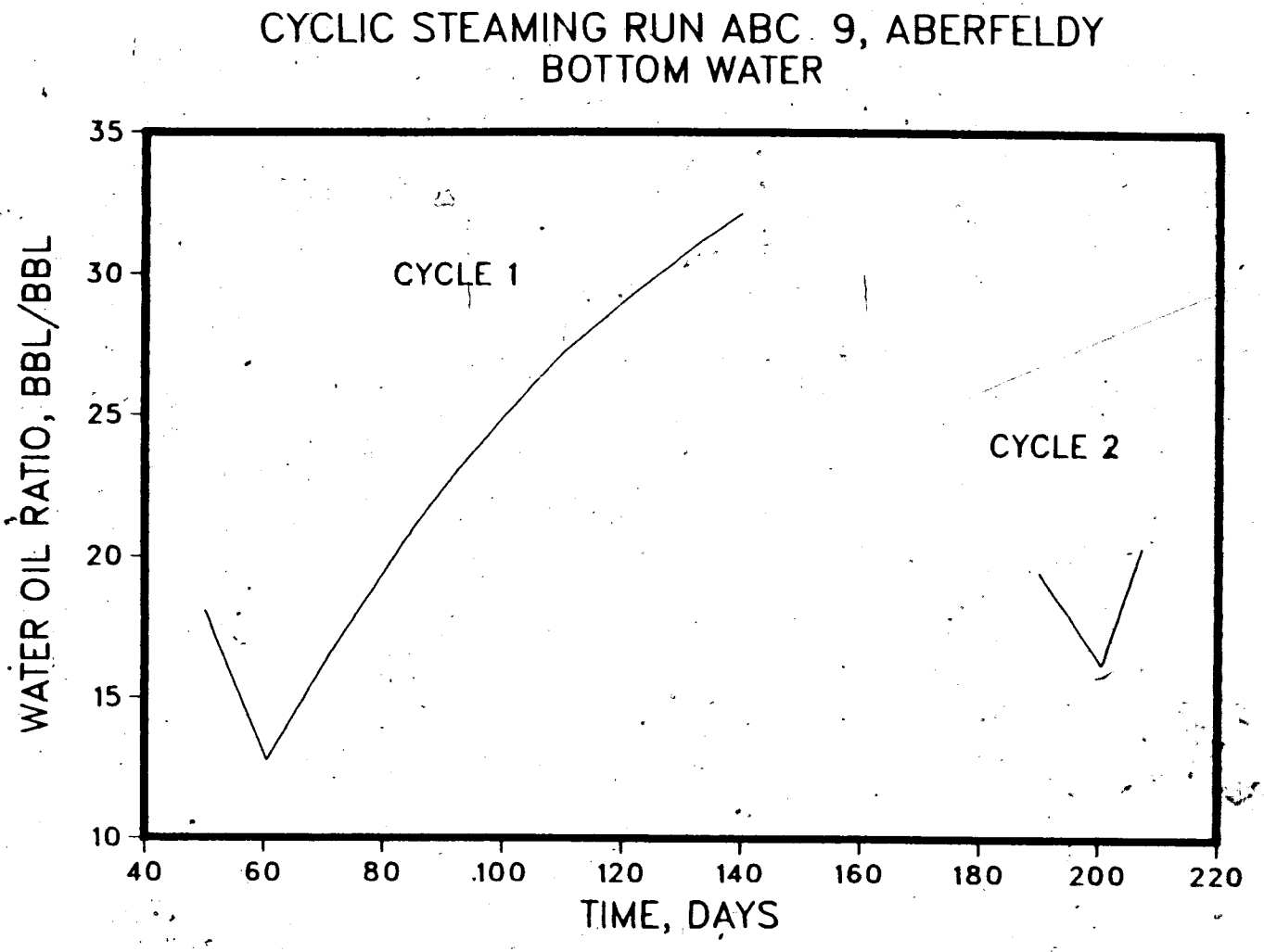

Figure 6.66 Water-Oil Ratio for Aberfeldy Cyclic Run ABC9, Bottom Water

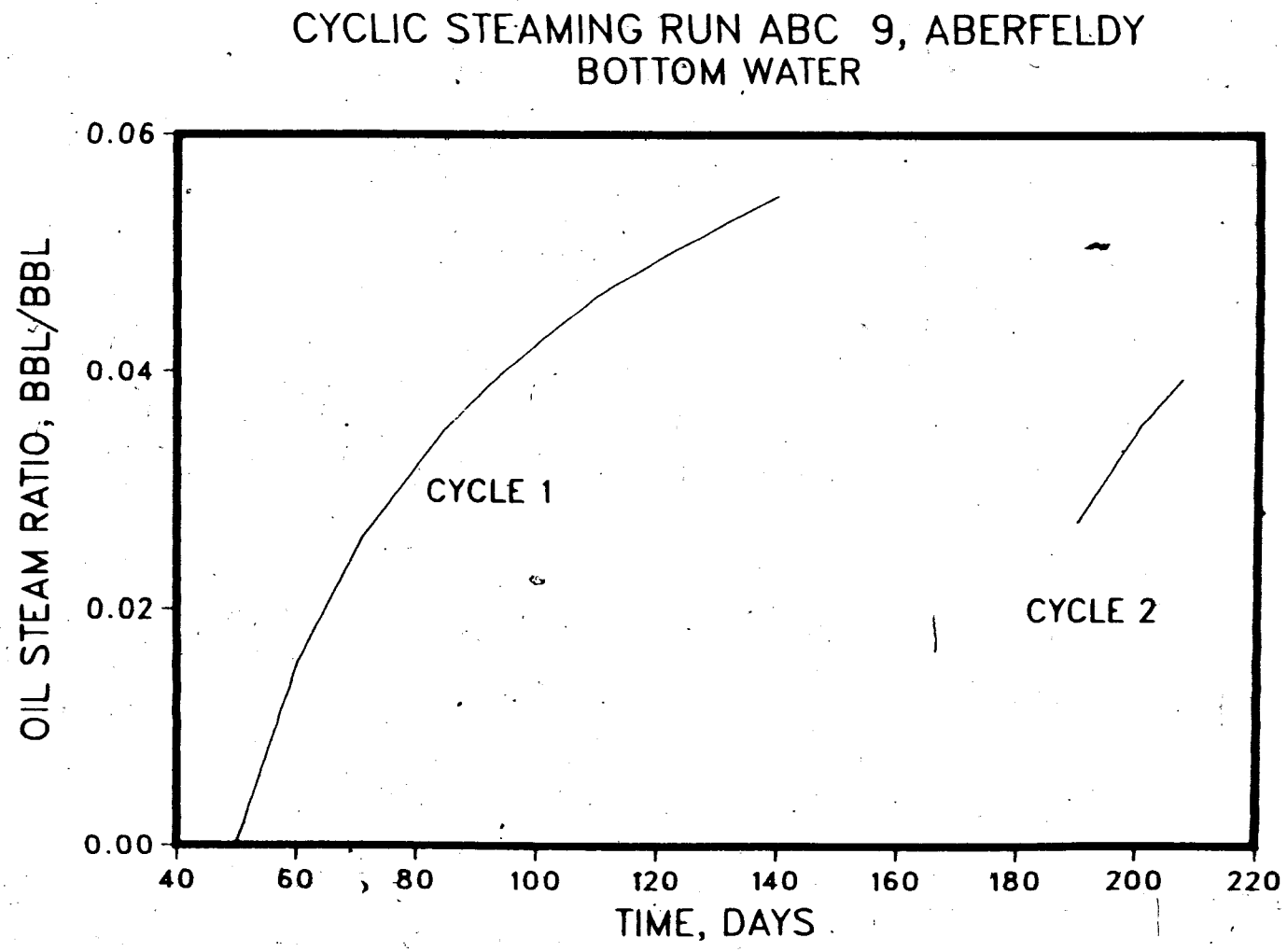

Figure 6.67 Oil-Steam Ratio for Aberfeldy Cyclic Run ABC9, Bottom Water

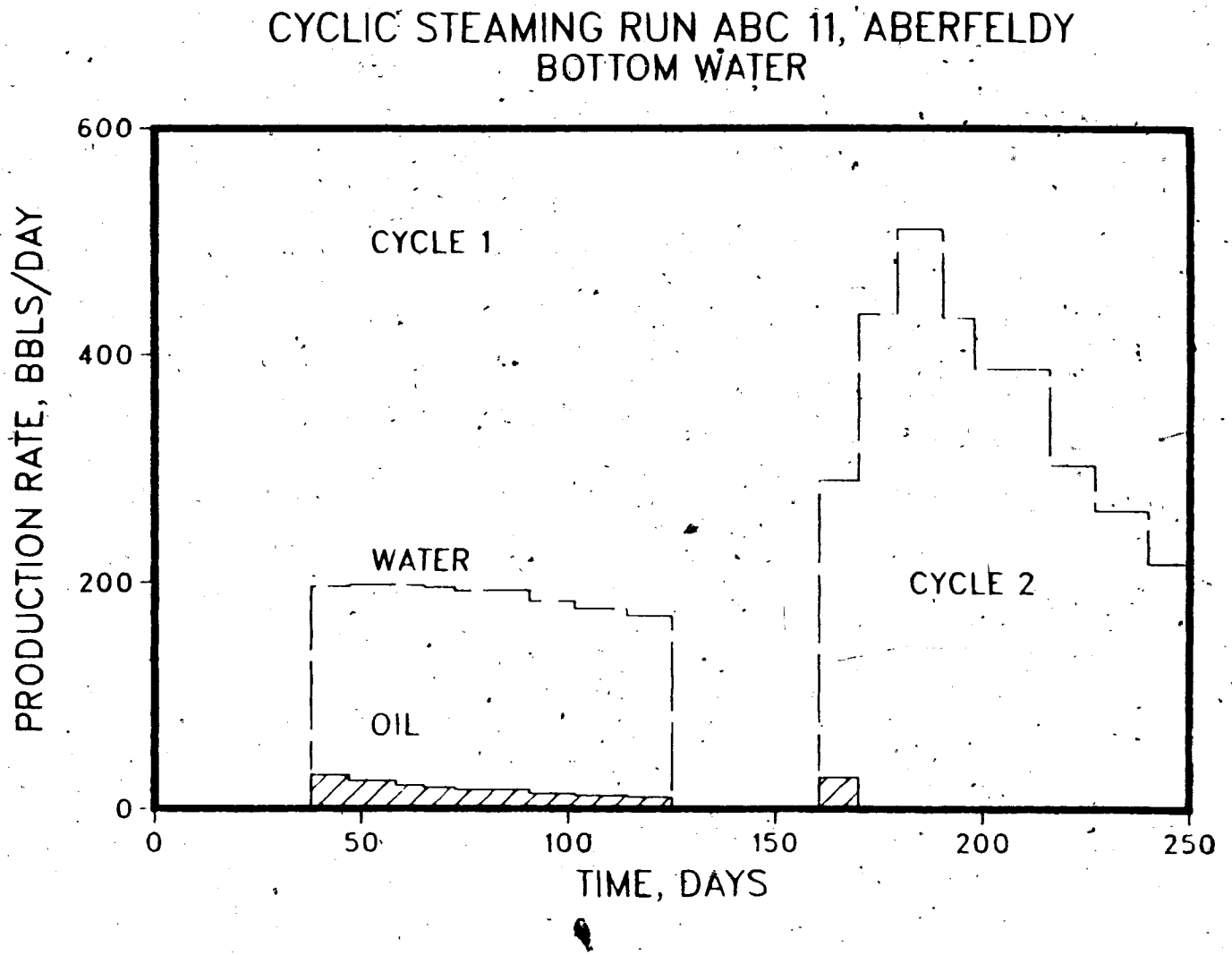

Figure 6.68 Production History for Aberfeldy Cyclic Run ABC11, Bottom Water

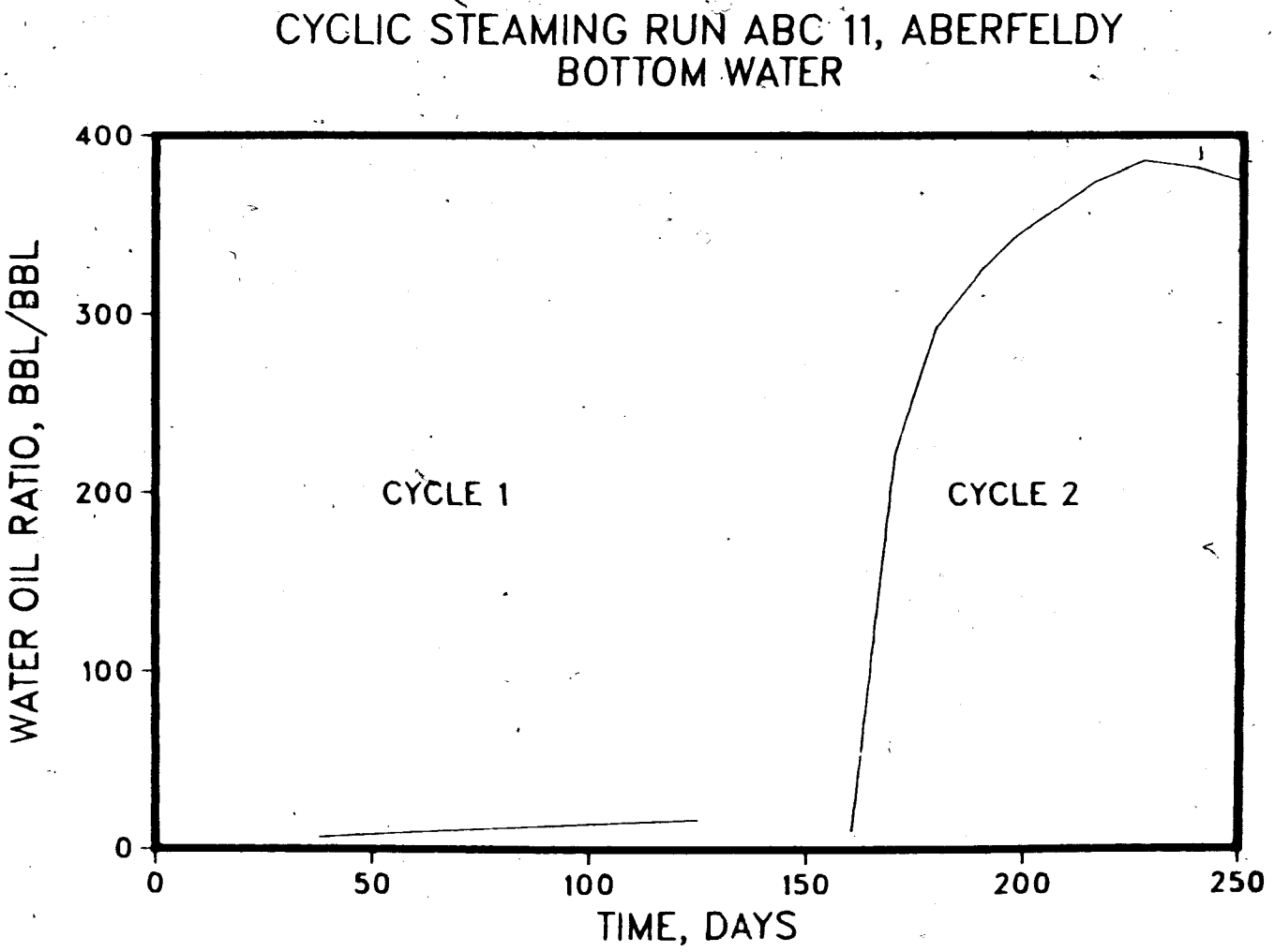

Figure 6.69 Water-Oil Ratio for Aberfeldy Cyclic Run ABC11, Bottom Water

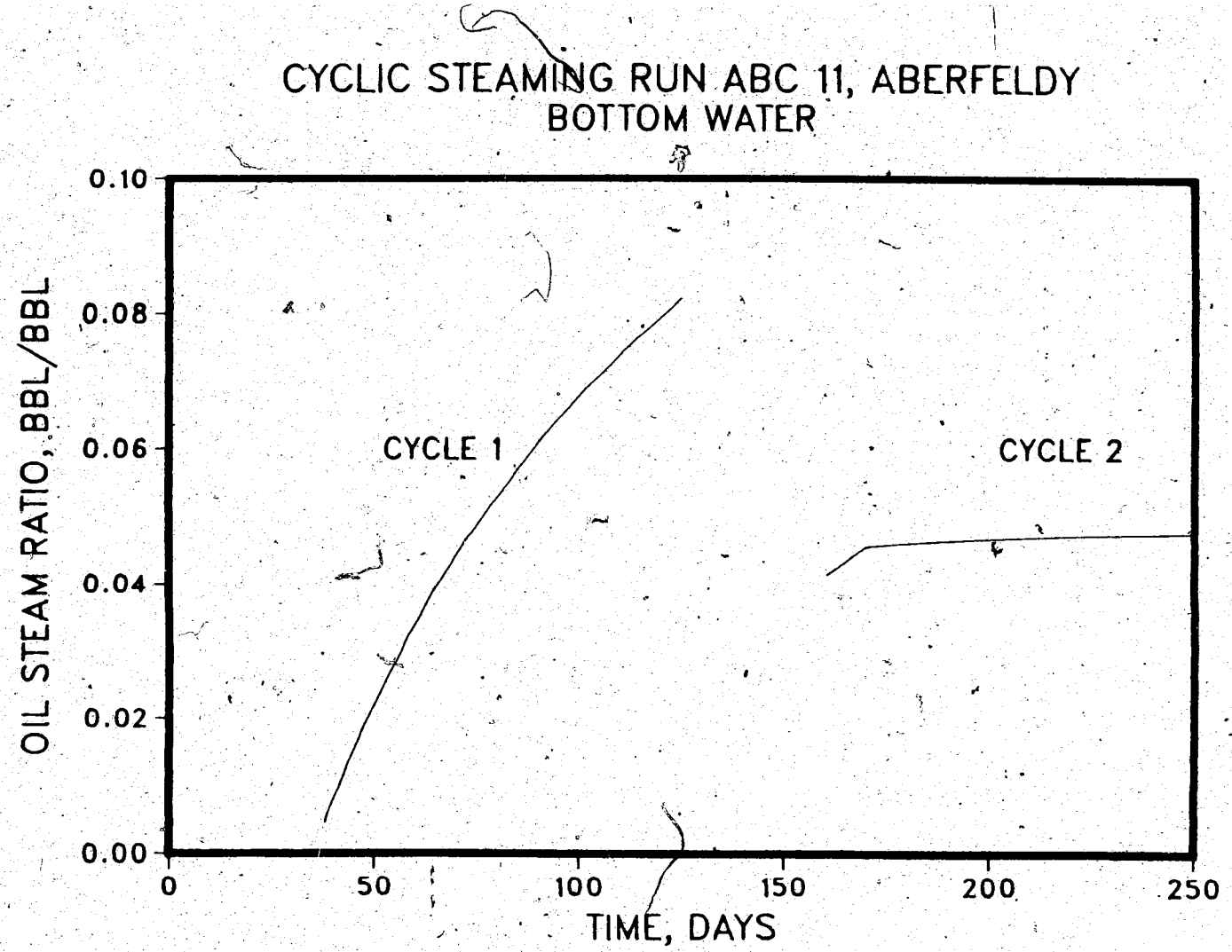

Figure 6.70 Oil-Steam Ratio for Aberfeldy Cyclic Run ABC11, Bottom Water

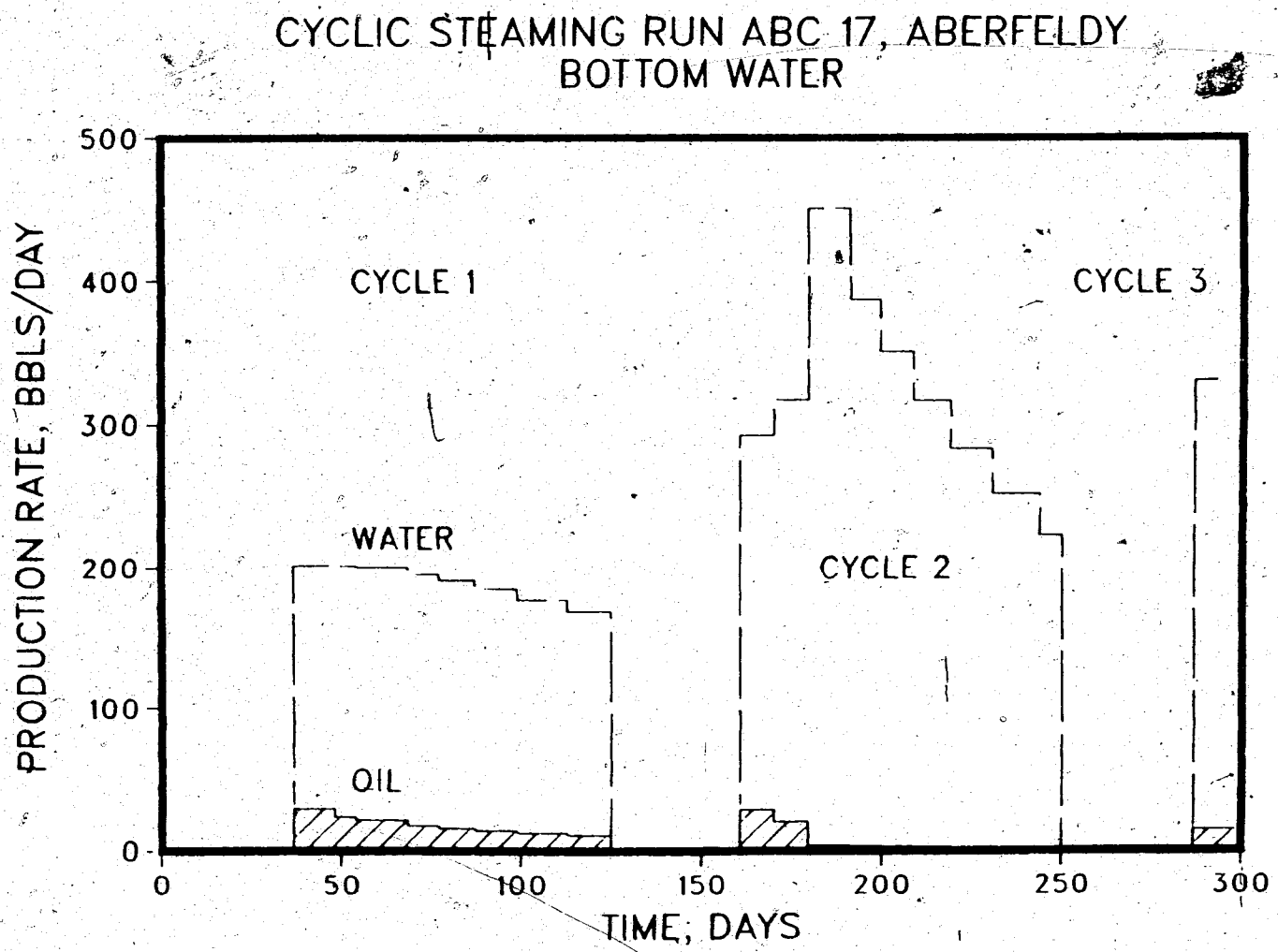

Figure 6.71 Production History for Aberfeldy Cyclic Run ABC17, Bottom Water

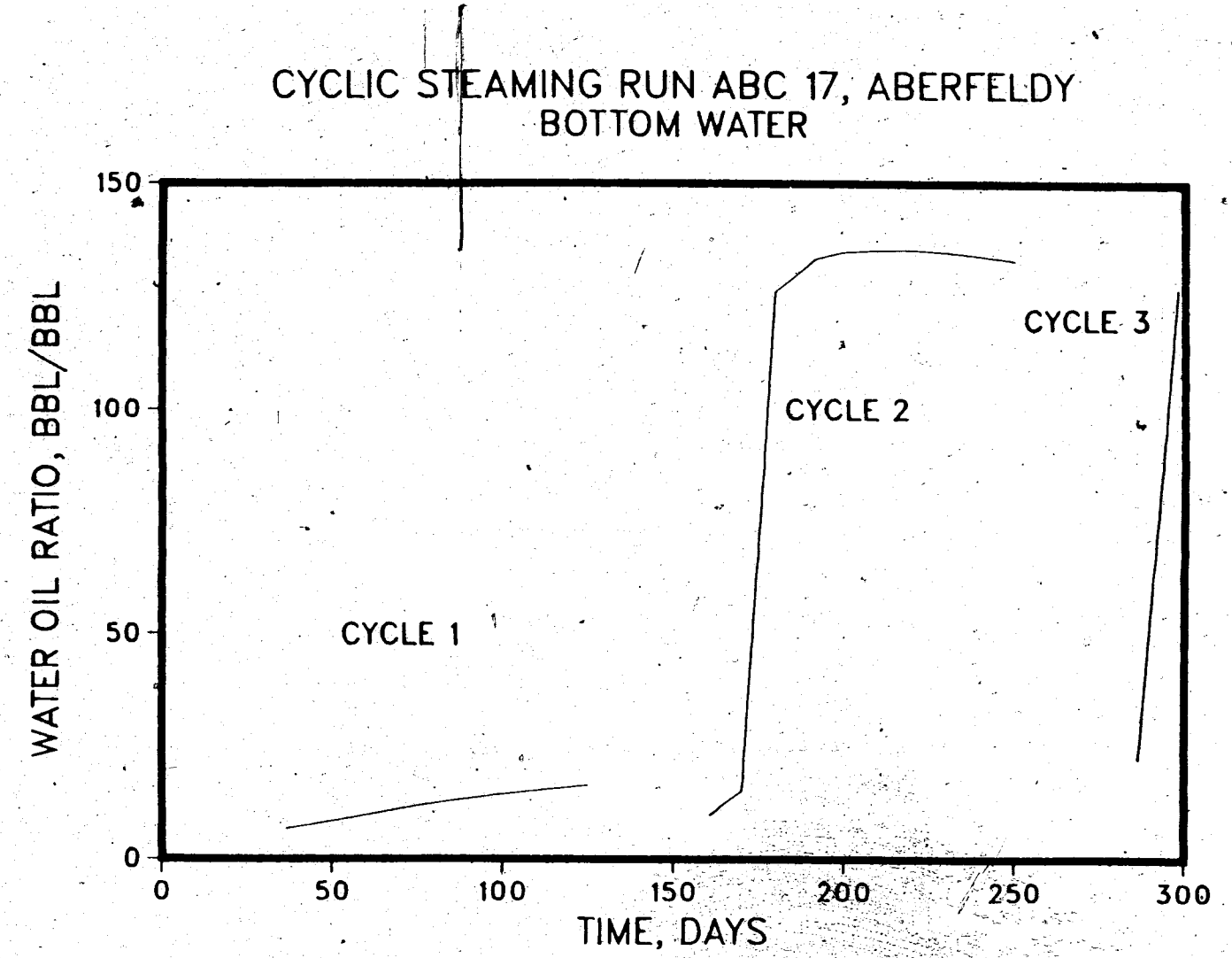

Figure 6.72 Water-Oil Ratio for Aberfeldy Cyclic Run ABC17, Bottom Water

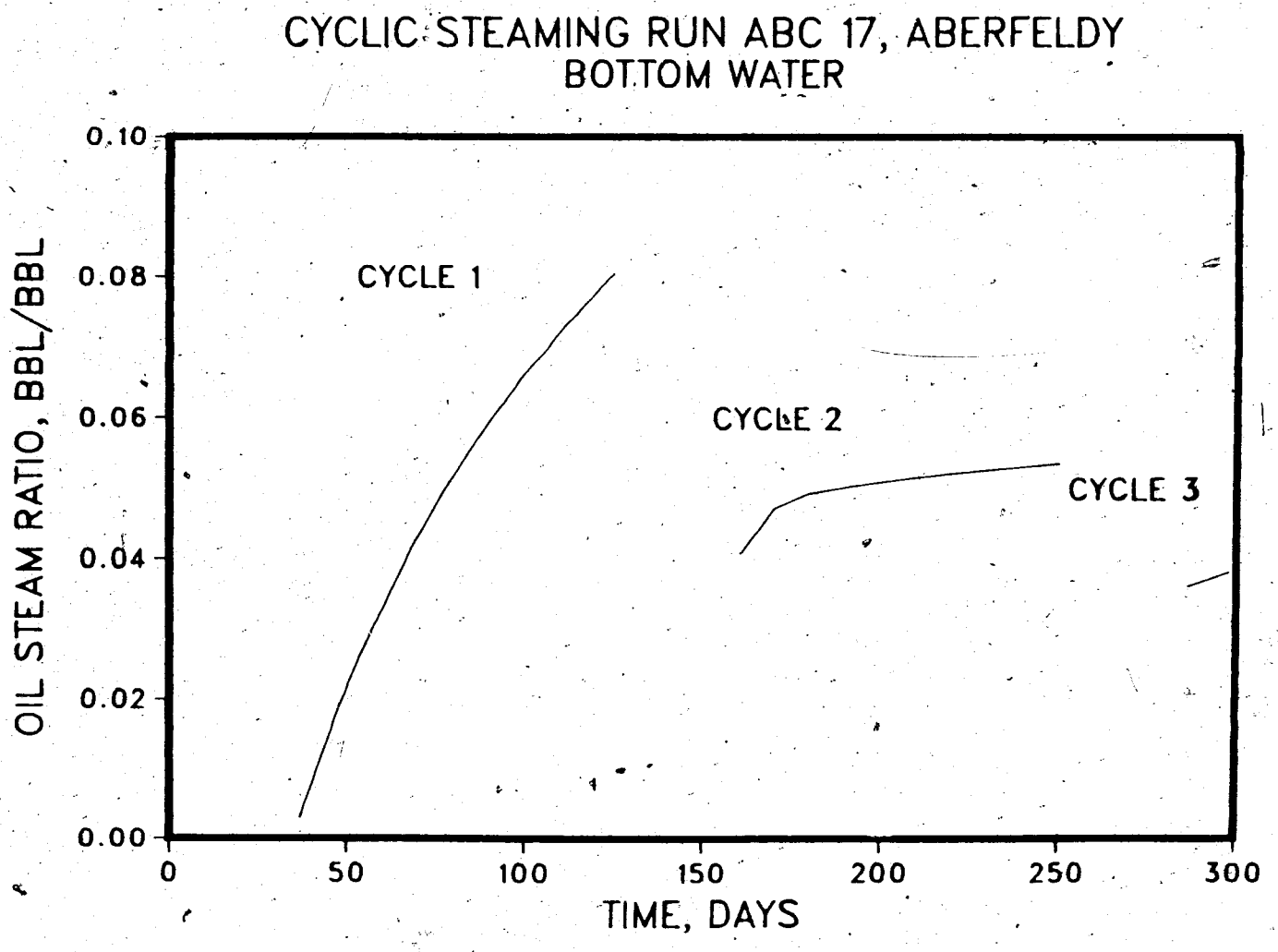

Figure 6.73 Oil-Steam Ratio for Aberfeldy Cyclic Run ABC17, Bottom Water

In Run ABC11, in the second cycle (Table C.21), the WORs are 200-400 (see Fig. 6.69, which shows the contrast between the first and second cycle WORs). This is mainly due to a much larger water zone in this case. At the same time, the steam slug used in the second cycle is twice as large as for the first cycle, i.e. 36000 bls, which also would increase water production rates. This trend is also evident from the performances of Runs ABC6 and ABC8 (Tables C.18 and 19, Figs. 6.60 and 6.63), where the WOR in the second cycle is higher when a larger volume of steam is injected. It is difficult to explain why the WOR in the second cycle of Run ABC8 is lower than that in the first cycle of the same run, although considerably more steam was injected in the second cycle. It is the result of complex interaction of the limited bottom water, conductive heating, and relative mobility/temperature relationships. The oil-steam ratio in the third cycle shows an improvement, because the conductive heating from the water layer to the oil layer above is starting to take effect.

Based upon the above, it may be said, that generally speaking, bottom water is undesirable in cyclic steaming, particularly when the bottom water thickness is large. Increasing steam slugs from cycle to cycle may have limited benefits, but it is more likely to give poorer performance than a constant slug. In fact, there may be some merit in reducing the steam slug size when bottom water is present. In all cases simulated, the oil-steam ratio was well below the minimum acceptable value of 0.10.

Cyclic Steam Simulations: Cold Lake

Several cyclic steam stimulation simulations were carried out for the Cold Lake Clearwater formation, three of which (Runs CLC1A, CLC6A, and CLC11A) are summarized in Tables C.23 to C.25, and in Figs. 6.74 through 6.82. The first run is for the no-bottom water case, while in the other two runs, bottom water thicknesses one-tenth and equal to the oil zone thicknesses are assumed.

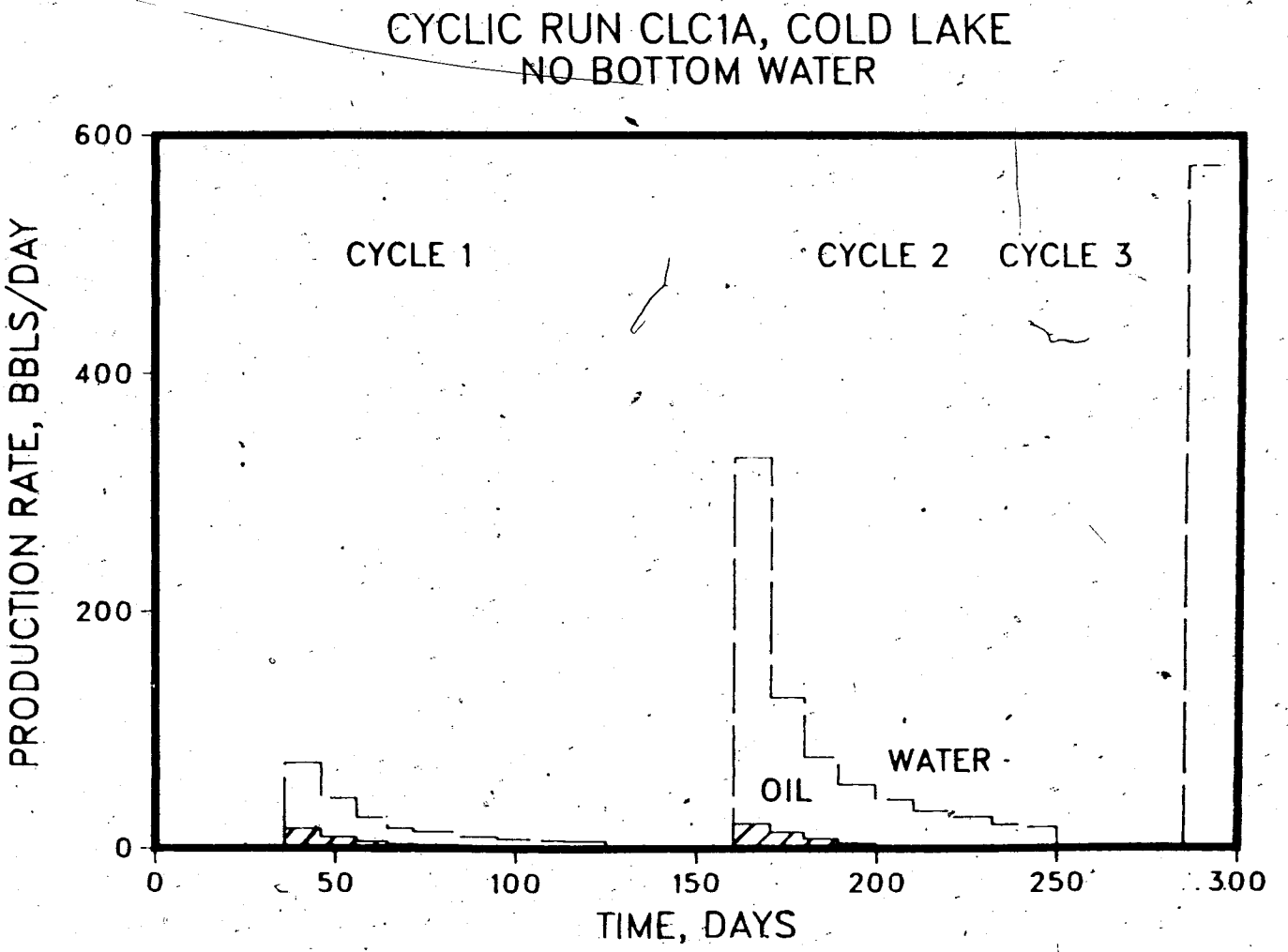

Figure 6.74 Production History for Cold Lake Cyclic Run CLC1A, No Bottom Water

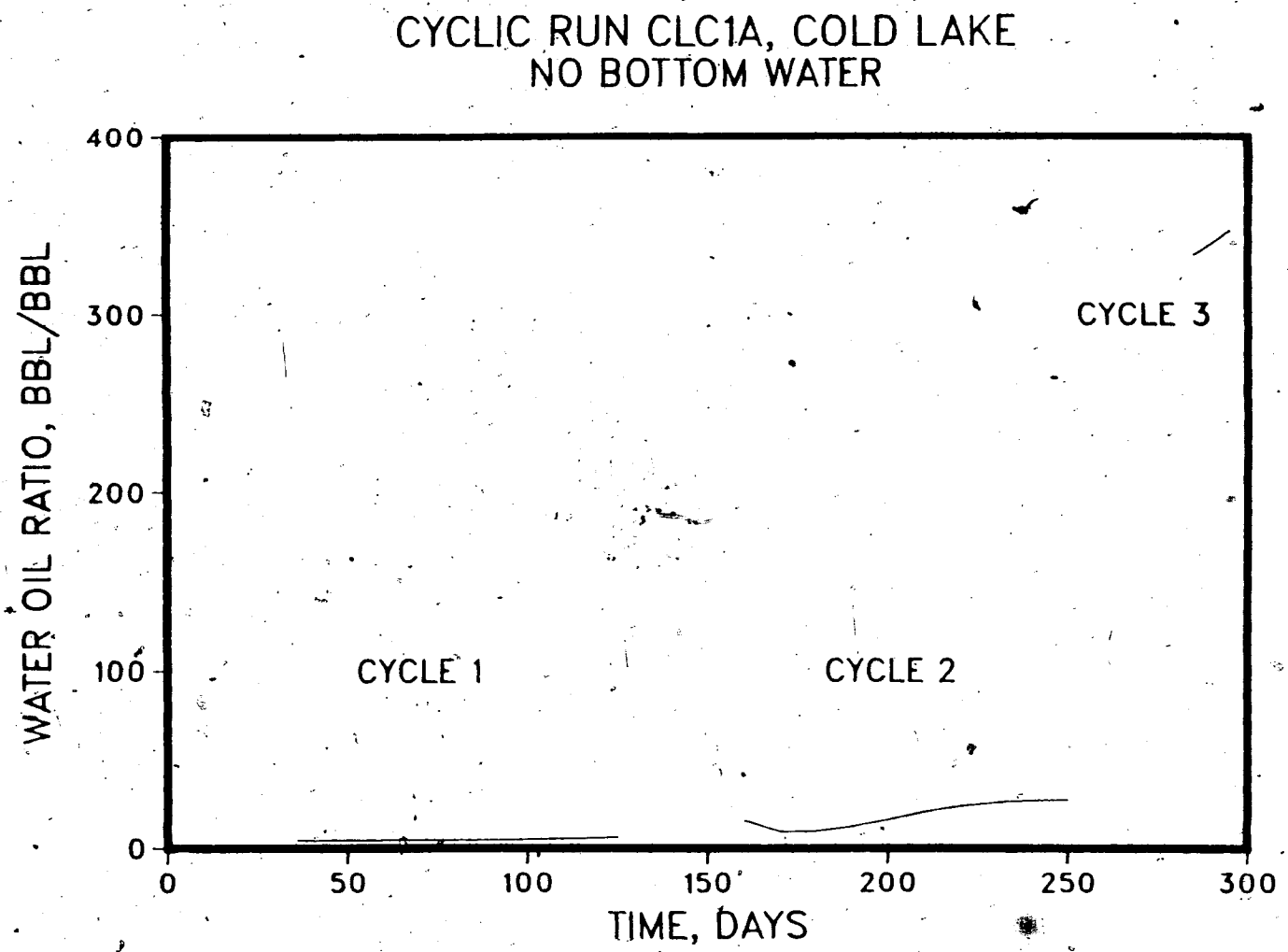

Figure 6.75 Water-Oil Ratio for Cold Lake Cyclic Run CLC1A, No Bottom Water

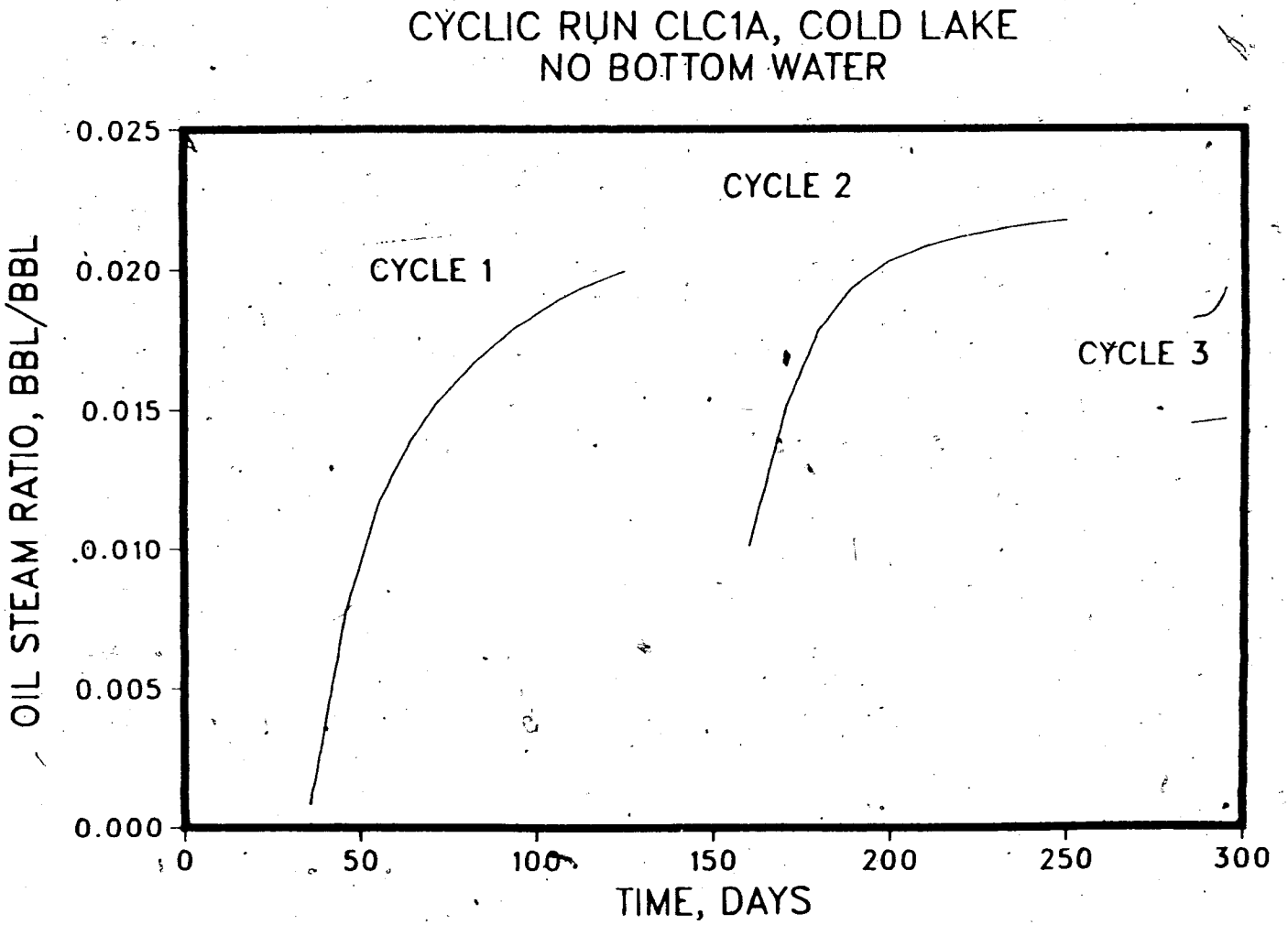

Figure 6.76 Oil-Steam Ratio for Cold Lake Cyclic Run CLC1A, No Bottom Water

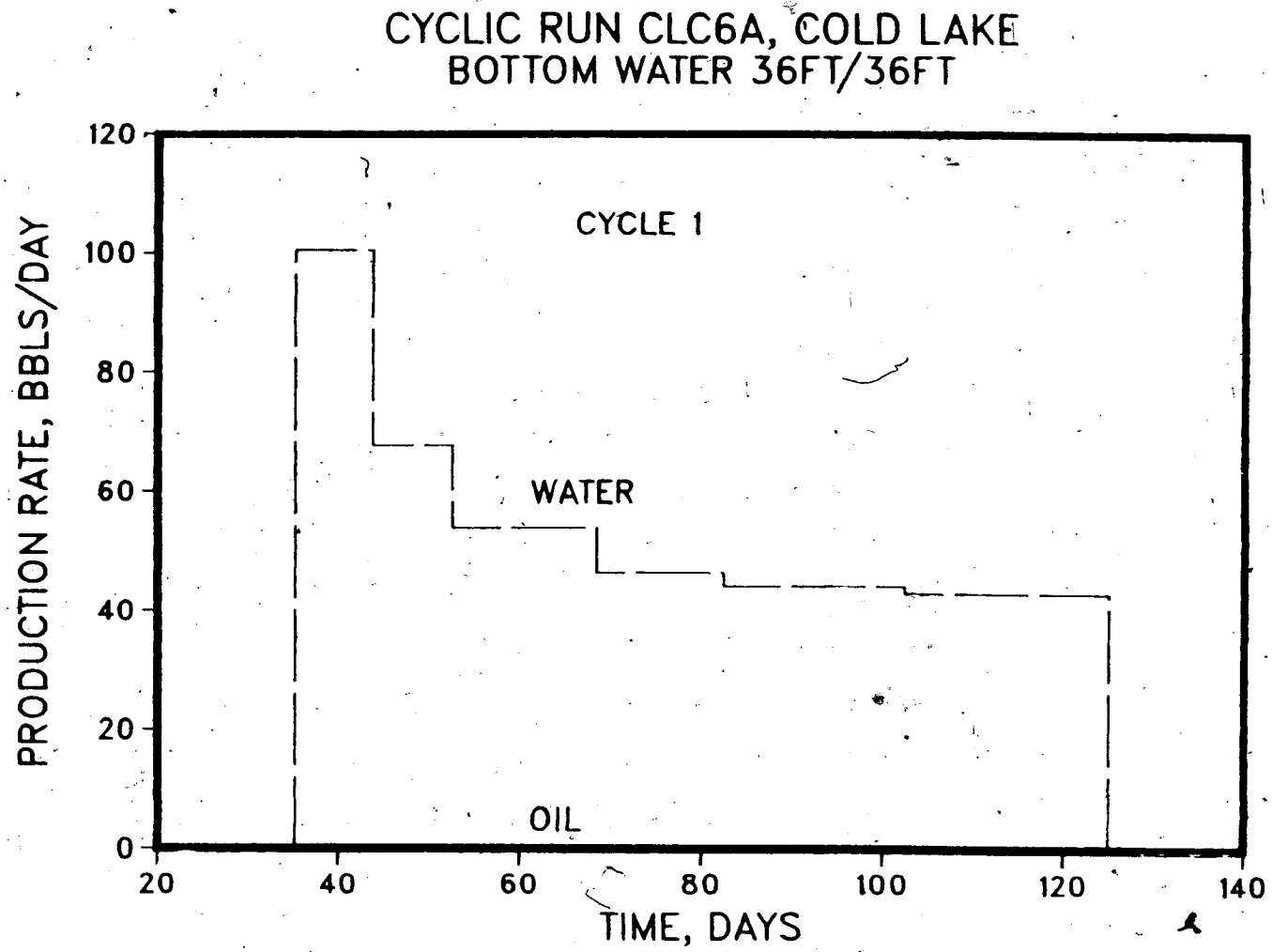

Figure 6.77 Production History for Cold Lake Cyclic Run CLC6A, Bottom Water

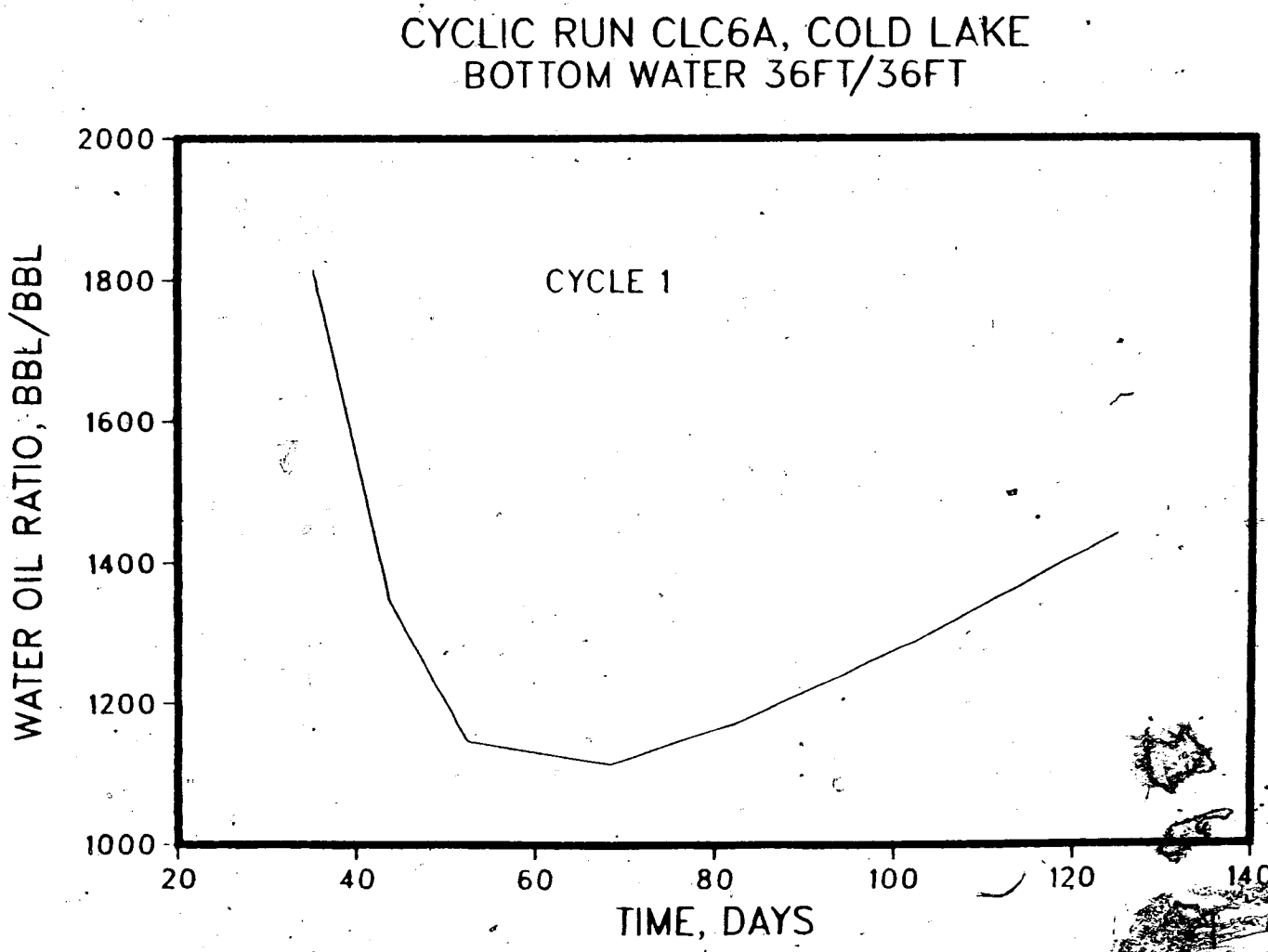

Figure 6.78 Water-Oil Ratio for Cold Lake Cyclic Run CLC6A, Bottom Water

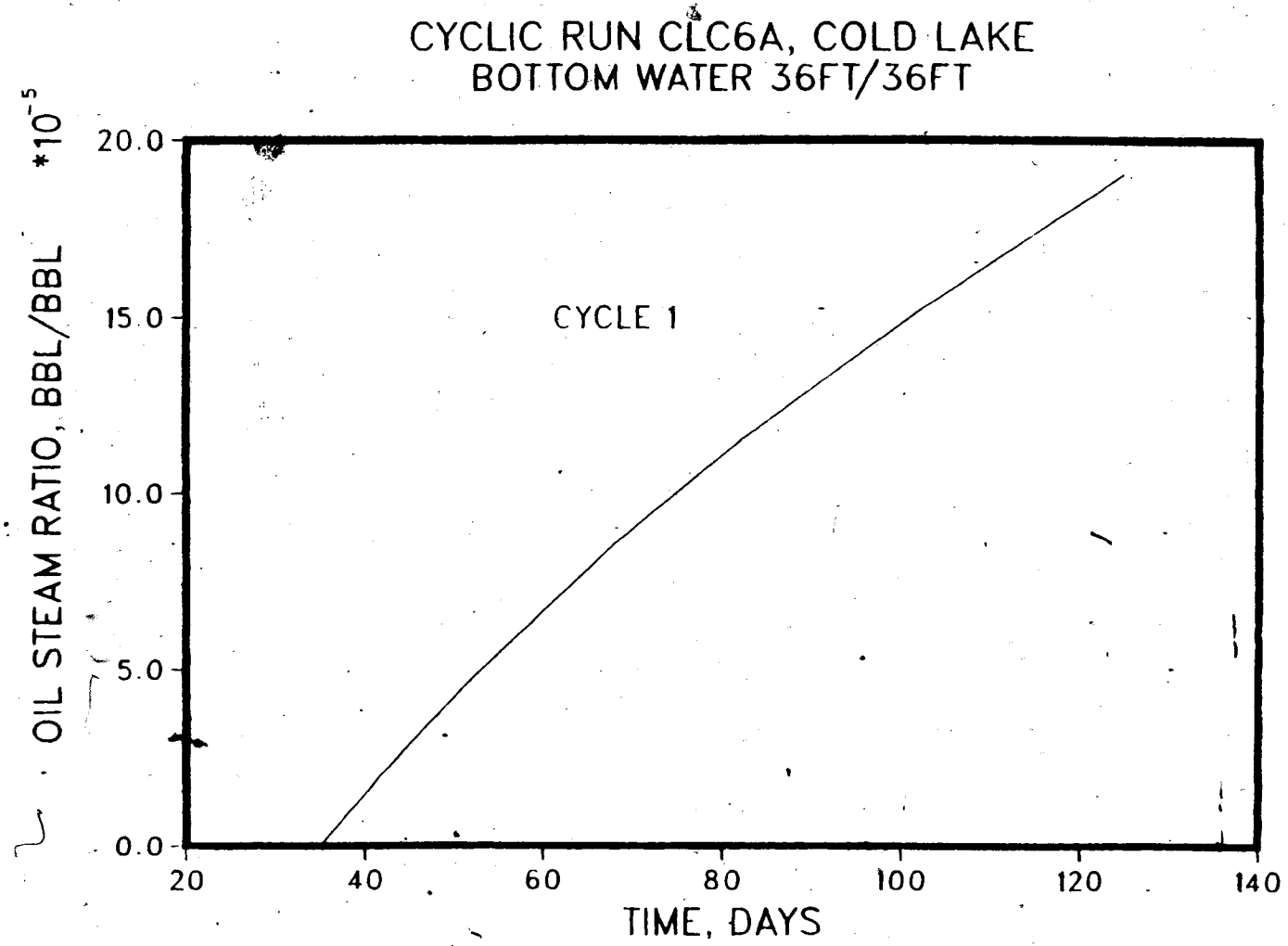

Figure 6.79 Oil-Steam Ratio for Cold Lake CAyclic Run CLC6A, Bottom Water

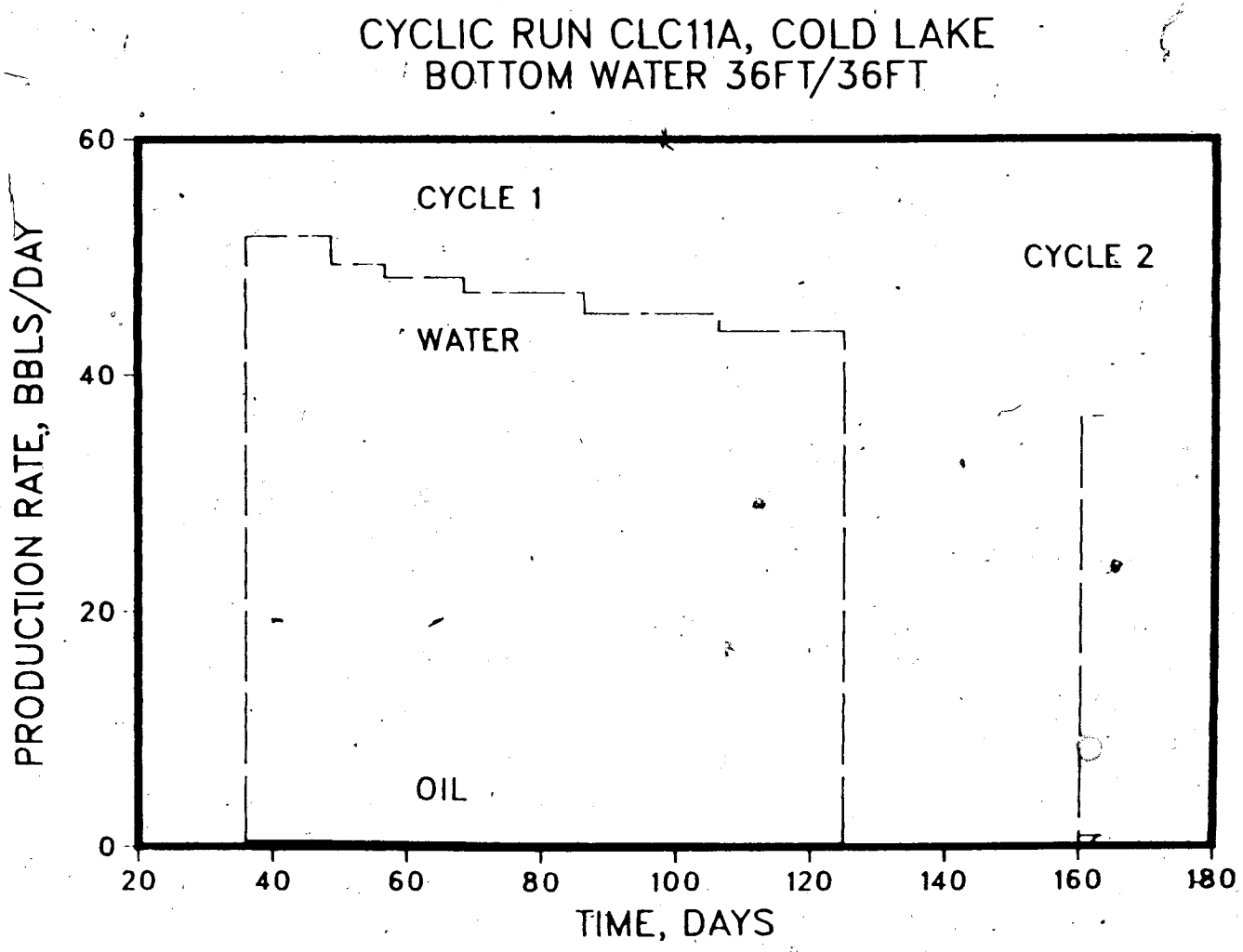

Figure 6.80 Production History for Cold Lake Cyclic Run CLC11A, Bottom Water

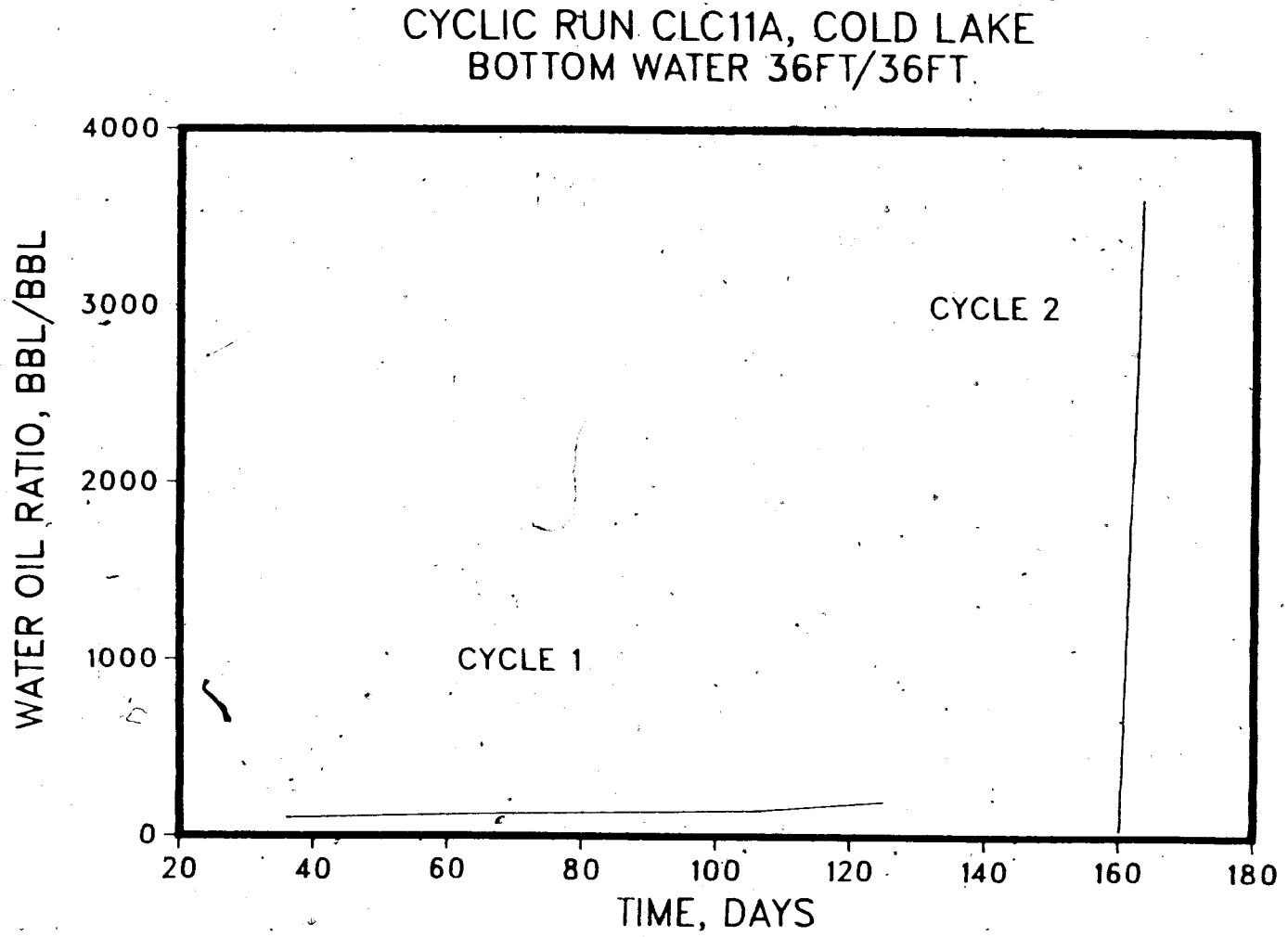

Figure 6.81 : Water-Oil Ratio for Cold Lake Cyclic Run CLC11A, Bottom Water

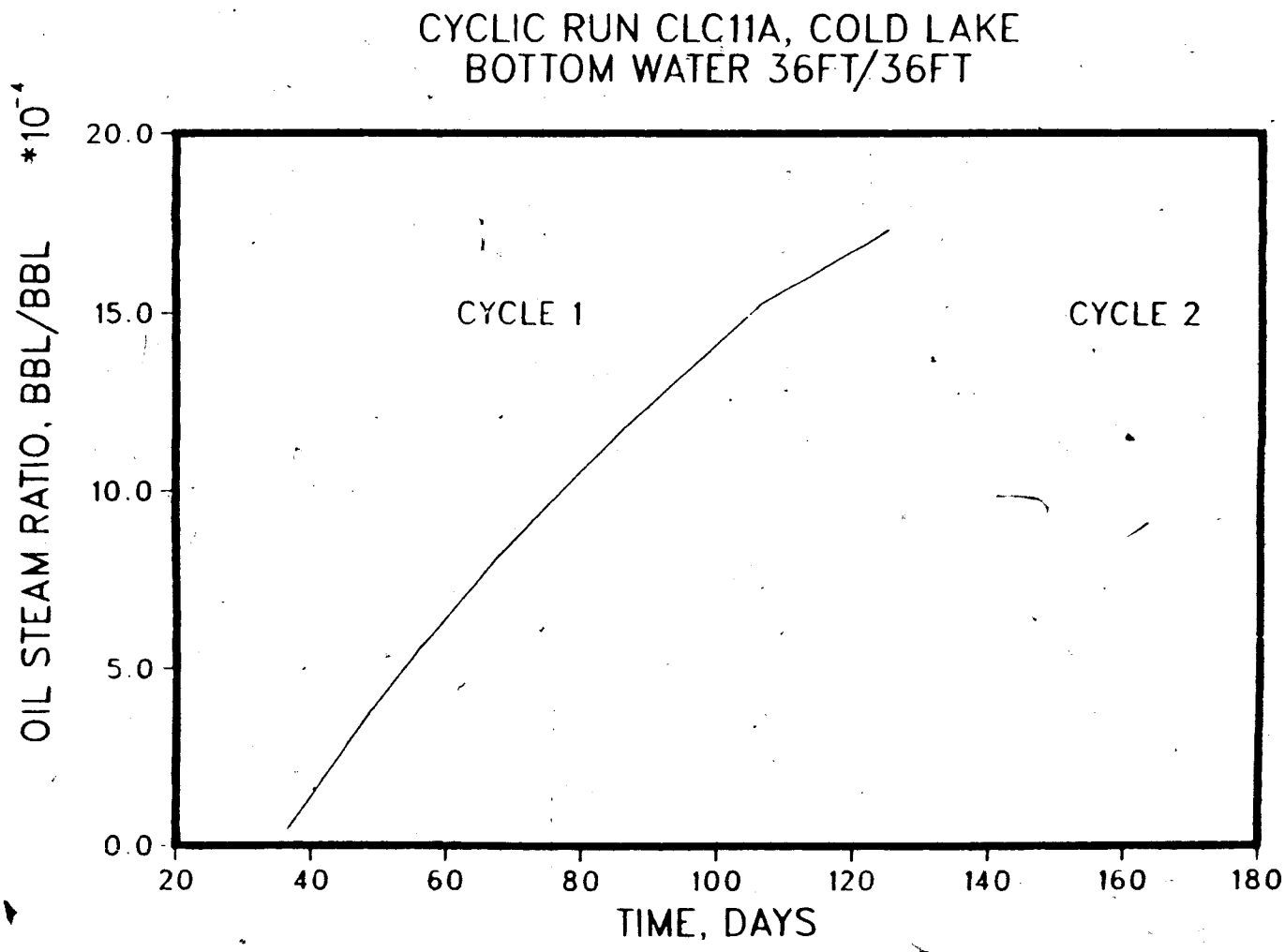

Figure 6.82 Oil-Steam Ratio for Cold Lake Cyclic Run CLC11A, Bottom Water

In the absence of bottom water, the performance in the three-cycle run (CLC1A) is rather poor, in view of the high oil viscosity in Cold Lake (125,000 cp). The overall oil-steam ratio is 0.0147. The heating of the formation was found to be quite uniform, with a higher steam saturation in the upper part of the formation. The terminal oil production rate was only 0.5 B/D, compared to 162 B/D for water. It should be noted that the cyclic steaming process that has been relatively successful in Cold Lake is a steam fracturing based process, whereas in the present simulations, uniform steam advance is assumed. Steam fracing helps to spread most of steam away from the wellbore, while in the present simulations, water saturation builds up around the wellbore.

Runs CLC6A and CLC11A were similar in performance, in that the oil-steam ratios were extremely low (0.0001 and 0.001, respectively, for the first cycle), although the bottom water thickness in the first run was much less. What these results show is that in the case of a very high viscosity oil, even a small amount of bottom water adversely affects performance.

The above results show, first, that the cyclic steaming performance simulation for Cold Lake, where steam parting is commonly used, cannot be realistically simulated by a non-frac simulator, such as the present one, and secondly, even small amounts of bottom water are likely to lower steam stimulation performance greatly for a very high viscosity oil.

Simulation of a Laboratory Steamflood

An important application of the simulators of the type developed in this work is their ability to interpret the results of laboratory experiments. In the present work, an attempt was made to evaluate a scaled model experiment of steamflooding, the data for which was reported by Proctor (1986). A scaled model is based upon scaling criteria derived from the partial differential equations of the process, in this case, steamflooding. First, the nonlinear equations must be simplified considerably before scaling criteria can be derived,

in order to minimize temperature and concentration dependence of various properties, and second, practical considerations make it difficult to satisfy all of the criteria derived. As a result, some of the scaling criteria must be relaxed. The question remains: what is the error due to neglecting these criteria? The steamflooding scaling criteria have been discussed by various investigators (e.g. Kimber et al. (1986)). It has been shown that in none of the cases considered can the scaling criteria be fully satisfied. Two different experimental approaches have been employed for steamflooding experiments: low pressure models, where the operation is at pressures close to the atmospheric pressure, and high pressure models, where the operation is close to the field conditions. Neither approach permits the use of the field porous media and fluids. (Kimber et al. showed that this would be feasible only if the model is geometrically distorted, and other groups relaxed). This is so because the model permeability must be scaled up by the geometric scaling factor. As a result, the model and field relative permeabilities are expected to be different (the end point saturations are different, for example), although these are assumed to be the same.

Over 25 steamflood simulations were carried out to try to simulate Proctor's Run 10, the conditions for which are listed in Table 6.4, and the production history for which is given in Table 6.5. Figure 6.83 shows the experimental and simulated production histories for this run. The history match runs were designed to match the experimental data without major adjustments in data. Block size, initial conditions, and transmissibilities were varied in these runs, with little success. Finally, only major adjustments in the critical saturations and transmissibilities permitted the match shown in Fig. 6.83. This match could have been further improved, but what is important is the finding that large adjustments of field relative permeabilities are necessary to achieve a match. Scaled model experiments using reservoir porous media and fluids are currently in progress, and it is too early to say whether they offer a solution to this problem.

Table 6.4

DATA USED FOR THE SIMULATION OF LABORATORY RUN 10

Dimensions of Porous Pack, ft	2.665 x 2.665
Thickness, ft	0.208
Initial Oil Saturation, %	70.0
Initial Pressure, psia	10.0
Permeability, darcy	4200
Porosity, %	30.23
Oil Compressibility, psi^{-1}	0.5×10^{-5}
Water Compressibility, psi^{-1}	0.3×10^{-5}
Oil Thermal Expansion Coefficient, $°F^{-1}$	0.5×10^{-3}
Water Thermal Expansion Coefficient, $°F^{-1}$	0.49×10^{-3}
Rock Compressibility, psi^{-1}	1×10^{-6}
Rock Thermal Conductivity, Btu/day-ft-°F	42.3
Thermal Conductivity of Overburden, Btu/day-ft-°F	35.3
Rock Matrix Density, lb/ft^3	165
Rock Matrix Specific Heat, Btu/lb-°F	0.20
Thermal Diffusivity of Overburden, ft^2/day	0.96
Specific Heat of Oil, Btu/lb-°F	0.50
Oil Density, lb/ft^3	58.5
Critical Gas Saturation, %	10.0
Residual Oil Saturation, %	20.0
Irreducible Water Saturation, %	7.5

Oil Viscosity (Oil: Faxam-100)

Temperature, °F	Viscosity, cp
33.8	9256
42.1	4066
59.2	653
75.2	208
95.0	91
180.7	9.4
325	2.8

Avg. Steam Injection Rate, B/D	2.084
Avg. Steam Injection Pressure, psia	15.0
Avg. Steam Quality, %	90.0

Table 6.5

EXPERIMENTAL DATA FOR RUN 10; STEAMFLOOD IN ABERFELDY MODEL

Type of Oil Used	Faxam-100 (208 mPa·s at 23°C)
Pore Volume	12700 cm^3
Porosity of Bead Pack	30.23%
Hydrocarbon Pore Volume	11680 cm^3
Initial Oil Saturation	92.00%
Irreducible Water Saturation	8.00%
Initial Model Temperature	4.07°C
Water Feed Flow Rate	199.8 cm^3/min
Boiler Feed Flow Rate	30.3 cm^3/min
Total Flow Rate of Steam	230.1 cm^3/min
Volume of Steam Injected	26850 cm^3 (2.114 PV)
Volume of Oil Recovered	3677 cm^3 (31.48% OOIP)

Cumulative Total PV Injected (cm^3)	Cumulative Total PV Injected (PV)	Cumulative Oil Produced (cm^3)	Cumulative Oil Produced (%OOIP)	Oil-Steam Ratio (cm^3/cm^3)
1100	0.087	540	4.62	0.4909
2830	0.223	895	7.66	0.2052
4280	0.337	1245	10.66	0.2414
6085	0.479	1690	14.47	0.2465
7575	0.596	1897	16.24	0.1389
9265	0.730	2027	17.35	0.0769
10760	0.847	2234	19.13	0.1385
12550	0.988	2399	20.54	0.0922
14240	1.212	2624	22.47	0.1331
16050	1.264	2749	23.54	0.0691
17745	1.397	2859	24.48	0.0649
19535	1.538	2998	25.67	0.0776
21335	1.680	3162	27.07	0.0911
23135	1.822	3304	28.29	0.0789
24030	1.892	3381	28.95	0.0860
24950	1.965	3422	29.30	0.0446
26850	2.114	3677	31.48	0.1342

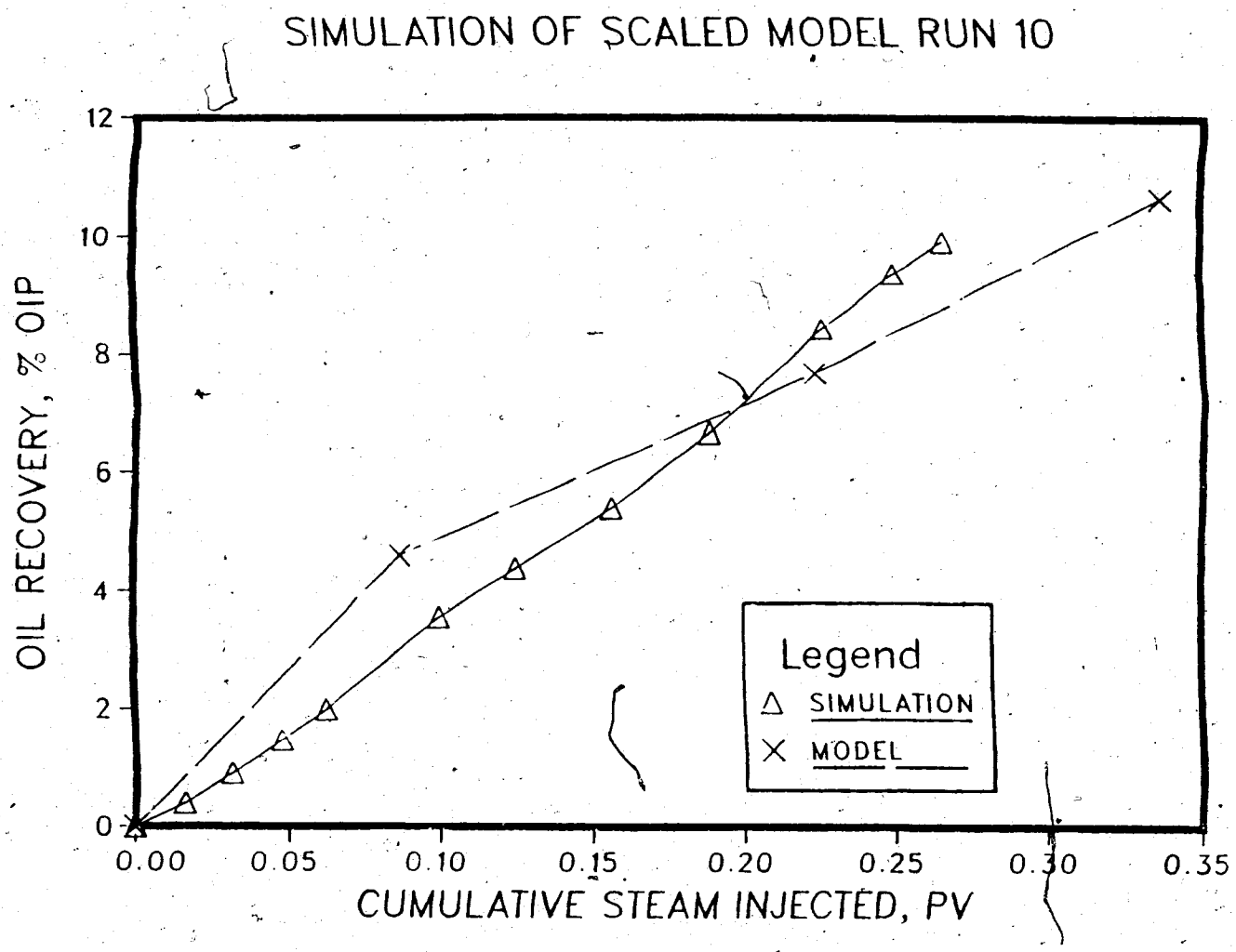

Figure 6.83 Simulation of Sclaed Model Steamflood [illegible]0, Oil Recovery vs. Steam Injected (Proctor).

Non-Newtonian Oil Viscosity Effects

In Chapter IV, a possible model was discussed for non-Newtonian oils. It has been claimed from time to time that certain Alberta, Saskatchewan and Venezeula oils behave in the non-Newtonian manner. In the present work, it is intended to show the effect of such oil rheology on steamflooding response. Table 6.6 gives the production performance summary for a base steamflood (SP1), with no bottom water, or any non-Newtonian or other effects. The oil/water production and oil-steam ratio plots are given in Figs. 6.84 and 6.85. The oil recovery at the end of 843 days is seen to be 12.47%, with a cumulative oil-steam ratio of 0.413.

Table 6.7 gives the production history of the same run, but with the assumption that the oil is non-Newtonian, with an exponent of 0.9, at all temperatures (Run SP5). The effect of such a value of the exponent will be to reduce the oil viscosity by one-half approximately, at typical shear rates involved. Figures 6.86 and 6.87 give the production histories and the oil-steam ratio for this run. It is seen that the oil recovery at the same steam injection time is 8.24% versus 4.15% for Newtonian behaviour (626 days). The corresponding oil-steam ratios are 0.367 and 0.185, respectively. The increase in oil recovery and the oil-steam ratio is due to decreased oil viscosity in the non-Newtonian case. It is important to note that within our assumptions, such a decrease is occurring regardless of temperature. In other words, the cold oil mobility is increased, and the oil behaves like a less viscous oil, although in a nonlinear manner. The observed improvements in performance would be obtained also if the steamflood is carried out in a less viscous oil.

In a typical steamflood, oil-water emulsions may form in certain temperature regions, although these were not considered in this work. Such emulsions would behave in a non-Newtonian manner. Depending on the rheology of such emulsions, they may not reduce oil mobility, if they are shear-thinning. Field experience in steamflooding shows that

Table: 6.6

BASE RUN: ABERFELDY (NO BOTTOM WATER) SP1
NO FOAM, NO LIPGRADING, NO NON-NEWTONIAN
INJ. RATE 600 BBLS/DAY STEAMFLOOD

Legend:

T : Time, Days
OPR : Oil Production Rate, Bbls/Day
WPR : Water Production Rate, Bbls/Day
WOR : Cumulative Water-Oil Ratio, Bbl/Bbl
CSI : Cumulative Steam Injected, 10^5 Bbls
ORec : Oil Recovery, %
OSR : Cumulative Oil-Steam Ratio, Bbl/Bbl

T	OPR	WPR	WOR	CSI	ORec	OSR
44	19.3	249	12.80	0.26	0.05	0.032
90	20.1	307	15.20	0.54	0.11	0.033
130	21.4	363	16.90	0.78	0.16	0.033
174	30.4	505	16.60	1.04	0.23	0.036
215	40.1	585	14.60	1.29	0.32	0.041
253	50.6	630	12.40	1.52	0.43	0.047
294	56.9	657	11.50	1.76	0.56	0.053
331	63.9	671	10.50	1.98	0.69	0.058
370	73.9	682	9.23	2.22	0.85	0.064
413	90.4	692	7.66	2.48	1.07	0.072
460	124.0	690	5.56	2.76	1.37	0.083
501	184.0	698	3.79	3.00	1.75	0.098
546	292.0	749	2.56	3.27	2.44	0.125
586	353.0	989	2.80	3.52	3.19	0.152
626	441.0	1246	2.82	3.76	4.15	0.185
667	474.0	960	2.02	4.00	5.28	0.221
703	542.0	775	1.43	4.22	6.38	0.253
742	633.0	720	1.14	4.45	7.75	0.292
788	737.0	664	0.90	4.73	9.66	0.342
820	860.0	696	0.81	4.92	11.20	0.381
843	1047.0	765	0.73	5.06	12.47	0.413

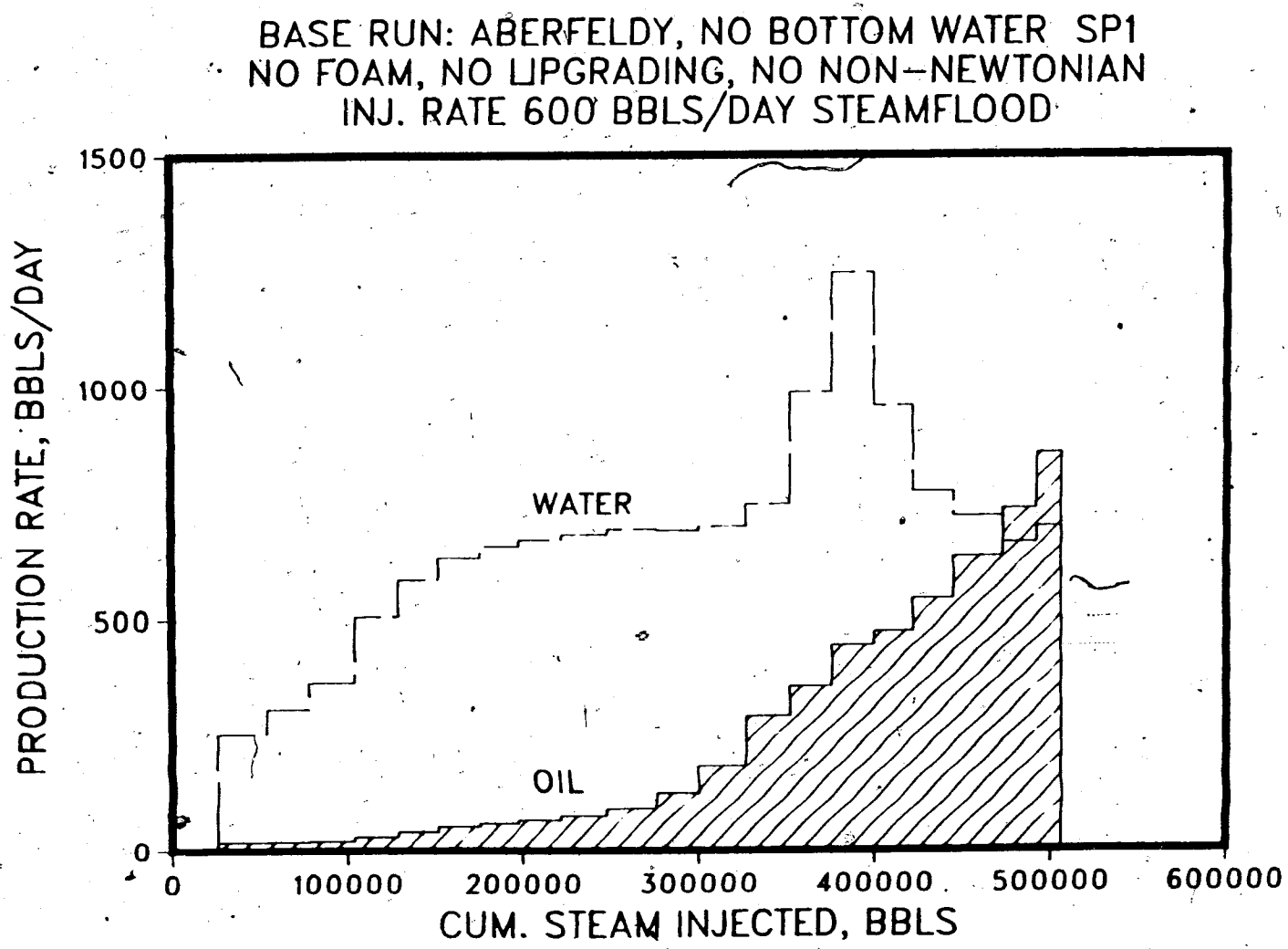

Figure 6.84 Production History of Base Aberfeldy Steamflood Run SP1, for Special Features Studies

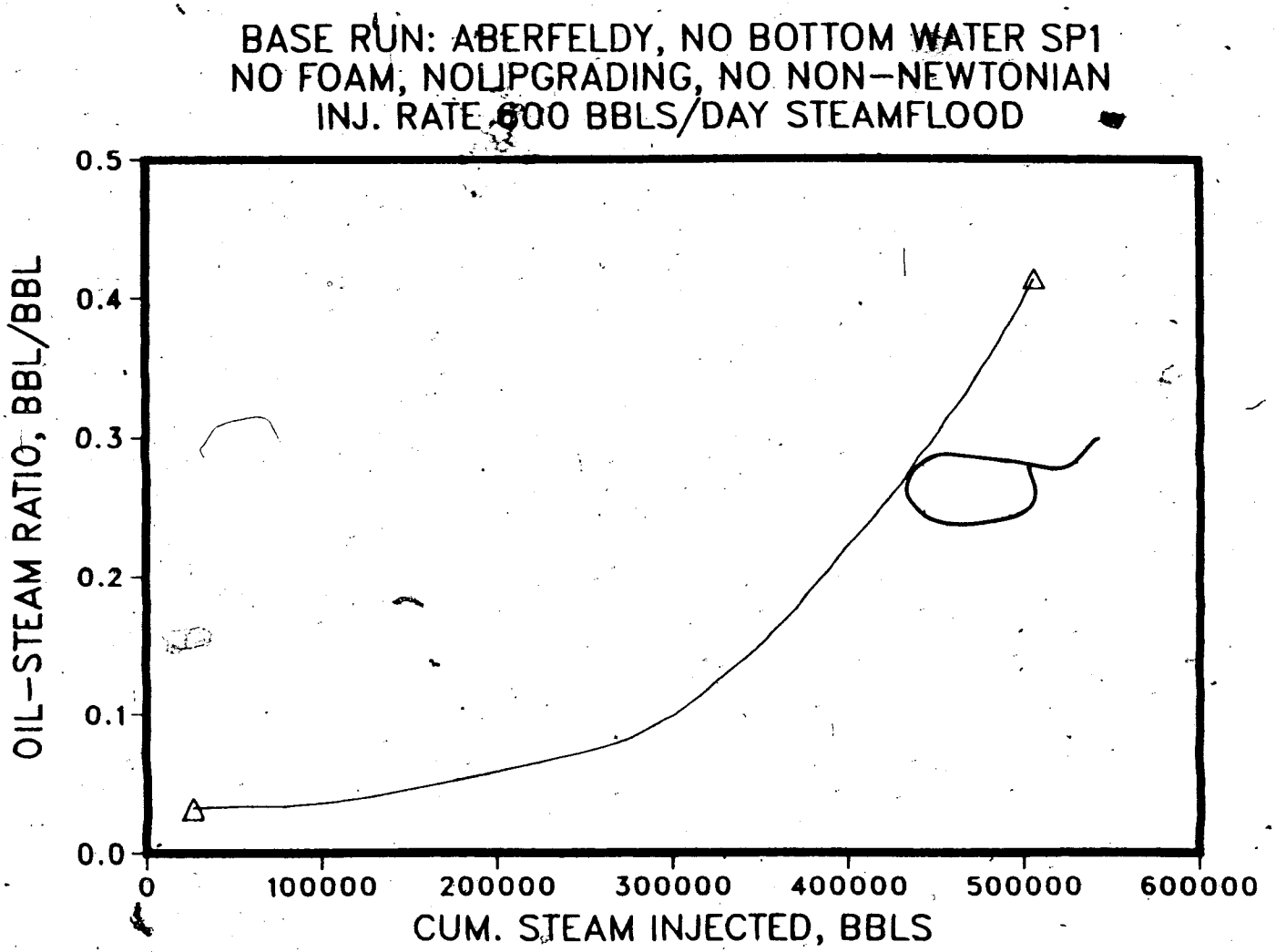

Figure 6.85 Oil Recovery of Base Aberfeldy Steamflood Run SP1, for Special Features Studies

Table: 6.7
NON-NEWTONIAN RUN: ABERFELDY (NO BOTTOM WATER) SP5
INJ. RATE 600 BBLS/DAY STEAMFLOOD

Legend:

T : Time, Days
OPR : Oil Production Rate, Bbls/Day
WPR : Water Production Rate, Bbls/Day
WOR : Cumulative Water-Oil Ratio, Bbl/Bbl
CSI : Cumulative Steam Injected, 10^5 Bbls
ORec : Oil Recovery, %
OSR : Cumulative Oil-Steam Ratio, Bbl/Bbl

T	OPR	WPR	WOR	CSI	ORec	OSR
42	47.0	242	5.13	0.254	0.12	0.0796
99	51.3	310	6.03	0.593	0.29	0.0813
128	54.2	348	6.41	0.770	0.38	0.0830
171	74.5	467	6.27	1.027	0.55	0.0894
213	97.6	541	5.54	1.279	0.77	0.1010
251	123.0	580	4.72	1.509	1.03	0.1140
294	137.0	605	4.41	1.766	1.36	0.1290
330	150.0	615	4.08	1.981	1.67	0.1410
369	169.0	622	3.68	2.216	2.05	0.1550
414	198.0	628	3.18	2.481	2.54	0.1720
459	246.0	630	2.56	2.753	3.16	0.1920
504	339.0	646	1.90	3.027	3.96	0.2190
546	566.0	850	1.50	3.273	5.04	0.2580
586	702.0	1245	1.77	3.516	6.61	0.3150
628	634.0	1042	1.64	3.770	8.32	0.3690

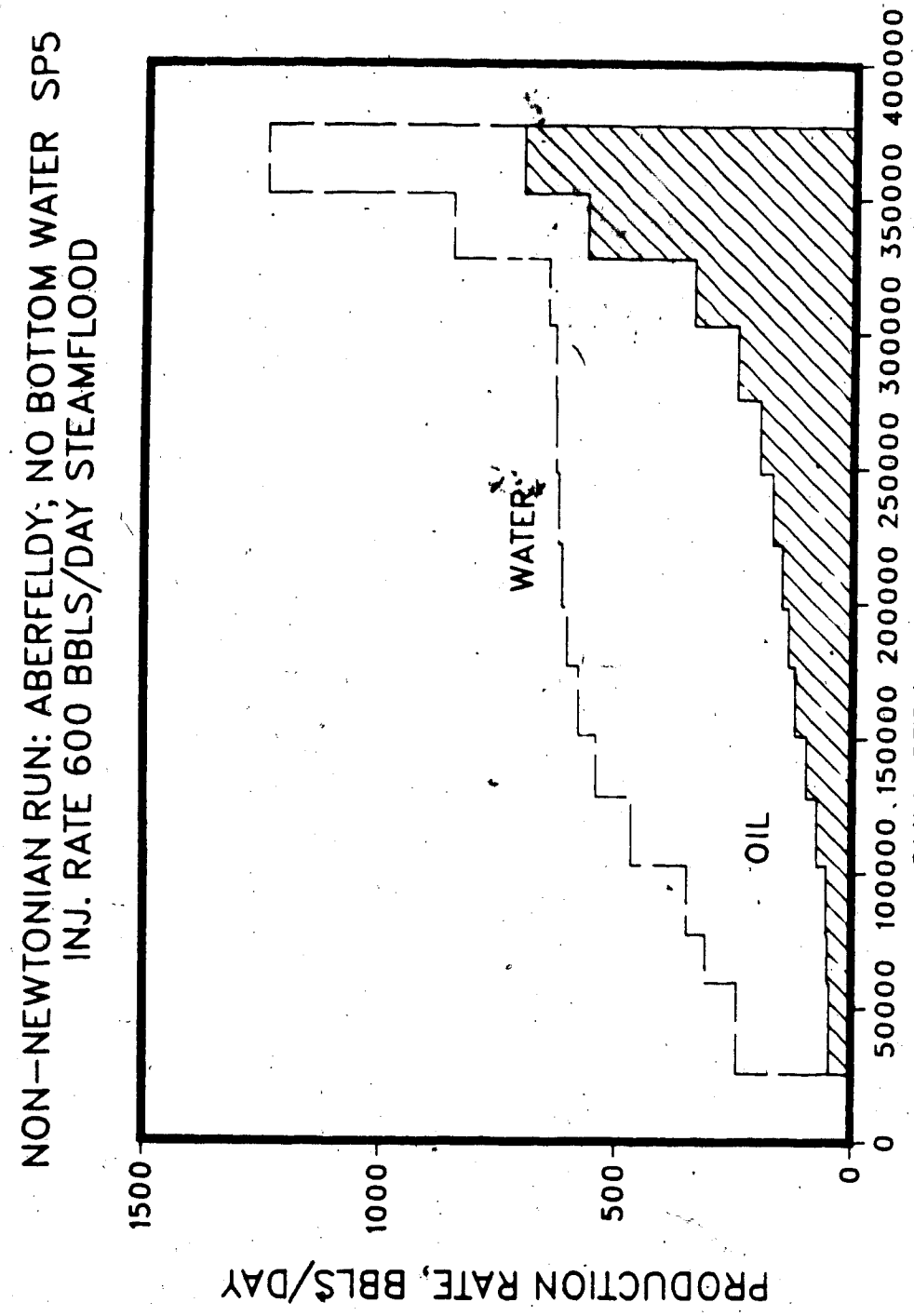

Figure 6.86 Production History of Aberfeldy Run SP5, for Non-Newtonian Oil (n = 0.9)

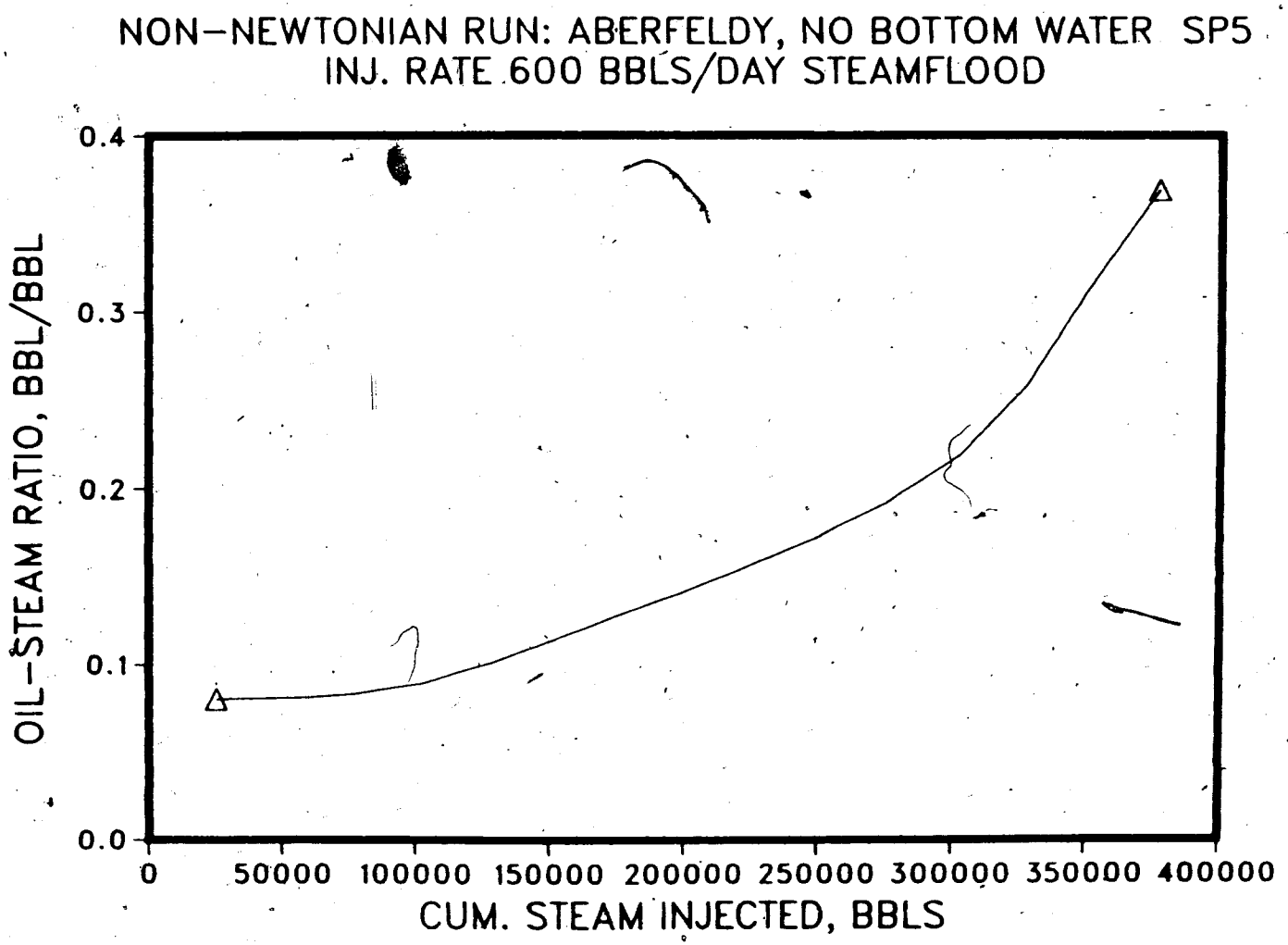

Figure 6.87 Oil-Steam Ratio of Aberfeldy Run SP5, for Non-Newtonian Oil (n = 0.9)

emulsions are not a serious problem. This is not so in fireflooding, where emulsions formed are highly viscous, and as a result, the rheology considered in the present simulation does not help much.

Thermal Upgrading

Thermal upgrading was discussed in Chapter IV, where a mathematical representation was given of the thermal upgrading process. Using the viscosity model developed, Run SP3 was carried out. The results were virtually the same as that for the base run (Table 6.6), with 0.1% higher oil recovery. An examination of the temperature profiles showed that the reason for no upgrading effect on oil recovery was the fact that the upgrading process lowered oil viscosity only in the parts of the reservoir with high temperatures, where the oil was mobile enough already. Upgrading had no effect on oil viscosity in the cold parts of the formation where it could have done some good. A second run (SP4) was carried out with slightly higher upgrading parameters. The simulation results are summarized in Table 6.8, and plotted in Figs. 6.88 and 6.89 for this run. There is a small improvement in this case, with oil recovery increasing to 13.02%.

It can be said that thermal upgrading is not likely to be significant in steamfloods of short duration, and prior to steam breakthrough. If a steamflood is continued after steam breakthrough, the oil around the producers would undergo some thermal upgrading leading to a reduction in viscosity. Also, in long-term projects, utilizing conductive heating of oil, thermal upgrading would be an important factor (e.g. Peace River project). It is thus desirable to include thermal upgrading effects in a steam injection simulator.

Foam Injection

Injection of a thermally stable foam prior to steam, or with steam, is being tested in the field. Foams are known to reduce the relative permeability to gas, without affecting oil relative permeability to any appreciable degree. In steam injection, foams are primarily

Table: 6.8

UPGRADING RUN: ABERFELDY (NO BOTTOM WATER) SP4
INJ. RATE 600 BBLS/DAY STEAMFLOOD

Legend:

T : Time, Days
OPR : Oil Production Rate, Bbls/Day
WPR : Water Production Rate, Bbls/Day
WOR : Cumulative Water-Oil Ratio, Bbl/Bbl
CSI : Cumulative Steam Injected, 10^5 Bbls
ORec : Oil Recovery, %
OSR : Cumulative Oil-Steam Ratio, Bbl/Bbl

T	OPR	WPR	WOR	CSI	ORec	OSR
44	21.6	248	11.50	0.262	0.06	0.0360
110	23.0	334	14.60	0.661	0.14	0.0367
130	23.8	361	15.20	0.781	0.17	0.0372
172	33.2	498	15.00	1.031	0.25	0.0403
211	42.9	574	13.40	1.264	0.34	0.0450
258	56.9	628	11.00	1.547	0.49	0.0528
295	63.4	652	10.30	1.771	0.62	0.0589
330	70.7	664	9.40	1.978	0.76	0.0645
366	81.1	675	8.33	2.199	0.93	0.0709
418	103.0	686	6.64	2.507	1.21	0.0812
458	135.0	684	5.05	2.751	1.51	0.0920
502	206.0	696	3.37	3.014	1.96	0.1090
546	320.0	740	2.31	3.278	2.70	0.1380
585	389.0	991	2.55	3.511	3.50	0.1670
626	481.0	1244	2.58	3.755	4.58	0.2040
667	506.0	952	1.88	4.001	5.78	0.2420
704	574.0	777	1.35	4.222	6.98	0.2770
741	645.0	707	1.10	4.448	8.36	0.3150
792	757.0	656	0.87	4.751	10.48	0.3700
824	885.0	694	0.78	4.947	12.08	0.4090
841	1024.0	748	0.73	5.045	13.02	0.4320

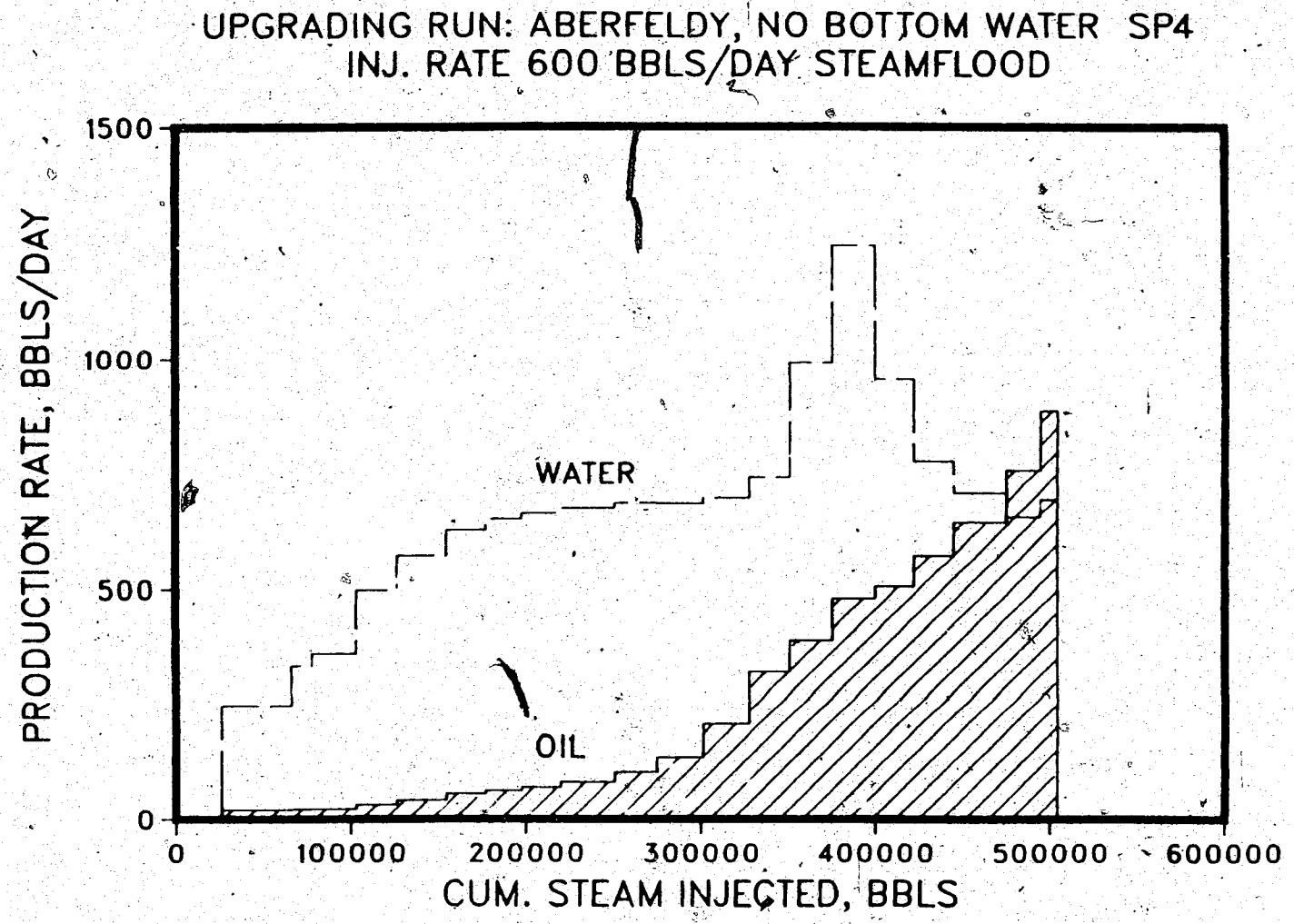

Figure 6.88 Production History of Aberfeldy Run SP4, for Oil Thermal Upgrading

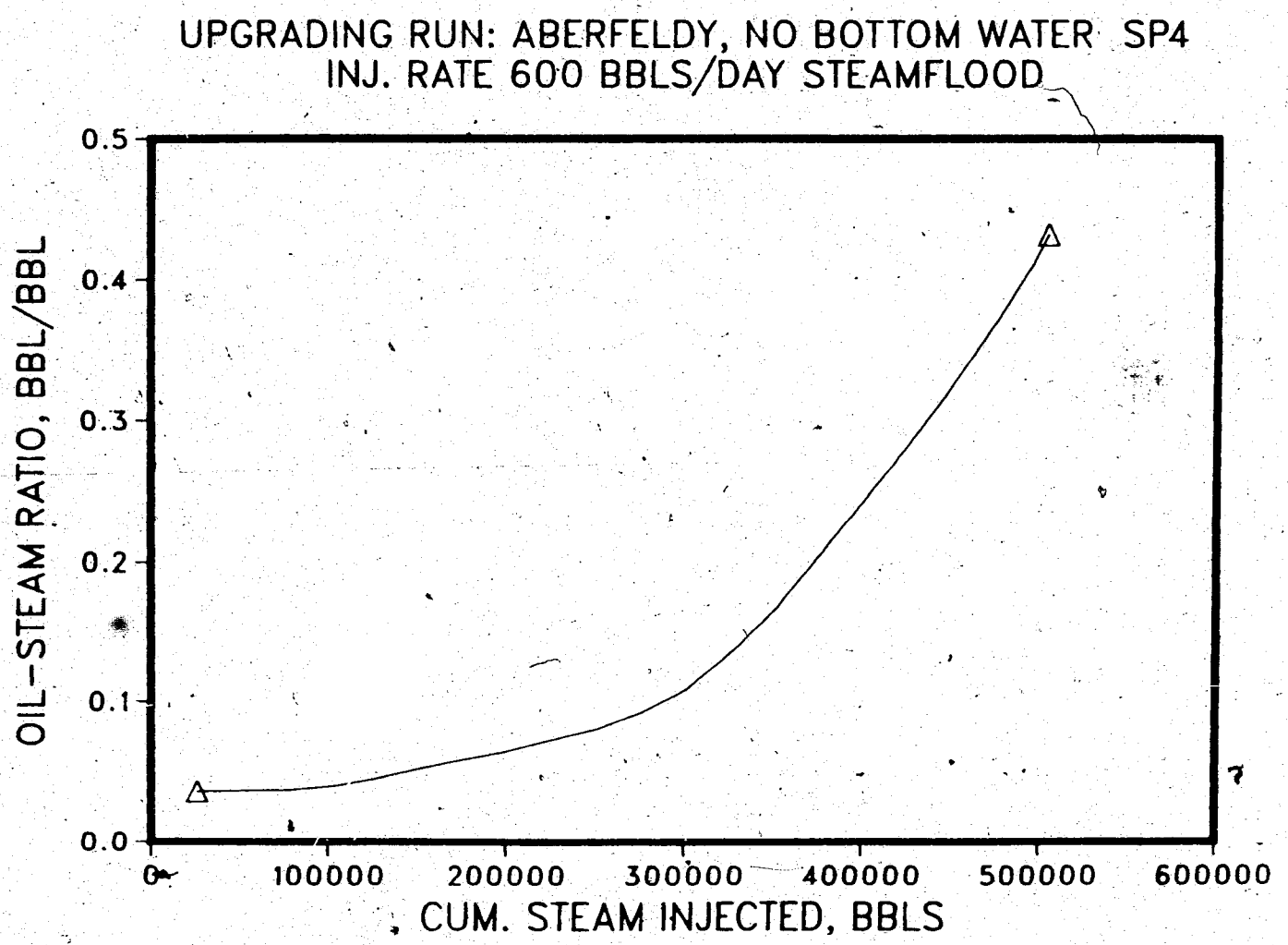

Figure 6.89 Oil-Steam Ratio of Aberfeldy Run SP4, for Oil Thermal Upgrading

being applied as diverting or blocking agents, with limited success. In the present work, a foam is considered to be a gas (steam) permeability reducing agent, plus a viscous material, the viscosity of which is shear-dependent. The foam model was discusssed in Chapter IV. Table 6.9 gives the results for a run, comparable to the base run (Table 6.6), in which foam was assumed to be injected. The production history and the oil-steam ratio plots are given in Figs. 6.90 and 6.91. It is seen that foam injection leads to an increase in oil recovery as well as oil-steam ratio, these being 13.69% and 0.453, respectively, as compared to 12.47% and 0.413 for the base run. The increase is not large, considering the additional expense of foam injection. Temperature and saturation profiles show that the foam did divert the steam into the lower part of the formation, where a considerable steam saturation developed. The representation of foam in this model is not rigorous. Very little useable and consistent data are available for high temperature foams. Quite apart from that, the inclusion of a foam breakdown temperature in the simulator limits the range of effectivenes of a foam injected with steam.

Effect of Gas Injection on Cyclic Steaming Response

The use of an additive gas with steam has been suggested for cyclic steaming operations. The injected gas may consist of natural gas, carbon dioxide, or a mixture of carbon dioxide and nitrogen. One long run was carried out to simulate gas injection following steam injection, for six cycles. In this simulation Cold Lake data were used with a formation thickness of 158 ft. The K-values were a function of pressure and temperature. Steam was injected at a rate of 550 B/D for 45 days, following which natural gas was injected at a rate of 500 Mscf/day for 5 days, before putting the well on production. This was repeated for each of the six cycles. The production history for the six cycles is shown in Fig. 6.92. The overall oil-steam ratio was 0.127, which is quite low compared to typical values in Cold Lake, without the use of a gas. It can be said that gas injection with steam does not appear to lead to a significant increase in oil-steam ratio.

Table 6.9
FOAM RUN: ABERFELDY (NO BOTTOM WATER) SP2
INJ. RATE 600 BBLS/DAY STEAMFLOOD

Legend:

T : Time, Days
OPR : Oil Production Rate, Bbls/Day
WPR : Water Production Rate, Bbls/Day
WOR : Cumulative Water–Oil Ratio, Bbl/Bbl
CSI : Cumulative Steam Injected, 10^5 Bbls
ORec : Oil Recovery, %
OSR : Cumulative Oil–Steam Ratio, Bbl/Bbl

T	OPR	WPR	WOR	CSI	ORec	OSR
5	19.6	28	14.50	0.03	0.01	0.032
44	19.4	249	12.80	0.26	0.05	0.032
90	20.2	301	14.90	0.54	0.11	0.033
129	21.6	364	16.90	0.78	0.15	0.033
172	30.5	506	16.60	1.03	0.23	0.037
214	40.1	586	14.60	1.28	0.32	0.041
252	50.8	630	12.40	1.51	0.43	0.047
293	57.1	657	11.50	1.76	0.56	0.053
330	64.1	671	10.50	1.98	0.69	0.059
369	74.0	682	9.21	2.21	0.86	0.065
412	90.5	692	7.65	2.47	1.07	0.072
458	123.0	691	5.59	2.75	1.37	0.083
502	189.0	704	3.73	3.01	1.78	0.099
546	293.0	751	2.56	3.27	2.45	0.125
586	353.0	988	2.80	3.39	3.51	0.152
626	450.0	1292	2.87	3.75	4.17	0.186
667	522.0	1044	2.00	4.00	5.37	0.224
702	634.0	779	1.23	4.21	6.58	0.262
742	765.0	690	0.90	4.45	8.27	0.311
792	872.0	717	0.82	4.75	10.71	0.377
821	988.0	792	0.80	4.93	12.36	0.420
842	916.0	634	0.69	5.05	13.69	0.453

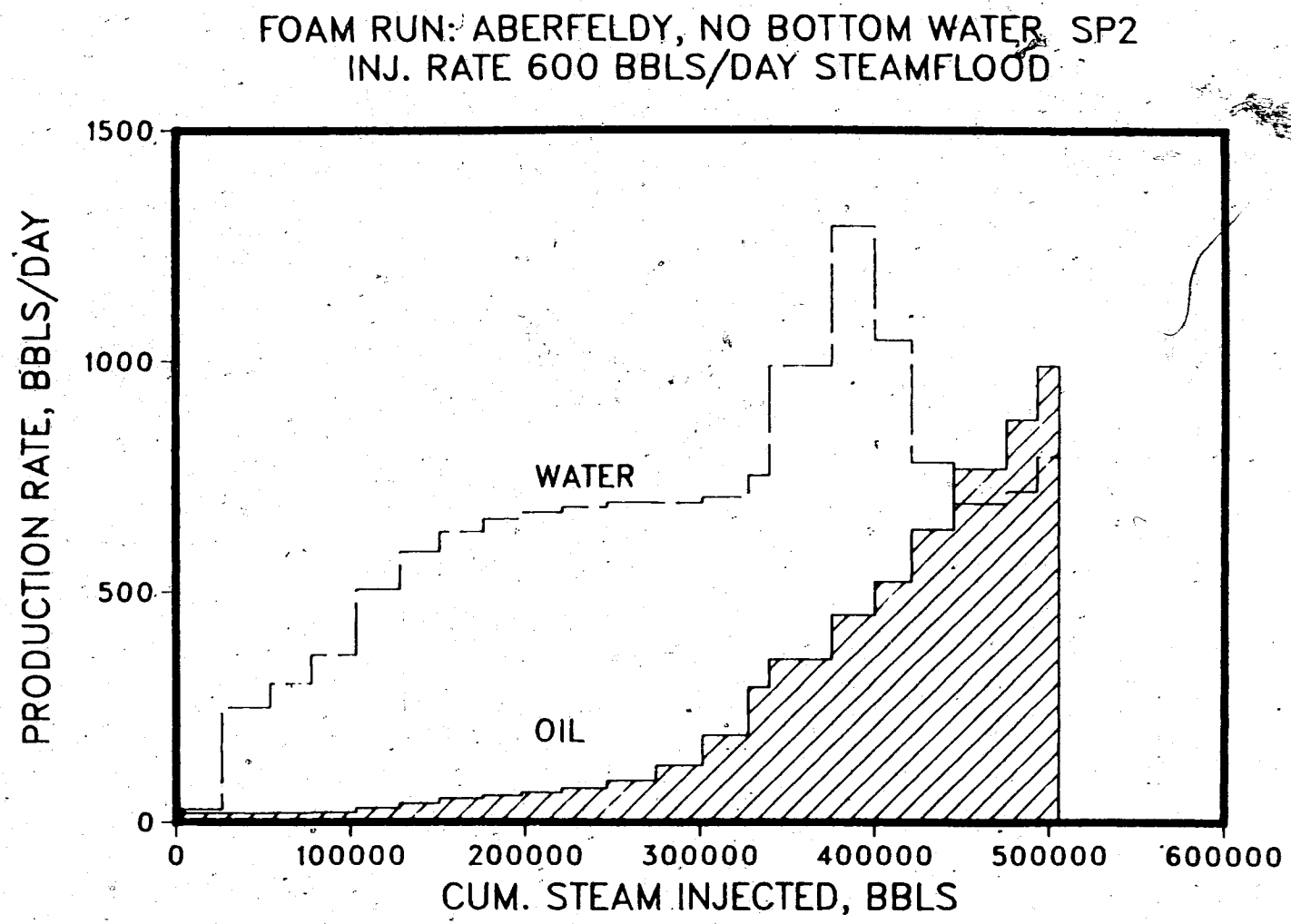

Figure 6.90 Production History of Aberfeldy Run SP2, for Steam Foam Injection

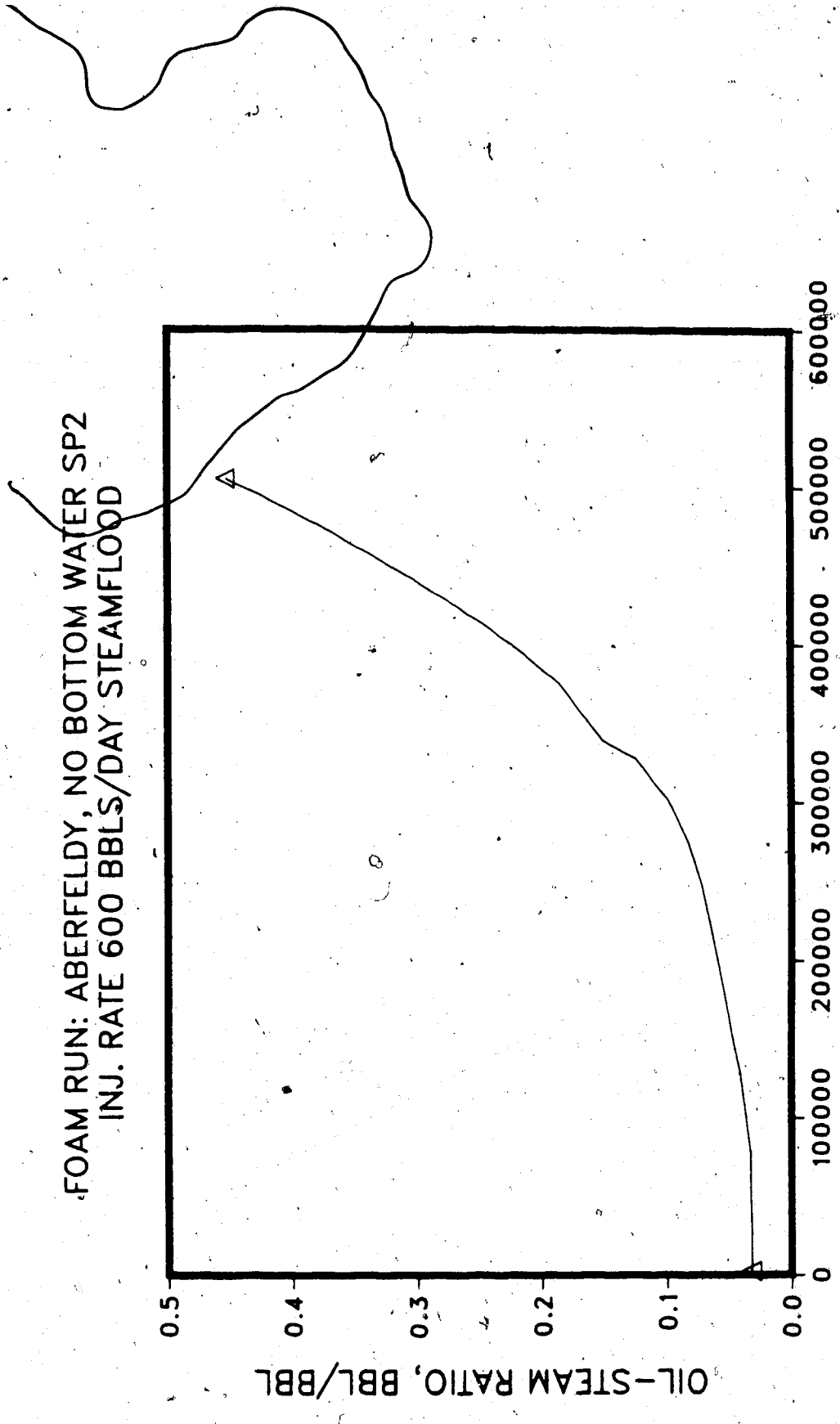

Figure 6.91 - Oil-Steam Ratio of Aberfeldy Run SP2, for Steam Foam Injection

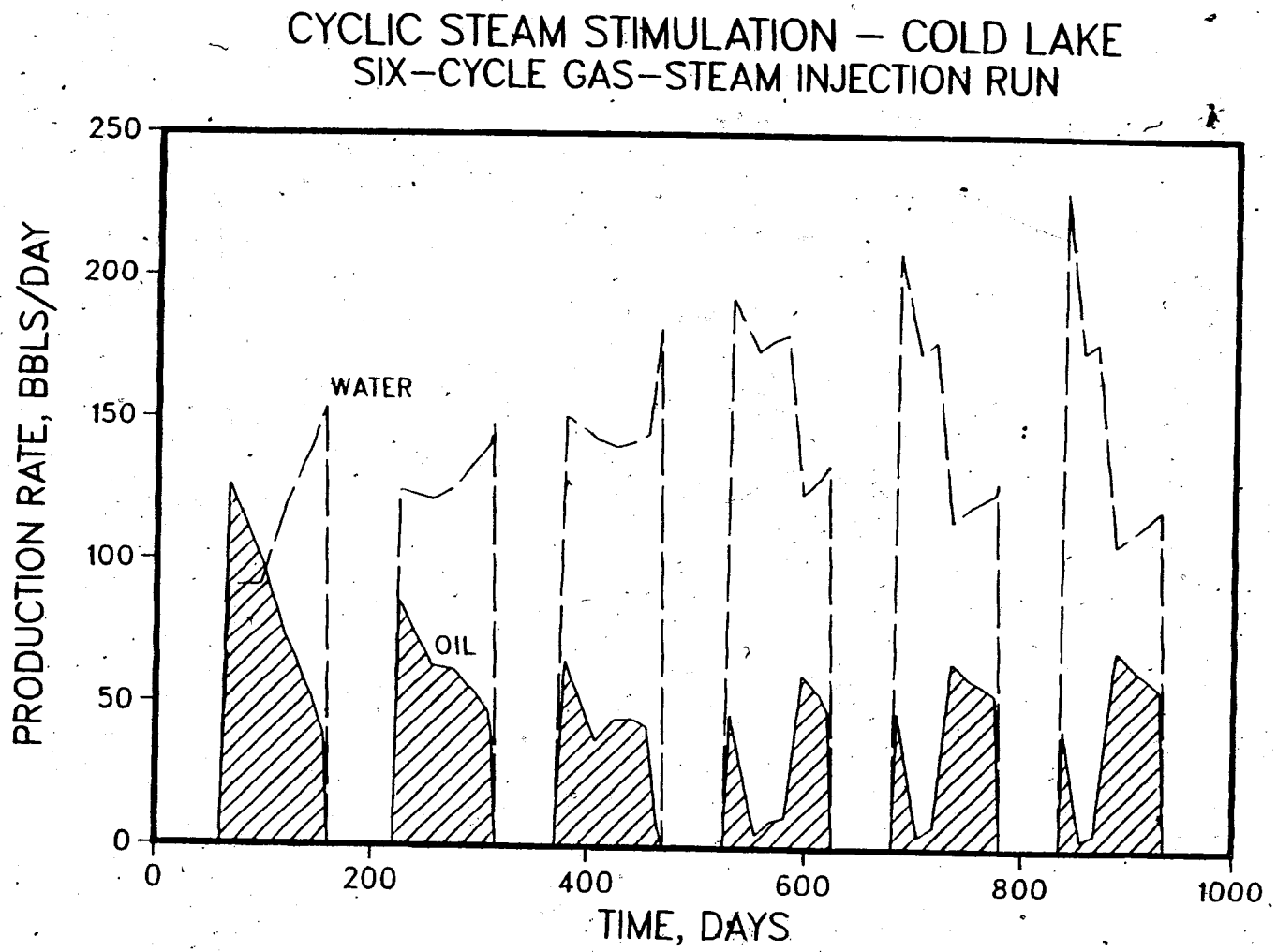

Figure 6.92 Production History of Six-Cycle Gas-Steam Injection Simulation for Cold Lake Reservoir.

Injection of gas following steam imparts additional production energy to the formation, which helps in oil production. It should be noted that the use of an additive gas has been tested over the years in Cold Lake. It has been found to be uneconomical, and is currently used only in special circumstances.

Steam Injection Using Partial Penetration

When bottom water is present, there may be some merit in completing injection and/or production wells partially into the formation. In classical reservoir engineering, partial penetration has been considered for special situations. Flow under partial penetration is a combination of radial and spherical flow. The latter is undesirable, unless special conditions necessitate that. In steam injection - cyclic and drive - the situation is complicated by heat injection. In this study, several runs were carried out to examine the effect of partial penetration on cyclic steaming and steamflooding response. Results of two runs are discussed below.

Run ABRS1B employs partial penetration in the absence of bottom water, and is comparable to Run ABRS1. Steam is injected over the lower one-half of the formation, while production is from the entire interval. Results for this run are plotted in Figs. 6.44 through 6.46, and are tabulated in Table C.27. It is seen that the oil-steam ratio and the oil recovery in the partial penetration case are lower (0.108 vs. 0.250 and 2.72% vs. 6.25%), at a given time (700 days). This is due to the fact that steam initially heats the lower part of the formation, and the oil viscosity is so high that steam segregation does not become a dominant feature because the oil mobility is too low to promote downward flow. This result is to be expected for a partially penetrating injection well. At long times, however, oil becomes mobile enough to flow downward, and the production rates increase rapidly. For example, the oil recovery at the end of 1100 days is 15.22%.

Figures 6.93 to 6.95, and Table C.28 give the production histories for a three-cycle simulation of the Aberfeldy reservoir, with partial completion (ABC18), when bottom

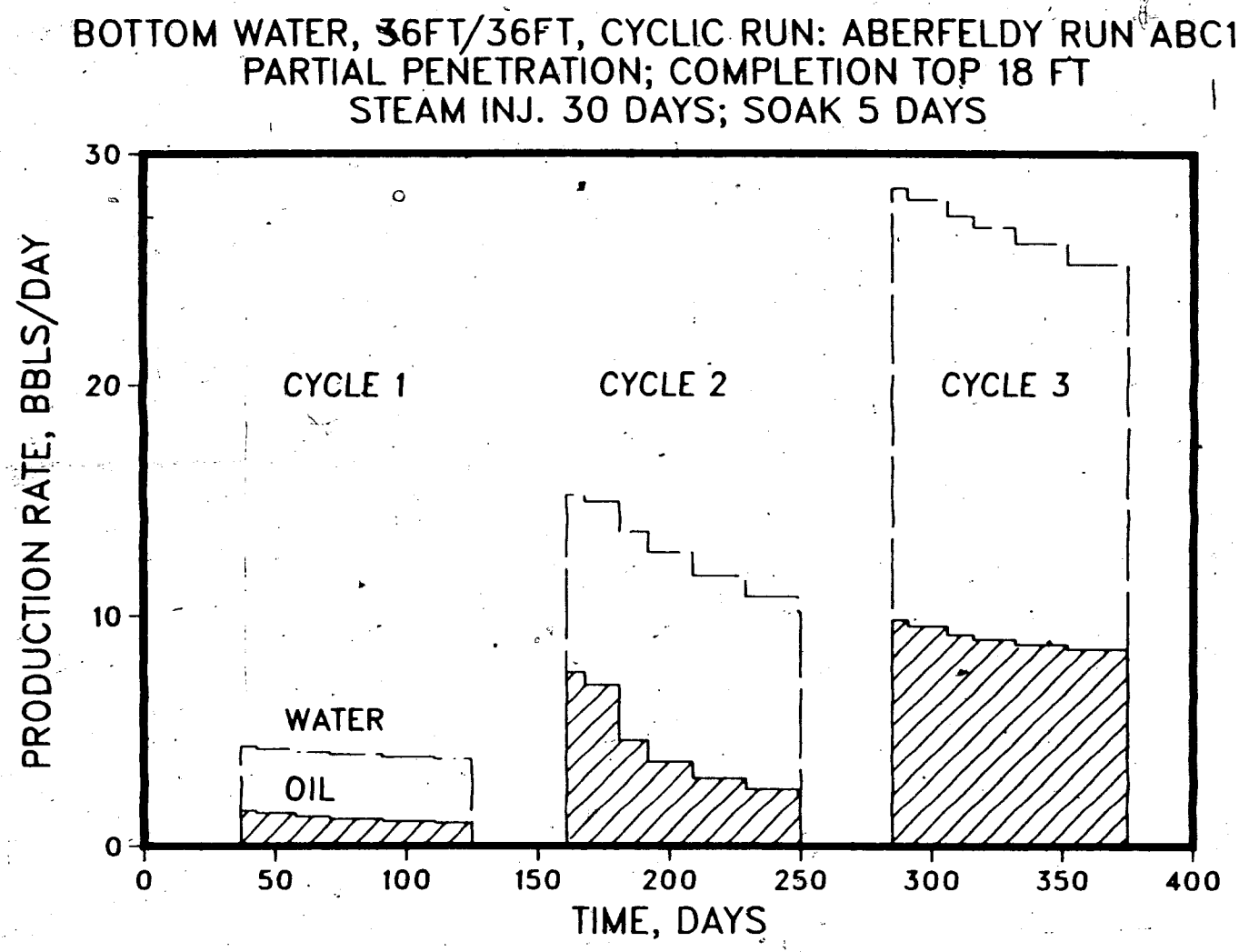

Figure 6.93 Production History of Aberfeldy Cyclic Run ABC18, for Partial Penetration

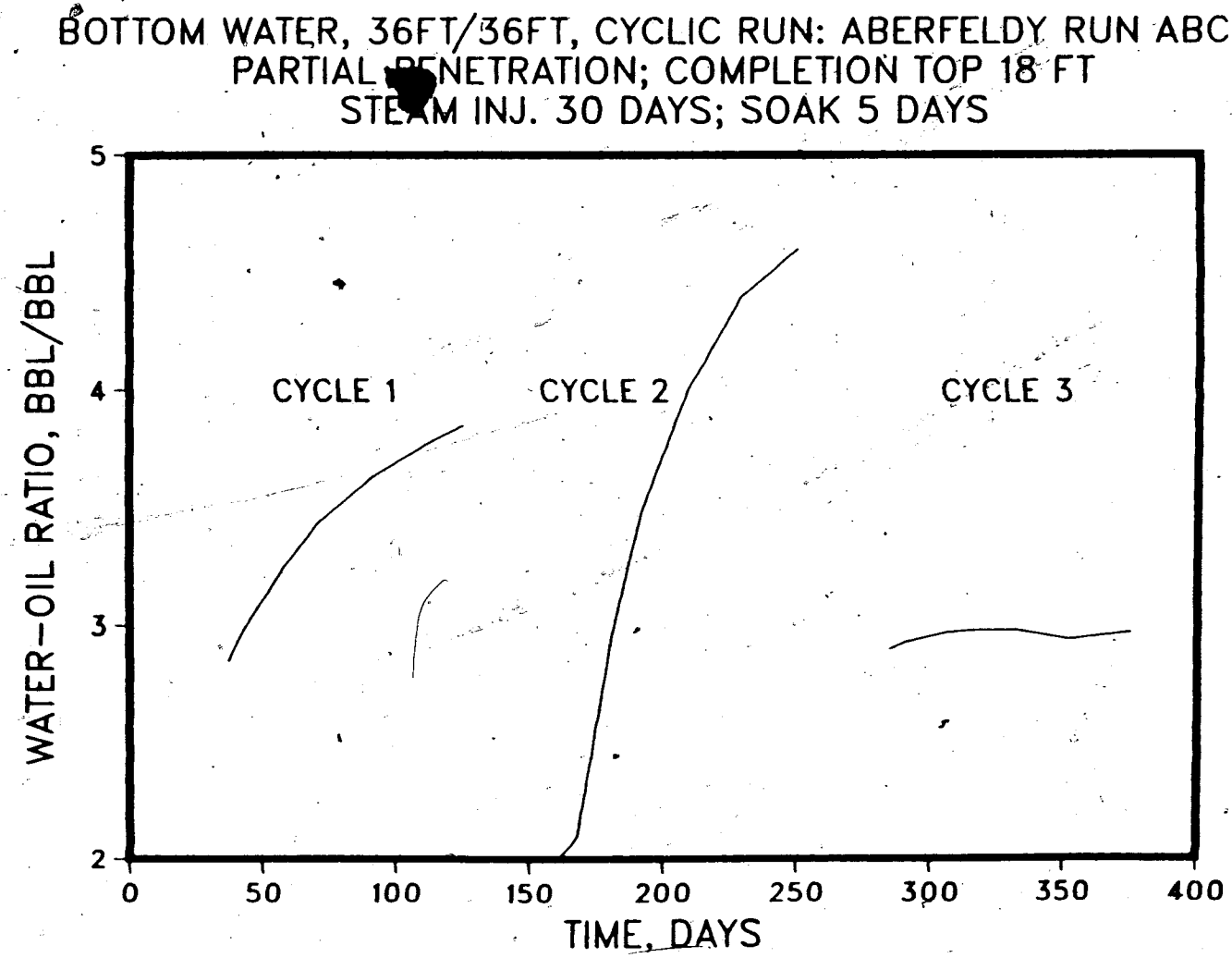

Figure 6.94 Water-Oil Ratio of Aberfeldy Cyclic Run ABC18, for Partial Penetration

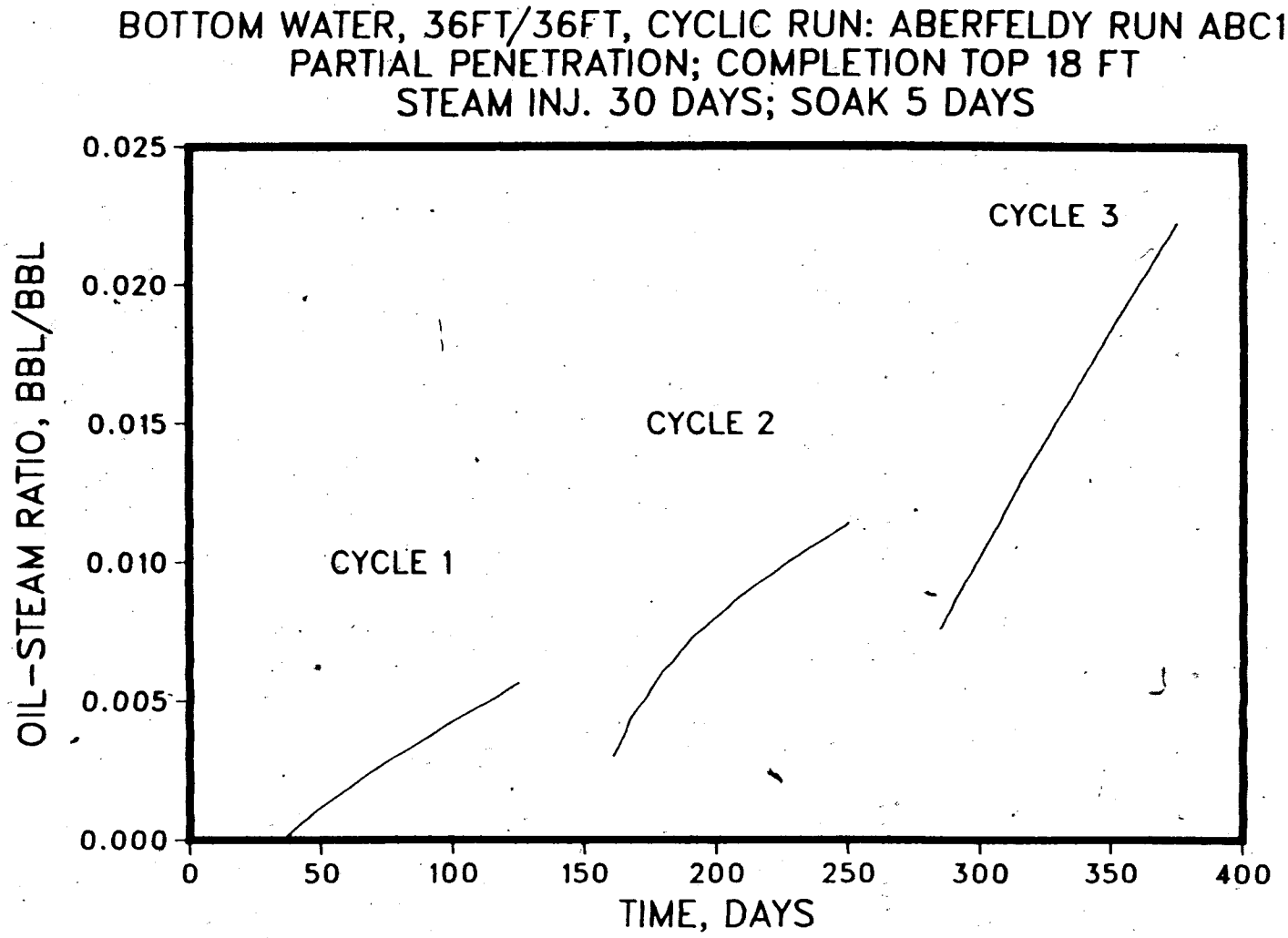

Figure 6.95 Oil-Steam Ratio of Aberfeldy Cyclic Run ABC18, for Partial Penetration

water is present. In this case, steam is injected into the top 18 ft. of the 36 ft. formation, at the base of which there is a water zone, 36 ft. in thickness. The results of this run are comparable to those of Run ABC17. A comparison of all Aberfeldy bottom water cyclic stimulation runs ABC6, 8, 9, 11, and 17 shows that the oil-steam ratio in all cases is higher than that in the case of the partial penetration run. The important difference is that in the full interval completion runs, the water-oil ratios are much higher, e.g. 3 in partial completion vs. 200-300 in full completion. It can be concluded that full interval completion may be practical only if the pumping capacity is large enough, and large volumes of the produced water can be handled.

Partially penetrating cyclic steaming wells do seem to have one advantage: they prevent communication with the bottom water zone, as seen from the low water-oil ratios. The very high water-oil ratios in the case of the full-interval completions in the bottom water situation are due to communication of the perforations with the bottom water zone. On the other hand, the oil production rate in the partial penetration case is very low. Table 6.3(b) shows that the oil production rate improves in succeeding cycles. The water production rates increases also, but the water-oil ratio declines. Possibly, partial penetration oil production would become competitive with the oil production of full-interval completion after many cycles. As such, partial penetration offers an interesting option in cyclic steaming under bottom water situations. Many more simulation studies are needed for fully evaluating partial penetration as an operating strategy in bottom water situations.

Sandface Steam Quality in Thick Formations with Multiple Offtake

General

In steam injection operations - both cyclic steaming and steamflooding - sometimes it is necessary to inject steam into one or more layers of a thick interval, from a single tubing, which is provided with multiple offtakes. In such a case, the bottomhole steam quality and

pressure at each offtake point will vary with time. In some cases, the steam inflow rate into each layer would also vary with time. These changes in steam quality, pressure, and possibly rate with time, at each injection point, are of importance in steam injection processes, especially in steamflooding. Very little field work has been done on this problem. Nothing has been published on the mathematical simulation of wellbore steam flow with multiple offtakes, or steam splitting. In this work, one of the objectives was to develop a mathematical model of steam injection in the wellbore, taking into account the pressure drop due to varying flow regimes, heat loss, and the steam quality. The model considers heat loss to the surrounding media in a rigourous manner.

In the following, first the computed results for steam quality variation with steam injection rate, steam pressure and steam splitting are discussed. Only one case of steam splitting (i.e. taking some of the steam off the tubing at intermediate points) is considered, where one-half of the injected steam is taken off at 1200 ft in a 1500- ft deep well. That is, the formation thickness is taken to be 300 ft. Other steam splitting ratios could have been considered, but it was not done in view of computer time limitations. The results of steam quality and pressure with time were used to carry out a steamflood simulation for the Aberfeldy reservoir conditions. Results for the assumption of a constant steam injection pressure and quality are compared with those for the steam and pressure and quality input from the wellbore simulator.

Table 6.10 lists the well data used in the simulations.

Effect of Steam Injection Rate and Flow Splitting on Steam Quality

Seventy-two runs were carried out for wellbore steam flow, half for no flow splitting, the other half for flow splitting. The results of the runs for bottomhole quality and pressure are summarized in Tables 6.11 and 6.12. The data versus depth are given in Table D.1 through D.24. Selected results are plotted in the following figures.

Table 6.10

CONDITIONS USED FOR WELLBORE HEAT LOSS CALCULATIONS

Pressure at Surface	260.0 psia
Atmospheric Temperature	80.0°F
Grid Points in R-Direction	5
Ratio of Radius of Grid	2.5
Time Elapsed	30.0 days
Thermal Conductivity of Annulas	0.0263
Emissivity of Tubing	0.9000
Density of Annular Fluid	0.0360 lb/ft^3
Tolerance of P	1.00 psia
Type of Flow	tion
Tubing Insulation	No
Type of Annulas Fluid	Gas
Casing Size	10.000 inch
Tubing Size	8.000 inch
Tubing Relative Roughness	0.00023
Depth	1400.0 feet
Reservoir Temperature	108.0°F
Grid Points in Z-Direction	11
Delz	140.0 feet
Deltim	3.0 days
Thermal Conductivity of Cement	0.5500
Emissivity of Casing	0.9000
Viscosity of Annular Fluid	0.0664 lbm/ft-hr
Tolerance of Q	0.010
Borehole Size	12.000 inch
Mass Flow Rate	558000.0 lb/hr
Geothermal Gradient	0.020 °F/ft
Thermal Conductivity of Earth	1.4000
Thermal Diffusivity of Earth	0.9600 ft^2/day
Specific Heat of Annular Fluids	0.2475 Btu/lb-°F
Tolerance of U	0.05

Table: 6.11
WELLBORE STEAM FLOW RUNS SUMMARY
DEPTH 1500 FT: STEAM OFFTAKE AT 1200 FT;
OFFTAKE RATE ONE-HALF FLOW RATE
SURFACE QUALITY 0.80

Legend:
RN : WB RUN NUMBER
T : Time, Days
SR : Steam Rate, Bbls/Day
IP : Inj. Pressure, psia
OR : Offtake Rate, Bbls/Day
SQ : Steam Quality, Frac at 1500 FT
SP : Steam Pressure, psia at 1500 FT

RN	T	SR	IP	OR	SQ	SP
1	100	600	1500	300	0.3298	1799.85
2	300	600	1500	300	0.3454	1800.05
3	500	600	1500	300	0.3458	1800.02
4	700	600	1500	300	0.3458	1800.02
5	900	600	1500	300	0.3458	1800.02
6	1100	600	1500	300	0.3458	1800.02
7	100	1200	1500	600	0.5674	1731.56
8	300	1200	1500	600	0.5751	1731.06
9	500	1200	1500	600	0.5753	1731.05
10	700	1200	1500	600	0.5753	1731.05
11	900	1200	1500	600	0.5753	1731.05
12	1100	1200	1500	600	0.5753	1731.05
13	100	1800	1500	900	0.6453	1699.40
14	300	1800	1500	900	0.6505	1698.93
15	500	1800	1500	900	0.6506	1698.92
16	700	1800	1500	900	0.6506	1698.92
17	900	1800	1500	900	0.6506	1698.92
18	1100	1800	1500	900	0.6506	1698.92
19	100	600	1500	0	0.4779	1774.34
20	300	600	1500	0	0.4897	1773.28
21	500	600	1500	0	0.4900	1773.25
22	700	600	1500	0	0.4900	1773.25
23	900	600	1500	0	0.4900	1773.25
24	1100	600	1500	0	0.4900	1773.25
25	100	1200	1500	0	0.6402	1707.33
26	300	1200	1500	0	0.6460	1706.96
27	500	1200	1500	0	0.6461	1706.95
28	700	1200	1500	0	0.6461	1706.95
29	900	1200	1500	0	0.6461	1706.95
30	1100	1200	1500	0	0.6461	1706.95
31	100	1800	1500	0	0.6934	1679.69
32	300	1800	1500	0	0.6972	1679.49
33	500	1800	1500	0	0.6973	1679.49
34	700	1800	1500	0	0.6973	1679.49
35	900	1800	1500	0	0.6973	1679.49
36	1100	1800	1500	0	0.6973	1679.49

Table: 6.12
WELLBORE STEAM FLOW RUNS SUMMARY
DEPTH 1500 FT: STEAM OFFTAKE AT 1200 FT;
OFFTAKE RATE ONE-HALF FLOW RATE
SURFACE QUALITY 0.80

Legend:
RN : WB RUN NUMBER
T : Time, Days
SR : Steam Rate, Bbls/Day
IP : Inj. Pressure, psia
OR : Offtake Rate, Bbls/Day
SQ : Steam Quality, Frac at 1500 FT
SP : Steam Pressure, psia at 1500 FT

RN	T	SR	IP	OR	SQ	SP
37	100	600	750	300	0.4603	1000.17
38	300	600	750	300	0.4714	999.31
39	500	600	750	300	0.4716	999.29
40	700	600	750	300	0.4716	999.29
41	900	600	750	300	0.4716	999.29
42	1100	600	750	300	0.4716	999.29
43	100	1200	750	600	0.6322	936.22
44	300	1200	750	600	0.6375	935.93
45	500	1200	750	600	0.6376	935.92
46	700	1200	750	600	0.6376	935.92
47	900	1200	750	600	0.6376	935.92
48	1100	1200	750	600	0.6376	935.92
49	100	1800	750	900	0.6878	910.38
50	300	1800	750	900	0.6913	910.24
51	500	1800	750	900	0.6914	910.23
52	700	1800	750	900	0.6914	910.23
53	900	1800	750	900	0.6914	910.23
54	1100	1800	750	900	0.6914	910.23
55	100	600	750	0	0.5672	970.33
56	300	600	750	0	0.5753	969.68
57	500	600	750	0	0.5755	969.67
58	700	600	750	0	0.5755	969.67
59	900	600	750	0	0.5755	969.67
60	1100	600	750	0	0.5755	969.67
61	100	1200	750	0	0.6838	915.68
62	300	1200	750	0	0.6878	915.49
63	500	1200	750	0	0.6879	915.49
64	700	1200	750	0	0.6879	915.49
65	900	1200	750	0	0.6879	915.49
66	1100	1200	750	0	0.6879	915.49
67	100	1800	750	0	0.7218	895.10
68	300	1800	750	0	0.7244	895.00
69	500	1800	750	0	0.7244	895.00
70	700	1800	750	0	0.7244	895.00
71	900	1800	750	0	0.7244	895.00
72	1100	1800	750	0	0.7244	895.00

Figures 6.96 through 6.101 show steam quality versus depth, for injection time of 100, 300, 500, 700, 900, and 1100 days, respectively. In each figure, quality is plotted for steam injection rates of 600, 1200, and 1800 B/D; for each rate there are two branches, one for zero offtake, and the other one for one-half steam offtake at 1200 ft. It is seen that the steam quality below the point of offtake is considerably lower than that in the absence of offtake. Furthermore, the relative quality drop becomes smaller as the steam injection rate increases. The plots for different times show that this trend persists, however, steam quality at all points increases with time. The reason for this behaviour is that when steam is taken off at a particular point in the wellbore, the remaining steam flows at a reduced velocity, with approximately the same temperature. Thus the heat loss rate, which is dependent on temperature is nearly the same, and it now acts on a reduced steam flow rate, resulting in a considerable quality drop. The situation is more complex, because steam pressure is also changing, causing a change in temperature, but this effect is not as important as the change in the steam flow, i.e. heat flow rate. It can be expected that at higher steam flow rates, the relative heat flow is increased, and hence the above effects are less important, as the curves in Fig. 6.96 through 6.101 show. It can be concluded that the steam quality is likely to drop below the point of offtake in a multiple layer steam injection well. The amount of drop will depend on the steam injection rate, the steam offtake rate, and steam pressure. Other variables of importance not examined in this work are: the type of well completion, heat loss reduction technique used, characteristics of the surrounding rocks, and the effect of a fluid level in the wellbore, which would also tend to restrict the uniform distribution of steam over the injection interval.

Effect of Steam Injection Rate and Flow Splitting on Steam Pressure

Figures 6.102 through 6.107 show graphs of steam pressure versus depth, for times of 100, 300, 500, 700, 900 and 1100 days, respectively. In each case, three curves are shown for steam injection rates of 600, 1200 and 1800 B/D. Each curve has two branches,

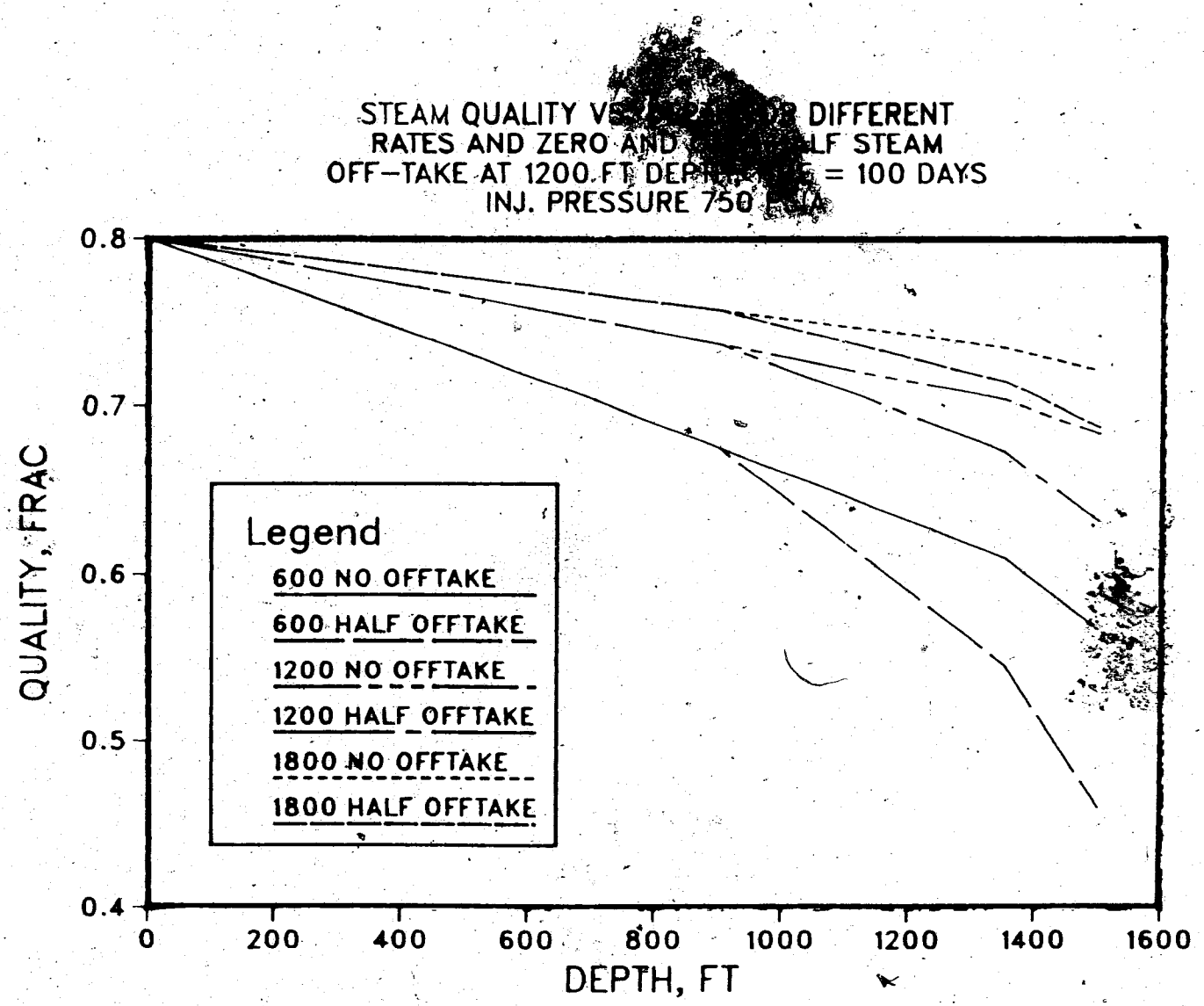

Figure 6.96 Wellbore Steam Quality for Zero and One-Half Offtakes (Time = 100 days)

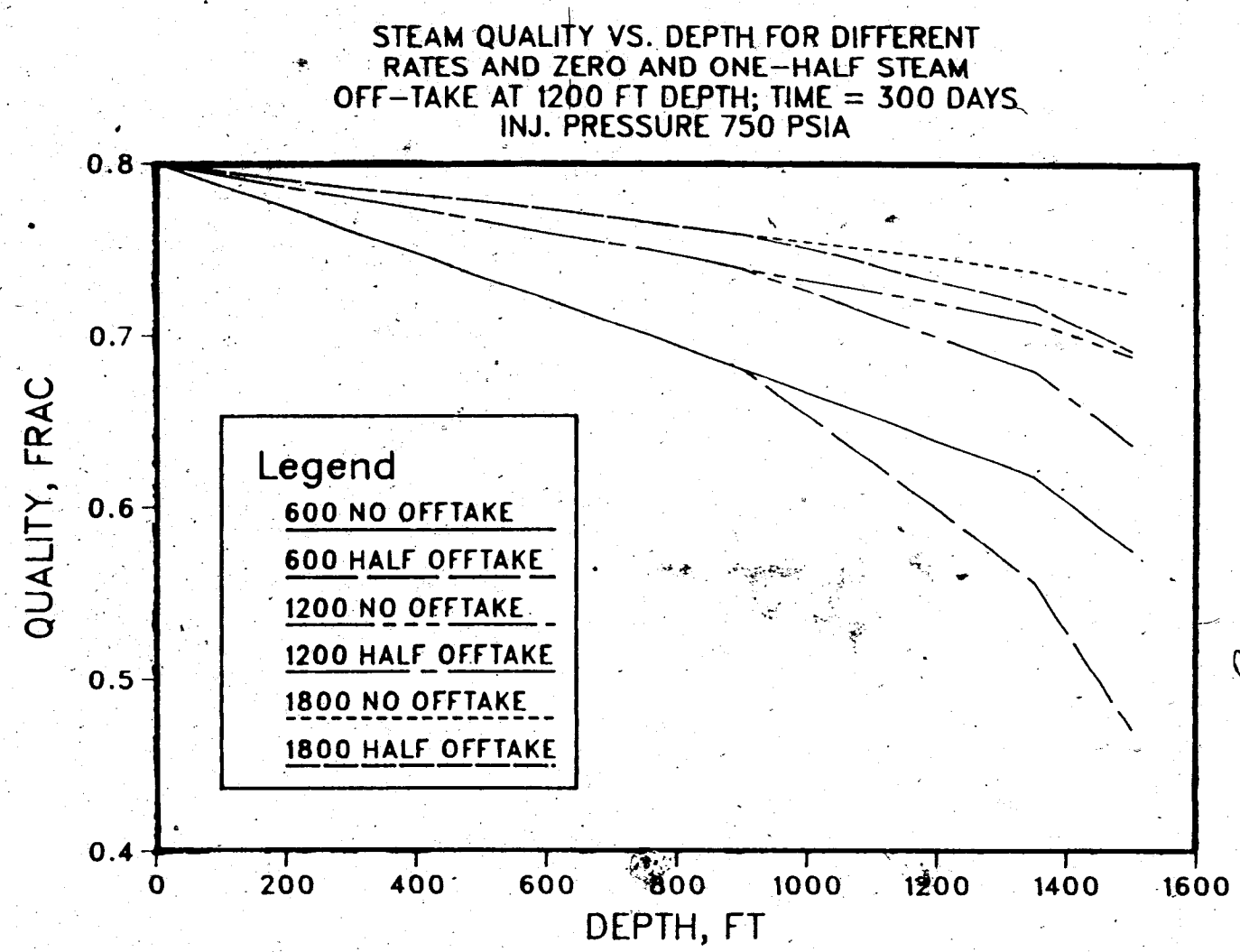

Figure 6.97 Wellbore Steam Quality for Zero and One-Half Offtakes (Time = 300 days)

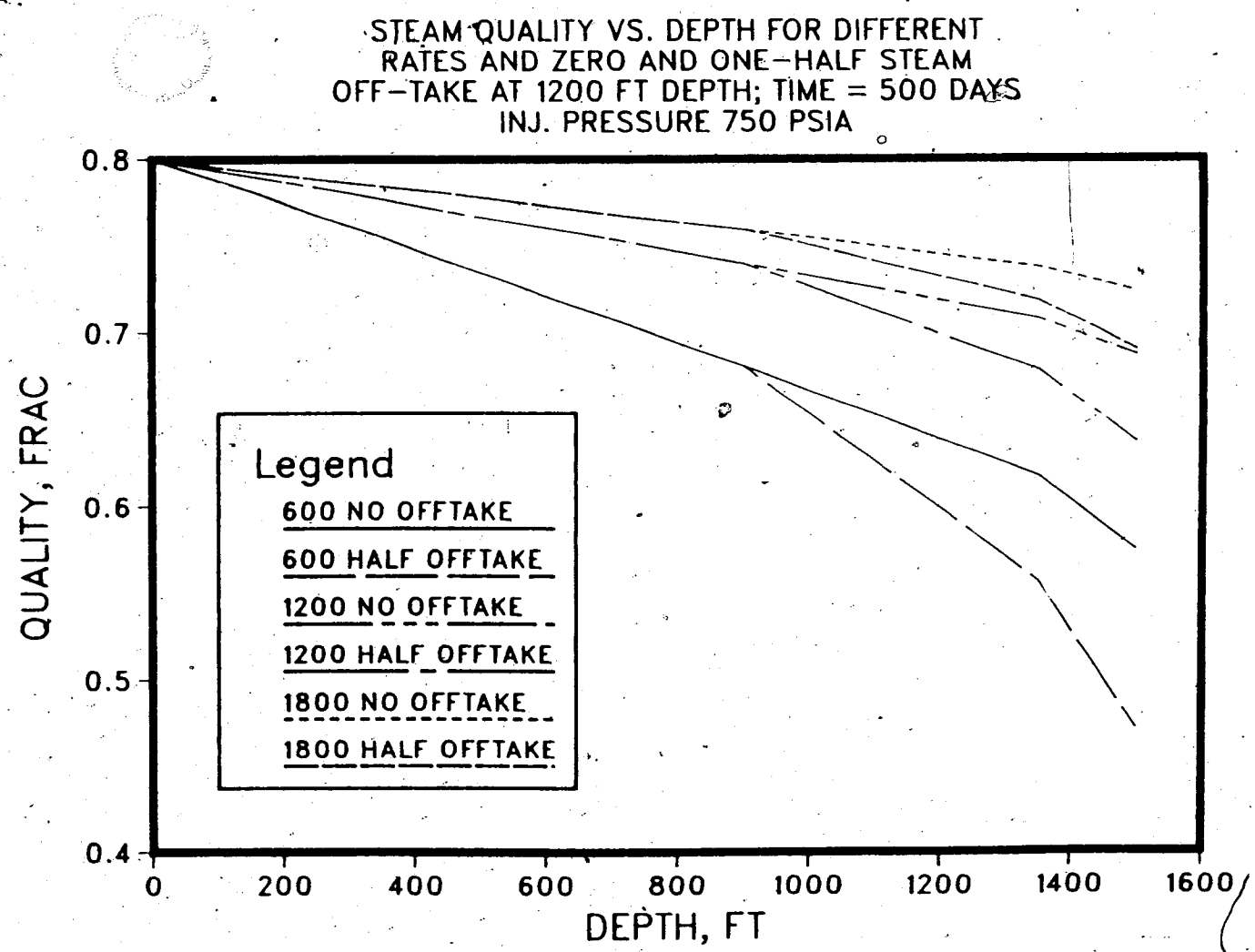

Figure 6.98 Wellbore Steam Quality for Zero and One-Half Offtakes (Time = 500 days)

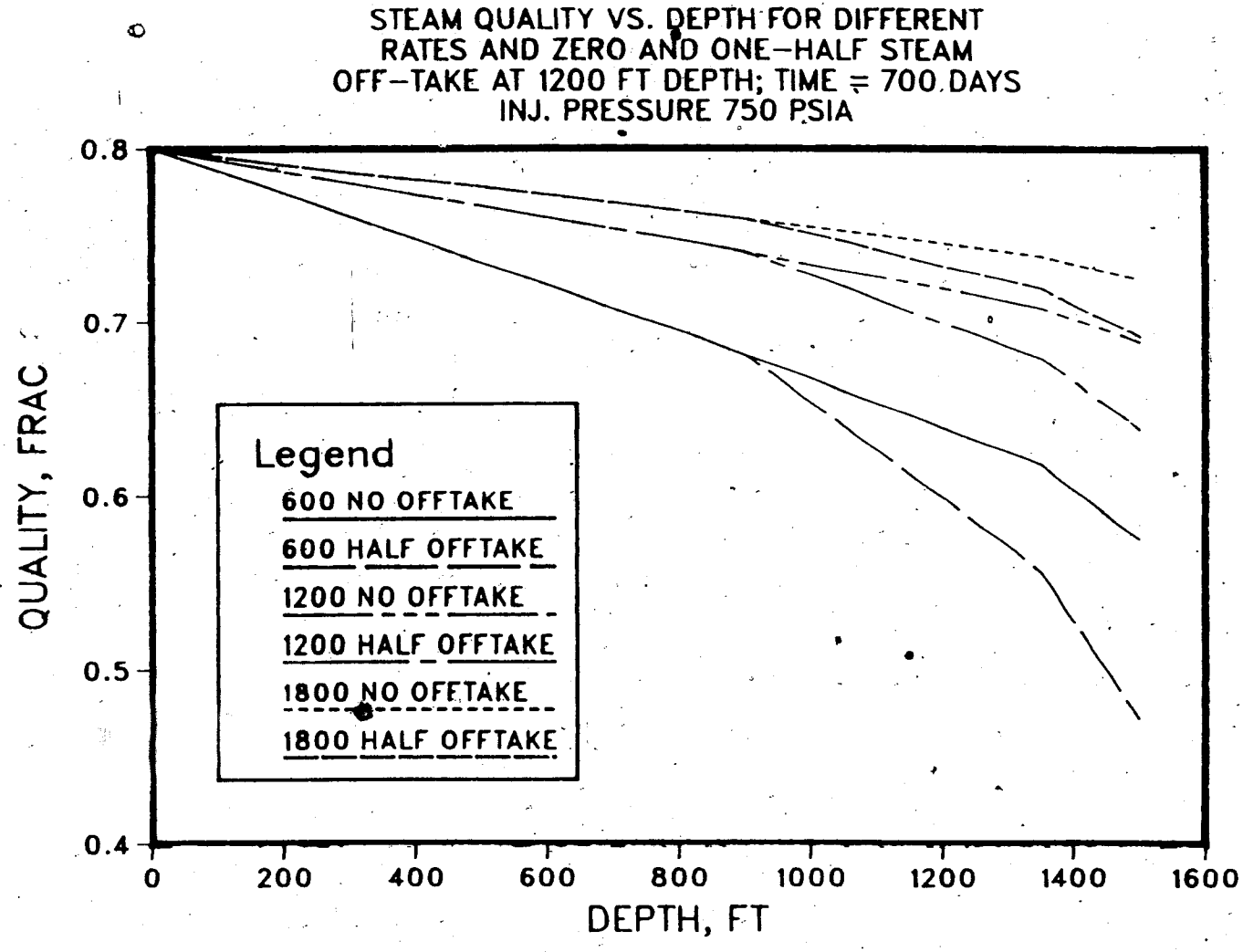

Figure 6.99 Wellbore Steam Quality for Zero and One-Half Offtake (Time = 700 days)

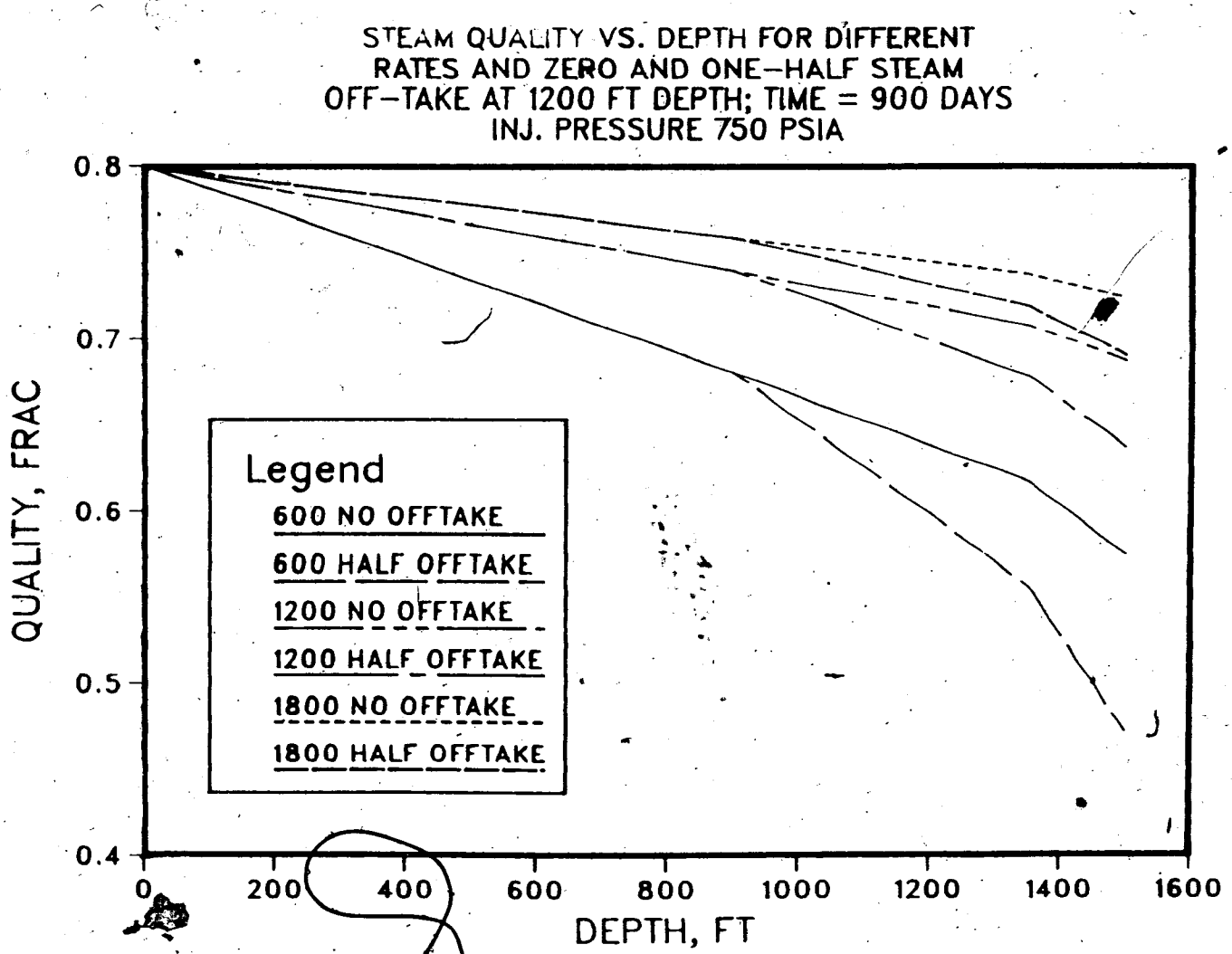

Figure 6.100 Wellbore Steam Quality for Zero and One-Half Offtakes (Time = 900 days)

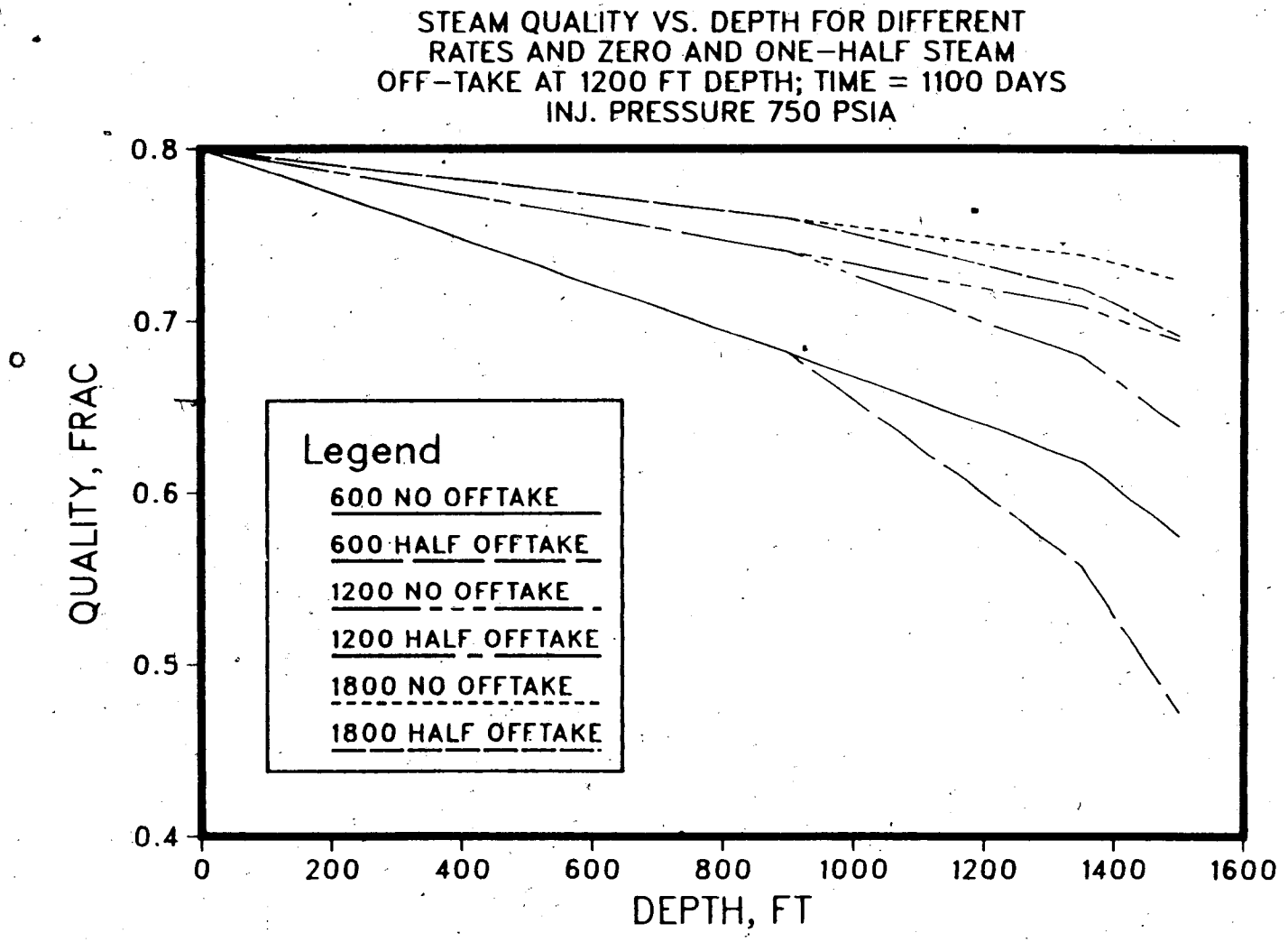

Figure 6.101 Wellbore Steam Quality for Zero and One-Half Offtakes (Time = 1100 days)

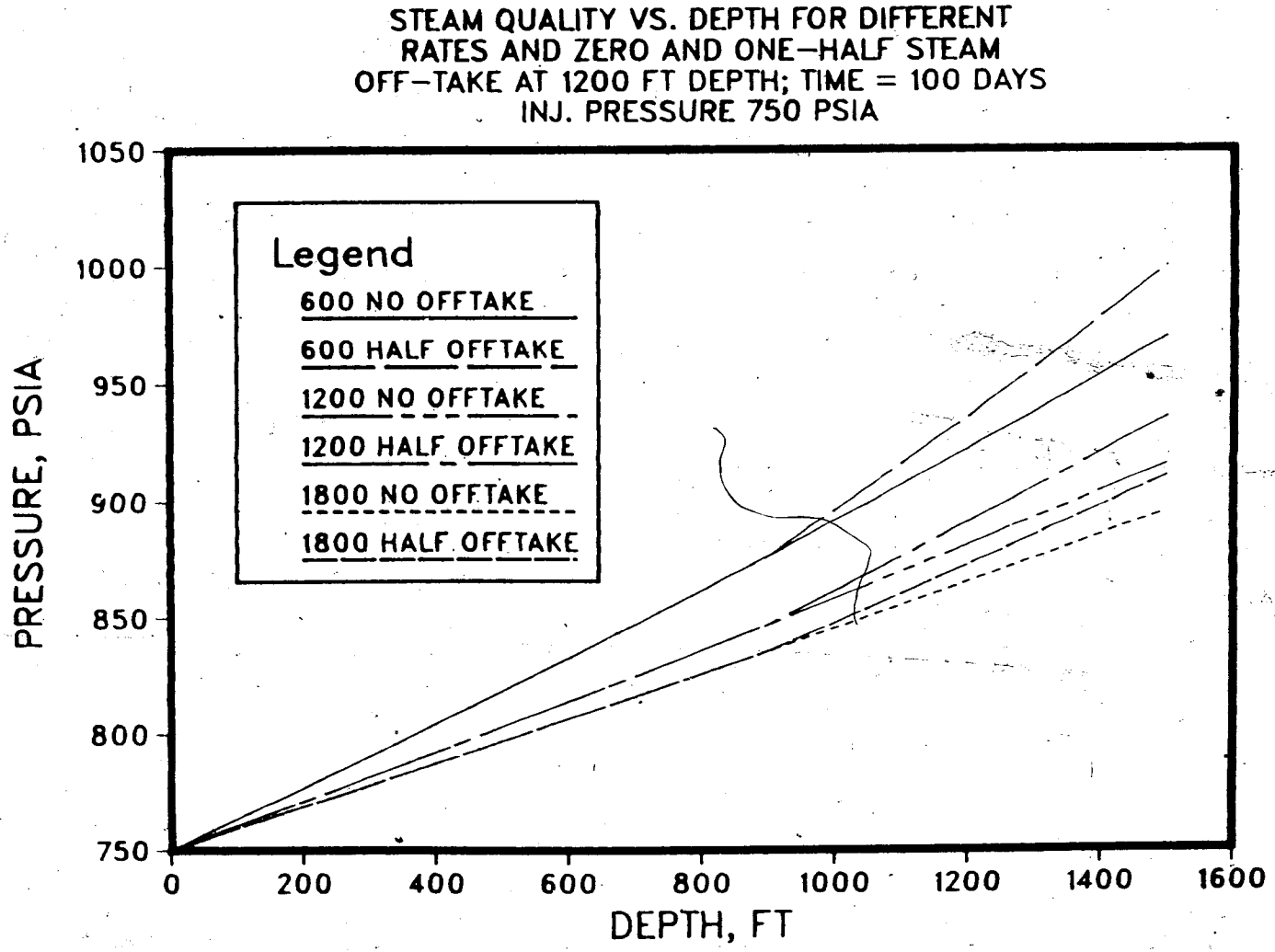

Figure 6.102 Wellbore Steam Pressure for Zero and One-Half Offtakes (Time = 100 days)

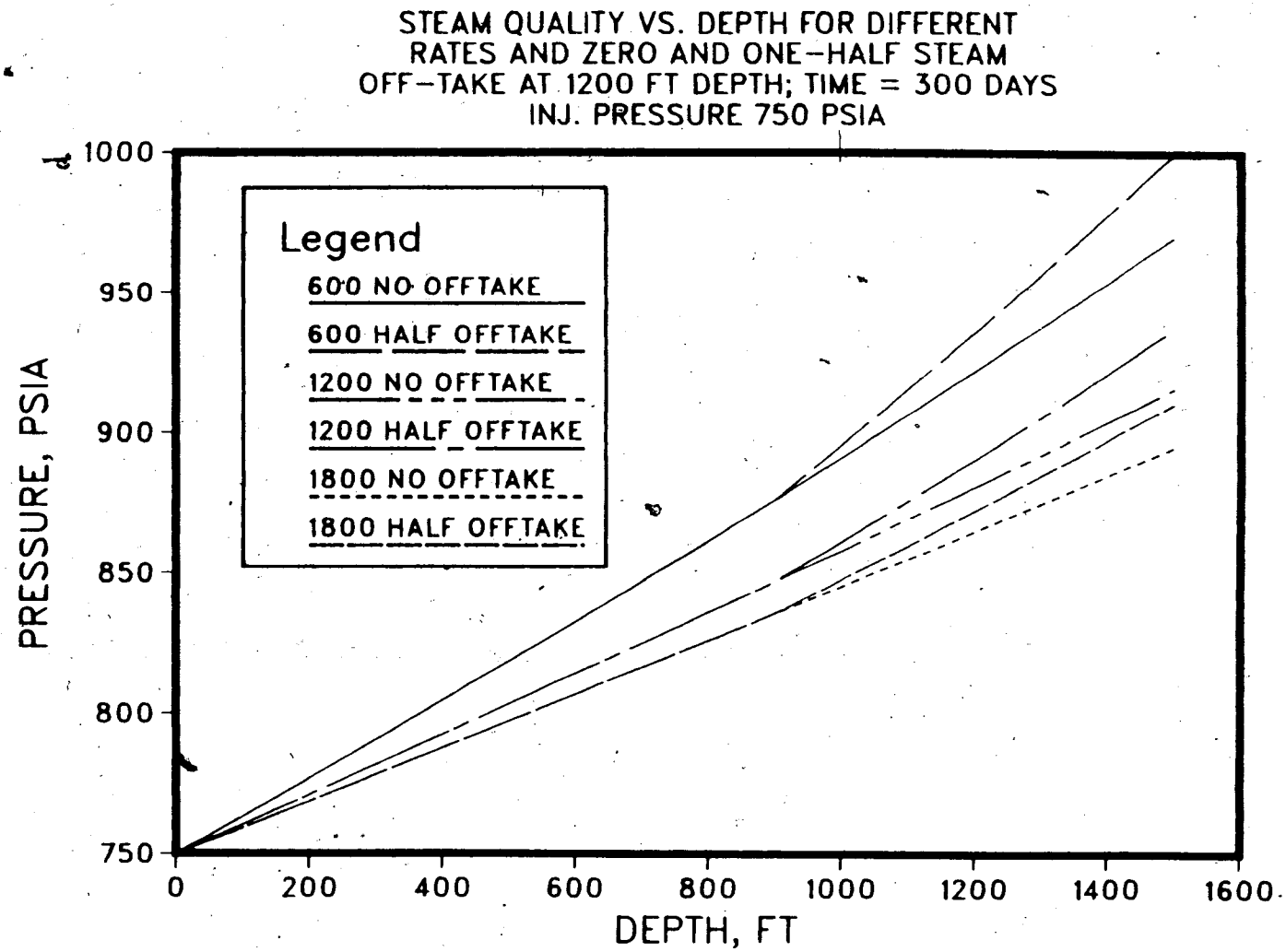

Figure 6.103 Wellbore Steam Pressure for Zero and One-Half Offtakes (Time = 300 days)

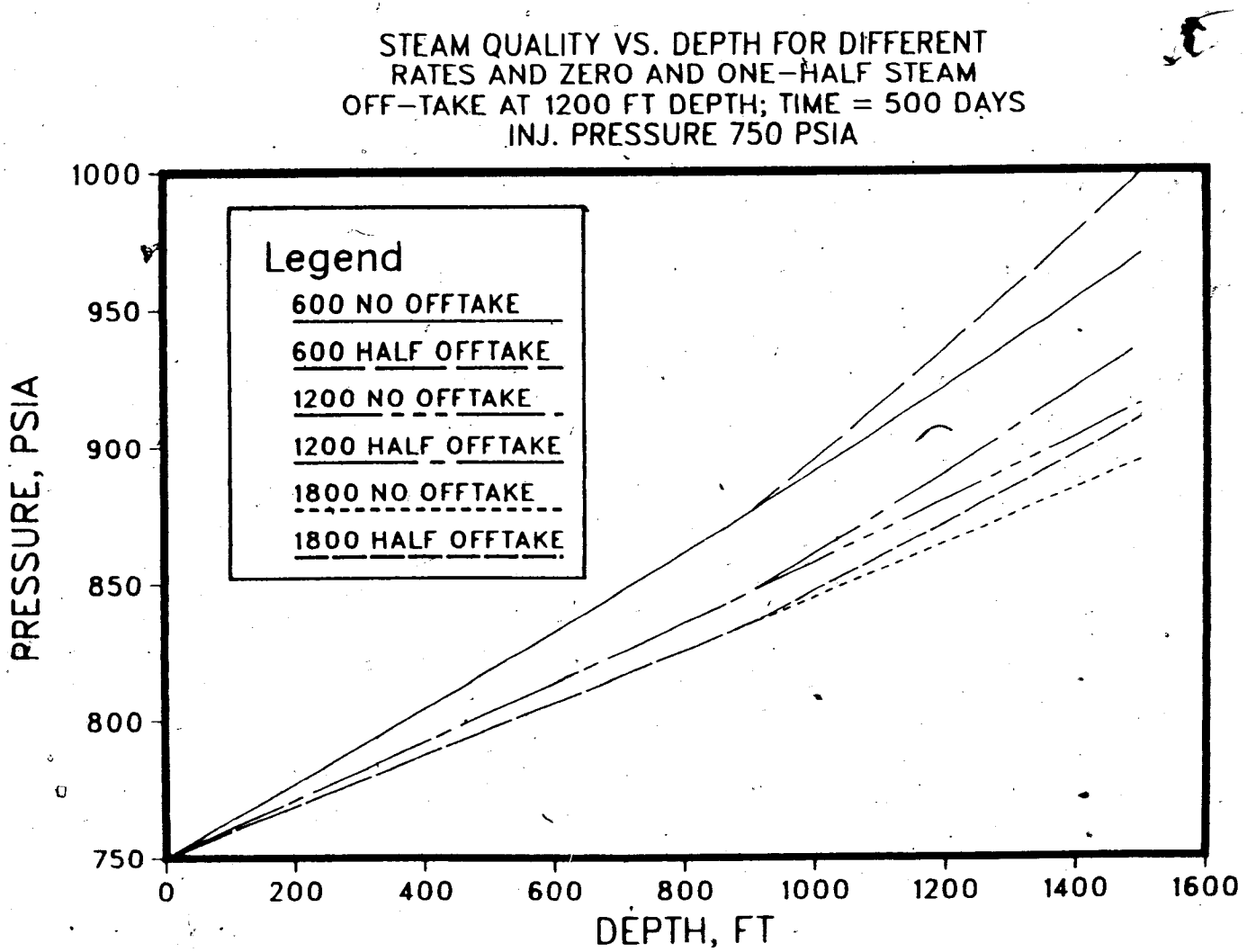

Figure 6.104 Wellbore Steam Pressure for Zero and One-Half Offtakes (Time = 500 days)

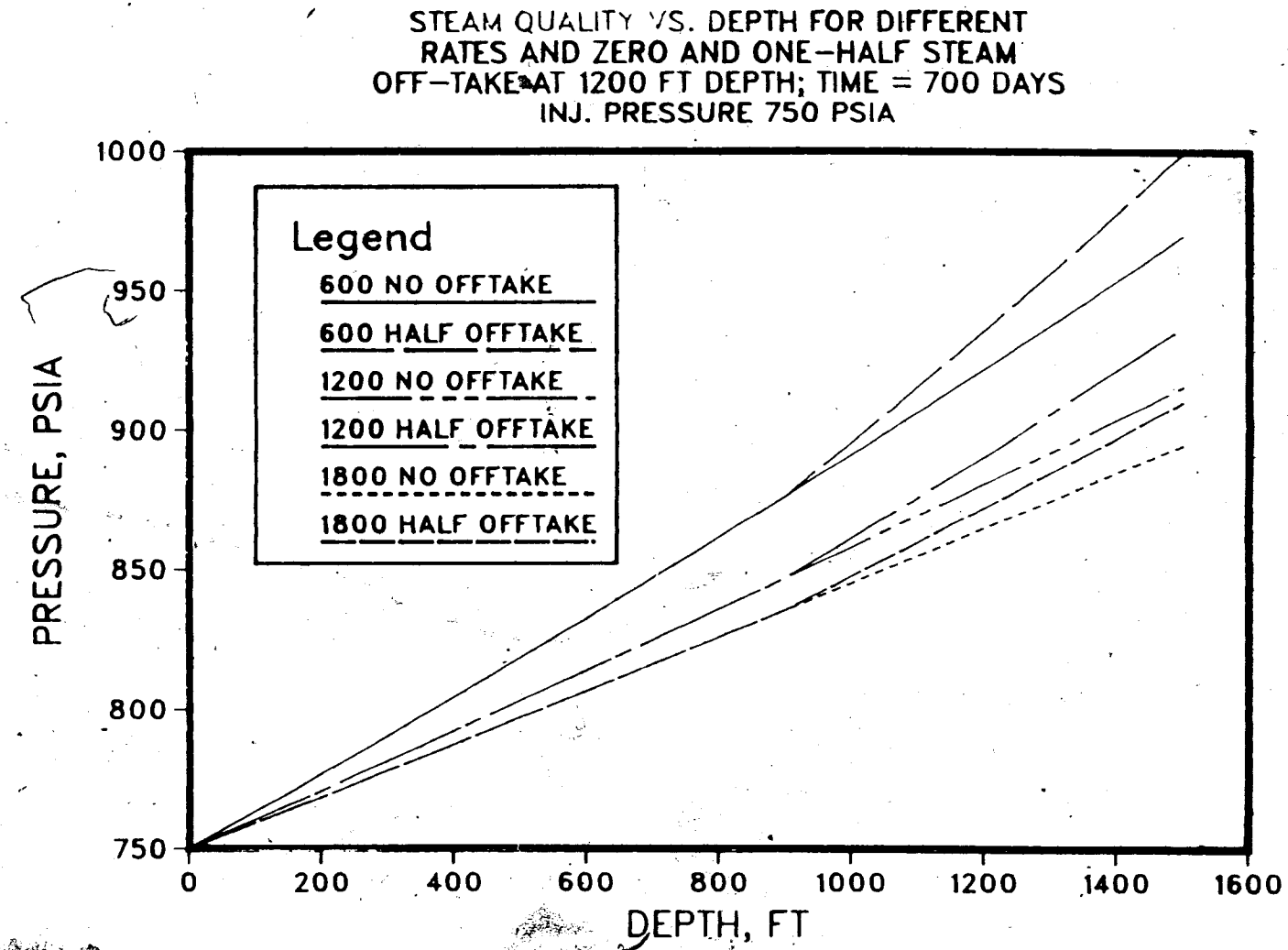

Figure 6.105 Wellbore Steam Pressure for Zero and One-Half Offtakes (Time = 700 days)

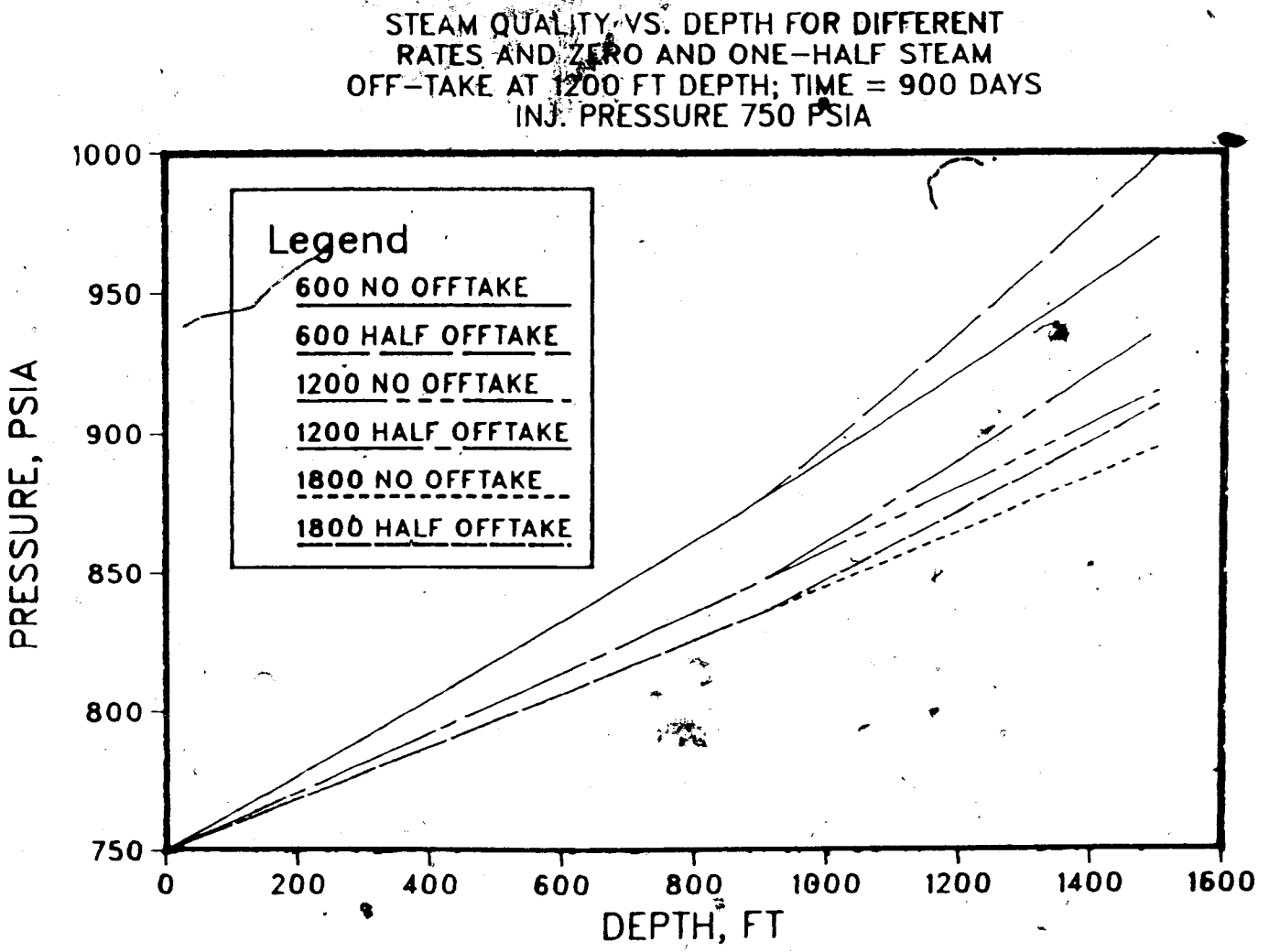

Figure 6.106 Wellbore Steam Pressure for Zero and One-Half Offtakes (Time = 900 days)

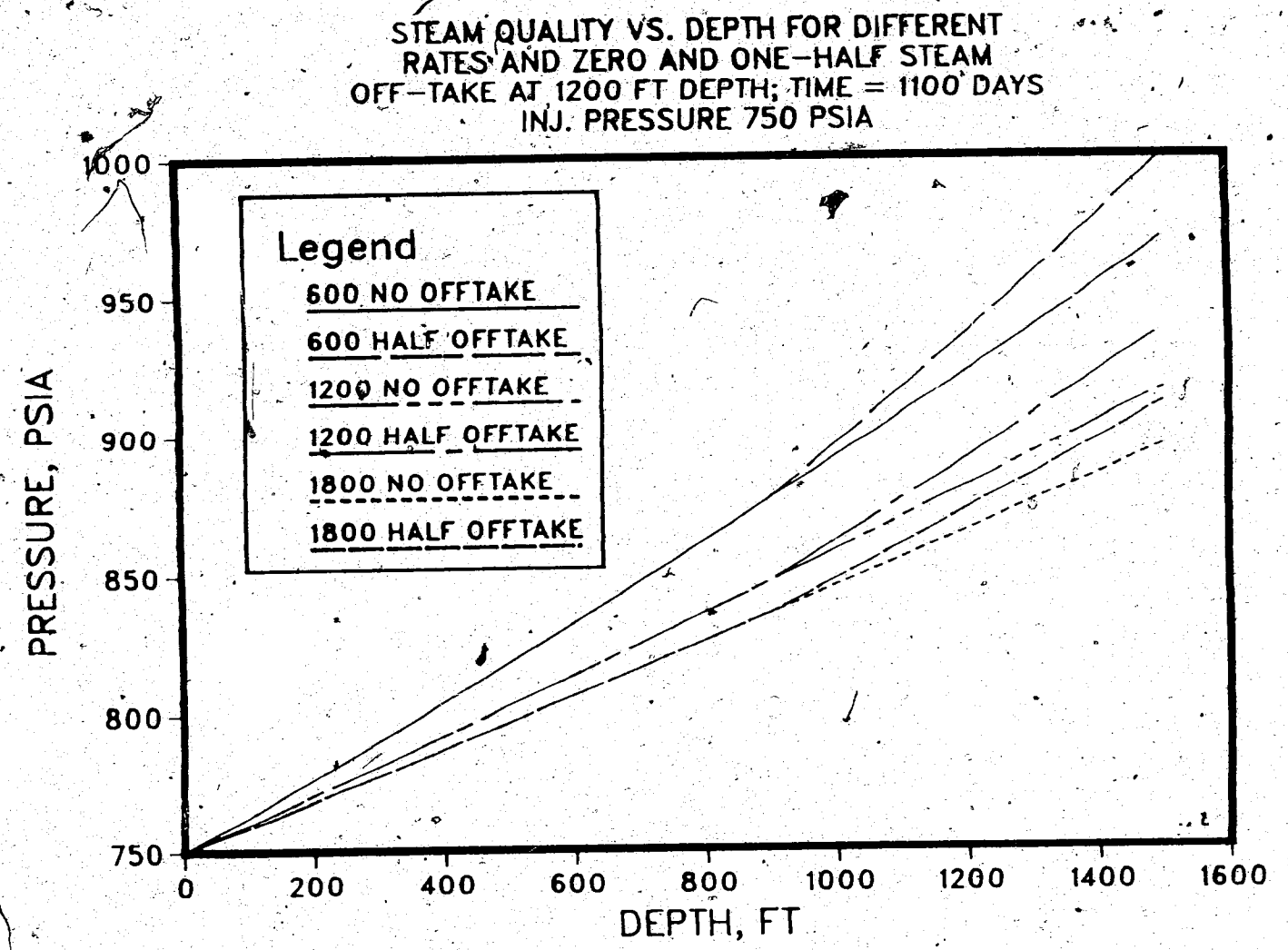

Figure 6.107 Wellbore Steam Pressure for Zero and One-Half Offtakes (Time = 1100 days)

one corresponding to a zero offtake, the other one corresponding to the offtake rate that is one-half of the steam rate. It is seen that in all cases, the steam pressures above the offtake point (1200 ft) are higher than those in the absence of offtake. This is due to the fact that steam quality decreases below the offtake point (as shown in the previous section), leading to an increase in the hydrostatic head, which causes an increase in steam pressure. This is further helped by the reduced frictional pressure drop due to the reduced velocity of steam below the offtake point. This effect becomes less important as the steam injection rate increases. In an actual multilayer injection operation, the situation would be more complex than the one described here. The increased steam pressure expected below the offtake point will lead to an increase in the steam flow rate below the offtake point with time. As a result, it is possible that the steam flow rate at the intermediate offtake point would continue to drop with time, and eventually reach some equilibrium value different from the design rate. It may be concluded that steam injection wells with multiple offtakes can be difficult to control as far as the steam inflow into individual layers is concerned.

Figures 6.108 and 6.109 summarize the results for bottomhole (1500 ft) steam quality, for offtake at 1200 ft, and for the two steam injection pressures considered (1500 and 750 psia). Again it is seen that the bottomhole qualities are lower when there is steam offtake. But the difference between the curves for increasing steam injection rates, or increasing steam injection pressures decreases, for reasons given above. It is evident that the effect of offtake examined here is important, and should be taken into account. Steam injection simulations carried out at the present time neglect steam quality changes in multilayer injection.

Temperature Distribution in the Surrounding Rock

A secondary feature of interest is the temperature distribution in the formation surrounding the wellbore, when multiple steam offtakes are employed. It is recalled that in the present work, the temperature distribution in the surrounding formation was calculated

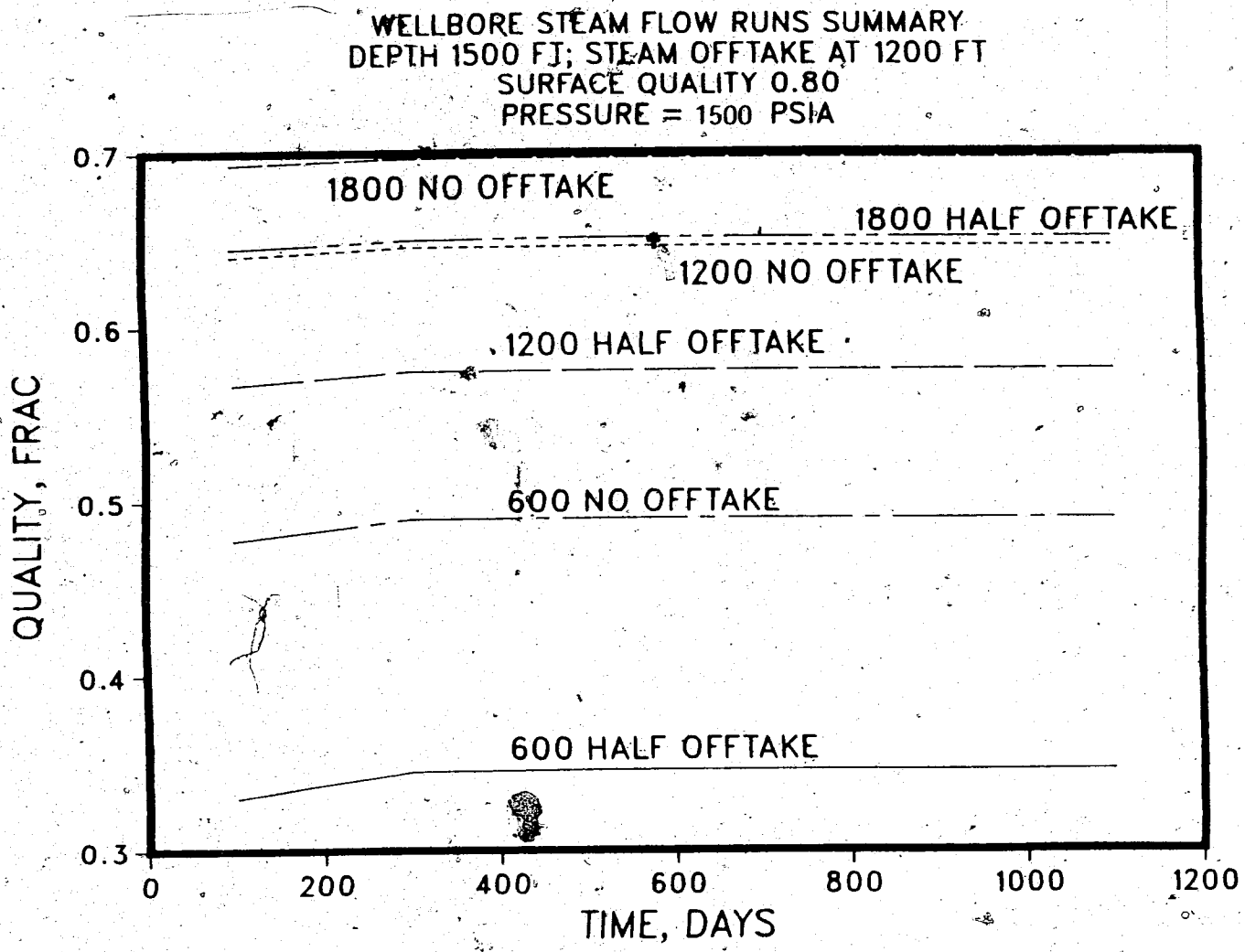

Figure 6.108 Wellbore Steam Quality vs. Time, for Surface Steam Pressure of 750 psia

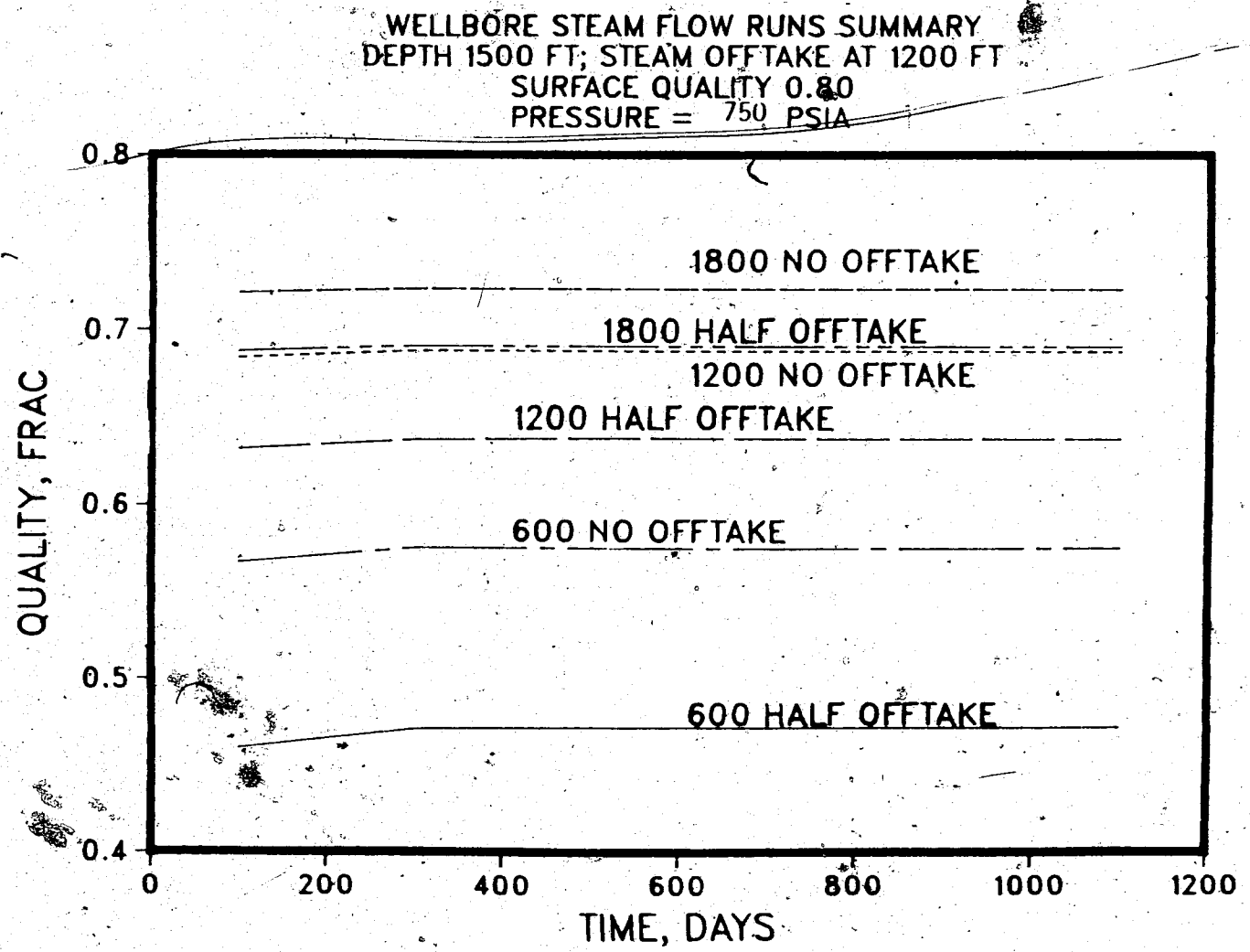

Figure 6.109 Wellbore Steam Quality vs. Time, for Surface Steam Pressure of 1500 psia

by the solution of the radial heat flow equation. It is thus expected that the temperature distribution in the formation will depend on the steam temperature in the wellbore. The temperature distribution was found to be relatively insensitive to offtake, and depends more on the injection time. Figure 110 shows the temperature distribution at a depth of 1200 ft at two different times.

Effect of Varying Steam Quality and Pressure on Steamflood Performance

Given a wellbore model such as developed here, it is possible to carry out a wide variety of coupled wellbore-reservoir studies. For the purpose of showing the effect of varying steam quality across the injection interval, one simulation of the Aberfeldy reservoir was carried out, where the wellbore steam quality and pressure for the 750 psia steam injection pressure and 600 B/D steam injection rate (CWE) history discussed above was used as a function of time. The remaining data were the same as used in the steam runs discussed previously.

Figures 6.111 through 6.118 show the oil/water production rates, water-oil ratio, and cumulative oil-steam ratio, and oil recovery, respectively, all versus cumulative steam injected, for the case of a uniform steam pressure and quality, and for variable values. The detailed production histories are shown in Tables 6.13 and 6.14, respectively. It is seen that the oil recovery is higher (42% vs. 28%) in the case of the uniform steam quality and pressure (in both layers, as well as in time) than that in the more realistic case. The main reason is that in the latter case, less dry steam is being injected in the lower part of the formation. However, the pressure is higher, and more hot water is going into the lower layer. On the whole, it can be said that the assumption of a constant steam quality over a multiple offtake injection tubing would give optimistic estimates of oil recovery.

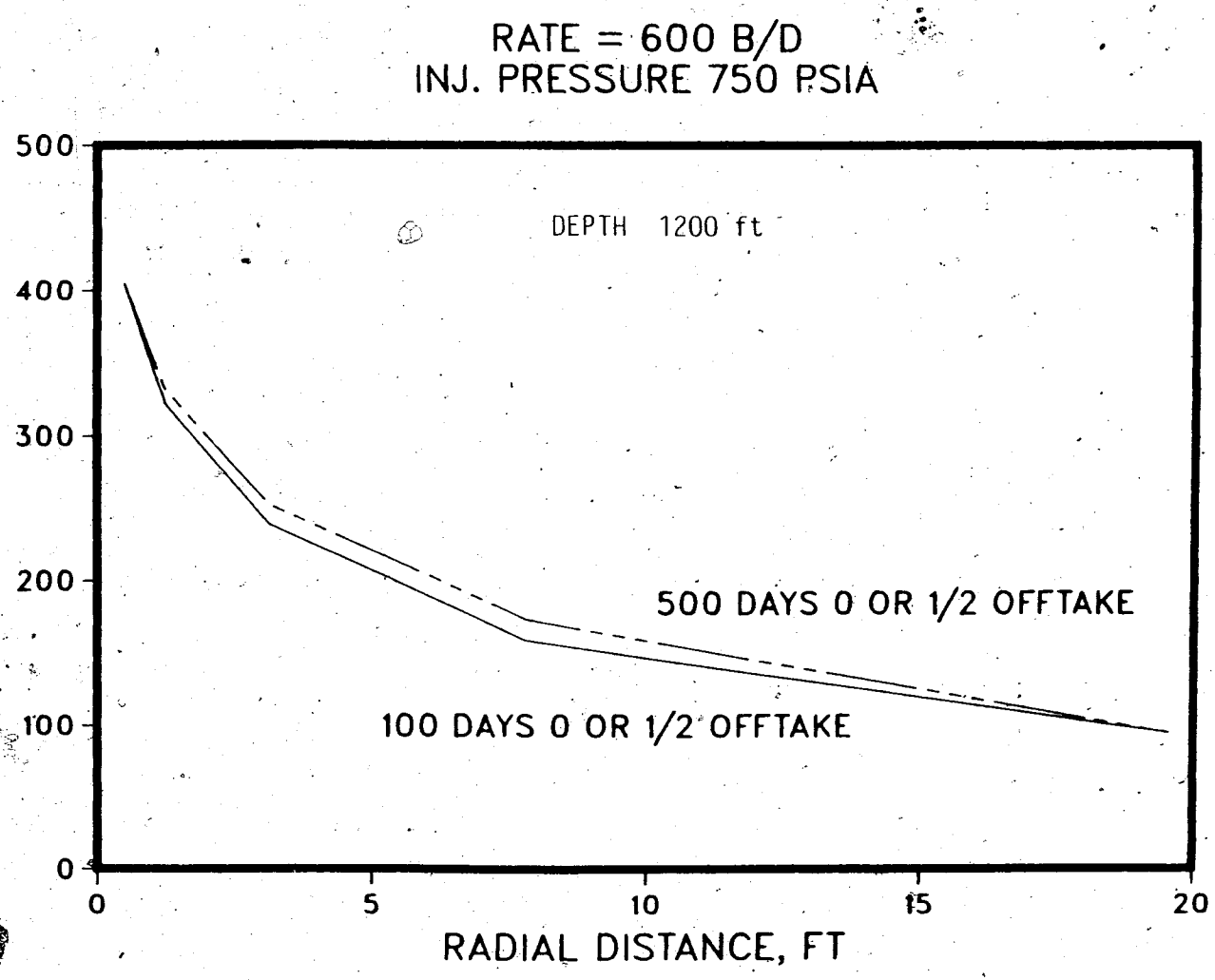

Figure 6.110 Temperature Distribution Around the Wellbore at 100 and 500 days

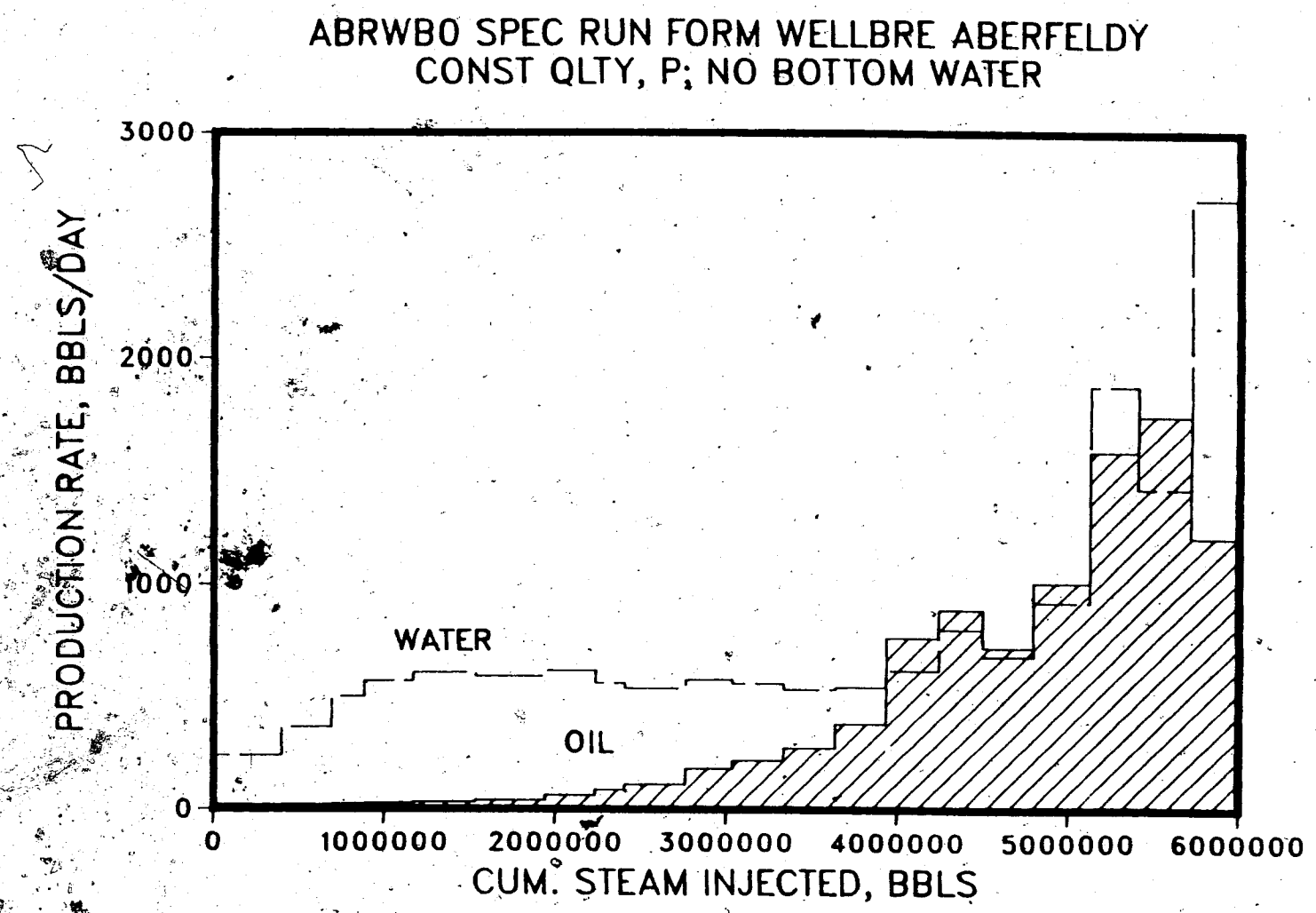

Figure 6.111 Production History for Steam Injection with a Uniform Steam Quality in the Wellbore, with Steam Offtake at Two Points

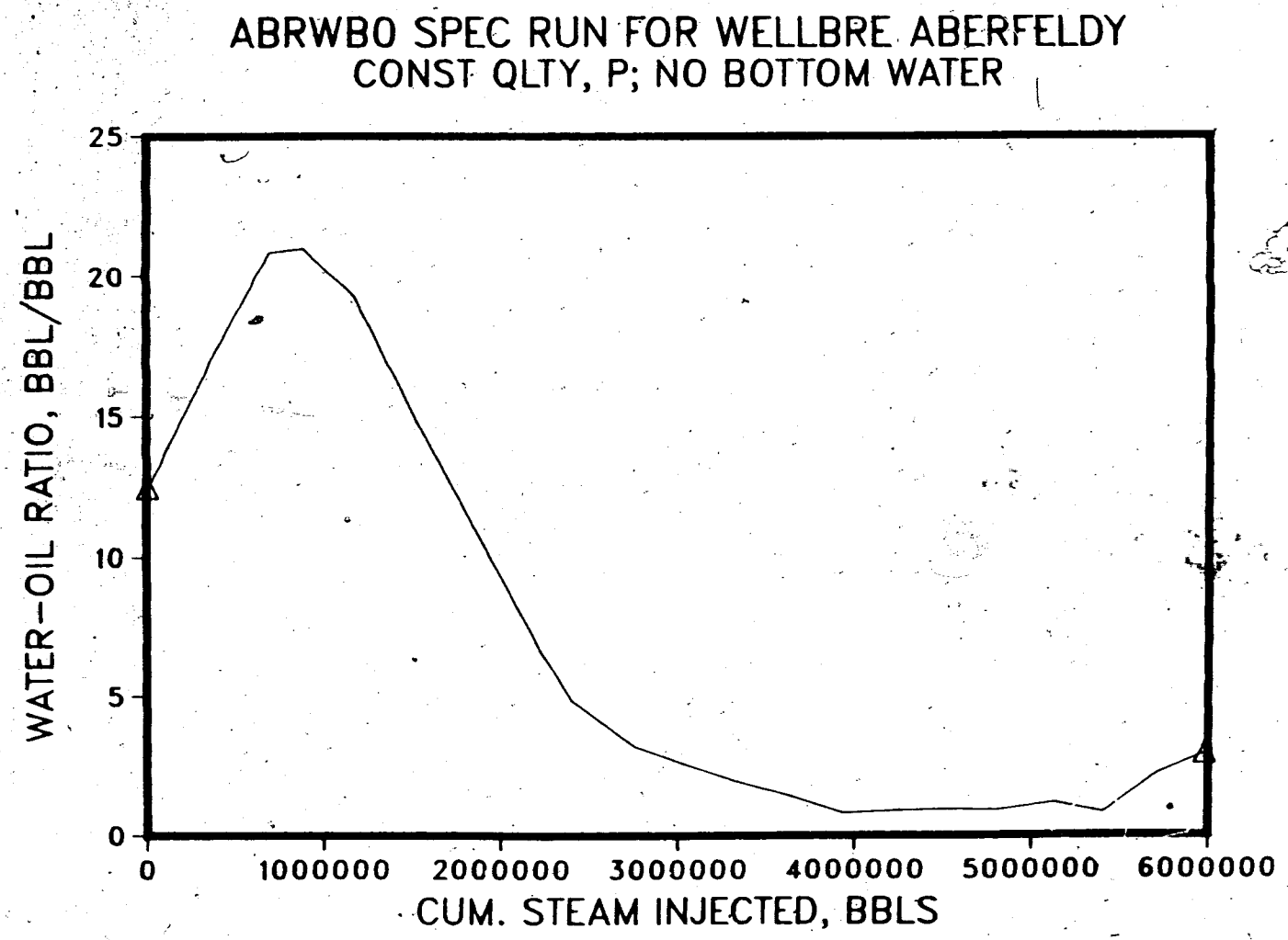

Figure 6.112 Water-Oil Ratio for Steam Injection with a Uniform Steam Quality in the Wellbore, with Steam Offtake at Two Points

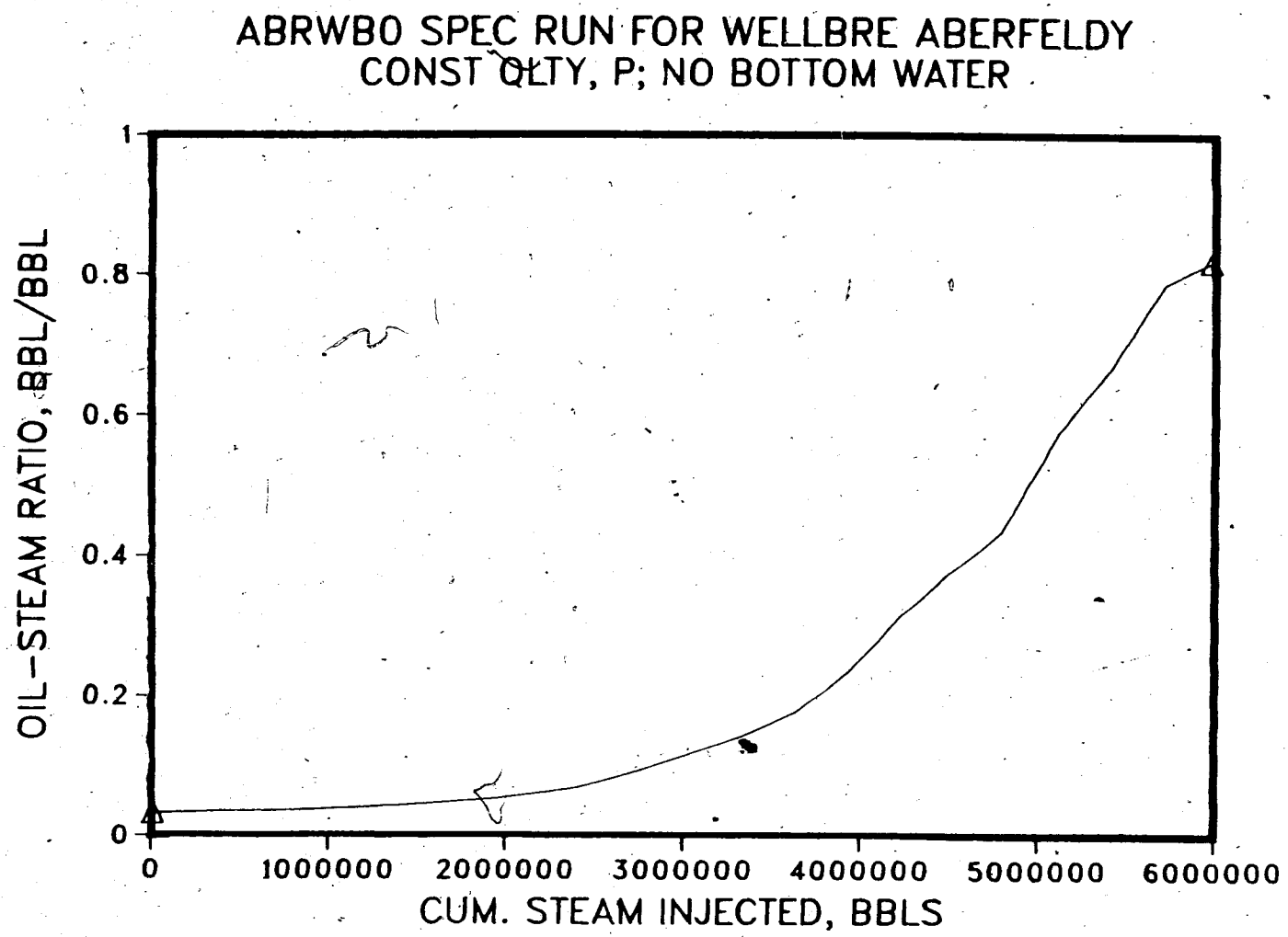

Figure 6.193 Oil-Steam Ratio for Steam Injection with a Uniform Steam Quality in the Wellbore, with Steam Offtake at Two Points

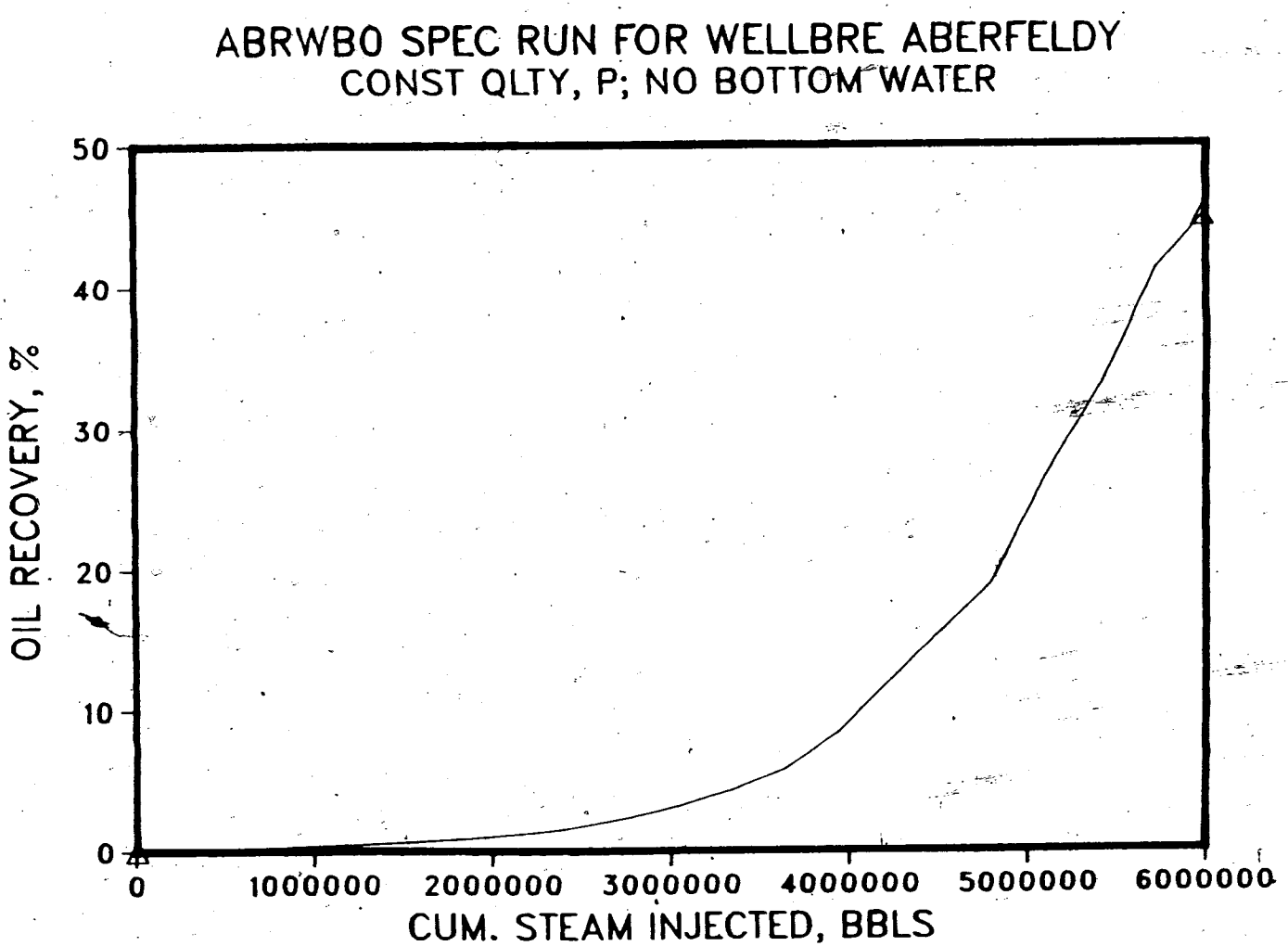

Figure 6.114 Oil Recovery for Steam Injection with a Uniform Steam Quality in the Wellbore, with Steam Offtake at Two Points

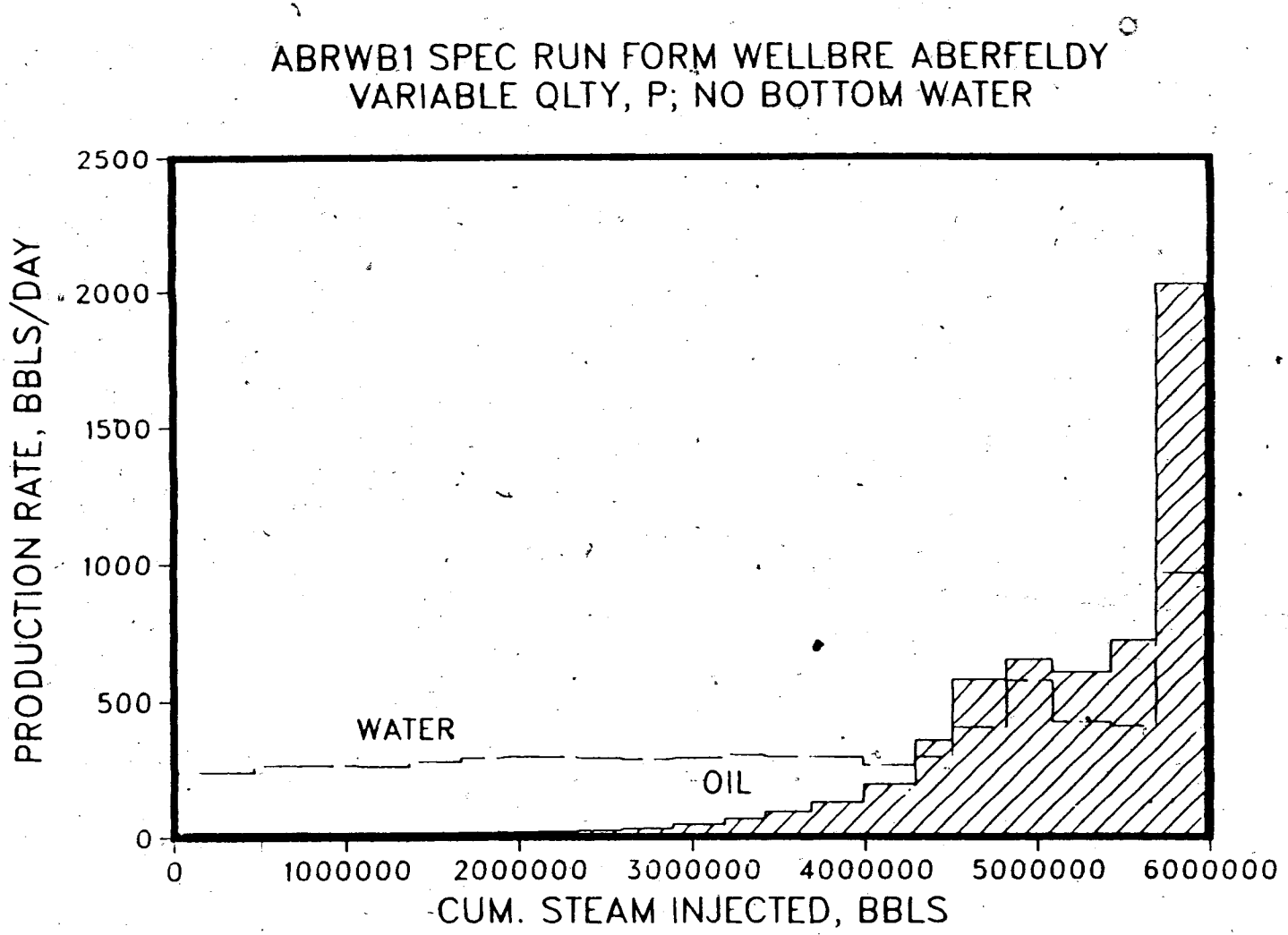

Figure 6.115 Production History for Steam Injection with a Variable Steam Quality in the Wellbore, with Steam Offtake at Two Points

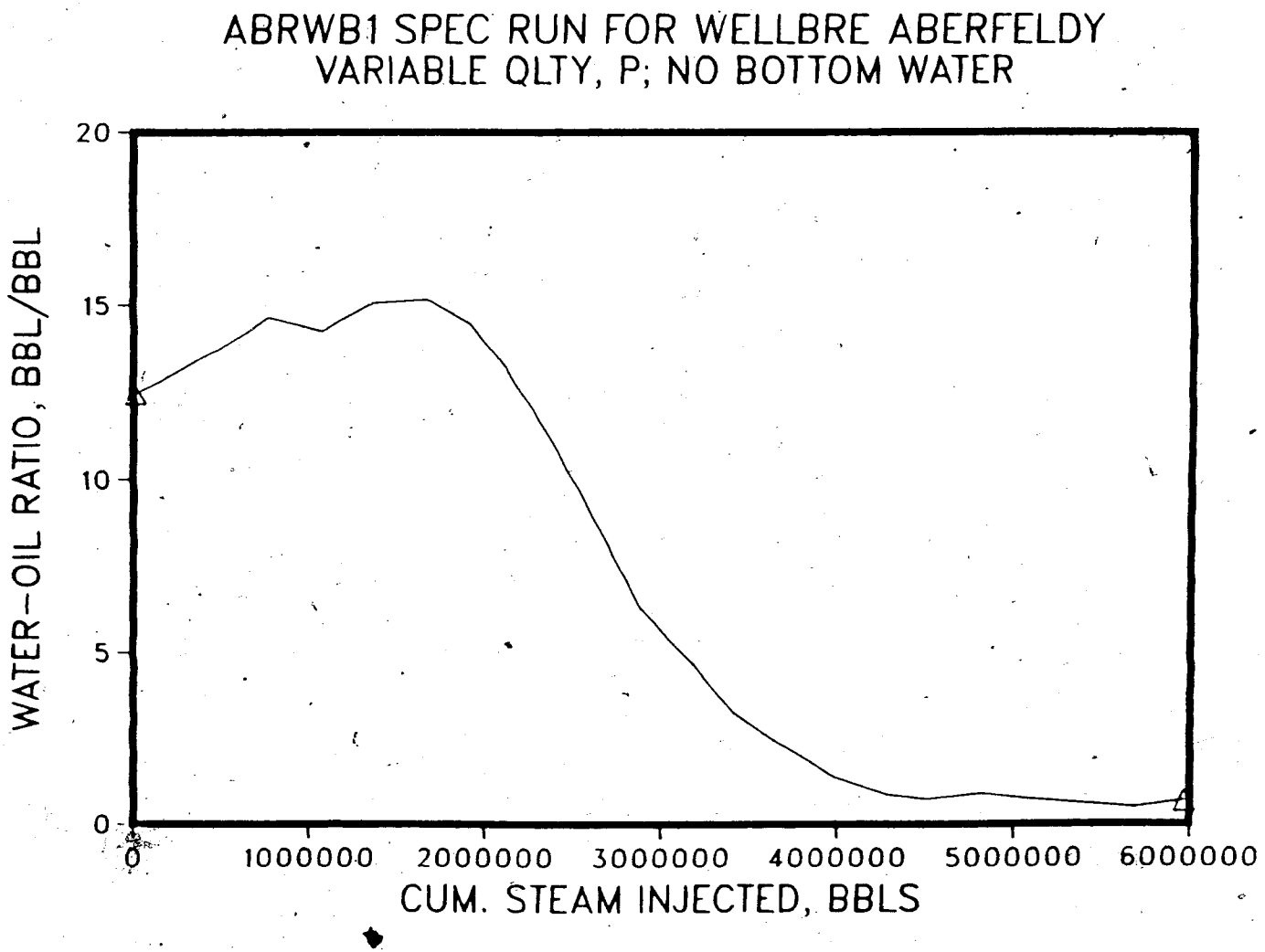

Figure 6.116 Water-Oil Ratio for Steam Injection with a Variable Steam Quality in the Wellbore, with Steam Offtake at Two Points

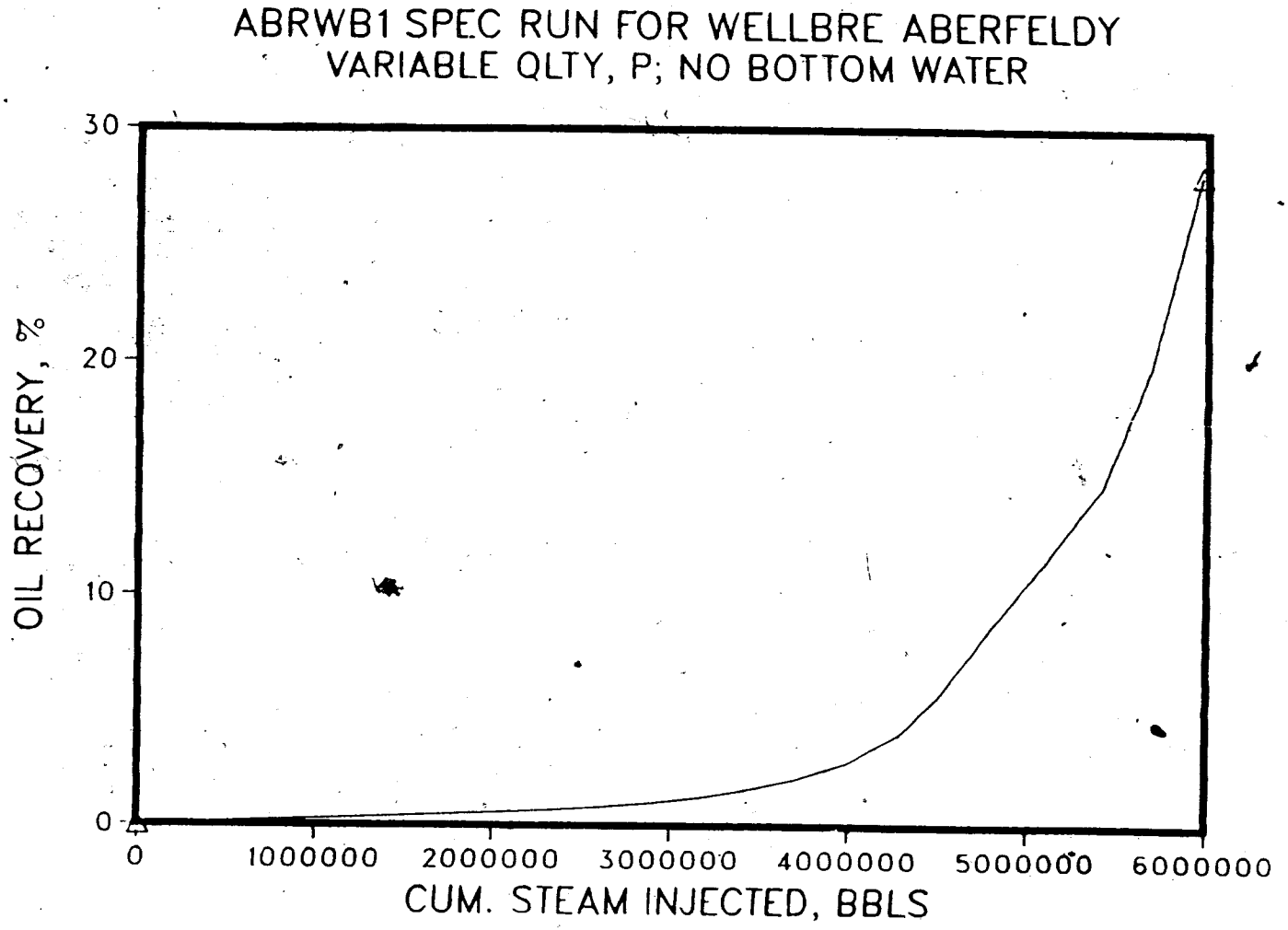

Figure 6.117 Oil-Steam Ratio for Steam Injection with a Variable Steam Quality in the Wellbore, with Steam Offtake at Two Points

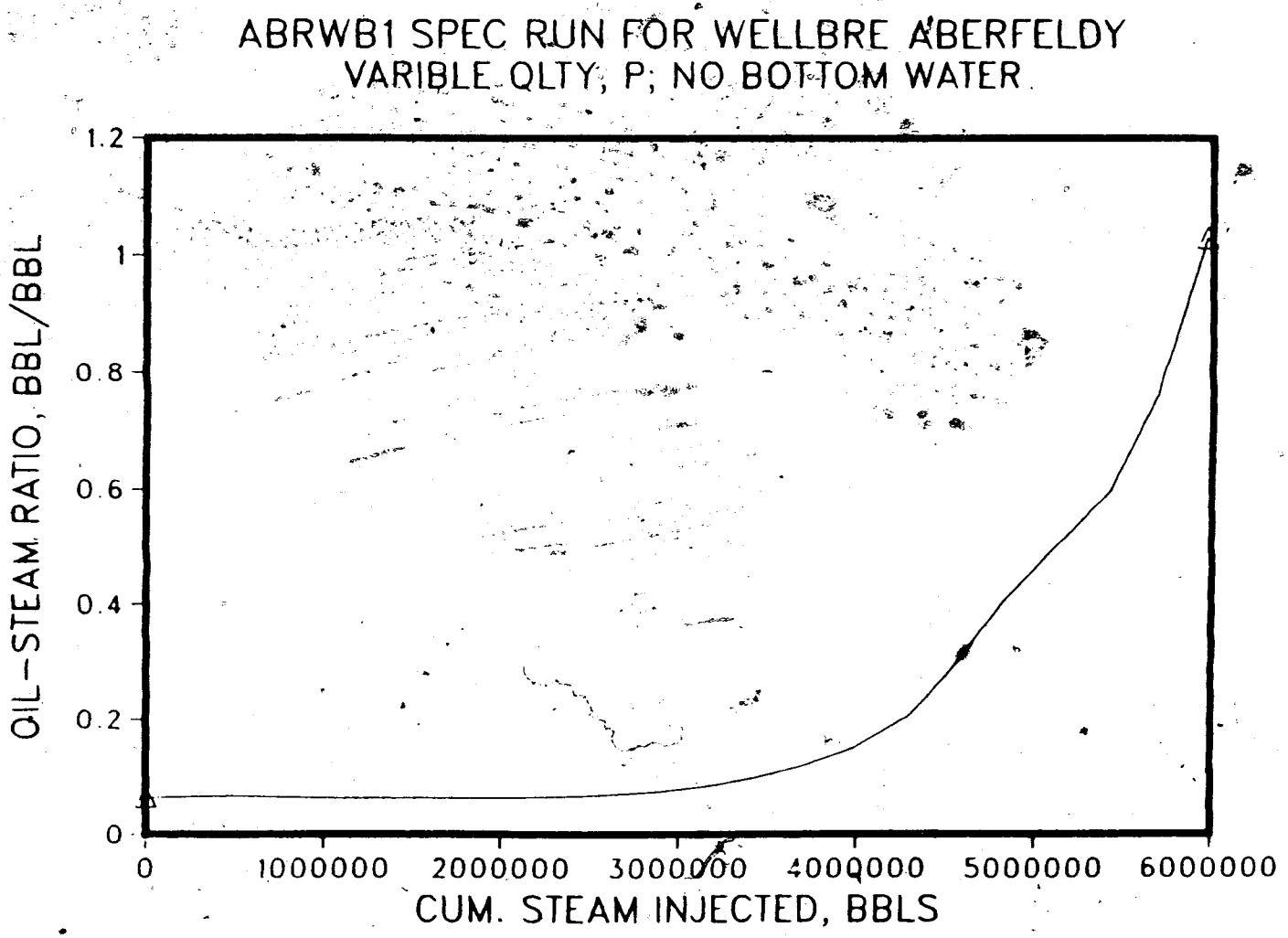

Figure 6.118 : Oil Recovery for Steam Injection with a Variable Steam Quality in the Wellbore, with Steam Offtake at Two Points

Table: 6.13
ABRWB0: SPEC RUN WELLBORE ABERFELDY; CONST QLTY, P NO BOTTOM WATER

Legend:

T : Time, Days
OPR : Oil Production Rate, Bbls/Day
WPR : Water Production Rate, Bbls/Day
WOR : Cumulative Water-Oil Ratio, Bbl/Bbl
CSI : Cumulative Steam Injected, 10^5Bbls
ORec : Oil Recovery, %
OSR : Cumulative Oil-Steam Ratio, Bbl/Bbl

T	OPR	WPR	WOR	CSI	ORec	OSR
13	19.1	238	12.44	0.079	0.002	0.0319
668	20.9	365	17.46	4.012	0.128	0.0348
1158	24.0	501	20.86	6.949	0.226	0.0355
1473	27.2	571	20.98	8.840	0.301	0.0372
1950	31.4	607	19.28	11.703	0.430	0.0401
2553	40.0	590	14.73	15.322	0.628	0.0447
3239	62.1	616	9.92	19.437	0.947	0.0532
3725	86.2	560	6.49	22.355	1.282	0.0627
4011	111.3	535	4.81	24.069	1.544	0.0701
4603	180.6	576	3.19	27.621	2.383	0.0942
5061	217.1	557	2.57	30.366	3.229	0.1162
5561	273.1	531	1.94	33.366	4.367	0.1430
6061	380.3	542	1.42	36.366	5.879	0.1766
6558	761.1	617	0.81	39.351	8.412	0.2335
7069	885.9	801	0.90	42.413	12.339	0.3178
7495	716.7	680	0.95	44.970	15.417	0.3745
7988	1010.3	920	0.91	47.931	18.981	0.4326
8544	1588.7	1875	1.18	51.265	27.202	0.5796
9014	1746.5	1425	0.82	54.085	33.035	0.6672
9529	1210.7	2709	2.24	57.179	41.283	0.7887
9967	663.4	1948	2.94	59.807	44.891	0.8200

Table: 6.14
ABRWB1: SPEC RUN FOR WELLBORE ABERFELDY; VARIABLE QLTY, P
NO BOTTOM WATER

Legend:

T : Time, Days
OPR : Oil Production Rate, Bbls/Day
WPR : Water Production Rate, Bbls/Day
WOR : Cumulative Water-Oil Ratio, Bbl/Bbl
CSI : Cumulative Steam Injected, 10^5 Bbls
ORec : Oil Recovery, %
OSR : Cumulative Oil-Steam Ratio, Bbl/Bbl

T	OPR	WPR	WOR	CSI	ORec	OSR
13	19.1	238	12.44	0.080	0.002	0.0638
779	19.2	263	13.68	4.676	0.143	0.0670
1279	17.9	262	14.63	7.676	0.227	0.0647
1779	18.0	258	14.27	10.676	0.310	0.0634
2279	18.4	278	15.07	13.676	0.393	0.0628
2779	19.2	292	15.18	16.676	0.479	0.0628
3181	20.5	297	14.46	19.088	0.553	0.0633
3512	22.2	295	13.27	21.076	0.618	0.0641
3896	25.3	290	11.45	23.378	0.702	0.0656
4317	31.1	285	9.14	25.906	0.812	0.0685
4809	46.3	291	6.28	28.854	0.988	0.0748
5309	65.1	302	4.64	31.854	1.247	0.0856
5697	91.5	294	3.21	[illegible]	1.536	0.0981
6147	127.0	293	2.31	36.882	1.996	0.1182
6647	192.9	262	1.36	39.882	2.742	0.1502
7147	354.8	296	0.83	42.882	4.004	0.2040
7505	574.5	402	0.70	45.028	5.659	0.2746
8026	653.5	570	0.87	48.160	8.859	0.4019
8474	605.3	423	0.70	50.846	11.385	0.4892
9038	721.1	407	0.56	54.232	14.752	0.5943
9473	2026.2	966	0.48	56.840	19.781	0.7604
9948	1804.4	1199	0.66	59.688	28.138	1.0299

Chapter VII

CONCLUSIONS

This investigation presented simulations of steam injection processes, with a number of novel features. The model examined such phenomena as thermal upgrading, non-Newtonian oil rheology and steam-foam injection in the context of steamflooding. The important problem of steamflooding and cyclic steaming bottom water reservoirs was investigated for the first time. Another contribution of this work is the study of wellbore steam flow, considering pressure and temperature changes, along with the prevailing flow regime, when steam is taken off the tubing at more than one point. The resulting steam pressure and quality variations were employed in steamflood simulations. Within the framework of this study, the following conclusions were reached:

1. The steam injection simulators developed can be used to simulate steamflooding, cyclic steam stimulation, in three dimensions, including effects such as thermal upgrading of oil, non-Newtonian oil rheology, and injection of a steam-based foam. A wellbore simulator can be used to simulate steam pressure and quality changes when multiple steam offtakes are employed in thick formations.

2. Thermal upgrading, non-Newtonian oil rheology, and foam flow are not necessarily important processes in steam injection, but should be included in any simulation. This observation is based upon rather few simulations and approximate representations of these processes. Thermal upgrading is effective in only the high temperature regions of a steamflood, over long periods. Non-Newtonian oil behaviour (in this case, shear-thinning) will affect oil viscosity over the entire reservoir, leading to an increase in oil recovery over the case where the oil viscosity is shear-invariant. Foam injection with steam was only a little more effective than steam alone, within the framework of the foam model used in this work.

3. In bottom water reservoirs, many factors affect steamflood and cyclic steaming performance, the most important of which are: bottom water zone thickness, its oil saturation, vertical and horizontal permeabilities, and completion interval. Vertical permeability makes a difference when it is one-tenth, or less of the horizontal; higher values do not seem to make much difference in performance. A mobile oil saturation in the bottom water zone, even though it may be low, can make a bottom water type heavy oil reservoir more attractive for steamflooding.

4. Partially penetrating wells can help avoid communication with a bottom water zone, but the oil-steam ratios would be low in the first few cycles, as compared to wells completed over the entire interval. The latter would produce oil at a much greater water-oil ratio.

5. If steam is taken off an injection tubing at more than one point, the steam quality at the lower points will be continue to drop. The extent of quality drop depends on the steam offtake rates, steam pressure, surface quality, and time. At a given offtake point in the tubing, the steam quality tends to stabilize with time. Assuming a constant steam quality for two, or more layers, as is the current practice in steam simulation, can lead to optimistic oil recovery estimates, compared to a more realistic simulation, as done in the present study, with the steam quality and pressure varying in time at each layer, with the offtake rates.

6. History matching of a scaled laboratory experiment of steamflooding showed that considerable adjustments in the "field" relative permeabilities must be made to obtain a match.

REFERENCES

Abdalla, A. and Coats, K.H.: "Three-Phase Experimental and Numerical Simulation Study of the Steam Flood Process", Paper SPE 3600, presented at 46th Annual Fall Meeting of Soc. Pet. Eng. of AIME, New Orleans, Louisiana, Oct. 3-6, 1971.

Abou-Kassem, J.: "Grid Orientation in a Steam Model", Ph.D. Thesis, U. of Calgary (1981).

Aktan and Farouq Ali: "A Comparison of Stone's and Naar-Henderson's Relative Permeability Equation", Unpublished Note (1972).

Ball, M.W.: The C[illegible]ist. of Mining & Metallurgy , Vol. 44 (1941) 58.

Bernard, G.G.: "Effect of Foam on Recovery of Oil by Gas-Drive", Producers Monthly (Jan. 1963) 18-21.

Bernard, G.G. and Holm, L.W.: "Effect of Foam on Permeability of Porous Media to Gas", Soc. Pet. Eng. J., Vol. 4 (1964) 267-274.

Bernard, G.G. and Holm, L.W.: "Effect of Foam on Permeability of Porous Media to Gas", presented at Soc. Pet. Eng. of AIME Annual Fall Meeting, Houston, Oct. 11-14, 1964.

Best, D.A., Tam, E.S., and Isaacs, E.: "A Discussion on the Mechanism of Foam Flow Through Porous Media", presented at the 3rd UNITAR Conf., Long Beach, Calif., Jul. 1985.

Bowen, W.B., and Patel, C.: "Use of a Numerical Simulator as an Aid to the Optimization of Steam Stimulation in a Typical 15° API Heavy Oil Reservoir", Paper 82-33-38, presented at the 33rd Annual Tech. Meeting of the Pet. Soc. of CIM, Calgary, Jun. 6-9, 1982.

Chiang, J.C., Sanyal, S.K., Castanier, L.M., Brigham, W.E., and Sufi, A.: "Foam as a Mobility Control Agent in Steam Injection Processes", Paper SPE 8912, presented at the California Regional Meeting, Los Angeles, Apr. 9-11, 1980.

Chierici, G.L., Ciucci, G.M., and Sclocchi, G.: "Two-Phase Vertical Flow in Oil Wells - Prediction of Pressure Drop", J. Pet. Tech. (Aug. 1974) 927-938.

Coats, K.H.: "Simulation of Steamflooding with Distillation and Solution Gas", Soc. Pet. Eng. J. (Oct., 1976) 235-247.

Coats, K.H.: "A Highly Implicit Steamflood Model", Soc. Pet. Eng. J. (Oct. 1978) 369-383.

Coats, K.H., George, W.D., Chieh, C., Marcum, B.E.: "Three-Dimensional Simulation of Steamflooding", Soc. Pet. Eng. J. (Dec. 1974) 573-592.

Crookston R.B., Culham, W.E., and Chen, W.H.: "A Numerical Simulation Model for Thermal Recovery Processes", Soc. Pet. Eng. J. (Feb. 1979), 37-58.

Diaz, J., and Farouq Ali, S.M.: "Effectiveness of Hot-Water Stimulation of Heavy Oil Formations", J. Can. Pet. Tech. Vol. 14, No. 3 (Jul.-Sept. 1975) 66-76.

Dietrich, J.K. and Bondor, P.L.: "Three Phase Oil Relative Permeability Models", Paper SPE 6044, presented at the 51st Annual Fall Meeting of Soc. Pet. Eng., New Orleans, Oct. 3-6, 1976.

Doscher, T.M., and Huang, W.: "Steam Drive Performance Judged Quickly for Use of Physical Models", Oil & Gas J. (Oct. 22, 1979) 52-57.

Duns, H. Jr., and Ros, N.C.J.: "Vertical Flow of Gas and Liquid Mixtures in Wells", Proc., Sixth World Pet. Cong., Frankfurt (1961) Sec. II, Paper 22-PD6 [illegible]

Egloff, G. and Morrell, J.C.: National Petroleum News, (Aug. 4, 1926) 43-[illegible]

Ehrlich, R.: "Laboratory Investigation of Steam [illegible]nt in the Wabasca Grand Rapids "A" Sand", Oil Sands of Canada-Venez[illegible] Calgary (1977) 364-379.

Eijiogu, G.C. and Fiori, M.: "High-Pressure Stea[illegible] Correlations", Paper SPE 15405, presented at the 61st Annual Fall Mee[illegible] Soc. Pet. Eng., New Orleans, Oct. 5-8, 1986.

Elson, T.D.[illegible] Marsden, S.S., Jr.: "The Effectiveness of Foaming Agents at Elevated Temp[illegible]ures Over Extended Periods of Time", Paper SPE 7116, presented at the California Regional Meeting of the Soc. Pet. Eng., San Francisco, Apr. 12-14, 1978.

Farouq Ali, S.M.: "Multiphase, Multi-dimensional Simulation of In Situ Combustion", Paper SPE 6896, presented at the 52nd Annual Fall Meeti[illegible] Soc. Pet. Eng., Denver, Oct. 9-12, 1977.

Farouq Ali, S.M., and Abad, B.: "Bitumen Recovery from Oil Sands, Using GCOS Synthetic Crude in Conjunction With Steam", J. Can. Pet. Tech. (Jul.-Sept. 1976) 1-11.

Farouq Ali, S.M., and Snyder, S.G.: "Miscible-Thermal Methods Applied to Two-Dimensional, Vertical Tar Sand Pack, With Restricted Fluid Entry", J. Can. Pet. Tech. (1974).

Ferrer, J. and Farouq Ali, S.M.: "A Three-Phase, Two-Dimensional Compositional Thermal Simulator for Steam Injection Processes", J. Can. Pet. Tech. (Jan.-Mar. 1977) 1-13.

Fried, A.N.: "The Foam Drive Process for Increasing the Recovery of Oil", R.I. 5866, U.S. Bureau of Mines, Pittsburgh (1961).

Garon, A.M., Geisbrecht, R.A., and Lowry, W.E.: "Scaled Model Experiments of Firefloading in Tar Sands", Paper SPE 9449, presented at the 55th Annual Fall Meeting of Soc. Pet. Eng., Dallas, Sept. 21-24, 1980.

Gogarty, W.B.: "Rheological Properties of Psuedoplastic Fluids in Porous Media", Soc. Pet. Eng. J. (Jun. 1967) 149-159.

Gould, T.L., Tek, M. Rasin, and Katz, D.L.: "Two-Phase Flow Through Vertical, Inclined, or Curved Pipe," J. Pet Tech. (Aug. 1974) 915-926.

Grove, C.S., Wise, G.E., Marsh, W.C. and Gray, J.B.: "Viscosity of Fire-Fighting Foam", Ind. and Eng. Chem. (May 1951) 1120-1122.

Harding, T.G.: "Oil Recovery by Steam and Gas Injection", Ph.D. Thesis, U. of Alberta (1986).

Henderson, J.H., and Weber, L.: "Physical Upgrading of Heavy Crude Oils by the Application of Heat", J. Can. Pet. Tech. (Oct.-Dec. 1965) 206-212.

Herning, F. and Zipperer, L.: "Calculation of the Viscosity of Technical Gas Mixtures from the Viscosity of Individual Components", Gas u. Wasserfach, Vol. 79, No. 49 (1936) 69.

Hirasaki, G.J. and Lawson, J.B.: "Mechanisms of Foam Flow in Porous Media - Apparent Viscosity in Smooth Capillaries", presented at the 58th Annual Fall Meeting of Soc. Pet. Eng., San Fransicso, Oct. 5-8, 1983.

Holm, L.W.: "The Mechanism of Gas and Liquid Flow through Porous Media in the Presence of Foam", Soc. Pet. Eng. J., Vol. 8 (1968) 359-369.

Huygen, H.H.A., and Lowry, W.E., Jr.: "Steamflooding Wabasca Tar Sand Through the Bottom Water Zone - Scaled Lab Experiments", Paper SPE 8398, presented at the 54th Annual Fall Meeting of Soc. Pet. Eng., Las Vegas, Sept. 23-26, 1979.

Irani, C.A., and Solomon, C.J., Jr.: "Slim-Tube Investigation of CO_2 Foams", Paper SPE14962, presented at the SPE/DOE 5th Symp. on EOR, Tulsa, Apr. 20-23, 1986.

Isaacs, E.E., Green, K., Reitman, V., and Malcolm, J.D.: "Laboratory Studies of Surfactant Additives to Steam for the Recovery of Bitumen from Oil Sands", Paper 85-36-25, presented at the Pet. Soc. of CIM Meeting, Edmonton, June 2-5, 1985.

Islam, M.R., and Bentsen, R.G., "A Dynamic Method for Measuring Relative Permeability", J. Can. Pet. Tech., Vol. 25, No.1 (Jan.-Feb. 1986) 39-50.

Ito, Y.: "A One-Dimensional Computer Model for Simulating Oil Recovery by Steamflooding", M.Sc. Thesis, U. of Calgary (Dec. 1976).

Jennings, R.R., Rogers, J.H., and West, T.J.: "Factors Influencing Mobility Control by Polymer Solutions", J. Pet. Tech. (Mar. 1971).

Johnson, E.F., Bossler, D.P. and Naumann, V.O.: "Calculations of Relative Permeability from Displacement Experiments", Trans. AIME, (1959) 370-372.

Kasraie, M., and Farouq Ali, S.M.: "Effect of Bottom Water and Gas Cap on Steam Injection Response", Paper SPE 13039, presented at the 59th Annual Fall Meeting of Soc. Pet. Eng., Houston, Sept. 16-19, 1984.

Kasraie, M., and Farouq Ali, S.M.: "Heavy Oil Recovery in the Presence of Bottom Water", Paper No. 84-35-122, presented at the Pet. Soc. of CIM Meeting, Calgary, Jun. 10-13, 1984.

Kasraie, M., and Farouq Ali, S.M.: "Application of Thermal Recovery Techniques to Marginal Reservoirs", Proc. of 3rd European Meeting on Improved Oil Recovery, Vol. 1, Rome, (1985) 379-389.

Kasraie, M., and Farouq Ali, S.M.: "Steamflooding Bottom Water Reservoirs", Second Tech. Conf. of the S. Sask. Sec. of the Pet. Soc. of CIM, Oct. 7-8, 1987.

Kimber, K.D., Puttagunta, V.R., and Farouq Ali, S.M.: "New Scaling Criteria and Their Relative Merits for Steam Recovery Experiments", Paper 86-37-22, presented at the Pet. Soc. of CIM Meeting, Calgary, Jun. 8-11, 1986.

Maini, B.B., and M[illegible]V.: "Relationship Between Foam Stability Measured in Static Tests and Flow Behaviour in Porous Media", Paper SPE 13073, presented at the 59th Annual Fall Meeting of Soc. Pet. Eng., Houston, Sept. 16-19, 1984.

Marsden, S.S. and Khan, S.A.: "The Flow of Foam Through Short Porous Media and Apparent Viscosity Measurements", Soc. Pet. Eng. J., (Mar. 1966) 17-25.

Mast, R.F.: "Microscopic Behavior of Foam in Porous Media", Paper SPE 3997, presented at the 47th Annual Fall Meeting of Soc. of Pet. Eng., San Antonio, Texas, Oct. 1972.

McKinley, R.M., Jahns, H.O., Harris, W.W. and Greenkorn, R.A.: "Non-Newtonian Flow in Porous Media", AIChE J. Vol. 12, No. 1 (Jan. 1966) 17-20.

Minssieux, L.: "Oil Displacement by Foams in Relation to Their Physical Properties in Porous Media", J. Pet. Tech., Vol. 26 (1974) 100-108.

Naar, J. and Henderson, J.H.: "Imbibition Model - Its Application to Flow Behaviour and the Prediction of Oil Recovery", 222, II-61; Soc. Pet. Eng. J. (Jun. 1961) 61.

Naar, J. and Wygal, R.J.: "Three-Phase Imbibition Relative Permeability", 222, II-254; Soc. Pet. Eng. J. (Dec. 1961) 254.

Naar, J., Wygal, R.J., and Henderson, J.H.: "Imbibition Relative Permeability in Unconsolidated Porous Media", 225, II-13; Soc. Pet. Eng. J. (Mar. 1962) 13.

Orkiszewski, J.: "Predicting Two-Phase Pressure Drops in Vertical Pipe," J. Pet. Tech. (Jun. 1967) 829-838.

Pacheco, E.F. and Farouq Ali, S.M.: "Wellbore Heat Losses and Pressure Drop in Steam Injection," J. Pet. Tech. (Feb. 1972) 139-144.

Patel, H.N., Masliyah, J.H., and Mathews, J.: "One-Dimensional Numerical Model For Cyclic Steam Injection in an Oil Reservoir", Oil Sands of Canada-Venezuela, CIM, Calgary (1977) 411-418.

Polikar, M., Ferracuti, F., DeCastro, V., Puttagunta, V.R., and Farouq Ali, S.M.: "Temperature Effects on Bitumen-Water Relative Permeabilities", Paper 85-36-14, presented at the Pet. Soc. of CIM Meeting, Edmonton, June 2-5, 1985.

Polikar, M., Puttagunta, V.R., DeCastro, V., and Farouq Ali, S.M.: "Relative Permeability Curves for Bitumen and Water in Oil Sand Systems", Paper No. 86-37-03, presented at the Pet. Soc. of CIM Meeting, Calgary, Jun. 8-11, 1986.

Poston, S.W., Ysrael, S., Hossain, A.K.M.S., Montgomery, E.F., III, and Ramey, H.J., Jr.: "The Effect of Temperature on Irreducible Water Saturation and Relative

Permeability of Unconsolidated Sand", Soc. Pet. Eng. J., Vol. 10, No. 2 (1970) 171-180.

Prats, M.: "Peace River Steam Drive Scaled Model Experiments", Oil Sands of Canada-Venezuela, CIM, Calgary (1977) 346-363.

Price, H.S. and Coats, K.H.: "Direct Methods in Reservoir Simulation", Trans. AIME, 257 (1974) 298.

Proctor, M.: "Steam Injection Experiments in a Scaled Physical Model", M.Sc. Thesis, U. of Alberta (1985).

Pursley, S.A.: "Experimental Studies of Thermal Recovery Processes", Proc. of Heavy Oil Symp., Maracaibo (1974).

Raza, S.H.: "Foam in Porous Media: Characteristics and Potential Applications", Soc. Pet. Eng. J., Vol. 10 (1970) 328-336.

Raza, S.H. and Marsden, S.S.: "The Steaming Potential and Rheology of Foam", Soc. Pet. Eng. J. (Dec. 1967) 359-368.

Shutler, N.D.: "Numerical Three-Phase Simulation of the Linear Steam Flood Process" Soc. Pet. Eng. J. (Jun. 1969) 232-246.

Shutler, N.D.: "Numerical Three-Phase Model of the Two-Dimensional Steam Flood Process", Soc. Pet. Eng. J. (Dec. 1970) 405-417.

Singh, B., Malcolm, J.D., and Hedrick, T.R.: "Injection-Production Strategies for Reservoirs Having a Bottom Water Zone", Paper SPE 13623, presented at the Calif. Regional Meeting, Bakersfield, March, 1985.

Spillette, A.G., Hillestad, J.G., and Stone, H.L.: "A High-Stability Sequential Solution Approach to Reservoir Simulation", Paper SPE 4542, presented at the 48th Annual Fall Meeting of Soc. Pet. Eng., Las Vegas, 1973.

Stegemeier, G.L. et al: "Representing Steam Processes With Vacuum Models", Soc. Pet. Eng. J. (Jun. 1980) 151-174.

Stone, H.L.: "Probability for Estimating Three-Phase Relative Permeability", Trans., AIME, 249 (1970) 214.

Stone, H.L.: "Estimation of Three-Phase Relative Permeability and Residual Oil Data", J. Can. Pet. Tech. (Oct.-Dec. 1973) 53.

Sufi, A.H., Ramey, H.J., Jr., and Brigham, W.E.,: "Temperature Effects of Relative Permeabiliites in Oil-Water Systems", Paper SPE 11071, presented at the 57th Annual Fall Meeting of Soc. Pet. Eng., New Orleans, Sept. 26-29, 1982.

Vinsomé, P.K.W.: "A Numercial Description of Hot-Water and Steam Drives by the Finite-Difference Method", SPE 5248, presented at the 49th Annual Fall Meeting of Soc. Pet. Eng. of AIME, Houston, Oct. 6-9, 1974.

Wang, G.C.: "A Laboratory Study of CO_2 Foam Properties and Displacement Mechanism", Paper SPE/DOE 12645, presented at the Fourth Symposium on Enhanced Oil Recovery, Tulsa, Oklahoma, Apr.15-18, 1984.

Weinbrandt, R.M., Ramey, H.J., Jr. and Casse, F.J.: "The Effect of Temperature on Relative and Absolute Permeability of Sandstones", Soc. Pet. Eng. J., Vol. 15, No. 5 (1975) 376-384.

Weinstein, H.G., Wheeler, J.A., Woods, E.G.: "Numerical Model for Steam Stimulation", Paper 4759, presented at Improved Oil Recovery Symposium, Tulsa, Apr. 22-24, 1977.

APPENDIX A

TREATMENT OF CONVECTIVE-DIFFUSION TERMS

$$\frac{\partial}{\partial x}(\rho_o v_{ox} T \Sigma (c_{pi} C_{io}))$$

$$= \frac{\partial}{\partial x}\left(\rho_o T \Sigma (c_{pi} C_{io}) \cdot \left(-\frac{k_x k_{ro}}{\mu_o} \frac{\partial \Phi_o}{\partial x}\right)\right)$$

$$= -\rho_o T \Sigma (c_{pi} C_{io}) \frac{\partial}{\partial x}\left(\frac{k_x k_{ro}}{\mu_o} \frac{\partial \Phi_o}{\partial x}\right)\Bigg|_i$$

$$-\left(\frac{k_x k_{ro}}{\mu_o} \frac{\partial \Phi_o}{\partial x}\right) \frac{\partial}{\partial x}(\rho_o T \Sigma C_{pi} C_{io})\Big|_i$$

$$= \rho_o T \Sigma (c_{pi} C_{io}) \quad \frac{A_x k_x k_{ro}}{\mu_o \Delta x}\Bigg|_{i+1/2} (\Phi_{o_{i+1}} - \Phi_{o_i})$$

$$- \frac{A_x k_x k_{ro}}{\mu_o \delta x}\Bigg|_{i-1/2} (\Phi_{o_i} - \Phi_{o_{i-1}})$$

$$- \frac{k_x k_{ro}}{\mu_o} \frac{\partial \Phi_o}{\partial x}\Bigg|_i S_{i-1} (\rho_o T \Sigma c_{pi} C_{io})_{i-1}$$

$$+ S_i (\rho_o T \Sigma c_{pi} C_{io})_i + S_{i+1} (\rho_o T \Sigma c_{pi} C_{io})_{i+1}$$

where for block i

$$\Delta x = 1/2 (\Delta x_i + \Delta x_{i+1})$$

$$\delta x = 1/2 (\Delta x_i + \Delta x_{i-1})$$

$$S_i = \frac{2(\Delta x_{i+1} - \Delta x_{i-1})}{(\Delta x_i + \Delta x_{i+1})(\Delta x_i + \Delta x_{i-1})}$$

APPENDIX B

FORTRAN 77 PROGRAM FOR SOLVING A 6X6 BLOCK DIAGONAL MATRIX

```
      C MAHNAZ KASRAIE * OCT. 10, 1986 * PGM TO SOLVE A 6X6 BLOCK BAND MATRIX
      C                  ARISING FROM A SYSTEM OF SIX IMPLICIT FINITE DIFF. EQNS.
      C WE LL DEFINE THE Z,B,D,E,F,H,S ARRAYS, WHICH COME FROM THE FDEQNS.
      C AND CREATE THE A BAND MATRIX; AND PRINT IT OUT TO SEE IF ALL THE A S ARE
      C IN THE RIGHT POSITIONS. Z=1, B=2, D=3, E=4, F=5, H=6, S=7,
      C AND THEN PROCEED TO OBTAIN THE SOLUTION VECTOR.
            IMPLICIT REAL*8 (A-H,O-$)
            DIMENSION Z(7,7,3,6,6),B(7,7,3,6,6),D(7,7,3,6,6),E(7,7,3,6,6),
           1F(7,7,3,6,6),H(7,7,3,6,6),S(7,7,3,6,6),X(882)
           2,NEL(500),M$(82000)
            DATA Z,B,D,E,F,H,S,X/5292*1.DO,5292*2.DO,5292*3.DO,5292*4.DO,
           15292*5.DO,5292*6.DO,5292*7.DO,882*0.DO/
            COMMON/XLB/A$(82000),Q$(500)
      C NEL(IROW) IS THE LAST A$( ) # IN ROW NO. IROW; NEQNS=IROW IS THE ROW #.
      C XX IS THE SUM OF ELEMENTS IN A ROW TO GENERATE THE CONSTANT VECTOR, Q$( )
      C FOR IROW;  ALL THESE ARE ONLY FOR TESTING; MAY BE REMOVED LATER;  THESE LINES
      C ARE IDENTIFIED BY A STATEMENT # BEGINNING WITH 9999- FOR CONVENIENCE.
      C
      C
      C     WRITE(6,1)
        1   FORMAT(/,'ENTER : NX, NY, NZ, NA')
      C
      C     READ*,NX,NY,NZ,NA
            NX=2
            NY=5
            NZ=5
            NA=6
      C
      11112 VAL=876579
            DO 11111 I=1,NX
            DO 11111 J=1,NY
            DO 11111 K=1,NZ
            DO 11111 L=1,NA
            DO 11111 M=1,NA
            U=URAND(VAL)
            Z(I,J,K,L,M)=Z(I,J,K,L,M)*U
            U=URAND(VAL)
            B(I,J,K,L,M)=B(I,J,K,L,M)*U
            U=URAND(VAL)
            D(I,J,K,L,M)=D(I,J,K,L,M)*U
            U=URAND(VAL)
            E(I,J,K,L,M)=E(I,J,K,L,M)*U
            U=URAND(VAL)
            F(I,J,K,L,M)=F(I,J,K,L,M)*U
            U=URAND(VAL)
            H(I,J,K,L,M)=H(I,J,K,L,M)*U
            U=URAND(VAL)
            S(I,J,K,L,M)=S(I,J,K,L,M)*U
      11111 CONTINUE
      C
            NXY=NX*NY
            NXZ=NX*NZ
            NYZ=NY*NZ
            NEQNS=NXY*NZ
      C
            IF(NXY.EQ.NEQNS.OR.NXZ.EQ.NEQNS.OR.NYZ.EQ.NEQNS)GO TO 12
      C
            NBANDS=NXY
```

```
      IF(NXZ.GT.NBANDS)NBANDS=NXZ
      IF(NYZ.GT.NBANDS)NBANDS=NYZ
      GO TO 13
C
   12 NBANDS=NX
      IF(NY.GT.NBANDS)NBANDS=NY
      IF(NZ.GT.NBANDS)NBANDS=NZ
C
      IF(NX.EQ.NEQNS.OR.NY.EQ.NEQNS.OR.NZ.EQ.NEQNS) NBANDS=1
      IF(NEQNS.EQ.1)NBANDS=0
C
   13 NBANDS=NBANDS*NA+NA-1
      NEQNS=NEQNS*NA
C
      MC=1+2*NBANDS
      MA=NEQNS*MC-NBANDS*(NBANDS+1)/2
      NFIN=MA-NBANDS*(NBANDS+1)/2
C
      DO 10 M=1,MA
   10 A$(M)=0.DO
C
      DO 11 M=1,NEQNS
   11 Q$(M)=0.DO
C
      NOFSET=0
      MOFSET=0
      INCR=0
C
      DO 101 K=1,NZ
C
      KK=NXY*(K-1)
C
      DO 101 J=1,NY
C
      JK=NX*(J-1)+KK
C
      DO 101 I=1,NX
C
      IJK=I+JK
C
      DO 101 M=1,NA
C
      NROW=(IJK-1)*NA+M
C
      DO 100 L=1,NA
C
      IJKL=(IJK-1)*NA+L
C
      A$(NOFSET+IJKL)=E(I,J,K,L,M)
      Q$(NROW)=Q$(NROW)+E(I,J,K,L,M)
C
      IF(I.EQ.1)GO TO 50
C
      A$(NOFSET+IJKL-NA)=D(I,J,K,L,M)
      Q$(NROW)=Q$(NROW)+D(I,J,K,L,M)
C
   50 IF(I.EQ.N*)GO TO 60
C
```

```
      A$(NOFSET+IJKL+NA)=F(I,J,K,L,M)
      Q$(NROW)=Q$(NROW)+F(I,J,K,L,M)
C
 60   IF(J.EQ.1)GO TO 70
C
      A$(NOFSET+IJKL-NA*NX)=B(I,J,K,L,M)
      Q$(NROW)=Q$(NROW)+B(I,J,K,L,M)
C
 70   IF(J.EQ.NY)GO TO 80
C
      A$(NOFSET+IJKL+NA*NX)=H(I,J,K,L,M)
      Q$(NROW)=Q$(NROW)+H(I,J,K,L,M)
C
 80   IF(K.EQ.1)GO TO 90
C
      A$(NOFSET+IJKL-NA*NXY)=Z(I,J,K,L,M)
      Q$(NROW)=Q$(NROW)+Z(I,J,K,L,M)
C
 90   IF(K.EQ.NZ)GO TO 100
C
      A$(NOFSET+IJKL+NA*NXY)=S(I,J,K,L,M)
      Q$(NROW)=Q$(NROW)+S(I,J,K,L,M)
C
100   CONTINUE
C
      MOFSET=MOFSET+NBANDS+1+INCR
      NEL(NROW)=MOFSET
      NOFSET=MOFSET
      IF(NROW.GT.NBANDS)NOFSET=MOFSET-(NROW-NBANDS)
      IF(NROW.LT.NEQNS-NBANDS)INCR=INCR+1
      IF(NROW.GT.NBANDS)INCR=INCR-1
C
101   CONTINUE
C
C PRINT OUT THE ORIGINAL MATRIX USING THE A$ ARRAY; WE HAVE NEQNS AND NEL(NEQNS)
      NST=1
      DO 200 I=1,NEQNS
      K=NEL(I)
      DO 210 MM=NST,K
210   M$(MM)=IDINT(A$(MM))
      NDIF=K-NST
      NQ$=IDINT(Q$(I))
      PRINT 300,I,NST,K,NDIF,NQ$,(M$(J),J=NST,K)
      NST=K+1
200   CONTINUE
301   FORMAT(' ',40(F3.1,1X))
300   FORMAT(' ',I3,1X,I4,1X,I4,1X,I4,1X,I3,1X,10811)
C
      PRINT*,NBANDS,NEQNS,NFIN,NEL(NEQNS)
      CALL XELB(NBANDS,NEQNS,NFIN)
      PRINT 33333,(Q$(I),I=1,NEQNS)
33333 FORMAT(' ',8(F9.7,1X))
C
C NBANDS IS    NO. OF DIAGONALS ABOVE MAIN DIAGONAL; NEQ IS NO. OF EQNS
C NFIN IS THE TOTAL NO. OF A'S; ONLY NEEDED FOR PRINTOUT IN XELB
      END
C
      SUBROUTINE    XELB(NX,NEQ,NFIN)
```

```
      IMPLICIT REAL*8(A-H,O-$)
      DIMENSION A(82000),BB(500)
      COMMON/XLB/A$(82000),Q$(500)
      EQUIVALENCE (A$,A), (Q$,BB)
C     PRINT*,(A$(I),I=1,NFIN)
C     PRINT*,(Q$(I),I=1,NEQ)
      M=NEQ
      N=1
      MUD=NX
      MLD=NX
      EPS=1.D-8
      IF(MLD)47,1,1
    1 IF(MUD)47,2,2
    2 MC=1+MLD+MUD
      IF(MC+1-M-M)3,3,47
    3 IF(MC-M)5,5,4
    4 MC=M
    5 MU=MC-MUD-1
      ML=MC-MLD-1
      MR=M-ML
      MZ=(MU*(MU+1))/2
      MA=M*MC-(ML*(ML+1))/2
      NM=N*M
      IER=0
      PIV=0.D0
      IF(MLD)14,14,6
    6 JJ=MA
      J=MA-MZ
      KST=J
      DO 9 K=1,KST
      TB=A(J)
      A(JJ)=TB
      TB=DABS(TB)
      IF(TB-PIV)8,8,7
    7 PIV=TB
    8 J=J-1
    9 JJ=JJ-1
      IF(MZ)14,14,10
   10 JJ=1
      J=1+MZ
      IC=1+MUD
      DO 13 I=1,MU
      DO 12 K=1,MC
      A(JJ)=0.D0
      IF(K-IC)11,11,12
   11 A(JJ)=A(J)
      J=J+1
   12 JJ=JJ+1
   13 IC=IC+1
   14 TOL=EPS*PIV
      KST=1
      IDST=MC
      IC=MC-1
      DO 38 K=1,M
      IF(K-MR-1)16,16,15
   15 IDST=IDST-1
   16 ID=IDST
      ILR=K+MLD
```

```
      IF(ILR-M)18,18,17
   17 ILR=M
   18 II=KST
      PIV=0.DO
      DO 22 I=K,ILR
      TB=DABS(A(II))
      IF(JB-PIV)20,20,19
   19 PIV=TB
      J=I
      JJ=II
   20 IF(I-MR)22,22,21
   21 ID=ID+1
   22 II=II+ID
      IF(PIV)47,47,23
   23 IF(IER)26,24,26
   24 IF(PIV-TOL)25,25,26
   25 IER=K-1
   26 PIV=1.DO/A(JJ)
      ID=J-K
      DO 27 I=K,NM,M
      II=I+ID
      TB=PIV*BB(II)
      BB(II)=BB(I)
   27 BB(I)=TB
      II=KST
      J=JJ+IC
      DO 28 I=JJ,J
      TB=PIV*A(I)
      A(I)=A(II)
      A(II)=TB
   28 II=II+1
      IF(K-ILR)29,30,30
   29 ID=KST
      II=K+1
      MU=KST+1
      MZ=KST+IC
      DO 33 I=II,ILR
      ID=ID+MC
      JJ=I-MR-1
      IF(JJ)31,31,30
   30 ID=ID-JJ
   31 PIV=-A(ID)
      J=ID+1
      DO 32 JJ=MU,MZ
      A(J-1)=A(J)+PIV*A(JJ)
   32 J=J+1
      A(J-1)=0.DO
      J=K
      DO 33 JJ=I,NM,M
      BB(JJ)=BB(JJ)+PIV*BB(J)
   33 J=J+M
   34 KST=KST+MC
      IF(ILR-MR)36,35,35
   35 IC=IC-1
   36 ID=K-MR
      IF(ID)38,38,37
   37 KST=KST-ID
   38 CONTINUE
```

```
      IF(MC-1)46,46,39
   39 IC=2
      KST=MA+ML-MC+2
      II=M
      DO 45 I=2,M
      KST=KST+MC
      II=II-1
      J=II-MR
      IF(J)41,41,40
   40 KST=KST+J
   41 DO 43 J=II,NM,M
      TB=BB(J)
      MZ=KST+IC-2
      ID=J
      DO 42 JJ=KST,MZ
      ID=ID+1
   42 TB=TB-A(JJ)*BB(ID)
   43 BB(J)=TB
      IF(IC-MC)44,45,45
   44 IC=IC+1
   45 CONTINUE
   46 RETURN
   47 IER=-1
      PRINT 48,IER
   48 FORMAT('0','IER=',I5)
      RETURN
      END
```

APPENDIX C

TABULATED DATA FOR SELECTED SIMULATIONS

Table: C.1
Simulation Results For Run ABRS 1 (No Bottom Water)
(ABERFELDY)

Legend:

T : Time, Days
OPR : Oil Production Rate, Bbls/Day
WPR : Water Production Rate, Bbls/Day
WOR : Cumulative Water-Oil Ratio, Bbl/Bbl
CSI : Cumulative Steam Injected, Bbls.
OSR : Cumulative Oil-Steam Ratio, Bbl/Bbl

T	OPR	WPR	WOR	CSI	OSR
44.1	19.39	248.98	12.84	26441	0.0324
72.4	19.74	280.34	14.20	43424	0.0325
110.2	20.67	335.40	16.23	66098	0.0330
159.5	27.52	468.79	17.03	95686	0.0352
201.8	36.50	562.39	15.41	121107	0.0395
241.2	49.14	618.93	12.59	144715	0.0451
275.7	53.91	645.91	11.98	165401	0.0504
318.9	61.44	666.86	10.85	191342	0.0567
363.0	71.94	680.37	9.46	217825	0.0634
397.2	83.58	689.04	8.24	238314	0.0692
438.6	105.51	696.03	6.60	263184	0.0778
483.0	154.13	680.26	4.41	289789	0.0910
515.3	218.08	718.76	3.30	309163	0.1047
559.8	292.39	762.70	2.61	335913	0.1339
599.7	391.77	1129.33	2.88	359838	0.1626
640.8	453.14	1171.98	2.59	384507	0.1983
679.3	495.10	872.89	1.76	407573	0.2315
720.9	582.36	747.13	1.28	432567	0.2701
758.1	657.15	670.27	1.02	454874	0.3082
802.9	788.31	671.95	0.85	481723	0.3592
840.3	1009.93	746.02	0.74	504158	0.4092

Table: C.2
Simulation Results For Run ABRS 2 Bottom Water
(ABERFELDY)

Legend:

T : Time, Days
OPR : Oil Production Rate, Bbls/Day
WPR : Water Production Rate, Bbls/Day
WOR : Cumulative Water-Oil Ratio, Bbl/Bbl
CSI : Cumulative Steam Injected, Bbls
OSR : Cumulative Oil-Steam Ratio, Bbl/Bbl

T	OPR	WPR	WOR	CSI	OSR
58.2	8.90	61.09	6.86	34938	0.0152
110.3	8.96	171.73	19.17	66199	0.0151
173.2	12.59	279.93	22.23	103926	0.0163
225.7	15.48	362.63	23.42	135427	0.0181
265.7	17.39	419.31	24.11	159427	0.0197
325.7	19.92	493.72	24.78	195427	0.0219
385.7	22.19	555.73	25.05	231427	0.0241
445.7	24.34	606.62	24.92	267427	0.0261
485.7	25.79	635.25	24.63	291427	0.0275
545.7	28.12	671.61	23.88	327427	0.0294
605.7	30.85	701.57	22.74	363427	0.0315
659.8	34.51	742.41	21.51	395888	0.0334
719.1	40.39	802.80	19.87	431452	0.0358
769.3	45.83	818.61	17.86	461611	0.0383
829.3	52.80	830.69	15.73	497611	0.0417
889.3	53.34	832.59	15.61	533611	0.0448
929.3	53.70	830.37	15.46	557611	0.0468
989.3	54.69	830.39	15.18	593611	0.0494
1045.6	56.07	832.00	14.84	627339	0.0517
1100.0	66.88	1016.96	15.20	660000	0.0542

Table: C.3
Simulation Results For Run ABRS 3 (No Bottom Water)
(ABERFELDY)

Legend:

T : Time, Days
OPR : Oil Production Rate, Bbls/Day
WPR : Water Production Rate, Bbls/Day
WOR : Cumulative Water-Oil Ratio, Bbl/Bbl
CSI : Cumulative Steam Injected, Bbls
OSR : Cumulative Oil-Steam Ratio, Bbl/Bbl

T	OPR	WPR	WOR	CSI	OSR
57.5	19.50	254.26	13.04	34514	0.0324
100.7	20.34	310.08	15.24	60399	0.0328
160.7	25.64	429.55	16.75	96399	0.0348
221.9	39.66	562.33	14.18	133138	0.0408
281.8	52.10	631.96	12.13	169060	0.0494
324.2	58.74	661.51	11.26	194500	0.0552
387.0	72.72	685.67	9.43	232198	0.0642
440.6	93.58	696.53	7.44	264387	0.0733
498.0	145.08	696.99	4.80	298816	0.0878
544.0	245.00	712.40	2.91	326410	0.1088
608.3	249.05	699.98	2.81	364982	0.1405
657.9	277.49	721.62	2.60	394728	0.1634
715.3	323.78	691.44	2.14	429155	0.1909
769.3	558.73	987.30	1.77	461566	0.2266
825.3	849.51	1083.01	1.27	495211	0.2935
881.2	786.55	743.81	0.95	528696	0.3732
935.3	702.34	657.65	0.94	561213	0.4183
989.8	792.09	661.19	0.84	593882	0.4658
1045.4	938.10	524.76	0.56	627264	0.5176
1100.0	1578.38	1237.53	0.78	660000	0.5915

Table: C.4
Simulation Results For Run ABRS 4 (No Bottom Water)
(ABERFELDY)

Legend:

T : Time, Days
OPR : Oil Production Rate, Bbls/Day
WPR : Water Production Rate, Bbls/Day
WOR : Cumulative Water–Oil Ratio, Bbl/Bbl
CSI : Cumulative Steam Injected, Bbls
OSR : Cumulative Oil–Steam Ratio, Bbl/Bbl

T	OPR	WPR	WOR	CSI	OSR
42.1	19.60	316.43	16.14	50574	0.0162
77.9	31.36	645.38	20.58	93445	0.0182
122.0	45.02	963.51	21.40	146468	0.0235
159.4	55.71	1126.44	20.22	191254	0.0280
201.5	71.43	1230.22	17.22	241780	0.0333
240.5	92.49	1285.60	13.90	288598	0.0393
283.9	106.92	1299.10	12.15	340739	0.0460
319.7	124.32	1293.96	10.41	383611	0.0518
360.3	182.41	1582.91	8.68	432352	0.0599
399.2	281.92	1796.82	6.37	479072	0.0731
437.8	358.56	1501.81	4.19	525347	0.0902
479.5	524.17	1339.84	2.56	575374	0.1147
519.3	720.12	1417.76	1.97	623202	0.1483
557.8	737.30	1316.03	1.78	669347	0.1800
597.1	777.80	1219.63	1.57	716472	0.2098
637.6	863.08	1087.38	1.26	765115	0.2402
681.4	969.37	1146.21	1.18	817738	0.2743
719.4	1096.35	1286.48	1.17	863308	0.3052
759.3	1154.36	1241.38	1.08	911195	0.3395
780.8	1184.55	1298.50	1.10	936935	0.3566

Table: C.5
Simulation Results For Run ABRS 5 Bottom Water
(ABERFELDY)

Legend:

T : Time, Days
OPR : Oil Production Rate, Bbls/Day
WPR : Water Production Rate, Bbls/Day
WOR : Cumulative Water-Oil Ratio, Bbl/Bbl
CSI : Cumulative Steam Injected, Bbls
OSR : Cumulative Oil-Steam Ratio, Bbl/Bbl

T	OPR	WPR	WOR	CSI	OSR
37.6	9.38	102.26	10.90	22554	0.0157
75.1	9.37	174.84	18.66	45074	0.0157
107.4	12.78	263.19	20.59	64421	0.0168
138.9	15.82	341.47	21.58	83349	0.0186
177.6	19.25	427.93	22.23	106553	0.0211
209.5	22.04	491.06	22.28	125685	0.0233
248.2	25.70	558.66	21.74	148905	0.0261
288.2	30.33	620.33	20.45	172905	0.0292
315.9	34.44	659.43	19.14	189535	0.0315
347.2	41.04	710.97	17.32	208309	0.0344
387.8	55.19	768.41	13.92	232697	0.0394
423.7	61.00	806.97	13.23	254250	0.0445
461.8	65.90	839.68	12.74	277065	0.0496
485.7	69.70	860.74	12.35	291414	0.0528
528.8	78.73	901.05	11.44	317291	0.0587
560.2	87.93	931.53	10.59	336105	0.0633
596.0	136.33	1384.36	10.15	357590	0.0704
630.3	192.01	1595.79	8.31	378176	0.0815
664.7	261.02	1474.04	5.65	398817	0.0969
689.2	450.65	1635.21	3.63	413546	0.1134

Table: C.6
Simulation Results For Run ABRS 6 Bottom Water
(ABERFELDY)

Legend:

T : Time, Days
OPR : Oil Production Rate, Bbls/Day
WPR : Water Production Rate, Bbls/Day
WOR : Cumulative Water-Oil Ratio, Bbl/Bbl
CSI : Cumulative Steam Injected, Bbls
OSR : Cumulative Oil-Steam Ratio, Bbl/Bbl

T	OPR	WPR	WOR	CSI	OSR
24.3	9.46	104.68	11.07	14611	0.0158
54.1	9.43	137.75	14.60	32470	0.0158
80.3	10.08	193.87	19.23	48172	0.0159
102.7	13.10	265.75	20.28	61640	0.0169
121.4	15.22	317.08	20.83	72853	0.0181
153.8	18.78	400.47	21.30	92267	0.0204
179.5	21.69	461.34	21.27	107715	0.0225
194.2	23.46	493.82	21.05	116501	0.0238
228.5	28.26	564.48	19.97	137097	0.0270
248.5	31.81	602.74	18.95	149097	0.0290
268.5	36.30	639.48	17.62	161097	0.0314
299.2	46.11	691.95	15.00	179549	0.0356
323.7	57.67	736.75	12.77	194233	0.0395
353.5	62.66	779.57	12.44	212103	0.0447
374.3	66.78	809.13	12.11	224581	0.0483
399.4	72.82	843.46	11.58	239657	0.0527
423.0	80.00	876.86	10.96	253829	0.0571
448.8	90.04	912.44	10.13	269290	0.0620
475.6	103.73	936.48	9.03	285383	0.0677
500.1	163.04	1361.15	8.35	300072	0.0751
525.2	246.88	1602.98	6.49	315107	0.0878

Table: C.7
Simulation Results For Run ABRS 7 Bottom Water
(ABERFELDY)

Legend:

T : Time, Days
OPR : Oil Production Rate, Bbls/Day
WPR : Water Production Rate, Bbls/Day
WOR : Cumulative Water–Oil Ratio, Bbl/Bbl
CSI : Cumulative Steam Injected, Bbls
OSR : Cumulative Oil–Steam Ratio, Bbl/Bbl

T	OPR	WPR	WOR	CSI	OSR
39.1	9.35	98.64	10.54	23468	0.0157
78.0	9.32	174.93	18.76	46827	0.0156
122.3	13.60	287.50	21.14	73397	0.0172
157.9	16.63	368.54	22.18	94739	0.0192
202.6	20.04	457.92	22.85	121576	0.0219
240.6	22.86	532.09	22.88	144385	0.0243
280.6	26.03	582.64	22.38	168385	0.0268
320.6	29.77	634.59	21.32	192385	0.0295
360.4	34.46	680.37	19.75	216222	0.0322
397.0	42.29	760.87	17.99	238233	0.0353
435.9	52.75	795.96	15.09	261525	0.0393
479.5	60.05	826.17	13.76	287715	0.0446
519.3	63.75	853.25	13.38	311562	0.0491
559.0	68.55	881.23	12.86	335407	0.0535
599.8	75.10	910.64	12.13	359888	0.0581
640.7	88.87	1009.91	11.36	384428	0.0629
679.8	130.50	1402.22	10.75	407867	0.0699
719.7	169.37	1494.25	8.82	431830	0.0799
760.5	214.39	1348.68	6.29	456314	0.0928

Table: C.8
Simulation Results For Run ABRS 8 (No Bottom Water)
(ABERFELDY)

Legend:

T : Time, Days
OPR : Oil Production Rate, Bbls/Day
WPR : Water Production Rate, Bbls/Day
WOR : Cumulative Water-Oil Ratio, Bbl/Bbl
CSI : Cumulative Steam Injected, Bbls
OSR : Cumulative Oil-Steam Ratio, Bbl/Bbl

T	OPR	WPR	WOR	CSI	OSR
38.5	33.52	461.44	13.77	46160	0.0216
79.5	47.18	826.17	17.51	95440	0.0284
117.1	57.06	1027.66	18.01	140531	0.0335
159.8	69.98	1148.05	16.40	191828	0.0389
199.0	88.09	1199.65	13.62	238788	0.0442
238.9	115.56	1231.61	10.66	286652	0.0514
276.7	132.21	1237.83	9.36	332011	0.0586
320.8	159.86	1224.63	7.66	385019	0.0675
355.1	195.73	1172.44	5.99	426088	0.0757
400.0	305.45	1414.04	4.63	479954	0.0900
440.0	458.05	1756.07	3.83	528015	0.1110
481.4	693.93	1631.70	2.35	577728	0.1420
519.1	841.99	1517.09	1.80	622967	0.1816
563.1	845.10	1322.64	1.56	675732	0.2222
600.4	873.02	1223.21	1.40	720464	0.2529
637.8	938.16	1086.45	1.16	765406	0.2825
680.1	1035.87	1143.88	1.10	816144	0.3163
719.2	1143.53	1263.57	1.10	863073	0.3487
762.3	1193.13	1236.52	1.04	914810	0.8351

Table: C.9
Simulation Results For Run ABRS 9 Bottom Water
(ABERFELDY)

Legend:

T : Time, Days
OPR : Oil Production Rate, Bbls/Day
WPR : Water Production Rate, Bbls/Day
WOR : Cumulative Water–Oil Ratio, Bbl/Bbl
CSI : Cumulative Steam Injected, Bbls
OSR : Cumulative Oil–Steam Ratio, Bbl/Bbl

T	OPR	WPR	WOR	CSI	OSR
23.0	9.46	105.19	11.12	13816	0.0159
54.2	9.44	135.75	14.39	32504	0.0158
80.5	9.86	188.56	19.12	48317	0.0159
103.0	12.87	259.55	20.16	61787	0.0168
121.7	15.00	310.63	20.71	73047	0.0179
154.3	18.59	394.03	21.19	92580	0.0202
180.2	21.55	455.21	21.12	108114	0.0223
194.9	23.35	487.96	20.89	116927	0.0236
224.9	27.55	552.25	20.04	134916	0.0262
247.0	31.58	602.73	19.08	148235	0.0283
273.0	37.70	656.80	17.42	163807	0.0312
294.8	44.86	697.72	15.56	176869	0.0341
326.9	59.05	755.42	12.79	196142	0.0399
343.8	61.92	779.88	12.59	206292	0.0430
373.8	67.87	822.75	12.12	224306	0.0484
402.1	75.06	864.50	11.52	241293	0.0536
427.6	83.34	902.16	10.83	256558	0.0584
451.2	93.34	936.68	10.04	270706	0.0631
475.6	110.95	1010.19	9.11	285386	0.0686
500.5	181.22	1497.22	8.26	300324	0.0772

Table: C.10
Simulation Results For Run ABRS 11 (No Bottom Water)
(ABERFELDY)

Legend:

T : Time, Days
OPR : Oil Production Rate, Bbls/Day
WPR : Water Production Rate, Bbls/Day
WOR : Cumulative Water-Oil Ratio, Bbl/Bbl
CSI : Cumulative Steam Injected, Bbls
OSR : Cumulative Oil-Steam Ratio, Bbl/Bbl

T	OPR	WPR	WOR	CSI	OSR
48.9	192.67	236.69	1.23	29347	0.3245
99.3	199.89	279.02	1.40	59577	0.3256
151.8	220.97	316.52	1.43	91108	0.3337
199.5	261.05	343.80	1.32	119725	0.3499
247.5	363.72	387.90	1.07	148533	0.3833
304.0	404.21	402.71	1.00	182414	0.4317
344.9	435.64	402.01	0.92	206922	0.4642
393.3	479.66	404.99	0.84	236013	0.5020
452.7	676.84	520.53	0.77	271605	0.5557
500.7	1152.53	841.73	0.73	300423	0.6478
550.5	1362.02	1001.65	0.74	330313	0.7903
599.5	792.25	621.85	0.78	359686	0.8643
649.1	566.81	472.01	0.83	389440	0.8835
701.1	512.01	439.67	0.86	420679	0.8829
749.4	535.22	449.78	0.84	449664	0.8819
802.6	760.10	534.26	0.70	481570	0.8943
848.5	1652.37	774.77	0.47	509115	0.9497
899.9	2364.58	1648.22	0.70	539967	1.1058
940.1	2749.35	1889.44	0.69	564061	1.2382

Table: C.11
Simulation Results For Run ABRS14 (No Bottom Water)
(ABERFELDY)

Legend:

T : Time, Days
OPR : Oil Production Rate, Bbls/Day
WPR : Water Production Rate, Bbls/Day
WOR : Cumulative Water–Oil Ratio, Bbl/Bbl
CSI : Cumulative Steam Injected, Bbls
OSR : Cumulative Oil–Steam Ratio, Bbl/Bbl

T	OPR	WPR	WOR	CSI	OSR
50.4	38.75	583.59	15.06	60456	0.0321
97.2	52.21	997.71	19.11	116623	0.0341
150.7	69.36	1223.28	17.64	180877	0.0403
198.5	90.99	1269.04	13.95	238179	0.0467
247.6	127.97	1280.89	10.01	297137	0.0560
300.4	172.30	1427.97	8.29	360446	0.0675
349.2	306.70	1861.59	6.07	419084	0.0859
397.0	433.40	1294.37	2.99	476394	0.1129
450.4	594.98	1185.37	1.99	540470	0.1514
499.2	886.99	1418.08	1.60	599095	0.1963
548.4	873.58	1344.27	1.54	658129	0.2481
603.2	855.08	1089.07	1.27	723979	0.2897
648.8	910.27	1056.50	1.16	778572	0.3215
700.0	943.83	1149.52	1.22	840023	0.3551
750.9	967.33	1137.50	1.18	901116	0.3849
800.4	2068.99	2563.11	1.24	960520	0.4319
850.9	2316.46	2453.75	1.06	1021036	0.5125
900.4	2166.26	2289.75	1.06	1080465	0.5989
949.8	1826.86	1694.96	0.93	1139819	0.6511
1000.4	1982.62	1667.34	0.84	1200529	0.6999
1050.1	3650.68	2456.51	0.67	1260107	0.7530

Table: C.12
Simulation Results For Run ABRS15 Bottom Water
(ABERFELDY)

Legend:

T : Time, Days
OPR : Oil Production Rate, Bbls/Day
WPR : Water Production Rate, Bbls/Day
WOR : Cumulative Water-Oil Ratio, Bbl/Bbl
CSI : Cumulative Steam Injected, Bbls
OSR : Cumulative Oil-Steam Ratio, Bbl/Bbl

T	OPR	WPR	WOR	CSI	OSR
32.6	9.38	97.79	10.42	19593	0.0158
56.5	9.38	137.23	14.63	33905	0.0157
93.6	11.35	227.63	20.05	56157	0.0161
122.1	14.26	301.31	21.13	73256	0.0175
144.4	16.34	355.25	21.74	86656	0.0189
184.6	19.86	443.32	22.32	110739	0.0216
218.0	22.79	507.85	22.28	130796	0.0239
237.8	24.64	542.57	22.02	142681	0.0253
277.8	28.94	606.34	20.95	166681	0.0283
297.8	31.57	635.48	20.13	178681	0.0300
330.9	37.12	683.52	18.41	198548	0.0328
361.1	45.51	750.68	16.50	216674	0.0360
393.2	58.03	788.86	13.59	235930	0.0402
420.2	60.71	812.49	13.38	252132	0.0440
450.1	64.33	840.27	13.06	270049	0.0480
478.7	68.58	867.79	12.65	287209	0.0518
512.2	74.89	900.63	12.02	307298	0.0563
540.6	81.77	927.24	11.34	324358	0.0602
570.7	94.80	1001.53	10.56	342396	0.0647
600.7	139.85	1397.79	9.99	360433	0.0713
630.1	186.54	1572.08	8.43	378071	0.0807
658.7	229.42	1455.15	6.34	395205	0.0922

Table: C.13
Simulation Results For Run ABRS16 Bottom Water
(ABERFELDY)

Legend:

T : Time, Days
OPR : Oil Production Rate, Bbls/Day
WPR : Water Production Rate, Bbls/Day
WOR : Cumulative Water-Oil Ratio, Bbl/Bbl
CSI : Cumulative Steam Injected, Bbls
OSR : Cumulative Oil-Steam Ratio, Bbl/Bbl

T	OPR	WPR	WOR	CSI	OSR
33.5	91.16	103.97	1.14	20134	0.1546
75.0	90.96	170.07	1.87	44992	0.1530
103.3	104.11	221.47	2.13	61968	0.1559
141.7	134.84	308.55	2.29	85004	0.1703
176.9	157.81	377.32	2.39	106129	0.1863
210.3	177.50	433.18	2.44	126181	0.2020
242.6	196.19	478.62	2.44	145545	0.2172
282.6	221.56	523.47	2.36	169557	0.2364
313.8	245.47	548.38	2.23	188261	0.2520
352.0	284.51	571.19	2.01	211228	0.2731
387.9	340.46	588.76	1.73	232725	0.2968
421.5	387.35	608.98	1.57	252887	0.3232
454.4	390.92	611.22	1.56	272634	0.3467
490.0	403.72	615.62	1.52	294025	0.3693
524.8	587.19	899.95	1.53	314879	0.3997
560.2	798.56	1125.00	1.41	336107	0.4483
595.5	910.61	1093.48	1.20	357277	0.5073
630.7	951.10	959.37	1.01	378428	0.5660
666.3	916.78	734.87	0.80	399766	0.6176

Table: C.14
Simulation Results For Cyclic Run ABC 1 (No Bottom Water)
(ABERFELDY)

Legend:

T : Time, Days
OPR : Oil Production Rate, Bbls/Day
WPR : Water Production Rate, Bbls/Day
WOR : Cumulative Water-Oil Ratio, Bbl/Bbl
CSI : Cumulative Steam Injected, Bbls
OSR : Cumulative Oil-Steam Ratio, Bbl/Bbl

T	OPR	WPR	WOR	CSI	OSR
		Cycle 1			
35.1	80.53	473.74	5.88	21000	0.0003
44.2	39.69	197.34	4.97	21000	0.0203
53.5	37.02	179.33	4.84	21000	0.0369
68.1	32.95	161.10	4.89	21000	0.0605
76.3	30.80	152.43	4.95	21000	0.0725
85.1	19.99	134.59	6.73	21000	0.0808
94.5	14.91	121.64	8.16	21000	0.0875
105.1	11.96	109.51	9.15	21000	0.0936
117.4	9.92	98.05	9.88	21000	0.0994
125.0	9.10	92.58	10.18	21000	0.1027

Table: C.15
Simulation Results For Cyclic Run ABC 2 (No Bottom Water)
(ABERFELDY)

Legend:

T : Time, Days
OPR : Oil Production Rate, Bbls/Day
WPR : Water Production Rate, Bbls/Day
WOR : Cumulative Water-Oil Ratio, Bbl/Bbl
CSI : Cumulative Steam Injected, Bbls
OSR : Cumulative Oil-Steam Ratio, Bbl/Bbl

T	OPR	WPR	WOR	CSI	OSR
		Cycle 1			
35.1	86.38	312.73	3.62	18000	0.0006
46.5	47.11	162.83	3.46	18000	0.0338
59.0	41.16	153.87	3.74	18000	0.0634
75.4	34.78	142.83	4.11	18000	0.0964
84.3	31.90	136.65	4.28	18000	0.1122
93.9	27.75	128.99	4.65	18000	0.1270
104.2	17.22	113.59	6.59	18000	0.1368
115.3	13.03	103.10	7.91	18000	0.1449
125.0	11.03	95.41	8.65	18000	0.1508
		Cycle 2			
170.2	62.52	297.34	4.76	42000	0.0649
180.1	21.12	330.67	15.65	42000	0.0746
190.0	7.04	376.25	53.41	42000	0.0775
200.3	9.53	482.61	50.62	42000	0.0797
210.3	8.05	387.97	48.16	42000	0.0818
221.7	4.97	301.72	60.69	42000	0.0836
229.4	3.67	260.38	70.95	42000	0.0843
242.3	2.64	202.88	76.88	42000	0.0852
250.2	2.30	177.67	77.34	42000	0.0857
260.0	2.00	153.94	76.87	42000	0.0861
		Cycle 3			
315.0	49.48	769.49	15.55	72000	0.0503
322.5	26.83	572.61	21.34	72000	0.0528

Table: C.16
Simulation Results For Cyclic Run ABC 3 (No Bottom Water)
(ABERFELDY)

Legend:

T : Time, Days
OPR : Oil Production Rate, Bbls/Day
WPR : Water Production Rate, Bbls/Day
WOR : Cumulative Water-Oil Ratio, Bbl/Bbl
CSI : Cumulative Steam Injected, Bbls
OSR : Cumulative Oil-Steam Ratio, Bbl/Bbl

T	OPR	WPR	WOR	CSI	OSR
		Cycle 1			
35.1	86.38	312.73	3.62	18000	0.0006
46.5	47.11	162.83	3.46	18000	0.0338
59.0	41.16	153.87	3.74	18000	0.0634
67.0	37.87	148.56	3.92	18000	0.0801
75.4	34.78	142.83	4.11	18000	0.0964
84.3	31.90	136.65	4.28	18000	0.1122
93.9	27.75	128.99	4.65	18000	0.1270
104.2	17.22	113.59	6.60	18000	0.1368
115.3	13.03	103.10	7.91	18000	0.1449
125.0	11.03	95.41	8.65	18000	0.1508
		Cycle 2			
150.0	78.50	509.26	6.49	30000	0.0905
160.2	32.58	197.72	6.07	30000	0.1061
170.1	12.52	180.14	14.38	30000	0.1134
180.2	9.86	257.05	26.06	30000	0.1164
191.5	9.80	234.15	23.88	30000	0.1202
200.0	9.18	207.64	22.63	30000	0.1228
209.7	8.60	182.39	21.21	30000	0.1257
221.1	6.85	150.87	22.03	30000	0.1285
227.7	5.74	138.11	24.05	30000	0.1298
240.0	4.57	119.84	26.19	30000	0.1317
		Cycle 3			
255.2	20.47	379.95	18.56	36000	0.1099
265.3	11.10	187.70	16.91	36000	0.1136
275.4	7.51	148.48	19.76	36000	0.1162
285.1	5.75	131.32	22.83	36000	0.1179
294.2	6.39	147.20	23.04	36000	0.1194
309.2	5.00	126.38	25.29	36000	0.1217
324.0	3.89	107.50	27.64	36000	0.1234
332.0	3.53	98.03	27.79	36000	0.1242
345.0	3.16	87.37	27.62	36000	0.1254

Table: C 17
Simulation Results For Cyclic Run ABC 4 (No Bottom Water)
(ABERFELDY)

Legend:

T : Time, Days
OPR : Oil Production Rate, Bbls/Day
WPR : Water Production Rate, Bbls/Day
WOR : Cumulative Water-Oil Ratio, Bbl/Bbl
CSI : Cumulative Steam Injected, Bbls
OSR : Cumulative Oil-Steam Ratio, Bbl/Bbl

T	OPR	WPR	WOR	CSI	OSR
		Cycle 1			
50.1	74.37	291.63	3.92	18000	0.0005
63.1	44.05	164.83	3.74	18000	0.0350
69.4	41.55	159.44	3.84	18000	0.0496
85.5	35.75	147.22	4.12	18000	0.0827
94.2	33.01	140.78	4.26	18000	0.0988
103.6	27.51	131.77	4.79	18000	0.1131
113.7	17.82	116.94	6.56	18000	0.1231
124.7	13.67	106.25	7.77	18000	0.1315
140.0	10.79	94.48	8.75	18000	0.1408
		Cycle 2			
190.2	53.52	627.32	11.72	36000	0.0707
200.0	32.82	344.70	10.50	36000	0.0816
210.0	11.62	291.76	25.11	36000	0.0874

Table: C.18
Simulation Results For Cyclic Run ABC 6 (Bottom Water)
(ABERFELDY)

Legend:

T : Time, Days
OPR : Oil Production Rate, Bbls/Day
WPR : Water Production Rate, Bbls/Day
WOR : Cumulative Water-Oil Ratio, Bbl/Bbl
CSI : Cumulative Steam Injected, Bbls
OSR : Cumulative Oil-Steam Ratio, Bbl/Bbl

T	OPR	WPR	WOR	CSI	OSR
		Cycle 1			
35.1	36.37	688.31	18.92	18000	0.0002
46.6	25.92	307.03	11.85	18000	0.0179
55.8	18.06	257.66	14.27	18000	0.0281
69.1	11.86	220.91	18.63	18000	0.0378
77.0	9.79	204.91	20.94	18000	0.0421
85.8	8.16	189.81	23.26	18000	0.0461
95.6	6.86	175.42	25.56	18000	0.0498
106.4	5.81	161.66	27.83	18000	0.0533
118.5	4.94	148.52	30.07	18000	0.0566
125.0	4.56	142.18	31.17	18000	0.0583
		Cycle 2			
160.2	49.05	753.48	15.36	36000	0.0294
170.1	34.74	301.60	8.68	36000	0.0407
180.0	20.69	269.63	13.03	36000	0.0477
190.0	13.36	217.49	16.27	36000	0.0528
200.2	2.81	209.64	74.56	36000	0.0549
212.6	3.23	262.16	81.14	36000	0.0560
225.9	3.21	228.31	71.17	36000	0.0571
234.5	3.22	209.84	65.11	36000	0.0579
244.2	3.20	191.84	59.93	36000	0.0588
250.0	3.16	181.87	57.57	36000	0.0593
		Cycle 3			
285.5	31.38	513.08	16.35	54000	0.0398
295.1	13.58	328.99	24.22	54000	0.0440

Table: C.19
Simulation Results For Cyclic Run ABC 8 (Bottom Water)
(ABERFELDY)

Legend:

T : Time, Days
OPR : Oil Production Rate, Bbls/Day
WPR : Water Production Rate, Bbls/Day
WOR : Cumulative Water-Oil Ratio, Bbl/Bbl
CSI : Cumulative Steam Injected, Bbls
OSR : Cumulative Oil-Steam Ratio, Bbl/Bbl

T	OPR	WPR	WOR	CSI	OSR
		Cycle 1			
35.1	36.37	688.31	18.92	18000	0.0002
46.6	25.92	307.03	11.85	18000	0.0179
55.8	18.06	257.66	14.27	18000	0.0281
69.1	11.86	220.91	18.63	18000	0.0378
77.0	9.79	204.91	20.94	18000	0.0421
85.8	8.16	189.81	23.26	18000	0.0461
95.6	6.86	175.42	25.56	18000	0.0498
106.4	5.81	161.66	27.83	18000	0.0533
118.5	4.94	148.52	30.07	18000	0.0566
125.0	4.56	142.18	31.17	18000	0.0583
		Cycle 2			
150.0	30.91	619.62	20.04	30000	0.0351
160.2	20.68	346.31	16.74	30000	0.0426
174.9	17.73	251.64	14.19	30000	0.0517
181.9	16.48	231.03	14.01	30000	0.0555
189.9	15.19	212.61	14.00	30000	0.0596
198.9	13.90	195.64	14.08	30000	0.0638
209.1	12.64	179.83	14.23	30000	0.0681
220.7	11.42	165.04	14.44	30000	0.0725
234.0	10.28	151.26	14.71	30000	0.0770
240.0	9.82	145.13	14.77	30000	0.0790
		Cycle 3			
255.2	17.38	388.90	22.38	36000	0.0659
265.1	13.07	253.49	19.39	36000	0.0698
277.4	11.43	203.85	17.83	36000	0.0739
287.2	10.73	181.80	16.95	36000	0.0769
299.6	9.88	162.78	16.47	36000	0.0804
310.6	9.18	149.71	16.31	36000	0.0832
327.2	7.81	131.43	16.82	36000	0.0870
337.5	7.36	126.45	17.17	36000	0.0891
345.0	7.00	119.83	17.11	36000	0.0906

Table: C.20
Simulation Results For Cyclic Run ABC 9 (Bottom Water)
(ABERFELDY)

Legend:

T : Time, Days
OPR : Oil Production Rate, Bbls/Day
WPR : Water Production Rate, Bbls/Day
WOR : Cumulative Water-Oil Ratio, Bbl/Bbl
CSI : Cumulative Steam Injected, Bbls
OSR : Cumulative Oil-Steam Ratio, Bbl/Bbl

T	OPR	WPR	WOR	CSI	OSR
		Cycle 1			
50.1	35.87	647.04	18.04	18000	0.0002
60.5	24.09	307.43	12.76	18000	0.0158
70.9	15.93	263.25	16.52	18000	0.0260
84.5	10.95	228.59	20.87	18000	0.0350
92.4	9.22	212.47	23.04	18000	0.0391
101.1	7.83	196.93	25.16	18000	0.0429
110.1	6.69	181.97	27.22	18000	0.0464
121.4	5.74	167.63	29.21	18000	0.0498
133.3	4.94	153.97	31.16	18000	0.0531
140.0	4.58	146.98	32.12	18000	0.0548
		Cycle 2			
190.0	41.36	805.69	19.48	36000	0.0274
200.6	25.05	406.59	16.23	36000	0.0357
207.3	15.58	317.76	20.40	36000	0.0395

Table: C.21
Simulation Results For Cyclic Run ABC11 (Bottom Water)
(ABERFELDY)

Legend:

T : Time, Days
OPR : Oil Production Rate, Bbls/Day
WPR : Water Production Rate, Bbls/Day
WOR : Cumulative Water-Oil Ratio, Bbl/Bbl
CSI : Cumulative Steam Injected, Bbls
OSR : Cumulative Oil-Steam Ratio, Bbl/Bbl

T	OPR	WPR	WOR	CSI	OSR
		Cycle 1			
37.8	30.51	196.40	6.44	18000	0.0048
47.0	25.61	197.74	7.72	18000	0.0184
58.4	21.23	197.21	9.29	18000	0.0325
65.1	19.20	195.47	10.18	18000	0.0396
72.5	17.29	192.67	11.14	18000	0.0468
90.5	13.77	183.59	13.33	18000	0.0613
101.5	12.16	177.13	14.56	18000	0.0688
114.2	10.72	170.18	15.87	18000	0.0764
125.0	9.75	164.58	16.87	18000	0.0822
		Cycle 2			
160.5	28.36	289.28	10.20	36000	0.0415
170.0	1.95	435.73	223.49	36000	0.0455
179.4	1.74	510.80	293.36	36000	0.0460
190.3	1.32	432.07	326.87	36000	0.0465
197.9	1.12	387.34	344.63	36000	0.0467
216.1	0.81	302.88	374.37	36000	0.0471
227.1	0.68	263.03	386.07	36000	0.0473
239.9	0.57	217.07	381.77	36000	0.0476
250.0	0.50	186.99	374.12	36000	0.0477

Table: C.22
Simulation Results For Cyclic Run ABC17 (Bottom Water)
(ABERFELDY)

Legend:

T : Time, Days
OPR : Oil Production Rate, Bbls/Day
WPR : Water Production Rate, Bbls/Day
WOR : Cumulative Water-Oil Ratio, Bbl/Bbl
CSI : Cumulative Steam Injected, Bbls
OSR : Cumulative Oil-Steam Ratio, Bbl/Bbl

T	OPR	WPR	WOR	CSI	OSR
		Cycle 1			
36.8	30.19	201.54	6.67	18000	0.0030
48.1	24.38	200.93	8.24	18000	0.0194
54.1	22.11	199.98	9.04	18000	0.0268
68.5	17.92	194.75	10.87	18000	0.0419
77.2	16.00	190.29	11.89	18000	0.0496
87.2	14.18	184.46	13.01	18000	0.0575
99.0	12.46	177.15	14.21	18000	0.0656
112.9	10.84	168.18	15.52	18000	0.0740
125.0	9.75	161.13	16.53	18000	0.0806
		Cycle 2			
160.7	29.67	292.63	9.86	36000	0.0409
170.0	21.00	316.48	15.07	36000	0.0472
179.6	3.58	451.36	125.99	36000	0.0493
191.3	2.91	387.27	133.17	36000	0.0503
199.6	2.60	350.67	134.78	36000	0.0509
208.8	2.34	316.10	135.17	36000	0.0515
219.0	2.09	282.80	135.30	36000	0.0521
230.6	1.87	251.27	134.65	36000	0.0527
243.8	1.66	221.38	133.44	36000	0.0533
250.0	1.57	208.57	132.79	36000	0.0536
		Cycle 3			
286.7	14.88	331.36	22.26	54000	0.0362
298.0	2.94	372.76	126.67	54000	0.0382

Table: C.23
Cyclic Run CLC1A (No Bottom Water)
(COLD LAKE)

Legend:

T : Time, Days
OPR : Oil Production Rate, Bbls/Day
WPR : Water Production Rate, Bbls/Day
WOR : Cumulative Water–Oil Ratio, Bbl/Bbl
CSI : Cumulative Steam Injected, Bbls
OSR : Cumulative Oil–Steam Ratio, Bbl/Bbl

T	OPR	WPR	WOR	CSI	OSR
		Cycle 1			
35.8	16.87	72.22	4.28	18000	0.0008
46.0	9.59	42.27	4.40	18000	0.0078
55.9	5.87	25.93	4.42	18000	0.0118
64.5	3.75	17.02	4.54	18000	0.0139
71.8	3.16	14.11	4.47	18000	0.0153
84.0	2.24	9.93	4.44	18000	0.0169
94.9	1.69	7.98	4.73	18000	0.0180
106.7	1.31	6.99	5.32	18000	0.0189
113.4	1.19	6.42	5.41	18000	0.0194
125.0	0.84	5.28	6.25	18000	0.0199
		Cycle 2			
160.2	21.17	330.79	15.62	36000	0.0101
170.5	13.86	127.92	9.23	36000	0.0152
179.8	8.22	77.32	9.41	36000	0.0179
189.2	4.50	54.31	12.06	36000	0.0194
199.6	2.58	41.39	16.04	36000	0.0203
210.1	1.55	31.76	20.52	36000	0.0208
220.0	1.14	26.60	23.31	36000	0.0212
231.9	0.78	20.12	25.71	36000	0.0215
239.7	0.67	17.75	26.37	36000	0.0216
250.0	0.51	13.73	26.77	36000	0.0218
		Cycle 3			
285.2	1.72	573.97	333.39	54000	0.0145
295.0	0.55	189.02	346.61	54000	0.0147

Table: C.24
Cyclic Run CLC6A (Bottom Water) 36FT/36 FT
(COLD LAKE)

Legend:

T : Time, Days
OPR : Oil Production Rate, Bbls/Day
WPR : Water Production Rate, Bbls/Day
WOR : Cumulative Water-Oil Ratio, Bbl/Bbl
CSI : Cumulative Steam Injected, Bbls
OSR : Cumulative Oil-Steam Ratio, 10^{-3} Bbl/Bbl

T	OPR	WPR	WOR	CSI	OSR
		Cycle 1			
35.2	0.06	100.46	1814.86	18000	0.0005
43.7	0.05	67.67	1344.86	18000	0.0253
52.5	0.05	53.89	1146.04	18000	0.0486
68.4	0.04	46.39	1115.95	18000	0.0865
82.4	0.04	44.10	1174.04	18000	0.1157
102.4	0.03	42.90	1290.09	18000	0.1526
125.0	0.03	43.02	1441.68	18000	0.1905

Table: C.25
Cyclic Run CLC11A (Bottom Water) 36FT/36FT
(COLD LAKE)

Legend:

T : Time, Days
OPR : Oil Production Rate, Bbls/Day
WPR : Water Production Rate, Bbls/Day
WOR : Cumulative Water-Oil Ratio, Bbl/Bbl
CSI : Cumulative Steam Injected, Bbls
OSR : Cumulative Oil-Steam Ratio, 10^{-3} Bbl/Bbl

T	OPR	WPR	WOR	CSI	OSR
		Cycle 1			
36.0	0.54	51.79	95.97	18000	0.0313
48.7	0.47	49.30	104.87	18000	0.3790
56.7	0.44	48.26	110.42	18000	0.5713
68.5	0.40	46.92	118.30	18000	0.8330
86.3	0.35	45.24	128.75	18000	1.1807
106.3	0.31	43.71	140.29	18000	1.5270
125.0	0.20	39.19	197.77	18000	1.7320
		Cycle 2			
160.1	0.89	36.56	41.26	36000	0.8696
163.4	0.03	90.82	3619.71	36000	0.9105

Table: C.26
BOTTOM WATER (36FT/36FT) STEAMFLOOD; ABERFELDY RUN ABRS2A
INJ. OVER ENTIRE INTERVAL; MOBILE OIL (50%) IN BW ZONE
INJ. RATE 600 BBLS/DAY

Legend:

T : Time, Days
OPR : Oil Production Rate, Bbls/Day
WPR : Water Production Rate, Bbls/Day
WOR : Cumulative Water-Oil Ratio, Bbl/Bbl
CSI : Cumulative Steam Injected, 10^5 Bbls
ORec : Oil Recovery, %
OSR : Cumulative Oil-Steam Ratio, Bbl/Bbl

T	OPR	WPR	WOR	CSI	ORec	OSR
47	13.8	168	12.20	0.283	0.03	0.0204
102	17.4	260	14.90	0.612	0.07	0.0239
152	20.0	340	17.00	0.911	0.11	0.0266
211	22.6	424	18.70	1.265	0.17	0.0293
251	24.3	471	19.40	1.504	0.21	0.0310
311	26.6	532	20.00	1.865	0.28	0.0333
351	28.1	567	20.20	2.105	0.33	0.0348
411	30.2	612	20.30	2.465	0.41	0.0369
451	31.7	638	20.10	2.705	0.47	0.0382
511	34.2	671	19.60	3.065	0.56	0.0403
551	36.1	690	19.10	3.305	0.62	0.0416
611	39.5	713	18.10	3.665	0.72	0.0438
651	42.4	728	17.20	3.905	0.80	0.0454
701	47.5	756	15.90	4.204	0.90	0.0476
754	56.8	822	14.50	4.522	1.03	0.0504
799	64.5	836	13.00	4.795	1.15	0.0534
849	64.6	826	12.80	5.094	1.30	0.0566
899	65.4	824	12.60	5.393	1.44	0.0594
959	67.4	830	12.30	5.753	1.62	0.0627
999	68.5	825	12.00	5.993	1.75	0.0647
1059	71.2	823	11.60	6.353	1.94	0.0677
1100	73.7	822	11.20	6.600	2.07	0.0697

Table: C.27
PARTIAL PENETRATION STEAMFLOOD: ABERFELDY RUN ABRS1B; NO BOTTOM WATER
INJ. RATE 600 BBLS/DAY; INJ. OVER LOWER ONE-HALF INTERVAL

Legend:

T : Time, Days
OPR : Oil Production Rate, Bbls/Day
WPR : Water Production Rate, Bbls/Day
WOR : Cumulative Water-Oil Ratio, Bbl/Bbl
CSI : Cumulative Steam Injected, 10^5 Bbls
ORec : Oil Recovery, %
OSR : Cumulative Oil-Steam Ratio, Bbl/Bbl

T	OPR	WPR	WOR	CSI	ORec	OSR
51	16.6	204	12.20	0.308	0.05	0.0277
108	17.2	298	17.30	0.646	0.11	0.0279
152	22.2	428	19.30	0.910	0.16	0.0294
212	28.4	543	19.10	1.272	0.25	0.0335
252	32.2	688	18.30	1.512	0.33	0.0363
304	37.8	621	16.40	1.823	0.44	0.0402
344	43.8	632	14.40	2.067	0.54	0.0436
413	61.0	641	10.50	2.479	0.75	0.0509
462	82.1	645	7.86	2.773	0.97	0.0586
518	95.1	642	6.74	3.111	1.28	0.0687
551	103.0	639	6.21	3.305	1.47	0.0745
610	129.0	690	5.35	3.658	1.88	0.0863
666	154.0	643	4.16	3.996	2.37	0.0995
701	184.0	683	3.70	4.205	2.72	0.1084
754	262.0	828	3.15	4.522	3.43	0.1270
804	336.0	778	2.32	4.823	4.33	0.1500
847	432.0	775	1.79	5.083	5.32	0.1750
901	668.0	821	1.23	5.406	7.08	0.2190
948	730.0	802	1.10	5.686	9.14	0.2690
1009	666.0	703	1.06	6.055	11.68	0.3230
1058	655.0	682	1.04	6.346	13.58	0.3580
1100	640.0	662	1.03	6.600	15.22	0.3860

Table: C.28
BOTTOM WATER (36FT/36FT) CYCLIC RUN: ABERFELDY RUN ABC18
PARTIAL PENETRATION; COMPLETION TOP 18 FT
(STEAM INJ. 30 DAYS; SOAK 5 DAYS)

Legend:

T : Time, Days
OPR : Oil Production Rate, Bbls/Day
WPR : Water Production Rate, Bbls/Day
WOR : Cumulative Water-Oil Ratio, Bbl/Bbl
CSI : Cumulative Steam Injected, 10^5Bbls
ORec : Oil Recovery, %
OSR : Cumulative Oil-Steam Ratio, Bbl/Bbl

T	OPR	WPR	WOR	CSI	ORec	OSR
			Cycle 1			
37	1.5	4.35	2.85	0.180	0.000	0.0001
43	1.4	4.24	2.99	0.180	0.001	0.0007
58	1.3	4.09	3.25	0.180	0.003	0.0017
71	1.2	3.99	3.44	0.180	0.005	0.0026
91	1.1	3.86	3.63	0.180	0.007	0.0037
111	1.0	3.77	3.77	0.180	0.009	0.0048
125	1.0	3.71	3.85	0.180	0.011	0.0056
			Cycle 2			
161	7.5	15.20	2.00	0.360	0.012	0.0030
168	7.0	14.90	2.10	0.360	0.017	0.0044
181	4.6	13.60	2.97	0.360	0.024	0.0062
192	3.6	12.70	3.49	0.360	0.028	0.0074
209	2.9	11.70	4.00	0.360	0.034	0.0087
229	2.5	10.80	4.40	0.360	0.039	0.0101
249	2.2	10.14	4.59	0.360	0.044	0.0113
250	2.2	10.10	4.60	0.360	0.044	0.0114
			Cycle 3			
285	9.8	28.50	2.90	0.540	0.044	0.0076
291	9.6	28.00	2.93	0.540	0.050	0.0087
306	9.2	27.30	2.97	0.540	0.065	0.0112
316	9.0	26.80	2.98	0.540	0.075	0.0130
332	8.8	26.10	2.98	0.540	0.090	0.0155
352	8.6	25.20	2.94	0.540	0.108	0.0187
375	8.1	24.10	2.97	0.540	0.129	0.0222

APPENDIX D

TABULATED DATA FOR WELLBORE HEAT LOSS

Table: D.1
STEAM QUALITY VS. DEPTH FOR DIFFERENT RATES AND ZERO AND ONE-HALF STEAM OFF-TAKE AT 1200 FT DEPTH; TIME = 100 DAYS INJ. PRESS. 1500PSIA

Legend:

D : Depth, FT
N O-T : No Off-Take
H O-T : Half Off-Take

Steam Quality, Fraction

	600 Bbls/Day		1200 Bbls/Day		1800 Bbls/Day	
D	N O-T	H O-T	N O-T	H O-T	H O-T	N O-T
0	0.8000	0.8000	0.8000	0.8000	0.8000	0.8000
150	0.7718	0.7718	0.7858	0.7858	0.7904	0.7940
300	0.7435	0.7435	0.7715	0.7715	0.7809	0.7809
450	0.7151	0.7151	0.7573	0.7573	0.7713	0.7713
600	0.6864	0.6864	0.7429	0.7429	0.7617	0.7617
750	0.6574	0.6574	0.7285	0.7285	0.7521	0.7521
900	0.6283	0.6283	0.7140	0.7140	0.7424	0.7424
1050	0.5989	0.5705	0.6995	0.6854	0.7327	0.7234
1200	0.5693	0.5120	0.6849	0.6566	0.7230	0.7042
1350	0.5394	0.4530	0.6702	0.6275	0.7132	0.6850
1500	0.4779	0.3298	0.6402	0.5674	0.6934	0.6453

Table: D.2
STEAM QUALITY VS. DEPTH FOR DIFFERENT RATES AND ZERO AND ONE-HALF STEAM OFF-TAKE AT 1200 FT DEPTH; TIME = 300 DAYS INJ. PRESS. 1500PSIA

Legend:

D : Depth, FT
N O-T : No Off-Take
H O-T : Half Off-Take

Steam Quality, Fraction

	600 Bbls/Day		1200 Bbls/Day		1800 Bbls/Day	
D	N O-T	H O-T	N O-T	H O-T	H O-T	N O-T
0	0.8000	0.8000	0.8000	0.8000	0.8000	0.8000
150	0.7731	0.7731	0.7864	0.7864	0.7909	0.7909
300	0.7461	0.7461	0.7728	0.7728	0.7817	0.7817
450	0.7188	0.7188	0.7592	0.7592	0.7726	0.7726
600	0.6914	0.6914	0.7454	0.7454	0.7634	0.7634
750	0.6638	0.6638	0.7317	0.7317	0.7542	0.7542
900	0.6360	0.6360	0.7178	0.7178	0.7449	0.7449
1050	0.6079	0.5808	0.7039	0.6905	0.7357	0.7267
1200	0.5796	0.5250	0.6900	0.6629	0.7264	0,7085
1350	0.5511	0.4685	0.6759	0.6352	0.7170	0.6901
1500	0.4897	0.3454	0.6460	0.5751	0.6972	0.6505

Table: D.3
STEAM QUALITY VS. DEPTH FOR DIFFERENT RATES AND ZERO AND ONE-HALF STEAM OFF-TAKE AT 1200 FT DEPTH; TIME = 500 DAYS INJ. PRESS. 1500PSIA

Legend:

D : Depth, FT
N O-T : No Off-Take
H O-T : Half Off-Take

Steam Quality, Fraction

D	600 Bbls/Day		1200 Bbls/Day		1800 Bbls/Day	
	N O-T	H O-T	N O-T	H O-T	H O-T	N O-T
0	0.8000	0.8000	0.8000	0.8000	0.8000	0.8000
150	0.7731	0.7731	0.7864	0.7864	0.7909	0.7909
300	0.7461	0.7461	0.7728	0.7728	0.7817	0.7817
450	0.7189	0.7189	0.7592	0.7592	0.7726	0.7726
600	0.6916	0.6916	0.7455	0.7455	0.7634	0.7634
750	0.6640	0.6640	0.7317	0.7317	0.7542	0.7542
900	0.6362	0.6362	0.7179	0.7179	0.7450	0.7450
1050	0.6081	0.5810	0.7040	0.6906	0.7357	0.7268
1200	0.5799	0.5253	0.6901	0.6631	0.7265	0.7086
1350	0.5514	0.4689	0.6761	0.6353	0.7171	0.6902
1500	0.4900	0.3458	0.6461	0.5753	0.6973	0.6506

Table: D.4
STEAM QUALITY VS. DEPTH FOR DIFFERENT RATES AND ZERO AND ONE-HALF STEAM OFF-TAKE AT 1200 FT DEPTH; TIME = 700 DAYS INJ. PRESS. 1500PSIA

Legend:

D : Depth, FT
N O-T : No Off-Take
H O-T : Half Off-Take

Steam Quality, Fraction

	600 Bbls/Day		1200 Bbls/Day		1800 Bbls/Day	
D	N O-T	H O-T	N O-T	H O-T	H O-T	N O-T
0	0.8000	0.8000	0.8000	0.8000	0.8000	0.8000
150	0.7731	0.7731	0.7864	0.7864	0.7909	0.7909
300	0.7461	0.7461	0.7728	0.7728	0.7817	0.7817
450	0.7189	0.7189	0.7592	0.7592	0.7726	0.7726
600	0.6916	0.6916	0.7455	0.7455	0.7634	0.7634
750	0.6640	0.6640	0.7317	0.7317	0.7542	0.7542
900	0.6362	0.6362	0.7179	0.7179	0.7450	0.7450
1050	0.6081	0.5810	0.7040	0.6906	0.7357	0.7268
1200	0.5799	0.5253	0.6901	0.6631	0.7265	0.7086
1350	0.5514	0.4689	0.6761	0.6354	0.7171	0.6902
1500	0.4900	0.3458	0.6461	0.5753	0.6973	0.6506

Table: D.5
STEAM QUALITY VS. DEPTH FOR DIFFERENT RATES AND ZERO AND ONE-HALF STEAM OFF-TAKE AT 1200 FT DEPTH; TIME = 900 DAYS INJ. PRESS. 1500PSIA

Legend:

D : Depth, FT
N O-T : No Off-Take
H O-T : Half Off-Take

Steam Quality, Fraction

	600 Bbls/Day		1200 Bbls/Day		1800 Bbls/Day	
D	N O-T	H O-T	N O-T	H O-T	H O-T	N O-T
0	0.8000	0.8000	0.8000	0.8000	0.8000	0.8000
150	0.7731	0.7731	0.7864	0.7864	0.7909	0.7909
300	0.7461	0.7461	0.7728	0.7728	0.7817	0.7817
450	0.7189	0.7189	0.7592	0.7592	0.7726	0.7726
600	0.6916	0.6916	0.7455	0.7455	0.7634	0.7634
750	0.6640	0.6640	0.7317	0.7317	0.7542	0.7542
900	0.6362	0.6362	0.7179	0.7179	0.7450	0.7450
1050	0.6081	0.5810	0.7040	0.6906	0.7357	0.7268
1200	0.5799	0.5253	0.6901	0.6631	0.7265	0.7086
1350	0.5514	0.4689	0.6761	0.6354	0.7171	0.6902
1500	0.4900	0.3458	0.6461	0.5753	0.6973	0.6506

Table: D.6
STEAM QUALITY VS. DEPTH FOR DIFFERENT RATES AND ZERO AND ONE-HALF STEAM OFF-TAKE AT 1200 FT DEPTH; TIME = 1100 DAYS INJ. PRESS. 1500PSIA

Legend:

D : Depth, FT.
N O-T : No Off-Take
H O-T : Half Off-Take

Steam Quality, Fraction

	600 Bbls/Day		1200 Bbls/Day		1800 Bbls/Day	
D	N O-T	H O-T	N O-T	H O-T	H O-T	N O-T
0	0.8000	0.8000	0.8000	0.8000	0.8000	0.8000
150	0.7731	0.7731	0.7864	0.7864	0.7909	0.7909
300	0.7461	0.7461	0.7728	0.7728	0.7817	0.7817
450	0.7189	0.7189	0.7592	0.7592	0.7726	0.7726
600	0.6916	0.6916	0.7455	0.7455	0.7634	0.7634
750	0.6640	0.6640	0.7317	0.7317	0.7542	0.7542
900	0.6362	0.6362	0.7179	0.7179	0.7450	0.7450
1050	0.6081	0.5810	0.7040	0.6906	0.7357	0.7268
1200	0.5799	0.5253	0.6901	0.6631	0.7265	0.7086
1350	0.5514	0.4689	0.6761	0.6354	0.7171	0.6902
1500	0.4900	0.3458	0.6461	0.5753	0.6973	0.6506

Table: D.7
STEAM QUALITY VS. DEPTH FOR DIFFERENT RATES AND ZERO AND ONE-HALF STEAM OFF-TAKE AT 1200 FT DEPTH; TIME = 100 DAYS INJ. PRESS. 1500PSIA

Legend:

D : Depth, FT
N O-T : No Off-Take
H O-T : Half Off-Take

Steam Pressure, psia

	600 Bbls/Day		1200 Bbls/Day		1800 Bbls/Day	
D	N O-T	H O-T	N O-T	H O-T	H O-T	N O-T
0	1500.0	1500.0	1500.0	1500.0	1500.0	1500.0
150	1525.0	1525.0	1519.6	1519.6	1517.2	1517.2
300	1550.5	1550.5	1539.4	1539.4	1534.6	1534.6
450	1576.4	1576.4	1559.5	1559.5	1552.2	1552.2
600	1602.9	1602.9	1579.8	1579.8	1569.9	1569.9
750	1629.9	1629.9	1600.3	1600.3	1587.7	1587.7
900	1657.5	1657.5	1621.2	1621.2	1605.8	1605.8
1050	1685.7	1692.0	1642.2	1647.9	1624.0	1628.6
1200	1714.5	1727.4	1663.6	1675.1	1642.4	1651.8
1350	1743.9	1762.4	1685.2	1702.9	1660.9	1675.3
1500	1774.3	1799.8	1707.3	1731.6	1679.7	1699.4

Table: D.8

STEAM QUALITY VS. DEPTH FOR DIFFERENT RATES AND ZERO AND ONE-HALF STEAM OFF-TAKE AT 1200 FT DEPTH; TIME = 300 DAYS INJ. PRESS. 1500PSIA

Legend:

D : Depth, FT
N O-T : No Off-Take
H O-T : Half Off-Take

Steam Pressure, psia

D	600 Bbls/Day		1200 Bbls/Day		1800 Bbls/Day	
	N O-T	H O-T	N O-T	H O-T	H O-T	N O-T
0	1500.0	1500.0	1500.0	1500.0	1500.0	1500.0
150	1525.0	1525.0	1519.6	1519.6	1517.2	1517.2
300	1550.4	1550.4	1539.4	1539.4	1534.6	1534.6
450	1576.3	1576.3	1559.4	1559.4	1552.2	1552.2
600	1602.8	1602.8	1579.7	1579.7	1569.9	1569.9
750	1629.7	1629.7	1600.3	1600.3	1587.7	1587.7
900	1657.2	1657.2	1621.0	1621.0	1605.7	1605.7
1050	1685.3	1691.5	1642.1	1647.7	1623.9	1628.5
1200	1713.9	1726.7	1663.4	1674.9	1642.2	1651.5
1350	1743.1	1763.0	1685.0	1702.5	1660.7	1674.9
1500	1773.3	1800.0	1707.0	1731.1	1679.5	1698.9

Table: D.9
STEAM QUALITY VS. DEPTH FOR DIFFERENT RATES AND ZERO AND ONE-HALF STEAM OFF-TAKE AT 1200 FT DEPTH; TIME = 500 DAYS INJ. PRESS. 1500PSIA

Legend:

D : Depth, FT
N O-T : No Off-Take
H O-T : Half Off-Take

Steam Pressure, psia

D	600 Bbls/Day		1200 Bbls/Day		1800 Bbls/Day	
	N O-T	H O-T	N O-T	H O-T	H O-T	N O-T
0	1500.0	1500.0	1500.0	1500.0	1500.0	1500.0
150	1525.0	1525.0	1519.6	1519.6	1517.2	1517.2
300	1550.4	1550.4	1539.4	1539.4	1534.6	1534.6
450	1576.3	1576.3	1559.4	1559.4	1552.2	1552.2
600	1602.8	1602.8	1579.7	1579.7	1569.9	1569.9
750	1629.7	1629.7	1600.3	1600.3	1587.7	1587.7
900	1657.2	1657.2	1621.0	1621.0	1605.7	1605.7
1050	1685.2	1691.5	1642.1	1647.7	1623.9	1628.5
1200	1713.9	1726.7	1663.4	1674.8	1642.2	1651.5
1350	1743.1	1762.9	1685.0	1702.5	1660.7	1674.9
1500	1773.2	1800.0	1706.9	1731.0	1679.5	1698.9

Table: D.10
STEAM QUALITY VS. DEPTH FOR DIFFERENT RATES AND ZERO AND ONE-HALF STEAM OFF-TAKE AT 1200 FT DEPTH; TIME = 700 DAYS INJ. PRESS. 1500PSIA

Legend:

D : Depth, FT
N O-T : No Off-Take
H O-T : Half Off-Take

	Steam Pressure, psia					
	600 Bbls/Day		1200 Bbls/Day		1800 Bbls/Day	
D	N O-T	H O-T	N O-T	H O-T	H O-T	N O-T
0	1500.0	1500.0	1500.0	1500.0	1500.0	1500.0
150	1525.0	1525.0	1519.6	1519.6	1517.2	1517.2
300	1550.4	1550.4	1539.4	1539.4	1534.6	1534.6
450	1576.3	1576.3	1559.4	1559.4	1552.2	1552.2
600	1602.8	1602.8	1579.7	1579.7	1569.9	1569.9
750	1629.7	1629.7	1600.3	1600.3	1587.7	1587.7
900	1657.2	1657.2	1621.0	1621.0	1605.7	1605.7
1050	1685.2	1691.5	1642.1	1647.7	1623.9	1628.5
1200	1713.9	1726.7	1663.4	1674.8	1642.2	1651.5
1350	1743.1	1762.9	1685.0	1702.5	1660.7	1674.9
1500	1773.2	1800.0	1706.9	1731.0	1679.5	1698.9

Table: D.11
STEAM QUALITY VS. DEPTH FOR DIFFERENT RATES AND ZERO AND ONE-HALF STEAM OFF-TAKE AT 1200 FT DEPTH; TIME = 900 DAYS INJ. PRESS. 1500PSIA

Legend:

D : Depth, FT
N O-T : No Off-Take
H O-T : Half Off-Take

Steam Pressure, psia

	600 Bbls/Day		1200 Bbls/Day		1800 Bbls/Day	
D	N O-T	H O-T	N O-T	H O-T	H O-T	N O-T
0	1500.0	1500.0	1500.0	1500.0	1500.0	1500.0
150	1525.0	1525.0	1519.6	1519.6	1517.2	1517.2
300	1550.4	1550.4	1539.4	1539.4	1534.6	1534.6
450	1576.3	1576.3	1559.4	1559.4	1552.2	1552.2
600	1602.8	1602.8	1579.7	1579.7	1569.9	1569.9
750	1629.7	1629.7	1600.3	1600.3	1587.7	1587.7
900	1657.2	1657.2	1621.0	1621.0	1605.7	1605.7
1050	1685.2	1691.5	1642.1	1647.7	1623.9	1628.5
1200	1713.9	1726.7	1663.4	1674.8	1642.2	1651.5
1350	1743.1	1762.9	1685.0	1702.5	1660.7	1674.9
1500	1773.2	1800.0	1706.9	1731.0	1679.5	1698.9

Table: D.12
STEAM QUALITY VS. DEPTH FOR DIFFERENT RATES AND ZERO AND ONE-HALF STEAM OFF-TAKE AT 1200 FT DEPTH; TIME = 1100 DAYS INJ. PRESS. 1500PSIA

Legend:

D : Depth, FT
N O-T : No Off-Take
H O-T : Half Off-Take

Steam Pressure, psia

	600 Bbls/Day		1200 Bbls/Day		1800 Bbls/Day	
D	N O-T	H O-T	N O-T	H O-T	H O-T	N O-T
0	1500.0	1500.0	1500.0	1500.0	1500.0	1500.0
150	1525.0	1525.0	1519.6	1519.6	1517.2	1517.2
300	1550.4	1550.4	1539.4	1539.4	1534.6	1534.6
450	1576.3	1576.3	1559.4	1559.4	1552.2	1552.2
600	1602.8	1602.8	1579.7	1579.7	1569.9	1569.9
750	1629.7	1629.7	1600.3	1600.3	1587.7	1587.7
900	1657.2	1657.2	1621.0	1621.0	1605.7	1605.7
1050	1685.2	1691.5	1642.1	1647.7	1623.9	1628.5
1200	1713.9	1726.7	1663.4	1674.8	1642.2	1651.5
1350	1743.1	1762.9	1685.0	1702.5	1660.7	1674.9
1500	1773.2	1800.0	1706.9	1731.0	1679.5	1698.9

Table: D.13
STEAM QUALITY VS. DEPTH FOR DIFFERENT RATES AND ZERO AND ONE-HALF STEAM OFF-TAKE AT 1200 FT DEPTH; TIME = 100 DAYS INJ. PRESS. 750PSIA

Legend:

D : Depth, FT
N O-T : No Off-Take
H O-T : Half Off-Take

Steam Quality, Fraction

D	600 Bbls/Day		1200 Bbls/Day		1800 Bbls/Day	
	N O-T	H O-T	N O-T	H O-T	H O-T	N O-T
0	0.8000	0.8000	0.8000	0.8000	0.8000	0.8000
150	0.7799	0.7799	0.7897	0.7897	0.7930	0.7930
300	0.7594	0.7594	0.7793	0.7793	0.7859	0.7859
450	0.7387	0.7387	0.7688	0.7688	0.7788	0.7788
600	0.7178	0.7178	0.7582	0.7582	0.7717	0.7717
750	0.6966	0.6966	0.7476	0.7476	0.7645	0.7645
900	0.6753	0.6753	0.7369	0.7369	0.7573	0.7573
1050	0.6537	0.6329	0.7262	0.7160	0.7500	0.7433
1200	0.6318	0.5899	0.7154	0.6949	0.7428	0.7292
1350	0.6098	0.5462	0.7045	0.6735	0.7355	0.7150
1500	0.5672	0.4603	0.6838	0.6322	0.7218	0.6878

Table: D.14
STEAM QUALITY VS. DEPTH FOR DIFFERENT RATES AND ZERO AND ONE-HALF STEAM OFF-TAKE AT 1200 FT DEPTH; TIME = 300 DAYS INJ. PRESS. 750PSIA

Legend:

D : Depth, FT
N O-T : No Off-Take
H O-T : Half Off-Take

Steam Quality, Fraction

	600 Bbls/Day		1200 Bbls/Day		1800 Bbls/Day	
D	N O-T	H O-T	N O-T	H O-T	H O-T	N O-T
0	0.8000	0.8000	0.8000	0.8000	0.8000	0.8000
150	0.7807	0.7807	0.7901	0.7901	0.7933	0.7933
300	0.7611	0.7611	0.7801	0.7801	0.7865	0.7865
450	0.7413	0.7413	0.7701	0.7701	0.7796	0.7796
600	0.7212	0.7212	0.7599	0.7599	0.7728	0.7728
750	0.7010	0.7010	0.7498	0.7498	0.7659	0.7659
900	0.6805	0.6805	0.7395	0.7395	0.7590	0.7590
1050	0.6598	0.6400	0.7292	0.7195	0.7520	0.7456
1200	0.6390	0.5989	0.7188	0.6992	0.7451	0.7321
1350	0.6178	0.5571	0.7084	0.6788	0.7381	0.7185
1500	0.5753	0.4714	0.6878	0.6375	0.7244	0.6913

Table: D.15
STEAM QUALITY VS. DEPTH FOR DIFFERENT RATES AND ZERO AND ONE-HALF STEAM OFF-TAKE AT 1200 FT DEPTH; TIME = 500 DAYS INJ. PRESS. 750PSIA

Legend:

D : Depth, FT
N O-T : No Off-Take
H O-T : Half Off-Take

Steam Quality, Fraction

	600 Bbls/Day		1200 Bbls/Day		1800 Bbls/Day	
D	N O-T	H O-T	N O-T	H O-T	H O-T	N O-T
0	0.8000	0.8000	0.8000	0.8000	0.8000	0.8000
150	0.7807	0.7807	0.7901	0.7901	0.7933	0.7933
300	0.7611	0.7611	0.7801	0.7801	0.7865	0.7865
450	0.7413	0.7413	0.7701	0.7701	0.7797	0.7797
600	0.7213	0.7213	0.7600	0.7600	0.7728	0.7728
750	0.7011	0.7011	0.7498	0.7498	0.7659	0.7659
900	0.6807	0.6807	0.7396	0.7396	0.7590	0.7590
1050	0.6600	0.6402	0.7293	0.7196	0.7521	0.7457
1200	0.6391	0.5991	0.7189	0.6993	0.7451	0.7322
1350	0.6180	0.5574	0.7085	0.6789	0.7381	0.7186
1500	0.5755	0.4716	0.6879	0.6376	0.7244	0.6914

Table: D.16
STEAM QUALITY VS. DEPTH FOR DIFFERENT RATES AND ZERO AND ONE-HALF STEAM OFF-TAKE AT 1200 FT DEPTH; TIME = 700 DAYS INJ. PRESS. 750PSIA

Legend:

D : Depth, FT
N O-T : No Off-Take
H O-T : Half Off-Take

Steam Quality, Fraction

D	600 Bbls/Day		1200 Bbls/Day		1800 Bbls/Day	
	N O-T	H O-T	N O-T	H O-T	H O-T	N O-T
0	0.8000	0.8000	0.8000	0.8000	0.8000	0.8000
150	0.7807	0.7807	0.7901	0.7901	0.7933	0.7933
300	0.7611	0.7611	0.7801	0.7801	0.7865	0.7865
450	0.7413	0.7413	0.7701	0.7701	0.7797	0.7797
600	0.7213	0.7213	0.7600	0.7600	0.7728	0.7728
750	0.7011	0.7011	0.7498	0.7498	0.7659	0.7659
900	0.6807	0.6807	0.7396	0.7396	0.7590	0.7590
1050	0.6600	0.6402	0.7293	0.7196	0.7521	0.7457
1200	0.6391	0.5991	0.7189	0.6993	0.7451	0.7322
1350	0.6180	0.5574	0.7085	0.6789	0.7381	0.7186
1500	0.5755	0.4716	0.6879	0.6376	0.7244	0.6914

Table: D.17
STEAM QUALITY VS. DEPTH FOR DIFFERENT RATES AND ZERO AND ONE-HALF STEAM OFF-TAKE AT 1200 FT DEPTH; TIME = 900 DAYS INJ. PRESS. 750PSIA

Legend:

D : Depth, FT
N O-T : No Off-Take
H O-T : Half Off-Take

Steam Quality, Fraction

	600 Bbls/Day		1200 Bbls/Day		1800 Bbls/Day	
D	N O-T	H O-T	N O-T	H O-T	H O-T	N O-T
0	0.8000	0.8000	0.8000	0.8000	0.8000	0.8000
150	0.7807	0.7807	0.7901	0.7901	0.7933	0.7933
300	0.7611	0.7611	0.7801	0.7801	0.7865	0.7865
450	0.7413	0.7413	0.7701	0.7701	0.7797	0.7797
600	0.7213	0.7213	0.7600	0.7600	0.7728	0.7728
750	0.7011	0.7011	0.7498	0.7498	0.7659	0.7659
900	0.6807	0.6807	0.7396	0.7396	0.7590	0.7590
1050	0.6600	0.6402	0.7293	0.7196	0.7521	0.7457
1200	0.6391	0.5991	0.7189	0.6993	0.7451	0.7322
1350	0.6180	0.5574	0.7085	0.6789	0.7381	0.7186
1500	0.5755	0.4716	0.6879	0.6376	0.7244	0.6914

Table: D.18
STEAM QUALITY VS. DEPTH FOR DIFFERENT RATES AND ZERO AND ONE-HALF STEAM OFF-TAKE AT 1200 FT DEPTH; TIME = 1100 DAYS INJ. PRESS. 750PSIA

Legend:

D : Depth, FT
N O-T : No Off-Take
H O-T : Half Off-Take

Steam Quality, Fraction

	600 Bbls/Day		1200 Bbls/Day		1800 Bbls/Day	
D	N O-T	H O-T	N O-T	H O-T	H O-T	N O-T
0	0.8000	0.8000	0.8000	0.8000	0.8000	0.8000
150	0.7807	0.7807	0.7901	0.7901	0.7933	0.7933
300	0.7611	0.7611	0.7801	0.7801	0.7865	0.7865
450	0.7413	0.7413	0.7701	0.7701	0.7797	0.7797
600	0.7213	0.7213	0.7600	0.7600	0.7728	0.7728
750	0.7011	0.7011	0.7498	0.7498	0.7659	0.7659
900	0.6807	0.6807	0.7396	0.7396	0.7590	0.7590
1050	0.6600	0.6402	0.7293	0.7196	0.7521	0.7457
1200	0.6391	0.5991	0.7189	0.6993	0.7451	0.7322
1350	0.6180	0.5574	0.7085	0.6789	0.7381	0.7186
1500	0.5755	0.4716	0.6879	0.6376	0.7244	0.6914

Table: D.19
STEAM QUALITY VS. DEPTH FOR DIFFERENT RATES AND ZERO AND ONE-HALF STEAM OFF-TAKE AT 1200 FT DEPTH; TIME = 100 DAYS INJ. PRESS. 750PSIA

Legend:

D : Depth, FT
N O-T : No Off-Take
H O-T : Half Off-Take

Steam Pressure, psia

D	600 Bbls/Day		1200 Bbls/Day		1800 Bbls/Day	
	N O-T	H O-T	N O-T	H O-T	H O-T	N O-T
0	750.0	750.0	750.0	750.0	750.0	750.0
150	770.0	770.0	765.7	765.7	764.0	764.0
300	790.4	790.4	781.6	781.6	778.0	778.0
450	811.3	811.3	797.6	797.6	792.2	792.2
600	832.5	832.5	813.9	813.9	806.5	806.5
750	854.2	854.2	830.3	830.3	821.0	821.0
900	876.4	876.4	847.0	847.0	835.5	835.5
1050	899.0	905.7	863.8	868.6	850.2	853.8
1200	922.2	936.0	880.9	890.6	865.1	872.3
1350	945.9	967.3	898.1	913.1	880.0	891.2
1500	970.3	1000.2	915.7	936.2	895.1	910.4

Table: D.20
STEAM QUALITY VS. DEPTH FOR DIFFERENT RATES AND ZERO AND ONE-HALF STEAM OFF-TAKE AT 1200 FT DEPTH; TIME = 300 DAYS INJ. PRESS. 750PSIA

Legend:

D : Depth, FT
N O-T : No Off-Take
H O-T : Half Off-Take

Steam Pressure, psia

D	600 Bbls/Day		1200 Bbls/Day		1800 Bbls/Day	
	N O-T	H O-T	N O-T	H O-T	H O-T	N O-T
0	750.0	750.0	750.0	750.0	750.0	750.0
150	770.0	770.0	765.7	765.7	764.0	764.0
300	790.4	790.4	781.6	781.6	778.0	778.0
450	811.2	811.2	797.6	797.6	792.2	792.2
600	832.4	832.4	813.9	813.9	806.5	806.5
750	854.1	854.1	830.3	830.3	821.0	821.0
900	876.2	876.2	846.9	846.9	835.5	835.5
1050	898.8	905.4	863.7	868.5	850.2	853.8
1200	921.8	935.6	880.8	890.4	865.0	872.3
1350	945.4	966.7	898.0	912.9	879.9	891.1
1500	969.7	999.3	915.5	936.9	895.0	910.2

Table: D.21
STEAM QUALITY VS. DEPTH FOR DIFFERENT RATES AND ZERO AND ONE-HALF STEAM OFF-TAKE AT 1200 FT DEPTH; TIME = 500 DAYS INJ. PRESS. 750PSIA

Legend:

D : Depth, FT
N O-T : No Off-Take
H O-T : Half Off-Take

Steam Pressure, psia

	600 Bbls/Day		1200 Bbls/Day		1800 Bbls/Day	
D	N O-T	H O-T	N O-T	H O-T	H O-T	N O-T
0	750.0	750.0	750.0	750.0	750.0	750.0
150	770.0	770.0	765.7	765.7	764.0	764.0
300	790.4	790.4	781.6	781.6	778.0	778.0
450	811.2	811.2	797.6	797.6	792.2	792.2
600	832.4	832.4	813.9	813.9	806.5	806.5
750	854.1	854.1	830.3	830.3	821.0	821.0
900	876.2	876.2	846.9	846.9	835.5	835.5
1050	898.8	905.4	863.7	868.5	850.2	853.8
1200	921.8	935.6	880.8	890.4	865.0	872.3
1350	945.4	966.7	898.0	913.9	879.9	891.1
1500	969.7	999.3	915.5	936.9	895.0	910.2

Table: D.22
STEAM QUALITY VS. DEPTH FOR DIFFERENT RATES AND ZERO AND ONE-HALF STEAM OFF-TAKE AT 1200 FT DEPTH; TIME = 700 DAYS INJ. PRESS. 750PSIA

Legend:

D : Depth, FT
N O-T : No Off-Take
H O-T : Half Off-Take

Steam Pressure, psia

D	600 Bbls/Day		1200 Bbls/Day		1800 Bbls/Day	
	N O-T	H O-T	N O-T	H O-T	H O-T	N O-T
0	750.0	750.0	750.0	750.0	750.0	750.0
150	770.0	770.0	765.7	765.7	764.0	764.0
300	790.4	790.4	781.6	781.6	778.0	778.0
450	811.2	811.2	797.6	797.6	792.2	792.2
600	832.4	832.4	813.9	813.9	806.5	806.5
750	854.1	854.1	830.3	830.3	821.0	821.0
900	876.2	876.2	846.9	846.9	835.5	835.5
1050	898.8	905.4	863.7	868.5	850.2	853.8
1200	921.8	935.6	880.8	890.4	865.0	872.3
1350	945.4	966.7	898.0	913.9	879.9	891.1
1500	969.7	999.3	915.5	936.9	895.0	910.2

Table: D.23
STEAM QUALITY VS. DEPTH FOR DIFFERENT RATES AND ZERO AND ONE-HALF STEAM OFF-TAKE AT 1200 FT DEPTH; TIME = 900 DAYS INJ. PRESS. 750PSIA

Legend:

D : Depth, FT
N O-T : No Off-Take
H O-T : Half Off-Take

Steam Pressure, psia

	600 Bbls/Day		1200 Bbls/Day		1800 Bbls/Day	
D	N O-T	H O-T	N O-T	H O-T	H O-T	N O-T
0	750.0	750.0	750.0	750.0	750.0	750.0
150	770.0	770.0	765.7	765.7	764.0	764.0
300	790.4	790.4	781.6	781.6	778.0	778.0
450	811.2	811.2	797.6	797.6	792.2	792.2
600	832.4	832.4	813.9	813.9	806.5	806.5
750	854.1	854.1	830.3	830.3	821.0	821.0
900	876.2	876.2	846.9	846.9	835.5	835.5
1050	898.8	905.4	863.7	868.5	850.2	853.8
1200	921.8	935.6	880.8	890.4	865.0	872.3
1350	945.4	966.7	898.0	913.9	879.9	891.1
1500	969.7	999.3	915.5	936.9	895.0	910.2

Table: D.24
STEAM QUALITY VS. DEPTH FOR DIFFERENT RATES AND ZERO AND ONE-HALF STEAM OFF-TAKE AT 1200 FT DEPTH; TIME = 1100 DAYS INJ. PRESS. 750PSIA

Legend:

D : Depth, FT
N O-T : No Off-Take
H O-T : Half Off-Take

Steam Pressure, psia

D	600 Bbls/Day		1200 Bbls/Day		1800 Bbls/Day	
	N O-T	H O-T	N O-T	H O-T	H O-T	N O-T
0	750.0	750.0	750.0	750.0	750.0	750.0
150	770.0	770.0	765.7	765.7	764.0	764.0
300	790.4	790.4	781.6	781.6	778.0	778.0
450	811.2	811.2	797.6	797.6	792.2	792.2
600	832.4	832.4	813.9	813.9	806.5	806.5
750	854.1	854.1	830.3	830.3	821.0	821.0
900	876.2	876.2	846.9	846.9	835.5	835.5
1050	898.8	905.4	863.7	868.5	850.2	853.8
1200	921.8	935.6	880.8	890.4	865.0	872.3
1350	945.4	966.7	898.0	913.9	879.9	891.1
1500	969.7	999.3	915.5	936.9	895.0	910.2

VITA

NAME: Mahnaz Kasraie
PLACE OF BIRTH: Kerman, Iran

POST-SECONDARY EDUCATION AND DEGREES:

University of Tehran
Tehran, Iran
1976
M.Sc. in Chemical Engineering

Pennsylvania State University
University Park, Pa., U.S.A.
1977 - 1979
M.S. in Petroleum & Natural Gas Engineering

RELATED WORK EXPERIENCE:

Chemical Engineer
Isiran Company, Tehran
1975 - 1977

Graduate Assistant
Pennsylvania State University
1977 - 1979

Instructor
University of Tehran
1979 - 1980

Research Assistant
Pennsylvania State University
1980 - 1982

Research and Teaching Assistant
University of Alberta
1983 - 1987

PUBLICATIONS:

"Simulation of Modified Steam Injection Processes Applied to Bottom Water Reservoirs", Ph.D. Thesis (1987).

"Steamflooding Bottom Water Reservoirs", Second Tech. Conf. of the S. Sask. Sec. of the Pet. Soc. of CIM, Oct. 7-8, 1987.

"Application of Thermal Recovery Techniques to Marginal Reservoirs", Proc. of 3rd European Meeting on Improved Oil Recovery, Vol. 1, Rome, 379-389 (1985).

"Effect of Bottom Water and Gas Cap on Steam Injection Response", Paper SPE13039, presented at the 59th Annual Fall Meeting of Soc. Pet. Engrs., Houston, Sept. 16-19, 1984.

"Heavy Oil Recovery in the Presence of Bottom Water", Proc. of 35th Annual Technical Meeting of CIM, Calgary, 753-761 (1984).

"Role of Immobile Phase Saturations in Tertiary Oil Recovery", Proc. SPE/DOE Fourth Symp. on Enhanced Oil Recovery, Vol. 1, Tulsa, 71-78 (1984).

"Influence of Rate and Various Immobile Fluid Saturations on the Mixing Coefficient in a Porous Medium", M.S. Thesis, Pennsylvania State University (Aug. 1979).

"Role of Polyesters in Industry", M.S. Thesis, University of Tehran (Feb. 1976).

"Food Additives and Essential Oils", University of Tehran (June 1974).

Membership of Professional Societies:

Society of Petroleum Engineers of AIME
Petroleum Society of Canadian Institute of Mining and Metallurgy